12th Symposium on

High-Performance Marine Vehicles

HIPER'20

Cortona, 12-14 October 2020

12th Symposium on

High-Performance Marine Vehicles

HIPER'20

Cortona, 12-14 October 2020

Edited by Volker Bertram

12th Symposium on High-Performance Marine Vehicles, Cortona, 12-14 October 2020, Hamburg, Technische Universität Hamburg, 2020, ISBN 978-3-89220-718-4

Schriftenreihe Schiffbau
Schwarzenbergstraße 95c
D-21703 Hamburg
http://www.tuhh.de/vss

TUHH
Technische Universität Hamburg-Harburg
Institut für Entwerfen von Schiffen und Schiffssicherheit
Schwarzenbergstraße 95 Gebäude C D-21073 Hamburg

Sponsored by

tutech.de

www.numeca.de

www.econowind.nl

www.alleantia.com

www.fleetcleaner.com

zestas.org

Index

Artificial Intelligence - Maritime Industries' Next Useful Idiot

Volker Bertram, DNV GL, Hamburg/Germany, volker.bertram@dnvgl.com

Abstract

This paper explains key technologies of Artificial Intelligence (AI), namely machine learning, expert systems, speech recognitions, gesture recognition, and related techniques. Capabilities and especially limits of capabilities of AI techniques are discussed. Techniques are illustrated by maritime examples taken from personal experience and literature. The conclusion is that AI techniques are a useful tool, but no silver bullet.

1. What is AI?

You've heard of it, and it is powerful, maybe threatening. Artificial Intelligence or "AI" is a term often used, yet little understood. What we don't know, often scares us, but sometimes we also have unrealistic hopes. Much of the common perception of AI comes through Hollywood movies: AI seems to have a nice female voice which lulls us into trusting "her", until "she" starts killing off humans, because somehow "she" developed "her" own mind. This makes generally for most entertaining movies, but has little in common with my experience and view of AI. It just seems to be a new version of the 1970s' misconception of computers and software: "he" (back then, it was generally a "he") says so and therefore it must be true.

The engineering truth behind the term or misnomer "Artificial Intelligence" is a set of tools that may do jobs better or handle tasks we could not handle at all in the past. The tools as such may fascinate; you may also worry what might be done when the tools are used by the wrong people; but the tools as such do not scare me.

There is no coherent definition of what "Artificial Intelligence" is. In its broadest sense, AI is concerned with the investigation and simulation of human intelligence with the ambition to replicate the processes in machines. A (not exhaustive) list of sub-branches of AI encompasses:

- machine learning / artificial neural nets / machine vision
- knowledge-based systems (expert systems, case-based reasoning, Bayesian networks)
- natural language processing / gesture processing
- robotics
- ...

In this paper, I will try to show that Artificial Intelligence is just another software technique, useful but not performing miracles. Maritime applications will illustrate how the techniques can be applied and contribute to engineering problem solving.

2. Machine Learning

2.1 Principle

Machine learning and data mining are closely related to computational statistics. In essence, we have glorified statistics here with new, catchy labels attached to it.

Traditionally, the human brain is very good at pattern recognition. Table I shows some x-y combinations which would remain meaningless if shown only for a second. Fig.1 shows the corresponding visualisation, *Zelasny (2011)*. Here we see immediately trends and unusual deviations. Such trend spotting and pattern recognition is a human intelligence ability that machine learning tries to mimic (and take further).

Table I: Sample x-y combinations

I	
X	Y
10.0	8.04
8.0	6.95
13.0	7.58
9.0	8.81
11.0	8.33
14.0	9.96
6.0	7.24
4.0	4.26
12.0	10.84
7.0	4.82
5.0	5.68

II	
X	Y
10.0	9.14
8.0	8.14
13.0	8.74
9.0	8.77
11.0	9.26
14.0	8.10
6.0	6.13
4.0	3.10
12.0	9.13
7.0	7.26
5.0	4.74

III	
X	Y
10.0	7.46
8.0	6.77
13.0	12.74
9.0	7.11
11.0	7.81
14.0	8.84
6.0	6.08
4.0	5.39
12.0	8.15
7.0	6.42
5.0	5.73

IV	
X	Y
8.0	6.58
8.0	5.76
8.0	7.71
8.0	8.84
8.0	8.47
8.0	7.04
8.0	5.25
19.0	12.50
8.0	5.56
8.0	7.91
8.0	6.89

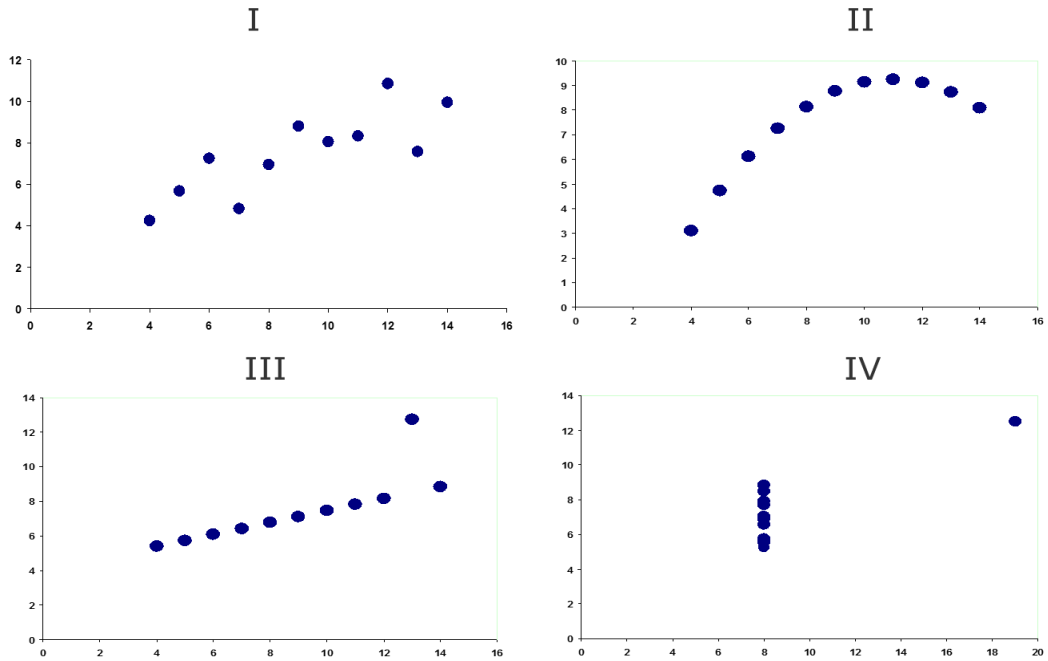

Fig.1: Visual equivalents to Table I – Here we see immediately the patterns, *Zelasny (2001)*

Our standard tools for evaluating such data, e.g. for simple design methods, have been rather primitive and inaccurate. We might have averaged to a single value (coefficient), used linear regression or nonlinear regression analysis based on polynomials, which had the unfortunate tendency to introduce unphysical oscillations for higher orders. These are the standard options Excel offers. And they all fail at least for some of the data sets in Table I.

Wouldn't it be nice to have some mathematical way of mimicking the curve we would instinctively draw through such data sets, ignoring implausible outliers and following the trends our eye sees, something flexible yet smooth and free of inappropriate oscillations? For the naval architect, this is old hat. We have approximated arbitrary point sets for centuries using first flexible thin beams (splines), Fig.2, and later using aptly named spline curves, which do not oscillate and form smooth curves and surfaces. See e.g. *Veelo (2004)* for an overview of such techniques for ship design, automotive engineering or the movie industry.

The machine learning community prefers other functions, such as sigmoid functions, Fig.3. Combining many of these, we have similar basic qualities of flexible approximation and avoiding oscillations.

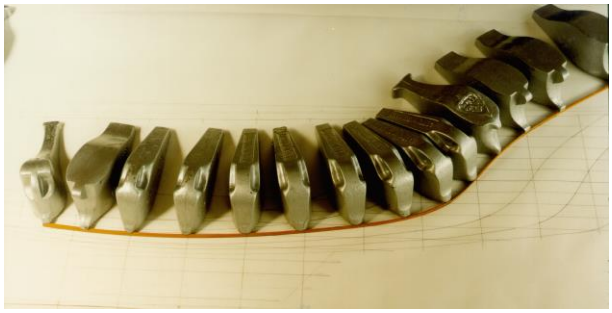

Fig.2: Traditional splines for ship design, source: TU Berlin

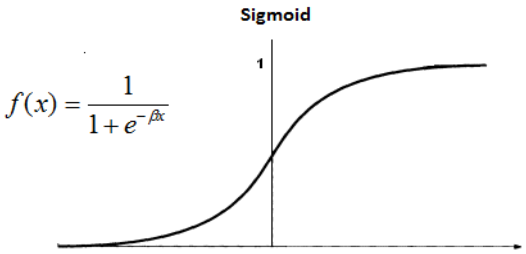

Fig.3: Sigmoid function

Conventional regression has been extensively used in naval architecture in system identification to provide required factors and coefficients. Based on databases of existing designs, coefficients are then interpolated or even extrapolated to calculate coefficients for a new application. This procedure requires the engineer to specify not only which input parameters mainly influence one or more output parameters, but also to specify the type of functional relation between input and output parameters. Most often in the past, simple linear relations have been chosen. Designers plotted data and by visual inspection sometimes chose also simple polynomial relations. This approach is cumbersome and unsuitable for many nonlinear relations. Shortcomings are especially apparent for multi-dimensional input/output data sets.

Artificial neural networks (ANNs) are the most popular technique in machine learning. ANNs can generally represent the mapping of multi-dimensional input/output data sets, i.e. an arbitrary number of input variables x_i and output variable y_i. An ANN structure consists of several layers; each layer consists of several nodes. In the example shown in Fig.4, we have the input layer, the output layer, and one hidden layer. The ANN is "trained" on data sets. This training process results in mathematical relationship output variables y_i and input variables x_i, e.g. of the form (for a single-input, single-output ANN):

$$y = c_0 + c_1 \cdot \mathrm{sig}\,[b_0 + b_1 \cdot \mathrm{sig}(a_{10} + a_{11} \cdot x_1 + a_{12} \cdot x_{2+\ldots}) + b_2 \cdot \mathrm{sig}(a_{20} + a_{21} \cdot x_1 + a_{22} \cdot x_{2+\ldots}) + \ldots] \qquad (1)$$

Here, sig denotes the sigmoid function, Fig.3. After sufficient training, adjusted values for the coefficients a, b, and c are derived and the non-linear relationship is determined. Now the ANN can very rapidly determine values y_i for given values x_i. One might also use the general functional expression of Eq.(1) and use least-square fit methods to determine the coefficients a, b and c. But then we would lose out on a wealth of wonderful jargon and might not be that impressed anymore.

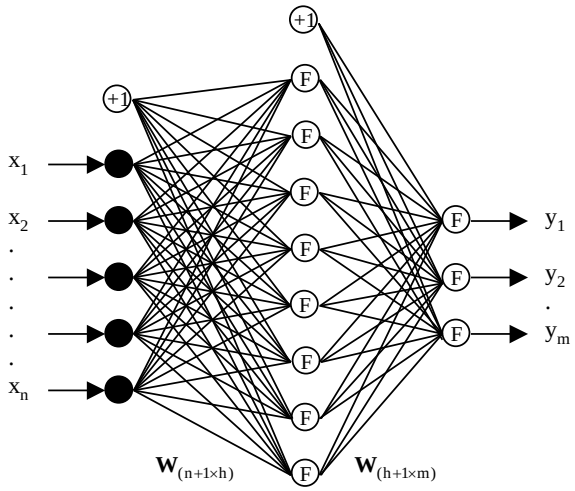

Fig.4: General structure of an Artificial Neural Network

There are countless applications for ANNs in the literature, as pattern matching or trending is needed in countless fields. Popular TV series may show fingerprint matching, facial recognition or machine reading of licence plates – all based on neural nets. General data mining, as found in major internet companies such as Google, Yahoo, Amazon, etc. will involve neural nets, and much of the large financial trading industries will rely on them. Game playing and decision making in some strategic games (chess, backgammon, poker, Go) is another popular application of ANNs.

Finally, "Deep Learning" is a more recent buzz word used when neural nets with two or more hidden layers are used.

2.2. Limitations

Artificial Neural Nets (as the most popular machine learning technique) have in principle no problem in handling arbitrary numbers of input variables. Hence the progress through them that has sometimes fuelled mythical confidence in what they can do. As any other tool, ANNs have their limitations:

- They can't predict the unpredictable. Random events, such as lottery numbers of next week, are by definition unpredictable. Many events involving highly nonlinear ("chaotic") behaviour are quasi-random. For example, crash-stop manoeuvres of ships are highly non-linear; small changes in the ambience at the begin of the manoeuvre result in largely varying tracks for the stopping manoeuvre, *Söding (1995)*, Fig.5. Subsequently, attempts to predict crash-stop paths using ANNs cannot succeed. If satisfactory agreement is published, e.g. *Moreira and Guedes Suares (2003)*, Fig.6, it is the luck of the draw taking only one of the possible tracks in sea trials for comparison.

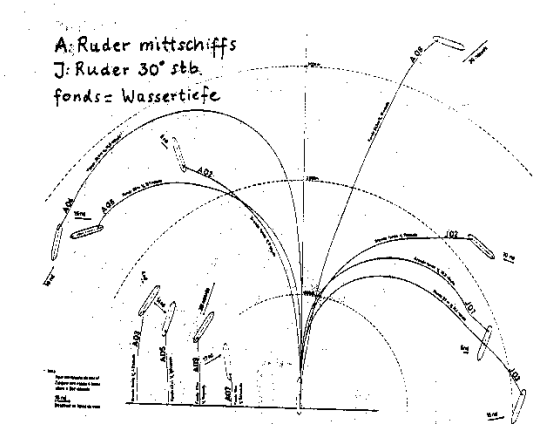

Fig.5: Sea trial results of repeated crash-stop manoeuvres for a tanker, *Söding (1995)*

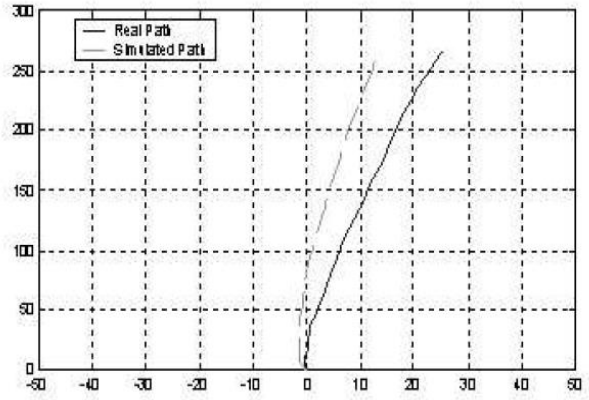

Fig.6: Satisfactory ANN prediction of crash-stop manoeuvre, *Moreira and Guedes Suares (2003)*

- Machine Learning is data greedy. Imagine an arbitrary curve, e.g. the sin-function sin(x) over one period. For us to recognize the function (= pattern), we would probably need ~10 points equidistantly spaced, and twice as many if we have some random selection. For a function of 2 input variables, we would then need 100-400 points to see the pattern or train a neural network. For n input variables, then 10^n-20^n data points are needed. For many real-world problems, we have many factors driving the problem; e.g. for hull performance monitoring we may look at changing operational conditions (speed, draft, trim, rudder angle) and ambient conditions (water depth, significant wave height, wave direction, wind speed, wind direction, possibly also current speed, current direction), leading to billions of data points to train a neural network properly.

  For many maritime problems, e.g. in ship design, we may have O(10)-O(100) data points. Then machine learning no longer works and we have to use natural intelligence, e.g. reducing the number of free variables using physical insight.

- Machine learning is not good for rare events. The relations found are fine for interpolating, especially in regions where we have many data points (= frequently occurring cases). Extrapolating often results in wrong predictions. Machine learning is based on experience, not theoretical reasoning. This may lead to problems in practice, *Bertram (2014)*: "[…], there was a shipowner who was looking for the best trim optimisation for his […] ships. He looked for suitable candidates and installed a CFD-based system [i.e. based on systematic simulations based on fluid dynamics physics] and a machine-learning system on one of his ships. One fine day, the captain asked both systems for advice. The CFD-based system said: 1m down by the bow. The machine learning system said: 1m down by the stern. […] the solution to the puzzle was that the comparison was made shortly after installation. The captain had never before driven the ship on that draft and at that speed other than with trim by stern. The machine learning system had, therefore, never "seen" that by trimming by bow the fuel consumption was lower and picked the best solution from its limited experience. Its knowledge base was patchy and thus its recommendation not good."

2.3. Maritime applications

ANNs are increasingly used in the maritime industries for system identification. *Hess and Faller (2000)* give an overview of early maritime ANN applications. *Mesbahi (2003)* gives an introduction to ANNs and some applications from ship design and marine engineering.

ANNs have been used in

- system identification, e.g. deriving body-force coefficients in ship manoeuvring from model tests or sea trials, e.g. *Moreira and Guedes Suares (2003)*, or diesel engine monitoring, *Mesbahi and Atlar (2000)*
- deriving design formulas from narrow-domain databases, e.g. power prediction for tugs, Fig.6, *Mesbahi and Bertram (2000)* or semi-planing hulls, *Bertram and Mesbahi (2004)*
- meta-modelling using ANNs to interpolate between data sets generated in expensive simulations, e.g. *Harries (2000), Couser et al. (2011)*; in a similar vein, ANNs can be used as to create response surfaces for interpolation of simulation results; e.g. in DNV GL's ECO Assistant for trim optimization, 300-500 CFD (Computational Fluid Dynamics) results of power as function of speed, draft and trim are connected smoothly in such a response surface.
- Automatic ship type identification, Fig.7, *Kumlu (2012)*
- Economic predictions, e.g. of freight rates, *Bruce and Morgan (2006)*

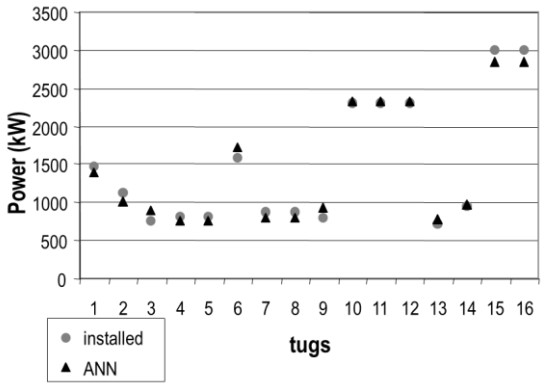

Fig.6: Tug power prediction, *Mesbahi and Bertram (2000)*

Fig.7: Automatic ship identification, *Kumlu (2012)*

The ANN software ICE (Intelligent Calculations of Equations) is provided free-of-charge by William Faller (Applied Simulation Technologies), *Roddy et al. (2006)*. The software is easy to use, tries automatically different architectures (i.e. number of layers and nodes per layer) to get best fits, and

allows exporting the resulting mathematical formulas directly to source code of widely used programming languages, *Bertram and Herradon (2016)*.

3. Expert Systems

3.1. Principle

Knowledge-based Systems (KBS) or expert systems (the terms are used here – as in many publications within the maritime industries – interchangeably) are Artificial Intelligence (AI) tools which reason within a narrow knowledge domain. Fig.8 shows the basic structure of an expert system, which might be best explained in its similarity to database management systems such as Excel:

- Knowledge base = a collection of knowledge sets, frequently in IF-THEN form; corresponding to data sets in a database management system; this part is domain specific.
- Human-machine interface = routines to type in knowledge sets, display knowledge sets, initiate action such as inference, etc.; corresponding to common interfaces in database management systems
- Optionally: sensor data; corresponding to automatic data import from sensors e.g. for onboard measurement campaigns
- Inference engine = core software that performs the key task of a knowledge-base system, i.e. bringing input data, sensor data and knowledge (rules) together to derive a conclusion; corresponding to the core database management system that sorts, filters, and performs other data management tasks; this part is domain independent.

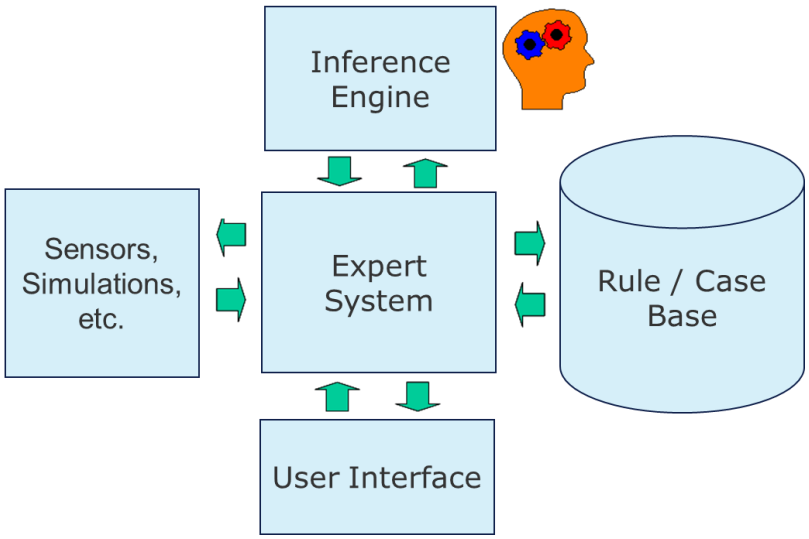

Fig.8: Basic structure of an expert system

'Production systems' are the most common way to represent knowledge in engineering. Production systems represent knowledge in IF-THEN rules, see the example in Fig.9. Many expert systems combine documented rules (taken e.g. from regulations or laws of physics) and heuristic knowledge, i.e. rules taken from common practice and experience. The KBS approach differs from conventional sequential computing approaches. The rule order in KBS is not critical for the result. However, it may affect the speed of execution significantly. KBS are often useful in developing a knowledge base as they allow rapid prototyping. Once a knowledge base has been established and is expected to remain constant for longer time, it may be incorporated in conventional programming approaches for much faster response times. Case-based reasoning (CBR) systems are special instances of knowledge-based systems. Here the approach is similar to that of lawyers or doctors: Find related cases and study them to derive the best strategy for the current case. (Intelligent) agents are swarms of simple expert systems working (communicating) together.

```
| ------------------------------------------
  DEFINE RULE   :   002-ENCLOSED_SUPERSTRUCTURE
| ------------------------------------------
  GOAL : 'HEIGHT_OF_ENCLOSED_SUPERSTRUCTURE'
| ----------------------------------------
    IF 'FREEBOARD_DECK' IS EQUAL TO 'SECOND DECK' THEN
       'HEIGHT_OF_ENCLOSED_SS' IS EQUAL TO 'DEPTH_TO_UPPER_DECK'
        MINUS 'DEPTH_TO_SECOND_DECK'
    RULE END

| ---------------------------------------
  DEFINE RULE   :   003-STABILITY_CRITERIA_4
| ---------------------------------------
  GOAL : 'AREA_BETWEEN_30_AND_DF_ANGLE'
| ------------------------------------
|  ASSUME THE STANDARD IMO CRITERIA APPLY
    IF 'DEFAULT_STABILITY_CRITERIA_REQUIRED' IS TRUE THEN
       'AREA_BETWEEN_30_AND_DF_ANGLE' IS EQUAL TO 0.030 METRE:RADIANS
    RULE END

| ---------------------------------------
  DEFINE RULE   :   015-DRAFT_RESTRICTION
| ---------------------------------------
  GOAL : 'MAXIMUM_DRAFT'
| ----------------------
    IF 'SCANTLING_DRAFT' IS GREATER THAN 'DRAFT_RESTRICTION' THEN
       'MAXIMUM_DRAFT' IS EQUAL TO 'DRAFT_RESTRICTION'
       OTHERWISE 'MAXIMUM_DRAFT' IS EQUAL TO 'SCANTLING_DRAFT'
    RULE END
```

Fig.9: Rules incorporated in INCODES in pseudo-English, *Welsh et al. (1990)*

Söding (1976) presented one of the earliest maritime knowledge-based system applications with his CHWARISMI compiler. Söding used the expression 'machine intelligence' for ship design rather than artificial intelligence, but the concept is the same: arbitrary rules (here functions and relations/constraints for optimization are given in arbitrary order and the CHWARISMI compiler turns them into a Fortran software code that will perform the formal optimization. Based on CHWARISMI, Gudenschwager developed the more user-friendly optimization shell DELPHI, *Bertram et al. (1998), Gudenschwager (2003).*

3.2. Limitations

The coding of an expert system is relatively simple in well-structured, rule-based domains with extensive, but documented expertise, e.g. fault diagnosis, medical diagnosis, or monitoring tasks. The challenge lies in getting all relevant rules together. This task can get daunting in the following cases:

- Implicit knowledge – Here the expert knows what to do, but cannot express the fundamental rule. For example, we may use the right prepositions in our mother tongue, but most of us will not be able to explain why we choose this or that preposition to a student of our language. We follow our 'feeling' of what sounds right. Here, knowledge engineers need to make implicit knowledge explicit, e.g. by observing experts, asking questions and trying to find fundamental rules. This can be a tedious, costly and sometimes error-prone approach. And sometimes, the expert may refuse to cooperate, e.g. for fear that he might be replaced by the expert system and lose his position.
- Fuzzy rules – Many rules are vague. Traffic rules, for example, require us to use headlights when visibility is 'poor'. Observe cars at dawn and dusk and you will see that this rule is subject to interpretation. Here, a solution may lie in showing a larger group of 'experts' a situation and ask for their assessment. Then you may take a typical (average), cautious (lower end) or daring (upper end) value and program this into your system. Again, using multiple experts possibly in multiple situations requires time and effort.

- Changing rules – For implicit and fuzzy rules, the preparation of rule sets may take considerable time. Rules may change within that time, e.g. due to political, economic or technical changes. Then the expert system becomes obsolete before it is finished – the "cathedral effect". As a general rule, the wider the domain, the more effort is needed and the more likely are changes somewhere within that domain.
- Lack of rules – In some domains, processes are not clearly structured. For example, look at art. Or design. It will be difficult to get three experts in these fields who agree on an approach or an assessment. Engineers like to think in IF-THEN categories, artists don't. Neither do almost artists, such as ship designers.

For case-based reasoning, the usefulness of a system depends on the number of cases and the associated tags or searching options. It is like a database. You need sufficient references in the system, you need to maintain the system feeding new cases in and you need some smart retrieval algorithms to find the 'right' cases.

3.3. Maritime applications

KBS have been proposed, developed and implemented for a variety of maritime applications, *Bertram (1998,2000,2013)*, including:

- Ship design (conceptual & detailed design, both for ship and components), e.g. *Erikstad (1996), Hees (1997), Es and Hees (2003)*
- Shipyard and port operations, e.g. *Simpson et al. (2003)*
- Ship operation, regular (collision avoidance, ballast control, cargo handling, predictive maintenance, …), e.g. *Bertram (1998), Statheros et al. (2008), Tam et al. (2009)*
- Ship operation, responsive (fault diagnosis for ship machinery, emergency response, …), *Kaeding and Bertram (1996), Lunau and Nielsen (1998)*

The main maritime applications of expert systems in practice are found for ship operation. This is not surprising; ship design is a creative and complex process in a rapidly changing economic and regulatory environment. In contrast, collision avoidance follows rules (COLREGs) that have hardly changed in the last 100 years and rules for emergency response are conveniently documented in emergency response plans and handbooks.

Expert systems for ship operation have enjoyed a renaissance in research interest, driven by the quest for autonomous/unmanned ships. With new technologies for sensor data and resulting situation awareness (e.g. automatic ship type recognition, AIS data, or LIDAR), it makes sense to review and update the solutions that have been developed since the 1990s, Fig.10. DNV GL works on combining machine vision and case-based reasoning for next-generation plan approval, Fig.11. The idea is to identify similar plans to the one submitted for approval, retrieve the corresponding cases, and derive recommendations based on these.

Fig.10: Collision avoidance on unmanned ship concept ReVolt by DNV GL

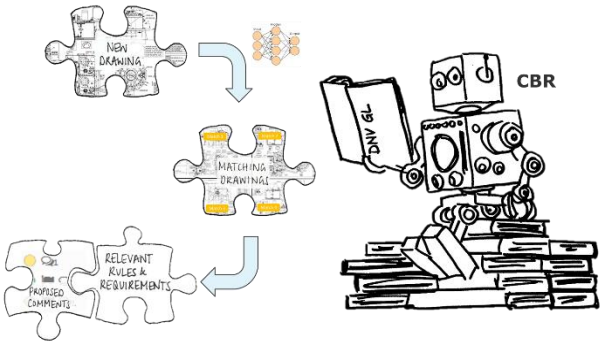

Fig.11: Next-generation plan approval combining pattern recognition and case-based reasoning

4. Speech & Gesture Recognition

4.1. Principle

Speech recognition works on “speech to text” and more recently also on “speech/text to meaning”. The task is simplified by limiting the vocabulary, e.g. just understanding the numbers 0 to 9, ‘yes’, ‘no’, and ‘help’ in phone company or credit card services. Speech recognition may involve system training on an individual speaker who has to read text or isolated vocabulary to the system. Such individual training reduces failure rate significantly. Speech recognition systems for companies or services with many customers cannot be personalized to individual speakers. Such ‘speaker independent’ systems may resort to other techniques to keep failure rates (and customer frustration) to an acceptable limit.

Accuracy of speech recognition may vary with the following:

- Vocabulary size and confusability (“foreign voices” vs. “for invoices”)
- Speaker dependence versus independence (Inspector Clouseau saying “massage”, “reum” or “dewg” would be understood saying “message”, “room” and “dog” by a system trained on Peter Seller’s fake French accent.)
- Discontinuous or continuous speech (“for – pause – invoices” would not be confused with “foreign – pause – voices”)
- Reading vs spontaneous speech (“ah”, “uh”)
- Adverse conditions (the ‘cocktail party’ effect with other people speaking, noisy industrial environment, etc.)

Like many AI techniques, speech recognition has been through manic-depressive cycles. In 2006, Microsoft had an epic blunder in demonstrating its speech recognition software. With time and funding, we have reached widespread acceptance, e.g. in Amazon’s Alexa Voice Service. However, Alexa’s intelligence is very limited in the sense that it performs only a handful of tasks (order online X; play music Y; read latest news; etc.) Nevertheless, the progress within a decade is significant.

Part of the motivation to fund research on speech recognition lies in practicalities of computer development. In “The Imitation Game”, Alan Turing (played by Benedict Cumberbatch) stands in front of the indeed colossal Colossus computer trying to crack the German codes. Today, smart phones have vastly more computing power than the Colossus (or even all of NASA back in 1969 when they put the first man on the moon). Yet, the computer part in the smartphone is only a small fraction of its volume – the size of a smartphone is driven by user interface and energy supply (largely driving the screen). As our hands remain roughly the same size, miniaturization of computers is limited as long as we need manual input and displays. Microphones and cameras can be miniaturized (as we know from our smartphones). Voice control is also useful when we are hands are busy (e.g. driving a car, piloting an airplane, etc.) or when we are handicapped.

Fig.12: Computer (1943); scene from the movie “The Imitation Game”

Fig.13: Smart phone (2016) with vastly more computing power than 1943 computer

Modern speech recognition uses a variety of techniques to understand speech. So do we actually. On the lowest level, you may see speech as a pattern of frequency and amplitude variations. Artificial neural nets may then perform their task of pattern matching and match sound modulation to words. If we have speaker-dependent training and concentrate on making pauses between words, we may get good results, say 95-98% word recognition success rate. Difficulties remain for homonyms, i.e. same or nearly same sounding words, for example C, see and sea. Here, we use context in the sense that we look at groups of words. 'Vitamin C', 'I can see clearly now' and 'deep blue sea' make it clear to us what homonym should be used. We just look at frequently used combinations of words (just like Google does) and decide to go with the most frequently used term. That may get us to 99% success rate. For rest, humans and computers will remain resigned to resorting to time honored strategies, such as asking to paraphrase or spell out.

Applications of speech recognitions range widely, including control of secondary equipment in airplanes and cars, automatic subtitling, automatic assistants (e.g. Apple's Siri), mobile email, speech-to-text reporting (e.g. in court reporting), pronunciation evaluation in language e-learning, hands-free user-interfacing with computers (e.g. in Virtual Reality applications and video gaming).

Gesture recognition is akin to speech recognition. It commonly focusses on hand or facial gestures (mimics). Like speech recognition, gesture recognition enables humans to interact with machines (computers, robots, etc.) without touching any controls. Fatigue detection software may look at eye openness patterns and use artificial neural networks to identify fatigue in drivers, pilots or machinery operators, Fig.14.

Gesture recognition is an obvious choice when silence is called for (e.g. in military operations) or imposed (e.g. for divers under water). Generally, the 'vocabulary' in gesture recognition is even more constraint than in speech recognition. Interpreting human emotions (such as frustration) is part of research for future man-machine interfaces; MIT's KISMET is an example for robots recognizing and expressing emotions, Fig.15, https://en.wikipedia.org/wiki/Kismet_(robot).

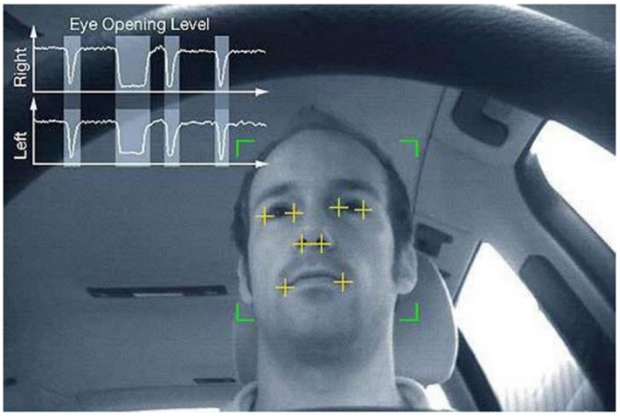

Fig.14: Fatigue recognition, www.eyealertgps.com

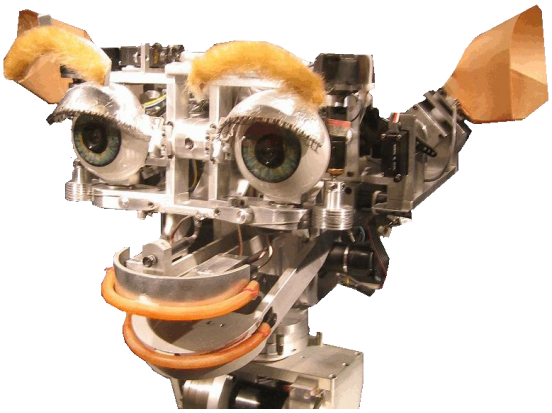
Fig.15: KISMET emotional robot

4.2. Limitations

Most commercial speech recognition software concern English. (Even here, we may get interesting results in the USA looking for ant or aunt killers.) For our purposes, this is good enough as English is the official language of international shipping and the maritime industries perform business largely in 'international' English. Most applications use small subsets of natural language with O(100) to O(1000) words. Humans may use a lot more words, but for the system they are just white noise until words from its vocabulary set are recognized. Most applications reach their limits when the 'sound quality' is not good, e.g. frequencies being cut off in (mobile) telephone sound transmission, ambient noise/echo, or accents (try YouTube Voice Recognition Elevator for a demonstration).

Gesture recognition requires cameras catching the gestures. For operators sitting in a fixed place (driver in a car, us sitting in front of our PC screen with a webcam), capturing the face is easy. For moving people, it is difficult. Emotional interpretation is culture dependent. Often, a specific sign language with clearly different signs has to be used.

4.3. Maritime applications

The voice-operated Super Bridge-X system of Mitsubishi allows in principle 'no-touch' operation of the ship, *Nagaya (1997), Fukuto et al. (1998)*. Here, the master is addressing the system by speaking (e.g. ordering changes in speed or course, changing displays on computers, etc.) and the system is announcing via a loudspeaker relevant information (e.g. confirmations of accepted orders, warnings and alarms, etc.). The advantages of voice-operation are obvious: The hands and eyes are free for other tasks, e.g. watching the traffic and checking sea charts. The interaction with the bridge system then becomes more like the traditional way of interacting with other humans on the bridge. The system is based only on Japanese as language, understanding ~30 commands or inquiries.

Wauchope (2003), Wauchope et al. (2003) present a speech-interactive virtual-reality environment for ship familiarization for the US Navy. Here, "speech interaction provides a highly natural alternative that offers minimal interference with the eyes/hands-busy task of virtual navigation."

In 2017, DNV GL announced the development of an AI-based customer support system using speech recognition and expert systems to support their DATE (Direct Access to Technical Expert) service, Fig.16.

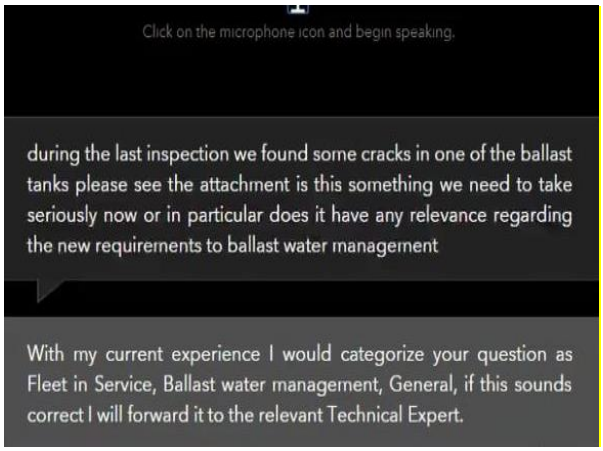

Fig.16: Speech recognition in DNC GL's customer assistant software

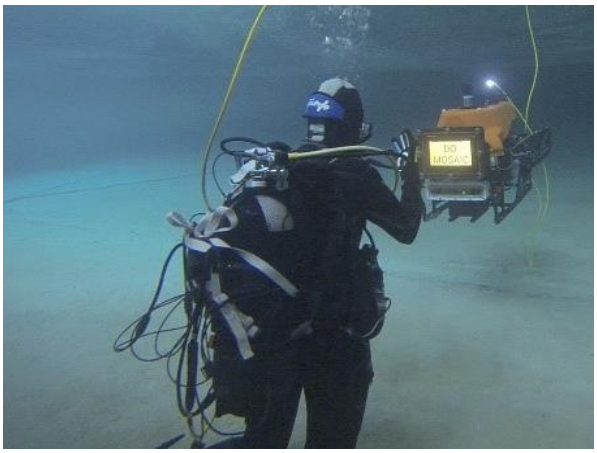

Fig.17: CADDY robot acknowledging diver command to do mosaic

Fig.18: Gesture recognition in CADDY diver support robot, http://www.caddy-fp7.eu/

The EU research project CADDY developed underwater gesture recognition for diver support, Figs.17 and 18. The divers need to wear special gloves with clear markings and use a special sign language, dubbed CADDIAN, with 52 symbols to send messages to the robot. The robot acknowledges with light signals and an LED screen displaying text.

5. Conclusion

Artificial Intelligence is a tool, sometimes using unnecessarily pretentious jargon. Like any other tool, it can be used for good or for bad purposes. Artificial Intelligence as such has no ethics, but it also has no mind or will of its own. Unlike a human, an AI software for playing Go brilliantly will not develop its own initiative or curiosity and start learning chess, for example.

The examples presented show that AI techniques can be put to good use for maritime applications. We can expect more and increasingly sophisticated applications to evolve in years to come.

References

BERTRAM, V. (1998), *Knowledge-based systems for maritime applications*, 26th WEGEMT School, Hamburg, www.wegemt.com/download/wegemt/26th_WEGEMT_School_Expert_Systems_for_Marine_Applications.pdf

BERTRAM, V. (2000), *Knowledge-based systems for ship design and ship operation*, 1st Conf. Computer and IT Applications in the Maritime Industries (COMPIT), Potsdam, pp.63-71, http://data.hiper-conf.info/compit2000_potsdam.pdf

BERTRAM, V. (2003), *Optimization in ship design*, OPTIMISTIC – Optimization in Marine Design, Mensch & Buch Verlag, Berlin, pp.29-56, http://www.wegemt.com/wp-content/uploads/2019/04/39th_WEGEMT_Summer_School_on_Optimistic_Optimization_in_Marine_Design.pdf

BERTRAM, V. (2013), *A survey of knowledge-based systems for ship design and ship operation*, Int. J. Intelligent Engineering Informatics (IJIEI) 2/1, pp.71-90

BERTRAM, V. (2014), *Trim optimisation – Don't blind me with science!*, The Naval Architect, September, pp.66-68, www.dnvgl.com/Images/2014_TheNavalArchitect_Bertram_TrimOptimization_tcm8-21468.pdf

BERTRAM, V.; HERRADON, E. (2016), *Predicting added resistance in wind and waves employing artificial neural nets*, 1st Hull Performance & Insight Conf. (HullPIC), Pavone, pp.14-22, http://data.hullpic.info/HullPIC2016.pdf

BERTRAM, V.; MESBAHI, E. (2004), *Estimating resistance and power of fast monohulls employing artificial neural nets*, 4th Conf. High-Performance Marine Vehicles (HIPER), Rome, pp.18-27, http://data.hiper-conf.info/Hiper2004_Rome.pdf

BIBULI, M.; BRUZZONE, G.; CACCIA, M.; CHIARELLA, D.; FERRETTI, R.; ODETTI, A.; RANIERI, A.; ZEREIK, E. (2017), *Cutting-edge underwater robotics - CADDY project challenges, results and future steps*, 16th Conf. Computer and IT Applications in the Maritime Industries (COMPIT), Cardiff, pp.101-114, http://data.hiper-conf.info/compit2017_cardiff.pdf

BRUCE, G.; MORGAN, G. (2006), *Artificial neural networks – Application to freight rates*, 5th Conf. Computer and IT Applications in the Maritime Industries (COMPIT), Oegstgeest, pp.146-153, http://data.hiper-conf.info/compit2006_oegstgeest.pdf

COUSER, P.; HARRIES, S.; TILLIG, F. (2011), *Numerical hull series for calm water and sea-keeping*, 10th Conf. Computer and IT Applications in the Maritime Industries (COMPIT), Berlin, pp.206-220, http://data.hiper-conf.info/compit2011_berlin.pdf

ERIKSTAD, S.O. (1996), *A decision support model for preliminary ship design*, Ph.D. thesis, NTNU, Trondheim

ES, K. van; HEES, M.T. van (2003), *Application of knowledge management in conceptual naval ship design*, 2nd Conf. Computer and IT Applications in the Maritime Industries (COMPIT), Hamburg, pp.350-362, http://data.hiper-conf.info/compit2003_hamburg.pdf

FUKUTO, J.; NUMANO, M.; MIYAZAKI, K.; ITOH, Y.; MURAYAMA, Y.; MATSUDA, K.; SHIMONO, N. (1998), *An advanced navigation support system for a coastal tanker aiming at one-man bridge operation*, on Control Applications in Marine Systems (CAMS '98), IFAC Proc. 31/30, pp.179-184, http://www.sciencedirect.com/science/article/pii/S1474667017384379

GUDENSCHWAGER, H. (2003), *Application and optimization in basic ship design*, OPTIMISTIC – Optimization in Marine Design, Mensch & Buch Verlag, Berlin, pp.173-190

HARRIES, S. (2010), *Investigating multi-dimensional design spaces using first principle methods*, 7th Conf. High-Performance Marine Vehicles (HIPER), Melbourne, pp.179-194, http://data.hiper-conf.info/Hiper2010_Melbourne.pdf

HEES, M.T. (1997), *Quaestor: Expert governed parametric model assembling*, PhD thesis, TU Delft

HESS, D.; FALLER, W. (2000), *Simulation of ship maneuvers using recursive neural networks*, 23rd Symp. Naval Hydrodynamics, Val de Reuil

KAEDING, P.; BERTRAM, V. (1996), *Artificial intelligence for ship automation – Technical and economical aspects of reduced crews*, IfS Report 572, Univ. Hamburg

KUMLU, D. (2012), *Autonomous ship recognition from color images*, MSc Thesis, Univ. Southern California, http://digitallibrary.usc.edu/cdm/ref/collection/p15799coll3/id/64052

LUNAU, C.P.; NIELSEN, J.K. (1998), *EMMA – Onboard emergency management system for ships*, 26th WEGEMT School, Hamburg, www.wegemt.com/download/wegemt/26th_WEGEMT_School_Expert_Systems_for_Marine_Applications.pdf

MESBAHI, E. (2003), *Artificial neural networks – Fundamentals*, 39th WEGEMT School OPTIMISTIC – Optimization in Marine Design, Mensch & Buch Verlag, Berlin, pp.191-216, www.wegemt.com/?wpfb_dl=45

NAGAYA, S. (1997), *Navigation support system with voice control and guidance*, Int. Marine Electrotechnology Conf., Shanghai

SIMPSON, D.; FURSTENBERG, L.; KALATHAS, E.; BERTRAM, V. (2003), *Virtual prototyping for developing South African ports*, 2nd Conf. Computer and IT Applications in the Maritime Industries (COMPIT), Hamburg, pp.235-246, http://data.hiper-conf.info/compit2003_hamburg.pdf

SÖDING, H. (1976), CHWARISMI I und II : Compiler für technische Entwurfsprobleme, ESS Report 15, TU Hannover

SÖDING, H. (1995), *Manövrierfähigkeit von Schiffen*, Lecture Notes, Institut für Schiffbau, Univ. Hamburg

STATHEROS, T.; HOWELLS, G.; McDONALD-MAIER (2008), *Autonomous ship collision avoidance navigation concepts, technologies and techniques*, J. Navigation 61, pp.129-142

TAM, C.K.; BUCKNALL, R.; GREIG, A. (2009), *Review of collision avoidance and path planning methods for ships in close range encounters*, J. Navigation 62, pp.455–476

VEELO, B. (2004), *Variations of Shape in Industrial Geometric Models*, PhD thesis, NTNU, Trondheim, https://www.sarc.nl/publications/variations-of-shape-in-industrial-geometric-models/

WAUCHOPE, K. (2003), *Interactive Ship Familiarization System: Technical Description*, Technical Report AIC-03-001, Navy Center for Applied Research in Artificial Intelligence, Washington, http://citeseerx.ist.psu.edu/viewdoc/download?doi=10.1.1.7.282&rep=rep1&type=pdf

WAUCHOPE, K.; EVERETT, S.; TATE, D.; MANEY, T. (2003), *Speech-interactive virtual environments for ship familiarization*, 2nd Conf. Computer and IT Applications in the Maritime Industries (COMPIT), Hamburg, pp.70-83, http://data.hiper-conf.info/compit2003_hamburg.pdf

WELSH, M.; BUXTON, I.L.; HILLS, W. (1990), *The application of an expert system to ship concept design investigations*, Trans. RINA, pp.99-113

ZELASNY, G. (2001), *Say It with Charts: The Executive's Guide to Visual Communication*, McGraw-Hill

Wind Propulsion – Assessment, Certification and Classification Services

Hasso Hoffmeister, DNV GL, Hamburg/Germany, hasso.hoffmeister@dnvgl.com

Abstract

This paper looks at the supporting services, a classification society (DNV GL) provides for wind assisted ships in times, where the related technology sees an encouraging revival. From engineering services supporting the design (or assessment), to IMO and Class certificates (type approval and notations), technical expertise of a third-party objective service provider plays a key role in enabling the implementation of wind assisted propulsion systems.

1. At the dawn of wind propulsion renaissance

The revival of wind propulsion seems to happen now; this is mainly driven by the quest for reducing emissions to counteract climate change, as obliged by the IMO. This renaissance of wind propulsion has been predicted by some visionary pioneers for decades. E.g. *Bertholdt and Riesch (1988)* pointed out that "…using the wind means using the most environmentally friendly energy source. Saving (fossil) fuel means emitting fewer pollutants. Time will come, in which this aspect will be considered more valuable than pure commercial interest."

Schenzle (2010) summarizes concepts for wind propulsion of ships. He convincingly argues that sea transportation particularly lends itself for first steps away from carbon combustion, for three reasons:

- Its uniquely low energy demand could be largely covered from solar sources [meaning the indirect solar energy source "wind"];
- Wind is easily available at sea and can directly drive ships without transformation losses;
- Weather routing and energy management can largely compensate for the variable input.

2. DNV GL as third-party competent service provider

DNV GL has accompanied wind propulsion technology for a long time, offering related certification services around sailing rig technology for more than 100 years, Fig.1. Friedrich Ludwig Middendorf, a former board member of Germanischer Lloyd, wrote a technical book about the design and construction of Tallship Rigs, *Middendorf (1903)*. More than 100 years later, it still stands valid and has been the basis for the DNV GL Standard "Tallship Rigs" which is enjoying worldwide reception in that industry.

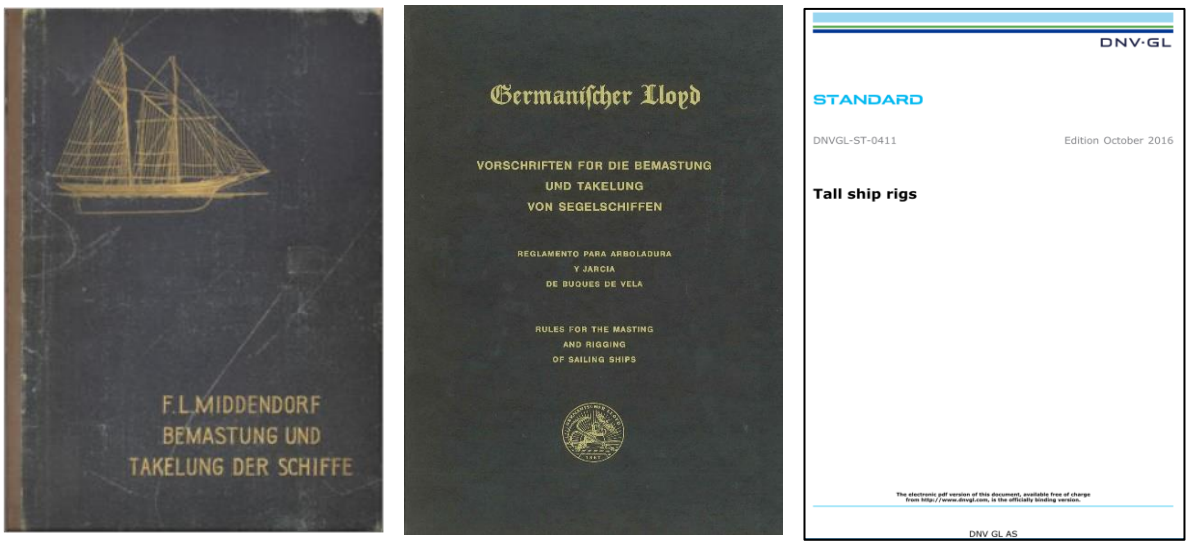

Fig.1: More than 100 years of accompanying wind propulsion technology

Over 25 years ago, DNV GL accompanied the pioneering age of composite materials, when carbon masts and (later) carbon rigging were introduced in the superyacht industry. Technical benchmark standards such as Germanischer Lloyd's "Guidelines for design and Construction of Large Modern Yacht Rigs" (2002) and DNV GL's "Design and construction of large modern yacht rigs" (2016), developed for the purpose of impartial assessment and certification, were adopted by most superyachts sailing today. Similarly, we are now using our collective experience to support the revival of wind assisted propulsion systems (WAPS) for cargo ships, Fig.2. Some WASP technologies are quite recent, with developments driven by competitive yacht racing such as the America's Cup (rigid wing sails), others by the need for shorthanded automated sailing (Dynarig). But some technologies have been dormant for almost a century (Flettner rotor) and are now enjoying renewed interest.

Fig.2: Typical wind assisted propulsion systems (WAPS)

3. Overview of WAPS certification

In response to the many inquiries for independent assessment of wind assisted propulsion systems, DNV GL developed the standard DNVGL-ST-0511 for the certification of WAPS, *DNVGL (2019a)*, and the additional class notation "WAPS", *DNVGL (2019b)*. The standard was developed typically for, Fig.2:

- Rotor sails
- Rigid wing sails
- Soft wing sails
- Soft sail systems
- Ventilated foil systems

The technical requirements in that Standard are generic enough to be applied for other types of WAPS, in close association.

4. DNV GL standard ST-0511

The core of this standard is the definition of structural design loads typical for large sail (or more general wind propulsion) installations on top of the deck of seagoing ships. It is distinguished between "in operation" and "out of operation" modes. The following loads are being considered:

- Wind loads (regular and extreme)
- Inertia loads (self-weight effect from ship motions)
- Green sea and spray water loads (for exposed structures)
- Snow and ice loads (in certain areas)
- Precession forces (for rotating systems)

The interaction of the WAPS with the ship's hull infrastructure can be quite complex and thus load combinations of the above listed loads need to be assessed. Evidence is requested in this standard, how WAPS cope particularly with extreme wind conditions, combined with other loads, particularly considering the large areas exposed to wind and possibly also green water on deck.

This is the reason why in before-hand, particularly for novel concepts, a risk analysis must be carried out, addressing all aspects of design, equipment and operation in order to identify detrimental effects in early design phase. By the standard, it is recommended to perform this risk analysis using a FMEA (Failure Mode Effect Analysis), giving rise to the possible consequences.

Depending on the "dominance" of the WAPS onboard a ship, i.e. the relative size between WAPS and ship, intact stability for the ship can get critical, when excessive aerodynamic loads cannot be controlled.

Technical aspects are generally subject to DNV GL certification/classification. These technical aspects include:

- structural design
- intact stability
- machinery installations
- electrical installations
- control systems

However, the standard addresses also other aspects with relevance to ship operation, as these are generally part of the Flag State authority's approval program:

- line of sight from bridge
- radar blind sector
- manoeuvrability

DNV GL Standard ST-0511 is intended for the certification of WAPS. It primarily serves WAPS Designers / Manufacturers for the purpose of having their systems independently assessed and certified. The Certification is offered in different levels and depths, depending on the demand:

- **Approval in Principle (AIP) -** An "approval in principle" is an independent assessment of a concept within an agreed framework, led by the Classification Society, by confirming that the design is feasible, and no significant obstacles exist to prevent the concept from being built. The basic design and operational concept will be reviewed and approved. The functionality of the system and restrictions of operation will be assessed and approved.

- **Type Approval Design Certificate (TADC) -** The Type Approval Design Certificate is a compliance document validating the compliance with all design requirements in all technical disciplines as defined by the standard. It does not cover surveys on construction.

- **Type Approval (TAC) -** A Type Approval Certificate is a compliance document including the scope of the TADC but amended with DNV GL production assessment and survey requirements on materials, components and the WAPS, once completed. The scope includes the survey of at least one sample from production.

One of the above certifications may suit a WAPS manufacturer demonstrating compliance with a recognized standard to the desired level.

If a ship owner decides to apply for the (new) additional class notation "WAPS", the minimum certification level required for the WAPS system is the TADC. Additional to that requirement, technical safety aspects of the ship's periphery associated with and affected by the installation of a WAPS unit will need to be approved according to the relevant class rules. The structural integration of the system will be reviewed in detail, especially the foundation, which has to carry substantial loads. Furthermore, the technical installations integrated into the ships systems, such as electrical, automation, and machinery are reviewed as well as safety aspects such as ship stability.

5. Conclusion

The full package of DNV GL certification services for wind assisted propulsion systems should provide key stakeholders with reasonable assurance on the technical and operational safety of such systems, installed on ships meeting the ambitious decarbonization targets of IMO.

Since we are all witness of the pioneering age, we are open to discuss even more unusual applications, be it new concepts or modifications or new technical challenges.

References

BERTHOLDT, J., RIESCH, H. (1988), *Windschiffe*, VEB Verlag Technik

DNVGL (2019a), *DNV GL Rules for Classification, Part 6, Chapter 2, Section 12, Wind Assisted Propulsion Systems WAPS*, DNV GL, ed. 7-2019

DNVGL (2019a), *Wind Assisted Propulsion Systems*, DNV GL Standard DNVGL-ST-0511, https://rules.dnvgl.com/docs/pdf/DNVGL/ST/2019-11/DNVGL-ST-0511.pdf

MITTENDORF, F.L. (1903), *Bemastung und Takelung der Schiffe [Masts and rigging of ships]*, Unikum

SCHENZLE, P. (2010), *Wind Ships in the 21st Century? - Current concepts for wind propulsion of ships*, Jahrbuch Schiffbau-Technische Gesellschaft, Springer, pp.55–65

New IT Technologies for a Sustainable Blue Growth

Emilio F. Campana, CNR, Rome/Italy, emiliofortunato.campana@cnr.it
Elena Ciappi, CNR, Rome/Italy, elena.ciappi@cnr.it
Volker Bertram, DNV GL, Hamburg/Germany, volker.bertram@dnvgl.com

Abstract

The paper presents an overview of technology trends for disruption in short and medium terms related to naval science and engineering, such as everywhere computing, predictive analytics, unmanned and autonomous vehicles, mixed reality, everywhere sensors, artificial intelligence and marine robotics.

1. Marine science & Marine technology

This paper shall focus on global technology trends related to marine science and technology. Before setting a course, it is good maritime practice to determine the position. So, where we are now?

Engineering is continually changing. New technologies are fusing the physical, digital, and biological worlds in what has been called the 4th Industrial Revolution. Today's researchers in marine science and technology stand on the cusp of dramatic advances in many fields: materials, communications and connectivity, Artificial Intelligence, information technology, robotics, energy, cybernetics, automation, manufacturing, simulation and HPC (high performance computing), etc. In addition, there are developments and challenges in areas we are generally not familiar with. Considerable progress is to be expected from research at the intersections of disciplines. This requires interdisciplinary teams made up from specialists in the respective disciplines, albeit with a mindset to communicate with and venture into other disciplines. For fruitful research, we also need "critical mass", i.e. a sufficient number of independent research teams working on similar interdisciplinary topics to allow cross-fertilization of ideas and perception of the research topic in the community.

Take for example the rapidly developing field of ship performance monitoring, www.hullpic.info. Here, state-of-the-art research combines advanced computational fluid dynamics, energy flow simulations, (big) data mining based on Artificial Intelligence, mathematical models, now-casting, uncertainty quantification, all that of course under consideration of cyber-security for the data flow from ubiquitous sensors on board ships to shore-based performance monitoring centers, Fig.1.

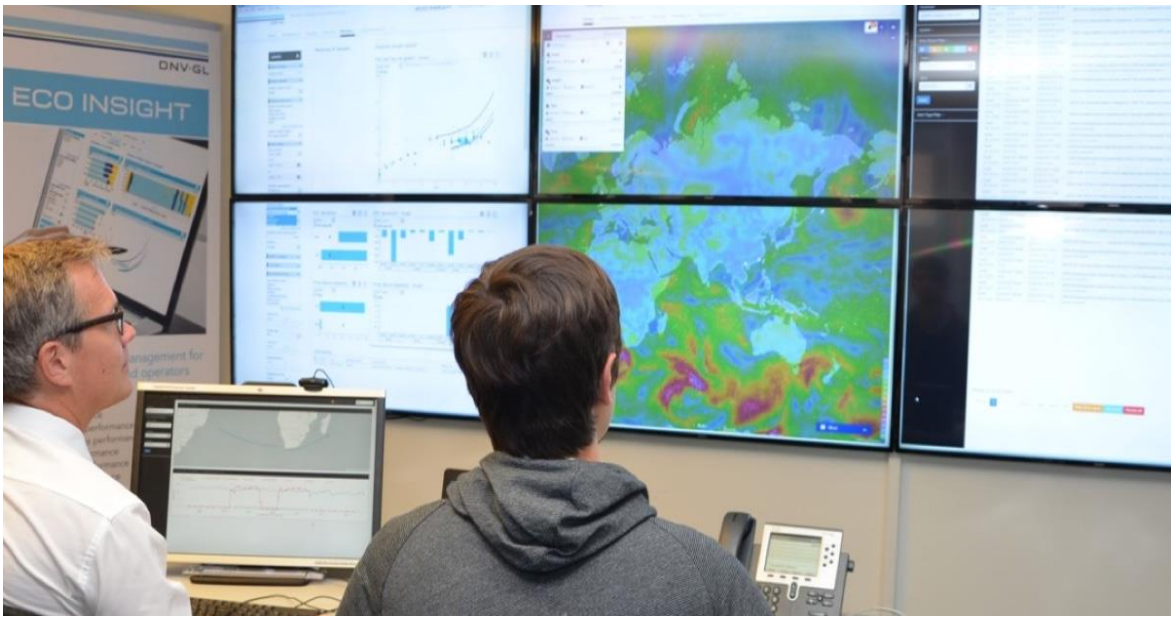

Fig.1: State-of-the art performance monitoring is a prime example of marine interdisciplinarity

The oceans are more than just a blue highway for ships to transport good around the world. They play a vital role for humanity and offer opportunities and challenges for the envisioned "Blue Growth", in areas traditionally featuring rather closed communities, even when it comes to R&D communities:

- Shipbuilding & Marine robotics (e.g. autonomous shipping)
- Renewable energies from the sea (e.g. offshore wind power)
- Marine biotic and abiotic resources (e.g. aquaculture, oil & gas and deep-sea mining)
- Blue technology (e.g. biofuel from algae farming)
- Marine environment and coastal zone (e.g. artificial reefs)

In addition, we should not overlook that most of the world's population lives in narrow coastal zones. Communities, their environment and culture, are tightly interwoven with the sea, which has affected our way of living, our weather, the development of humankind and even the arts.

Marine science and technology focusses on the following:

- Marine science (climate changes and adaptation) with
  - Challenges arising from anthropogenic pressure and impact
  - Challenges arising from human health and well-being
- Marine technology (key enabling technologies) with
  - Challenges related to sustainable designs
  - Challenges related to sustainable policy

2. Technology trends for disruption

"Prediction is very difficult, especially if it's about the future", said Nobel prize winner Niels Bohr. However, reviewing fundamental research and avantgarde technology applications, one can extrapolate where we may be one or two decades from now. Various publications have helped us in forming our perspective. Some were focussed on marine science and technology, such as *DNVGL (2014), LR (2015), Matsuo (2017),* and *Waterborne (2016a,b,c).* Others covered more basic fields of science and engineering, such as *EFFRA (2013), EU (2019), NAE (2017,2018), NAP (2017), NATO (2017), NRC (2013),* and *West (2017).*

The technology trend report of *NATO (2017)* has been a particular source of insight and inspiration for our work. This report introduced a helpful structure of looking at technologies in terms of short, medium and long term. Key technologies with maritime relevance and associated horizons discussed in the report include:

- Technology trends for disruption in the short term (less than 6 years)
  - Additive manufacturing (a.k.a. 3d printing)
  - Everywhere computing
  - Predictive analytics
  - Social media
- Technology trends for disruption in the medium term (6-20 years)
  - Advanced materials
  - Mixed Reality
  - Ubiquitous sensors
- Technology trends for disruption in the long term (more than 20 years)
  - Artificial Intelligence

In general, we will see the virtual world and the real converge more and more towards a cyber-physical world. This will be discussed in more detail in the following.

2.1. Cyber-Physical Convergence (Digital Twins)

The cyber-world and the physical world are more and more intertwined, with continuous interactions and mutual impact between the two, Fig.2. The convergence of the two worlds is enabled diffusion of mobile devices and IoT (Internet of Things) and the pervasive availability of wireless networks.

Data (and data analytics) are central to this process, as they:

- Represent characteristics and evolution of the physical world
- Extract knowledge in the cyber-world
- Enable feedback and control through actions

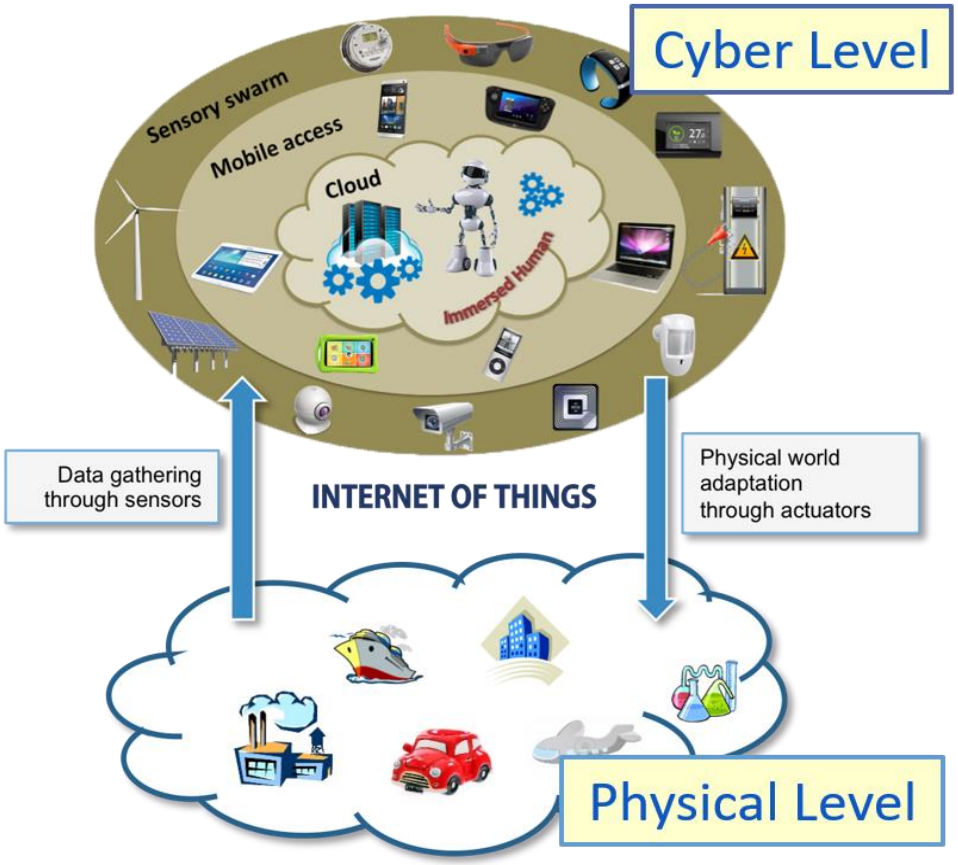

Fig.2: Cyber-world and physical world

The cyber-physical convergence leads us to Digital Twins. In our understanding, Digital Twins are digital simulation models that update and change as their physical counterparts change. Consequently, a Digital Twin (worthy of its name):

- Continuously learns and updates itself from multiple sources to represent its near real-time status, working condition or position;
- Learns autonomously, using sensor data that convey various aspects of its operating condition from:
    - human experts;
    - other similar machines;
    - other similar fleets of machines and;
    - the larger systems and environment in which it may be a part of;
- Integrates historical data from past machine usage to factor into its digital model.

In industrial use, Digital Twins optimize the operation and maintenance of physical assets, systems and manufacturing processes. They are a formative technology for the industrial IoT, where physical objects can live and interact with other machines and people virtually.

An early maritime example of the Digital Twin approach is given in *Cabos et al (2008)*, where a ship's structure is mirrored in a ship structure model, which is updated after the ship is built and then combines information from thickness measurements to update the plate thickness of each structural member which diminishes due to corrosion. The changing condition is not only recorded in the ship condition model, Fig.3, but the finite-element model for its strength is correspondingly updated allowing adjusting residual fatigue strength of the aging ship.

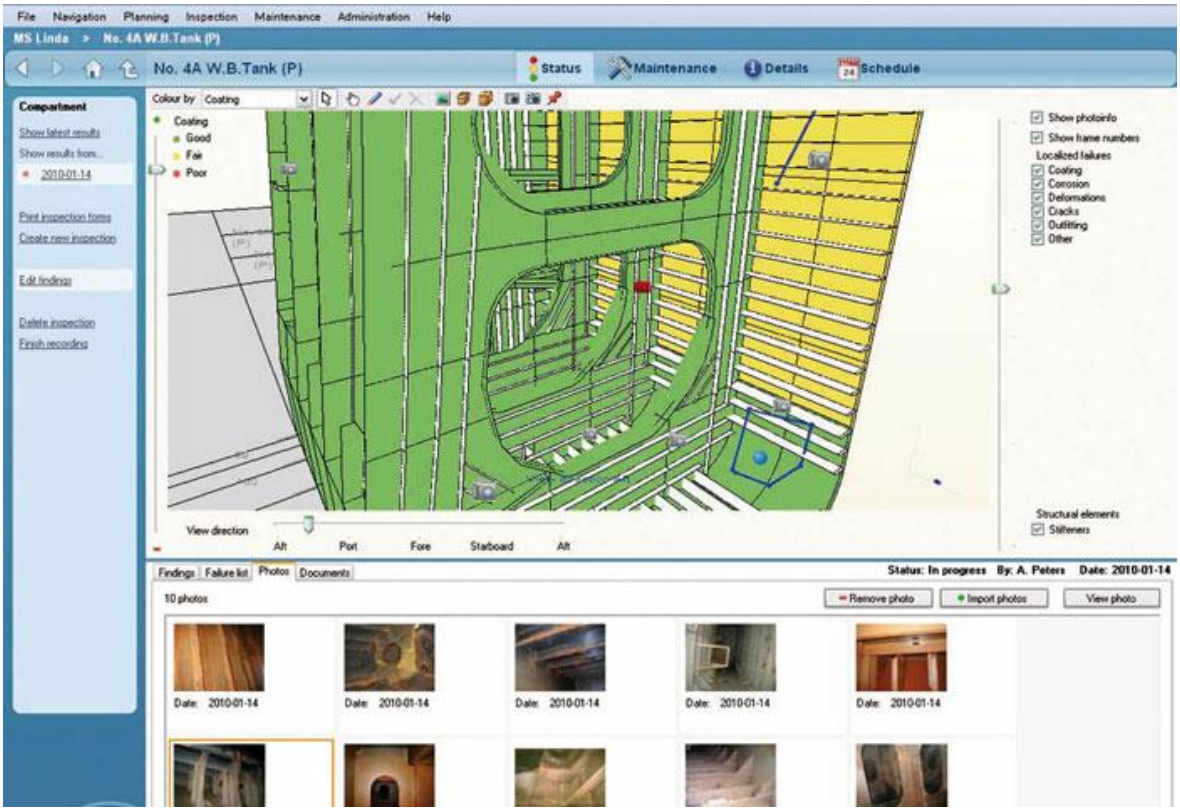

Fig.3: Digital Twin concept updating ship structure model as ships rusts in time

2.2. Everywhere computing – Networking trends

Extreme distribution of networking and computing at the edge of the network is fuelled by the omni-presence of mobile devices (smartphones, tablets, …) and their computational and networking capabilities, Fig.4. In networking, the trend is for capacity and coverage to become more and more pervasive. There are two factors contributing to this dynamic growth:

- Densification of mobile infrastructure: we see the development towards more and more (small) cellular stations, e.g. one per house, each serving a limited number of devices providing high capacity.
- Mobile devices as providers of networking services:
  - "mobile access points", e.g. in cars, trains, or busses, become portable access points for other devices nearby
  - D2D (device-to-device): devices communicate directly with other, already standardised in LTE, https://en.wikipedia.org/wiki/LTE_(telecommunication)

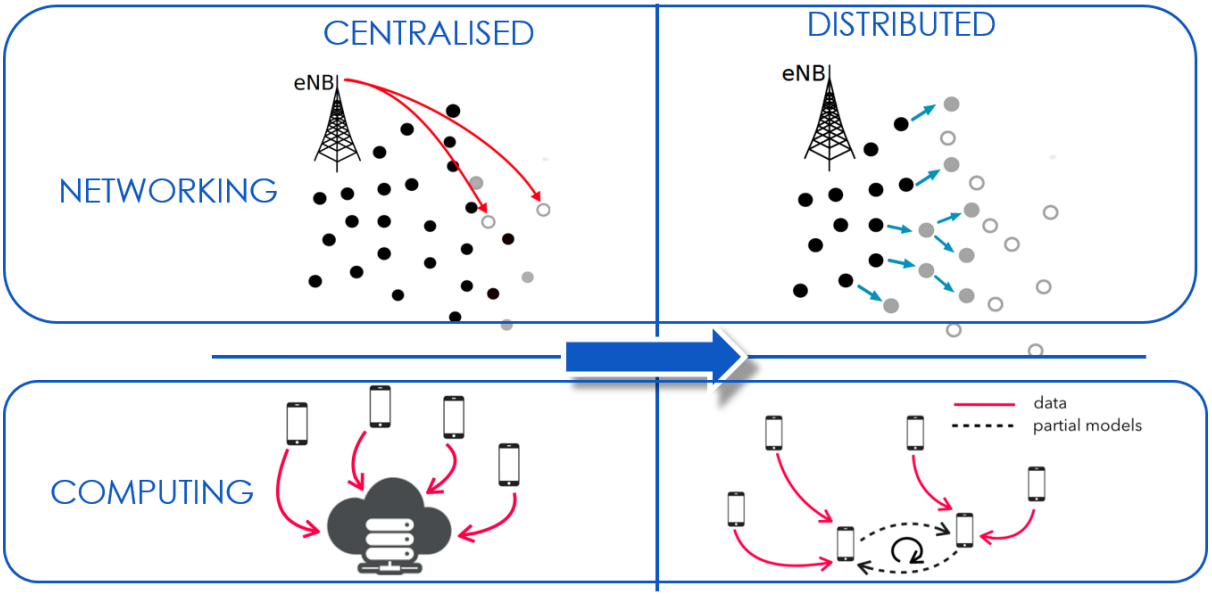

Fig.4: Everywhere computing with omnipresent mobile devices with increasing computational power

Omnipresent networks of computing enhance present applications and opens the door for new applications:

- Infrastructure bandwidth: current occasional scarcity of infrastructure bandwidth may be overcome by increased satellite links and cellular networks (with LTE in perspective). However, as capacity increases, so do bandwidth-hungry applications. Occasional bandwidth shortage may then stay with us.
- Range extension: mobile and small local access points will create "bridge heads" of network access, adding coverage at the boundaries of traditional infrastructure coverage
- Localised communications: The technology trends support groups of devices communicating in a given physical environment, e.g. within company premises or at a conference site.
- Public safety: D2D can work also without any infrastructure, e.g., in case of attacks or natural catastrophes destroying the traditional cellular base stations.

In ubiquitous computing, the macro-trend is from centralised to distributed computing at the edge.

The current cloud-based computing model can be described as follows:

- any device in the physical world can have a virtual proxy in the cloud
- data flows between the devices and the cloud thanks to omnipresent wireless networks
- cloud-based applications and services exploit the data and control the behaviour of the devices

It pushes data to the centre. There are various challenges in this approach:

- Data gravity: Data gravity describes the phenomenon that data and applications are attracted to each other, like physical objects are attracted to each other by physical gravity. As datasets grow larger and larger, they become harder and harder to move. With exponential growth of devices at the edge, an enormous amount of data is generated at the edge. Then applications and processing power should move to where the data is.
- Wireless network capacity, on the other hand, will only scale linearly. The gap between exponential data traffic increase and linear data traffic infrastructure increase is already causing problems.
- Data ownership: This is an issue for many industrial applications; in the maritime context, an example is performance monitoring: Sensors from various equipment manufacturers installed on a ship owned by company A, chartered by company B, deliver data to a performance

monitoring application run and monitored by a service provider, who compares performance with similar ships to assess the performance of an antifouling coating supplied by paint manufacturer who is paid according to this performance. Who owns the data?

- Privacy: Social media and assorted scandals around leaks of data have led to a "cultural" lack of trust in global cloud platforms. Orwellian scenarios are part of a wide-spread mindset and result in legislation that tries to recapture spheres of privacy, such as the General Data Protection Regulation of the EU.
- Relevance of data: Finally, are all data of global relevance? Of course not. In the context of performance monitoring, a torque meter for measuring the delivered power may have 4 sensors, recording data every second, giving 345600 data sets per day. But the 4 sensors are just used to give redundancy; and for performance monitoring, we just need 1 data set per day, where errors have been filtered and averaged out. It is only this 1 data set that is need at the onshore performance monitoring centre.

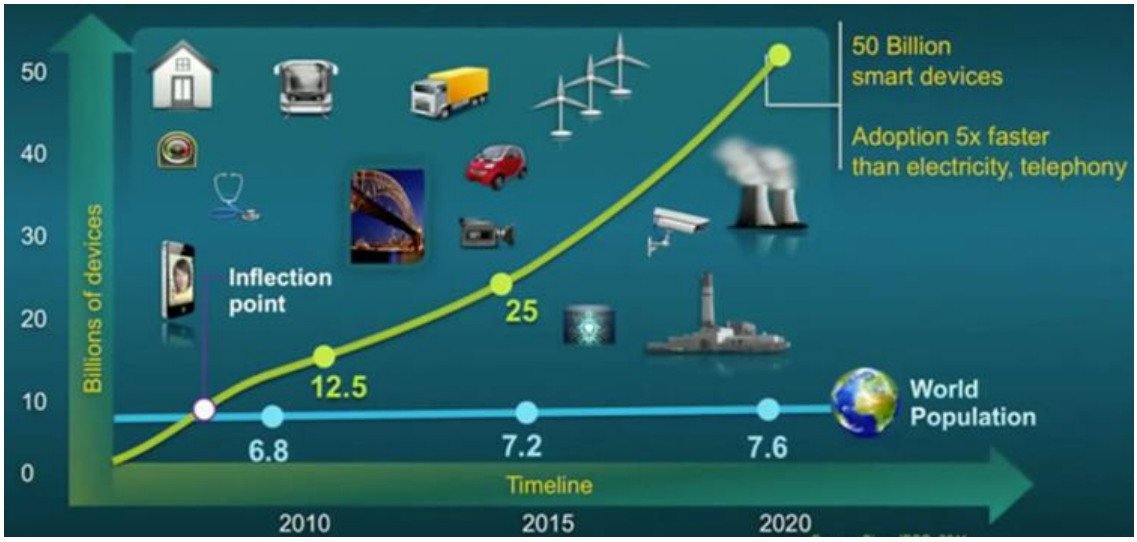

Fig.5: The Internet of Things (IoT) has already arrived, *Evans (2011)*

The natural solution and IT evolution is edge computing, i.e. moving the applications processing the data to where the data are first generated (the sensors and mobile devices). Multi-Edge Computing (MEC) features:

- Cloud functions are distributed at the edge of the network
- Edge gateways (typically, cellular base stations) become “micro data centres”
- Faster response compared to centralised cloud solutions
- More control on data, as data are processed close to where they are generated

“Fog computing” denotes the same basic idea as edge computing, when further distributing the computation on to mobile devices.

With MEC/Fog computing, we move from centralised computing models (where we collect all data in a central location and perform the computing task on the entire dataset) to distributed computing models (where we collect partial datasets at multiple locations, perform computations on each dataset (e.g., use machine learning on a partial dataset) and exchange aggregated information (trained data models) across nodes to refine them). For example, Google’s Federated Learning follows this approach, https://ai.googleblog.com/2017/04/federated-learning-collaborative.html.

2.3. Predictive (and prescriptive) analytics

Data science distinguishes four types of analytics:

1. Descriptive Analytics ("What is happening") mines data to understand what has happened
2. Diagnostic Analytics ("Why it happened") adds intelligence (data analytics) to understand why
3. Predictive Analytics ("What will happen") predicts the future evolution of systems
4. Prescriptive Analytics ("Why will it happen?") predicts the effect of specific interventions, and supports decisions

The first two items are sometimes clustered as "data exploration", the last three as "advanced analytics".

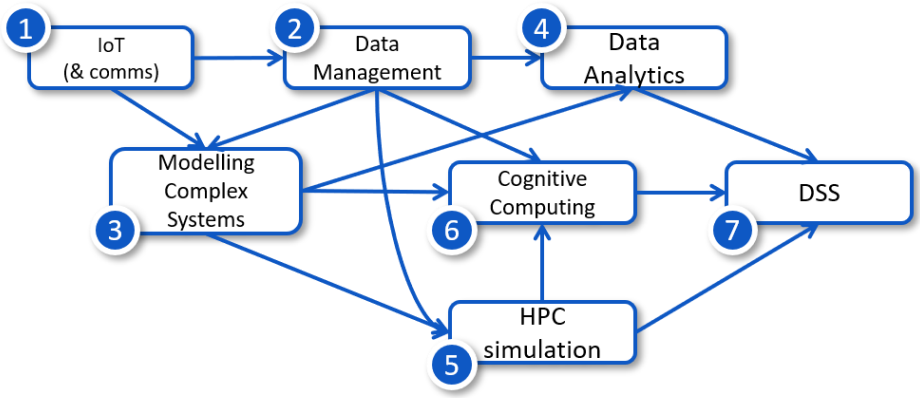

Fig.6: Conceptual framework of predictive analytics technologies

Predictive (and prescriptive) analytics lies at the intersection of different technologies that work together, such as, Fig.6:

1. IoT (& communications) to sense the status of the physical system and collect data into designated collection points (cloud/edge)
2. Data management for advanced distributed storage and replication technologies
3. Modelling of complex systems to create Digital Twins of the physical systems
4. Data Analytics processing Big Data for diagnostic and predictive steps
5. HPC simulation of the physical system behaviour for predictions based on current status
6. Cognitive computing for knowledge extraction, inference/reasoning and human collaboration
7. Decision Support Systems predicting the impact of decisions and selecting optimum strategies under uncertainty

A typical maritime application of the above framework would be an intelligent collision avoidance system, as discussed e.g. in *Bertram (2000)*:

1. Radar, ARPA, electronic charts, ship engine data, ship speed (via GPS and log) and transponders to other ships are automatically and continuously supplied data.
2. These will be processed on board to condense data to key information for own and target ships
3. Beforehand, CFD (Computational Fluid Dynamics) will have created a Digital Twin for the manoeuvring characteristics of the ship. Manoeuvring characteristics of target ships will be obtained either by communicating their Digital Twin data (if available) or by surrogate models derived from data mining of databases for similar ships.
4. The data will be processed for collision risks, considering transponder information of course plans of target ships and prediction of typical behaviour based on machine learning, e.g. based on AIS data, as outlined in *Mestl and Dausendschön (2016)*.
5. See point 3
6. A knowledge-based system processes COLREGs (the traffic rules of the sea) and human expert behaviour extracted in nautical simulator tests, e.g. for rules on last-minute manoeuvres to avoid collision if the target ships does not follow COLREGs.
7. The decision support system displays recommended paths and executes autonomously if crew fails to take last-minute actions

2.4. Artificial Intelligence

The short-term perspective for Artificial Intelligence (AI) is rather sobering. The key application of AI is machine learning, mostly based on Artificial Neural Networks (ANNs). The machine learning is applied to (Big) data, requiring sometimes considerable computing power (HPC). In essence, the current applications have evolved from what was called 'numerical statistics' some 30 years ago.

No radical novel breakthroughs are expected in the machine learning techniques per se in the near future. But the applications will grow in scope and sophistication as more data becomes more widely available and more members of the maritime community become familiar with machine learning technology and tools.

Many of the technologies described so far support the adoption of A.I. for a multitude of applications:

- Everywhere computing for distributed machine learning (which may also be motivated by consideration of proprietary information, where only the gist of the data is to be shared, but not the data itself)
- Predictive Analytics employing machine learning, Big Data and HPC

On a larger scale affecting us all, social networks and media analysis is largely based on A.I. technologies and the multi-billion social-media industry is driving and funding much of the R&D for A.I. techniques and tools.

Maritime applications of machine learning include, *Bertram (2020)*:

- system identification, e.g. deriving body-force coefficients in ship manoeuvring from model tests or sea trials
- deriving design formulas from narrow-domain databases, e.g. power prediction for a given ship type
- meta-modelling using ANNs to interpolate between data sets generated in expensive simulations
- Automatic pattern recognition such as ship type identification or crack identification in drone inspections
- Economic predictions, e.g. of freight rates

In the longer term, we expect to see omnipresent cognitive systems in cyber-physical systems. Mobile devices will act as proxies of their users in the cyber-world, acting as their users would if 'encountering' the same information in the physical world. The inference machine (the 'brain') in these devices will exploit efficient and effective decision-making rules, based on cognitive heuristics (expert system rules in older parlance).

The goal is to design ICT systems embedding human cognitive functions. Unlike ANNs, these envisioned systems would embed functional, not physiological models of the brain's behaviour. Thus, they would be much more lightweight and suitable to be embedded also in personal and miniaturised devices. As an example, your smartphone may filter data "around you" (as your brain does) to quickly tell apart relevant from irrelevant information, predict diffusion of injected information based on your social relationships, and drop irrelevant data and analyses the rest via ANNs optimised for resource limited devices.

2.5. Cyber-security

With increasingly interconnected cyber infrastructure and omnipresent and embedded computers, cyber security gains similarly in importance. Cyber security poses assorted challenges:

- Our private and business world relies more and more on cyber-systems, e.g. energy distribution, transport, defense, healthcare, etc. Failures can potentially affect millions of people.
- Cyber-attacks may come from different countries, even from hostile governments, making legal prosecution difficult.
- A huge effort is needed to prevent, detect and react to cyber-attacks.
- Cyber systems often have specific needs, e.g. confidentiality for defense, banking and industrial systems.
- With "everyone" relying on cyber systems and rapid changes in technologies and cyber-attack modes, large parts of the users will not be cyber security aware or IT savvy enough to detect cyber attacks and respond appropriately.

In the maritime field, we see autonomous systems in ship operation increasing in scope and level of autonomy, including "hidden" cyber systems, such as in barcode scanners, electronic sea-charts, etc. Various service providers have addressed the issue. E.g. DNV GL has issued awareness training, consulting services, guidelines for ship design operation, *Rossi et al. (2018), DNV GL (2016).*

2.6. E-Infrastructure

Comprehensive ICT infrastructures that are needed to enable the complex, multi-disciplinary and globalized practice of modern science.

The European Open Science Cloud (EOSC) is a federated, globally accessible environment where researchers, innovators, companies and citizens can publish, find and re-use each other's data and tools for research, innovation and educational purposes under well defined, secure and trusted conditions, supported by a sustainable and just and value-for money model. Key objectives of the EOSC are:

- Developing an open and evolving federation of research supporting infrastructures and other resources:
  - Generic network, computing and data infrastructures
  - Domain-specific research infrastructures
  - Thematic platforms, e.g. the Copernicus* Data & Information Access Services (DIAS)
- Supporting multidisciplinary and cross-disciplinary research
- Facilitating fair data management
- Enabling cooperation and early sharing of research results

The European Data Infrastructure (EUDAT) was launched to target a pan-European solution to the challenge of data proliferation in Europe's scientific and research communities.

World-class HPC capability and high-speed connectivity as well as leading-edge services benefitting from these European data initiatives.

2.7. Marine robotics

Marine robots fall into three categories:

- Remotely Operated Vehicles (ROVs), e.g. for underwater cleaning, Fig.7,
- Autonomous Underwater Vehicles (AUVs), e.g. for offshore underwater inspections,
- Autonomous Surface Vehicles (ASVs), e.g. for surveillance tasks.

They are used for both civilian and military purposes to perform missions that cannot be easily done by other marine vehicles or by humans because of the harsh environment or because they involve risky operations such as monitoring and maintenance of submerged structures, identification of mines and unexploded ordnance, etc., *Bibuli et al. (2020)*. On the other side, when the human element is essential

as in SAR operations, cooperation between humans and robots can improve the effectiveness of the action.

In addition, aerial drones are used for surveillance, or more recently surveys of ship structures such as large bulk carrier cargo holds. Here machine learning for machine vision is used to automatically identify cracks and other deficiencies in the structure, *Xie et al. (2018)*, Fig.8.

Fig.7: Hullskater for in-water hull cleaning

Fig.8: Drone inspection of cargo hold

The marine environment poses specific problems to underwater marine robotics, *Zereik et al. (2018)*:

- High pressure and low temperature;
- Difficulties in underwater communications (for ROVs); acoustic devices are unreliable and have limited bandwidth and range;
- Long-term missions require the capability of energy generation from the working environment.

AUVs are increasingly used also for scientific purposes such as environmental and biological monitoring and observations and are considered the most promising technology to discover the secrets of the deep ocean, to date, almost completely unknown. Moreover, if designed to mimic biological systems, AUVs can offer stealth (invisibility and silence) in maritime surveillance operations.

Research is active on cooperative robotics, sensing and perception, navigation, guidance and control, energy generation, storage and optimum management, innovative and efficient propulsion systems, new materials and marine IoT. R&D trends are, *Zereik et al. (2018)*:

- Cooperative master-slave robots that allow changing system morphology through modular design and reconfiguration, to perform different tasks in different scenarios, as outlined e.g. in *Bibuli et al. (2020)*;
- Autonomous robotic teams with decisional autonomy, capability to harvest energy from environment and cognitive ability to adapt to changes in environment and mission objectives;
- Underwater data exchange and dynamically adapting network capability for multi-robot systems using acoustic and optic communication

Unmanned surface vessels (USVs) have been used for many years in military applications and oceanography, *Manley (2008)*. Over the past 10 years, these USVs have gained more and more autonomous decision capability. Transatlantic crossings of such ASVs seem to be within reach, as IBM's MARS (Mayflower Autonomous Research Ship) project demonstrates, Fig.9 (left).

The ambitious concept of autonomous, unmanned ships is a vision on the threshold of becoming reality. The technology needed goes far beyond autonomous navigation and collision avoidance, *Bertram (2016)*. However, the ICT technologies come together reaching sufficient maturity, as the first "autonomous-ready" containership "Yara Birkeland" is entering active service, Fig.9 (right).

Fig.9: Long-range ASV technology (left) paves the way for autonomous cargoships (right)

3. Technology vs. Responsibility

3.1. A new world to destroy?

We know that the oceans are vital for life on this planet, and especially for us humans. They are not just the main source of food for many people and blue highways for the exchange of goods of our world economy; phytoplankton, for example, produces more than half of the oxygen of the world, far more than the Amazon rain forest.

Yet, we know precious little about the oceans. Two thirds of the Earth's surface are covered by deep sea (> 200 m water depth), yet the deep sea seems to be similarly unexplored as outer space: <10% has been mapped, <0.001% has be studied for biodiversity, although we estimate >90% of the biosphere to be in the deep sea.

Our ignorance is risky. We start to explore and to exploit the last Terra Incognita (or better Mare Incognita) on our planet, without adequately understanding it. Inadvertently, we may destroy this last "new world" in a mixture of ignorance, short-term thinking and greed. Our track record is not promising.

An incomplete list of threats that we pose for the oceans includes: Climate change and its impacts, deep-sea mining disrupting biotopes, ships as vectors for biological invasions, marine pollution, microplastics, overfishing, altered food chains, etc.

We engineers are both the disease and the only cure and hope against climate change and ocean pollution. We need to live up to our responsibilities and use our skills and expertise to contribute to a sustainable future for the planet.

3.2. Social networks vs. Real world

Social networks and new media are another example of cyber-physical systems, where the interaction between physical world and cyber-world becomes stronger and stronger – and affects the way we work. Our physical world is driven by a multitude of human social relationships, the cyber-world connects and interconnects in social networks, also in the professional arena, using LinkedIn, ResearchGate, Xing, etc. And there is continuous interaction between the two worlds.
Online social networks have been a key driver of Artificial Intelligence and advanced data analysis techniques. They collect huge amounts of data, which can be analysed by Big Data (machine learning) techniques to distil knowledge. E.g. mobile phone data can be used for traffic analyses, e.g. spotting traffic jams in real time. On a smaller scale, mobile phone data have been used for improving inland shipping, identifying slow traffic and back-logs at locks, *Bons et al. (2015)*. Techniques used for pedestrian traffic monitoring in shopping centres can be applied also to cruise ships to analyse and signal e.g. busy times for restaurants.

Online social networks have also impacted how we learn (continuously) and how we find information, also in the business context. Most of time, we do not notice the change consciously, but how do we:

- Find the colleague, who is an expert in XYZ, within our own company or network of maritime contacts?
- Get daily news on what is happening in the maritime world?
- Get cross-referencing publications or see who has referenced my publications and may work on a similar topic
- Obtain publications from colleagues working on similar topics
- …

Much happens these days through push information from (professional) social networks, embedded social network functions in company intranets, or social network functions embedded in online training platforms.

4. Conclusion

Engineering is continually changing. In the second decade of the millennium, new technologies are fusing the physical, digital, and biological worlds in what has been called the Fourth Industrial Revolution.

Today's researchers in marine and naval science stand on the cusp of dramatic advances in materials, communications and connectivity, artificial intelligence to augment human capabilities, information, robotics, energy, control, automation, manufacturing, simulation, etc. Researchers must be able not only to thrive in an environment of rapid technological change and globalization but also to work on interdisciplinary teams, since research is being done at the intersections of engineering disciplines, and successful researchers must be aware of developments and challenges in areas that may not be familiar to them.

A new age of sustainable prosperity can be propelled by these advances, through technological innovation coupled with its thoughtful application and use for the benefit of society.

Acknowledgements

Many colleagues have supplied input helping to shape this paper. Thanks are due to Fred Stern (University of Iowa), Ki-Han Kim, Thomas Fu, Woei-Min Lee, Pat Purtell (ONR), (CNR), Matteo Diez, Andrea Serani, , Andrea Passarella, Massimo Caccia, Lidia Armelao, Donatella Castelli, Paola Carrara, and Paolo Bulgarelli (CNR).

References

BERTRAM, V. (2000), *Knowledge-based Systems for Ship Design and Ship Operation*, 1st Conf. Computer and IT Applications in the Maritime Industries, Potsdam, pp.63-71, http://data.hiper-conf.info/compit2000_potsdam.pdf

BERTRAM, V. (2016), *Unmanned & Autonomous Shipping – A Technology Review*, 10th HIPER Conf., Cortona, pp.10-24, http://data.hiper-conf.info/Hiper2016_Cortona.pdf

BERTRAM, V. (2020), *Artificial Intelligence - Maritime Industries' Next Useful Idiot,* 12th HIPER Conf., Cortona, pp.7-20, http://data.hiper-conf.info/Hiper2020_Cortona.pdf

BIBULI, M.; BRUZZONE, G.; CACCIA, M.; CERVELLERA, C.; FERRETTI, R.; GAGGERO, M.; ODETTI, A.; ZEREIK, E.; VIVIANI, M.; ALTOSOLE, M. (2020), *Evolution of Autonomous Surface Vehicles,* 19th Conf. Computer and IT Applications in the Maritime Industries, Pontignano, pp.26-37,

http://data.hiper-conf.info/compit2020_pontignano.pdf

BONS, A.; WIRDUM, M.v.; MARK, R.v.d. (2015), *Collaborative Data for Improved Performance of Inland Shipping*, 14th Conf. Computer and IT Applications in the Maritime Industries, Ulrichshusen, pp.433-442, http://data.hiper-conf.info/compit2015_ulrichshusen.pdf

CABOS, C.; JARAMILLO, D.; STADIE-FROHBÖS, G.; RENARD, P.; VENTURA, M.; DUMAS, B. (2008), *Condition Assessment Scheme for Ship Hull Maintenance*, 7th Conf. Computer and IT Applications in the Maritime Industries, Liege, pp.222-243

CAITI, A.; CALABRÒ, V.; MEUCCI, D.; MUNAFÒ, A. (2012), *Underwater robots: Past, present and future*, 11th Conf. Computer and IT Applications in the Maritime Industries, Liege, pp.422-437, http://data.hiper-conf.info/compit2012_liege.pdf

DNVGL (2014), *The future of shipping*, Whitepaper, DNV GL, Høvik, https://www.dnvgl.de/publications/the-future-of-shipping-21028

DNVGL (2016), *Cyber security resilience management for ships and mobile offshore units in operation*, Recommended Practice, DNV GL, https://www.dnvgl.com/maritime/dnvgl-rp-0496-recommended-practice-cyber-security-download.html

EFFRA (2013), *Factories of the future*, European Factories of the Future Association, European Commission, https://www.effra.eu/sites/default/files/factories_of_the_future_2020_roadmap.pdf

EU (2019), *Horizon Europe – The next EU research & innovation programme (2021-2027)*, European Commission, https://ec.europa.eu/info/sites/info/files/research_and_innovation/strategy_on_research_and_innovation/presentations/horizon_europe_en_investing_to_shape_our_future.pdf

EVANS, D. (2011), *The Internet of Things: How the Next Evolution of the Internet Is Changing Everything*, Whitepaper, Cisco Internet Business Solutions Group (IBSG), San Jose, https://www.cisco.com/c/dam/en_us/about/ac79/docs/innov/IoT_IBSG_0411FINAL.pdf

LR (2015), *Global marine technology trends 2030*, Lloyd's Register, QinetiQ, Univ. Southampton, http://info.lr.org/l/12702/2015-09-04/2bxfbc/12702/131118/55046_LR2030_WEB_LR_25mb.pdf

MANLEY, J. (2008), *Unmanned surface vehicles, 15 years of development*, Oceans 2008 Conf., Quebec City, http://ieeeoes.org/history/080515-175.pdf

MATSUO, K. (2017), Innovative Technologies for Maritime Industry & Future Scenario, 11th HIPER Conf., Zevenwacht, pp.160-177, http://data.hiper-conf.info/Hiper2017_Zevenwacht.pdf

MESTL, T.; DAUSENDSCHÖN, K. (2016), *Port ETA prediction based on AIS data*, 15th Conf. Computer and IT Applications in the Maritime Industries, Lecce, pp.331-338, http://data.hiper-conf.info/compit2016_lecce.pdf

NAE (2017), *Frontiers of engineering*, National Academies Press, Washington DC

NAE (2018), *Autonomy on land and sea and in the air and space*, National Academies Press, Washington DC

NAP (2017), *The frontiers of machine learning*, National Academies Press, Washington DC

NATO (2017), *Tech trends report 2017*, Science and Technology Org., NATO, https://www.nato.int/nato_static_fl2014/assets/pdf/pdf_topics/20180522_TTR_Public_release_final.pdf

NRC (2013), *The mathematical sciences in 2025*, National Academies Press, Washington DC

ROSSI, P.; PEREZ, W.; CSORBA, M.; JØRGENSEN, A. (2018), *Cyber Security by Design - A proposed approach applied to modern cruise ship newbuilding*, DNV GL, https://www.dnvgl.com/maritime/publications/paper-security-by-design-complex-vessels.html

WATERBORNE (2016a), *ICT maritime opportunities 2030 - Maritime Connected and Automated Transport - Maritime Europe Strategic Action*, EU MESA project brochure, https://www.waterborne.eu/images/documents/mesa-project-documents/files/mesa-brochure-2016.pdf

WATERBORNE (2016b), *Global trends driving maritime innovation*, EU MESA project brochure, https://www.waterborne.eu/images/documents/mesa-project-documents/files/global-trends-driving-maritime-innovation-brochure-august-2016.pdf

WATERBORNE (2016c), *Maritime innovations for the 21st century*, EU MESA project brochure, https://www.waterborne.eu/images/documents/mesa-project-documents/files/tra-2016-brochure-final.pdf

WEST, G. (2017), *Scale: The Universal Laws of Growth, Innovation, Sustainability, and the Pace of Life in Organisms, Cities, Economies, and Companies*, Penguin Press

XIE, J.; HAMRE, G.; STENSRUD, E.; RAEISSI, B. (2018), *Automated Crack Detection for Drone-based Inspection Using Convolutional Neural Network*, 17th Conf. Computer and IT Applications in the Maritime Industries, Pavone, pp.69-83, http://data.hiper-conf.info/compit2018_pavone.pdf

ZEREIK, E.; BIBULI, M.; MISKOVIC, N.; RIDAO, P.; PASCOAL, A. (2018), *Challenges and future trends in marine robotics*, Annual Reviews in Control 46

Digital Maritime Training in Corona Times and Beyond

Tracy Plowman, Volker Bertram, DNV GL, Hamburg/Germany, tracy.plowman@dnvgl.com

Abstract

The paper discusses digital postgraduate and professional training in maritime technologies, which experienced significantly increased demand since the outbreak of the Covid-19 pandemic. After a description of key options for live training and self-paced training, some experience and lessons learnt are shared. Options range from "simple" videoconferencing to sophisticated 3d Virtual Reality based training.

1. Introduction

Teaching environments and techniques have changed since the Covid-19 pandemic, Fig.1. Like it or not, the training community had to embrace digital, remote forms of training rapidly.

Fig.1: Before Covid-19 (left) and during Covid-19 (right)

The first response to the lock-down of physical classrooms has been employing ad-hoc measures such as delivering PowerPoint lectures in videoconferences. But at the same time, a more fundamental discussion has started on

- how to provide quality training if the pandemic stays with us for longer;
- whether we should return to traditional classroom training even if we could; or whether the experience with currently deployed remote methods indicates that a change towards more digital training methods is called for anyway.

2. Bringing management expectations and technology developments together

Classification Societies are big on rules and regulations. Training is no exception. Plan approval engineers and surveyors need proof of appropriate qualification to perform certain tasks, e.g. verifying the proper installation of an exhaust gas cleaning system ("scrubber"). Without record of such a qualification (= participation in a training with a successful assessment of acquired knowledge), a surveyor may not perform the task and a customer may have to wait or go to a different port to get his required survey in turn.

This system had been challenging already in pre-Covid-19 times, as surveyors around the globe need to be trained, with highly qualified trainers usually located in our headquarters in Hamburg and Høvik, and training demand often coming in at short notice and by very few trainees. Covid-19 brought essentially a shut-down of travel outside your own country, and temporarily also a ban on

meetings and classroom training. The latent management strategy for a digital transformation also for training turned in this situation into a pressing necessity for action. The key requirement was a rapid solution of delivering training remotely.

We had already a wide portfolio of options employed in digital training, *Bertram and Plowman (2017,2019).* But with the pandemic came also a rapid development of software solutions responding to the special circumstances that the pandemic brought. Especially the software for live online teleconferencing has taken off since the Covid-19 outbreak. Tools like Skype and Zoom boomed massively, as they addressed the need for face-to-face meetings without physical meetings, in private applications, in schools and universities, and in the business world. The existing infrastructure for 1-to-1 chats and business meetings just needed to be enhanced by a few features to address specific training needs, such as enabling small-group in (digitally) secluded environments, so-called break-out rooms. We reviewed a variety of competing option for live online training, including Microsoft Teams, Zoom, GoToTraining, Webex, and Adobe Connect. Zoom was best in functionality but had initial cyber-security issues. Teams has initially inferior functionality but has been adding features similar to Zoom to become a comparably useful tool. We now use Teams and Zoom in our trainings, where the choice often depends on what the trainer is familiar with.

Looking at the required effort in terms of time and cost for different options, Fig.2, it became quickly apparent that live online training and self-paced online learning were the most obvious choices. Software solutions for developing self-paced online training had been improved significantly over the past few years, reducing required effort significantly. Namely the move from Articulate's Storyline to Rise brought down development times and costs, while at the same time improving trainee satisfaction with the "look and feel" of the training products.

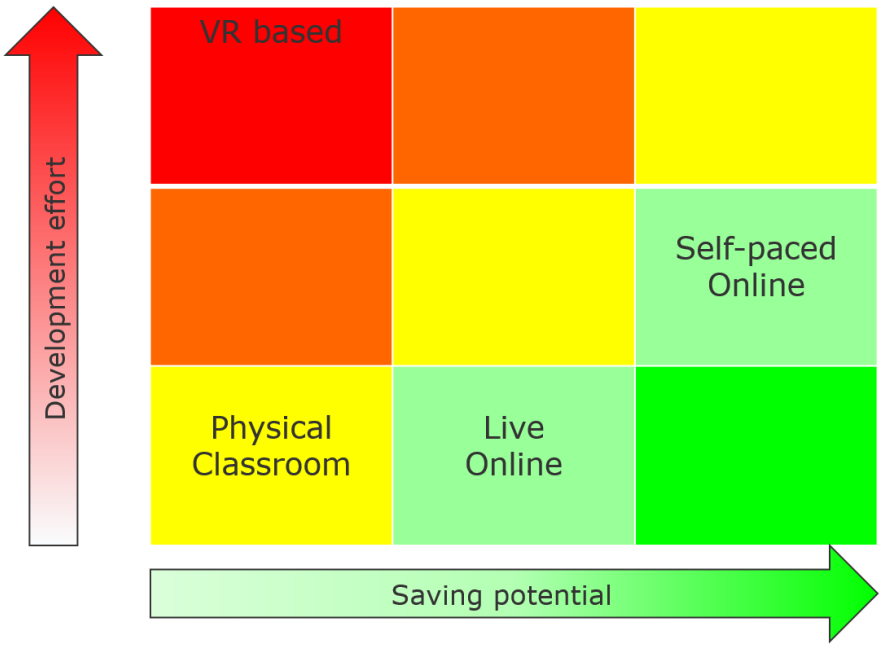

Fig.2: Live online training is an attractive option – at least as short-term option

Most trainings employ a blend of different training options. We used self-paced online training based on Rise predominantly for the following applications:

- resource libraries with reading material (pdf files or hyperlinks) and videos, often referencing to publicly available sources, such as IMO websites
- assessment tests, mainly in the form of multiple-choice tests, for self-assessment as well as formal assessment for compliance purposes
- secondary topics, such as background knowledge or historical developments

We used live online training (using Teams or Zoom) for the following purposes:

- Kick-off and closure of trainings
- Question & Answer sessions
- Short group activities
- Material that needed live commentary of trainers and was most likely to spark interactivity such as questions from trainees with fast response from trainer

The next chapter will discuss the considered choices for digital training solutions in more detail, always within the context of the Covid-19 constraints.

3. (Realistic) Options for digital training at Maritime Competence Learning & Academy

3.1. Traditional vs. Digital training

Until fairly recently, DNV GL's training experience was based on classroom courses, where frontal teaching has been interspersed with various tasks to actively involve and engage the learners. Class size is usually limited to 15-20 people to allow small-group interaction, but training groups may be as small as 3-5 persons.

Over the past few years, we have responded to the increasing demand for "e-learning", a frequently used term by laymen expressing "something on the computer where my employees don't have to travel and sit in your classroom". The demand for such digital distance learning has skyrocketed with the outbreak of the Covid-19 pandemic.

Table I compares traditional training with digital options. Although real world and digital world are never quite the same, we have largely equivalent options for traditional methods.

Table I: Traditional training elements with their closest digital equivalents

	Traditional	**Digital**
Reading	book, lecture notes	e-book, pdf, online reading
Frontal training	Lecture, presentation	Online lecture, webinar
Exercises	(group) exercises	(virtual) breakaway rooms
Assessment	written exam	online quiz
Social networking	Coffee breaks, etc.	Social media

Of course, virtually all training will combine elements of frontal training, exercises and assessment. And virtually all "traditional trainings" will have most of the training material in digital format, such as presentation material in PowerPoint, often with videos, handouts (reading, group work instructions, assessment) at least originally in Word or pdf.

Correspondingly, most digital training will combine various techniques to arrive at the learning objectives, e.g. self-paced studies and live online lectures and teleconferencing for face-to-face discussions.

If a traditional training is well designed using visually stimulating material with interspersed activities for the trainees, the conversion to digital equivalents is straightforward. Only the coffee breaks with real coffee and initial social bonding are vastly better in the real world…

We discuss our experience with various options in the following subchapters, updating *Plowman (2017)* with our experience of the past three years.

3.2. Self-paced online learning

3.2.1. Self-paced online courses (classical e-learning)

These days, most people think of self-paced, click-through self-paced online learning when they hear terms like “e-learning”, “digital training solutions” or “digital transformation of classroom training”. Alas, it is just one of our tools, albeit a powerful and useful one if properly employed.

A key risk with self-paced learning is that the trainee does not study, whether it is an old-fashioned book or an e-learning. Purely self-paced online courses generally have less impact than classroom training where individual feedback is possible and where learners generally have a higher attention rate.

Longer courses are generally subdivided into modules of typically 20-60 minutes’ duration. Due to their longer duration, web courses generally employ a wider range of techniques to avoid fatigue. The training material employs techniques akin to PowerPoint presentations – text (sometimes animated), images, embedded videos.

Short courses with typical durations of 5-10 minutes are called “nano-learning”. They are often employed for quick once-off instructions, e.g. when a new software is rolled out inside the company or a short safety instruction is needed and a pdf one-page instruction is ruled out, e.g. because some short video clip is needed.

In principle, all good advice for designing PowerPoint presentations for classroom training also applies to designing e-learnings. In addition, some self-paced online training software allows information on demand (e.g. mouse-over pop-up explanations, magnifying of images, links to websites or pdf documents). Information on demand allows decluttering slides with faster progress for those who don’t need that information detail.

3.2.2. Videos

Videos are frequently used in e-learning, varying from small add-on to complete lecture recording. For training purposes, it is advisable to split longer videos into shorter chunks. Beyond 30-60 s, most brains start to wander.

Basic options for videos are:

- Recorded lecture: This option gives high focus on the trainer, making the perception much closer to classroom training. Blue-screen recordings of the speaker may be overlaid with slides (PowerPoint) while the trainer talks and advances slides as in traditional training, Fig.3 (left). While blue or green screens are quite cheap, you need a quiet room with proper lighting, a good camera on a tripod, good microphones, etc. for the recording. Alternatively, at significantly lower cost, the expert may self-recorded with a webcam, using standard PowerPoint features, clicking through the slides and running a natural narrative, Fig.3 (right). Typically, 2-3 takes are necessary to get a useful recording.
- Technical video: For special, usually promotional purposes, video production is outsourced. Prices depend always on content and length, but order of magnitude is 1000-3000 € per minute of video, *Bertram and Plowman (2017)*. For most training purposes, the production of such videos is prohibitively expensive. However, existing videos may be re-used, embedding or hyperlinking them. Videos on public websites (such as YouTube) are best hyperlinked. This avoids many legal issues and makes the own training material “light”, i.e. reduces file size and required bandwidth for acceptable response.

- Animation video: Rather dry (technical or regulatory) material may be made more entertaining by using animated, cartoon-type videos. We use Vyond, Fig.4. As a rule of thumb, 1 minute of an animated videos costs 200-400 € to produce.

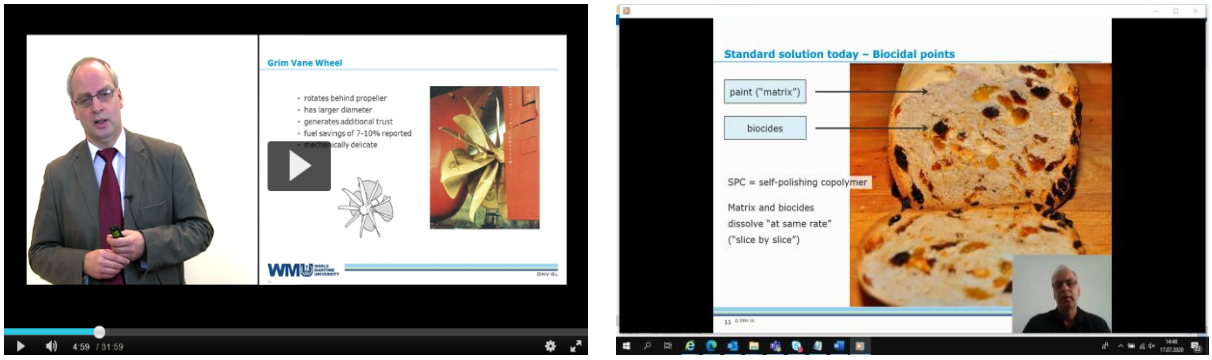

Fig.3: Video recording using blue-screen technique (left) and using ppt & webcam (right)

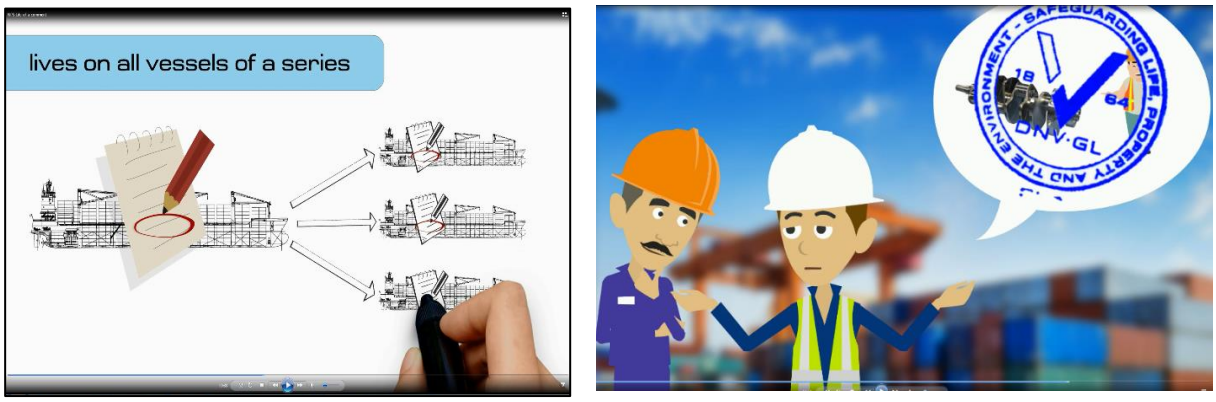

Fig.4: Stills from e-learning videos merging cartoon-like animations with tailored image elements

Producing new videos adds significant costs. It should thus be considered in each case whether a video is "nice to have", "important" or "essential" in the context of the learning goals. On the other hand, it is recommended to re-use existing videos (in full or in part) wherever this supports the learning goals: pay once (for the development), use many times. For video formats, wmv and mp4 seem to give the least technical problems. There are free online tools to convert older video formats to mp4.

3.2.3. Online reading

While e-learnings should be strongly visual, there is usually text information that needs to be transmitted. Various options exist:

- Full text: All text information is given as full text, as pdf attachment, embedded or as links to websites. This is the easiest and cheapest way to produce; trainees do not need audio, i.e. they can use the training also in crowded areas (commuting, open-plan office, etc.) without headphones. For short trainings, like nano-learnings, this is a good option.
- Keywords on slides + audio narrative: This is akin to classroom training. However, the trainees then need headphones. Due to narrower audio bandwidth and unavoidable accent challenges in multinational settings, trainees need to concentrate harder and fatigue faster.

Our preference has moved towards "silent" reading options, based on the feedback from our multinational, mostly non-native speaker trainee customer-base.

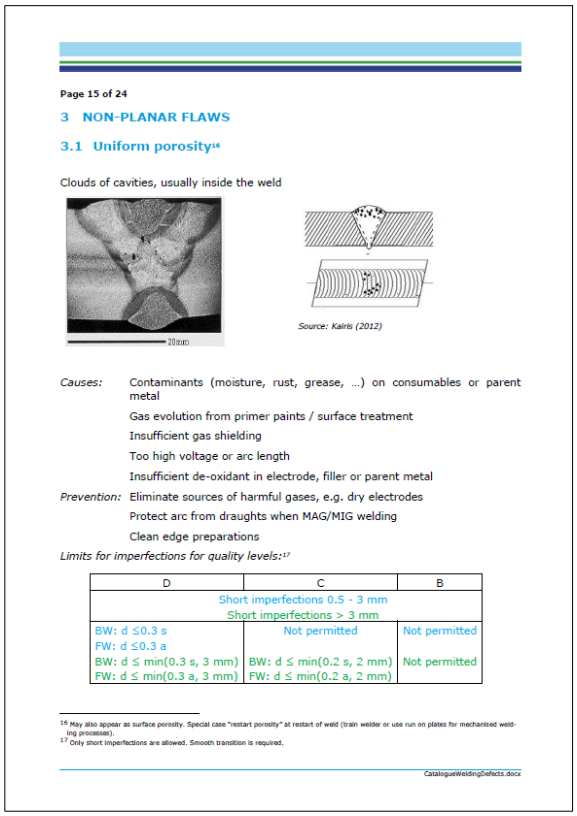

Page 15 of 24

3 NON-PLANAR FLAWS

3.1 Uniform porosity[16]

Clouds of cavities, usually inside the weld

Source: Kalris (2012)

Causes: Contaminants (moisture, rust, grease, ...) on consumables or parent metal
Gas evolution from primer paints / surface treatment
Insufficient gas shielding
Too high voltage or arc length
Insufficient de-oxidant in electrode, filler or parent metal

Prevention: Eliminate sources of harmful gases, e.g. dry electrodes
Protect arc from draughts when MAG/MIG welding
Clean edge preparations

Limits for imperfections for quality levels:[17]

D	C	B
Short imperfections 0.5 - 3 mm Short imperfections > 3 mm		
BW: d ≤0.3 s FW: d ≤0.3 a	Not permitted	Not permitted
BW: d ≤ min(0.3 s, 3 mm) FW: d ≤ min(0.3 a, 3 mm)	BW: d ≤ min(0.2 s, 2 mm) FW: d ≤ min(0.2 a, 2 mm)	Not permitted

[16] May also appear as surface porosity. Special case "restart porosity" at restart of weld (train welder or use run on plates for mechanised welding processes).
[17] Only short imperfections are allowed. Smooth transition is required.

CatalogueWeldingDefects.docx

Fig.5: Typical reference knowledge in pdf

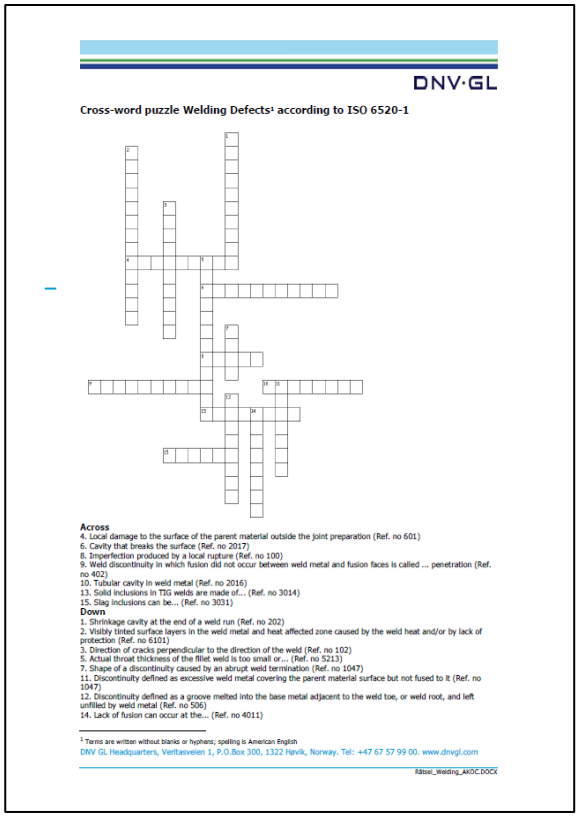

DNV·GL

Cross-word puzzle Welding Defects[1] according to ISO 6520-1

Across
4. Local damage to the surface of the parent material outside the joint preparation (Ref. no 601)
6. Cavity that breaks the surface (Ref. no 2017)
8. Imperfection produced by a local rupture (Ref. no 100)
9. Weld discontinuity in which fusion did not occur between weld metal and fusion faces is called ... penetration (Ref. no 402)
10. Tubular cavity in weld metal (Ref. no 2016)
13. Solid inclusions in TIG welds are made of... (Ref. no 3014)
15. Slag inclusions can be... (Ref. no 3031)

Down
1. Shrinkage cavity at the end of a weld run (Ref. no 202)
2. Visibly tinted surface layers in the weld metal and heat affected zone caused by the weld heat and/or by lack of protection (Ref. no 6101)
3. Direction of cracks perpendicular to the direction of the weld (Ref. no 102)
5. Actual throat thickness of the fillet weld is too small or... (Ref. no 5213)
7. Shape of a discontinuity caused by an abrupt weld termination (Ref. no 1047)
11. Discontinuity defined as excessive weld metal covering the parent material surface but not fused to it (Ref. no 1047)
12. Discontinuity defined as a groove melted into the base metal adjacent to the weld toe, or weld root, and left unfilled by weld metal (Ref. no 506)
14. Lack of fusion can occur at the... (Ref. no 4011)

[1] Terms are written without blanks or hyphens; spelling is American English

DNV GL Headquarters, Veritasveien 1, P.O.Box 300, 1322 Høvik, Norway. Tel: +47 67 57 99 00. www.dnvgl.com

Rätsel_Welding_AKOC.DOCX

Fig.6: Crossword puzzle as media break

While not glamorous, pdf files and online reading text are often a good and cost-effective option:

- Short instructions: **"**Sometimes it makes more sense to deliver new training content in the form of a job aid. Don't stretch out a small amount of content in order to create an hour elearning course," *Ferriman (2013)*. If you have little to say, put it on one page.
- Reference knowledge as add-on: A cardinal sin in training is 'slidumentation', *Duarte (2008)*, the mixing of slides with documentation. Much of our traditional training material contains reference knowledge. Nobody can seriously expect trainees to retain this knowledge after brief exposure: Catalogues of welding defects, Fig.5, pages of regulations applicable if A exceed this threshold and B that. All the trainee should learn is where to find that documentation and how to work with it. Transferring classroom training to digital solutions, we often include links to pdf files or websites, where the reference knowledge is found, and focus on the learning goals "I know this resource exists", "I know where to find it" and "I know how to work with it". Referenced websites should not be short-lived; few things frustrate trainees more than clicking on hyperlinks and getting error messages. Websites under your own control and rather stable links (Wikipedia, IMO regulations, ISO standards, etc.) work well, though.
- Lecture notes: Online trainings cannot be printed as traditional PowerPoint training material. However, most participants feel a need for take-home reading material for later reference in their professional life. More or less extensive lecture notes as pdf downloads from online training are popular and make pedagogical sense. The lecture notes can be updated frequently and cost effectively, much faster and cheaper than programming an e-learning. In one extreme case, we converted an older e-learning, which was text-heavy with many technical drawings, into a pdf-attachment of lecture notes (96 pages) and a lean e-learning consisting essentially of a page for the download of the lecture notes and a quiz to ensure that trainees had studied the material.
- Instructions for activities: Pdf files may also be used for interspersed tasks or case studies. For example, after an e-learning has presented material for 20 minutes, you may attach a pdf with a crossword puzzle reflecting the presented material, Fig.2. Time for a coffee, a pen and let's

crack that crossword. Such media breaks work well and generally receive positive feedback from the trainees.

Pdf files come with some inherent advantages:

- They can be downloaded and printed. We get a lot of reading down during our commuting to and from work. And we often prefer reading a paper version, where we can work with a pen or a highlighter, and where the strain of reading seems less after hours spent in front of computer screens.
- They are standard software from a major supplier, in an open format based on ISO 32000. As such, it can be expected that in decades to come, we will still be able to open and read pdf files, with free and easily available software.
- The standard reader for pdf software comes with a search function, which is particularly useful in large documents.

3.2.4. Online assessment

Often the trainees are "motivated" by a test at the end required to get the formal qualification. It may not follow a feel-good modern view on pedagogy, but it has been proven to work - and our industry is used to it. For such an assessment, there are various options:

- Ungraded quiz: The softest option: Have a quiz (usually programmed in the e-learning software) with tasks, most often multiple-choice questions, and give immediate feedback to the trainee whether the answer was correct or incorrect, possibly giving additional explanations on the correct answer. This type of quiz is intended to give just voluntary assessment to the trainee how much or little has been learnt. It also breaks the habit of just clicking 'continue' again and again.
- Graded quiz: As above, but this time there is an overall grade at the end, most often without additional details. The trainee gets the final score and whether this was enough to pass. The assessment result is entered automatically in the learning platform and possibly an e-certificate is issued and emailed or offered for download. This is our standard option for courses. If the certificate is important (e.g. a university degree, a formal license, etc.), this approach is not suitable as it is difficult to ensure the identity of the person taking the test.
- Classroom quiz after e-learning: In cases where the identity of a candidate must be checked and ensured that no external help was received, we have not found an alternative to classroom testing under supervision. The knowledge acquisition may be based on digital solutions, but the knowledge assessment in classroom makes the approach "blended learning".
- Human evaluation of free text: In some cases, the assessment may be in the form of a free text (essay). We use this option in our joined post-graduate diploma courses with World Maritime University,. This approach comes with significant time required from the subject matter expert, but allows checking more advanced reasoning and documentation skills, as e.g. needed in auditing.

3.3. Live online training

In response to the Covid-19 pandemic, we needed to develop training solutions rapidly. Often lecture series of 8-12 modules (of 1.5 h each) had to be converted from face-to-face classroom teaching to digital solutions, Fig.7.

The first task was generally a critical review of what could be rapidly converted to self-paced study, e.g. quizzes and historical background information. Such a partial conversion gave well-received breaks from online face-to-face videoconferencing, for training purposes a.k.a. "virtual classrooms". The remaining parts, which involved strongly discussion between expert and trainees, and "off-the-record" lively comments by the expert, were kept as live online training.

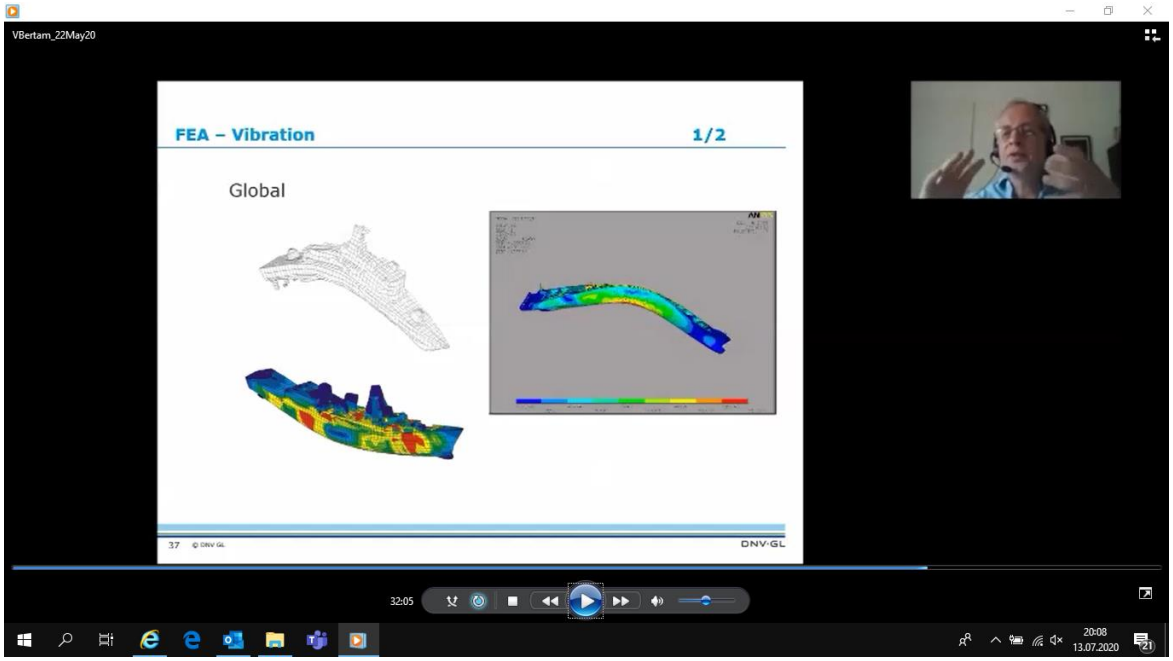

Fig.7: Volker Bertram (DNV GL) in live online lecture from Hamburg to students in Valdivia/Chile

Unlike business videoconferencing, the training options of e.g. Microsoft Teams and Zoom offer some additional features, such as digital breakaway rooms allowing smaller subsets of the trainee group to discuss a task in private with possibility of the trainer entering virtually each sub-group. Overall, the experience is that this type of training is more tiring, possibly due to reduced audio and visual resolution. It is recommended to reduce conventional full days in classrooms to half-days online while doubling the course duration in calendar days.

- Subject matter experts (SMEs) are much more open to online live training. Webinars are often enthusiastically embraced, as they allow direct contact to customers.
- SMEs are generally neither communication nor webinar technology experts. Presentation material (PowerPoint) generally needs reworking for online delivery.
- Most often, a second person is needed to support periphery work, e.g. monitoring chats.
- Live online training may be combined with prior or follow-up reading material, e.g. trainer and trainee introduction.
- Teaching material should be strongly visual and cut down on reading text, Fig.8.
- After 5-10 minutes speaking time, an interactive element (e.g. a "poll", Fig.9) should stimulate the audience to refocus on the topic. Otherwise the temptation to multi-task (i.e. read incoming emails, etc.) becomes overwhelming for most people.

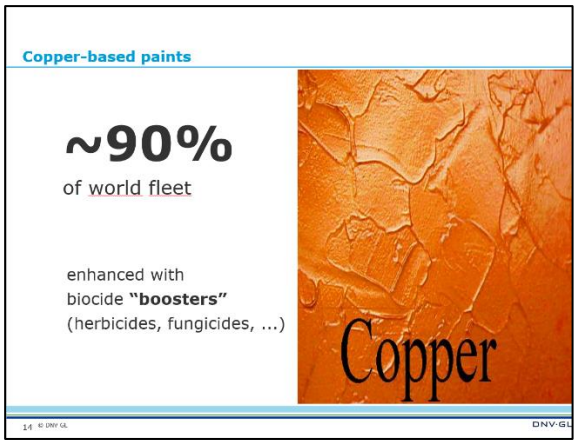

Fig.8: Typical webinar slide

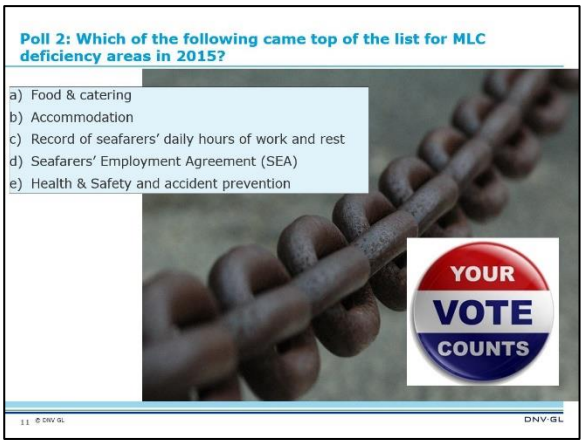

Fig.9: "Polls" stimulate audience to think

While recordings can be offered after a broadcast, in our experience virtually nobody downloads these recordings.

Short "conference-style" presentations of 20-30 minutes have often been converted into online webinars. As with classroom/conference presentations, there are good ones and bad ones. Bad ones are of the format "you look at PowerPoint slides while the expert drones on". Participants often zone out, doing other things like checking their emails, passively absorbing the audio and tuning back into the webinar occasionally. The good ones are relatively brief, focused on a single, tangible topic with a clear take-home message, and strong user interaction. In our line of training, we often must respond rapidly to new developments, e.g. new regulations coming into force. We have found that webinars are an attractive addition to our toolbox of training solutions in this respect. DNV GL's line of external webinars is called smart-ups.

Lessons learnt about live online training include:

- Live online training always comes with live audio. That makes them easy to prepare and generally livelier that e-learning but introduces the accent and charisma challenge: Listening to a voice from another nationality requires more concentration that listening to someone from your own language. The first few minutes our brain tunes into to a different accent; native English speakers are often the hardest to understand for non-native speakers. A charismatic trainer may capture his audience much longer than a boring trainer. This is already experienced in classroom, but even more so in live online training.
- Presentations can be broadcast with or without webcam video of the speaker. Having an inserted window with a speaker makes a webinar more personal. Lip reading also helps with comprehension; it is good to have a close-up of the speaker for that purpose. Having webcams turned on for the trainees has been proven to help both with maintaining trainee focus and with trainer liveliness.
- Chats function are good for trainees to write down immediate questions, but disruptive for the trainer. Regular breaks need to be planned for the trainer to review questions and respond to them. Responses may be live or via a chat or email.
- Live online training software allows tracking user behaviour and exporting statistics e.g. to Excel files. Information gathered includes trainee registration information, time of joining, time of leaving, attention rate (percentage of time when window with webinar was active), questions asked, what was answered in polls. Both for training and marketing purposes, such statistics can be very interesting.

Webinars have become a standard tool for many companies. The problem is that we all get flooded with emails, touting upcoming webinars. As a simple self-defense, webinar invitations often land in the spam folder. In order to avoid this fate, best use a specific invitation from a known colleague/ manager and find a title for the webinar that raises curiosity or motivation to join.

3.4. Gamification & Virtual Reality

Gamification of teaching using video game technology has attracted a lot of attention. Virtual Reality (VR) is seen as a key technology for (maritime) training, *Plowman (2017). Bertram and Plowman (2018).* Virtual Reality is not only fascinating and fun; it is also a powerful tool for training, especially when it comes to visual assessment and human interaction, e.g. judging when to initiate action in maneuvering, crane operation, etc.

However, the price of developing VR-based training is high. Models need to have the right level of detail, balancing realism and response time. Import/export from CAD systems or other models (e.g. finite-element models) may save time, but is never as straightforward as hoped for or promised by vendors. VR-based training is generally well received by trainees and effective; but it comes at high costs. Having a ship modelled over several decks, along with equipment, interactivity, training tasks

and solutions, assessment, etc. may take 100,000 to 1,000,000 €. Such an investment needs either subsidizing from R&D projects, opportunistic recycling of available, suitable models or a mass market willing to pay premium fees for training, such as firefighting.

DNV GL has developed SuSi (Survey Simulator), a VR-based training solution for ship inspections, *Bertram and Plowman (2020)*. SuSi provides realistic and cost-efficient 3D training software for survey inspections, using Virtual Reality technology and detailed models of ships and offshore structures, Fig.10. The virtual inspection gets trainees exposed to deficiencies that would take years for a surveyor to experience in real life. An inspection run can be recorded and discussed in a debriefing with an experienced supervisor/trainer, pointing out oversights and errors by the trainee.

Fig.10: Level of detail in DNV GL's SuSi (Virtual Reality based survey simulator)

Fig.11: VR-based training works better with trainer supervision, *Bertram et al. (2020)*

Besides the cost issue, there are other aspects to consider with VR-based training:

- Cyber-sickness, with symptoms akin to motion sickness, may occur, especially if using head-mounted displays,

- Trainee group coherence may be lost due to varying IT savviness. Much is intuitive for video gamers, nothing for digital immigrants aged 50+.

VR-based training does not seem suitable for self-paced learning without support.

A pragmatic approach where the trainer guides the class collectively through the ship (e.g. with a single PC and a data projector, or a shared screen) and trainees interrupt when they spot a deficiency has been well received by participants from industry across a wide range of nationalities (cultures), educational backgrounds, management levels and age groups, Fig.11.

3.5. Social media

Training (from school over university to life-long training) always has a social aspect, making friends and meeting them again. Overlooking this aspect with a tunnel vision on "we want them to answer these questions correctly" would be a mistake.

As response to an invitation to a webinar, we received the following reply: "I shall not register to the webinar, whatever the topic, for the simple reason that I do not see the point… no networking, no coffee, no time out of the office." This echoes a widely shared feeling: people miss the exchange of experience, the maritime gossip, the networking. Can social media step in and help? In DNV GL, we employ two technologies (besides video conferences which were covered above) to "reach out and stay in touch" within groups of people interested in a certain theme:

- Yammer, a social networking service for private communication within organizations. For training purposes, it is thus limited to internal training. There are mixed feelings about using a platform like Yammer as add-on in digital training solutions:
  - Use Yammer (like any other social media platform) selectively. As a posting platform for occasional nuggets of information ("I was recently at a conference on our theme and the proceedings can be found here") or specific questions ("Has anybody any experience with…?"), it works well in small and coherent groups.
  - It works better for younger groups than for older groups.
  - The more Yammer groups you subscribe to, the more messages pop up. Soon people react in mental self-defence and no longer open any of them.

  In some cases, only time will tell whether a social media channel like Yammer works for its intended training purpose or not.
- Email: Emails work well for pre- and post-training contact if they are concise and relevant. You can for example send short personal presentations of trainer and trainees before a training to establish a rapport and identify special areas of interest. Or a trainer may email a special publication in response to a question during the training. Email may also work as an electronic hotline; often specific questions come sometime after a training, when trainees have to solve a specific problem in their line of work. If it so specific that it is of little interest to the rest of the trainees, individual emails work better than a Yammer.

4. Conclusions - Combine and conquer

You can achieve Death by Powerpoint, i.e. boring training based on PowerPoint. But trainees may die many deaths, i.e. irrespective of platform, you can be boring: in classroom presenting, using pinboards and flipcharts, talking in videoconferences or accumulating a multitude of videos.

Make it relevant, make it short, make it fun – in traditional training as in digital training. And most of the time, variety adds to making it fun and tailoring learning objectives to the training platform. No media is per se evil, and no media is per se perfect. Combine (training options) and conquer (the hearts of the trainees).

The Covid-19 situation has forced us to adopt digital training options, whether we wanted it or not. Due to time pressure, not all options worked as well as we expected and wanted. But other things worked surprisingly well; one trainer perceived more audience focus on the training than in classroom training. This is probably due to shorter training session and longer breaks for the trainees allowing them to check email and respond to urgent requests otherwise preying on their minds.

We learnt some lessons and, for sure, we are not at the end of our exploration of the digital universe of teaching. But we are convinced the after Covid-19, we will not simply return to the pre Covid-19 modus operandi. The virus has changed our private world, our business world, and also our training world. Deal with it!

Acknowledgements

We thank my colleagues of the developer team in the MCLA (Maritime Competence Learning & Academy) department for their support and help over the years in shaping my skills and my view on training in the specific maritime world, namely Ulrich, Bernie, Torsten, and Margit. And special thanks to Volker, who twisted my arm into presenting again at Hiper. He is a force of nature…

References

BERTRAM, V.; PLOWMAN, T. (2017), *Maritime training in the 21st century*, 16th Conf. Computer and IT Applications in the Maritime Industries (COMPIT), Cardiff, pp.8-17, http://data.hiper-conf.info/compit2017_cardiff.pdf

BERTRAM, V.; PLOWMAN, T. (2019), *A Hitchhiker's Guide to the Galaxy of Maritime e-Learning*, 18th Conf. Computer and IT Applications in the Maritime Industries (COMPIT), Tullamore, pp.7-23, http://data.hiper-conf.info/compit2019_tullamore.pdf

BERTRAM, V.; PLOWMAN, T. (2018), *Virtual Reality for maritime training – A survey*, 17th COMPIT Conf., Pavone, pp.7-21, http://data.hiper-conf.info/compit2018_pavone.pdf

BERTRAM, V.; PLOWMAN, T.; FEINER, P. (2020), *Survey simulator – A Virtual Reality training tool for ship surveys*, 19th Conf. Computer and IT Applications in the Maritime Industries (COMPIT), Pontignano, pp.7-15, http://data.hiper-conf.info/compit2020_pontignano.pdf

DUARTE, N. (2008), *Slide:ology: The Art and Science of Creating Great Presentations*, O'Reilly & Assoc.

FERRIMAN, J. (2013), *9 things people hate about elearning*, LearnDash, https://www.learndash.com/9-things-people-hate-about-elearning/

PLOWMAN, T. (2017), *Maritime e-Training – Matching Requirements to Solutions*, 11th Symp. High-Performance Marine Vehicles (HIPER), Zevenwacht, pp.55-65, http://data.hiper-conf.info/Hiper2017_Zevenwacht.pdf

Options for the Post-Biocide Era of Antifouling

Volker Bertram, DNV GL, Hamburg/Germany, volker.bertram@dnvgl.com

Abstract

This paper surveys maritime antifouling solutions recent developments for biocide-free antifouling solutions. Super-hydrophilic coatings, nano-coatings, surface treated coatings combined with robotic cleaning, flocked surfaces, and ultra-sound transducers are some of the alternatives that have started to emerge. Robotic cleaning shows rapid growth in technological and business maturity.

1. Old problem, new solutions?

Marine growth can decrease ship performance drastically, resulting in a 30-50% increase of fuel consumption (and associated emissions) compared to a smooth hull. Hull fouling is also responsible for the spread of invasive species, even more so than ballast water. Antifouling, i.e. any measure to prevent or reduce fouling, is thus both an economic and ecological necessity. Note that here is use the term "antifouling" for any measures that inhibits fouling, while traditionally paint manufacturers and many operators use the term to denote biocidal paint coatings.

Fouling has been a headache for shipping since ancient times. An Aramaic scroll dated from around 400 BC stated: "the arsenic and sulphur have been well mixed with Chian oil … with the mixture evenly applied to the vessels sides so that she may speed through the blue waters freely and without impediment.", *NN (1952).* Oh well, the ancient Egyptians tried, the Phoenicians tried, so did Columbus and Horatio Nelson, *Doran (2019)*, while today's top operators continue to test the latest solutions. See *Bertram and Yebra (2017)* for a more comprehensive historical perspective with focus on antifouling paints.

2. Biocide-based antifouling paints - A bridging technology

World War II brought important progress also in the field of coating technologies, including modern antifouling paints. The basic principle was the same as in most of today's antifouling paints: In contact with seawater, antifouling paint releases biocides which form a toxic boundary layer preventing marine growth. A certain concentration of these toxins must be maintained for effective protection. As the ship moves through water, the toxins are washed off and the paint must re-supply the protective boundary layer with new toxins. Most antifouling paints are so-called self-polishing copolymers (SPCs), where the coating matrix containing the biocides dissolved slowly in water, Fig.1. As the hosting matrix film dissolves, the surface remains smooth and an almost constant leaching rate of the biocides is obtained. The most popular toxin was TBT (tributyltin), an organotin compound. Due long-term accumulation of this biocide in seafood, it has been banned by IMO since 2003/2008.

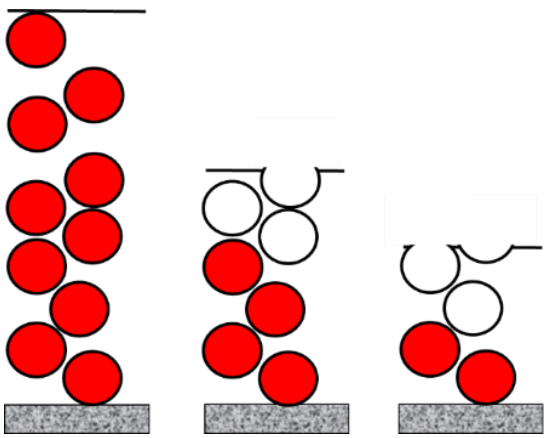

Fig.1: Principle of self-polishing co-polymers with biocides (red) and leached layer (empty circles)

After the TBT-ban, copper compounds have become the predominant antifouling biocide. Various herbicides and fungicides are added to address plant fouling, which is not affected by copper compounds. These additional toxins are dubbed 'boosters'. Some of the boosters (including Irgarol 1051 and Diuron) have come under scrutiny, resulting in regional bans and proposals to add them to the list of antifouling substances banned by IMO.

Biocidal antifouling coatings have fueled also a debate on in-water cleaning of ships. Over the past decade, a steadily increasing number of port authorities have banned in-water cleaning in their ports. This is partly due to the fear that aquatic invasive species may be released and spread uncontrollably threatening the local ecosystem, but another concern is that the cleaning will release biocides and paint particles which will settle and contaminate the soil.

As such, biocidal antifouling paints are now widely seen as a bridging technology. But what could be on the other side of the bridge? World shipping moves slowly, but steadily towards sustainable shipping. Leaching copper and micro-plastics (the dissolved ingredients of today's standard SPC coatings) into the world oceans is not sustainable. *Dafforn et al. (2011)* argue "that the way forward is to phase-out metals and organic biocides from [antifouling] paints and to adopt non-toxic alternatives. […] However, we call for caution in the time-frame for making these changes." There is no shortage of ideas, but the road from concept to deployment is often a long one. This is especially true for antifouling, where a product's success and effectiveness are generally measured over five years, the standard docking interval.

3. The Teflon principle may not stick much longer

The surface energy is a measure of how easy or difficult it is to stick to a material. Low-surface energy coatings (LSE), a.k.a. 'foul release' or 'silicone' coatings, use the same principle as Teflon pans: making adhesion (of fouling organisms) difficult. As such, the coating does not prevent fouling, Fig.2. However, such 'non-stick' coatings are much easier to clean, e.g. by wiping or low-pressure rinsing. On speed boats the surface may be self-cleaning, however, cleaning is necessary on most other ships, especially in niche areas (such as bow thruster tunnels and sea chests). LSE coatings, like Teflon, are mechanically sensitive and fouling starts rapidly after the coating has been scratched. Even if the coating avoids surface damage the silicone film weathers over time, rendering it less effective. In a case study, Hempel reports that a large tanker which used such non-toxic coatings in sea trials achieved 8% fuel savings, but average fuel savings over a five-year period, between dockings, amounted to 4%. While the star of classical silicone coatings seems to be waning, with some new twists the idea lives on.

Fig.2: Teflon pan encrusted in fouling, source: Burkhard Watermann

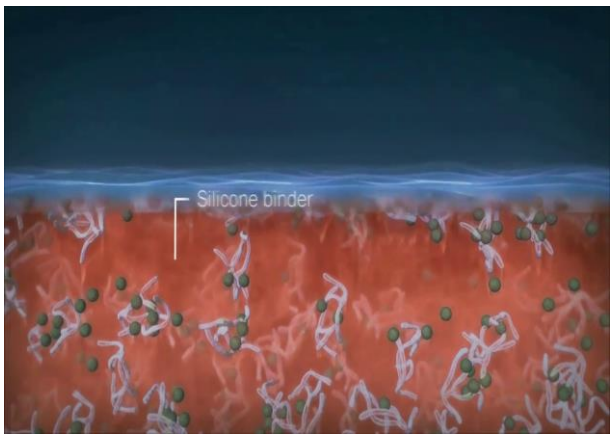

Fig.3: 'Hydrogel' technology, source: Hempel

LSE coatings are super-hydrophobic (i.e. water repellent). At the other extreme, super-hydrophilic (i.e. water attracting) surfaces also impede fouling. Such 'hydrogel' coatings are akin to soft contact

lenses. Many fouling organisms mistake the surface of a hydrogel for water; in other words, the hull surface becomes invisible for them. Combined with a mechanism to trap biocides on the hull surface, this approach can reduce biocide leaching by a factor of 10-20 over conventional antifouling coatings with virtually constant performance between docking intervals, *Yebra (2016)*. The best-known example of this technology is Hempel's ActiGuard®, Fig.3, *Sørensen et al. (2012)*, which is also marketed as "fouling defense".

'Nano-coatings' use bio-inspired microscopic surface structures (e.g. shark skin, lotus effect, etc.) to make adhesion difficult for organisms. Several such products are already on the market, such as Ultra Ever Dry, Fig.4, but research is continuing to present new ideas. There are assorted efforts to recreate biomimetic effects industrially for ship coatings. *Stenzel et al. (2016)*, *Kluwe et al. (2019)* describe Riblet-coatings, mimicking the skin of a shark, and compliant dolphin-like coatings. The EU project eSHaRk (eco-friendly Ship Hull film system with fouling Release and fuel saving properties) works on self-adhesive foils inspired by shark skin microstructures. Similar projects are working on mimicking shark-skin structures in Japan and the USA, Fig.5.

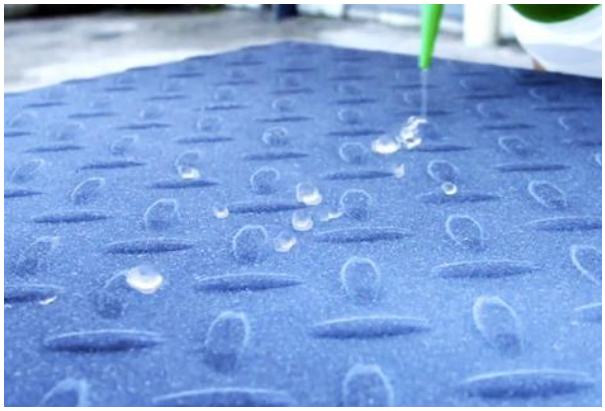

Fig.4: Nano-coating, source: Ultra Ever Dry

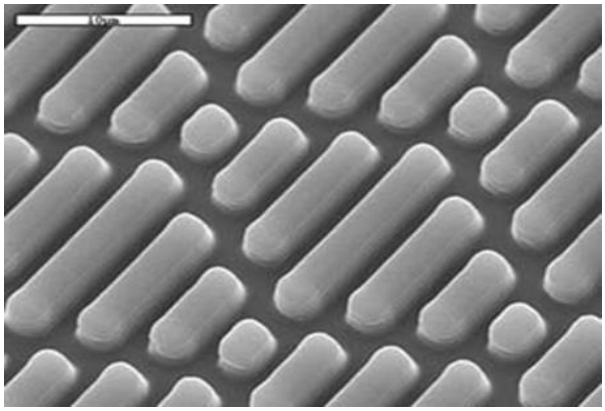

Fig.5: Coating mimicking shark skin, source: University of Florida

Fig.6: Salvinia traps air for a passive insulation, source: CML Fraunhofer

Fig.7: Flocked surface applied to ship, source: Micanti

The CML Fraunhofer institute in Hamburg is developing new coatings mimicking floating ferns (Salvinia), which trap a fine film of air, Fig.6, *Oeffner et al. (2020)*. While the focus here is on reducing resistance through passive air lubrication, *Silberschmidt et al. (2016)* indicate that air lubrication may substitute antifouling coatings. Similarly, the Dutch company Micanti offers films with flocked surfaces (resembling Velcro in surface texture), Fig.7. The microfibers prevent settling of fouling organisms even at zero ship speed. Despite the increase in surface due to the fibers, the company claims that there is no increase in friction resistance and thus no speed penalty, based on model tests. A possible explanation is that air was trapped when the test specimen was immersed in water and air lubri-

cation cancelled with added surface. There is no verified performance gain in longer operation (when any initially trapped air will have gone into solution again) yet.

3. Robots ahead

Appropriate cleaning strategies depend on the coating used. Copper-based antifouling paints release biocides under shear forces. Thus, cleaning with brushes will release more biocides, leading to premature depletion of the coating. However, frequent pro-active cleaning or grooming to remove the biofilm allows soft cleaning techniques with no or low abrasive forces. “Frequent” may mean every two weeks, to give an idea. Such frequent cleaning would remove biofilms before advanced calcareous fouling can develop; thus, it addresses issues of aquatic invasive species, a concern of ports and reason to prohibit in-port cleaning. But we do have neither enough divers worldwide to serve all or even many ships, nor would the ship operators be willing to pay every few weeks for traditional cleaning by divers.

But robots may change the game. You have seen swimming pools cleaned by robots. You have seen lawns mowed by robots. Couldn’t robots clean ships every time they are in port, too? Yes, they could! But the cleaning techniques and coating should be adapted to it and current hull cleaning robots must learn a few more tricks, most notably teamwork.

Recent developments on robotic cleaning, such as the FleetCleaner in the Netherlands and Belgium, Fig.9, *Noordstrand (2018)*, the HullWiper in the United Arab Emirates, *Doran (2019)*, or the Norwegian Hull Skating Solutions, Fig.10, indicate a larger trend towards softer, more frequent, more robotized cleaning with collection and disposal of removed waste. Although the technology is available, it needs to be rolled out and made widely available at competitive prices. But time is on the side of robotics, and so is industry interest.

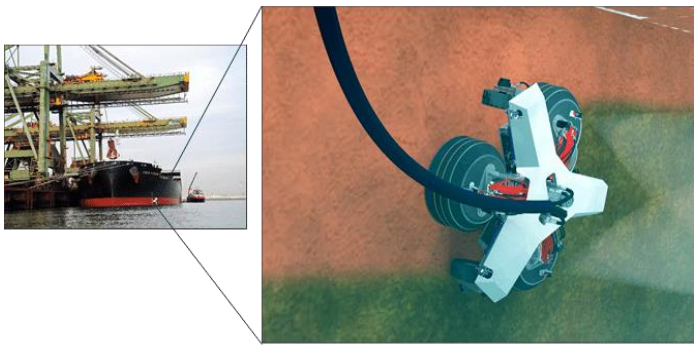

Fig.9: Fleet Cleaner

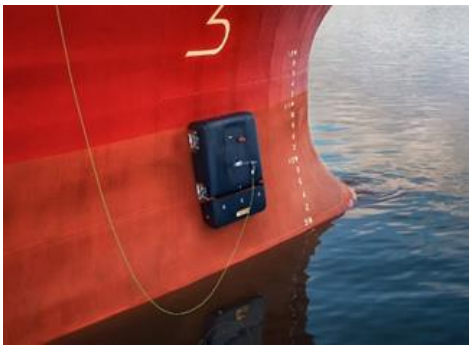

Fig.10: Hull Skater

4. New ideas waiting in the wings

Alternatives to biocide-based antifouling paints have been proposed for decades. Ideas which appeared as impractical or even exotic in the past may be reviewed in the light of changing technology and develop to viable contenders in the game of antifouling.

Ultrasonic vibrations cause very high accelerations, which destroy cell structures of fouling. The technology has progressed from research to industrial applications, Fig.11, *Kelling (2017a,b)*. So far, ultrasonic antifouling requires oscillators (‘transducers’) every 6-8m. For a cargo-ship, this would mean hundreds of transducers, many in areas that are difficult to access. Reliable operation in double bottoms filled with water or fuel may need more research. But already, transducers are a very attractive complementary technology to protect recessed areas, such as cooling-water pipes or sea chests. These areas are difficult to paint and to clean, an issue that will become an even larger headache when currently regional biofouling management regulations (e.g. for Australia or California) are applied on a wider global scale. A strong point of ultrasonic protection is that it offers biocide-free protection for ships even at zero speed.

Fig.11: Ultrasonic transducer, source: Hasytec

Fig.12: UV-based antifouling, source: AkzoNobel

Ultraviolet (UV) radiation is widely used in ballast water treatment. It has been proposed for hull antifouling decades ago, *Benson et al. (1973)*. The rapid attenuation of UV radiation and relatively high initial and operational costs has made this option rather unattractive for external antifouling applications. This may change now. AkzoNobel and Philips are jointly developing a novel fouling prevention solution, based on the generation of UV light by LEDs embedded in a transparent layer, Fig.12. The LEDs form thin tiles, relatively light-weight and thin. The tiles are 100% watertight and powered via wireless power transfer, thus substantially reducing any chance of electrical shorts. The technology is in the prototype stage.

Electric antifouling systems were already proposed by Edison in 1891, *Benson et al. (1973)*. The idea was revived and refined in 1990s, most notably by Mitsubishi's MAGPET system, *Bertram and Yebra (1973)*. Probably due to high installation costs, this approach was not accepted by the market. However, more recently, the German Fraunhofer institute researched (in 2016) a variation on the same theme: Nano-particles conduct weak current with electrolysis with alternating poles. This results in pH stress for marine organisms. The approach does not seem to have matured beyond the research stage yet.

Finally, we may use non-lethal chemicals in traditional paints. Selektope® (generic substance name Medetomidine) has been promoted as a non-toxic alternative to copper compounds, *Chabaane et al. (2019)*. The working principle is described as "pharmaceutical" as opposed to biocidal: barnacle larvae are stimulated to kick their legs, preventing settling on any surface. The substance is rather specific against barnacle fouling with much narrower spectrum of action than e.g. cuprous oxide, *Yebra (2016)*. It thus requires boosters to offer broad-band protection.

5. Conclusions

Biocide-based coating might remain king for years and maybe decades, but a host of more sustainable solutions is challenging the current standard approach. These "young challengers" are maturing with a growing number of in-service reference applications preparing the ground for wider acceptance, and ultimately a post-biocide era of antifouling.

References

BENSON, P.H.; BRINING, D.L.; PERRIN, D.W. (1973), *Marine fouling and its prevention*, Marine Technology 10/1, pp.30-37

BERTRAM, V. (2000), *Past, Present and Prospects of Antifouling*, 32nd WEGEMT School on Marine

Coatings, Plymouth, pp.87-97, http://www.wegemt.com/wp-content/uploads/2019/04/32nd_WEGEMT_School_on_Marine_Coatings.pdf

BERTRAM, V.; YEBRA, D.M. (2017), *Past, Present and Prospects of Maritime Antifouling*, 11th HIPER Conf., Zevenwacht, pp.32-43, http://data.hiper-conf.info/Hiper2017_Zevenwacht.pdf

CHAABANE, P.; CATHERINE, A.; ISAKSSON, D.; WEIGENAND, O.; OHLAUSON, C. (2019), *Application of Biotechnology in Antifouling Solutions for Hard Fouling Prevention*, 4th HullPIC Conf., Gubbio, pp.301-311, http://data.hullpic.info/HullPIC2019_gubbio.pdf

DAFFORN, K.A.; LEWIS, J.A., JOHNSTON, E.L. (2011), *Antifouling strategies: History and regulation, ecological impacts and mitigation*, Marine Pollution Bulletin 62/3, pp.453-465

DORAN, S. (2019), *A Short History of Hull Cleaning and Where Do We Go Now*, 4th HullPIC Conf., Gubbio, pp.97-102, http://data.hullpic.info/HullPIC2019_gubbio.pdf

KELLING, J. (2017a), *Ultrasound-based antifouling solutions*, 2nd HullPIC Conf. (HullPIC), Ulrichshusen, pp.43-49, http://data.hullpic.info/hullpic2017_ulrichshusen.pdf

KELLING, J. (2017b), *Ultrasonic Technology for Biocide-Free Antifouling*, 11th HIPER Conf., Zevenwacht, pp.70-77, http://data.hiper-conf.info/Hiper2017_Zevenwacht.pdf

KLUWE, F.; SCHRADER, L.U.; BRETSCHNEIDER, H. (2019), *From Bow to Stern: Hydrodynamic Measures for Increased Hull Performance*, 4th HullPIC Conf., Gubbio, pp.65-75, http://data.hullpic.info/HullPIC2019_gubbio.pdf

NN (1952), *Marine Fouling and its Prevention*, Report 580, Ch.11, Woods Hole Oceanographic Institute, https://darchive.mblwhoilibrary.org/handle/1912/191

NOORDSTRAND, A. (2018), *Experience with Robotic Underwater Hull Cleaning in Dutch Ports*, 3rd HullPIC Conf., Redworth, pp.4-9, http://data.hullpic.info/hullpic2018_redworth.pdf

OEFFNER, J.; HAGEMEISTER, N.; JAHN, C.; BRETSCHNEIDER, H.; SCHMALE, J. (2020), *Reducing friction with passive air lubrication: Initial experimental results and the numerical validation concept of AIRCOAT*, 12th HIPER Conf., Cortona, http://data.hiper-conf.info/Hiper2020_Cortona.pdf

SILBERSCHMIDT, N.; TASKER, D.; PAPPAS, T.; JOHANNESSON, J. (2016), *Silverstream system – Air lubrication performance verification and design development*, 10th HIPER Conf., Cortona, pp.236-246, http://data.hiper-conf.info/Hiper2016_Cortona.pdf

SØRENSEN, K.F.; HILLERUP, D.; BLOM, A.; OLSEN, S.M. (2012), *ActiGuard®: Novel technology to improve long-term performance of silicone-based Fouling Defence coatings*, Hempel, www.hempel.com/~/media/Sites/hempel/files/marine/technical-papers/ActiGuardtechnology.pdf

STENZEL, V.; SCHREINER, C.; BRINKMANN, A.; STÜBING, D. (2016), *Biomimetic approaches for ship drag reduction – Feasible and efficient*, 10th Symp. High-Performance Marine Vehicles (HIPER), Cortona, pp.131-140, http://data.hiper-conf.info/Hiper2016_Cortona.pdf

YEBRA, D.M. (2016), *Future directions towards low-friction hulls*, 10th Symp. High-Performance Marine Vehicles (HIPER), Cortona, pp.217-224, http://data.hiper-conf.info/Hiper2016_Cortona.pdf

Antifouling Treatment with Nano-Ceramic-based Coatings

Andrea Ratti, Politecnico di Milano, Milan/Italy, andrea.ratti@polimi.it
Federico Maggiulli, Politecnico di Milano, Milan/Italy, federicoluigi.maggiulli@polimi.it
Federico Veronesi, ISTEC-CNR, Faenza/Italy, federico.veronesi@istec-cnr.it
Cristiano Bighetti, Boero Group, Genova/Italy, cristiano.bighetti@boero.it
Simone Garofoli, Boero Group, Genova/Italy simone.garofoli@boero.it

Abstract

This paper presents the experimentation on new applications of materials with a nano-ceramic structure with the aim of reducing the development of biological agents on yacht hulls in both fresh and saline water. The project stems from the growing need to find an alternative to classic antifouling paints based on biocides that would represent a real eco-friendly solution during the entire life cycle of the product. The general objective of the research is to develop innovative solutions for the protection of boat hulls from bio-fouling. The program included the development of laboratory activities and reale scale testing campaign on water with comparative analysis of static samples and the use of a testing sailing boat.

1. Introduction

Antifouling product technologies are in a phase of great transformation due to progressive regulatory restrictions limiting the use and content of biocides and high active substances with potential impact in terms of environmental toxicity. These restrictions aim to cancel, or at least limit, the potential release into the environment of substances with possible effects on marine biology, as well as on the health of shipyard workers involved in the application of such products and the maintenance of vessels. Also potentials risk of antifouling painting are well known, *Bellotti et al. (2010), Ratti and Bionda (2015)*, and, in particular after the IMO International Convention on the Control of Harmful Anti-fouling Systems on Ships, *IMO (2001)*, the attention of the international scientific community is concentrated on nontoxic alternative to biocidal coatings.

The International Maritime Organization estimated that, without corrective actions and introduction of new technologies, air emissions due to increased bunker fuel consumption by the world's shipping fleet could increase by between 38% and 72% by 2020, *IMO (2000)*.

For this reason, various strategies are being developed for the development of new technologies to guarantee antifouling properties, not based on the presence of active ingredients in the formulation and therefore with little or no environmental impact.

The objective of the research programme was therefore to test new coatings able to prevent or slow down the formation of the bacterial chain that allows the development of microorganisms on the surface and consequently the vegetative growth on the immersed hulls in total absence of release of contaminants into the water.

A secondary, but no less important effect of the tests carried out in the research programme, is the improvement in performance in terms of reduced resistance of the hull, with a consequent reduction in fuel consumption and further limitation of environmental impact. The challenge consists in replacing conventional coatings (containing biocides) with coatings that possess structural and functional stability during application and yet effectively prevent growth of fouling organisms, avoiding any major environmental impact, *Nurioglu et al. (2015)*. Environmentally benign AF coatings would not only save the marine industry huge sums of money invested in fuel, maintenance, and labor, but would also have significant benefits for citizens and society, *Selim et al. (2019)*.

2. Project strategies

The experimental path, developed as part of a collaboration between the Department of Design, the Department of Materials Chemistry of the Politecnico di Milano, the CNR-ISTEC of Faenza and the Boero Company, has included the application of coatings with nano-ceramic structure on immersed samples made of in rigid PVC that were exposed for a period of 6 months in fresh water (at the nautic base of Dervio (LC)) and in saline water (in the Gulf of La Spezia). The program included a first test campaign in the 2019 and a subsequent one, currently underway, focused on the products and processes that performed better during the first phase. The specific objective is the selection of combinations of coatings with nano-ceramic structure and their evaluation according to criteria of effectiveness, durability, ease of application.

The comparison activity was therefore carried out using standard samples of antifouling applied to both static samples in immersion and on the hull of the experimental boat as a reference, which made it possible to obtain feedback on the self-cleaning factors of the surfaces due to motion.

2. 1. Project objectives

The purpose of the test program was to investigate the following performances:

A. Bacterial chain adhesion and growth factor and subsequent formation of micro organisms and vegetation on the surface of immersed samples (both in fresh and saline water) and on the testing boat by direct comparison of the performances of alternative treatments compared to a commercial antifouling product used as a reference. The observations were carried out at monthly intervals since the dive(1 and the subsequent comparative evaluations were carried out using photographic analysis with image processing according to standards already developed in previous research on the antifouling properties of polymeric films, *Ratti and Bionda (2016)*.
B. Check of the self-cleaning properties of the different surfaces under investigation by dragging samples in water at a speed of 5 knots (speed measured by GPS instrumentation) for an extension of half a mile. At the end of each drag, the samples were subjected to the same process of evaluation of the residual vegetation translated in percentage of surface cover and consequently comparable with the initial situation.

2. 2. Application procedures

The project focused on the antifouling properties of surfaces treated with ceramic nanoparticles. Below is a brief description of the application procedures.

Water-repellent hybrid coatings with low surface energy, consisting of a layer based on ceramic nanoparticles and an organic layer. The overall thickness of these coatings is less than the micrometer. Initially, we worked with 3-4 different formulations preliminarily evaluated according to the adhesion to the selected substrates and their full scale application transferability also according to the required post-cure steam processes.

More precisely, the coatings were applied on different types of substrates, but made homogeneous through the surface application of an epoxy primer in order to simulate a realistic application situation:

- Fluorinated polymeric resin based coating (Sample 1)
- Hybrid coating consisting of a ceramic layer similar to the previous point and a layer of alkyl silane with fluorinated aliphatic chains and heat application (Sample 2)
- Hybrid coating similar to the previous one, with the addition of a lubricating oil that penetrates the surface structure and homogeneity and heat application (Sample 3)
- Hybrid coating consisting of a ceramic layer based on nanoparticles and a layer of alkylsilane, possibly with fluorosubstituted aliphatic chains (Sample 3bis)

- Coating with textured primer (print through peel-ply) + Coating 3 (3PP sample)
- Hybrid coating similar to the previous one with addition of a different lubricating oil and heat treatment (Sample 4)

While the sample used as a reference was a commercial Boero product (AV sample), Table I summarises the formulations of each composition, the presence or absence of heat application and lubricating oils.

Table I: Application sequences

Sample	fluorinated polymeric resin	ceramic nanoparticles	Heat treatment	Alkyl silane fluorinated	alkylsilane	lubricating oil A	lubricating oil B	Peelply
1	X							
2		X	X	X				
3		X	X	X		X		
3BIS		X		X		X		
4		X	X		X		X	
3PP		X	X	X		X		X

2.3. Test protocol

The test protocol identifies the instruments, how and when to prepare samples and perform tests. The seat of the trials is the municipal port of Santa Cecilia in the Larian town of Dervio (LC) and the port of Le Grazie (SP).

The products for the tests in static immersion were applied on PVC supports of the dimensions 12.5 x 23.5 cm. treated with epoxy primer. For each product combination, 6 applications were made, 3 of which were intended for immersion in fresh water and the remaining in saline water.

Fig.1: Frame with samples ready for diving

In addition, the project included the application of the samples tested on the hull of the experimental craft. The support boat for the execution of the full scale tests is a 7 mt sailing boat with wooden construction. The boat hull surfaces and appendages in which the test products were used were sanded, grouted and treated with an epoxy primer and then cleaned of any residual dust and oil.

The quantity and type of attack from external Biofouling agents was investigated through a monthly photographic survey and the images processed following a procedure already experimented in a previous research project, *Ratti and Bionda (2015)*. The images of the results were processed using photo-editing and computer analysis tools to define the percentage of biofouling saturation. In particular, the following steps were performed:

- adjustment of brightness (-10%) and contrast (+ 100%);
- correction of the tone values for the exclusion of reflected light;
- exposure adjustment to highlight the biofouling in the background color of the film (+ 9%, 0%, 5%);
- color abandonment with a selective filter of green and yellow channels;
- black and white channels are reversed;
- proportion of the black channel to 200,000 pixels.

Fig.2: The order of test samples on the Testing hull

3. Analysis and evaluation of the results

After the first quarter of immersion in fresh and saline water, the first photographic surveys were carried out on all the samples. In the second quarter (August - September - October), the samples showed almost total coverage of the exposed surface, Fig.3. Fig.4 shows the coverage percentages measured on a monthly basis.

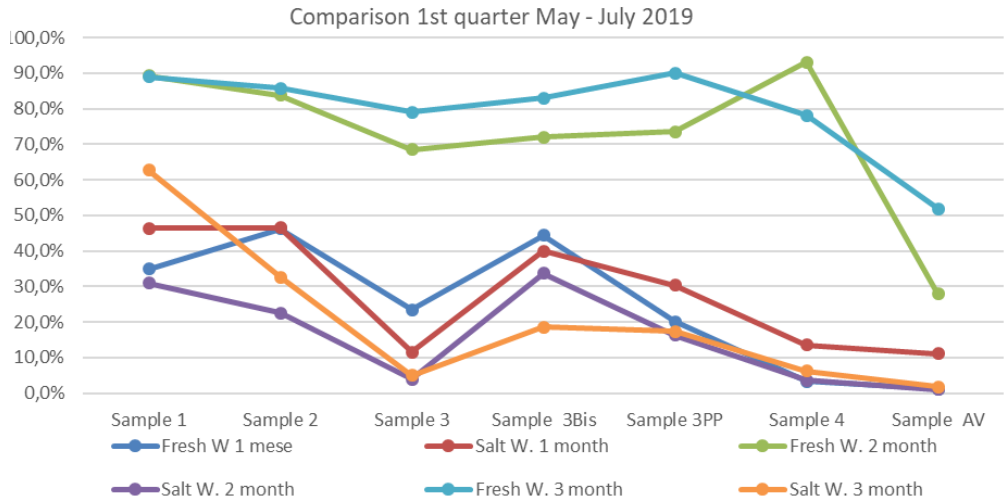

Fig.4: Coverage for different samples

Fig.3: Coverage perceptage for three consecutive months

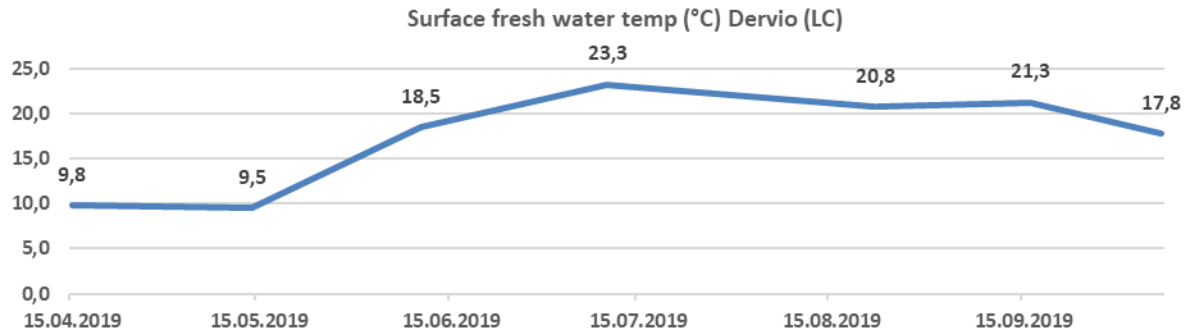

Fig.5: Seawater temperature

Fig.6 to Fig.9 show the sample frames in September and October in both test areas: the coating is characterized by incrustations of considerable thickness, except for the panels treated with traditional antifouling. We can also notice the substantial difference between the marine and lake biological attacks; in fact, the marine ones, created an initial sludgey substrate, similar to the lake one; then, the surfaces were attacked by other agents that thickened the biological covering layer, generating a real microhabitat made by vegetable and animal agents. In lake samples, on the other hand, the coating stopped at the sludgey consistency without generating further developments. This aspect makes the lacustrine attacks have less tenacity to the surface and therefore easily removable with a pressure washer. Precisely for these reasons it was not possible to make a "B/W contrast" comparison as done in previous months because the coating would have been close to 100% for all samples, moreover, as can be seen from the images of the marine samples, some biological agents are white and this would have distorted the contrast, resulting in an incorrect assessment of the coverage.

In addition, for samples exposed in fresh water the level of saturation affects all the samples including the reference sample which, vice-versa, preserves antifouling power in saline water.

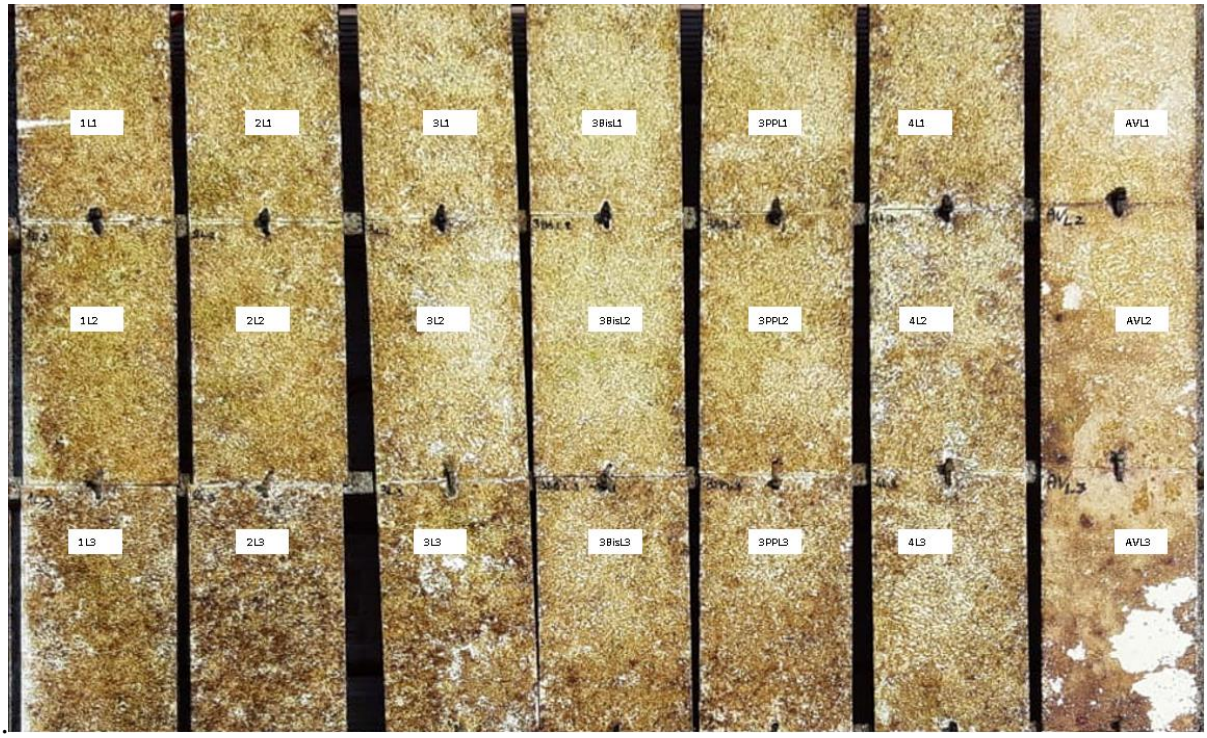

Fig.6: Panel test Dervio (LC) 5th month (September 2019)

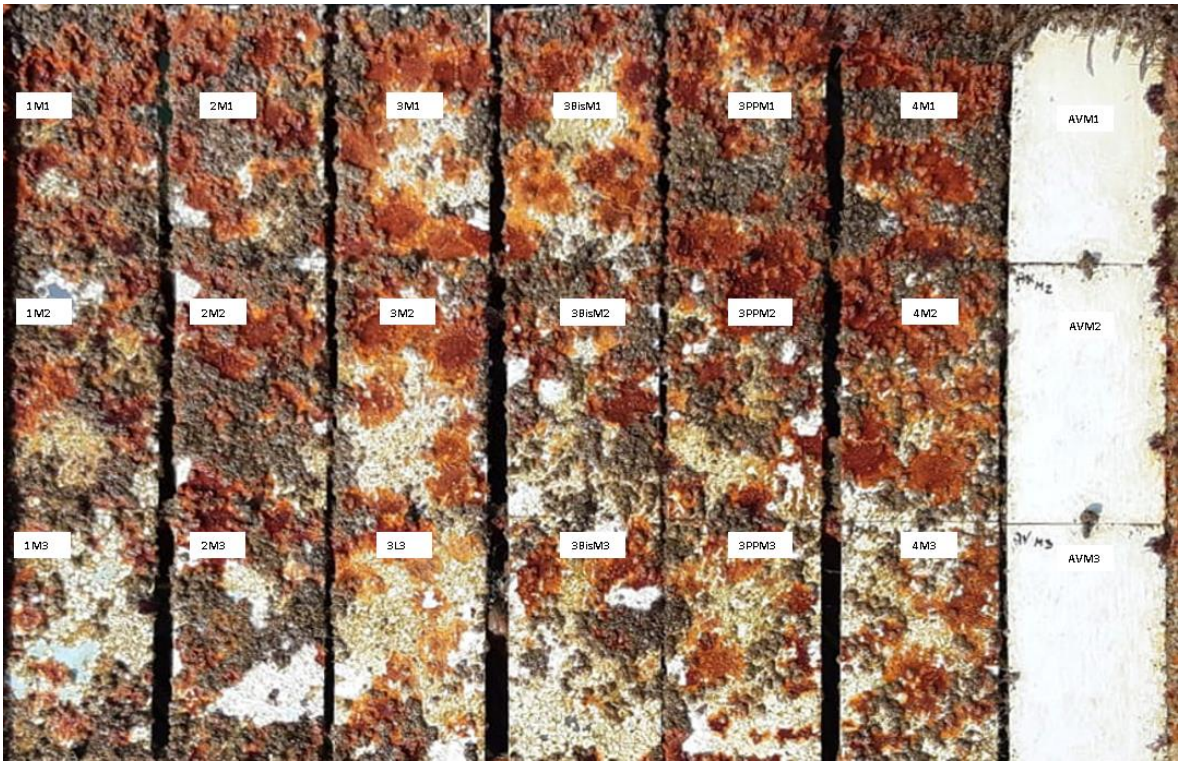

Fig.7: Panel test La Spezia 5th month (September 2019)

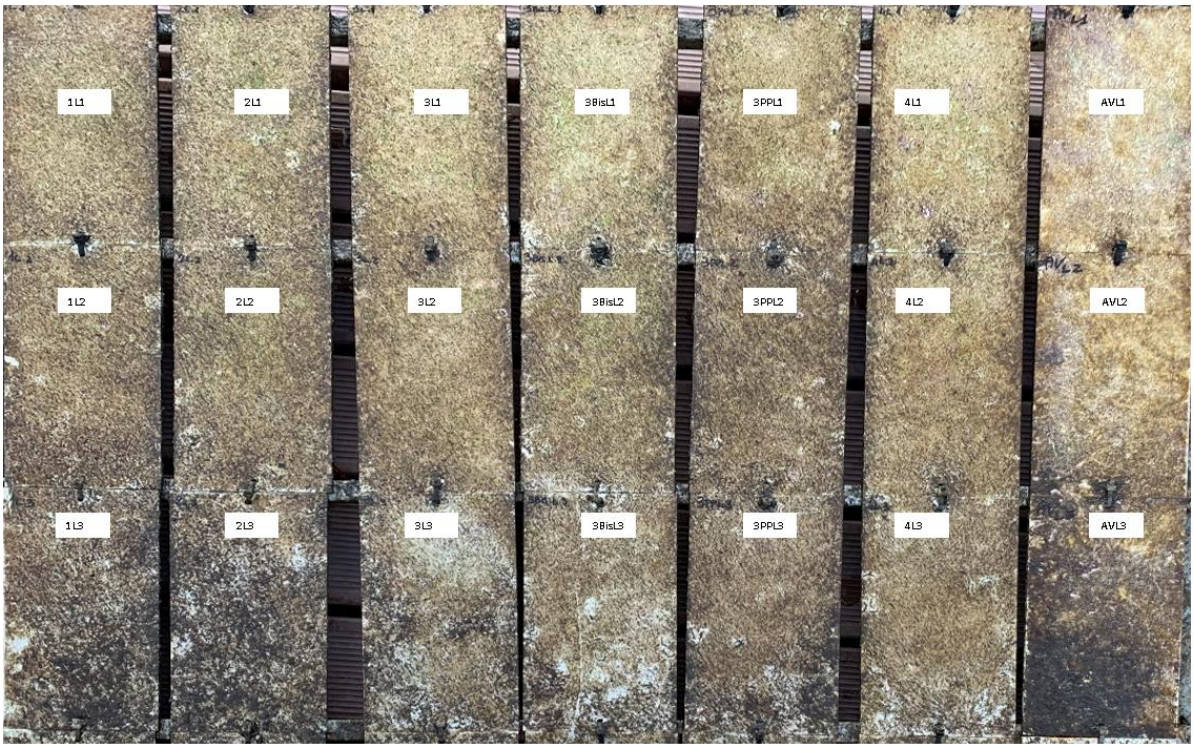

Fig.8: Panel test Dervio (LC) 6th month (October 2019)

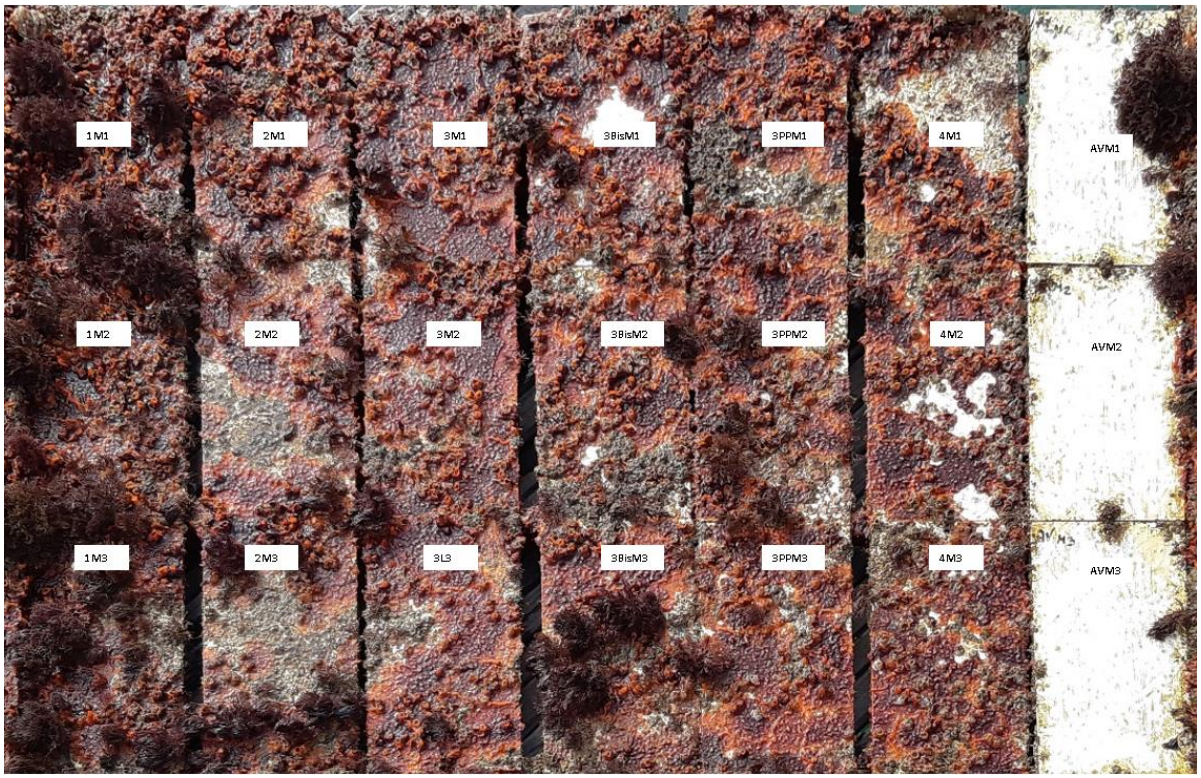

Fig.9: Panel test La Spezia 6th month (October 2019)

4. Relief on Testing boat hull

As previously described, all the nano-ceramic coatings under investigation were applied to the hull of the Testing sailing boat (Gullisara) for cross-sections from stern to bow, avoiding the application of the materials to the appendages (keel and rudder) which were maintained with anti-fouling reference treatment (Tradictional AF). Unlike the panels, which were measured on a monthly basis, on the hull of the Testing boat, photographic surveys were carried out quarterly for logistical reasons. It was chosen to analyse two distinct areas of the hull: the area near the waterline, and therefore the shoreline, and the bottom of the hull to assess the differences due to exposure to light and surface oxygenation. From the comparative graphs based on photographic surveys at 1 month (May 2019), 3 months (July 2019) and at the end of the project after 6 months (October 2019) it is evident that the attack of biological agents is lower on the hull of the boat compared to the panels immersed on the frame, Fig.10, Table I.

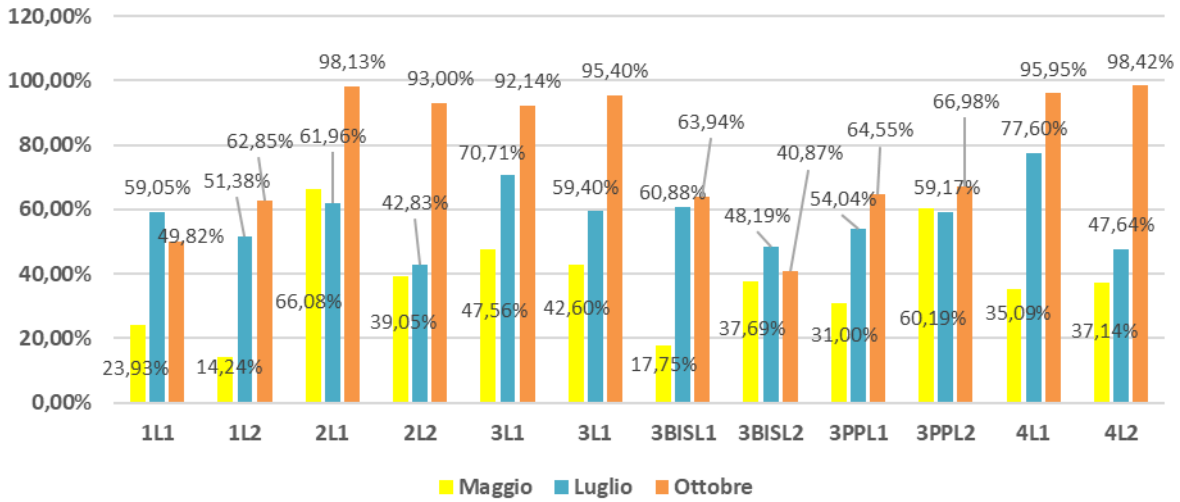

Fig.10: Hull relief May – July - October

Table I: Hull relief (covering %)

	May	July	October
1L1	23,93%	59,05%	49,82%
1L2	14,24%	51,38%	62,85%
2L1	66,08%	61,96%	98,13%
2L2	39,05%	42,83%	93,00%
3L1	47,56%	70,71%	92,14%
3L1	42,60%	59,40%	95,40%
3BISL1	17,75%	60,88%	63,94%
3BISL2	37,69%	48,19%	40,87%
3PPL1	31,00%	54,04%	64,55%
3PPL2	60,19%	59,17%	66,98%
4L1	35,09%	77,60%	95,95%
4L2	37,14%	47,64%	98,42%

The factor is evidently related to the movement of the boat itself, which in the period May-July made transfers and participated in regattas with a frequency of use that in any case did not exceed 5 days/month. It is therefore reasonable to attribute the result to the activation of a self-cleaning mechanism also highlighted in the drag tests carried out and described in the following paragraph. A further factor found is the lower involvement of the horizontal surfaces of the hull characterised by lower levels of light exposure and water oxygenation. In the tables we also notice, especially from the third month, a recurring different level of vegetation between sample 1 (found on the waterline) and sample 2 (found on the bottom of the hull), both refer to the left side, exposed to the south-west during the mooring in port of the boat.

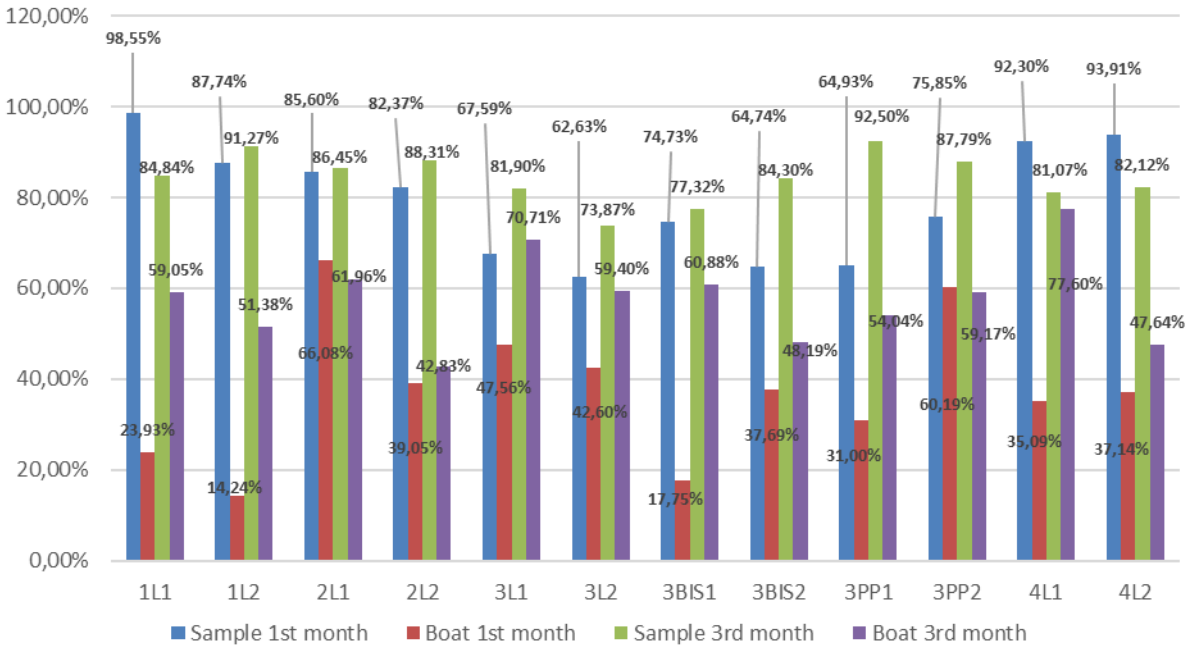

Fig.11: Comparison sample – Boat fresh water (Dervio)

In the last photographic survey carried out at the end of the project, in mid-October, the hull showed a widespread coverage by biological agents, due not only to the dive time, but also to the static nature of the boat. Since the end of July the boat has always been at berth in increasing water temperature conditions that this year have exceeded 23°C.

5. Drag tests and self-cleaning

In order to test the level of adhesion of the biological agents on the samples and the self-cleaning capacity due to the motion of the hypothetical boat, a drag test was carried out using one of the immersed samples for each type of coating. The test consisted in photographing the samples before and after the dragging in water at a speed of 5 knots (speed measured by GPS instrumentation) for an extension of half a mile, with specimens applied to a support that guaranteed their stability in navigation. Below are the results obtained with the image processing that allow to evaluate the degree of coating of the surface.

Table II: Data collected 14.6.2019 (Dervio – Como Lake) – Frag and self-cleaning tests

	%before	%after drag.	abate-ment
1L3	81,54%	68,19%	13,35%
2L3	83,30%	60,78%	22,52%
3L3	75,45%	43,66%	31,79%
3bisl3	76,75%	58,68%	18,07%
3PPL3	79,81%	50,52%	29,29%
4L3	93,31%	87,05%	6,26%
AVL3	27,47%	13,53%	13,94%

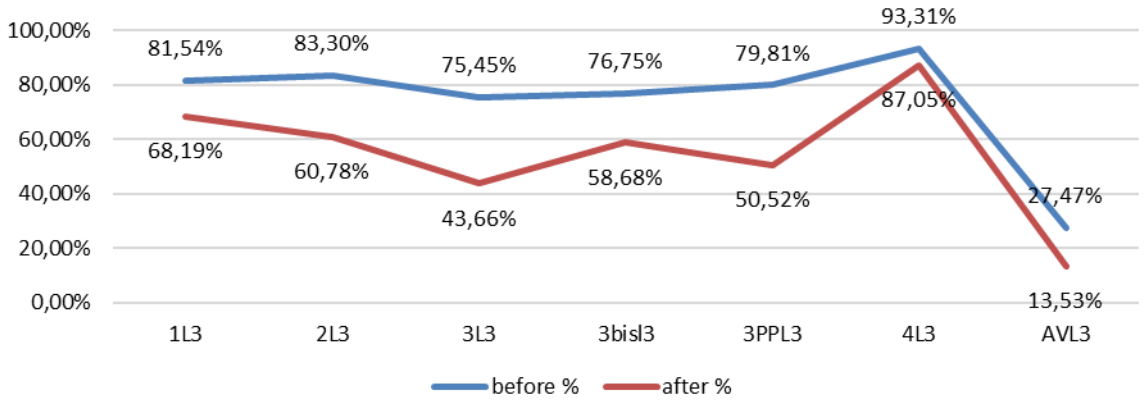

Fig.12: Self-cleaning test fresh water 16.6.2019

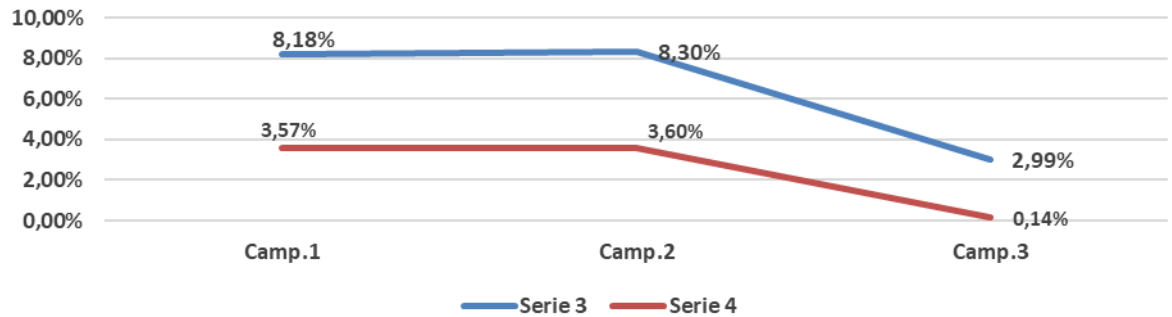

Fig.13: Self-cleaning test salt water 17.6.2019

Regarding the drag test carried out in seawater, it was considered appropriate to focus attention exclusively on the samples that showed the best performance, i.e. sample 3 and sample 4. In particular, of the 3 panels treated and exposed in the frame, coating 3 was dragged according to the specification adopted in the test carried out at the lake and then compared with the other two panels with the same surface treatment. The graph below shows how even a dragging at a modest speed of 5 knots (9.26 km/h) significantly reduces the presence of microorganisms in surface deposition.

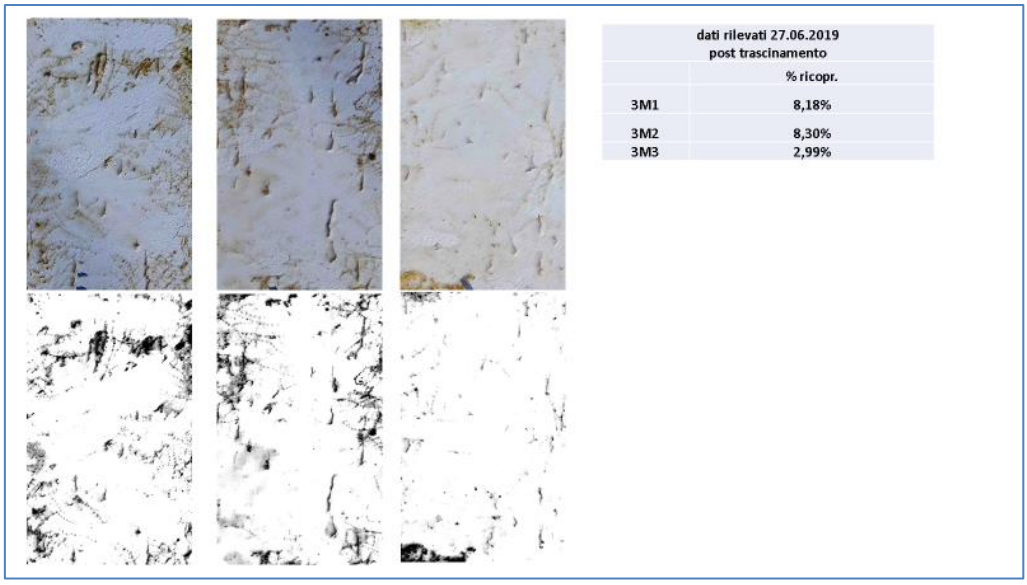

Fig.14: Sample 3 after drag test in salt water (June 2019)

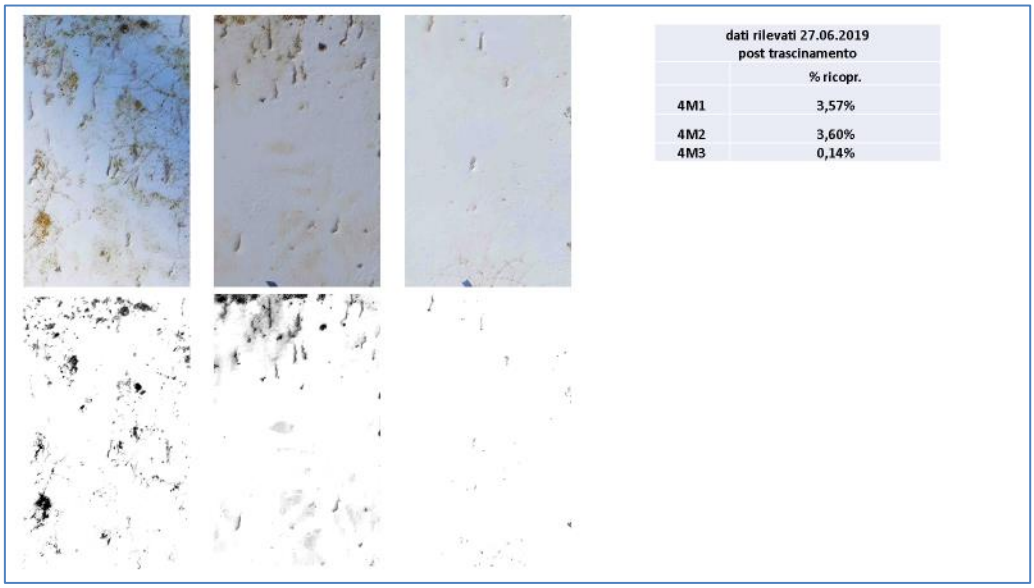

Fig.15: Sample 4 after drag test in salt water (June 2019)

Following the dragging tests in the lake and sea water, a series of tests and laboratory analyses were carried out on the samples subjected to dragging and to washout with a pressure washer to assess their surface condition. In particular, the results obtained on samples 3 and 4 have been studied in depth because they were considered, at a first analysis in the field, more promising.
On these samples, two types of characterization of wettability properties were performed:

1. Measurement of contact angle hysteresis (CAH) to understand the level of wear of the coating following cleaning procedures;
2. Calculation of surface energy (SE) to know the potential antifouling properties of surfaces.

Laboratory tests have shown that the coatings produced on the field differ from those obtained in ISTEC laboratories, with a substantial loss of the infused oil.

In addition, CAH measurements have shown that the type 3 coating is damaged by cleaning procedures (washout test with pressure washer), while the type 4 coating remained substantially unchanged. Never-

theless, SE measurements indicated that the Type 3 coating remained potentially superior to Type 4 in terms of antifouling capacity.

These considerations left room for some feedback on coating fabrication processes such as:

1. Improvement of the heat treatment process in order to ensure better structure of the alumina layer and increase capillary oil retention;
2. Use of less volatile oils for type 3 samples. The same is not possible with type 4 coatings since alkanes higher than hexadecane (e.g. ottadecane) are solid.

6. Results and conclusions

After the test period carried out between April 2019 and October 2019 both in the lake area of Dervio (LC) and in the marine environment in La Spezia, some evidences emerged:

1. Samples 3 and 4 were the samples that showed the most comparable efficacy, in the first months of exposure, to the antifouling reference. Both had a first layer of Aluminium Al2SO3, both were subjected to heat treatment and as a surface finishing film a lubricant.
2. Sample 3 proved particularly effective in fresh water, while sample 4 showed excellent potential in both environments.
3. The samples maintained a behaviour worthy of observation up to about 3 months, after which the biological attack was such as to generate a total coating of the samples. As can be seen in the graph of water temperatures in Dervio (LC), this dead line corresponds to the peak water temperature passing from 9.8°C to 23.3°C within 3 months. This "collapse" also affected the surfaces treated with antifouling both on the samples and even more so on the hull.
4. Drag tests and the first surveys carried out on the boat in July revealed a considerable propensity for self-cleaning, i.e. the ease of cleaning the hull thanks to the boat's motion. This is evident both from the dragging tests carried out on the panels, at a speed of only 5 knots, and on the hull of the testing boat. It is therefore important to consider how the self-cleaning factor represents a topic to be dealt with and studied in depth as a potential key to understanding the performance offered by the formulations under investigation.
5. As further confirmation of this, it should be noted that the samples that showed the best performance were also those that showed the best self-cleaning skills with particular reference to sample 3. Further consideration to be taken into account in this regard is that the first drag test took place after 2 months of static immersion and it is therefore reasonable to believe that without such a long period of static permanence, but with a greater frequency of motion from the first moments of immersion, the results can be expected to improve appreciably.

References

BELLOTTI, N.; DEYA, C.; AMO, B.; ROMAGNOLI, R. (2010), *Antifouling paints with zinc "Tannate"*, Ind. Eng. Chem. Res. 49

IMO (2000), *Study of Greenhouse Gas Emissions from Ships,* International Maritime Organization, London

IMO (2008), *International Convention on the Control of Harmful Anti-fouling Systems on Ships*, International Maritime Organization, London

NURIOGLU, A.G.; ESTEVES, A.C.C.; DE WITH, G. (2015), *Non-toxic, non-biocide-release antifouling coatings based on molecular structure design for marine applications*, J. Mater. Chem. B 3 (32), pp.6547-6570

RATTI, A., BIONDA, A. (2015), *New solutions for biofouling prevention,* 18th Int. Conf. on Ships and Shipping Research - Advanced Solutions for Yachts Efficiency Symp., Lecco

RATTI, A.; BIONDA, A. (2016), *Antifouling wrap: a sustainable solutions for biofouling prevention,* Sustainable Energy for All by Design, Cape Town

SELIM, M.S.; EL-SAFTY, S.A.; SHENASHEN, M.A. (2019), *Superhydrophobic Foul Resistant and Self-cleaning Polymer Coating,* Chapter in Superhydrophobic Polymer Coatings: Fundamentals, Design, Fabrication, and Applications, Elsevier Science BV

The Silent Revolution in Biocide-Free Antifouling

Jan Kelling, **Xavier Mayorga**, HASYTEC Electronics GmbH, Schönkirchen/Germany,
j.kelling@hasytec.com

Abstract

Future biocide-free biofouling management solutions are evolving rapidly. For internal systems and niche areas, ultrasonic systems have proven to be an attractive option in this context. The paper describes the basic approach of the Dynamic Biofouling Protection system and illustrates its effectiveness for various applications with case studies from different vessel.

1. Introduction

Fouling develops in stages, where the initial stage is a microscopic fouling, which collectively may form a biofilm visible to the human eye, Fig.1. See *Kelling (2017a,2018)* for a more extensive discussion. If the biofilm formation is inhibited, the subsequent stages of macrofouling will not develop. Much of the focus of recent research and development into biofouling management have been focused – rightfully and logically – then on inhibiting biofilm formation and development.

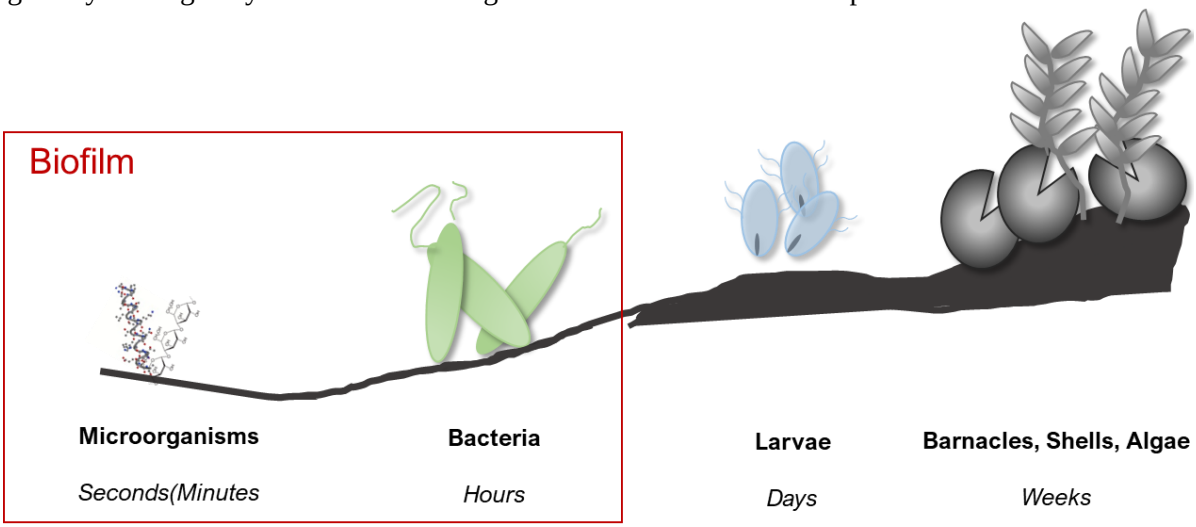

Fig.1: Biofilm as the initial step of marine growth

The classical approach to combat biofouling on ships has been using biocide-containing paints, *Bertram and Yebra (2017)*. In relation to the IMO convention "International Convention on the control of harmful Anti-Fouling Systems on Ships (2001)", the European Union finalized the EU Regulation No. 528/2012. This regulation on biocide containing products regulates the marketing and use of biocide containing products, which due to the activity of the active ingredients contained in them for the protection of humans, animals, materials or products against harmful organisms such as pests or bacteria, may be used. The aim of the regulation is to ensure a better functioning of the biocide containing products market in the EU, while ensuring a high level of protection for human health and for the environment. As an example, almost no copper based active substance will get permission to be used in the future. Every system must be approved to be marketed and the environmentally harmful systems shall be sorted out. This leaves essentially two options:

- taking the risk of using less effective antifouling systems which leads to higher costs for maintenance and repair as well as to higher fuel expenses
- looking for alternatives to replace the currently used antifouling systems

While robotic cleaning solutions are often a cost-effective solution for large, smooth areas, niche areas are unsuited for robotic cleaning. However, niche areas are particularly critical in terms of biofouling

and the threat of aquatic invasive species. This is explicitly addressed in IMO's biofouling management guideline. Niche areas are also the focus of inspections of authorities already enforcing biofouling management policies, such as Australia, New Zealand, California and Hawaii State. A complementary solution is needed, and the Dynamic Biofilm Protection (DBP) based on ultrasound is the perfect match for the requirements of IMO's biofouling guideline. It will be described in the following.

2. Dynamic Biofilm Protection

Using low-powered ultrasound (which does not cause cavitation in a certain combination of frequencies, altitudes and power consumption) avoids biofilm formation on any liquid carrying surface, *Kelling (2017b)*. This working principle is still relatively unknown in the shipping industry, but it has large potential and enjoys a rapidly growing customer base.

The Dynamic Biofilm Protection based on ultrasonic protection against biofouling may be used for external spaces, such as pipes, heat exchangers, sea chests, or tanks, Fig.2. But they may also be used for hull protection. For smaller vessels, the complete hull may be protected, but for large cargo vessels, the typical applications focus on niche areas, such as side thrusters, sea chests, etc.

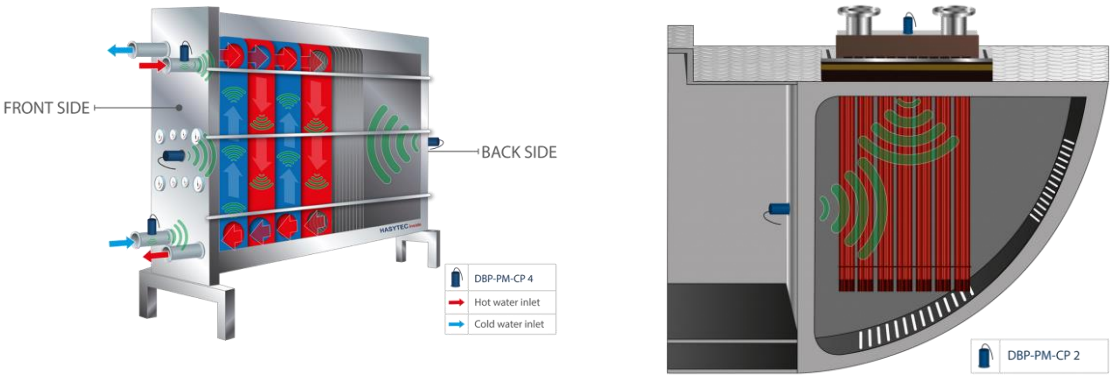

Fig.2: Internal biofouling protection using DBP. Small blue cylinders are 'transducers'

The ultrasonic vibrations are brought into the water via 'transducers', Fig.3, which are attached to the steel hull on the inside, e.g. in the engine room where electrical supply to the transducers is easy. Transducers are relatively low-powered, e.g. 12 W per transducer for average output, 20 W per transducer for maximum output.

Fig.3: Examples of installed transducers

Figs.4 to 7 show results from sample installations, demonstrating the effective protection against biofouling. More such results from shipping industry applications are found in *Kelling (2017a,b).*

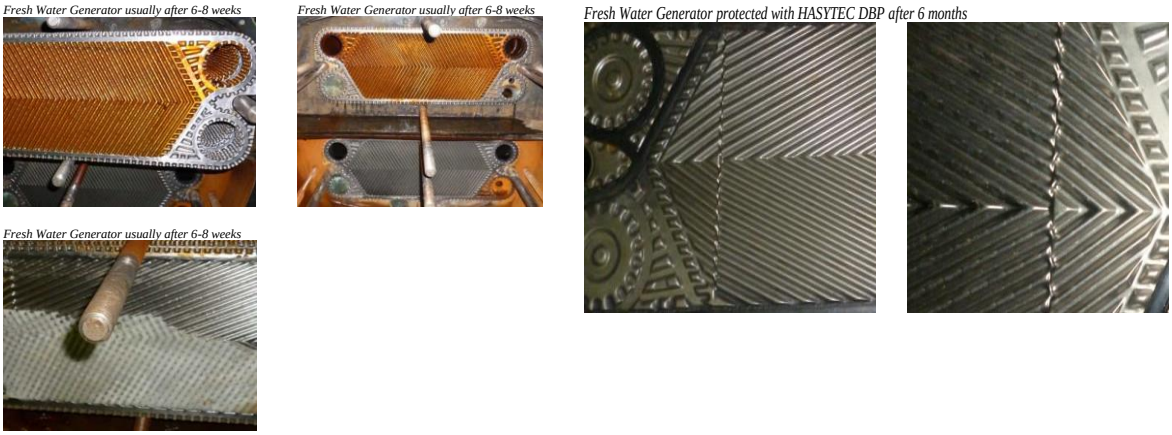

Fig.4: Fresh-water generator after 6-8 weeks without DBP / after 6 months with DBP

Fig.5: Sea Chest view from outside after 3.5 years in operation with DBP

Fig.6: Propeller after 6 months without DBP and comparable propeller after 3 years with DBP

Fig.7: Side thruster before (left) and after (right) installing DBP

3. Summary

Ultrasonic biofouling management continues to gain traction in the maritime industry. We have more then 4500 transducers installed, on a total of more than 230 ships. In a nutshell, the Dynamic Biofouling Protection system is summarized as follows:

- environmentally friendly and sustainable
- maintenance free
- reducing OPEX
- increasing lifetime of vessel`s components & operational safety
- design following shipping industry standards and IP 68 approved

Acknowledgements

HASYTEC electronics GmbH has enjoyed great support from customers and media which have accompanied us from the beginnings of a small start-up to where we are now: the technology leader in maritime ultrasonic biofouling protection. We are grateful for the many awards bestowed upon us: Environmental Performance Award (2017), Hansa Maritime Innovator Award (2017), PitchBlue Jury and Audience Awards (2018), Ocean of Opportunities Award (2018), SEATRADE Engineering Award (2019), and Deutscher Innovationspreis (2020). Thank you.

References

BERTRAM, V.; YEBRA, D.M. (2017), *Past, Present and Prospects of Maritime Antifouling*, 11th HIPER Conf., Zevenwacht, pp.32-43, http://data.hiper-conf.info/Hiper2017_Zevenwacht.pdf

KELLING, J. (2017a), *Ultrasound-based antifouling solutions*, 2nd HullPIC, Ulrichshusen, pp.43-49, http://data.hullpic.info/hullpic2017_ulrichshusen.pdf

KELLING, J. (2017b), *Ultrasonic Technology for Biocide-Free Antifouling*, 11th HIPER Conf., Zevenwacht, pp.70-76, http://data.hiper-conf.info/Hiper2017_Zevenwacht.pdf

KELLING, J. (2018), *Ultrasound – The Silent Revolution in Antifouling*, 3rd HullPIC Conf., Redworth, pp.346-353, http://data.hullpic.info/hullpic2018_redworth.pdf

How Covid-19 Will Affect the Cruise Ship Projects

Massimo Musio-Sale, University of Genova, Genova/Italy, musio-sale@arch.unige.it
Valerio Ruggiero, University of Messina, Messina/Italy, vruggiero@unime.it

Abstract

This paper analyses the problems observed on cruise ships during the Covid-19 pandemic and proposes a series of changes in the design of passenger ships to face similar pandemics to allow the cruise ship market to re-open. The hospital facilities on board play a key role in this.

1. Introduction

The spring 2020 will be remembered for the spread of a viral pandemic, called SARS-2 COVID-19. This pandemic is hitting every country all over the world, involving all the aspects of transportation with heavy consequences: planes, trains, buses, passengers ships, all have been touched and all the governments all over the world made significant changes to ensure the safety of passengers.

In some cases, the mean of transportation, like for example a ship or an airplane became the place to start an infection causing a lot of causes among the passengers. One of the most prominent examples have been the passenger ship "Diamond Princess" where an important outbreak occurred, causing the spread of the infection up to over 20% of the people on board, with over 700 cases out of about 3700 people. In the spring 2020, there were over 20 cruise ships with cases of contagion on board, and all shipping companies such as Viking cruises, Princess cruises, MSC, etc. announced a suspension of their cruises.

Some cruise companies started again some cruises in summer 2020, but with a lot of limitations and on short routes, and without knowing yet the exact impact of the situation on the market. During the first months of the pandemic dozens of Cruise ships were stopped, with over 80.000 member of the crew on board, under quarantine.

According to the opinion of scientists, architects and cruise experts, the need of a high level of interactivity among design, passenger management, marketing, medical aspects is obvious. The 2020 COVID situation showed the requirement of a total new approach at the design of cruise ships. In the initial phase, for all the ships involved there was the problem of containing contagion on board, in order to allow the landing and subsequent treatment in safety conditions of the staff. It is well known that on board all passenger ships are naturally equipped with an emergency hospital, in order to guarantee the necessary medical assistance to passengers or to the on-board staff requesting it. But evidently these hospital facilities are not sized to cope with a situation like the one that has arisen. This article therefore aims to give an analysis of the situation, give an analysis of the general arrangement of a Passenger ships and propose a methodology for the development and implementation of a hospital unit for Passenger Ships that can be of assistance in situations such as the one currently underway.

The ships have always had to deal with the problem of containing contagious diseases due to their characteristics of transporting people with a high density of human beings per square meter of available surface. In the past, unfortunately, this problem was difficult to solve, due to the limited responses that Technology could offer to medical Knowledge, which of course was also a limit. The classic "yellow flag", corresponding to the letter "Q", indicated a ship subject to “quarantine” for the presence on board of contagious diseases. The disembarkation of the boats was therefore forbidden until quarantine end.

The possibility to adapt the design of an existing passenger ship into a support vessel or to face pandemic disease had already been studied, *Cohen and Sokolvsky (1980), Reitherman (1986), Van*

Ommeren et al. (2005), Ruggiero et al. (2011), Carter and Moizer (2011), Yang (2013), Zhao et al. (2015), Hameed et al. (2016), and this possibility, on a different vessel, has been just realized in the Port of Genova in March 2020.

This paper will focus on the relevant data of the problems that passengers ships actually may have to face during a contagious disease spreading on board, and also to demonstrate how the new passengers ships could be adapted, during the construction process, to improve the operations in case of infection diseases on board.

2. Description of the COVID-19 Situation

The international situation due to the COVID-19 pandemic is well known and does not need to be described in this article. We only want to recall the main points useful to define a chronological schedule and necessary to define the covered topics.

In February 2020 Mn Diamond Princess was placed in quarantine in the port of Yokohama in Japan, because of the occurrence of the cases of COVID-19 on board. Medical tests performed on 3711 people on board (passengers and crew) confirmed 712 cases of contagion.

Passenger companies around the world immediately and carefully monitored the situation, reporting suspicious cases and trying to isolate them, as far as allowed by the on-board logistic accommodations. As a consequence of the new emergence cases, all the shipping companies have immobilized their ships and suspended the cruises already scheduled. At the end of April 2020, Fig.1 an examination of www.marinetraffic.com showed dozens of passenger units, anchored off the coast of Florida, waiting for the emergency to end. It is estimated that more than 80,000 people, members of the parked ships crews, were blocked on board, awaiting new provisions, to ensure the necessary minimum and safe operations of the stationed units.

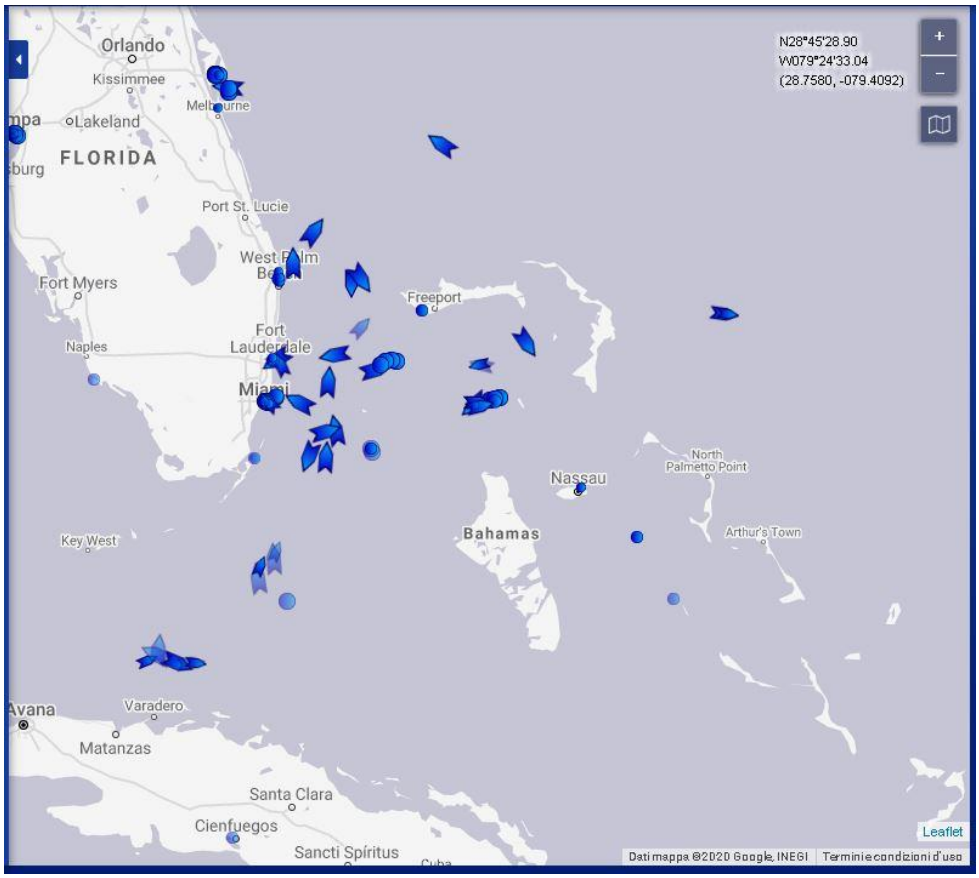

Fig.1: www.marinetraffic.com image

At the same time the shipping companies, organized the returns home for the infected crew and passengers, simultaneously adopting preventive measures on board such as carrying out tests to verify the positivity to the virus and isolation, in order to organize the returns in the safest possible way.

Following the facts happened, the world scientific community underlined the importance to adopting preventive measures in order to, in the event of future contagious diseases within a community, to be able to prevent a rapid growth of the infections as quickly as possible. Surely these recommendations will have an impact on the design of existing passenger ships and new constructions. Some of these measures have been adopted already in summer 2020, during the first attempts to restart the cruise activities. These measures can be summarized as:

- Preventive hygiene measures: adoption of devices to maintain correct and easy personal hygiene (for example: hand sanitizer gel dispensers).
- Social distancing measures: based on the study of the disposition of people within common spaces, in order either to limit or to prevent the spread of contagion by air.
- Isolation of suspected cases. Isolation of anyone with suspicious symptoms, in order to avoid transmissions of the infection.

These are the fundamental measures. Obviously in a particular environment such as a passenger ship it is necessary to adopt an extremely interactive approach among the elements of design, social engineering, engineering, marketing, to make these measures economically sustainable by the cruise operators and psychologically acceptable by passengers.

3. Analysis of the State of the Art

Today the distribution of spaces in a state-of-the-art cruise ship today involves the division of areas according to the different criteria of use and safety. As far as use is concerned, the main subdivision consists in the separation of the areas dedicated to the crew, compared to those of the passengers. But this separation is functional to the needs of exercise and is not the result of a specific analysis of containment of infectious diseases, *Zignego (2009)*.

Naval architecture mainly deals with the maintenance of safety factors, aimed at safeguarding both the ship and its occupants mainly in the event of accidents such as a breach in the hull or a fire on board. It is common knowledge that the main reference standards for this aim are: the rules issued by the IMO, (International Maritime Organization, UN body), the requirements of the SOLAS Convention (Safety Of Life At Sea), the requests of the Classification Registers (LR, RINA, ABS, DV, etc) which have the classification of the ship, the requests of the Flag Administration, that is, of the nation in the Registers of which the ship is registered and the prescriptions that the insurances recommend to every shipowner, builder or designer to be scrupulously followed as for the construction and operation of passenger ships.

Both in the case of a leak and a fire, there are specific compartments capable of limiting the loading of the water, rather than the spread of the fire on board, in order to guarantee the protection of the ship and passengers possibly avoiding the evacuation (a ship evacuation is supposed to occur in a short time from the occurrence of the accident such as leak or fire. Therefore, the ship's project, from the point of view of naval architecture, provides for the interactivity between the need to meet the requirements listed above and the needs of interior design and functionality of the same. So the interior spaces of the ship are designed through a process of comparison with the positions of the watertight bulkheads, with the structural needs to create large spaces such as cinemas and theaters, with the needs of the onboard systems such as air conditioning, water, lighting, etc.

Nowadays, however, there are no plans regarding to the presence of infectious diseases on board the ship, because in modern times the history of navigation has never recorded any significant phenomenon of this kind to justify the study of the resolving protocol dedicated for this purpose, both

on a logistic way and on the infrastructures prepared on board.

Without a procedure prepared for the purpose, or a structural predisposition of the ship to be able to stem the phenomenon emergencies have happened with the pandemic COVID-19, that the chronicles have highlighted starting from the best known case of the DIAMOND PRINCESS in Yokohama, followed by many other cases recorded on numerous cruise ships, in Southeast Asia, as in the Caribbean or Mediterranean.

Economically, this technical unpreparedness leads to a very negative return, both on the managerial level of the current tourist season and on the image of the entire cruise sector with respect to the potential of future seasons, if functional preventing solutions were not foreseen and implemented. to promptly stem the contamination of the disease and to effectively treat those people who have tested positive for the infection.

3.2. Critical Points related to the Current Configuration of Cruise Ships

Preventing contagion, curbing contagion, managing emergencies: these are the absolute three priorities to be observed and implemented with determination in the future management of cruises in order to recover credibility on the market and demonstrate the reliability of cruises, compared to any other kinds of holidays on the mainland.

Furthermore, these three priorities are those that have been applied in the case of “Diamond Princess”, but clashing with the lack of original predisposition of the unit: such as, for instance, the limited sectioning capacity of the ventilation and air conditioning system and, also, the lack of adequate spaces to be used for the hospitality of those passengers infected or suspected of being infected, certainly facilitating the spreading of the infection.

We will, therefore, examine the consequences of this situation, also evaluating the possible consequences on the cruise market, if the design of the ships is not changed.

It is natural to imagine that, after what we had to witness for cruise ships in the current year, it is natural to imagine that public opinion has been led to negatively evaluate this kind of holiday by imagining the consequences of quarantine and health risks which have characterized the contamination of the disease on board a microcosm, such as a passenger ship, in a more dangerous way. The idea of being obliged to sail as outcasts, without being able to find a safe landing place and a port to land and return home in case of contagion, is the aspect that, above all, can frighten the passengers and make them move away from that kind of holiday.

It is therefore imperative to find effective solutions to be adopted in a very short time, either on the operative units which already sail the sea and must foresee future seasons of operation possible with some retrofit intervention, or on the units that will be designed and built from here on and who, benefiting from this experience, will be able to implement a whole series of measures designed to minimize the effects of disease contagion, just as there are measures to minimize leaks or fires.

These solutions will require further increase in interactivity among various elements of engineering, architecture and medicine.

We have therefore decided to expose the various solutions, which can be adopted by examining, in succession, two distinct scenarios: the adoption of measures that fall into a "retrofitting" situation, i.e. capable of integrating with the current arrangement of existing passenger ships with low impact modifications and subsequently a re-designing measure to consider the possibility of an infection occurring on board and the need to have a ship with an interior design allowing a more incisive intervention from a medical point of view.

4. Possible Containment Interventions

4.1. Contact Prevention

In this section, our aim is to group together all the fit measures to be adopted, even in the immediate future, to raise the level of safety of a cruise, trying to prevent access on board by infected and contagious passengers. Such measures can include:

- Extended installation of boarding sanitary check-up stations as a scanner-gate to detect people's temperatures. From the operational point of view, these stations must integrate the reception operations, in order to avoid unpleasant psychological repercussions.
- Extended distribution of hand sanitization devices. This distribution requires minimal changes in terms of on-board system, but also a correct integration of the interior design.
- Disposition of the use of masks and gloves for passengers during some activities that involve public gathering. This provision must be coordinated with the onboard services, and adequately supported at the marketing level, to be accepted with the least possible impact.
- Distribution of health masks to passengers. These masks must be studied through a synergy with marketing, in order to contain elements that can guarantee a low psychological impact, for example cheerful motifs, labeling and so on.
- Distribution of hygienic gloves for passengers (Every day always changed in the cabin).
- Provision of medical masks and gloves for the crew to be worn according to their jobs.

The adoption of the above-described measures would have a limited impact from the plant engineering and logistical point of view on board, but could significantly contribute to limit the risk of disease transmissions. These measures could be adopted immediately. Many of them, such as the adoption of masks for the crew, would be always adopted regardless of the emergency examined by this paper. Subsequently, to further increase the level of safety, the following measures could be adopted, even if with new planning of the logistics of the onboard spaces:

- Study of the distribution of restaurant spaces and management of meals by four turns.
- Study of the distribution of sun and swimming pool spaces, assigned on the basis of a turn schedule.

4.2. Measures to Stem Infection

In this chapter, we will examine the possibility in which, in spite of the preventive measures, the presence of infection on board the vessel is nevertheless verified. The examined case of the DIAMOND PRINCESS is emblematic: as was initially explained, cruise ships adopt centralized ventilation systems, that is the air treatment is not carried out by many machines each of them serving either a cabin or, in any case, a limited group of cabins, but by a main machine with subsections, however dedicated to a large number of users.

As per legislation, there are subdivision devices, which are mainly dedicated to the maintenance of the Main Vertical Zones, that is, of vertical development areas dedicated to the containment of fires, possibly adopting bulkheads or subdivisions, at transversal level, to prevent a fire or fumes propagating longitudinally along the ship. In the event of contagion, however, it is necessary to stem the phenomenon by circumscribing it in an area on board in order to separate the outbreak of infections from the uncontaminated environments, *Hoffman et al. (2004), NN (2008)*. In this sense, the timeliness of the intervention represents a determining circumstance for the success of the operation. On board of current passenger ships, there is an area intended for “hospital” use, but, as shown in Fig.2, this area has a rather limited extension. In addition, the medical and paramedical staff on board is limited to a few units for thousands of passengers on board: therefore, it would be appropriate to provide to increase such staff.

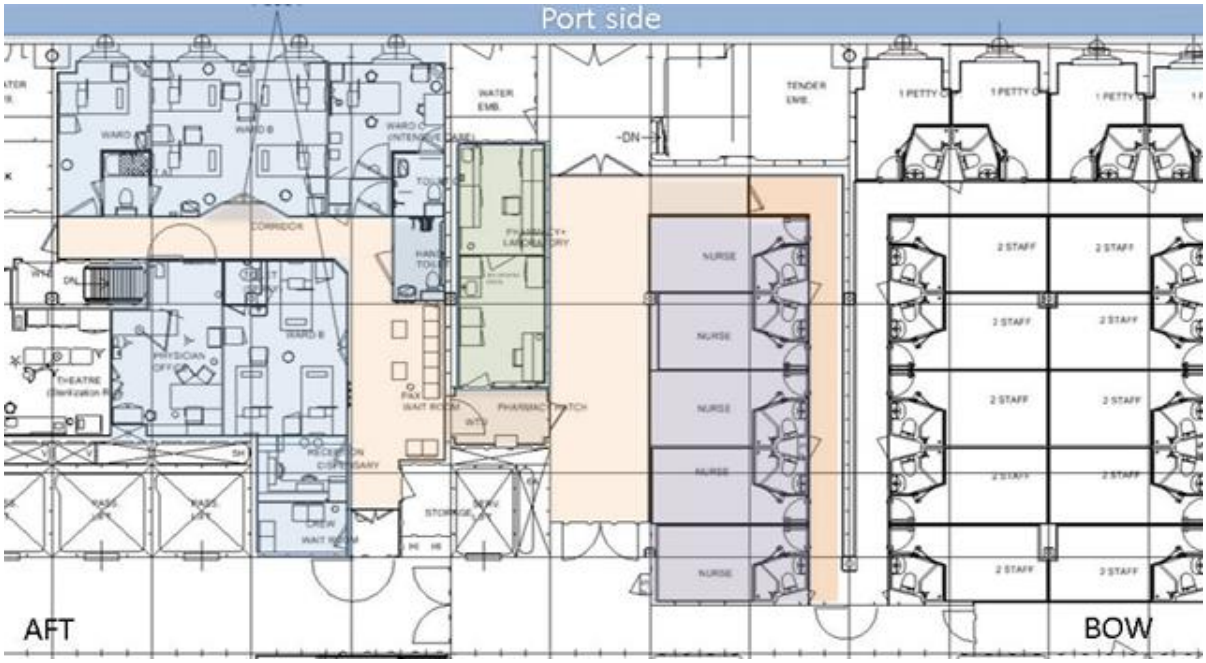

Fig.2: Hospital area, modern passenger ship

So, in order to contain a suspected contagion, it would be necessary to set up on board a delimitation area for the suspected cases and possibly to get a partition of the areas:

- Distribution of remote-control devices for the health of passengers (electronic bracelets) and provision of an on-board network for tele-control of movements. From the design point of view, the definition of this containment area is the aspect of very important interest because, in this way, this area should offer the possibility.
- To circumscribe and isolate this area through filter zones, beyond which to be able to host the full-blown cases. These areas must comfortably have all the on-board services to carry out the daily activities, such as a canteen and an entertainment service (reading, television, video communication, etc.).

For the whole ship, but in particular for the contagion treatment areas, interventions must be studied and implemented on the treatment of the air conditioning system of indoor spaces (such as public and cabins) fit to create contagious pressurized environments, discharging the stale air into the external environment only after an adequate sanitation and purification treatment. Supply the ship with equipment fit for the specialization of contagion areas such as (for instance) medical clothing and specific defence equipment for the employed sanitary and paramedical staff. The particular characteristics of this area will be examined below as a "Case study" with a more detailed analysis of the necessary design interventions.

5. New Design for Emergency Management

The possible cases of medical emergency that might occur on board are numerous, and variable according to the triggering cause: viral, bacterial, etc. We decided to take inspiration from the situation generated by COVID-19 and to create a type of "case study" on an existing and recently built cruise ship, to evaluate the possible countermeasures. The starting point was the propagation of COVID-19 on board the Diamond Princess, involving a large number of subjects and the relative impossibility to achieve an effective separation among the infected people and the rest of the present staff, while the epidemic progressed. This aspect largely reflects the medical knowledge of the state of the art. The COVID-19 case requires the isolation and treatment of the patients with anti-inflammatory and antiviral drugs, according to current acknowledges and to the experience and sensitivity of the medical staff.

In the most serious cases forced ventilation has proved essential to allow the patient in intensive care to be able to overcome the criticality of the disease and find the minimum survival conditions independently from machine assistance. It could also reasonably be expected to equip large cruise ships with ventilation devices for assisted breathing in an adequate number to deal with a contained and controlled emergency. Even imagining having 30 units (0.5% of people on board) this could represent a reasonable solution for the COVID-19 emergency, but it does not guarantee us in front of a different form of infection, such as another type of disease, which perhaps triggers the symptoms on the biliary tract and therefore requires other intensive treatments, such as dialysis. For this reason, a greater on-board equipment of pulmonary ventilation machines is an appropriate condition, but not sufficient to counteract any case of infectious disease present on board.

Specifically also for breathing devices, the high oxygen consumption required by these therapies should be taken into account, with the consequent need to store large quantities of medical oxygen on board. This solution, even assuming to adopt on-board oxygen production systems, *WHO (2020), Giddey et al. (2010),* would not be easy to implement. While therefore thinking of increasing towards an "adequate" number of equipment for clinical equipment, for the staff trained for this purpose and for hospital beds, while dedicating a part of the ship capable of being easily converted into a hospital containment lazar The infection, the essential conditions for expecting a reasonable success of the epidemic emergency management firm, remain linked to the timeliness of prevention and containment actions.

However, it would be possible to hypothesize an intervention on the current type of interior distribution, in order to hypothesize not the creation of real hospital areas, but of areas of normal use that could offer a valid contrast to the spread of diseases with contagion by air. The concept design on which we worked is to prepare part of the ship's accommodation, perhaps intended for the staff, with characteristics that can be quickly transformed into a "Quarantine Zone".

6. Case Study of the Recommendations and Solutions

The "Case study" under consideration is a large cruise ship and the possible transformations to be adopted. The large cruise ships currently in service offer hospitality for about 5000 people including on-board staff (1500) and passengers (3500), hosted on about 17 decks, Fig.3.

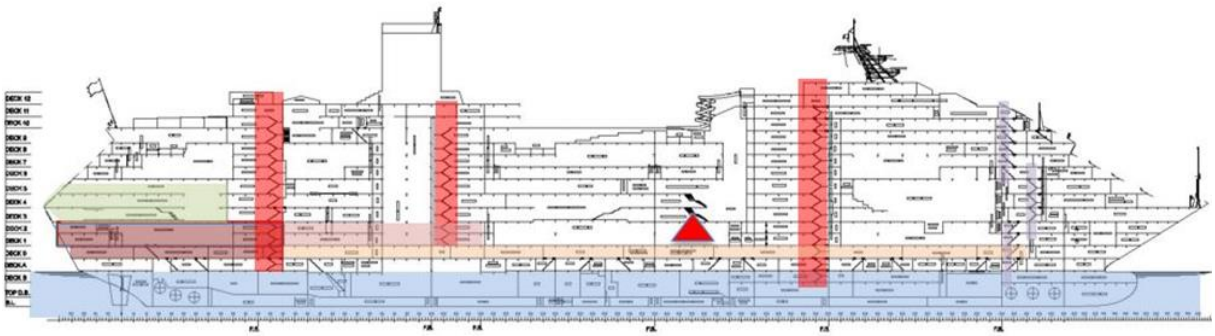

Fig.3: Typical vertical section in dark red the area modified, see Fig.7

Passenger boarding generally takes place at the center of the ship on the fifth level above the compartments (Deck 3) in correspondence with the launch of the live-saving appliances, Figs.3-6. That of the crew takes place on deck 0, three levels below the launch of the launches (see below). The entrance to the ship's main foyer is located between the ship's center and the first third from the bow. The foyer is an environment developed in height for three-four levels and on it converge the main lift columns (about 10) that connect the level to the two lower decks and the remaining bridges up to the top of the ship. On the same bridge of the foyer there are: towards the bow the theater (elevated on three levels) which can be accessed through galleries of shops, while, towards the stern you enter the first of the restaurant rooms, followed by the kitchen (in some cases full width) and then to a second

aft room, articulated on two levels, which is accessed from the upper deck, which connects the entire length of the ship. On this level, in addition to the mezzanines of all the aforementioned rooms (in the center of the ship's body), long closed walks extend sideways alongside the lifeboats and put all the ship's vertical connections in direct communication.

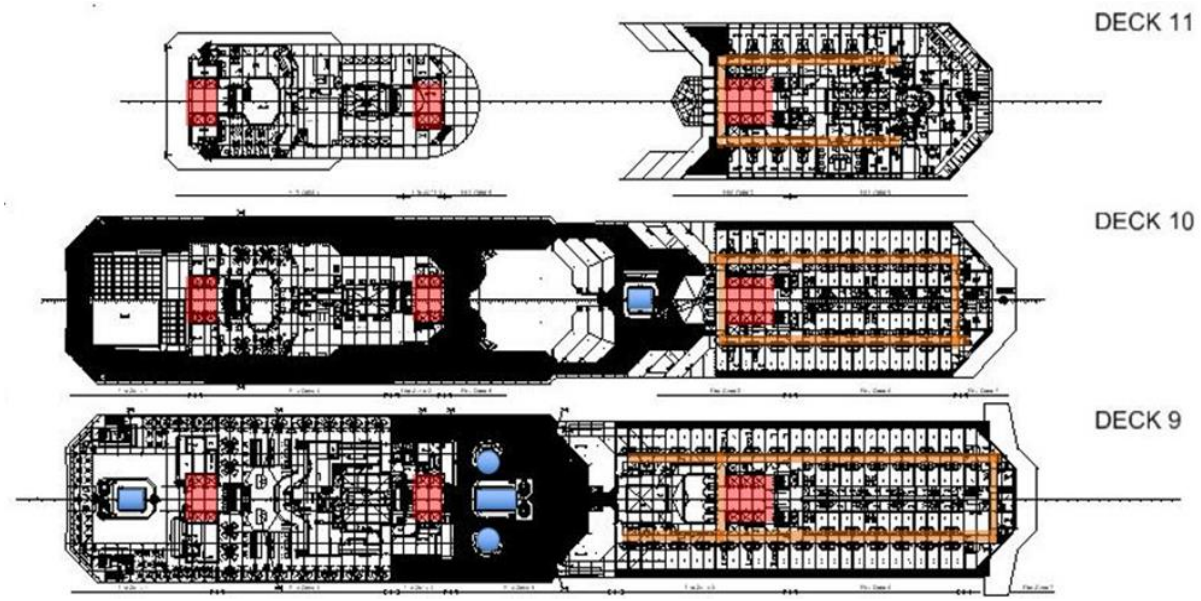

Fig.4: Deck 9 to 11

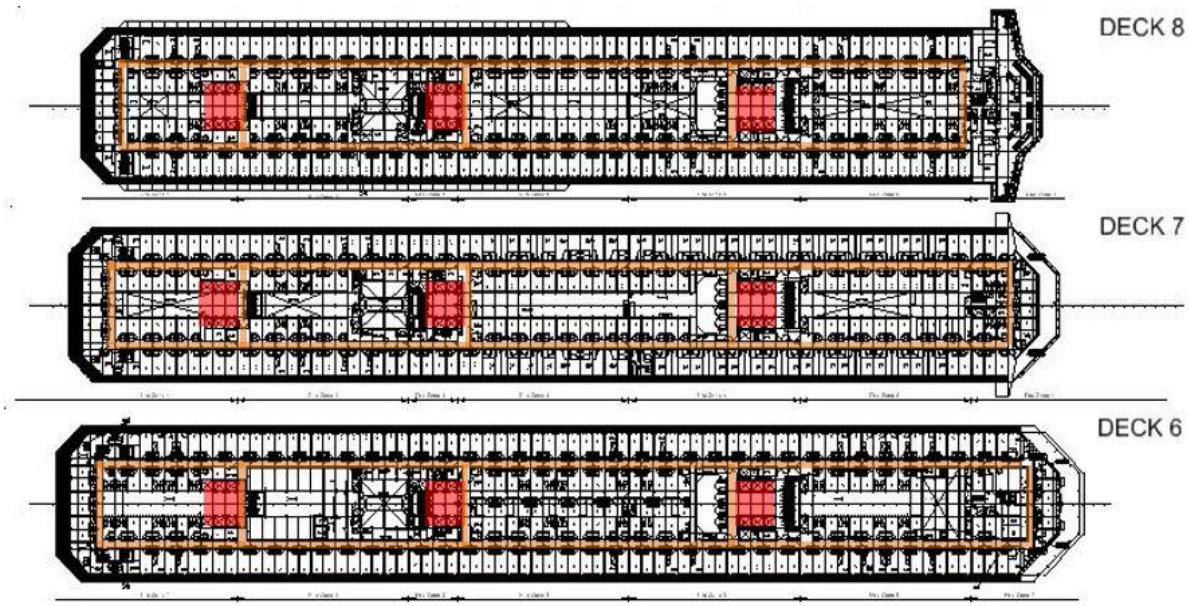

Fig.5: Deck 6 to 8

From deck 6 to deck 11 there are the most valuable passenger accommodations, Figs.4 and 5. The main swimming pool is located in the center of deck 9, while the secondary one is developed in the stern area. Between the two pools there is an open bar with a hot table which serves informal meals at any time of the day (and night). From deck 9 to climb, the cabins are present only in the forward area of the ship. The main galley of the ship is located on deck 3. It is connected to the galley on deck 9 through a dedicated series of lifts and elevators articulated around the fumes discharges also coming from the engine room. This stern column is very important from a technical point of view because it brings together both the vertical connection of passengers with stairs and 4 to 6 lifts, and the technical connection of the crew hoists that also link the distribution of on-board supplies. The main crew bridge is Bridge 0. This bridge is very important because it represents the nerve center of the ship. All

technical connections and crew routes go through this level. Its wide corridor represents a real highway on board (or if we want the subway connecting the whole ship).

On board 0 there is also the on-board hospital, Fig.2. Currently this area is capable of hosting about ten patients and gravitating between two and three medical officers and three to six nurses. Normally this capacity is adequate to cope with current healthcare, but completely inadequate compared to a viral emergency such as that of COVID-19. Going into the merits of the discussion, considering inadequate a transformation of the entire ship into a floating hospital, to keep the ship's body as functional as possible to carry out the cruise activities, it is necessary to think of flexible solutions that can be quickly implemented in case of emergency without upsetting the main board structure.

Referring to the naval tradition, in emergency conditions the ship tends to position itself always and in any case with the bow in the wind, perhaps held back by anchors, if it is unable to moor in a port. If in the worst-case scenario, a partial (or total) electrical black-out were also detected, the ventilation of all the rooms would still follow the direction of the wind. In this way it is reasonable to think that the stale air on board would tend to be discharged outboard from the stern.

For this simple reason, the ancient passenger ships had called lazaretto precisely that last leeward district from which the poisons of the on-board contamination could not go up the wind, plaguing the rest of the ship. Even the modern distribution of the cruise ship could help us if we thought of dedicating the stern area of the ship to a possible hospital, where to obtain accommodation and public spaces sufficient to accommodate 10% of the people on board resulting contaminated, making the remaining 90 % can be safeguarded from infection.

It would be a matter of working on the lodgings on the levels corresponding to the fire-zones 1, 2 and 3 of Bridges 1 and 2 obtaining about 150 beds, Fig.6.

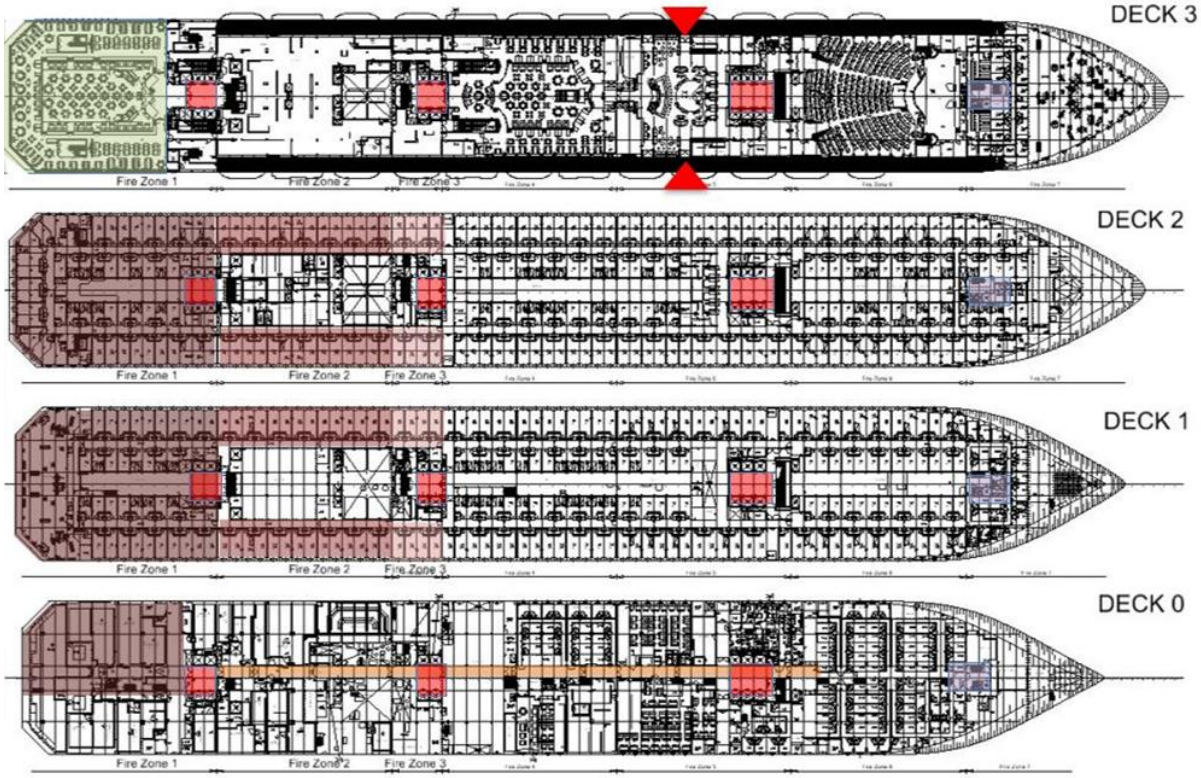

Fig.6: Areas that could be modified with separate systems

Extending the hospitality of the contaminated to fire-zone 4 could also increase the hospitality of another 100 people, bringing the capacity to 250 patients. The entire stern restaurant on both levels could be dedicated to them, having to consider that this environment would have the function of a

canteen and a living room in emergency.

The use of a subdivision based on the already existing Fire Main Zones is dictated by a convenience from an engineering point of view: as already explained the Main Vertical Zones are ship subdivisions adopted to contain a possible fire that may occur on board. The spread of fires involves the containment of flames but also of the fumes that have developed, therefore the Vertical Zones already provide structural and plant engineering sections for suspended ceilings, ventilation ducts, etc. in order to prevent the propagation of toxic fumes.

Obviously, these separations do not have the required sanitary characteristics, but from the point of view of feasibility, there would still be a great advantage in exploiting this predisposition. It is more difficult to grant patients an open space, if not the cockpit of the stern maneuver which, when the ship is sailing or at anchor, is normally unused on the technical front. These spaces could (with reasonable ease) be refitted with devices, furnishing materials and adduction filters to make them easily operational for an emergency transformation. At this point, in parallel with the compartmentalization interventions, special procedures for the management of on-board accommodation must be studied.

In the event of an emergency, sick passengers are already isolated in their cabins with pressurized pneumatic diving suits. A turn-over is imperatively ordered with passengers in the areas set up for reception in isolation. Once the passenger cabins found sick are sanitized with specially implemented room sanitation procedures, decks 1 and 2 can be freed for the fire-zones (previously illustrated). These will be extended based on the extent of the infection in order to create the hospital area (off-limit) for passengers and uninfected staff.

Regarding the compartmentalization of the new ships (or the more structural refitting of the existing ones) it would certainly be useful to maintain the location of the hospital area at Bridge 0, but it will be appropriate to also include the inclusion of an intensive care unit, imagining the arrangement in proximity of fire zones 1, 2 and 3, moving it aft from the current location, which instead is part of the fire zone 5.

7. Conclusions

Our conclusions demonstrate the possibility, in the current state of the art, of modifying the design of passenger ships, significantly raising the level of health safety in the event of contagious diseases, through the implementation of structured interventions on 2 levels. The first level, that can be already applied in the present situation to restart the cruise market, provides adoption of preventive measures, with low environmental impact on the ship, and immediate installation, to remedy the foreseeable need to reassure passengers immediately.

The second level is more invasive but with more time lasting effects, and provides for the adoption of a design intervention, redefining the distribution of on-board spaces, with an impact on the on-board systems that is certainly significant, but technically sustainable, which allows to significantly increase the degree of safety, creating an impact that would affect however, a percentage of passengers varying between 5% and 10%, therefore economically and marketing sustainable by the shipping companies. Currently, the cruise industry is trying to restart, and it should not be forgotten that the order portfolio of cruise ships, for the next 10 years, involves the construction of dozens of units.

The timely adoption of changes, on the basis of what is proposed, could allow saving both existing units or those in the completion phase, and those still in the project, with changes that could be studied in an interactive way with sectors of medicine and engineering as scientific studies progress.

Adopting these modifications (both for retro-fitting and newbuildings) would constitute a valuable reference flag for the shipbuilding companies for the quality of the ship: an essential condition to be advertised on the market to obtain the relaunch of the cruise offered, with the guarantee of health safety requirements that are decidedly higher and more reliable than what has happened so far.

References

CARTER, D.; MOIZER, J.D. (2011), *Simulating the impact of policy on patrol policing: introducing the emergency service incident model*, Syst. Dyn. Rev. 27, pp.331-357

COHEN, C.I.; SOKOLVSKY, J. (1980), *Social Engagement Versus Isolation: The Case of the Aged in SRO Hotels*, Gerontologist 20, pp.36-44

GIDDEY, S.; CIACCHI, F.T.; BADWAL, S.P.S. (2010), *High purity oxygen production with a polymer electrolyte membrane electrolyser*, J. Membr. Sci.

HAMEED, J.M.; McCAFFREY, R.L.; McCOY, A.; BRANNOCK, T.; MARTIN, G.J.; SCOUTEN, W.T.; BROOKS, K.; PUTNAM, S.D.; RIDDLE, M.S. (2016), *Incidence, Etiology and Risk Factors for Travelers' Diarrhea during a Hospital Ship-Based Military Humanitarian Mission: Continuing Promise 2011*, PLoS One 11

HOFFMAN, P.N.; WEINBREN, M.J.; STUART, S.A. (2004), *A practical lesson in negative-pressure isolation ventilation*, J. Hospital Infection 57/4, pp.345-346

NN (2008), *Isolation Rooms & Pressurization Control*, Penn State Department of Architectural Engineering, The Pennsylvania State University

REITHERMAN, R. (1986), *How to prepare a hospital for an earthquake*, J. Emerg. Med. 4, pp.119-131

RUGGIERO, V.; GUGLIELMINO, E.; ORTECA, V.; CUCINOTTA, F. (2011), *A new idea for an Italian fast support ship for peacekeeping and assistance in case of events in enlarged Mediterranean scenario*, HSMV (High Speed Marine Vehicles) Conf., Naples, pp 1-6

VAN OMMEREN, M.; S. SAXENA, S.; SARACENO, E. (2005), *Aid after disasters*, The BMJ 330
WHO (2020), *Clinical management of severe acute respiratory infection (SARI) when COVID-19 disease is suspected: Interim guidance*, World Health Organization

YANG, L.B. (2013), *Study of Maritime Traffic Patrol and Rescue Ships Configuration Amount*, Ship Engineering

ZHAO, F.B.; WANG, Y.; XIE, X.L. (2015), *A Novel Approach of Patrol Ship Configuration and Fleet Planning*, Appl. Mech. Mater. 1761, pp.744-746

ZIGNEGO, M.I. (2009), *Cruise Vessels Design*, DOGMA, Genova

Practical Use of A.I. Technologies Applied in Ship Design & Production

Rodrigo Pérez Fernández, SENER, Madrid/Spain, rodrigo.fernandez@sener.es
Jesus A. Muñoz Herrero, SENER, Madrid/Spain, jesus.munoz@sener.es
Alicia Ramírez, SENER, Madrid/Spain, alicia.ramirez@sener.es

Abstract

Artificial Intelligence (A.I.) could be applied in ship design and ship production in many aspects. The management and access to all the information necessary for the correct and efficient execution of a ship project is one of the aspects where A.I. could have a strong impact in access all the rules, design guides, best practices, lessons learnt, etc., in a fast and intelligent way. A.I. is one of the enabling technologies of digital transformation that probably has the greatest potential among those that make up the fourth industrial revolution. Knowing their characteristics and possibilities, is essential to identify their application to certain processes and products, especially industrial ones and very particularly those related to the marine sector. It is important to identify the value that A.I. could provide to this transformation by identifying the use cases where it could be applied. The use of A.I. in industrial environments, such as the naval one, is just beginning. There is still a long way to go in the field of design, optimization of projects, maintenance of data and results. Fields such as the recognition of images, for their conversion into models; the automatic intervention in the validation of the requirements; or the optimal exploitation of the processes inherent to naval engineering, are still practically unexplored. A.I. is present in our day life and its presence will be growing for years to come. It is necessary to have a correct knowledge about what actually is A.I and what are the capabilities that could offers to business, processes and normal life. We will even see A.I. applications that we would not have ever imagined before. Once it is understood what A.I. is, the key is to find the way this could be applied to different aspects of our life and what is the benefit given by it. But ant the end, we will continue to need intelligent people, people who are smart and have critical thinking, because the essence of the human being could never be embedded in artificial intelligence.

1. Introduction

Gartner, Fig.1, on the most strategic trends in technology included Artificial Intelligence (A.I.) technologies in the first three positions: Applied A.I., Intelligent apps, and Smart things, https://www.gartner.com/smarterwithgartner/gartners-top-10-technology-trends-2017/.

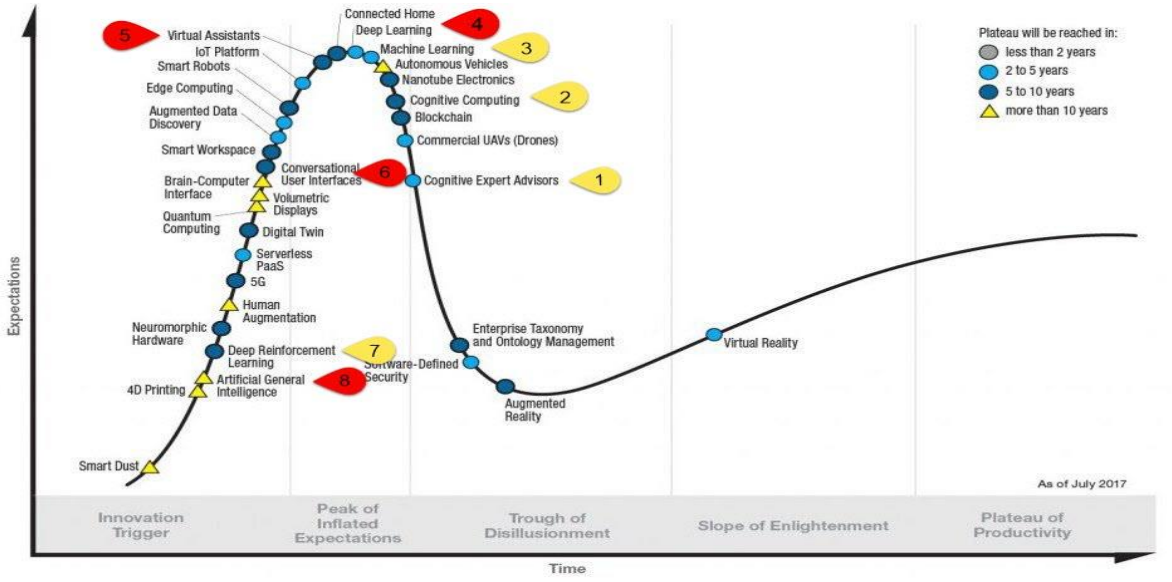

Fig.1: Gartner Hype Cycle 2017, https://www.gartner.com/smarterwithgartner/top-trends-in-the-gartner-hype-cycle-for-emerging-technologies-2017/

A hasty analysis indicates that their position in the intended cycle of expected maturity suggested that they would reach maturity in an interval of 5-10 years, in order to be exploited effectively.

Three years later, the hype cycle shows a specialization of A.I. in subsets of itself, Fig.2. One wonders what happened to those A.I.-related technologies that seemed to be reaching maturity in 2017 and have now banished. The reality is A.I. is specializing and evolving accordingly to the applications of this technology in real use cases. Furthermore, the algorithms related with M.L. are being grouped into complexity areas with different levels of maturity and in this way, there are several trends of this technology under observation:

- Explainable A.I.
- Embedded A.I.
- Responsible A.I.
- Generative A.I.
- Composite A.I.
- Adaptive M.L.
- Others related….

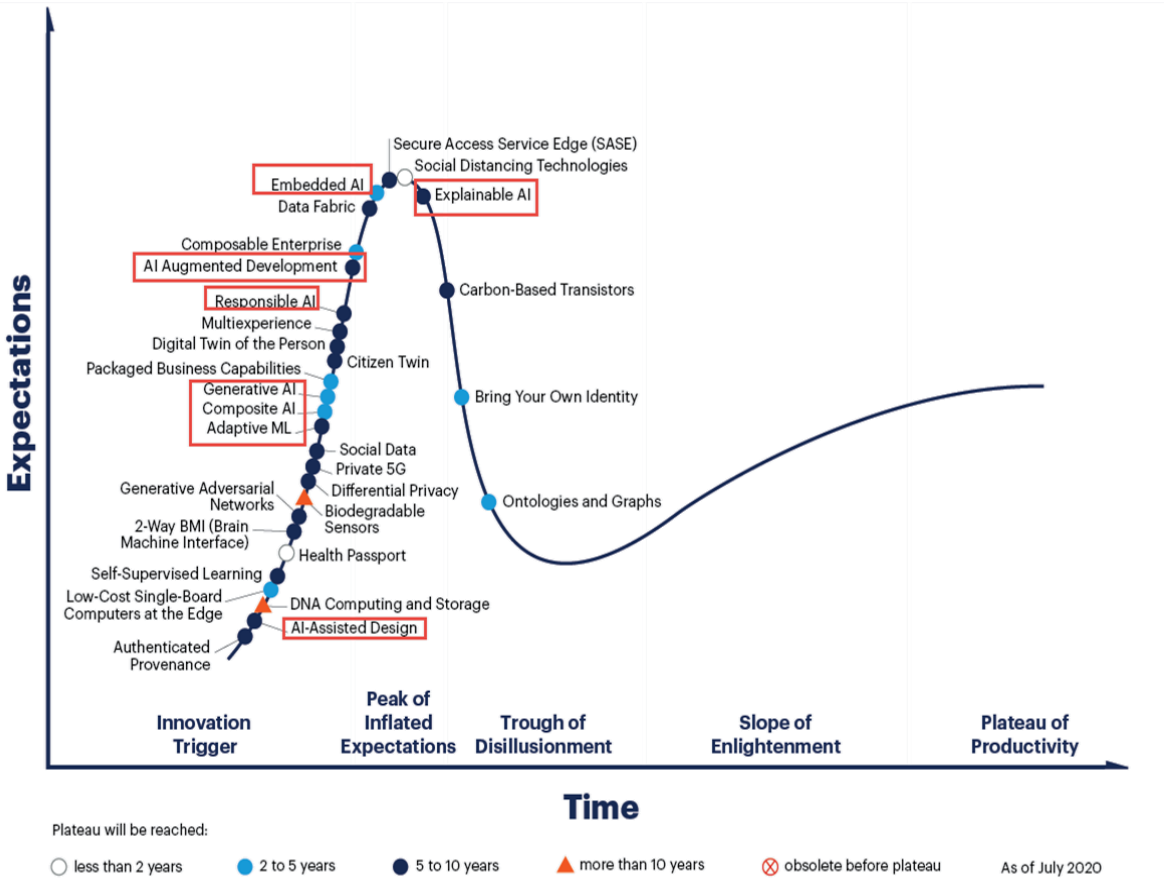

Fig.2: Gartner Hype Cycle for emerging technologies 2020, https://www.gartner.com/smarterwithgartner/5-trends-drive-the-gartner-hype-cycle-for-emerging-technologies-2020/

Leaving aside the criticisms that could be made to the loop of Gartner technologies (Gartner Hype Cycle) as explained in Michael Mullany´s blog and the suspicions that may appear after reading the aforementioned article; it seems sensible to think that A.I. -related technologies are going to continue having a strong impact on our lives. This is something that we have already seen. Let us not forget the

situation arising from the pandemic produced by COVID-19. A.I. technologies are being used for predicting its evolution and in the vaccines development cycle or helping to decide political decisions that could be made in the different aspects of our current lives.
There is no doubt that technological evolution is approaching a future that a few years ago was only on out imagination and in fictional movies. The concept of A.I. opens up a wide field subject of hours of study. The following, aims to make an analysis of what these technologies are, how they are influencing society, how they will influence it in the future and what could be done now to obtain a value from them, by seeking their application to the shipbuilding sector and more specifically to naval design. In any case, for finding practical and real use cases, it is essential to understand well what A.I. is and what are its foundations.

2. Background

It is clear that there is not a unique origin to the concept known as A.I., and therefore there is no consensus on how to define this concept. Nevertheless, in order to understand any of the definitions that apply, it is convenient to know, at least briefly, the most important facts and some of the milestones in its history.

It could be considered that A.I. was born as a philosophical study on human intelligence supported by man´s concern to imitate the behaviour of other beings with capacities beyond the reach of humans (such as flying or diving), reaching the point of trying to imitate Likewise. In this sense, we could say that A.I. is the search to imitate human intelligence. It is clear that it has not yet been fully achieved, but it is also true that we are increasingly closer.

2.1. A little of history

The first man who became aware of his own existence and that he was capable of thinking, surely wondered how his thinking would work and would conclude the idea of "superior creator", an intelligent being capable of creating another. In this sense, the idea of a virtual design for intelligence is as remote as human thought. In 1920, the Czech writer Karel Čapek published a science fiction play called "Rossum's Universal Robots". It is about a company that builds organic artificial humans in order to lighten the workload of other people. Although in the play these artificial men are called robots, they are more similar to the modern concept of android or clone. These are creatures that look like humans and have the ability of thinking, *Capek (2017)*. In 1950, the English mathematician Alan Turing published an article entitled "Computing Machinery and Intelligence" which opens the doors to AI. The article itself began with the simple question: "Can machines think?", *Turing (1950)*. Later Turing proposed a method to evaluate whether machines could think, which became known as the Turing test. This test, or "Imitation Game", as it was called in the paper, was presented as a simple test that could be used to judge whether machines could think.

In 1956 the Dartmouth conference called by McCarthy was held and in which the term "Artificial Intelligence" was born. Researchers from Carnegie Mellon University and IBM attended the conference, among others: Minsky, Newell and Simon. At this conference, ten-year predictions were made, but unfortunately never fulfilled. It occurred an almost total abandonment of investigations for fifteen years on this topic, giving rise to what is now known as "the winter of Artificial Intelligence", https://www.kdnuggets.com/2018/02/birth-ai-first-hype-cycle.html. In the late 1970s, A.I. re-emerged with the appearance of "expert systems". These programs answer questions and solve problems in a specific domain. They emulate an expert in a specific branch and are capable of solving problems by rules. There are two types of knowledge engines in expert systems. Firstly, there is the knowledge engine, which represents facts and rules on a specific topic. Secondly, there is the inference engine, which applies the rules and facts of the knowledge engine to new facts. As an illustration of this: In 1981, an expert system called SID® (Synthesis of Integral Design) designed 93% of the logic gates of the VAX 9000® CPU. This system was build based on 1,000 hand-coded rules. The final design of the CPU took around 3 hours of calculations and outperformed human experts in many ways. As an example, the SID® produced a faster 64-bit adder than the one designed manually. The error rate of the

human experts was one error per 200 doors while that of the SID® was around one error per 20,000. However, these expert systems required high computing capacity and the rise of desktop personal computers made these expert systems lose the interest of investors, causing the downfall of companies that were dedicated to building hardware and software for these systems, leading to what is known as the second winter of A.I.

On May 11th, 1997, IBM´s Deep Blue computer defeated Gary Kasparov with three Deep Blue wins to two Kasparov wins and a draw. In 2011, IBM's Watson® system beat out two of the most successful human contestants on the long-running American game show Jeopardy, which requires participants to do a question in response to general knowledge clues. At the event, Watson® marked a breakthrough in A.I. with its understanding of natural language and the ability to make sense of a large amount of written human knowledge. In June 2018, IBM´s Watson® system participates in a debate to demonstrate the progress of the Project Debater project that IBM has been developing since 2012. In one of the debates, the IBM computer argued with Noa Ovadia, a former national debate champion from Israel. The debate was based on the following statement: "Should we subsidize space exploration?" If you are interested in finding out who won, check out some of the many references you could find on the internet, such as: "What is it like to see an IBM A.I. successfully debate with humans".

Since the beginning of the 21st century, the progress of A.I. has been unstoppable, driven by hardware improvements that make it possible to handle enormous amounts of data in ever-shorter times, as well as the efficient use of neural networks, and full connectivity of devices through high-speed internet. In this sense, what once was required a long time is now practically immediate, https://www.livescience.com/47544-history-of-a-i-artificial-intelligence-infographic.html. Fig.3 shows the vision of the history of computing from the perspective of IBM, the leading company in A.I. development with its set of solutions called Watson®. According to Juan Ramón Gutiérrez, head of industrial solutions at IBM, the evolution of A.I. could be divided into three stages, with us now entering the cognitive era.

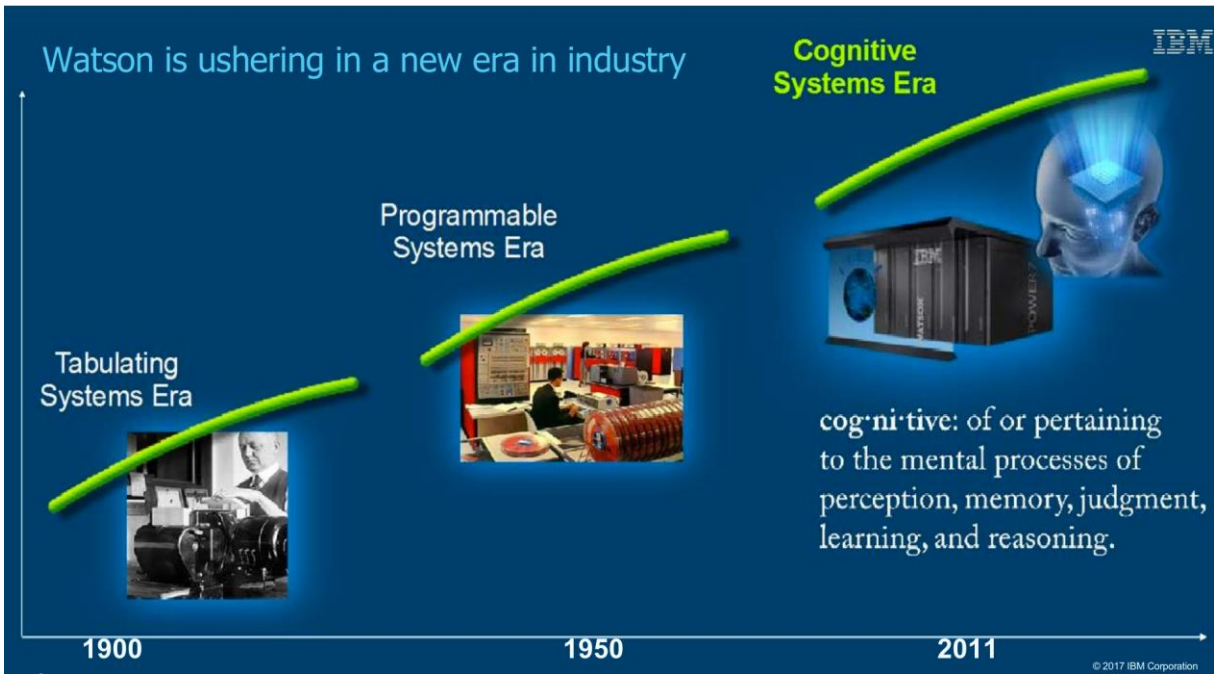

Fig.3: Stages of computer science, source: IBM

2.2. Present

In recent years, the most important companies have begun to position themselves in the use of A.I., by acquiring specialized companies, start-ups and technologies; as well as developing them, seeking applications that could add value to their investments.

It is interesting to pay attention to the acquisitions of companies, many of them start-ups, that have been taking place, in order to position themselves before this reality. Fig.4 shows the purchases of companies by large corporations that have opted for A.I. until 2017.

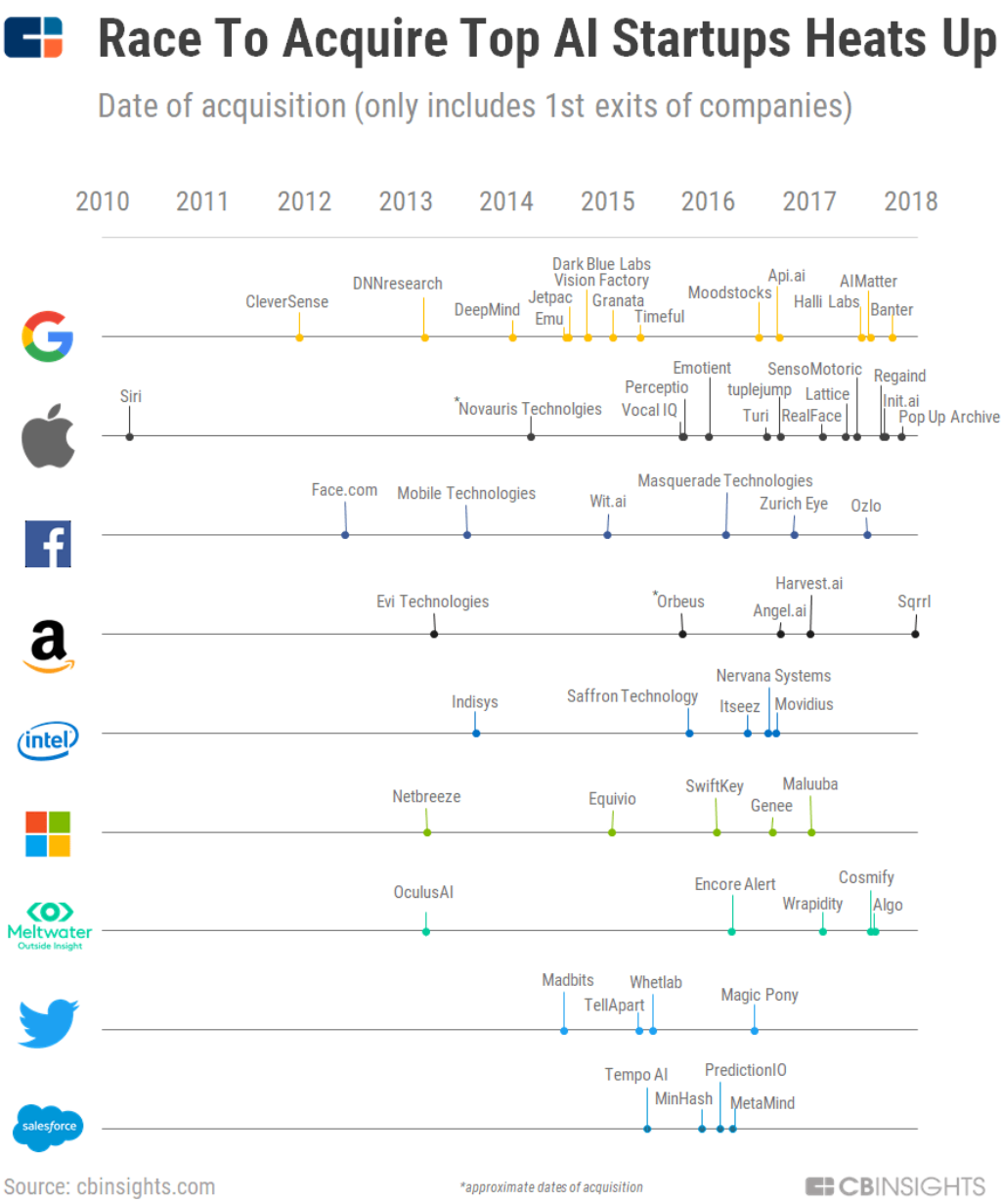

Fig.4: A.I. Start-ups acquisitions, source: CBINSIGHTS

The development is obvious. We could say there is a real race to obtain start-ups with the most potential within A.I. technologies. As stated in the CBINSIGHT report "Large corporations in all industries, from retail to agriculture, are trying to integrate Machine Learning into their products. But at the same time, there is an acute shortage of Artificial Intelligence talent", https://app.cbinsights.com/research/top-acquirers-ai-startups-ma-timeline/.

It is also significant to observe how this technology has been positioning itself: through virtual assistants. Large techno-logical companies such as Google, Apple, IBM, Facebook, Amazon or Microsoft make marketing of their assistants as a banner to attract the attention of companies and markets. Apple with Siri®, Google with Google Assistant®, Microsoft with Cortana®, Amazon with Alexa® or IBM with Watson® project, that goes far beyond what could be expected from virtual assistants.

Other well-known personalities are also gambling on the future of A.I., trying to ensure that there is a certain standardization of technologies. Elon Musk promoted a project called OpenAI, which tries to unify all A.I. developments in a single project that being free and open could overcome the restrictions of commercial products. Interesting research projects could be found under this project, but where it has found a fertile field to grow is in MOBA (Multiplayer Online Battle Arena), online games among many players who are changing the rules of leisure and even sports, https://www.esportsunlocked.com/especiales/open-ai-la-inteligencia-artificial-que-nos-daria-una-paliza-en-cualquier-moba/. In any case, it is still far from being able to make decisions in a minimum reaction time, as many of these games require in certain circumstances. It is necessary to mention that Elon Musk decided to abandon this initiative to avoid "future conflicts of interest", http://fortune.com/2018/02/21/elon-musk-leaving-board-openai/.

3. Basic Concepts

Before going further, we must establish some order on related concepts. Firstly, it is important to state that A.I. could be found on products or applications frequently but small percentages. This is simply because A.I. cannot be a solution in itself. This concept is what they refer to as general A.I., which in Gartner´s famous cycle appears far from its expected maturity (more than ten years), that is, the most immature of all. To such an extent, it is true that already in 1995, A.I. was already emerging as one of the strategic technological trends, but there is still progress to make. The latter has an explanation that will be discussed later.

3.1. What is Artificial Intelligence?

A.I. and Machine Learning (M.L.) have finally gone mainstream, and it is also a fact that people know very little about it. We hear about many concepts and tend to simplify and understand A.I. as an agglomeration of concepts and technologies that could mean different things to different people: virtual assistants, robots that imitate humans, M.L., self-driving cars, etc.; and its applications are everywhere. We need to identify the basic elements that constitute A.I.

What is the right definition for A.I.? As Vicenç Torra points out in one of his articles, the first definition of artificial intelligence was given in the document prepared by J. McCarthy, M. Minsky, N. Rochester and C.E. Shannon for the preparation of the meeting held in Darthmouth (United States) during the summer of 1956 and in which the term "artificial intelligence" appears for the first time. According to the author of the article, "It appears that this name was given at the urging of J. McCarthy. The proposal cited above from the meeting organized by J. McCarthy and his colleagues includes what can be considered as the first definition of artificial intelligence. The document defines the problem of artificial intelligence as that of building a machine that behaves in such a way that if the same behaviour were carried out by a human being, this would be called intelligent", *Torra (2011)*.

Nevertheless, there are other definitions not based on human behaviour:

- Act like people. This is McCarthy´s definition, where the model to follow for the evaluation of programs corresponds to human behaviour. The so-called Turing Test (1950) also uses this point of view. The Eliza system®, a conversational bot (software program) is an example of this.
- Think as people. What is important is how the reasoning is carried out and not the result of this reasoning. The proposal here is to develop systems that reason in the same way as people. Cognitive science uses this point of view.
- Reason Rationally. In this case, the definition also focuses on reasoning, but based on the premise that there is a rational way of reasoning. Logic allows the formalization of reasoning and is used for this purpose.

- Act Rationally. The objective is the results, but now evaluated objectively. For example, the objective of a program in a game like chess will be to win. To meet this objective, the way to calculate the result is irrelevant.

At this point, one might wonder in which of all the meanings the help systems available in our mobile phones fit on this definition. We could think of the famous (although a little outdated) Turing test to determine if when talking with Siri® on your mobile phone and getting a reasonable answer, you are in a position to say you are dealing with an A.I.

According to *Kirkpatrick (2018)*, A.I. is a compound that covers multiple technologies designed to provide computers with human-like capabilities on listening, vision, reasoning and learning. These techniques, Fig.5, including M.L., Deep Learning (D.L.), Computer Vision (C.V.), Natural Processing Language (N.P.L.) or Natural Language Understanding (N.L.U.), unmask hidden patterns in large data sets and later, using complex algorithms, find the similarities between apparently unrelated variables.

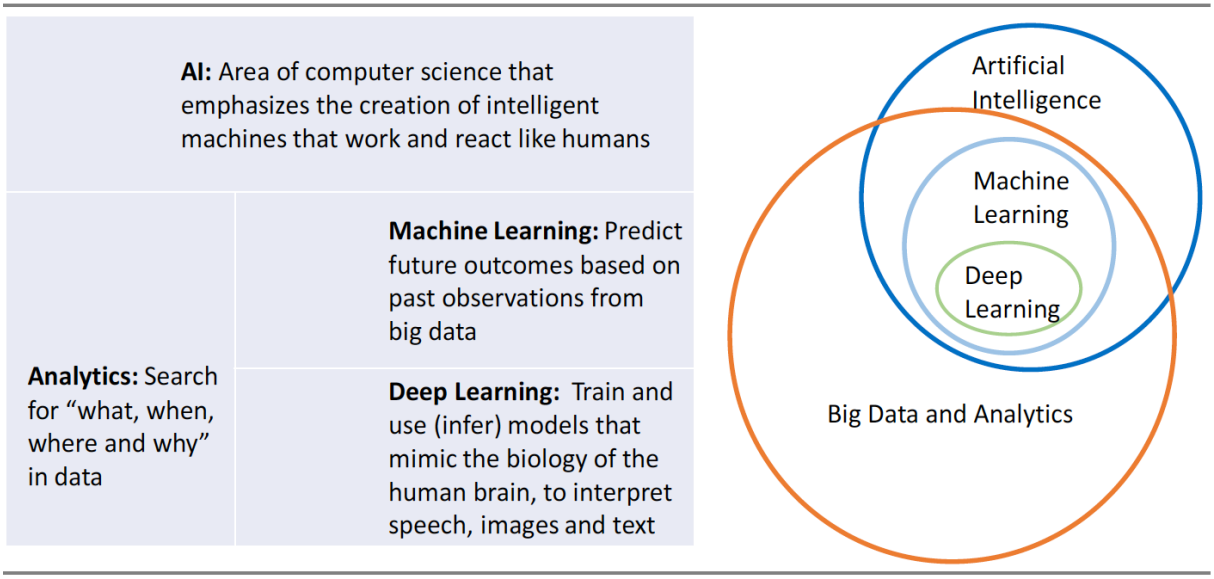

(Source: Cray, Inc.)

Fig.5: A.I. Techniques, *Kirkpatrick (2018)*

Leaving aside Big Data techniques and analytics, and focusing exclusively on A.I., three fundamental elements could be detected:

- A.I. covers everything that allows computers to behave like humans. The main techniques included are M.L., N.P.L., language synthesis, computer image recognition, robotics, sensorization and analysis of results, optimization and simulation.
- M.L. is the subset of A.I. that deals with the extraction of patterns from data sets. In this subset, we could find D.L., support vector machines, decision trees, Bayes learning, k-means clustering, association rule learning, regression algorithms, etc.
- D.L. is a specific class of M.L. algorithms that use complex neural networks. In a sense, it is a group of related techniques comparable to a group of decision trees or support vector machines. Thanks to the progress made in parallel computing, these have become accessible to common use. Its components include artificial neural networks, convolutional neural networks, recursive neural networks, long short-term memory, deep belief networks and many more.

3.2. Why is Artificial Intelligence important?

There are many reasons to underpin the importance of A.I., but to focus on something more relevant, we share the vision of DataRobot, for which "Artificial Intelligence systems are essential for companies that seek to extract value from data by automating and optimizing processes or producing actionable

insights. Artificial Intelligence systems powered by Machine Learning allow companies to leverage their vast amounts of available data to uncover insights and patterns that would be impossible for one person to unravel, enabling them to deliver more specific and personalized communications, predict critical care events, identify probable fraudulent transactions, and more", https://www.datarobot.com/wiki/artificial-intelligence/.

Companies that do not embrace A.I. and M.L. technologies are bound to be left behind:

- Global spending on A.I. will grow by 50% compounded annually and will reach 50 billion euros by 2021.
- Industries such as retail, marketing, healthcare, finance, insurance and others will not only benefit from A.I. and M.L., but those that do not adopt it will disappear.
- Starting in 2020, companies that bet on data management within A.I. will get 1.2 trillion dollars a year from those that do not do so because they do not have the same vision.
- 83% of early adopters are already gaining value from A.I. and M.L. initiatives.
- The net gain in jobs resulting from the adoption of A.I. will be above 5 million.

These facts are overwhelming. As it is remarked by *McAffe and Brinjolfsson (2017)* "The effects of Artificial Intelligence. will expand over the next decade as manufacturing, retail, transportation, finance, healthcare, advertising, insurance, entertainment, education, and virtually every other industry will transform your core processes and business models to leverage Machine Learning".

4. Artificial Intelligence Applications

After all that has been explained in this article, you could understand how A.I. relies on three fundamental pillars: data, algorithms and computing power. This explains that the greatest development of applications is found in those sectors in which there are many data that could be analysed and the conclusions extracted serve for a specific purpose in time. In other words, that the application of A.I. to data analysis provides significant value to the sector, company or individual that uses its results.

There are innumerable sectors in which the application of A.I. could be realised. Companies around the world are trying to take advantage of A.I. to optimize their processes for higher revenues and profits. What are they doing and in which sectors? It is known that some of the applications that we use every day use A.I. for their operation, such as Netflix®, Spotify® and Siri®, among others. Here are some examples to illustrate the scope that has been reached:

- Chatbots: "A computer program designed to simulate conversations with human users, especially over the Internet". These elements are applications that interact with A.I. programs and provide an almost human conversation, answering the most frequently asked questions from users. Chatbots save time and effort by automating the first line of customer service. Gartner forecasts that by 2020, more than 85% of customer interactions will be handled without a human. However, the opportunities provided by Chabot systems go beyond providing answers to customer inquiries. Chinese WeChat® bots could now schedule medical appointments, call a taxi, send money to friends, check in for a flight, and many more. They are also used for other business tasks, such as collecting information about users, helping organize meetings, and reducing overhead costs. It´s no wonder that the size of the chatbot market is growing exponentially. It is important to note that chatbots are actually the interface between A.I. and humans, that is, they are a tool used by A.I. to materialize.
- E-commerce: E-commerce programs that include A.I. tag, organize, and visually search for content, allowing shoppers to discover associated products, whether in size, colour, shape, or even brand. This technology allows companies of any size to reach an extraordinarily wide market.
- Human Resources (H.R.) Management: A.I. and M.L. is used in companies that have progressed most in human resource management through specific computer programs. The reasons why these technologies have become so widespread in this area must be sought in two aspects. First, because of the amount of data handled in human resources, and secondly, because of the need to increase

efficiency in an essential area of the company. A.I. takes care of the most labour-intensive work in H.R. (screening, paperwork, data entry, reporting, etc.), as well as offering powerful analytics tools to automatically generate high-quality data for H.R. departments.

- Medicine: A.I. programs could leverage data collected from patients to provide clinical decision support during critical medical situations, as well as document those events electronically in real time. A.I. improves the reliability, predictability, and consistency of clinical trial data and results, being a tremendous aid for decision-making.
- Communication and collaboration: A.I. allows integrating employee communication and collaboration, improving interaction with data, providing translation even in real time, improving calendar management or activating meetings by electronic means, etc.
- Energy: Interconnected power plants that obtain data on operation, consumption, climatic circumstances that influence energy needs or their generation.
- Automotive: Autonomous vehicles will use A.I. for their operation and it is something that will be seen in the medium term. However, you don´t have to wait for some capabilities, such as in-vehicle assistants that anticipate the needs of the driver and passengers, or mechanical and driving monitoring to increase safety.

These are just some of the fields of application, although there are others in which the application of A.I. is generating good results or raising enormous expectations: Intelligent cybersecurity, logistics and supplies, leisure, sports betting, etc.

4.1. Artificial Intelligence Applications on the Industry

Looking at the applications of A.I. on the industry, it is difficult to separate what is purely industrial from all other areas that help the development of industrial business. The digitization of industrial processes, robotization, improvements in data collection and analysis that allow better decisions and reduce risks, etc. All this, without a doubt, are indirect applications of A.I. in the development of the industry. However, what type of A.I. could be found in the industry? Moreover, where could we find it in the particular case of the marine industry?

In order to find a more direct application in the industry, one must focus on the phases of the life cycle of manufactured products and look for opportunities for the application of A.I. in them. If we consider that, the phases of the life cycle of a product are the following:

- Definition
- Design
- Development and production
- Operation
- Dismantlement

In all of them, applications of A.I. could be discovered.

During the definition phase, A.I. tools linked to “Big Data” and analytics allow specifying what the customer wants, help to predict market behaviour and build a strong business case. For this phase, several of those applications explained above are perfectly applicable.

The design stage, the one in our opinion that lacks the most A.I. applications with direct impact on generating value. It must be taken into account that the design phase is the one that most commits the resources necessary for the development and operation of the product. There are two points of view when it comes to seeing the possibilities of applying A.I. in the design phase: A.I. applications that help to design properly and A.I. applications that help make a good design.

If A.I. helps make a good design, it will have saved time and probably reduced errors. This means adding value to the product by reducing its cost and being able to transfer improvement to the consumer,

obtaining a more competitive product. Since at present the designs are made with Computer-Aided Design tools, known by its acronym in English, CAD, either office automation or management, such as Life Cycle Managers (PLM), and Documentaries (PDM), etc. You have to look in these tools for possible applications of A.I., and honestly, at present it is not easy to find them. As *Naoyuki et al. (2017)* suggests, "Artificial Intelligence technology applied to product design in Monozukuri (Japanese form of manufacturing) aims to provide computerized support for various tasks in product development that currently rely on human expertise". Given that this has its limitations, they propose a platform in the cloud that allows data to be collected and to manage the learning models extracted from that data in order to take advantage of them in the design of new products. In this article, they propose cases and an implementation plan. Truth be told, to date there are no results yet.

Large generalist or mechanical design CAD companies have tried to position themselves by advertising A.I. tools integrated in their CAD, such as Solidworks® which recently announced character and feature recognition capabilities, although their practical application in CAD is unknown. More interesting is the EXALEAD OnePart proposal that offers a product to recognize similarities in parts and informs the user to avoid duplication. This product is integrated with 3DEXPERIENCE®, and although the gain of reducing and simplifying a model is evident, it is a tool that works afterwards, that is, once time has been invested in designing it. The powerful Autodesk has a research project known as Dreamcatcher underway that seeks to ease the design of hundreds of alternatives that meet the designer's specifications. In their own words, "Dreamcatcher is a generative design system that allows designers to elaborate a definition of their design problem through objectives and limitations. This information is used to synthesize alternative design solutions that meet the objectives. Designers could explore the trade-offs between many alternative approaches and select design solutions for manufacturing. "This project is supported by various ideas such as the DreamSketch interface that "combines the expressive qualities of the sketch and free forms with the computational power of generative design algorithms", *Rubaiat Habib (2017)*. Finally, the interesting approach proposed by the Laboratory of Artificial Intelligence for Design (LAI4D) "LAI4D is an R&D project whose objective is to develop an Artificial Intelligence capable of understanding the user's ideas regarding spatial imagination". On their WEB page, they have a web application, Fig.6, that allows them to experience the scope they have reached.

As conclusion, there is still a wide field of improvement in the application of A.I. to the technique to make the design and the main challenge is in how to obtain value from that application.

A.I. also has as a field of application to make a good design and that goes far beyond being able to parameterize the designs, collect usage and performance data and evaluate them. This is precisely the great difficulty faced by the expansion of A.I. in this field, since there is still not enough information collected or parameterized on those designs that we want to carry out.

When it comes to development and production, there are countless existing applications. It is precisely in this area where the implementation of work methodologies that use A.I. to obtain improvements in the production process has advanced the most. The boost that governments are giving for the digital transformation of the industry through what is known as Industry 4.0 has made many initiatives materialize. However, not all initiatives are purely A.I., nor those that are, produce value to the product. There are repetitive tasks or tasks that require a certain programmable logic that could be automated through the use of A.I. applications. Industrial production could improve from the re-compilation of operating data, analysis of the results and the use of applications that, using A.I. algorithms, detect inefficiencies in the production chain. For example, evaluating defective products could reveal which specific machines produce them or whether the production design is wrong.

The great leap of A.I. in the industry has been given by the hand of what is known as the Internet of Things (IoT) or internet of things and the impulse of Industry 4.0 to improve the operation of products. All companies have launched into their products, sensors and connectivity with platforms that collect a multitude of data to draw conclusions about their operation, improve and extend their operational life. The companies that supply the products in this way sell what they call the industrial operating system.

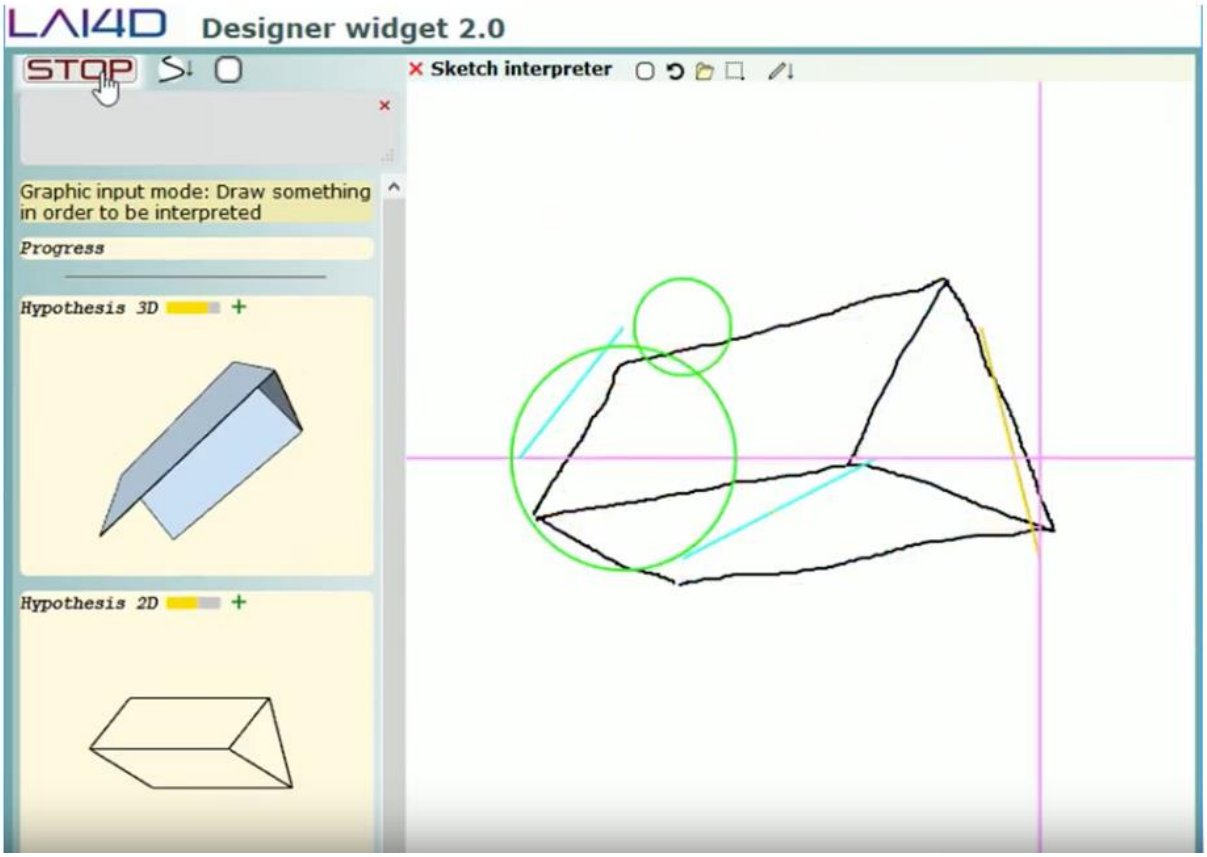

Fig.6: Sketchers analyzer, source: LAI4D

Thus, the giant Siemens offers MindSphere®, "the open and cloud-based IoT operating system from Siemens that connects its products, plants, systems and machines, allowing it to take advantage of the large amount of data generated by IoT with advanced analysis", https://www.siemens.com/global/en/home/products/software/mindsphere.html. It should be noted that 'open' does not mean that any other product could be connected to such cloud unconditionally. One of the aspects that significantly impede the progress of the extension of A.I. is the absence of open standards, which anyone could use for their products and applications. Not only Siemens offers this approach, also PTC or IBM among others have developed their connectivity and analytics platforms enhanced with A.I. applications.

We must not forget about the entire waste treatment or recycling industry, which like any other industry could make use of A.I. applications to optimize its processes.

4.2. Artificial Intelligence Applications on the Marine Industry

The naval industry has always been very traditional and seems to be on the rear of the implementation of improvements that in other industries have previously matured. This fact has a reasonable explanation in the difficulty that the naval industry has to turn investments into profits. The shipbuilding industry is not risk-friendly, even more so when the simple fact of making ships is a huge risk in itself. On the other hand, the naval industry includes, to a greater or lesser extent, all other industries and it is conceivable that what is good for the others must also be good for this one.

Once the essentiality of having data available for A.I. to be able to conclude the disposal of users has become clear, one of the difficulties faced by the shipbuilding industry in taking advantage of A.I. could be understood. When focusing on the shipbuilding industry, we come across some major limitations, including the scarcity and the confidentiality of the data. The marine industry is oriented towards immediate results, looking very quickly for a solution, dispenses with storing the data, and results in a systematic way that allows it to be reused in subsequent similar scenarios. The development of powerful

algorithms requires that they could be applied in similar conditions with some recurrence. The data must be correctly structured and reasonably clean so that it could be used profitably, *Muñoz et al. (2018)*. Nevertheless, the products of the naval industry are not for mass consumption. In the most successful cases, limited series of boats may be produced that have the same characteristics. It is difficult to find a systematic use of data, but even so, there are interesting contributions that occur in the different phases of the life cycle of a naval project.

4.1.1. Artificial Intelligence on Ship Design

The first stage in the life cycle of ships and naval artefacts is naval design. Interesting approaches to the use of A.I. could be found in this phase. It is important to remark that some of them are quite old and date back to the time of the first explosion of interest in A.I. In 1989, the United States Defense Agency for Advanced Research and Projects (DARPA) promoted a workshop that was held at Rutgers University, New Brunswick, N.J. to support hydrodynamic ship design research initiatives. One of the goals was to clarify the relationships between hydrodynamic ship design issues and A.I. research areas related to the design and analysis of complex systems. Results were not very promising, since they concluded in the need to acquire Computational Fluid Mechanics Analysis tools, known by its acronym in English, CFD, and integrate them into the processes. Design and effective control of design processes, with an emphasis on concurrent design and including approaches to explore feasible design space configurations and record and store results systematically, *Amarel and Steinberg (1990)*. However, expectations remained open and unrealized.

Subsequently, proposals have been made to apply A.I. to the resolution of complex design problems through expert systems and the appropriate selection of them for certain problems such as the dynamics of structures or vibrations, *Díez de Ulzurrum (1992)*.

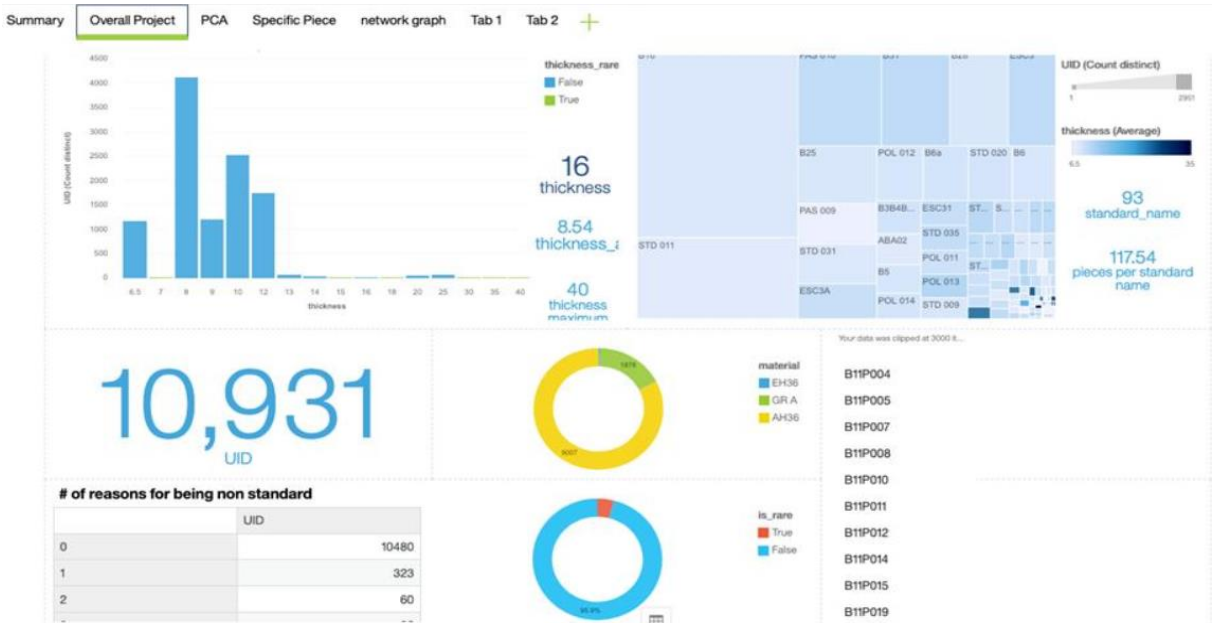

Fig.7: Dashboard for analysis of standard parts versus thickness of plates

Where a greater variety of proposals could be found is in the task of optimizing designs by means of A.I. algorithms that analyse the design space of certain ships in which a systematic parameterization of the variables that allow to define different design alternatives. One of the examples could be found in the article, *Abramowsky (2013)*, for the application of A.I. in cargo ships.

However, it is not easy to find applications of A.I. to truly systematic processes that are in use in a real way, beyond purely academic or research attempts that have not finally materialized in the field of

design. The reason could be found in the difficulty in developing these tools and the low returns that companies and organizations derive from them.

The company SENER proposes a use of the data generated during the design to identify singularities in the designed elements and in this way prevent early the appearance of anomalies that reach the manufacturing and assembly phase. Avoiding the appearance of singularities also allows optimizing the supply and logistics of materials. FORAN® insights is a set of tools that, working with the data of a FORAN® project, provides visual results of the singularities detected in the elements designed based on design or manufacturing parameters, Fig.7.

4.1.2. Artificial Intelligence on Marine business

Some more tangible applications and with some validity could be found in the field of the operation of ships, that is, the operation and management of transport. In this sense, the initiatives are much more numerous, although some are in the research or prototype phases, others are in more advanced stages of implementation.

Prototypes of unmanned vehicles could be found that are used in very hostile environments and that require the support of A.I. This is well described by M.I.T. professor Henrik Schmidt in his course "Unmanned Marine Vehicle Autonomy, Sensing and Communications". On these types of artefacts that operate on difficult environments, such as icy waters, where communication is an impossible limitation to overcome, the role of A.I. is crucial, http://news.mit.edu/2017/unlocking-marine-mysteries-artificial-intelligence-1215.

Another interesting field of application of A.I. is described in an article on the use of A.I. techniques for the detection of small vessels, *Del-Rey et al. (2017)*. The approach is interesting because it raises a situation in which the ship is the subject of the observation, but it could also be the owner of the application. Having on board systems with techniques for detecting other vessels, based on A.I., opens the horizon for unmanned vessels and their possibilities of realization.

A.I. is also being integrated into modern ships´ combat systems as essential elements for identifying threats. The STARTLE® software from the company Roke was selected by the Royal Navy for threat management and is described as a software that continuously monitors the ship's environment in short, medium range, processes the data it receives, and using A.I. techniques, it helps crews to make decisions. "It is inspired by the way the human brain works, emulating the mammalian conditioned fear response mechanism. Rapidly detects and assesses possible threats, the software significantly increases the situational awareness of the human operator in complex environments", https://aerospacedefence.electronicspecifier.com/marine/artificial-intelligence-to-play-key-role-in-maritime-combat. Recently, the Rolls-Royce company has signed a partnership agreement with Google to use the latter´s M.L. engine to improve the company´s intelligent awareness systems, https://www.ship-technology.com/features/rolls-royce-teams-google-ai-driven-ship-awareness/.

A.I. applications could also be found in management systems for the use of energy at sea or in the proposals of companies dedicated to energy in ships. Recently the company Eco Marine Power announced that it would begin to use the Neural Network Console provided by Sony Network Communications Inc., as part of a strategy to incorporate (A.I. in various technology projects related to the ship, including the further development of the patented Aquarius MRE® (Marine Renewable Energy) and EnergySail® propulsion system, https://www.marineinsight.com/shipping-news/eco-marine-power-study-use-artificial-intelligence-research-projects/.

One of the great references in the naval field is the marine area of Rolls Royce that is trying to promote the application of A.I. in ships in two lines: intelligent asset management that encompasses energy, health, data and fleet management, and a second business line of remote and autonomous operations. The latter includes intelligent detection or reconnaissance, remote operations, autonomous navigation systems and connection with ships, https://www.rolls-royce.com/products-and-services/marine/ship-

intelligence.aspx#/. As could be seen on their website, not all lines of work are in operation, but some are under development.

4.2. The Future of Artificial Intelligence in the Marine Sector

The exploitation of the marine business has an unquestionable growth field for A.I. There are many IT solutions that, based on the operating data of the different ship systems could help to manage the assets in a more optimal way. The application of IoT to ships provides both data collection and the ability to act on assets to obtain their best performance, *Muñoz and Pérez (2017)*. For this reason, it is necessary to have essential elements. First, it is necessary to have comprehensive solutions that cover all aspects of connectivity and integrate them in a coherent way. It is also essential to have sensor devices, connectivity and adequate representation-based models that allow adequate interactivity with end users. IBM with its Maximo® program and SENER with FORAN® are developing a proposal that integrates the reality of the model made during the initial design stage, with IBM´s solution to combine asset management with the power of IoT data obtained from sensors, devices and people to have visibility of them in real time. Having a ship model in a single database allows obtaining virtual reality and augmented reality images on which the data obtained could be superimposed and their comparison with the technical performance measures expected for each supervised element of the ship. In this way, it will be possible to act accordingly in each situation. Another interesting field of work for the future of A.I. is image recognition. In this sense and putting the focus on the naval industry, two fields of application appear. The identification of images in autonomous vehicles that could help their mission and operation. Although it does not only have application in ships and unmanned devices, it could also be used in surveillance systems and detection of possible threats or risks in manned ships. Part of this is what one of the projects that have been mentioned above covers, *Mathews (2016)*.

Image recognition through A.I. is also of interest at design stages. The need to have virtual models of the objects that are part of a project means that real models could be scanned and later recognized to create the virtual model. This is of particular interest in ship retrofits. There is a real need to have a virtual model based on a real one in order to evaluate the possibilities of retrofitting or re-motorization, including the processes and manoeuvres necessary to carry out said operations. Although point cloud treatment programs are capable of working with that amount of visual information, they have not yet passed the threshold of identifying the elements that appear in the scene and converting them into analytical geometric representations or not, on which measurements could be obtained or manipulated as a whole. An extension of this could be applied to component models that are used in the design stages by CAD programs. Nowadays, it is very common that the components that are going to be modelled in CAD are obtained through external files that, for the most part, have been obtained for marketing purposes. These are surface representations of many faces that do not have a geometric and parametric representation. This, which is useful simply to see a model, makes it useless or even a problem to carry out projects, since it is necessary to have metadata that only exists when the models have a formal geometric representation. That is, it is not the same to handle the six faces of a cube, than the cube as a whole. This limitation opens up a field of action for A.I. programs that are capable of recognizing that certain faces form a particular surface, or that certain surfaces form a solid. At the moment, the available programs help the user, but it is finally the this one who will validate the conversion. However, A.I. programs could learn from this type of recognition made by a human in order to be more precise each time.

Carrying out a ship project is certainly complex, and not only because of its transversally but also because of the number of tools that must be handled and the limitations imposed by design rules or regulations of various kinds: construction, safety, etc. CAD systems provide more and more tools, but they are also increasingly complex to be used optimally. Along with this scenario, marine engineering companies and shipyards have very demanding delivery times and templates, or very young people who, although they are familiar with new technologies, do not know the art of naval engineering or, with very old people more reluctant to work with the most current CAD programs and with new capabilities. For this reason, it would be interesting to have a virtual assistant that could provide all the necessary information to do the job correctly. SENER and IBM are developing a project that integrates

the cognitive capabilities of Watson® with the functionalities of CAD in the different design stages, as shown in Fig.8.

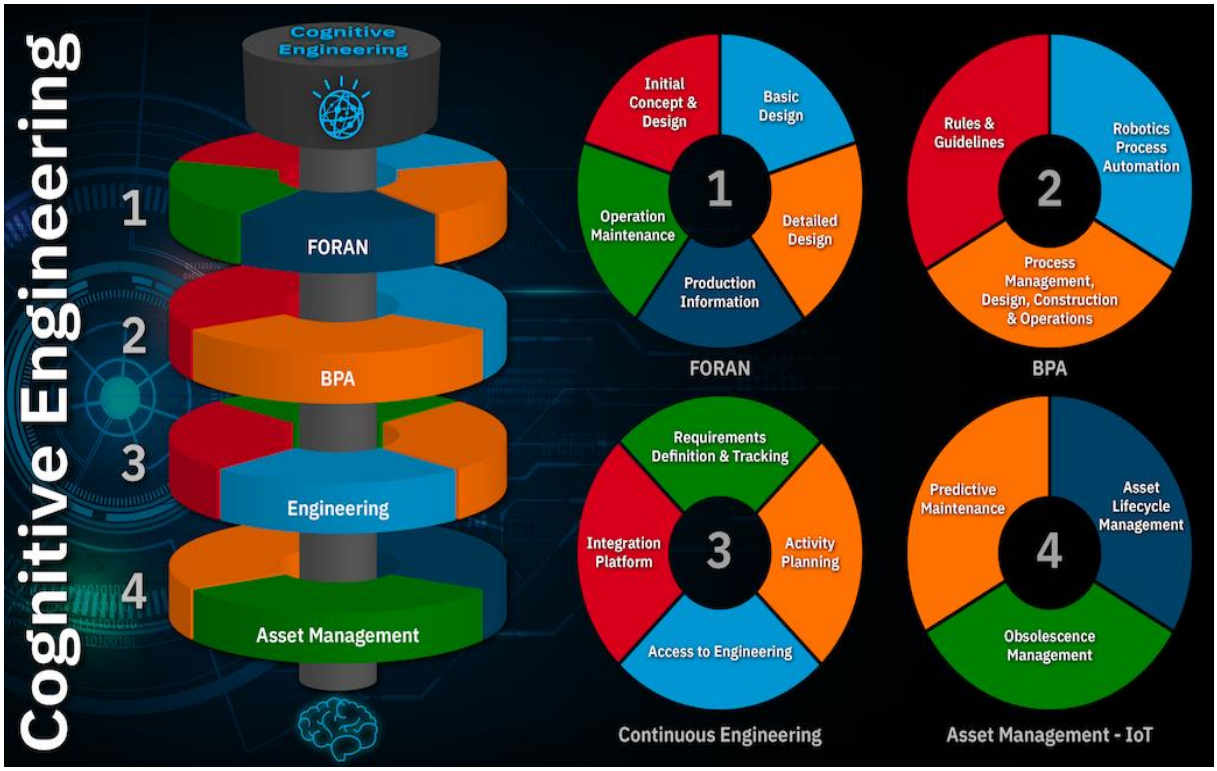

Fig.8: Cognitive engine in FORAN, source: IBM and SENER

Watson®'s platform will have a corpus of information and data that will integrate everything necessary to use the FORAN® system correctly and optimally, but will also include all the regulations applicable to the different types of ships, such as IMO regulations, firefighting, pollution, safety regulations, etc. It could even integrate the shipyard's own design and work rules, so that CAD users could carry out designs in accordance with all applicable regulations and standards at different levels: administration, construction, ship-owner. This system will be trained to learn to provide the appropriate information to each type of intention and will be able to learn and be trained in different and new things that may affect the design. The integration could be carried out at different levels, completely decoupled from the CAD or coupled to it so that the performance of certain operations in the CAD triggers events that are captured by the listening system and this in turn links to the virtual assistant to provide the information or data that is linked to those operations. Interaction with the system may also be on demand or taking advantage of the natural language processing capabilities of the Watson® system. This project makes it possible to increase the capacities of FORAN® to have the cognitive and analytical capacities of the Watson® system and make them available to the naval industry to put it in the field of 4.0 digitalization.

Just as we have found possibilities for the application of A.I. in the realm of design, it will also be possible to see realities of A.I. in manufacturing processes soon. Perhaps the first progress we will see is related to the ability of machines to select the manufacturing material. Machines that select cutting plates to take advantage of the material according to the remaining pieces or robots capable of organizing the movements of intermediate products in the workshop. The novelty of A.I. will be that these machines and robots will not have to be programmed, but will receive the data or objects with which they have to work and will know how to act. "In the future, robots will no longer have to be expensively programmed in a time-consuming way with code pages that provide them with a fixed procedure for assembling parts. We will only have to specify the task and the system will automatically translate these specifications in a program", https://www.siemens.com/innovation/en/home/pictures-of-the-future/industry-and-automation/the-future-of-manufacturing-autonomous-assembly.html.

5. Conclusions

The concept of A.I. has evolved over the years, developing multiple related technologies and specialized uses. There is no doubt that a technological evolution in this sense has become a reality to which companies must adapt in order to evolve.

In recent years, many companies have invested enormously on A.I., by acquiring start-up companies or developing applications themselves. This factor is key, and, although we still do not know the whole extent of applications in the industry, it is common sense that all companies that do not embrace A.I. and M.L. technologies are bound to be left behind in the race.

In the specific case of the Marine Industry, applications of A.I. are becoming a reality at slow pace, because it is necessary to identify clearly in what areas to apply and what is the benefit. These two aspects compromise the investment and increase the uncertainty of the A.I. projects. Assuming a similar progress to other industries, the digitalization of industrial process, robotization and usage of data by the A.I. will become a reality in this specific industry in a mid-term.

In the case of ship design, applications using A.I. are being more difficult to develop, as the complexity of the projects becomes a real handicap when trying to solve design and automation issues. Nevertheless, this area of development in A.I. will be key for the future of digitalization of ships end to end lifecycle.

References

ABRAMOWSKY, T. (2013), *Optimization, Application of Artificial Intelligence Methods to Preliminary Design of Ships and Ship Performance*, https://www.researchgate.net/publication/259361068_Application_of_Artificial_Intelligence_Methods_to_Preliminary_Design_of_Ships_and_Ship_Performance_Optimization

AMAREL, S.; STEINBERG, L. (1990), *Artificial Intelligence and Marine Design*, AI Magazine 11(1), pp.14-17

CAPEK, K. (2017), *R.U.R. (Robots Universales Rossum)*, Libros Mablaz. https://es.wikipedia.org/

DEL-REY, N.; MATA, D.; JARABO, M.P. (2017), *Artificial intelligence techniques for small boats detection in radar clutter*, https://www.sciencedirect.com/science/article/pii/S0952197617302610

DÍEZ DE ULZURRUN, I. (1992), *Aportaciones al diseño dinámico de buques*, Universidad Politécnica de Madrid

KIRKPATRICK, K. (2018), *Considerations for getting started with AI*, TRACTICA LLC (Cray Inc.)

McAFFE, A.; BRINJOLFSSON, E. (2017), *What´s driving machine learning explosion*, Harvard Business Review

MUÑOZ, J.A. ; PÉREZ, R. (2017), *Design of smart things for the IoT*, 2nd Int. Conf. Internet of Things, Data and Cloud Computing, New York

MUÑOZ, J.A.; PÉREZ, R. ; GUTIERREZ, J.R. (2018), *Design rules evaluation through technologies of treatment of Big Data.* COMPIT Conf., Pavone

NAOYUKI, N.; KONNO, E.; SATO, M.; SAKAIRI, M. (2017), *Application of Artificial Intelligence Technology in Product Design*, Fujitsu Science Technology 53(4), pp.43-51

RUBAIAT HABIB, A. (2017), *DreamSketch: Early Stage 3D Design Explorations with Sketching and Generative Design*, ACM Symp. User Interface Software & Technology

TORRA, V. (2011), *La inteligencia Artificial*, LYCHNOS - Cuadernos de la Fundación General CSIC(7), pp.14-18

TURING, A. (1950), *Computers and Thought*, Mind 49, pp.433-460

Parametric Modelling Method based on Knowledge Based Engineering: The LNG Bunkering Vessel Case

Nikoleta Dimitra Charisi, TU Delft, Delft/ Netherlands, N.D.Charisi@tudelft.nl
Hans Hopman, TU Delft, Delft/Netherlands, J.J.Hopman@tudelft.nl
Austin Kana, TU Delft, Delft/Netherlands, A.A.Kana@tudelft.nl
Nikos Papapanagiotou, C-Job Naval Architects, Hoofddorp/Netherlands, n.papapanagiotou@c-job.com
Thijs Muller, C-Job Naval Architects, Hoofddorp/Netherlands, t.muller@c-job.com

Abstract

This paper proposes a parametric modelling method based on Knowledge Based Engineering (KBE) for an LNG bunkering vessel (LNGBV). Parametric models aim to define the geometry and main systems configuration of the vessel starting from the principle that the vessel should be able to perform its mission successfully. The adoption of KBE in combination with parametric modelling is expected to improve the current practice by automating the generation of the parametric models based on the design requirements. The results showed that different design alternatives can be rapidly generated which in turn gives the possibility to the designer to perform a wide exploration of the preliminary design space.

1. Introduction

Nowadays, advanced design solutions need to be developed with ever shorter lead-times due to the enhanced competitiveness of the shipping industry resulting from digitalization, https://www.shipfinance.dk/media/1817/shipping-market-review-may-2018.pdf, and the stringent regulatory framework (Global Sulphur Cap 2020, IMO's strategy for reducing greenhouse gas emissions). To support this, the designer must perform a broad exploration of the preliminary design space to develop improved design solutions. Parametric models form a core element of the preliminary design process designed to facilitate this exploration. Specifically, parametric models are connected with design optimization routines and analysis performed by dedicated software tools. By developing different configurations associated with a design problem and predicting their performance, the designer is able to make efficient trade-offs, *Duchateau (2016)*. Parametric models provide a visualization of the designed vessel, which helps the designer understand the design problem, create relevant design solutions, and evaluate potential solutions that have been developed, *Dahl et al. (2001)*.

The European ship design industry puts effort into developing large and expansive knowledge-bases to support design, engineering and manufacturing, *Bruinessen et al. (2013)*. The stored knowledge regarding preliminary ship design contains previous design cases and existing vessel data, generalised design cases, templates, syntactic knowledge, rules and facts, and problem solving methods, strategy and tactics, *Erikstad (2007)*. The common practice for parametric modelling is that parametric models are developed via the combination of different geometric primitives (points, lines, surfaces, etc). This practice requires a lot of manual effort and repetitive non-creative engineering work. However, the efficient exploitation of design knowledge gives the potential to automate parametric modelling. Consecutively, the developed parametric models can be used as an input to the most suitable software packages, including CAD packages and analysis tools.

Knowledge Based Engineering (KBE) is a method used to identify, record, and re-use relevant engineering knowledge in product design, *van Tooren et al. (2003)*. The improvement resulting from its adoption is that the proposed parametric modelling method is based on the development of knowledge building blocks, called High Level Primitives (HLPs), rather than geometric primitives. The HLPs are instantiated according to the design requirements and decisions and combined to form a design solution. In order to form another design solution, the HLPs can be re-instantiated according to the designer's decisions.

As a case study, the proposed parametric modelling method is applied to the preliminary design of an LNG bunkering vessel (LNGBV). From a design point of view, the LNGBV design case is interesting due to the fact that there are only a few LNGBVs built at the moment and as a consequence, the design can not be reliably based on reference data.

2. Parametric Modelling in early design stages

Parametric models have been widely researched and applied in many different fields of product design such as aerospace, *Wei (2016)*, automotive, *Wan et al. (2005)*, and architecture, *Hernandez (2006)*. By employing the parametric design procedure, the design and optimization of a mechanical engineering system can be automated by the elaboration of sets of design parameters defined by the designer or an optimisation algorithm, *Papanikolaou (2019)*. Regarding early-stage ship design, naval architects use parametric modelling to establish a consistent parametric description of the vessel in terms of its dimensions and other descriptive parameters, *Parsons (2004)*. The parametric models must be flexible and generic to apply to many design alternatives, *Kanellopoulou et al. (2019)*. Regarding the design of large integrated systems such as a ship, the development of parametric models is a complicated task in order to ensure their integrity, accuracy, robustness and functionality, *Papanikolaou (2019).*

There are a few commercially available software tools exploiting the capabilities of parametric modelling. The different approaches vary from commercially available ship parametric modelling tools such as FRIENDSHIP-Modeler via integration of parametric capabilities to a well-established ship design system such as NAPA to more restricted methods like the parametric definition of shape deformation functions (GMS/Facet), *Maisonneuve et al. (2003)*. Regarding the case study presented in this paper, NAPA software will be used for the development of the parametric models.

Several studies are dedicated to the parameterization of the hull. The generation of the parametric model of the hull is used for hydrodynamic optimization. *Biliotti et al. (2011)* developed a framework for the automatic optimization of the fore hull forms of a fast frigate. *Brizzolara et al. (2015)* researched global hull optimization by using CFD. *Timur (2015)* developed a parametric modelling tool in Java programming for rapid hull geometry generation. *Sanches (2016)* presented a method for parameterization regarding different merchant vessel types by using FRIENDSHIP framework.

Several studies are examining parametric modelling from the holistic design approach perspective. The holistic design approach is explained in *Papanikolaou (2014)*. Parametric models for different vessel types are created in the studies *Papanikolaou (2010), Papandreou and Papanikolaou (2015), Priftis et al. (2016), Marzi et al. (2018), Kanellopoulou (2019)*. The developed models were further optimized by optimization algorithms. The software used for the parameterization is either NAPA or CAESES. In the context of SHOPERA project *Kanellopoulou (2019),* a series of parametric models have been generated for various types and sizes of ships, such as RoPax ships, cruise ships, tankers, bulk carriers, container ships and general cargo carriers using Computer-Aided Ship Design (CASD) software tools. Furthermore, the H2020 European Research project – HOLISHIP – Holistic Optimisation of Ship Design and Operation for Life Cycle (2016-2020), *Papanikolaou et al. (2020),* aims to achieve improved vessel concepts for the 21st century.

Parametric models have also been developed based on the Design Building Block (DBB) approach. More specifically, in the context of Low Carbon Shipping and Shipping in Changing Climates, the Whole Ship Model (WSM) was developed. The model combines a parametric model with the operational profile and a range of performance-enhancing or emissions-reducing technologies, *Calleya et al. (2016)*.

Therefore, engineers are effectively using parametric modelling in a wide variety of applications in the ship design field. Depending on the way of setting up the parametric models, they can reflect different design methodologies and adapt to various design problems. The present paper examines the application of a parametric modelling method based on KBE for preliminary ship design. The

proposed approach differentiates itself from the traditionally established method based on CAD. The difference between KBE and CAD is highlighted in *La Rocca (2012)*.

3. Knowledge Based Engineering (KBE)

KBE is defined as a technology that allows capturing product and process multidisciplinary knowledge employing integrated software applications that can automate the repetitive design activities, and as a result, reduce engineering time and cost, *La Rocca and van Tooren (2010)*. The core of KBE is the identification, record, and re-use of engineering knowledge by combining Artificial Intelligence (AI) techniques, IT tools and Object-Oriented methodologies, *van Tooren et al. (2003)*.

KBE which was developed as part of Knowledge Based Systems (KBSs) in the field of Artificial Intelligence (AI), dates back to 1970s, *Sobieski et al. (2015)*. Regarding engineering applications, KBSs faced two major limitations, namely the inability for geometry manipulation and data processing, *La Rocca (2012)*. The technological advancements in the field of CAD and CAE systems addressed these limitations, and the concept of KBE began to be widely applied in product design, *La Rocca (2012)*. Nowadays, KBE tools are being used by many companies operating in the automotive and aerospace sector. In the aerospace industry, Airbus, *Cooper et al. (2001)*, Fokker Elmo, *van den Berg (2013)*, are some examples, to mention but a few.

The KBE product model represents the core of every KBE application, and it consists of a structured and dynamic network of classes where both product and process knowledge, both geometry-related and non-geometry related are modelled using a broad typology of rules *La Rocca (2012)*. The KBE product model consists of High Level Primitives (HLPs), which are objects containing product and engineering knowledge that can be used and re-used in different configurations *La Rocca and van Tooren (2006)*. The HLPs can be seen as functional blocks that allow the designer to define a product as a result of a structured set of HLPs. These functional blocks are a set of rules using parameters to initiate objects that represent the product under consideration or to apply an engineering process to the initiated object *Schut and van Tooren (2007)*. A clear example of different aircraft configurations resulted from the combination of the re-instantiation of the same five HLPs is shown in Fig.1.

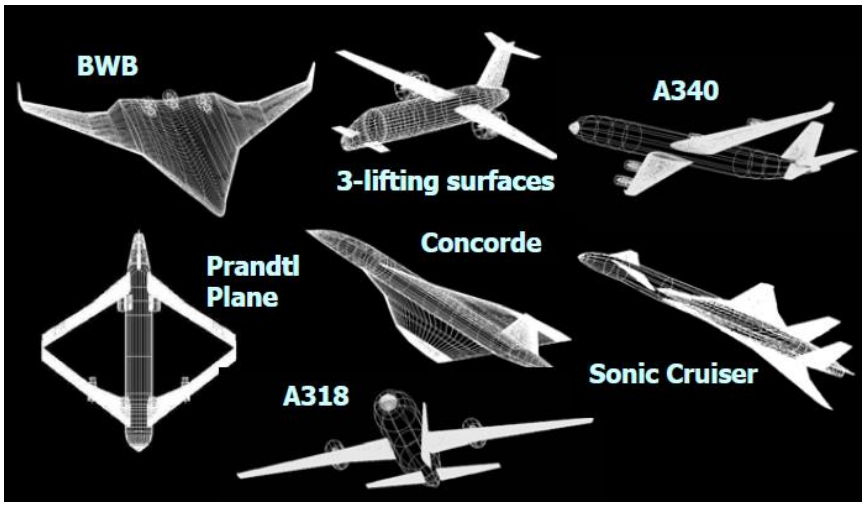

Fig.1: Design variations for the aircraft's preliminary design *van Tooren et. al (2003)*

Knowledge is the core element of every KBE model. Knowledge can be defined as relations between facts and becomes central when it comes to reasoning processes *Rehn (2018)*. Design supporting knowledge includes the methods and data (presented in forms of handbooks), software for recording analysis (CAD and CFD software) and humans experts *van Tooren et al. (2003)*. The challenges of the method can be identified in the identification of the knowledge in an organization, its capture, and formalization in reusable rules and the way of embedding them in the KBE system.

KBE has been extensively researched and applied in preliminary aircraft design. More specifically, the Design Engineering Engine (DEE), which is an integrated design support tool, was developed for the aircraft's conceptual design at TU Delft *van Tooren et al. (2003)*. The DEE consists of an initiator, an optimization algorithm, and the relevant analysis tools connected with aerodynamics, structures, and manufacturing. Further information can be found in *Schut and van Tooren (2008)*.

Ship design is a suitable field for the application of KBE due to its associated complexity. However, the applications of KBE in the maritime field are limited due to the high level of customization. The study of *Wu and Shaw (2011)* suggested a basic (preliminary) ship design knowledge-model for information storage and retrieval using KBE and developed a semantic inquiry function that allows users to use the retrieved information immediately. The acquired knowledge was collected from experienced engineers or information from journals and theses. In addition, KBE methodology has been also used for ship hull structural member design *Yang et al. (2012)*. The concept of exploiting gained knowledge in ship design forms a part of current scientific research. The data-driven design developed by *Gaspar (2018)*, make use of data regarding both the product (ship) and the process (design) to extract information and knowledge. Also, *Arendt and van Uden (2011)* developed a decision-making module for enhancing automation in ship design. The selected method for the creation of the database was the Analytic Hierarchy Process (AHP), which was applied in the selection of the temperature sensors in a fuel transport system.

Following the KBE principles applied in aircraft's preliminary design, the proposed parametric modelling method was developed. It is expected that the method will improve parametric modelling by the automation of the models' generation.

4. Proposed Method

The method consists of eight steps, and its flowchart is depicted in Fig.2. The method consists of the following steps:

1. Identification of the design requirements
   The first step of the research procedure is to determine the design requirements. These are dependent on the vessel type, its associated functions, and the specific design problem. In general, for commercial vessels, the design requirements focus on deadweight, speed, and building cost of the vessel. The design requirements correspond to the input variables, which lead to the tuning of the parametric model.

2. Main drivers analysis
   The main drivers analysis is conducted to identify the way that the vessel should be parameterized. The main drivers analysis mainly depends on the vessel type and its associated functions. In this step, the vessel's functions are mapped to the required systems.

3. Determine the HLPs
   The third step consists of the determination of the HLPs (the 'building blocks') of the examined vessel. The principles of KBE will be used for the definition and modelling of the HLPs. The HLPs form the toolkit from which different parts can be combined to form the different vessel's alternatives.

4. Qualitative description of the HLPs
   The fourth step is associated with the way that the HLPs are parameterized. The qualitative description will be the guideline for the mathematical representation.

5. Mathematical representation of the HLPs
   The mathematical description of the HLPs is derived from their qualitative description. Here their interrelations are defined, and from this, the vessel's architecture can be created.

6. Define the HLPs for each “total ship” architecture
   The selected HLPs from the vessel's toolkit are combined to form the “total ship” architecture according to the design decisions of the Naval Architect. The different design decision combinations lead to different solutions in the design space.

7. Tune the HLPs to fit the design problem
   The selected HLPs are then tuned to fit the specific design problem. The design requirements are used as guidelines to form feasible and suitable design solutions for the design problem.

8. Extract and evaluate the geometric model
   The output of the framework is the geometric model of the vessel for the Naval Architect to visualize their ideas and use the model as an input for analysis. The case study presented here uses NAPA software for this visualization; however, this step can be performed by other software packages as well according to design needs and preferences. Besides, a first weight and stability analysis based on semi-empirical methods should also be included in this step to give an idea about the feasibility of the design solution.

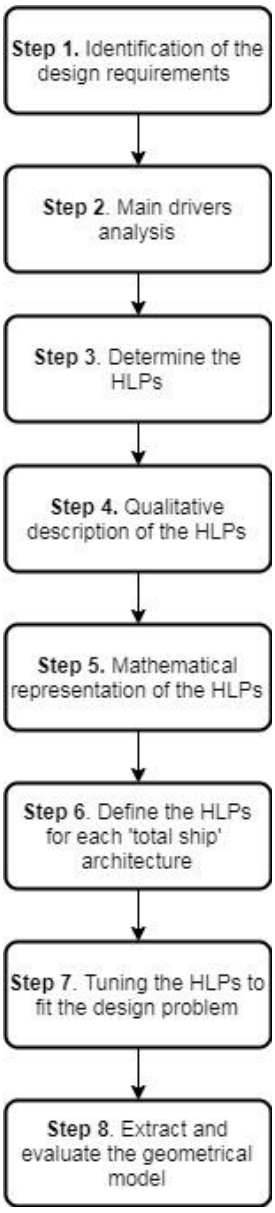

Fig.2: Flowchart of the proposed method

The proposed method was developed generically to apply to different vessel types and to fulfil different design problems. However, to bound the research work, a proof of concept was built based on the parametric modelling of an LNGBV. In addition, the case study was tailor-made for C-Job Naval Architects. In the context of C-Job design tools, all the relevant knowledge was gathered to be used for the building of the HLPs and the tailoring of the case study according to the company's design process. Further information can be found in *Charisi (2019)*.

The sources of the company's intellectual capital, which were used, included:

- Interviews from Naval Architects to understand the company's design process and design way of thinking.
- Datasets of machinery components from manufacturers.
- RefWeb tool (in-house developed data visualization tool for design intelligence and big data analysis).
- Naval architectural empirical design rules.
- Classification rules and regulations.

5. Case study: Preliminary design of the LNGBV

The preliminary design of the LNGBV is examined as a case study. The LNGBV was selected to be examined because there are just a few vessels built and as a consequence, its design can not be reliably based on design trends of reference vessels. In addition, the demand for building LNGBVs is expected to increase due to the wider adoption of LNG as a marine fuel; the use of LNG lowers the polluting emissions, and thus, the compliance with the stringent IMO's regulatory framework can be achieved, *Kim et al. (2019)*. The LNG bunkering infrastructure forms a key point on the establishment of LNG as a marine fuel, *Jingjing et al. (2015)*. However, the ship-to-ship (S-T-S) bunkering around the world brings new opportunities as unlike a fixed LNG terminal, it is not dependent on location. At the moment, several LNG bunkering vessels are operating worldwide, which are either custom-built, small LNG carriers converted to bunkering vessels, or bunker barges (pushed or self-propelled), *Charisi (2019)*.

From a design point of view, the LNGBV has similarities with the LNG carrier. However, there are also significant differences, such as their operational profile. The LNG carrier is an ocean-going vessel transporting cargo worldwide, while the LNGBV aims to bunker other vessels. Thus, the LNGBV has less capacity and sails for short distances. According to naval architects at C-Job, the significant components of both of these vessels are the following: the LNG cargo containment system, the propulsion system, the boil-off gas (BOG) handling system, the inert gas system, the bunkering equipment, the S-T-S equipment, and the superstructure. A unique characteristic of the propulsion unit of the LNG carriers is that the BOG from the cargo can be used in different ways. The most common way is that the BOG is being used as a fuel source for propulsion. The LNGBV differentiates itself from the LNG carrier in its high manoeuvrability capabilities connected with safety during port operation and S-T-S bunkering process.

5.1 Application of the proposed method to the design of the LNGBV

The proposed method is applied step-by-step to the design of an LNGBV. A detailed description of the steps is given.

5.1.1 Identification of the design requirements

In order to define the design requirements, a real design problem of C-Job was considered. A detailed description contains proprietary details. Thus, the detailed client's requirements were simplified to approach a more generic form of the problem. Design requirements were set related to the following:

1. The LNG cargo capacity and the LNG cargo handling system layout.
2. The required service speed and propulsion layout
3. Manoeuvrability characteristics.
4. Compliance with the applicable regulations, codes and standards related to the preliminary design stage.
5. The technical systems for the BOG treatment and the inert gas system.
6. The crew accommodation.
7. Ballast water storage.

5.1.2 Main drivers analysis

The main drivers analysis aims to identify the vessel's parts, which will be parameterized. The starting point is the identification of the vessel's required functions resulting from the design requirements. Regarding the LNGBV, the required functions of the vessel are to float, move, manoeuvre, navigate, transport LNG cargo, bunker other vessels, accommodate crew, and ensure safe operation. Thus, these functions were mapped to the required vessel's systems, Table I.

Table I. Mapping LNGBV functions to LNGBV systems

	Float	Move	Manoeuvre	Navigate	Transportation of LNG cargo	Bunkering operations	Accommodate crew	Ensure safety
Hull	✓							
Propulsion system		✓	✓					
Cargo handling system					✓			
Bunkering equipment						✓		
BOG handling system								✓
Inert gas system								✓
Ballast water system						✓		
Thrusters		✓	✓					
Rudder			✓					
Superstructure							✓	
Bridge				✓				

Specifically, the hull of the vessel ensures that the vessel is floatable. The propulsion system and the thrusters (if azimuth thrusters are selected) are responsible for the sailing of the vessel. The main systems influencing the vessel's manoeuvrability are the selected propulsion system, the thrusters (azimuth and bow), and the rudder. The LNG cargo handling system should also be included in order to ensure the transportation of the LNG cargo. The bunkering equipment and the ballast water system ensure bunkering operations. Safety is a significant aspect to be taken into account for the design of this vessel's type; therefore, BOG handling system and inert gas system are also included. Finally, the superstructure and the bridge are included in the design to accommodate the crew and to enable navigation.

5.1.3 Determine the HLPs

Following the main drivers analysis, the HLPs are defined. The HLPs can be seen as the building blocks, which can be combined to form the LNGBV. The HLPs can be re-shaped following different design decisions to form another design solution. The required systems resulted from the main drivers analysis are the hull, the propulsion system, the cargo handling system, the bunkering equipment, the

BOG handling system, the inert gas system, the ballast water system, the thrusters, the rudder, the superstructure, and the bridge. For this specific case study, these systems were filtered and translated into HLPs by taking into account the properties of the expected outcome, the NAPA geometric model. The hull was translated into three different HLPs, namely the afthull, midhull, and forehull. This decision was made to enhance the flexibility of generating different hull shapes. The HLP Engine Room corresponds to the propulsion system of the vessel. Similarly, the HLP Cargo Space is equivalent to the cargo handling system. The inert gas system and the BOG handling system are combined to form the HLP of the Technical Space. The ballast water system results from the vessel's design. Thus, it is not an influential design entity that should be taken into account. The HLP Superstructure contains the superstructure and the bridge. The bunkering equipment, the stern thrusters, and the rudder are not taken into account since these entities do not add information to the geometric model at this design stage. The HLP Bow Thruster Room was developed to accommodate the bow thruster system. Finally, the HLPs Aftpeak and Forepeak were defined for geometrical purposes.

To summarize, the HLPs which will be used for the synthesis of the LNGBV are the following:

1. Engine room
2. Cargo space
3. Superstructure
4. Technical space
5. Bow thruster space
6. Aftpeak space
7. Forepeak space
8. Afthull part
9. Midhull part
10. Forehull part

5.1.4 Qualitative description of the HLPs

The qualitative description of the HLPs forms the basis for their mathematical representation. In order to proceed with the qualitative description of the HLPs, the sub-parts of the HLPs which should be taken into account should be defined.

An example is given for the engine room. A detailed description of this step can be found in *Charisi (2019)*. According to Wärtsilä Encyclopedia of Marine Technology, the engine room is defined as the compartment onboard a ship that includes the main propulsion machinery as well as the control room, the auxiliary machinery, and other equipment. The engine room layout, design, and arrangement are governed by SOLAS- International Convention for the Safety of Life at Sea Ch.II-1 Part C, and IGF code.

According to *Klein Woud and Stapersma (2002)*, the following spaces will form the typical layout of the engine room of a small cargo vessel:

- a main machinery space including the propulsion engine, gearbox transmission, diesel generators and auxiliaries
- a steering gear room, which is located above the rudder
- a workshop, in which maintenance is carried out
- a control and/or main switchboard room

Regarding the required level of detail for the preliminary design phase, the following aspects are considered to be the design drivers for the engine room layout:

- type of propulsion
- selected machinery components
- type of propulsor(s)

- required propulsive power
- required electrical power
- requirements for manoeuvrability

An example layout for the direct mechanical drive engine room for the LNGBV is shown in Fig.3.

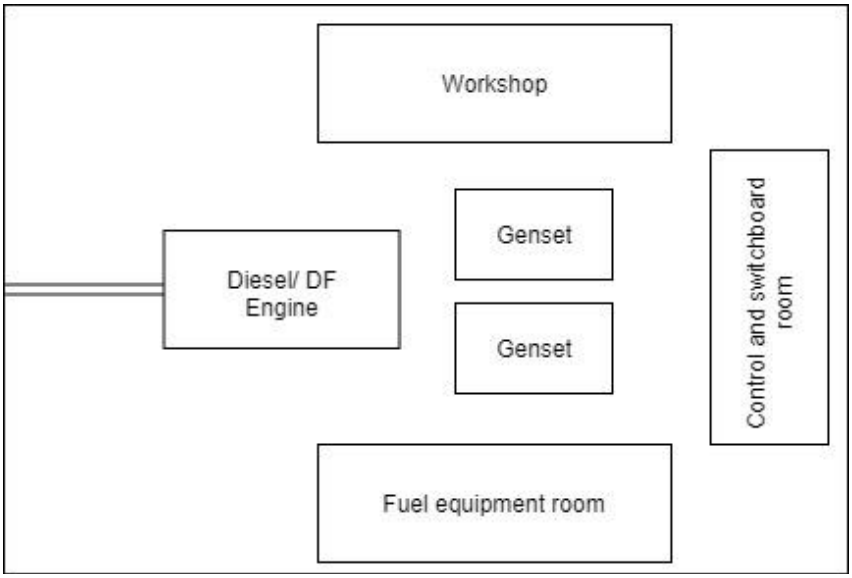

Fig.3: Direct mechanical drive engine room layout

5.1.5 Mathematical representation of the HLPs

Each HLP forms a class containing the relevant attributes and methods which are required to create the design solution. Regarding the case study, the expected outcome is the NAPA parametric model of the vessel and an estimation to ensure initial stability and buoyancy. Therefore, four different methods were developed for each HLP associated with their definition, tuning, geometrical representation, and weight estimation.

In general, for each HLP the following equations apply:

$$Lenght_i = f1_i(IndependentVariables_i)$$
$$Width_i = f2_i(Independent\ Variables_i)$$
$$Height_i = f3_i(Independent\ Variables_i)$$
$$Weight_i = f4_i(Independent\ Variables_i)$$
$$GeometricModel_i = f5_i(Independent\ Variables_i)$$

Therefore, the main dimensions of the vessel are defined as follows:

$$Lpp = \sum Lenght\ Inner\ Blocks$$
$$Beam = \max(Width\ Inner\ Blocks)$$
$$Height = \max(Height\ Inner\ Blocks)$$
$$Depth = Draft + Min\ Required\ Freeboard$$

The HLPs are modelled based on Object Oriented Programming (OOP) principles. Python was chosen for the development of the HLPs. The reasoning is that Python is a user-friendly coding language, which is open-source and is supported by an active and growing community of users.

5.1.6 Define the HLPs for each "total ship" architecture

Metaphorically, step 6 can be visualized as picking the appropriate "lego bricks" from the vessel's

"tool kit". To do this, there are three sub-processes. Firstly, the design requirements and the naval architect's decisions are defined. Then, the relevant knowledge is retrieved from the company's databases. Finally, the required HLPs are defined.

5.1.7 Tune the HLPs to fit the design problem

It should be noted that up to this step, all the dimensions of the HLPs are set to zero. Step 7 is associated with the method of tuning the HLPs to form a solution suitable for the specific design problem. The process consists of two sub-processes, namely the tuning of the parameters of each HLP, and the balancing of the parameters of the individual HLPs to create a feasible design solution.

The sub-process of tuning the parameters for the individual HLPs starts with the load balance analysis for the LNGBV. The primary electric consumers for this vessel are the inert gas system, nitrogen generation system, the bunkering systems, the voyage fuel supply system, the bow thruster and the general ship systems (deck equipment, engine room equipment, ventilation, heating, workshop, domestic facilities, cargo room equipment). A first prediction of the required propulsion power is taken from the reference vessel's data stored in the RefWeb. In turn, the individual HLPs are tuned and as a result, the design solution is developed. By taking this design solution as a starting point, the HLPs are re-tuned in order to form a balanced design solution.

5.1.8 Extract and evaluate the geometrical model

The subprocesses of the final step can be divided into the development of the parametric model and its assessment. For the development of the parametric model, the geometric model of the HLPs is created in NAPA. For the assessment of the design solution, the regulation regarding the minimum freeboard area, the initial stability, the manoeuvrability requirement, the ballast capacity are checked.

5.2 Results

The design of an LNGBV of 7,500 m^3 capacity with a service speed of 12 kn, high manoeuvrability, and accommodation for 14 crew members is examined. Different design options were developed by adopting different options for the LNG cargo handling system layout, the propulsion layout, the positioning of the technical spaces and the superstructure. Indicatively, the parametric models for 4 different designs are shown in Figs.4-7. Their characteristics are presented in Table II. It should be noted that each design is developed within five to ten minutes.

For the first design solution, the propulsion system consists of a hybrid drive (two dual-fuel (DF) engines, two electric motors, and four generator sets). For the storage of the cargo, two bilobe tanks were considered. The superstructure was positioned fore to improve visibility. The technical space, which includes the inert gas system and the GCU, is positioned on the forepart of the vessel. There is also the option to include a reliquefaction plant placed on the deck.

Regarding the second design solution, the use of a membrane tank for the cargo handling system was examined. Direct mechanical drive consisting of two DF engines and two fixed pitch propellers (FPP) was selected. Two generator sets provided the required power for electric consumers. The superstructure is positioned on the aft part of the ship. A bow thruster was included to enhance manoeuvrability and compensate for the limited manoeuvrability of the mechanical drive propulsion system. The technical space was placed on the deck.

For the third design solution, it was decided to examine the use of cylindrical tanks for the LNG storage. For the propulsion layout, it was selected to use a mechanical drive consisting of two diesel engines driving two FPP. A bow thruster is also included and the superstructure was placed in the aft since more deck space was available at the afthull. For the fourth design option, the use of four cylindrical tanks was examined. Diesel-electric propulsion was selected (the generator sets were positioned on the engine room on the forepart), and the technical spaces were placed on the aft (inert

gas system and GCU). The superstructure was placed in the fore to enhance visibility. The developed NAPA models are functional and can be used for further stability and strength calculations within NAPA.

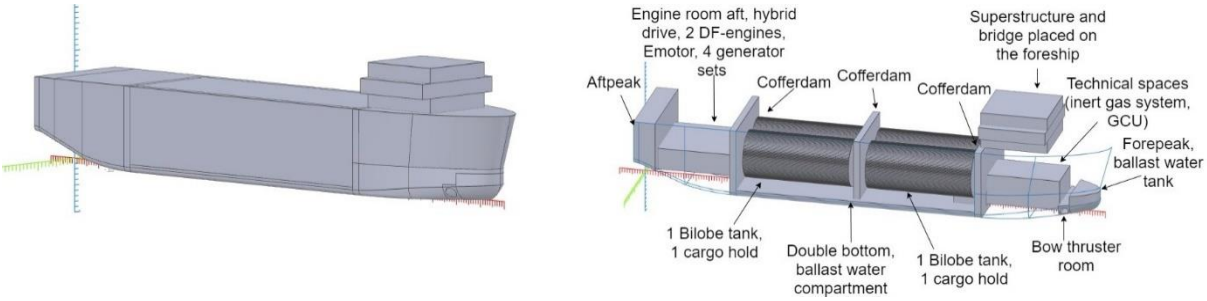

Fig.4: Design solution I (bilobe tanks, hybrid propulsion system)

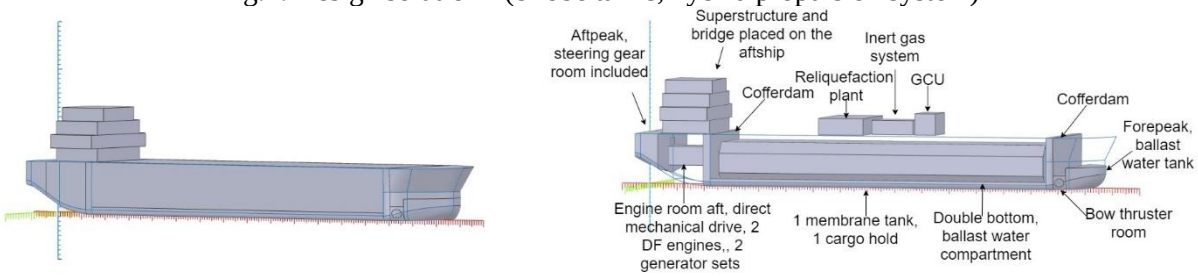

Fig.5: Design solution II (membrane tank, mechanical propulsion system)

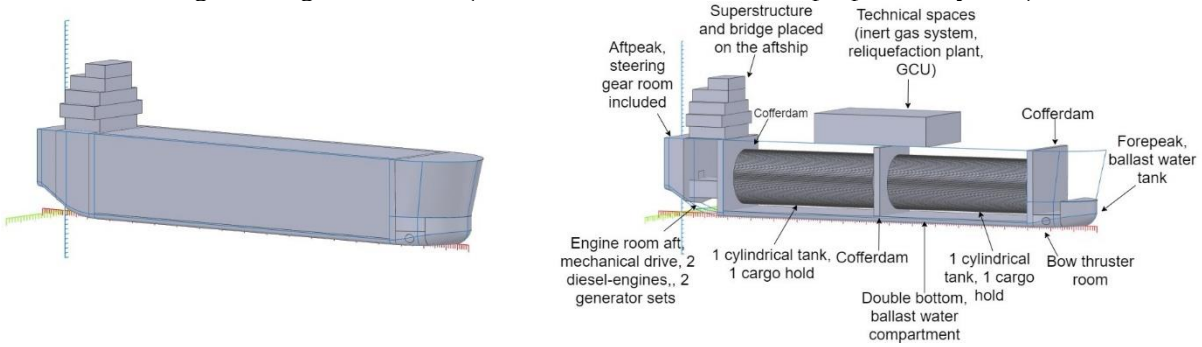

Fig.6: Design Solution III (cylindrical tanks, mechanical propulsion system)

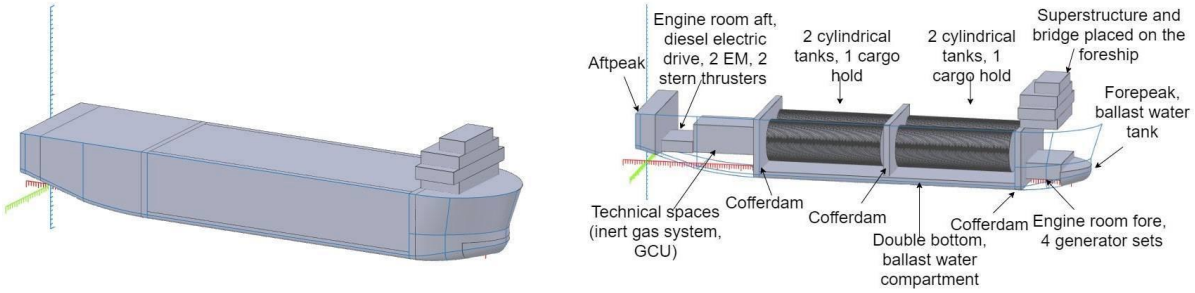

Fig.7: Design Solution IV (cylindrical tanks, diesel-electric propulsion system)

By taking into account the design cases, it can be seen that the leading factor for determining the length and the beam of the vessel is the cargo room layout. Other influential parameters were the selection of the propulsion layout and the positioning of the technical spaces on the forehull, afthull, or on the deck. Therefore, by developing different variations of the HLPs and using them to create different design solutions the naval architect can visualize and understand the impact of the major design decisions to the vessel, the LNGBV in this case.

Table II. Characteristics of the design solutions

LNGBV 7500 LNG				
	*Design Solution **I** (bilobe tanks, hybrid propulsion system)*	*Design Solution **II** (membrane tank, mechanical propulsion system)*	*Design Solution **III** (cylindrical tanks, mechanical propulsion system)*	*Design Solution **IV** (cylindrical tanks, diesel-electric propulsion system)*
GENERAL				
Length overall	109.54m	102.87m	110.40m	115.82m
Length b.p.p	106.86m	100.36m	107.71m	113.00m
Beam moulded	22.00m	24.00m	19.00m	27.00m
Height	16.00m	11.00m	18.00m	15.00m
Depth(min)	6.5m	5.8m	7.5m	5.50m
Draft	5.13m	4.6m	6.07m	4.10m
Lightshipweight	6350t	4740t	6680t	6680t
Block Coefficient	0.80	0.73	0.80	0.81
Deadweight	3750t	3750t	3750t	3750t
Total installed power	3300kW	2700kW	3570kW	3600kW
Inert gas system	YES	YES	YES	YES
GCU	YES	YES	YES	YES
Reliquefaction plant	OPTION	YES	YES	OPTION
TANK CAPACITIES				
Ballast water	3900 m^3	4480m^3	5300m^3	5330m^3
PERFORMANCE				
Speed (at the design draft and 100% MCR)	12 knots	12 knots	12 knots	12 knots
PROPULSION SYSTEM				
	Hybrid drive, 4 diesel generator sets, 2 electric motors driving the 2 azimuth thrusters	Mechanical drive, 2 diesel generator sets, 2 DF engines, 2 FPP	Mechanical drive, 2 diesel generator sets, 2 DF engines, 2 FPP	Diesel electric drive, 4 diesel generator sets, 2 electric motors, 2 azimuth thrusters
ACCOMMODATION				
Crew (Single Cabins)	14 people	14 people	14 people	14 people

6. Discussion and Conclusions

The present research work proposes a parametric modelling method based on the principles of KBE. The case study focused on the preliminary design of the LNGBV. The main idea of the technique was the development of the parametric models based on the combination of the different building blocks, the HLPs. The HLPs can be seen as lego bricks, which can change shape, size, and re-order according to the design case and the Naval Architect's decisions.

The significant benefit of the proposed method is that each parametric model is automatically developed within a few minutes. In turn, the generated solutions can be further evaluated with analysis tools. As a result, the Naval Architect is able to perform a broader exploration of the design space and thus, come up with improved designs developed in shorter lead times. In contrast to repetitive engineering work for developing the parametric models, the Naval Architect is committed to creative tasks such as figuring out which design decisions should be examined for each design problem, which is their impact to the final design, which different design variations should be further

examined and optimized.

7. Recommendations for future research

The results of the application of the proposed method to the LNGBV are promising. The presented case study is a self-contained proof of concept, which shows potential in the automation of parametric modelling by using the KBE methodology. However, further research is suggested to harness its full potential.

From a design perspective, it is worthwhile to develop an HLP toolkit to address the design of different ship types. As a first step, the proposed parametric modelling method should be validated for the design of different vessel types with geometrical similarities. As a next step, it is suggested to develop a parametric modelling method to address the design of vessels with radically different geometrical features. This improvement will lead to the exploration of more innovative design concepts.

In order to compare the different solutions, their performance should be assessed. Therefore, research and integration of performance functions into the proposed framework will enable the assessment of the developed design variations. The interface of the proposed framework with the suitable state-of-the-art analysis tools will enable the calculation of each design's performance. Finally, an optimization loop can be also implemented to generate optimized designs according to the design problem. In the context of C-Job Naval Architects, it is suggested to develop the connection with the Accelerated Concept Design (ACD), which is the in-house developed optimization tool based on a surrogate assisted optimization algorithm, the Constrained Efficient Global Optimization (CEGO) algorithm, *de Winter et al. (2019a,b)*.

Acknowledgements

The present paper is part of the research carried out in the context of the first author's Master thesis, which was conducted in TU Delft in cooperation with C-Job Naval Architects.

References

ARENDT, R.; VAN UDEN, E. (2011), *A decision-making module for aiding ship system automation design: A knowledge-based approach. Expert Systems with Applications*, 38(1), pp.410-416

BILIOTTI, I.; BRIZZOLARA, S.; VIVIANI, M.; VERNENGO, G.; RUSCELLI, D.; GALLIUSSI, M.; MANFREDINI, A. (2011), *Automatic Parametric Hull Form Optimization of Fast Naval Vessels*, 11th Int. Conf. Fast Sea Transportation (FAST 2011)

BRIZZOLARA, S.; VERNENGO, G.; PASQUINUCCI, C.; HARRIES, S. (2015), *Significance of parametric hull form definition on hydrodynamic performance optimization*, MARINE 2015 - Computational Methods in Marine Engineering VI, pp. 254-265

BRUINESSEN, T.; HOPMAN, H.; SMULDERS, F. (2013), *Towards a Different View on Ship Design: The Development of Ships Observed Through a Social-Technological Perspective*, Int. Conf. Offshore Mechanics and Arctic Engineering - OMAE. 1, 10.1115/OMAE2013-11585

CALLEYA, J.; PAWLING, R.; RYAN, C.; GASPAR, H. (2016), *Using Data-Driven Documents (D3) to explore a Whole Ship Model*, 11th System of Systems Engineering Conf. (SoSE), 10.1109/SYSOSE.2016.7542947

CHARISI, N.D. (2019), *Parametric Modelling Method based on Knowledge Based Engineering: The LNG Bunkering Vessel Case*, MSc thesis, TU Delft, http://resolver.tudelft.nl/uuid:5321df04-39e6-4128-9eec-c3adcac8a68a

COOPER. S.; FAN. I.; LI. G. (2001), *Achieving competitive advantage through knowledge based engineering – a best practice guide*, Department of Trade and Industry

DAHL, D.; CHATTOPADHYAY, A.; GORN, G. (2001), *The importance of visualisation in concept design*, Design Studies 22/1, pp.5-26

DE WINTER, R.; VAN STEIN, B.; DIJKMAN, M.; BÄCK, T. (2019a), *Designing ships using constrained multi-objective efficient global optimization*, Machine Learning, Optimization, and Data Science, Springer, pp.191–203

DE WINTER, R.; FURUSTAM, J.; BÄCK, T.; MULLER, T. (2019b), *Optimizing Ships Using the Holistic Accelerated Concept Design Methodology*, 14th Int. Symp. Practical Design of Ships and Other Floating Structures (PRADS 2019), Yokohama

DUCHATEAU, E.A.E. (2016), *Interactive evolutionary concept exploration in preliminary ship design*, PhD, TU Delft, https://doi.org/10.4233/uuid:27ff1635-2626-4958-bcdb-8aee282865c8

ERIKSTAD, S.O. (2007), *Efficient Exploitation of Existing Corporate Knowledge in Conceptual Ship Design*, Ship Technology Research 54/4, pp.184-193

GASPAR. H.M. (2018), *Data-Driven Ship Design*, COMPIT Conf., Pavone

JINGJING X.; DAVID T.; PROSHANTO K. M. (2015), *The Use of LNG as a Marine Fuel: The International Regulatory Framework*, Ocean Development & International Law 46/3, pp.225-240

HERNANDEZ, C. (2006), *Thinking parametric design: Introducing parametric Gaudi*, Design Studies 27, pp.309-324

KANELLOPOULOU, A.; KYTARIOLOU, A.; PAPANIKOLAOU, A.; SHIGUNOV, V.; ZARAPHONITIS, G. (2019), *Parametric ship design and optimisation of cargo vessels for efficiency and safe operation in adverse weather conditions*, J. Marine Science and Technology 24/4, pp.1223-1240

KIM, K.; PARK, K.; ROH, G.; CHUN, K. (2019), *Case Study on Boil-Off Gas (BOG) Minimization for LNG Bunkering Vessel Using Energy Storage System (ESS)*, J. Marine Science and Eng. 7/5, 130

KLEIN WOUD, H.; STAPERSMA, D. (2002), *Design of Propulsion and Electric Power Generation Systems*, IMarEST publications, IMarEST

LA ROCCA, G.; VAN TOOREN, M. (2010), *Knowledge-based engineering to support aircraft multidisciplinary design and optimization*, J. Aerospace Eng. 224/9, pp.1041-1055

LA ROCCA, G. (2012), *Knowledge based engineering: Between AI and CAD. Review of a language based technology to support engineering design*, Advanced Engineering Informatics 26, pp.159-179

LA ROCCA, G.; VAN TOOREN, M.J.L. (2006), *A Modular Reconfigurable Software Modelling Tool to Support Distributed Multidisciplinary Design and Optimisation of Complex Products*, 16th CIRP Int. Design Seminar, Kananaskis

MAISONNEUVE, J.J.; HARRIES, S.; MARZI, J.; RAVEN, H.C; VIVIANI, U.; PIIPPO, H. (2003), *Towards optimal design of ship hull shapes*, IMDC Conf., pp.31-42

MARZI, J.; PAPANIKOLAOU, A.; CORRIGNAN, P.; ZARAPHONITIS, G.; HARRIES, S. (2018), *HOLISTIC Ship Design for Future Waterborne Transport*, 10.5281/zenodo.1436316.

NOWACKI, H. (2010), *Five decades of Computer-Aided Ship Design*, Computer-Aided Design 42, pp.956-969

PAPANDREOU, C.; PAPANIKOLAOU, A. (2015), *Parametric Design and Multi-objective Optimization of SWATH*, 5th Int. Symp. on Ship Operations, Management and Economics, Athens

PAPANIKOLAOU, A.; ZARAPHONITIS, G.; BOULOUGOURIS, E.; LANGBECKER, U.; MATHO, S.; SAMES, P. (2010), *Multi-objective optimization of oil tanker design*, J. Marine Science and Technology 15, pp.359-373

PAPANIKOLAOU, A. (2014), *Ship Design - Methodologies of Preliminary Design*, Springer

PAPANIKOLAOU, A. (2019), *A Holistic Approach to Ship Design Volume 1: Optimisation of Ship Design and Operation for Life Cycle*, Springer

PAPANIKOLAOU, A.; FLIKKEMA, M.; HARRIES, S.; MARZI, J.; NENA, R.; TORBEN, S.; YRJANAINE, A. (2020), *Tools and Applications for the Holistic Ship Design*, Transport Research Arena TRA2020 - Rethinking Transport, Helsinki

PARSONS, M.G. (2004), *Parametric Design*, Ship Design and Construction, SNAME

REHN, C.F. (2018), *Ship design under uncertainty*, PhD, NTNU, Trondheim

PRIFTIS, A.; PAPANIKOLAOU, A.; PLESSAS, T. (2016), *Parametric Design and Multiobjective Optimization of Containerships*, J. Ship Production and Design 32, pp.1-14

SANCHES, F.M. (2016), *Parametric modelling of hull form for ship optimization*, MSc thesis, TU Lisbon, Lisbon

SCHUT, E.J.; VAN TOOREN, M.J.L (2007), *A Knowledge Based Engineering approach to automation of conceptual design option selection*, 10.2514/6.2007-968.

SCHUT, E.J.; VAN TOOREN, M.J.L. (2008), *Engineering Primitives to Reuse Design Process Knowledge*, 4th AIAA Multidisciplinary Design Optimization Specialist Conf., Schaumburg

SOBIESKI, J.; MORRIS, A.; VAN TOOREN, M.J.L. (2015) *Multidisciplinary Design Optimization Supported by Knowledge Based Engineering*, J. Wiley & Sons

TIMUR, M. (2015), *A parametric modelling tool for high speed displacement monohulls*, MSc thesis, https://dspace.mit.edu/handle/1721.1/100091

VAN DEN BERG, T. (2013), *Harnessing the potential of Knowledge Based Engineering in manufacturing design*, MSc thesis, TU Delft, https://repository.tudelft.nl/islandora/object/uuid%3Ad44876fe-45dd-44ae-8947-622613eb963c

VAN TOOREN, M.J.L; LA ROCCA, G.; KRAKERS, L.; BEUKERS, A. (2003), *Design and technology in aerospace. Parametric modelling of complex structure systems including active components*, 13th Int. Conf. Composite Materials, San Diego

WAN, J.; WANG, N.; GOMEZ-LEVI, G. (2005), *Parametric modeling method for conceptual vehicle design*, 25th Computers and Information in Eng. Conf., Long Beach, Vol.3, pp.403-410

WEI, J.H. (2016), *Parametric modelling for determining aircraft stability & control derivatives*, MSc thesis, TU Delft, https://repository.tudelft.nl/islandora/object/uuid:cd095318-3272-400a-822d-

e7990480a904?collection=education http://resolver.tudelft.nl/uuid:cd095318-3272-400a-822d-e7990480a904

WU, Y.H.; SHAW, H.J. (2011), *Document Based Knowledge Base Engineering Method for Ship Basic Design*, Ocean Engineering 38/13, pp.1508-1521

YANG, H.Z.; CHEN, J.F.; MA, N.; WANG, D.Y. (2012), *Implementation of knowledge-based engineering methodology in ship structural design*, Computer-Aided Design 44, pp.196-202

Support for the Selection of Environmental Impact Abatement Equipment in the Early Stage Design

Jeroen Pruyn, Delft University of Technology,Delft/Netherlands, j.f.j.pruyn@tudelft.nl
Ivar van Grootheest, Delft University of Technology, Delft/Netherlands, I.V.vanGrootheest@outlook.com
Frans Hendrik Lafeber, MARIN, Wageningen/Netherlands, F.Lafeber@marin.nl
Marco Scholtens, NMT, Rotterdam/Netherlands scholtens@maritimetechnology.nl

Abstract

Stricter regulations for shipping on the emission to air and water are introduced. To deal with this, a part of the Horizon2020 NAVAIS project is devoted to the identification of relevant regulations and the design of a tool to select the optimal combination of abatement options to achieve or go beyond the limits set by these regulations. It is an early-stage design tool, which includes the mutual influences of abatement options on each other, allowing/giving a deeper understanding of trade-offs to be made. The results of this tool show the trade-off between emission abatement and costs.

1. Introduction

The environmental impact of shipping is significant, *Buhaug et al. (2009)*. A process of further and further regulating both emissions to the air and to the water is ongoing (e.g. EU's Good Environmental Status). The most well-known emissions are greenhouse gasses (GHG), Nitrogen Oxides (NO_x), Sulphur Oxides (SO_x) and particulate matter (PM), *Buhaug et al. (2009)*, *EEA (2012)*. Also, pollution of the water with sewage or oil is banned, more recently ballast water needs to be treated to avoid spreading organisms into new habitats, *IMO (2004)*. Less known is noise pollution, which is receiving more attention recently as well, *McKenna et al. (2012)*.

Methods to comply with these regulations and limitations are not evident. In many cases, reducing one element increases another. For example, reducing NO_x will result in either more PM when working with the engine load, or it will result in more CO_2 when actively filtering the exhaust gasses. Furthermore, all these systems require space (besides additional investments and running costs) in the vessel and should be considered in an early stage of the design to not end up with space issues in a later design stage. This was also recognised by the European Commission and has led to the NAVAIS project. Within this project, a tool to support this early stage design with a selection tool was developed. This tool was named TEchnology Selection Tool for Emission Reduction (TESTER). In Section 2 both the relevant regulations and already available tools and approaches will be discussed. In Section 3 the methodology is described in detail, followed by two applications in Section 4. Finally, Section 5 will conclude and give recommendations for further research.

2. Literature Review

The literature review contains two important parts, the first part is an overview of regulations and an assessment of the relevance and type of compliance especially considering the early stage of the design. The second part focusses on identifying relevant research on how to select the best combination of equipment to comply with the selected regulations.

2.1. Regulations

Three different levels of regulations are in force in the maritime sector; international, national and local. For this study, the international (International Maritime Organisation, IMO) regulations are assessed. To identify the potential impact of national regulations, also the regulations of Canada, Norway and the European Union (EU) have been studied. It was currently beyond the scope of the project to also study

local legislations, which can differ per port or state. Local regulations are relevant when designing for a concrete situation and the option to include specific local regulations is a requirement for the TESTER development.

Table I shows all identified emissions to either water or air. The first column identifies the type of emission, the second column refers to the relevant regulation. In some cases local regulations are added to show stricter limits may apply. These limits are presented in the third column. In some cases, there is not one specific limit, but a formula. Especially in the case of the EEDI, NO_x and URN (underwater radiated noise), the limits are usually represented graphically. These will not be repeated in this paper; for these figures, we refer to the reference indicated in the fourth column. Finally, in the last column, the applicability for the NAVAIS project, but also for the TESTER tool is indicated. If a "No" is indicated, the text behind the arrow shortly explains the reason for this. The most common reason is that the implementation has no interaction with other systems, however, TESTER's key contribution is the integration of system impacts. In several cases the early-stage design is not the moment to address an issue as more detailed information is required to estimate the impact. For checking compliance with underwater radiated noise (URN) limits, for example, details of the propeller design are needed, which are not available in the early design phase. Finally, in some cases, no limits were identified and therefore the emissions will not be included.

Table I: Identified legislation for emissions to air and water from ships

Environmental impact	**Regulations**	**Limit**	**References**	**Applicable for TESTER**
Oil	MARPOL Annex I, Ch.3, Pt. C, Reg. 15	<15 ppm	*IMO (2017)*	Yes
	Canada – TP12301	<5 ppm		
Noxious liquid substances	MARPOL Annex II	Various limits	*IMO (2017)*	No => No system dependency
Harmful substances in packaged form	MARPOL Annex III	List of threats	*IMO (2017)*	No => No system dependency
Sewage	MARPOL Annex IV	0.00926*V*D l/min	*IMO (2017)*	Yes
	Canada – TP15211E, Annex I, Sec. 5.3	<14 Particle count/ml		
Garbage	MARPOL Annex V	Various limits	*IMO (2017)*	No => No system dependency
Nitrogen Oxides (NO_x)	MARPOL Annex VI, Ch. 3, Reg. 13	Variable limit	*IMO (2017)*	Yes
Sulphur Oxides (SO_x)	MARPOL Annex VI, Ch. 3, Reg. 14	0.1 %	*IMO (2017)*	Yes
Particulate Matter (diameter smaller than 2.5 μm, $PM_{2.5}$)	MARPOL Annex VI, Ch. 3, Reg. 14	0.5 %	*IMO (2017)*	Yes
Volatile Organic Compounds (VOC)	MARPOL Annex VI, Ch. 3, Reg. 15	No limit for methane-slip (LNG)	*IMO (2017)*	Yes => the impact can be established even without legal limits.
Carbon Dioxide (CO_2)	MARPOL Annex VI, Ch. 3, Reg. 20/21–EEDI	Variable limit	*MEPC (2012), IMO (2017)*	Yes
Underwater radiated noise (URN)	IMO MEPC.1/Circ. 833	Currently: all voluntary.	*DNVGL (2018b), IMO (2014b, JOMOPANS (2017), GM (2017), OSPAR (2017), LR (2018), RINA (2017), ABS (2018), POV (2017), BV (2018)*	No => More detailed design required
	EU Marine Strategy Framework Directive for Good Environmental Status – Descriptor 11			
	OSPAR/JOMOPANS, BIAS, Green Marine, Classification			

Above water noise	IMO Resolution MSC.337(91)	Only local	*IMO (2014a)*	No => More detailed design required
Surface waves	Only local	Limits on wash or speed	*Bolt (2001), Feldtmann (2000), Kirkegaard et al. (1999), Murphy et al. (2006), Raven and Valkhof (1998)*	No => N system dependency, but hull shape dependent
Electromagnetic radiation	International Commission on Non-Ionizing Radiation Protection (ICNIRP), International Committee on Electromagnetic Safety (ICES)	Regulated at the equipment level	*Mitson (1995)*	No => Equipment is approved separately
Heat	No legislation found	N/A	N/A	No => No legislation
Light – visible / Infrared (IR)	Part C of COLREG72, CAP437 and Annex 14, IMO SOLAS	Only requirements on required light, no limitations. IR limitation focus on naval ships only.	*Authority (2016), Commandant (1999), MSC (2006)*	No => No limitations
Ballast water	BWM-2004, D-2 standard	D-2 Standard	*IMO (2004)*	No => Local operations

2.2. Ship Design Solutions

In the maritime industry, the use of an optimisation algorithm for the selection of abatement options can be traced back to the research done in 2005 by *Winebrake et al. (2005)*. This study uses a nonlinear optimisation algorithm to find a cost-effective combination of technologies for ferries. A lot of attention has also been paid to this optimisation problem by *Balland et al. (2010,2012,210*4,2015). These authors use an integer linear optimisation algorithm for the selection of abatement options. They also addressed several decision factors such as changing regulations over time, uncertainty in emission reductions and the simultaneous selection of the mechanical systems and other aspects. The simultaneous selection of abatement options and machinery systems is also an option, *Trivyza et al. (2018), Wagner (2005)*. In their study, they use a genetic algorithm to find the most cost-effective combinations of energy systems over the ship's life cycle. This indicates that a variety of algorithms have already been applied for this type of optimisation problem. A key advantage of OR (Operations Research) techniques is that a clear answer is provided, the major drawback is the amount of data required to evaluate and select options.

The Multi-Criteria Decision-Making (MCDM) approach solves this data issue by working with relative weights, rather than absolute numbers. In that way, multiple unrelated aspects can be combined. The analytical hierarchy process (AHP), which uses a pairwise comparison to determine the weight of each element and choice is the most popular, *Hansson et al. (2019), Ren and Lützen (2015), Schinas and Stefanakos (2014), Yang et al. (2012)*. Distance-based and other weight-based methods have also been applied, *Corbett and Chapman (2006), Ölçer and Ballini (2015), Vakili (2018)*. Despite the multi-criteria approaches used in the developed models, they always contain some degree of subjectivity. Therefore, an optimisation approach was chosen for the selection tool. For clarity, the studied approaches have been combined in an overview in Fig.1 (left).

In addition to the selection approaches of individual aspects, it is also important to consider how to select the optimal combination. As can be seen in Fig.1 (right) three main approaches were identified in the literature. Some are purely economic, such as a Net Present Value (NPV), *Balland et al. (2015), Corbett and Chapman (2006), Ölçer and Ballini (2015), Schinas and Stefanakos (2014)* calculation, or life cycle costing (LCC), *Trivyza et al. (2018), Wang et al. (2005)*. Others only consider the environmental aspects in a life cycle assessment (LCA), while two mixed approaches were identified,

cost-benefit analysis (CBA), *Balland et al. (2014), Bari et al. (2011), Hansson et al. (2019), Ren and Lützen (2015), Vakili (2018), Yang et al. (2012)* and Marginal Abatement Cost Curves (MACC), *Calleya et al. (2015), Wang et al. (2010), Winebrake et al. (2005)*. Interesting are the options offered by LCC and LCA to compare the environmental impacts of different kinds with each other, either using the concept of costs to society, or an indicative value such as ecopoints.

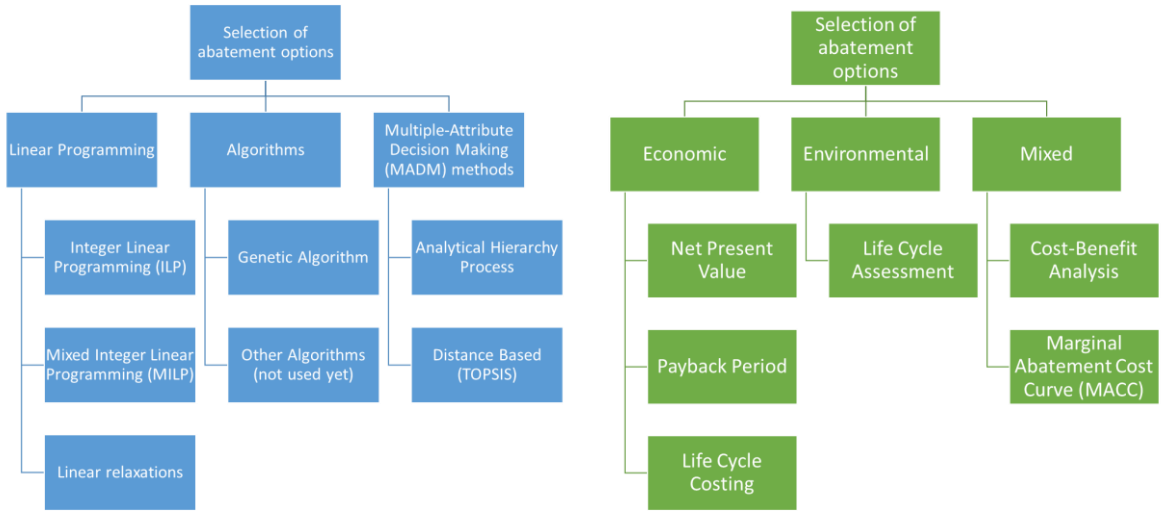

Fig.1: Taxonomy of decision-making techniques used in the reviewed literature. Optimisation (left) and Evaluative (right)

The MACC compares costs and impacts as measures are sorted by costs and the environmental impact is shown. In a MACC graph, the achieved impact reduction is shown on the horizontal axis and on the vertical the costs per unit of reduction is presented. The measures are sorted by the costs (cheapest first) and the costs could even be negative. This way a shipowner can identify options that will not only reduce the impact but also save money. A second stage could be to increase the impact reduction until a break-even is reached between costs and profits of emission reduction measures. Although the MACC is a very useful first step, a crucial element is missing in the selection process; some abatement options are mutually exclusive or influence each other. Also, the available methods are often limited to GHG, without taking into account other regulations and impacts.

Finally, based on the literature described above, four major elements for the abatement can be identified. The first is the energy systems, these deliver the power for the activities of the ship. The main groups within these elements are internal combustion engines, batteries and fuel cells. The second, related, element is the fuel. The main groups identified here are traditional fuels, transitional fuels (biodiesel, LNG) and alternative fuels. The last group currently has a low Technology Readiness Level (TRL) in general, *Hansson et al. (2019).* The next element is the energy efficiency increasing options. Primarily ship design and additional power and propulsion systems (waste heat recovery, solar panels, sails) fall in this group. The fourth element is the emission-reducing systems. Here, the primary methods are related to the engine (reducing the creation of emission), while the secondary measures are related to capturing emission in the exhaust gas. An overview of the systems with their advantages (third column) and disadvantages (last column) is presented in Table II (FC is Fuel Consumption).

Table 2: Abatement Systems

Main Element	System	Advantage	Disadvantage
Energy systems	Diesel engine	High specific power	Noise and high NO_x emissions
	Gas engine	High specific power and lower NO_x	Noise and CH_4 emissions
	Batteries	No emissions and noise,	Low specific power and energy
	Ultracapacitor	High specific power and no emissions	Low specific energy
	Flywheel	High specific power and no emissions	Complex design, not for main propulsion
	Hydrogen fuel cell	No emissions and low noise	Low specific power
Fuels	Diesel fuels (high sulphur content)	High energy density; low fuel cost	High SOx, CO_2 emissions
	Diesel fuels (low sulphur content)	High energy density, low SO_x	High fuel costs, CO_2 emissions
	LNG	Low SO_x; lower CO_2, PM and NO_x	Dimensions and costs, CH_4 slip
	Biofuels	Lower CO_2; No system impacts	Increase of FC, affects (fuel) system
	LPG	Low SO_x; lower CO_2, PM and NOx	Safety, Butane slip
	Methanol	Reduction of CO_2, NOx and PM	Corrosive, low energy density
	Ammonia	No CO_2	Low energy density, toxic
	Hydrogen	No emissions in fuel cell	Low energy storage density
energy-efficiency	Lightweight construction	Reduction of FC	High investment costs
	Optimisation of hull form	Reduction of FC	High investment costs, in refit
	Hull coating	Reduction FC and URN	Extra investment
	Air (cavity) lubrication	Reduction of FC	Less effective off-design
	Waste Heat Recovery (WHR)	Reduction of FC	High costs and efficiency
	Propeller (flow) optimisation	Reduction of URN and/or FC	Trade-off between URN and efficiency
	Wind recovery systems	reduction of FC	Limited operational envelope and space
	Solar panels	reduction of FC	Low and variable energy yield
	Energy-efficient lighting	Reduction of FC	-
emission-reduction	Humid Air Motor (HAM)	Reduction of NO_x	Increase of FC
	Fuel Water Emulsion (FWE)	Reduction of NO_x and PM	Increase of FC, corrosive
	Direct Water Injection (DWI)	Reduction of NO_x	Increase of FC
	Exhaust Gas Recirculation (EGR)	Reduction of NO_x and CH_4	Increase of FC and PM
	Selective Catalytic Reduction (SCR)	Reduction of NO_x and PM	Increase of FC
	Diesel Particulate Filter (DPF)	Reduction of PM	Increase of FC, sulphur
	Diesel Oxidation Catalyst (DOC)	Reduction of PM	Sulphur in fuel
	Exhaust gas scrubber	Reduction of SO_x and PM	Dimensions, Increase of FC

3. Methodology

In this section, a selection of approaches and methods will be made based on the advantages and disadvantages identified in the literature study. Also, the setup of the TESTER (TEchnology Selection Tool for Emission Reduction) tool will be discussed.

The chosen approach should deal with four important elements:

1. The model includes the influences of systems on each other.
2. The model evaluates more environmental impacts than only GHG.
3. An optimisation is preferred over MADM and
4. The selected reduction options are all available in the model.

These requirements have a huge impact on the choice of optimisation approaches as the problem becomes highly non-linear, excluding LP (Linear Programming) solutions. To combine or compare the environmental impact, the costs-to-society (CTS) approach was taken from the LCA and LCC approaches. As external costs are primarily to compare different impact categories and not intended to function as real costs for the shipowner, the choice was made to use a multi-objective optimisation. This is then split between external costs and direct expenses for the owner (investment in equipment and operational costs). The first objective is the minimization of internal (company-related) costs, while the second objective is the external (environment-related) virtual costs. This allows the different costs to remain separated and to be able to adjust their impact using weights. The four requirements implicate that the model can deal with complex interactions and administrate various emissions side by side.

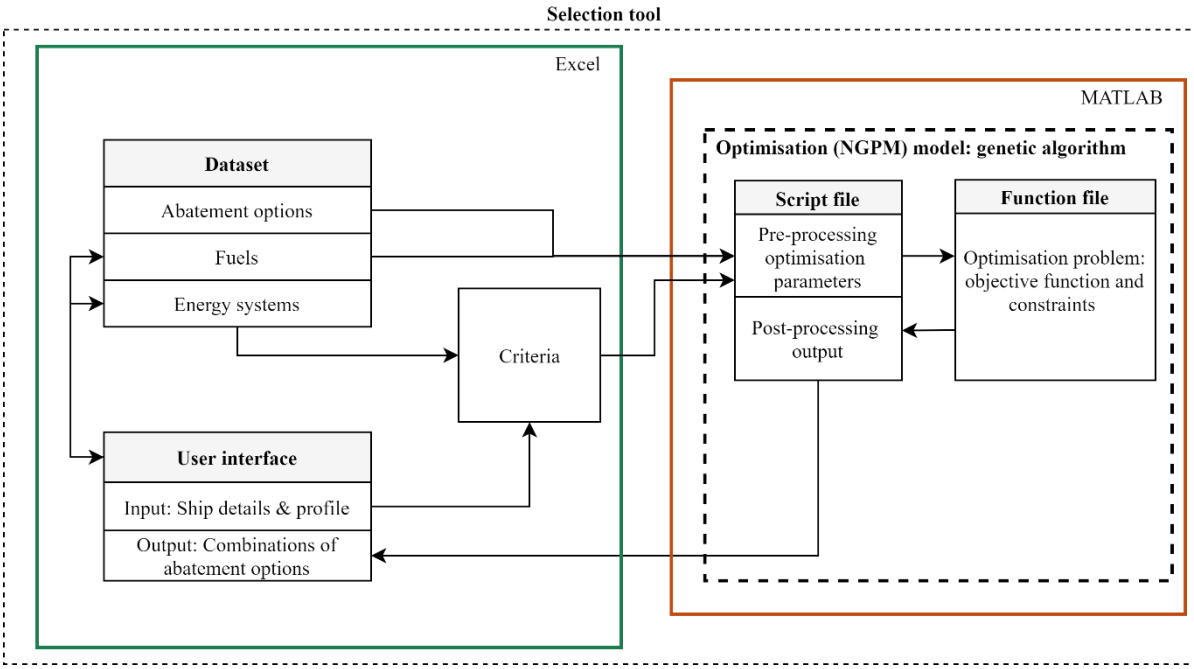

Fig.2: Flow chart of the selection tool

The result is TESTER; a model with two components the input, output and background data is managed in Microsoft excel® for relatively easy use and control. The optimisation is done in Mathworks MATLAB® making use of the non-dominated sorting genetic algorithm II solver. The solver is suitable for the problem described, although a more in-depth study of potential solvers should be executed in the future to identify the optimal solver. The final model is presented in Fig.2.

The actual implementation and verification of this model can be found in the publicly available deliverables D4.1 and D4.2 of the NAVAIS project, *Pruyn (2019).*

4. Case Studies

The NAVAIS project focusses on improving the environmental impact of a family of road ferries and a family of workboats. Due to this focus, TESTER was tested on two instances, one of each ship type. In Section 4.1 the road ferry and the optimisation results will be discussed, whereas in Section 4.2 the selected workboat and optimisation will be discussed.

4.1. Road Ferry

The electric "Road Ferry 9819" has been chosen as the reference vessel for the case study because it has similar characteristics to the intended concept design in the NAVAIS project. This type is also a double-ended ferry configuration, which has a comparable passenger/car capacity and has full-electrical propulsion.

Some information about this reference vessel is given in Table III and Fig.3. The energy system configuration of the road ferry 9819 is full-electric, in which the four azimuth thrusters are electrically driven. The road ferry has back-up diesel generator sets which are required by SOLAS regulations for passenger vessels as an emergency generator for redundancy, but they are not used during normal operation. Additionally, the reference ship is designed for an operational area that can have ice conditions. In that case, the diesel generators can be used to give an extra boost in addition to the power obtained from the batteries. However, the aforementioned scenarios are rare, so it can be assumed that the road ferry will mainly sail electrically with the power being obtained from the batteries.

Fig.3: Damen road ferry 9819, *Damen (2020a)*

Table III: Ship specifics (Road ferry 9819) and operational profile, *Damen (2020a)*

Length	98.4 m
Beam	20.2 m
Azimuth thrusters	4*520 kW
Diesel generator sets	2*565 ekW
Battery pack	4000 kWh
Free Sailing	15 min
Manoeuvring	4 min
At berth/charging	11 min

Therefore, only the performance of the full-electric battery mode is evaluated as the benchmark. The environmental and economic performance of the reference vessel is evaluated based on the annual operational profile. The annual profile is based on 97% availability, in which 10 days per year can be reserved for maintenance work. The operational profile is divided into three conditions: free sailing, manoeuvring, and at berth. The assumed operational profile for a one-way trip of 30 minutes is given in Table III. At berth, the electric ferry will use shore power for recharging the batteries.

The assumed energy consumption is estimated at around 550 kWh per trip. This is based on the required propulsion power to drive the four azimuth thrusters (e.g. distribution of 70% aft and 30% forward), an effective efficiency, trip time and an assumed auxiliary load (~50 kWh per trip). It is assumed that the

road ferry is operational for 15 hours a day, resulting in a total of 30 trips. This gives a total energy consumption of 16.5 MWh per day and 5841 MWh per year. 85% of the annual energy consumption is used for propulsion power and the other 15 % is used for the auxiliary energy consumption such as Heating Ventilation and Air Conditioning (HVAC).

The internal costs and external costs of the benchmark energy system are summarised in Table IV. This table shows the build-up of the internal costs on an annual basis, which is a summation of the annual depreciation and interest costs and the operational costs. Furthermore, it shows that the annual investment costs are of the same order as the operational costs (280.0 k€ investment costs and 351.8 k€ Operational costs). The benchmark electricity is assumed to be produced from a European mix of energy sources, including more polluting sources such as coal. This electricity has upstream emissions (WTT) from the production, which are based on a European average carbon intensity (emission) factor of 466 gCO2-eq/kWh, *Gilbert et al. (2018), Moro and Lonza (2018).* A European average industrial electricity (mix) price of 70 [€/MWh] is used, which is based on values from, *EC (2019).* TTP are emissions of the energy system on board. The Costs to Society (CTS) factors are taken from, *Lafeber (2019).*

Table IV: Benchmark performance of the road ferry

B	C	D
Selected energy system		**Batteries (lithium-ion)**
Predefined fuel		**Electricity[mix]**
Energy delivered by energy system [MWh/year]		**3564**
Fuel consumption [MWh/year]		**4950**
Internal (investment+operational) costs		
Total investment (equipment+installation) costs [k€]	**k€**	**2800.0**
Annual investments costs [k€/year]	**k€|y**	**280.0**
Operational costs: fuel cost factor [€/MWh]	**€**	**70.00**
Operational costs: fuel costs [k€/year]	**k€|y**	**346.5**
Operational (maintenance) costs [k€/year]	**k€|y**	**5.3**
Total operational costs [k€/year]	**k€|y**	**351.8**
Total annual internal costs [k€/year]	**k€|y**	**631.8**
External costs of (WTT+TTP) emissions		
External costs of upstream (WTT) emissions		
E_CO_2-eq [ton/year] & External costs CO_2-eq [k€/year]	**t|y 2316.6**	**k€|y 125.1**
External costs of operational (TTP) emissions		
E_NO_x [ton/year] & External costs NO_x [k€/year]	**t|y -**	**k€|y -**
E_SO_x [ton/year] & External costs SO_x [k€/year]	**t|y -**	**k€|y -**
E_PM [ton/year] & External costs PM [k€/year]	**t|y -**	**k€|y -**
E_VOC [ton/year] & External costs VOC [k€/year]	**t|y -**	**k€|y -**
E_CO_2 [ton/year] & External costs CO_2 [k€/year]	**t|y -**	**k€|y -**
Total external costs (WTT+TTP) [k€/year]		**k€|y 125.1**

The optimisation algorithm is tested for different population sizes and numbers of generations, as this is case dependent. The population size largely determines the variability in the solutions. However, a larger population size together with a larger amount of generations increase the solution time. For this type of decision context, the emphasis is not on the exact solution, but on scanning and finding a feasible design space for possible combinations within a reasonable calculation time. Using the MATLAB Graphical User Interface (GUI), it was determined after how many generations the algorithm had converged. Furthermore, the number of solutions and solution time were noted.

The test overview for the road ferry is presented in Table V. It shows that the optimisation run has often converged in about 10 generations, therefore the number of generations for the optimisation is set to 20 to include a margin. Furthermore, it appears that the results remain the same if the population size increases. Therefore, the selected population size is 50.

Table V: Determination of population size and number of generations for road ferry case

Population Size	Nr. Of generations	Convergence after generation.#	Nr of Solutions	Solution Time (s)	Obj 1 (k€/year)	Obj 2 (k€/year)
50	10	10	18	3.3	673.6	92.6
50	20	15	28	6.9	664.4	95.5
50	30	13	25	7.6	664.4	95.5
100	20	10	21	11.4	664.4	95.5
200	20	11	21	15.6	664.4	95.5

The final solution is visualised in Fig.4. This figure shows the benchmark performance in terms of internal costs and external costs. It shows how the combinations (blue circles) lead to a reduction of the external costs of emissions and how these combinations impact the internal costs. In the output, two sets of solutions can be distinguished. These solutions are studied in more detail below. In Table VI the solution with the lowest internal cost (far left bullet) and the solution with the lowest external costs (far right bullet) are compared to the initial benchmark.

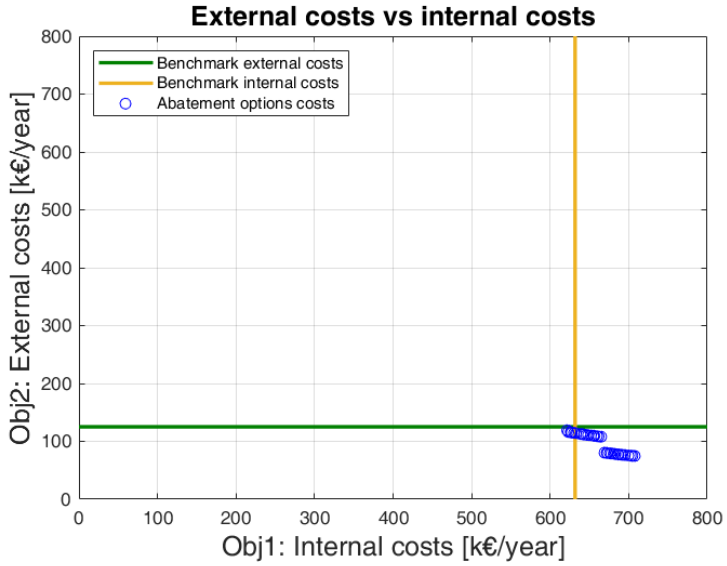

Fig.4: output case study road ferry relative to the benchmark

Table VI: Comparison of the optimised solution with the benchmark for the road ferry.

Element	Benchmark	Min. Internal Costs	Min. External Costs
Internal Costs (k€/year)	631.8	621.6	707.7
External Costs (k€/year)	125.1	119.2	74.8
Abatement Options			
System 1	Electricity [EU mix]	Electricity [EU mix]	Electricity [Renewable energy]
System 2		Hydrodynamically optimised hull form and appendages	Hydrodynamically optimised hull form and appendages.
System 3			Propeller optimisation - Higher efficiency, higher URN
System 4			Solar panels

For the solutions with the lower internal costs, hydrodynamic design optimisation is responsible for a decrease in overall costs, as this is a relatively cheap option, but could impact the operational costs positively for many years. In the minimal external costs, the solar panels are an investment in the future; it will make the ship more expensive, but the ship's impact is reduced further. In this situation, "green" electricity is also considered. In a sensitivity study, it was identified that both lowering the costs of green electricity and lowering the upstream emissions would cause the optimiser to find more optimal solutions adopting green electricity instead of the current "grey" electricity mix currently available in Europe.

Since the ferry was already electric, no major improvements were achieved in these optimisations. Still, two relevant abatements systems or approaches were identified to lower emissions further without increasing the benchmark costs: Hull Optimisation and High-efficiency propellers. The latter will most likely increase the Underwater Radiated Noise, but without any strict regulations available yet, the efficiency gain seems preferable at this moment in time.

4.2. Workboat

The Damen workboat "UV 4312", Fig.5, Table VII, is chosen as the reference vessel for this case study because the UV 4312 has similar dimensions to the intended NAVAIS subject. The vessel has a gross tonnage of 499 GT. The energy system configuration is diesel-electric, in which two azimuth thrusters with ducted propellers are electrically driven by two electric motors. The vessel has three diesel gensets (Volvo D16) with a rated power of 470 ekW each, *Damen (2020b)*. The reference vessel also has a smaller diesel genset (Volvo D7) of 139 ekW. This small diesel genset can support the main diesel gensets or provide the power for smaller loads. The diesel-electric configuration with a total of four diesel gensets provides flexible power supply for the 750 kW propulsion system and other loads on board. The high-speed diesel engine is the most suitable type for this type of workboat, because of the power range and since there is limited space in the machinery room.

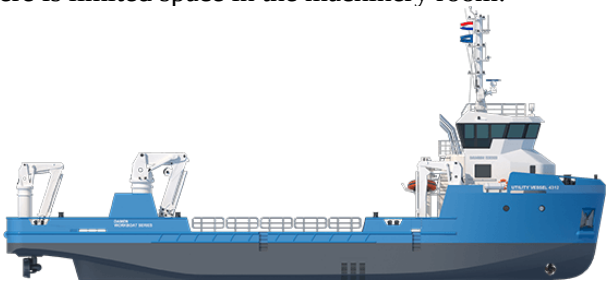

Fig.5: Reference vessel Damen workboat UV 4312, *Damen (2020b)*

Table VII: Ship specifics (UV 4312) and operational profile, *Damen (2020b)*

Length	43.27 m
Beam	12 m
Azimuth thrusters	2
Bow thrusters	1
Electric motors	2*375 ekW
Main diesel gensets (Volvo D16)	3*470 ekW
Small diesel genset (Volvo D7)	1*139 ekW
Free sailing	5 h (100% use of 2*D16 @ 90% MCR)
Station keeping (Dynamic Positioning)	2 h (80% use of 2*D16 @ 90% MCR)
Moored (different tasks)	5 h (70% use of 2*D16, 1*D7 @ 90% MCR)

The workboat is almost always operational on year-basis and is laid-up for maintenance and classification every five years. Therefore, the assumed annual operational profile is based on 354 operational days. The operational profile of a workboat can vary greatly. The reference vessel is designed for an endurance of a maximum of two weeks. The assumed average operational profile is based on 12 h a day and is given in Table VII. The profile is divided into three operational phases: free sailing, station keeping and moored. The table shows the assumed operational characteristics of diesel gensets. The time factor is the relative operational time of the diesel gensets and the load factor is expressed with respect to Maximum Continuous Rating (MCR). In free sailing, two diesel gensets are capable to generate the propulsion power of 750 ekW. In station keeping, both the azimuth thrusters and the bow thruster can be used, requiring slightly less power. In the moored phase the load can be significant, e.g. due to the required power for deck machinery. If necessary, depending on the location and occupation of the ship, the energy demand during the night for Heating Ventilation Air Conditioning (HVAC) can be generated by the small diesel generator (D7).

The benchmark performance including internal costs and external costs is summarised in Table VIII. The upstream (CO_2 equivalent) emissions are based on an emission factor of 43 gCO_2-eq/kWh for (LS) MGO, *DNVGL (2018a), Verbeek et al. (2011).* The quantified emissions are in the same order as other studies, e.g. *Ammar and Seddiek (2017), Madsen et al. (2011).* The fuel cost of (LS)MGO (610 €/ton) is based on bunker prices for Rotterdam, https://shipandbunker.com/prices/emea/nwe/nl-rtm-rotterdam. The total annual internal costs (404 k€/y) and the total external costs (307 k€/y) are in the same order of magnitude. It is important to note that the benchmark design is not fulfilling the current regulations for NO_x emissions.

Table VIII: Benchmark performance of the workboat

	B	C	D
51	**Selected energy system**	**HS-4s Diesel (CI) engine (Tier II)**	
52	Predefined fuel	**LSMGO**	
53	Energy delivered by energy system [MWh/year]	**3594**	
54	Fuel consumption [MWh/year]	**7375**	
55	**Internal (investment+operational) costs**		
56	Total investment (equipment+installation) costs [k€]	**k€ 423.0**	
57	Annual investments costs [k€/year]	**k€|y 16.9**	
58	Operational costs: fuel cost factor [€/ton]	**€|t 610**	
59	Operational costs: fuel costs [k€/year]	**k€|y 379.7**	
60	Operational (maintenance) costs [k€/year]	**k€|y 7.2**	
61	Total operational costs [k€/year]	**k€|y 386.9**	
62	Total annual internal costs [k€/year]	**k€|y 403.8**	
63	**External costs of (WTT+TTP) emissions**		
64	**External costs of upstream (WTT) emissions**		
65	E_CO_2-eq [ton/year] & External costs CO_2-eq [k€/year]	**t|y 318.6**	**k€|y 17.2**
66	**External costs of operational (TTP) emissions**		
67	E_NO_x [ton/year] & External costs NO_x [k€/year]	**t|y 15.9**	**k€|y 119.8**
68	E_SO_x [ton/year] & External costs SO_x [k€/year]	**t|y 1.2**	**k€|y 12.0**
69	E_PM [ton/year] & External costs PM [k€/year]	**t|y 1.5**	**k€|y 49.0**
70	E_VOC [ton/year] & External costs VOC [k€/year]	**t|y 0.6**	**k€|y 1.7**
71	E_CO_2 [ton/year] & External costs CO_2 [k€/year]	**t|y 1995.7**	**k€|y 107.8**
72	**Total external costs (WTT+TTP) [k€/year]**		**k€|y 307.4**

The optimisation algorithm has been run using the following settings: the initial population size of 300 and a total number of 40 generations. These values are both much higher than in the electrical ferry case. The more extensive set of relevant abatement options is responsible for this. The output of a genetic algorithm can vary for different optimisation runs. Therefore, the optimisation output with the lowest objective values is selected and the corresponding output data is also noted. First of all, the 11 generated solutions are all feasible. The solution time of this optimisation run was 65.6 seconds and the optimisation converged after 32 generations. The last generation is visualised in Fig.6. This last generation gives a mean distance of 463, a mean objective 1 of 452 [k€/year] and a mean objective 2 of 176 [k€/year]. The figure also shows the benchmark performance in terms of the internal costs and

external costs, although this system does not meet the regulations at this moment. The solutions are close to the internal costs of the benchmark because the extra investment costs are offset by lower operational expenses, primarily fuel costs. The objective values of these solutions are studied in more detail below. In Table IX the solution with the lowest internal cost (far left bullet in Fig.6) and the solution with the lowest external costs (far right bullet) are compared with the initial benchmark.

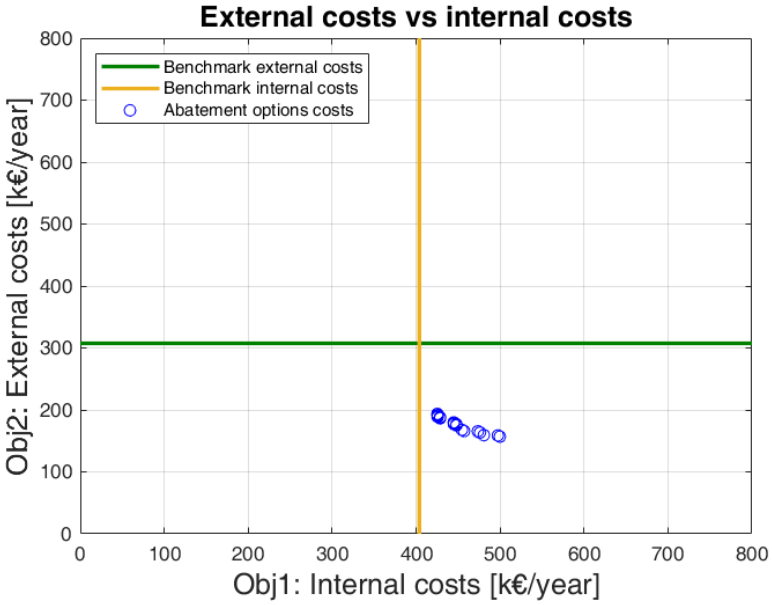

Fig.6: output case study workboat relative to the benchmark

Table IX: Comparison of the optimised solutions with the benchmark for the workboat.

Element	**Benchmark**	**Min. Internal Costs**	**Min. External Costs**
Internal Costs (k€/year)	404	425	500
External Costs (k€/year)	307	194	160
Abatement Options			
System 1		Marine Diesel Oil 0.1%S (MDO)	Marine Gas Oil 0.1%S (LSMGO)
System 2		Selective Catalytic Reduction (fuel <1.5 %S) (SCR)	Fuel Water Emulsification (FWE or WIF)
System 3		Hydrodynamically optimised hull form and appendages.	Selective Catalytic Reduction (fuel <1.5 %S) (SCR)
System 4		Hull coating	Hydrodynamically optimised hull form and appendages.
System 5		Energy-efficient light system	Hull coating
System 6			Propeller optimisation - Higher efficiency, higher URN
System 7			Waste Heat Recovery (WHR)
System 8			Energy-efficient light system

The Selective Catalytic Reduction (SCR) can be found in any combination since SCR is the most suitable abatement option for the high-speed diesel engine to reduce the NO_x emissions to meet IMO Tier III requirements. In both solutions, the hull optimisation, hull coating and energy-efficient lighting are also identified as having positive impacts on the total costs and emissions. MDO as a fuel is much cheaper than the Low Sulphur MGO, hence it is the choice for low internal costs, whereas LSMGO improves the environmental performance a little more. The high-efficiency propeller and Waste Heat

Recovery (WHR) do not deliver enough potential to be earned back economically but can be relevant in stricter owners. The WHR is more suitable for larger ships, as it takes up quite some space. The space availability was not yet considered in this optimisation, on the other hand, a WHR might not even fit on the selected workboat.

Since the benchmark workboat did not meet the legal limits for NO_x it may seem to outperform the optimisation for internal costs. However, the optimisation could be said to identify the impact of the increase from Tier II to Tier III for NO_x regulations. The environmental impact is significant, whereas the operational impact is limited. However, this does assume that, for example, a hull form optimisation was not already performed for the benchmark. It seems unrealistic to expect a further voluntarily reduction by installing extra measures as the impact is limited, and the cost increase significantly. Furthermore, LNG was tested for the benchmark ship as well, resulting in internal costs of 260 k€/year and external costs of 154 k€/year. In both cases, further improvement compared to the presented optimisations. However, there is not enough room to store the LNG and therefore it was excluded from the optimisation. Still, it explains the current popularity of LNG as an abatement fuel, despite the methane slip.

5. Conclusions

The developed selection tool TESTER can select a combination of abatement options taking into account their interactions and optimising for a given set of limits. The potential of TESTER was shown in two case studies, one on an electric road ferry and one for a diesel-electric workboat. In both cases a set of relevant solutions allows the user to study the impact of different combinations of emission abatement options. Also, unconventional or future options and regulations can easily be added to the model to identify the impact of such developments.

A drawback of the current tool is that the space impacts on the ship design are not yet taken into account. It is left up to the designer in the next iteration to further clarify the design of the ship. Of course, once executed the tool could be used again to further select emission and cost reduction options, by manually taking into account e.g. space limitations.

The selection tool TESTER has demonstrated that, as with the MACC approach, sets of solutions can be identified, improving both costs and emissions. These support tools show that there is still significant potential for ship design measures, which perform well both economically and ecologically.

For the future, an integration with a ship design system is planned and an extension or update of the abatement options is crucial to the proper functioning of the selection tool for future ship designs.

Acknowledgements

The research presented in this paper is part of the EU-funded Horizon 2020 project NAVAIS (New, Advanced and Value-Added Innovative Ships, contract No.: 769419) and we would like to acknowledge all partners for their contributions.

References

ABS (2018), *Guide for the Classification Notation Underwater Noise*, ABS, Houston

AMMAR, N.R.; SEDDIEK, I.S. (2017), *Eco-environmental analysis of ship emission control methods: Case study RO-RO cargo vessel*, Ocean Engineering 137, pp.166-173

AUTHORITY, C.A. (2016), *Standards for offshore helicopter landing areas*, TSO

BALLAND, O.; ERIKSTAD, S. O.; FAGERHOLT, K. (2014), *Concurrent design of vessel machinery system and air emission controls to meet future air emissions regulations*, Ocean engineering 84,

pp.283-292

BALLAND, O.; GIRARD, C.; ERIKSTAD, S.O.; FAGERHOLT, K. (2015), *Optimized selection of vessel air emission controls—moving beyond cost-efficiency*, Maritime Policy & Management 42, pp. 362-376

BALLAND, O.; ERIKSTAD, S.O.; FAGERHOLT, K. (2012), *Optimized selection of air emission controls for vessels*, Maritime Policy & Management 39, pp.387-400

BALLAND, O.; SOLEM, S.; HAGEN, A.; ERIKSTAD, S.O. (2010), *A decision support framework for the concurrent selection of multiple air emission controls*, 9th COMPIT Conf., Gubbio

BARI, M.E.; ZIETSMAN, J.; QUADRIFOGLIO, L.; FARZANEH, M. (2011), *Optimal deployment of emissions reduction technologies for construction equipment*, J. Air & Waste Management Association 61**,** pp.611-630

BOLT, E. (2001), *Fast ferry wash measurement and criteria*, FAST'2001 Conf., pp.135-148

BUHAUG, Ø.; CORBETT, J.J.; ENDRESEN, Ø.; EYRING, V.; FABER, J.; HANAYAMA, S.; LEE, D.S.; LEE, D.; LINDSTAD, H.; MARKOWSKA, A.Z. (2009), 2nd IMO GHG Study, IMO, London

BV (2018), Rule Note NR 614 DT R02 E, Underwater Radiated Noise (URN), Bureau Veritas, Paris

CALLEYA, J.; PAWLING, R.; GREIG, A. (2015), *Ship impact model for technical assessment and selection of Carbon dioxide Reducing Technologies (CRTs)*, Ocean Engineering 97, pp.82-89

COMMANDANT, U. (1999), *International regulations for prevention of collisions at sea, 1972 (72 COLREGS)*, US Dept. of Transportation, US Coast Guard, COMMANDANT INSTRUCTION M, 16672

CORBETT, J.J.; CHAPMAN, D. (2006), An environmental decision framework applied to marine engine control technologies, J. Air & Waste Management Association 56, pp.841-851

DAMEN (2020a), *Road ferry 9819*, https://products.damen.com/-/media/Products/Images/Clusters-groups/Ferries/Passenger-Car-Ferry/Road-Ferry/DRFe-9819/Downloads/Product_Sheet_Damen_Road_Ferry_9819_E3.pdf

DAMEN (2020b), *Utility vessel (UV) 4312*, https://products.damen.com/-/media/Products/Images/Clusters-groups/Workboats/Utility-Vessel/UV4312/Documents/Product_Sheet_Damen_Utility_Vessel_4312_01_2017_.pdf

DNVGL (2018a), *Assessment of selected alternative fuels and technologies*, DNV GL Guidance Paper 5

DNVGL (2018b), *Rules for Classification – Ships – Part 6 Additional class notations. Ch. 7*, DNV GL

EEA (2012), *Air Quality in Europe*, European Environmental Agency

EC (2019), *Energy prices and costs in Europe*, European Commission

FELDTMANN, M. (2000), *In the wake of wash restrictions*, RINA Conf. on the Hydrodynamics of High Speed Craft–Wake Wash and Motions Control

GILBERT, P.; WALSH, C.; TRAUT, M.; KESIEME, U.; PAZOUKI, K.; MURPHY, A. (2018), *Assessment of full life-cycle air emissions of alternative shipping fuels*, J. Cleaner Production 172,

pp.855-866

GM (2017), *Advancing Environmental Excellence,* Green Marine https://green-marine.org/

HANSSON, J.; MÅNSSON, S.; BRYNOLF, S.; GRAHN, M. (2019), *Alternative marine fuels: Prospects based on multi-criteria decision analysis involving Swedish stakeholders*, Biomass and Bioenergy 126, pp.159-173

IMO (2004), *International convention for the control and management of ships' ballast water and sediments*, IMO, London

IMO (2014a), *Code on Noise Levels on Board Ships*, IMO, London

IMO (2014b), *Guidelines for the reduction of underwater noise from commercial shipping to address adverse impacts on marine life*, IMO, London

IMO (2017), *The International Convention for the Prevention of Pollution from Ships*, IMO, London

JOMOPANS (2017), *Joint Monitoring Programme for Ambient Noise North Sea (JOMOPANS)* https://northsearegion.eu/jomopans

KIRKEGAARD, J.,;KOFOED-HANSEN, H.; ELFRINK, B. (1999), *Wake wash of high-speed craft in coastal areas*, Coastal Engineering

LR (2018), *ShipRight Design and Construction – Additional Design Procedures: Additional Design and Construction Procedure for the Determination of a Vessel's Underwater Radiated Noise*, Lloyd's Register, London

MADSEN, R.T.; JON, P.; MARKESTAD, L.; DAVID, P.; LARSEN, W. (2011), *144-Car Ferry LNG Fuel Conversion Feasibility Study for Washington State Ferries*, Seattle

McKENNA, M.F.; ROSS, D.; WIGGINS, S.M.; HILDEBRAND, J.A. (2012), *Underwater radiated noise from modern commercial ships*, J. Acoustical Society of America 131, pp.92-103

MEPC (2012), *Guidelines on the method of calculation of the attained energy efficiency design index (EEDI) for new ships*, Resolution MEPC 212, IMO, London

MITSON, R. (1995), *Underwater noise of research vessels: review and recommendations*, ICES Cooperative Research Report No. 209

MORO, A.; LONZA, L. (2018), *Electricity carbon intensity in European Member States: Impacts on GHG emissions of electric vehicles*, Transport and Environment 64, pp.5-14

MSC (2006), *Adoption of amendments to the international convention to the safety of life at sea, 1974, as amended*, Resolut. MSC 216, IMO, London

MURPHY, J.; MORGAN, G.; POWER, O. (2006), *Literature review on the impacts of boat wash on the heritage of Ireland's inland waterways*, Moore Group

ÖLÇER, A.; BALLINI, F. (2015), *The development of a decision making framework for evaluating the trade-off solutions of cleaner seaborne transportation*, Transport and Environment 37, pp.150-170

OSPAR (2017), *OSPAR Commission*, https://www.ospar.org/about/introduction

POV (2017), *Enhancing Cetacean Habitat and Observation (ECHO) Program*, Port of Vancouver

https://www.portvancouver.com/environment/water-land-wildlife/echo-program/

RAVEN, H.; VALKHOF, H. (1998), *Ship Wash*, MARIN Report, Wageningen

REN, J.; LÜTZEN, M. (2015), *Fuzzy multi-criteria decision-making method for technology selection for emissions reduction from shipping under uncertainties*, Transport and Environment 40, pp.43-60

RINA (2017), *Amendments to Part A and Part F of the "Rules for the Classification of Ships": New additional class notation: "DOLPHIN QUIET SHIP" and "DOLPHIN TRANSIT SHIP"*, RINA, Genova

SCHINAS, O.; STEFANAKOS, C.N. (2014), *Selecting technologies towards compliance with MARPOL Annex VI: The perspective of operators*, Transport and Environment 28, pp.28-40

TRIVYZA, N.L.; RENTIZELAS, A.; THEOTOKATOS, G. (2018), *A novel multi-objective decision support method for ship energy systems synthesis to enhance sustainability*, Energy Conversion and Management 168, pp.128-149

VAKILI, S. (2018), *Under-water noise pollution sources, mitigation measures in commercial vessels: the trade-off analysis in the case of study for trans mountain project*, Port of Vancouver

VERBEEK, R.; KADIJK, G.; VAN MENSCH, P.; WULFFERS, C.; VAN DEN BEEMT, B.; FRAGA, F.; AALBERS, A. (2011), *Environmental and Economic aspects of using LNG as a fuel for shipping in The Netherlands*, TNO, Delft

WAGNER, C.G. (2005), *Basic combinatorics*, Dept. Math., The University of Tennessee, Knoxville

WANG, H.; FABER, J.; NELISSEN, D.; RUSSELL, B.; ST. AMAND, D. (2010), *Reduction of GHG Emissions from ships–Marginal abatement costs and cost effectiveness of energy efficiency measure*, Document MEPC, IMO, London

WANG, W.; ZMEUREANU, R.; RIVARD, H. (2005), *Applying multi-objective genetic algorithms in green building design optimization*, Building and environment 40, pp.1512-1525

WINEBRAKE, J.J.; CORBETT, J.J.; WANG, C.; FARRELL, A.E.; WOODS, P. (2005), *Optimal fleetwide emissions reductions for passenger ferries: An application of a mixed-integer nonlinear programming model for the new york–new jersey harbor*, J. Air & Waste Management Association 55, pp.458-466

YANG, Z.L.; ZHANG, D.; CAGLAYAN, O.; JENKINSON, I.; BONSALL, S.; WANG, J.; HUANG, M.; YAN, X. (2012), *Selection of techniques for reducing shipping NOx and SOx emissions*, Transport and Environment 17, pp.478-486

Modular Conceptual Synthesis of Low-Emission Ships

Benjamin Lagemann, NTNU, Trondheim/Norway, benjamin.lagemann@ntnu.no
Stein Ove Erikstad, NTNU, Trondheim/Norway, stein.ove.erikstad@ntnu.no

Abstract

With the ambition of lowering emission from shipping, today's ship designers face both the freedom and challenge to select from a large set of different ship system concepts during the conceptual design stage. In order to design competitive vessels, these options need to be assessed in an efficient and systematic way. Building upon established ship design methodologies, this paper presents a combined synthesis model adapted to low-emission ship design. By making extended use of modularity, namely component swapping and combinatorial modularity, the model enables flexibly synthesizing diverse ship configurations. To illustrate how the model can be used, we show how it can be implemented computationally and apply it to a RoRo transport case for the route Rotterdam - Halifax. An efficient discrete event simulation enables immediate performance evaluation. The ship designer can thus directly foresee the consequences of decisions and elucidate requirements on an informed basis.

1. Introduction

'How can we reach the IMO 2050 ambition, *IMO 2018*, for ship GHG emissions?' is an increasingly urgent question. Given the most optimistic projections in terms of least presumed emissions, shipping GHG emissions in 2050 will be as high as in 2008, *IMO (2015)*. Such a scenario already implies a high uptake rate of efficiency measures. In this light, the IMO GHG emission goals for 2050 may seem ambitious. Yet, they represent what is deemed as shipping's fair contribution to the Paris agreement, *UN (2015)*.

Translation of the IMO ambitions into a per-ship-basis is currently under discussion. Generally, we can identify three main levers for GHG emission reductions in shipping, Fig.1.

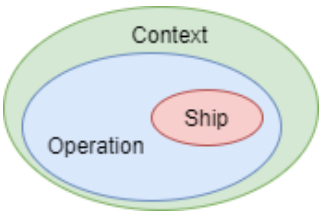

Fig.1: Levers for shipping emission reduction

Operative measures, such as speed reductions, are debated, *IMO (2018)*, and in some cases already implemented voluntarily. Green technologies are said to significantly advance emission reductions in the future. In many cases, these advanced technologies make use of synthetic fuels produced by electric energy. Local emissions can thus be avoided, but well-to-tank emissions need to be assessed. Hence, the context the ship operates in (external infrastructure etc.) determines whether the technology will achieve reductions in practice or not.

The focus of this paper is on ship GHG emission reductions that can be achieved during the design phase. More specifically, we will look into the conceptual design phase (also called early, preliminary design or feasibility study), where not only a large fraction of costs is determined, but also the main concept for the ship is set. The design space, and thereby the freedom for change, gradually reduces from preliminary design to manufacturing, *Mistree et al. (1990)*. Hence, we find the largest lever to reduce ship emissions in the conceptual design phase.

All three levers shown in Fig.1 will influence ship emissions. As both context (e.g. refueling locations or regulations) and operation (e.g. required speed) impose requirements upon the ship, these need to

be thoroughly examined. One should at the same time keep in mind that the ship is in fact serving a purpose different from emission reduction. Emissions are thus a by-product while achieving the ship's intended purpose.

Fig.2: Wind-power car carrier, developed jointly by KTH Stockholm, SSPA Gothenburg and Wallenius Wilhelmsen

There are numerous proposals for ships, built or under design, that each serve a distinct mission while maintaining low-emission levels: Wind-power cargo vessels as proposed by NEOLINE, https://www.neoline.eu/wp-content/uploads/2019/07/NEOPOLIA_NEOLINE_2019_07_PressRelease.pdf, and KTH, https://www.kth.se/en/aktuellt/nyheter/ett-hallbart-fartyg-kommer-lastat-1.965511, Fig.2, or hydrogen-driven solutions as investigated by *Raucci et al. (2015)*. Those examples prove that large emission reductions can be achieved. Thanks to their low emission levels, some of the presented solutions could likely be part of a shipping fleet in 2050. However, when tasked with a new ship design today, we will quickly get to the question “What is a better ship?”, *Ulstein and Brett (2015)*: Would a hydrogen-powered vessel be the preferred choice? Could even a purely wind-powered solution be feasible? Couldn't we design a ship that can be retrofitted in 10 years, when a certain technology is likely to be more mature?

Ship design requirements are different from case to case. Thus, achieving emission reductions is not as straightforward as taking a marginal abatement cost curve to find the best solution, *Kesicki and Strachan (2011)*. Its underlying assumptions are most likely different from the design task at hand. Consequently, as part of the requirements elucidation process, *Andrews (2003,2011)*, the previous 'better ship' questions need to be answered for each new design case. Due to the large number of different alternatives and their many interactions and intersections, the design process appears to be ill-structured, *Simon (1973)*, *Pettersen et al. (2018)*, and complex. *Gaspar et al. (2012)* identify five complexities of ship design: structural and behavioral complexities associated with the ship (components and their emerging behavior); contextual and temporal complexities as the ship subject to changing operations and context over time; perceptual complexity referring to diverse and possibly contradictory stakeholder expectations.

We have outlined the three main levers for emission reductions in shipping, Fig.1, as well as how they relate to the complexities in ship design. All three factors should be incorporated in the requirements elucidation process. For this to be done successfully, we need both a holistic life-cycle analysis, *Papanikolaou (2010)*, as well as a conveniently fast ship synthesis model. The present paper will focus on the ship synthesis part, keeping context and operation constant. After recalling the generic design process, we will review a set of ship design approaches with respect to their applicability to low-emission conceptual design. Based on the reviewed methodologies, we will then attempt to formulate a combined ship synthesis model considering emission performance from the very beginning of the design process. We will describe how this model can be implemented computationally and illustrate its use by quickly synthesizing a conventional diesel- and an ammonia-driven RoRo ship.

2. The generic design process

Simon (1996) defines design as “changing existing situations into preferred ones”. Thus, design starts with a need to change a situation. As for engineering design, such a need is usually met by the specification of an artifact. This artifact attempts to meet the stated need by means of certain functions which are enabled by the artifact's form. *Coyne et al. (1990)* and *Suh (1990)* illustrate this process as a mapping from need via function to form:

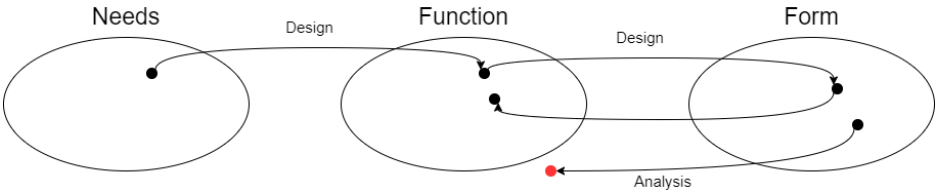

Fig.3: Design as a mapping between different domains

We can see that design is different from analysis. No straightforward deductive step from function to form exists. If we propose a certain form, we can evaluate if its attained performances meet the intended ones. If that is not the case, we need to alter the form and verify it again. Design thus often represents an iterative process with changes on form and perhaps even functions. If we realize that our intended performance (e.g. high speed at low emission levels) is not attainable or too costly, we might be willing to change them. *Andrews (2003,2011)* refers to this process as 'requirements elucidation'.

3. Established ship synthesis models

Within this section, we will briefly review and compare three influential ship synthesis models: system-based ship design (SBSD), *Levander (1991)*, the design building block approach (DBB), *Andrews and Dicks 1997)*, and the packing approach, *van Oers (2011)*. These synthesis models have been widely discussed and used in the past. They are not mutually exclusive, rather they share many common ideas and thus can often be combined. Van Oers' packing approach for instance builds upon the design building block methodology as a parametric ship description.

Ship design is often seen as a subset of engineering design or systems design. Nevertheless, ship design also features a spatial, architectural aspect. In order to be precise about terminology when comparing the synthesis models, we will use a discrimination inspired by *Kroes et al. (2008):*

- Architectural design: Concerned with the spatial arrangement
- (Systems) engineering design: A reductive, hierarchical perspective emphasizing (sub-) system interactions

The architectural aspect has historically been more influential for service ships (e.g. cruise ships or warships) than for cargo ships. It is still is to be proven that this will also be the case potentially unconventional, low-emission ship designs in the future.

Within systems engineering, we additionally define the term topology as:

- System topology: “connectivity between parts of the ship”, *van Oers (2011)*

Mission - We have outlined in Section 2 that design originates from a purpose. For a ship, this purpose is usually described as a mission. The focus of SBSD has been civil ship missions (transport and service missions), whereas both the DBB and the packing approach are targeting service vessels (civil and naval) that are considered more architecturally complex. A mission statement translates into requirements. *Van Oers (2011)* underlines that the negotiable ones of these can be subject to an exploration.

Functional and system breakdown - Both SBSD and the DBB start out with a functional breakdown. Due to the unlike target missions, the breakdowns are somewhat differing:

Table I: Functional breakdown structure of SBSD and the DBB methodology

SBSD, *Levander (2012)*		DBB, *Andrews and Dicks (1997)*			
ship functions	payload functions (for cargo)	float	move	fight/operations	infrastructure
structure equipment accommodation machinery tanks	cargo units cargo spaces cargo handling cargo treatment				

The detail of the functional breakdown in SBSD is increased for a specific ship mission and then mapped into a system breakdown. Such detailed breakdowns ease the handling of systems and enable a quick weight and space estimate. If used in a spreadsheet fashion, this type of breakdown however appears to be somewhat rigid when exploring a wide solution space. The designer seems to be somewhat locked to certain system topology that hampers a wide exploration. Hence, maintaining flexibility for the system breakdown is key for low-emission ship design. As for the DBB approach, the functional groups are mapped to so-called super building blocks. The selection of super building blocks is denoted "major feature selection", *Andrews and Dicks (1997)*, and represents the most important conceptual design decisions. Building blocks can be assembled and architecturally positioned. According to *Pawling (2007)*, this procedure particularly fosters the exploration of innovative, unconventional designs. *Andrews et al. (2010)* enhance the DBB approach with a library for different system options. Again, this strongly supports innovative system compositions and enables concurrent investigation of diverse concepts, Fig.4. *Calleya (2014)* presents a "ship impact model" to assess the impact of certain carbon reducing technologies on a given ship model. This enables a case-based impact assessment, but does not consider emissions from the very beginning, i.e. integrated into the design DBB design methodology.

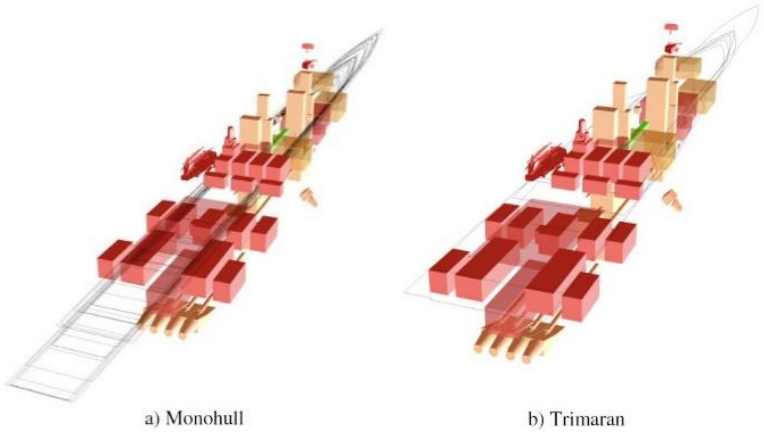

Fig.4: DBB visualization of two different ships for the same mission, *Andrews et al. (2010)*

Generating diverse configurations - The intention of SBSD and the DBB methodology is to systematically support the designer in the preliminary design phase. The main decisions (what systems, where to place) are thus to be taken by the designer a-priori to design evaluation. As illustrated by Fig.4, the DBB methodology encourages generating diverse configurations. Van Oers' packing approach does not relief the designer of making decisions. The key difference however is that decisions are made a-posteriori to the synthesis phase: A set of diverse ship configurations is generated and evaluated by a search algorithm. Only non-negotiable requirements (e.g. positive GM) are considered as a threshold. Negotiable requirements are not considered as a threshold, but can be elucidated a-posteriori to the design evaluation. Hence, when the designer faces the proposed designs generated by the search algorithm, performance data is directly accessible and can guide the process of (negotiable) requirements elucidation.

Engineering and architectural design aspects - All three design approaches contain a numerical ship description and make use of experience to estimate system parameters. SBSD reveals relevant system parameters (e.g. weight/kW for an engine) to the designer, while the packing approach makes use of *van der Nat's (1999)* sizing functions containing hard-coded experience. Similar relations are used for sizing DBBs. Rather than on numerical relations, the focus of the DBB and the packing approach is on architectural design aspects. Although *van Oers (2011)* describes certain overlap rules supplied to the search algorithm, he notes that architectural aspects are often negotiable and will lack completeness when stated a-priori. SBSD does not directly focus as much on architecture as the two other approaches. Nevertheless, its open and simple system descriptions have proven to be useful for design of architecturally complex vessels too, as they enable repositioning and quick estimations for the center of gravity for instance, *Levander (2009).*

Hull design - Both SBSD and the DBB adhere to a "wrapping" approach for hull design: "Instead of fitting systems into a hull we fit a hull to the system description already made", *Levander (1991)*. Van Oers, within his search algorithm, employs a "packing" strategy. That is, all systems are positioned within a given hull form. If hull dimensions are selected as variables for the search algorithms, different hull sizes for the same systems can be generated, yielding different packing densities and covering diverse configurations.

Modular aspects - All three design approaches make use of basic concepts of modularity, which is further discussed in Section 4.2. Weight, space and position attributes are assigned to each system and the particularly the DBB approach fosters interactive positioning of such modules. Van Oers notes that systems can be exchanged for alternative systems to generate diverse system topologies.

Triggering unconventional designs - The goal of the three preliminary design approaches is to trigger exploration of diverse configurations - including potentially unconventional ones. Their respective means to do so, are however slightly different:

- SBSD uses a simple and parametric system description. Not only does it provide the designer with a list of required systems, but also reveals the most important system characteristics.
- The DBB methodology uses an interactive block assembly of ship systems, providing necessary numerical tools one the side. The designer can thus focus on generating diverse designs and particularly elucidate architectural requirements.
- Elucidating requirements is a notion shared by the packing approach. The key difference is the speed of doing this: With an a-posteriori selection approach, the designer is relieved from manually balancing and evaluating designs. Requirements are thus elucidated by directly revealing decision implications.

The three presented design approaches provide a stepwise design methodology, starting with a mission, proceeding via functions and finally specifying a form. Generally, the questions 'where to place systems?', 'what system size?' and 'what implications?' seem to be widely covered. What appears to be missing is how to rapidly generate and investigate diverse system typologies, in particular for those systems that drive emissions. In the next section, will attempt to combine the successful features of these three synthesis models by extending the use of modularity.

4. A combined modular synthesis model

Our combined synthesis model shall in principle target the same missions as SBSD. Yet, we slightly adapt the 'crux of the task', *Pahl et al. (2007)*: Synthesize diverse ship configurations for a given mission, paying due regard to required emission reduction measures and goals. Albeit still generic, our combined synthesis model will naturally be biased towards this problem description. More specifically, it shall address the necessary flexibility for generating diverse system topologies.

4.1 Ship functions

We have outlined that a generic and flexible function-system mapping is crucial in order to not limit the solution space. However, functions need to be provided by specific systems. Hence concrete, precise functions would be desirable. Before discussing the high-level functional breakdown, we shall briefly take a look at aviation. The flexible mapping issue from function to form is shared by aircraft designer and depicted by *Esdras and Liscouet-Hanke (2015)*:

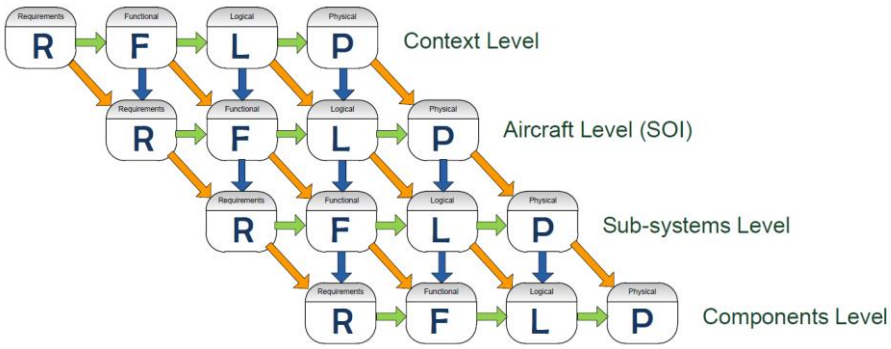

Fig.5: Proposed RFLP model in alignment with the left-hand part of the systems engineering V-model, *Esdras and Liscouet-Hanke (2015)*. (R=requirements; F=functional; L=logical; P=physical)

As illustrated in Fig.5, the functional decomposition at the aircraft level (SOI, system of interest) influences the logical system structure, but similarly the functional and requirements structure at the sub-system level.

Introducing a logical layer is similar to the combination of different working principles, *Pahl et al. (2007)*. Working principles do not refer to a specific embodiment (e.g. an M10 bolt), but rather refer to the underlying logical concept (e.g. frictional connection). Thanks to this abstraction, a logical item becomes less specific but more flexible. It can represent a number of different embodiments grouped under the same working principle, without necessarily implying a specific form. Abstracting the underlying physical concept, a logical representation can thus simplify an entity's interface. *Simon (1996)* claims that most artifacts, being artificial or not, bear such simple interfaces and they facilitate combination into more complex structures: ”The more complex [systems] arise out of a combinatoric play upon the simpler”, *Simon (1996)*. We should keep in mind, however, that eventually also the more flexible logical entities need to be mapped to specific physical items (the physical space in Fig.5).

In order to facilitate a more flexible synthesis model, we shall now apply such a logical layer in between the mapping from functions to concrete systems. Inspiration for the functional breakdown is taken from both SBSD and the DBB methodology (see Table I). Due to the differing 'crux of the task', our functional breakdown will be somewhat different. We show the functional breakdown and its mapping to logical systems for a RoRo transport vessel, Fig.6. Before discussing the proposed mapping between functions and logical systems, we shortly introduce each of the functions and logical systems shown in Fig.6.

A generic vessel will require the high-level functions 'provide vertical force', 'provide volume', 'provide stability', 'provide strength' in order to be present. With these functions, the vessel can float at a certain immersion in equilibrium condition and will not collapse. For the vessel to become a ship, we generally need to 'provide thrust' and to 'avoid resistance'. The latter function seems rather parasitical than useful, but will always be present to a certain extent. Moreover, a moving ship needs to be controlled in some way. *Papanikolaou (2010)* terms the functions described so far as “inherent”. For a RoRo cargo ship, we then add the functions 'load/unload' and 'cargo voyage handling' to the portfolio. For other ship types - e.g. service ships - these functions would need to be replaced by their

respective mission-specific functions as shown by *Levander (1991, 2012)* and *Erikstad and Levander (2012)*.

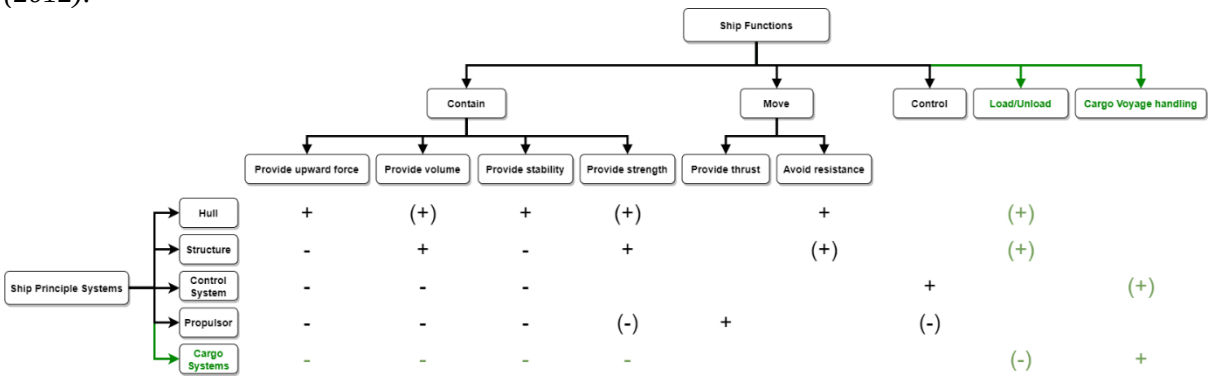

Fig.6: Proposed mapping from functions to logical systems for a RoRo cargo ship (generic=black, mission-specific=green)

The logical systems that fulfil the basic functions of a generic ship are termed 'hull', 'structure', 'control system' and 'propulsor'. For our specific RoRo cargo ship, we will add 'cargo systems' to the list. This division may not seem obvious, as the hull generally describes the shape of the structure and these two cannot directly be separated. However, these logical systems coincide well with the decision-based design paradigm, *Mistree et al. (1990)*, and the 'major feature selection', *Andrews and Dicks (1997)*, during the preliminary design phase: What kind of hull shape would be suitable? What structural concept and material should be used? Should the vessel be operated by humans or be controlled autonomously? What kind of propulsion system should propel the vessel? What cargo system do we need? In theory, these decisions can be made independently from each other which is why we specify them as separate 'logical systems'. We will discuss their dependencies and relations now to clarify this issue.

4.1.1 Function - logical systems mapping

The function ‘provide upward force’ is generally enabled by the hull lift concept (buoyancy, hydrodynamic, aerodynamic). All other systems consume the upward force by their weight. For a balanced ship, consumption consequently needs to match supply.

The ‘provided volume’ is generally not directly limited by the hull form - at least not for surface ships. In most cases, the hull determines the projected area upon which volume can be extruded. But this is not a strict limitation either. Instead, it is often (but not always) the structure that provides the total volume needed for all other systems. Alike *Liscouet-Hanke and Huynh's (2013)* “equivalent design volume” for aircraft systems, each system will consume a certain amount of the provided volume.

‘Stability’ is a ship property affected by the hull form and center of gravity as well as the spatial arrangement (bulkheads, decks, down-flooding points etc.) of the ship. If we focus on linear intact hydrostatics in the preliminary design phase, we can neglect the influence of the compartmentation. In other words, we do not make any premises with respect to the internal subdivision. In this case, stability becomes a property of the hull form ($KM = \frac{I_{WL}}{\nabla} + KB$) as a supplier and the systems as consumers in terms of KG.

Global ‘strength’ is a compromise of hull form, structural material and application, and the cargo to be loaded. Different propulsive means or other systems can affect this function too, but more on a local than global level. Given a specific hull form and cargo storage concept (large open deck areas for our RoRo case), we could say that the structural concept needs to be compatible with these two. For a fast and small RoRo vessel for instance, we could imagine the same cargo storage and loading concept (roll-on-roll-off cargo on large open decks) and the same hull concept (say catamaran in this

case) but with different structural concepts: Steel, aluminum and perhaps even composite structures might all be feasible and could be worth an investigation.

'Providing thrust' is often the largest source of ship life cycle emissions. However, this is only true for particular kinds of propulsive systems: While a propeller will need rotational power supplied and therefore most likely some energy stored onboard, a sail will generally not require the storage and conversion of chemical energy.

For most ships, 'resistance' is mainly determined by the hull form. Wind resistance, as a result of volume above the free surface, is generally a smaller fraction. Hence, we will neglect it for now, but acknowledge that it could in principle be associated with the structure.

A ship's 'control' can be plied by humans as well as artificial computer systems. Different criteria with respect to usability and safety will arise, but both solution principles can theoretically exercise the control function.

'Loading and unloading cargo' is often done by port operators in the case of RoRo ships. Hence, loading requirements upon the ship can be seen as comparatively low - only the hull and structural concept need to be suitably chosen for this function. Again, we could describe this as a combinatorial issue.

'Cargo voyage handling' is a function with different requirements for each specific ship. In case refrigerating units or ventilation are required, the specific magnitude of these functions needs to be supplied by the cargo systems.

We have discussed our proposed mapping from functions to logical systems and seen that some of the interactions (those marked in parentheses in Fig.6) can either be neglected in the preliminary design phase or are of a combinatorial nature. This has often been observed by system theorists, claiming that systems can be divided into "leaky modules", *Goel and Pirolli (1989)*, and have "near decomposability", *Simon (1996)*: "the `inner environment' of the whole system may be denoted by describing its functions, without detailed specification of its mechanisms, so the 'inner environment' of each of the subsystems may be defined by describing the functions of that subsystem, without detailed specification of its submechanisms", *Simon (1996)*. This theoretical hook seems to fit well here. Certain interactions - vertical force, volume and stability - apply to all systems and can only be neglected when we exclude the architectural aspect. In the next section, will explain how modularity can be (and has been) used to align these interactions with 'simple interfaces'.

4.2 Modularity

"The primary action of modularity is to enable heterogeneous inputs to be recombined into a variety of heterogeneous configurations", *Schilling (2000)*. Modularity can thus help to decompose systems into recombinable parts, often called blocks or modules. Modularity is frequently employed for producing customized products, such as different product variants in the automotive industry for instance, *Salvador et al. (2002)*. Salvador et al. define four different concepts of modularity by classifying with respect to interface and platform, Fig.7.

In shipbuilding, modularity has already been used to some extent, e.g. when assembling pre-manufactured blocks or cruise cabins. Some ships, such as the research vessel 'Jacob Brei', https://www.shipandoffshore.net/news/shipbuilding/detail/news/hydrographic-swath-for-estonia.html, use component swapping modularity in order to enable easy retrofit.

Choi and Erikstad (2017) and *Choi et al. (2018)* found that modularity, thanks to its recombination capabilities, often proves useful to cope with future uncertainty. However, *Erikstad (2019)* reminds us that "modularity in most cases comes at a cost. These include less optimized physical architecture, and correspondingly increased weight and size."

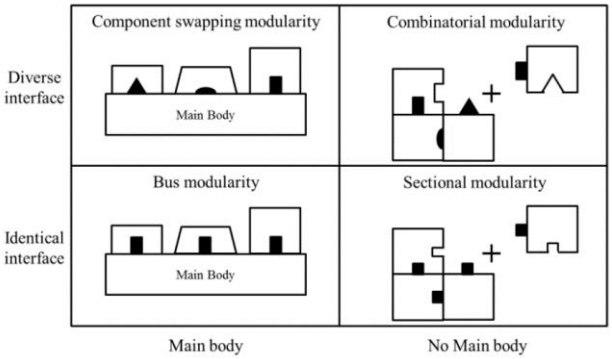

Fig.7: *Salvador et al. (2002)*'s different types of modularity from *Choi and Erikstad (2017)*

Some aspects of modularity have already been employed within the SBSD, DBB and packing approach. We will analyze their use of modularity within the next section and argue how and why using modularity should be increasingly used within our synthesis model.

4.2.1 Extending modularity as a conceptual synthesis concept

In all three reviewed synthesis models as well as our proposed function - logical systems mapping, certain ship functions are influenced by all systems: These functions mainly concern provision and consumption of vertical force, space and stability. Corresponding to *Salvador et al. (2002)*, we may formalize these common interactions as 'bus modularity'.

In addition, we have seen that certain ship functions (e.g. provide thrust) only relate to specific systems. Depending on their logical nature, these systems can require secondary systems: A propeller will need some system to provide rotational energy which, in case of an electric motor, requires some kind of electric energy provider. For the ship as an integration platform, these subsequent functions are less relevant. They mainly concern interactions between systems and are dependent on the logical type of the systems. We have outlined that a systematic combination of entities is facilitated by simple interfaces, collected for instance in a design catalog. The multitude of possible combinations, however, quickly grows and complicates the use of design catalogs. Instead, we can make use of diverse interface concepts of modularity. That is, 'component swapping modularity' to relate an overall function to suitable logical entities and 'combinatorial modularity' to combine different logical entities on the same hierarchical level.

Pahl et al. (2007) represent functions as discrete modular entities with specified inputs and outputs. Based on the IDEF0 methodology, *Esdras and Liscouet-Hanke (2015)* additionally assign controls and mechanisms at the entity's parent and child level respectively. Controls in our case can be functions that require a logical entity and mechanisms can be sub-functions that are specific to the logical entity at hand. For our current task of structuring and (re-)combining logical systems, we consequently propose the representation shown in Fig.8.

Whether a secondary system should be modeled as an input (combinatorial modularity) or sub-system (component swapping modularity), is determined by whether it can be seen as part of the system of interest or not: Assume that our current system of interest was one that provides rotational power to a propeller. We choose an electric engine as a module to provide this energy as output to the propeller. In this case, we would need a system to provide electric power to the engine. It is easiest to model the system as an input system, since it does not directly constitute the electric engine. Rather, the electric engine is fairly flexible with respect to where the electric energy comes from. Many options are conceivable and could be investigated. By modeling a battery as an input system, we ease the systematic combination of logical systems, as it is the intention of a design catalog.

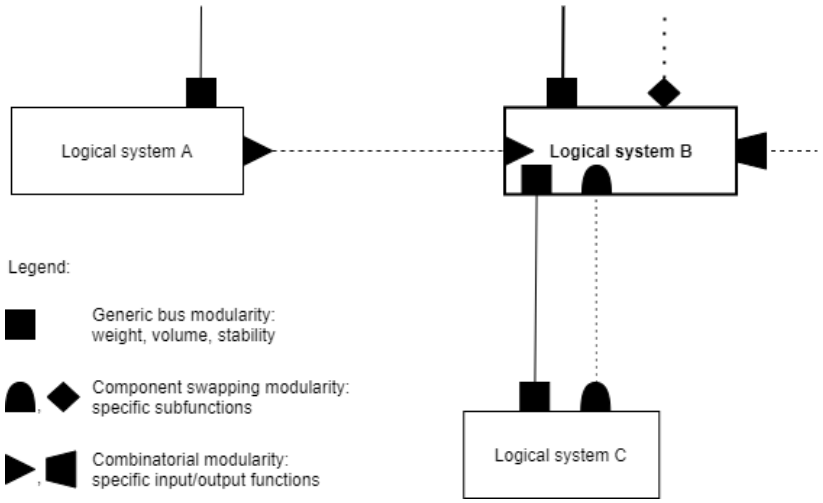

Fig.8: Representation and combination of logical systems

So far, we have illustrated our extended use of modularity to build up 'logical system' structures. Our logical system topology is now 'modifiable' (modifiable and scalable according to *Ross et al. (2008)*. The design task however is to come up with a specification of an artifact. Hence, we need to map our logical entities to concrete, 'physical systems'. We can achieve the mapping to physical specification by means of 'scalable' modules: Scalable modules contain a parametric description, whose parameter values can be adapted for each design case. The idea of scalability is also covered by SBSD and the DBB approach.

4.3 Summary

Our combined synthesis model formalizes system interactions by different types of modularity. In addition to 'bus modularity' aspects as used by SBSD and the DBB approach, we propose using 'component swapping' and 'combinatorial modularity' as a synthesis concept. Component swapping modularity enables exchanging (sub-)systems and combinatorial modularity facilitates combining different systems on the same hierarchical level. Alike in SBSD and the DBB, scalable modules can help making our knowledge operable and - as opposed to design catalogs - allow case-based reasoning.

So far, the outline of our combined synthesis model has been rather theory-laden. We will therefore illustrate how it can be applied by means of object-oriented programming. Also, we will explain how the implementation helps to realize our initial goal of systematic systems combination together with a case-based assessment.

5. Implementation and application of a modular synthesis model

We have seen that interfaces are important to facilitate a systematic combination of logical entities. Relying on interfaces makes a type-safe, class-based object-oriented programming language particularly suitable for implementation. In this way, we can capture our logical module interactions (bus modularity, component swapping modularity and combinatorial modularity) by means of an abstract class' interface. By deriving abstract classes (or abstract interfaces, depending on the programming language), we can assign a parametric, scalable system description to this interface. Once instantiated and scaled, the instance of a concrete class represents a mapping into the physical form space. The following figure depicts the basic object structure:

We can assign different spatial architectures to the same system topology. Certain functions (such as stability) will be largely dependent on the ship's architecture. We have already formalized these simple interactions numerically be means of the generic bus. A 3-dimensional architectural representation however, such as the DBB's implementation in Paramarine, can be much more revelatory than

only providing numerical feedback. Due to the lack of completeness when stating requirements a-priori, a 3-dimensional representation can help to unveil and elucidate requirements.

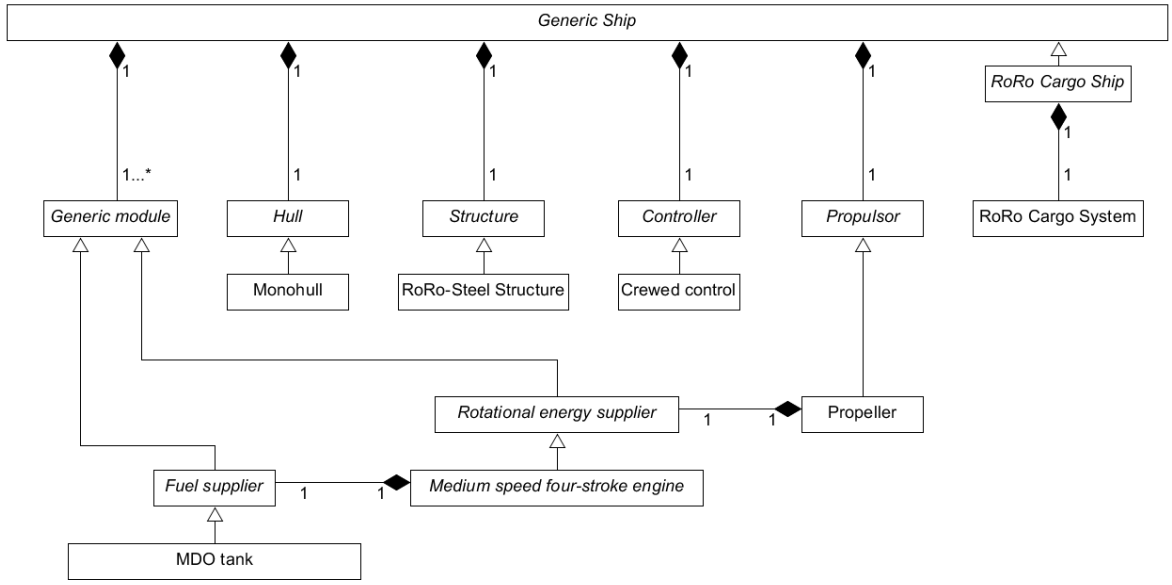

Fig.9: UML representation of proposed synthesis model

For our illustrative implementation, we have chosen to implement our logical system model in Java and couple it with the open-source JavaScript library vessel.JS, *Gaspar (2018)*, to address the architectural aspect with a 3-dimensional representation. The mapping between the two is achieved by serializing the Java system configuration to JSON which is read by vessel.JS. As shown by Figs.10 and 11, we thus have a system view (logical entities and respective topology) and an architectural view on our configuration.

5.1 Illustrative ship mission

When defining our functional breakdown structure in Section 4.1, we have taken a generic ship RoRo transport mission as an example. The generic functional breakdown is still valid. We now define a specific ship mission for our example:

- Transport 5500 cars on a bi-weekly schedule from Rotterdam to Halifax.

The distance between the two ports of call is assumed to be 2800nm, which results in an average speed of about 17 knots. This ship mission assigns numerical values to some if its functions (speed for moving and the cargo capacity). Hence, we can use our predefined function-systems mapping, implemented within the class structure, and turn towards synthesizing two ship configurations that fulfill our mission.

5.2 Ship synthesis

When synthesizing a ship configuration, we start with instantiating a ship. For our RoRo ship case, the RoRo ship class implements the functional breakdown shown in Fig.6 and provides component swapping slots for corresponding logical modules. Next, we instantiate our logical systems and integrate them into an overall topology. The manual input required for instantiation is relatively limited as shown in the Table II. As proposed by *Levander (1991)*, experience data is used for implementation of both design and analysis.

Table II: Module implementation

ship module slot	selected module type	required input parameters	design knowledge and experience data used for implementation
cargo system	RoRo cargo system	position, number of cars	per car: mass 2 t, 2.3 m width, 5 m length; 2.5 m height from deck to deck
structure	steel structure for RoRo monohull	total displacement, cargo system height	weight estimated acc. to Papanikolaou (2014), $VCG = 40\% \; of \; side \; depth$
propulsor	single-screw propeller	position	$\eta_D = 0.67, diameter = 2 \cdot VCG$
control system	crewed control	position	12 $pers$ 1000 $USD/day * person$, 3 $t/pers$, 75 $m3/pers$
generic	four-stroke engine	position	$b_e \triangleq 250 \; gMDO/kWh$, 3.2 $tCO2/tMDO$, 15% MCR at max power
generic	MDO tank	position	42.7 MJ/kg, $\rho_{MDO} = 890 \; kg/m^3$, 5% margin on volume and weight for systems, 300 $USD/tMDO$
generic	pressurized ammonia tank	position	18.6 MJ/kg, $\rho_{Ammonia} = 610.3$ kg/m3, 20% margin on tank weight, 27% margin on tank space, 850 $USD/tNH3$, exhaust heat used for ammonia evaporation
hull	monohull	L, B, T, C_B, C_P	Holtrop and Mennen (1982) for calm water resistance, STawave-1 (ITTC 2014) for R_{AW}, 15% sea margin for power sizing

One can recognize that we have not used any advanced analysis method and our design experience data can be termed (very) rough. It is therefore easy to come up with more accurate analysis methods or better data. The point here is not to propose any specific analysis method or design data, but rather to see them as a complementary part for the synthesis model. Yet, more advanced methods will not fundamentally change the modules' interfaces. They may require a more detailed description of the hull form, but the function of a hull is still to provide a vertical force, stability and low resistance. The goal of these simplistic implementations is to focus on the most important decisions to be made ("major feature selection" according to *Andrews and Dicks (1997)* in the preliminary design phase.

Sizing and balancing can be triggered once our system topology is established, Figs.10 and 11. As outlined in Table II, the manual input for sizing is rather simple: The cargo system is directly sized according to our requirements specification; the hull requires a few main particulars; similarly, the structure. In order to size the remaining systems correspondingly, we can make use of van der Nat's idea of sizing functions which we assign to an abstract class's interface. For the propulsor slot, the methods 'sizeForEndurance(SailingLeg)' and 'sizeForPower(SailingLeg)' have thus been added to the class interface. The argument for both methods is a sailing leg, a concatenation of discrete events.

Since all systems communicate through the main bus in terms of weight, volume and COG, one can easily check the ship's balance after sizing and positioning the systems. That being said, we can position the objects before assigning a hull ('wrapping' strategy, *Andrews (1986)*) or place them inside a given envelope ('packing' strategy, *van Oers (2011)*). Those systems that rely on information of the hull (the propulsor with all connected systems), will not be able to size automatically until a hull is instantiated. If we alter or exchange the hull module, we can update the size of the propulsion-related systems directly. Most importantly, this procedure is responsive to changes in both requirements and system configuration. In order to synthesize diverse configurations, we can

- assign different input parameters to the same logical entity, see *van Oers (2011)*, for exploration of alternative arrangements)
- exchange the logical entity against another one (if compatible), keeping the overall topology equal
- change the logical system topology

For our illustrative case, we will stick to the same spatial concept and similar system topology, but exchange the diesel oil fuel tank against an ammonia fuel tank (option 2). The system topology and ship architecture of our configurations is depicted in Figs.10 and 11.

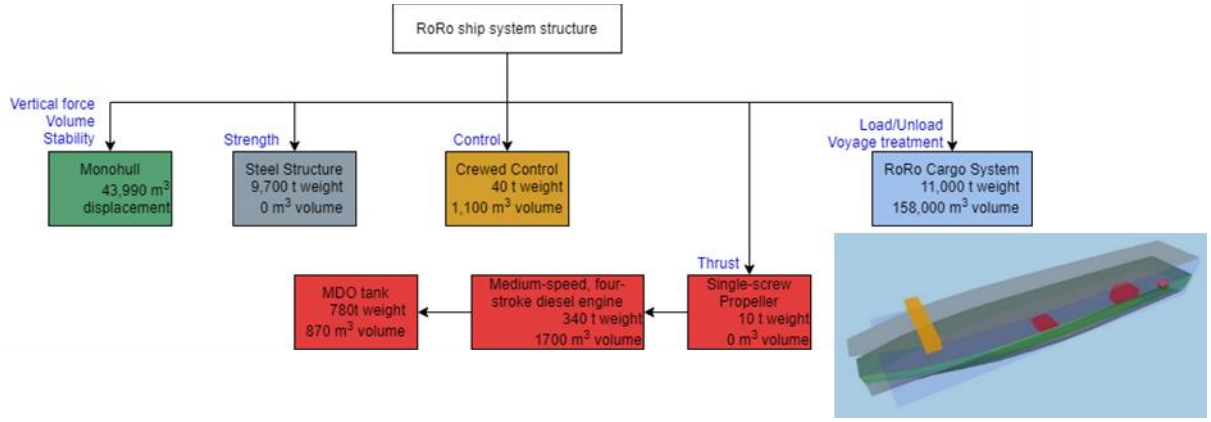

Fig.10: Systems engineering and architectural representation for MDO-driven configuration

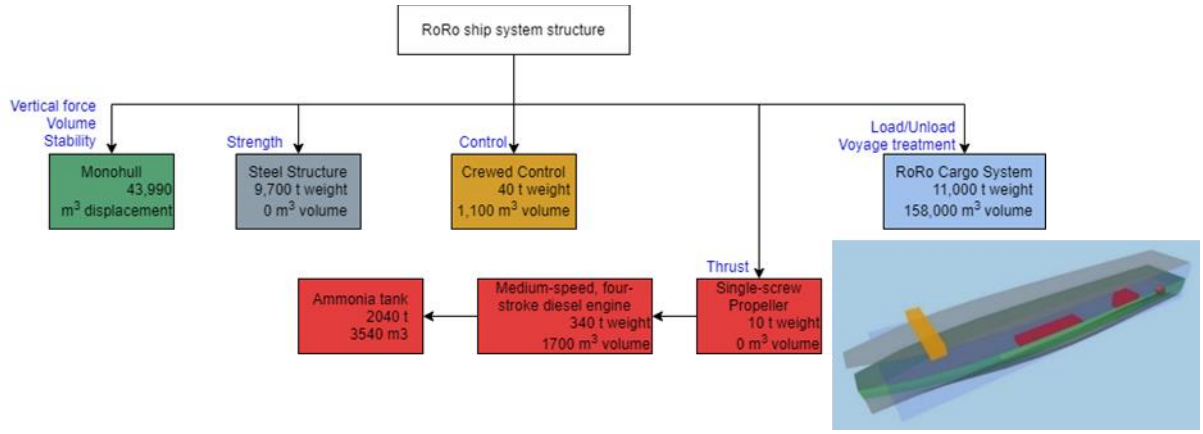

Fig.11: Systems engineering and architectural representation for ammonia-driven configuration

5.3 Simple analysis and evaluation

Once all systems are sized and the configuration is deemed to be balanced, we can analyze our system with a discrete event simulation. Not only is this method increasingly used to simulate more realistic conditions, *Sandvik et al. (2018)*, but also a necessity if we wish to analyze the response of wind- or wave-propelled configurations in the future, *van der Kolk et al. (2019)*. In order to create a sample concatenation of discrete events, we employ the wave scatter diagram, *DNVGL (2018)*, and divide the voyage into discrete events that represent the proportional time spent in each sea state. This is most likely is not a realistic voyage simulation, as a captain would certainly avoid extreme sea states and will alter the route along the way. We shall only use it for our simple illustration.

Our generated sample sailing leg from Rotterdam to Halifax contains approximately 2500 discrete events. The complete sailing leg is handed over to the ship that will execute the voyage and forward information to its sub-modules. The ship controls communication between its slot modules which themselves can communicate with their corresponding inputs, outputs and submodules: For each discrete event, the ship requests the hull to compute its resistance. The propulsor slot will then receive this information and request required rotational power from the engine etc. Throughout the course of discrete events, all modules can post relevant information, such as instantaneous power, fuel consumption or CO2 emissions.

Table III shows a compilation of posted data for one voyage in our illustrative design case.

Table III: Compiled results for one voyage

	economics			environmental impact	
ship configuration	crew costs [USD]	fuel costs [USD]	total costs [USD]	consumed fuel [t]	tank-to-wake CO2 emissions [t]
MDO-driven	91 000	209 000	300 000	700	2 240
ammonia-driven	91 000	639 000	730 000	1 600	0

With our rough and simplified experience data in mind, we clearly cannot claim the produced data to be accurate. Nevertheless, we can see a clear trend: With today's fuel prices, ammonia is not likely to the preferred economical choice. The cost relations indicate similar magnitudes as found by *de Vries (2019)* for today's fuel prices. On the other hand, if we limited ourselves to these two options only, ammonia would be the only viable way to reduce tank-to-wake emissions. For this reason, order-of-magnitude estimations are likely to be sufficient in the preliminary design phase. With a computational time well below 0.1s, we may consider the effort to see the implications of our decisions appropriate.

Our goal is not to argue in favor or against ammonia- or MDO-propelled ships here. We only use these technologies to highlight the need of a quick ship synthesis model as a necessity for a wide exploration in combination with a holistic analysis to find truly optimal solutions – or rather dismiss inferior ones before spending many resources in subsequent design stages. If we wish to reduce emissions significantly, we need to be able to predict their magnitudes at least approximately from the very beginning of the design phase.

Getting back to our illustrative case, one may justifiably raise the question 'what will happen if we were obliged to pay a certain carbon tax and ammonia prices drop significantly?'. In such a scenario, an ammonia-propelled option could come within reach. ‘But what if we relaxed our speed requirement, would that render a wind-powered ship feasible? Alternatively, what if we retrofit the vessel in 8 years from now? What would be the most energy-efficient solutions if we considered different synthetic e-fuels?' This discussion directly relates to the process of requirements elucidation, *Andrews (2011),* and is one that will likely be required for future-proof ships. We subscribe to *van Oers' (2011)* notion, that the feedback time between making a decision and seeing its implications needs to be as short as possible. Our modular synthesis model shall help to predict the implications of our decisions. It is responsive to changes in requirements and choice of systems and can thus support the preliminary, explorative design phase of low-emission ships.

6. Conclusion

By reviewing a set of ship synthesis models, we have seen the difficulty of efficiently and systematically synthesizing low-emission ships. Hence the need for a more flexible yet systematic approach to investigate the various options for low-emission shipping. Our proposed modular synthesis model in many ways resembles ideas of established synthesis models; most importantly SBSD and the DBB methodology. In addition to these models, our proposed synthesis model formalizes the mapping from functions to logical systems as component swapping modularity and the interaction between different systems as combinatorial modularity. Scalable modules eventually map logical systems to form. These means enable us to flexibly synthesize a wide range of ship system configurations.

To make appropriate decisions, the designer needs to know their implications on the specific design task, *van Oers (2011)*. Coupled to a discrete event analysis, our model can predict the consequences of decisions within short time (0.1s). By supporting such direct feedback on decision implications, the model can serve as a conceptual synthesis platform to not only configure different systems, but also elucidate requirements - potentially in an interactive way. Nevertheless, the proposed synthesis model is far away from a describing a complete design model. At best, it could be a small brick within a larger, holistic design process. We thus foresee different research directions for the future:

- Refining the module implementation: Naturally, a balance between accuracy and computational speed needs to be sought. The simulation time indicates that a slight balance shift towards accuracy is reasonable and advantageous to create more believable solutions.
- Adding more logical systems: A necessity if we wish to synthesize more configurations to get closer to global optimum solutions. With a larger component library, coupling to a guided search algorithm, as presented by *van Oers (2011)*, becomes interesting.
- Application to different ship missions: The methodology has been illustrated for a RoRo cargo ship mission. Its applicability and use with different functional breakdowns still needs to be proven.
- A holistic life-cycle perspective: As *Papanikolaou (2010)* argues, a life-cycle perspective is required to understand the full consequences of each design. Future uncertainty could be integrated by means of scenarios.
- Retrofittability and modularity: With a holistic life-cycle perspective in place, we could investigate the impact of changes along the ship's lifetime, *Rehn et al. (2018)*. A relevant, exemplary question is 'should we equip the ship with physical modularity to enable exchanging the power system for instance?'
- Design process integration: Given that we had the ability to synthesize and analyze different ship configurations in different scenarios, how can we best use this in the design process involving different stakeholders? A combination with an interactive evaluation, *Duchateau (2016)*, *Calleya et al. (2016)*, is a promising approach.

We recognize the long way ahead and at the same time acknowledge that fundamental research on most the above-mentioned topics has already been undertaken. For the future, we thus wish to build upon this research and integrate its concepts into a future-proof design process. Being a prescriptive design methodology, we can expect our presented synthesis approach to face obstacles and undergo alterations when applied to real-world problems. We thus appreciate future case studies to correct, adapt and expand the proposed methodology and continuously learn from practitioners.

Acknowledgement

The research presented in this paper has received funding from the Norwegian Research Council, SFI Smart Maritime, project number 237917.

References

ANDREWS, D. (1986), *An Integrated Approach to Ship Synthesis*, Trans. RINA, pp.73-102

ANDREWS, D. (2003), *Marine design - requirements elucidation rather than requirement engineering*, 8th IMDC Conf. Vol. 1, pp.3-20

ANDREWS, D. (2011), *Marine Requirements Elucidation and the Nature of Preliminary Ship Design*, Int. J. Mar. Eng. 153, pp.23-39

ANDREWS, D.; Dicks, C. (1997), *The Building Block Design Methodology Applied to Advanced Naval Ship Design*, 6th IMDC Conf. Vol.1, pp.3-19

ANDREWS, D.; McDONALD, T.P.; PAWLING, R.G. (2010), *Combining the Design Building Block and Library Based Approaches to improve Exploration during Initial Design*, 9th COMPIT Conf., pp.290-303

CALLEYA, J.N. (2014), *Ship Design Decision Support for a Carbon Dioxide Constrained Future*, PhD thesis, University College London

CALLEYA, J.N.; PAWLING, R.J.; RYAN, C.; GASPAR, H.M. (2016), *Using Data Driven Docu-*

ments (D3) to explore a Whole Ship Model, 11th System of Systems Eng. Conf. (SoSE), pp.1-6

CHOI, M.; ERIKSTAD, S.O. (2017), *A module configuration and valuation model for operational flexibility in ship design using contract scenarios*, Ships and Offshore Structures 12, pp.1127-1135

CHOI, M.; REHN, C.F.; ERIKSTAD, S.O. (2018), *A hybrid method for a module configuration problem in modular adaptable ship design*, Ships and Offshore Structures 13, pp.343-351

COYNE, R.D.; ROSENMAN, M.A.; RADFORD, A.D.; BALACHANDRAN, M.; GERO, J.S. (1990), *Knowledge-based design systems*, Addison-Wesley

DE VRIES, N. (2019), *Safe and effective application of ammonia as a marine fuel*, Master's thesis, Delft University of Technology

DNV GL (2018), *DNVGL-CG-0130 Wave loads*, DNV GL, Høvik

DUCHATEAU, E.A. (2016), *Interactive evolutionary concept exploration in preliminary ship design*, PhD thesis, Delft University of Technology

ERIKSTAD, S.O. (2019), *Design for Modularity*, A Holistic Approach to Ship Design: Optimisation of Ship Design and Operation for Life Cycle Vol. 1, Springer

ERIKSTAD, S.O.; LEVANDER, K. (2012), *System Based Design of Offshore Support Vessels*, 11th IMDC, pp.397-410

ESDRAS, G.; LISCOUET-HANKE, S. (2015), *Development of Core Functions for Aircraft Conceptual Design: Methodology and Results*, Bombardier Product Development Engineering

GASPAR, H.M. (2018), *Vessel.js: an open and collaborative ship design object-oriented library*, 13th IMDC Conf. Vol.1, pp.123-133

GASPAR, H.M.; RHODES, D.H.; ROSS, A.M.; ERIKSTAD, S.O. (2012), *Addressing Complexity Aspects in Conceptual Ship Design: A Systems Engineering Approach*, J. Ship Production And Design 28, pp.145-159

GOEL, V.; PIROLLI, P. (1989), *Motivating the Notion of Generic Design within Information-Processing Theory: The Design Problem Space*, AI Magazine 10, pp.19-36

HOLTROP, J.; MENNEN, G.G. (1982), *An approximate power prediction method*, Int. Shipbuilding Progress 29

IMO (2015), *Third IMO Greenhouse Gas Study 2014*, Int. Mar. Org., London

IMO (2018), *Resolution MEPC.304(72)*, Int. Mar. Org., London

ITTC (2014), *Recommended Procedures and Guidelines: Analysis of Speed/PowerTrial Data*, Int. Towing Tank Conf.

KESICKI, F.; STRACHAN, N. (2011), *Marginal abatement cost (MAC) curves: confronting theory and practice*, Environmental Science & Policy 14, pp.1195-1204

KROES, P.; VERMAAS, P.E.; LIGHT, A.; MOORE, S.A. (2008), *Design in Engineering and Architecture: Towards an Integrated Philosophical Understanding*, Philosophy and Design: From Engineering to Architecture, Springer, pp.1-17

LEVANDER, K. (1991), *System-based Passenger Ship Design*, 4th Int. Marine Systems Design Conf. Vol.1, pp.39-53

LEVANDER, K. (2009), *Cruise Ships - Success factors for the design*, 10th IMDC Conf. Vol.1, pp.16-35

LEVANDER, K. (2012), *System based ship design*, NTNU, Trondheim

LISCOUET-HANKE, S.; HUYNH, K. (2013), *A Methodology for Systems Integration in Aircraft Conceptual Design - Estimation of Required Space*, SAE 2013 AeroTech Congress & Exhibition

MISTREE, F.; SMITH, W.; BRAS, B.; ALLEN, J.; MUSTER, D. (1990), *Decision-Based Design: A Contemporary Paradigm for Ship Design*, SNAME Trans. 98, pp.565-597

NEOLINE. (2019). NEOLINE selects Neopolia's offer for the construction of its first two 136m sailing cargo ships in Saint-Nazaire. Retrieved from

PAHL, G.; BEITZ, W.; FELDHUSEN, J.; GROTE, K.-H. (2007), *Engineering Design: A Systematic Approach*, Springer

PAPANIKOLAOU, A. (2010), *Holistic ship design optimization*, Computer-Aided Design 42, pp.1028-1044

PAPANIKOLAOU, A. (2014), *Ship Design: Methodologies of Preliminary Design*, Springer

PAWLING, R.G. (2007). *The application of the design building block approach to innovative ship design*, PhD thesis, University College London

PETTERSEN, S.S.; REHN, C.F.; GARCIA, J.J.; ERIKSTAD, S.O.; BRETT, P.O.; ASBJØRN-SLETT, B.E., ... RHODES, D.H. (2018), *Ill-structured commercial ship design problems: The responsive system comparison method on an offshore vessel case*, J. Ship Production and Design 34, pp.72-83

RAUCCI, C.; CALLEYA, J.; FUENTE, S.; PAWLING, R.J. (2015), *Hydrogen on board ship: a first analysis of key parameters and implications*, Int. Conf. Shipping in Changing Climates

REHN, C.F.; AGIS, J.J.; ERIKSTAD, S.O.; DE NEUFVILLE, R. (2018), *Versatility vs. retrofitability tradeoff in design of non-transport vessels*, Ocean Engineering 167, pp.229-238

ROSS, A.M.; RHODES, D.H.; HASTINGS, D.E. (2008), *Defining changeability: Reconciling flexibility, adaptability, scalability, modifiability, and robustness for maintaining system lifecycle value*, Systems Engineering 11, pp.246-262

SALVADOR, F.; FORZA, C.; RUNGTUSANATHAM, M. (2002), *Modularity, product variety, production volume, and component sourcing: Theorizing beyond generic prescriptions*, J. Operations Management 20, pp.549-575

SANDVIK, E.; GUTSCH, M.; ASBJØRNSLETT, B.E. (2018), *A simulation-based ship design methodology for evaluating susceptibility to weather-induced delays during marine operations*, Ship Technology Research 65, pp.137-152

SCHILLING, M.A. (2000). *Toward a General Modular Systems Theory and Its Application to Interfirm Product Modularity*, The Academy of Management Review 25, pp.312–334

SIMON, H.A. (1973), *The structure of ill structured problems*, Artificial Intelligence 4, pp.181-201

SIMON, H.A. (1996), *The sciences of the artificial*, MIT Press

SUH, N.P. (1990), *The Principles of Design (Vol. 6)*, Oxford University Press

ULSTEIN, T.; BRETT, P.O. (2015), *What is a better ship? – It all depends*, 12th IMDC Conf. Vol.1

UN (2015), *Paris Agreement*, United Nations, New York

VAN DER KOLK, N.; BORDOGNA, G.; MASON, J.C.; DESPRAIRIES, P.; & VRIJDAG, A. (2019), *Case study: Wind-assisted ship propulsion performance prediction, routing, and economic modelling*, Int. Conf. Power & Propulsion Alternatives for Ships

VAN DER NAT, C.J. (1999), *A knowledge-based Concept Exploration Model for Submarine Design*, PhD thesis, Delft University of Technology

VAN OERS, B.J. (2011), *A Packing Approach for the Early Stage Design of Service Vessels*, PhD thesis, Delft University of Technology

Performance Prediction and Weather Routing of Wind Assisted Ships

Nils Hagemeister, Fraunhofer CML, Hamburg/Germany, nils.hagemeister@cml.fraunhofer.de
Tina Hensel, Fraunhofer CML, Hamburg/Germany, tina.hensel@cml.fraunhofer.de
Carlos Jahn, Fraunhofer CML, Hamburg/Germany, carlos.jahn@cml.fraunhofer.de

Abstract

This paper describes the integrated performance prediction and weather routing tool developed by Fraunhofer CML for the VINDSKIP® wind assisted hybrid propulsion concept. The performance prediction approach utilizes a constraint optimization routine to balance aerodynamic and hydrodynamic forces to determine the total resistance while satisfying the equilibrium condition for three degrees of freedom. For the weather routing an implementation of the A-algorithm on a dynamic grid is utilized, including avoidance of land masses and harsh weather according to IMO guidelines. The results of the performance prediction and weather routing are presented.*

1. Introduction

With the pressure for decarbonisation of the shipping industry steadily increasing, sail assist systems are gaining increasing popularity. There are a number of different systems being developed, tested or marketed at the moment, each with their own individual characteristics. However, one common aspect is that weather routing should be utilized to realise each system's full emission reduction potential. In its simplest form this might be the consideration of favourable wind angles in the route planning. However, neglecting the hydrodynamic response to the aerodynamic forces can cause significant errors in the prediction of the propulsion power demand and the corresponding fuel consumption. This paper presents an approach for integrated performance prediction and weather routing for the example of the VINDSKIP® wind assisted ship concept.

2. The VINDSKIP® concept

2.1. Main features

The VINDSKIP® is a unique wind assisted PCTC concept, combining wind and hybrid propulsion. Fig.1 shows an illustration of the concept. The main feature of the concept is the aerofoil shape adopted for the ship's superstructure, transforming it into built-in sail area. The stability required for safe sailing is created through a trimaran configuration consisting of the main hull and one small float on either side of the vessel, https://ladeas.no/.

Fig.1: Illustration of the VINDSKIP® concept, https://ladeas.no/

Table I lists the main dimensions of the VINDSKIP®.

Table I: VINDSKIP® main dimensions, *Lade AS (2013)*

Quantity	Units	value
Length	[m]	199.0
Breadth	[m]	49.0
Design Draft	[m]	8.5
Displacement	[m³]	24550
Service Speed	[kts]	14.0
Car capacity	[-]	6600

2.2. Fluid dynamic characteristics

This study uses the concept of force areas (A) and moment volumes (V) to describe the fluid dynamic characteristics of the vessel. In contrast to force and moment coefficients for which reference areas and lengths are considered, these quantities are derived from experimental and simulation data by normalizing forces F and moments M only with dynamic pressure.

$$A = \frac{F}{\frac{\rho}{2}u^2};\ V = \frac{M}{\frac{\rho}{2}u^2}$$

The coordinate convention used is a right-handed, ship-fixed cartesian coordinate system with the longitudinal axis pointing aft along the centerline and the vertical axis pointing upwards.

2.2.1. Aerodynamic characteristics

Fig.2 shows the aerodynamic characteristics consisting of resistance area A_{xaero}, sideforce area A_{yaero} and yaw moment volume V_{zaero} of the VINDSKIP® as function of the Apparent Wind Angle (AWA). It can be observed that at very small AWAs the ship experiences aerodynamic resistance. With increasing AWA, the resistance starts to decrease, becomes negative (i.e. thrust) at just below 20° and continues to decrease further until reaching a minimum of approximately -700m² at an AWA of about 90°. Between the minimum and an angle of attack of 160° the resistance area increases to -500m² and then stays approximately constant for the remaining range of AWAs.

Starting from zero at AWA = 0° the sideforce area increases to just below 9000m² at an AWA of 60°. From there it decreases steadily until it is back at zero at AWA = 180°. The yaw moment volume is also zero at 0° AWA and then decreases to about -180.000 m³ at AWA = 40°. It then starts to increase, changing signs at approximately 80° AWA, reaching a maximum of 280.000m³ at about AWA = 140° and goes back to zero at AWA = 180°.

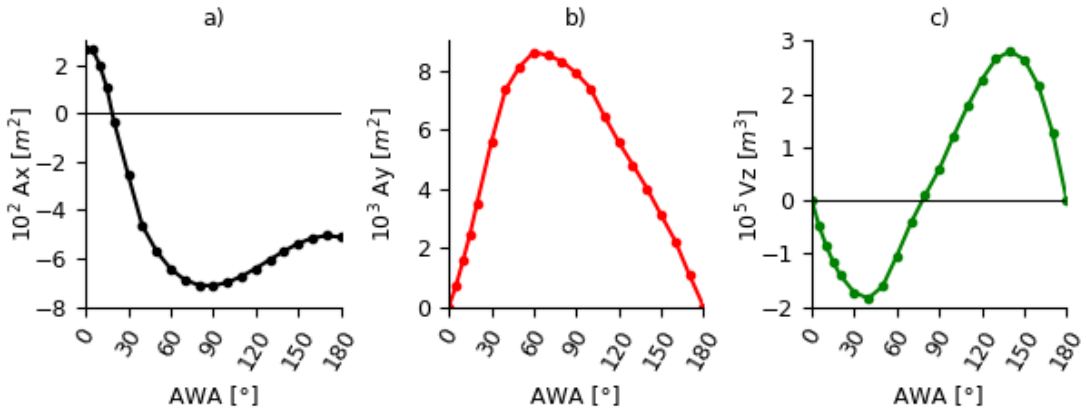

Fig.2: a) aerodynamic resistance area A_{xaero}, b) aerodynamic sideforce area A_{yaero} and c) aerodynamic yaw moment volume V_{zaero} over apparent wind angle (AWA)

2.2.2. Calm-water resistance

Fig.3 shows a plot of the calm-water resistance area A_{xcwr} as a function of speed. As can be observed the available data only covers speeds between 7.2 m/s and 8.7 m/s, which represents the range considered relevant for ocean crossings. The resistance area varies between approximately 0.015 m² and 0.017 m² for these speeds.

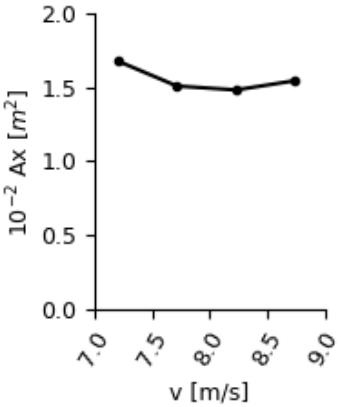

Fig.3: Calm water resistance area A_{xcwr} over velocity

2.2.3. Response to yaw

Fig.4 shows the hydrodynamic responses to leeway at a velocity of 16.0 knots for yaw angles (β) between 0° and 6°. The longitudinal force is expressed as delta in relation to the calm water resistance. It can be observed that the delta A_{xhydro} becomes negative at small yaw angles between 0.5° and 4.5°, indicating a decreasing resistance force, before it starts to provide a net increase from about 5.0° onwards. This may seem counterintuitive, as leeway is usually associated with additional resistance. However, the reader is reminded that the underlying coordinate system is fixed to the ship, which means that while the force along the centerline when assuming a yaw angle may drop slightly, it does not represent the total force in the direction of motion anymore.

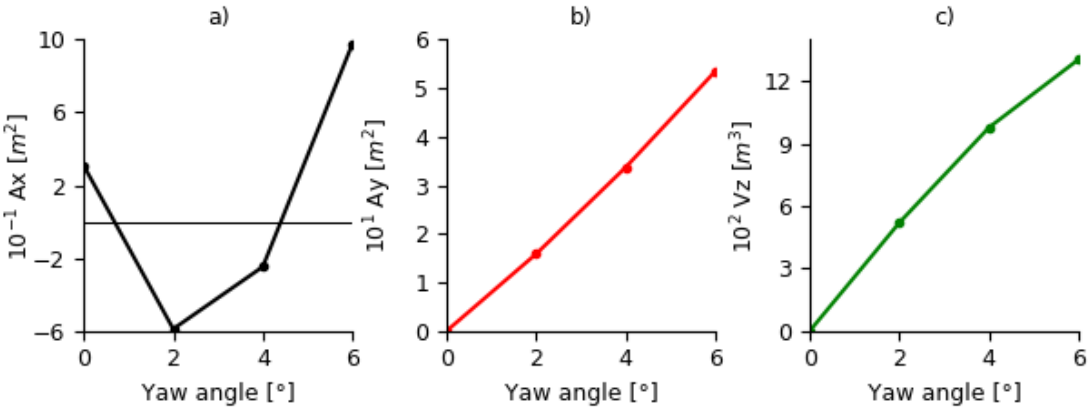

Fig.4: a) hydrodynamic resistance area A_{xhydro}, b) hydrodynamic sideforce area A_{yhydro} and c) hydrodynamic moment volume V_{zhydro} over yaw angle β

The transverse force area A_{yhydro} increases approximately proportionally to the yaw angle, starting from zero at 0° of yaw and reaching a value of about 53 m² at 6° of yaw.

The yaw moment volume V_{zhydro} is 0m³ at 0° of yaw and also progresses almost proportional to the yaw angle in the plotted range. However, with the slope of the curve slightly decreasing between each pair of consecutive data points, this observation is not expected to hold at larger yaw angles.

2.2.4. Rudder forces

Fig.5 shows the rudder resistance area A_{xr} and sideforce area A_{yr} over rudder angle γ. The plot shows the typical characteristics of a finite, symmetric wing: The sideforce (respectively the lift) increases proportionally with the rudder angle until the curve starts to flatten when approaching the stall angle, which in this case is about 35°. After exceeding the stall angle the sideforce starts to drop and this trend continues up to the highest rudder angles considered here. In contrast, the resistance at first increases only slightly with increasing rudder angle. From a rudder angle of 10° onwards the slope of the resistance increases continuously until the stall angle is reached. Above the stall angle the resistance area continuous to increase at a decreasing rate. At a rudder angle of 45° sideforce and resistance are of equal magnitude.

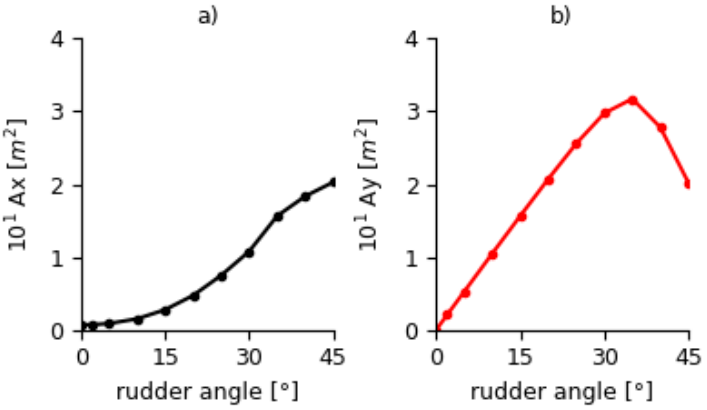

Fig.5: a) rudder resistance area A_{xr} and b) rudder sideforce area A_{yr} as functions of rudder angle γ

2.2.5. Added forces due to seastate

For this project the wave forces caused by the seastate have been calculated for two ship speeds and one loadcase with wave periods varying between 3 s and 25 s and encounter angles changing in 5° increments from 0° to 180°. Two methods, a strip theory and an asymptotic approach, have been employed to consider forces arising from low and high frequency waves.

Following the approach of *Clauss et al. (1994)*, the second order wave forces can be assumed to vary with so-called seaway envelope $a(t)^2$. Accordingly, a wave force in the time domain can thus be determined from the following expression where ρ denotes the density, g gravitational acceleration, L a reference length and α^2 a non-dimensional wave force coefficient. Since this study considers a specific ship, the constants have been integrated into the force coefficient c_{wf} and moment coefficient c_{wm}, respectively.

$$F(t) = \frac{\rho}{2} * g * L * \alpha^2 * a(t)^2 = c_{wf} * a(t)^2$$

Fig.6 illustrates the second order wave forces and moments normalized by the seaway envelope as functions of encounter angle δ and wave period T for a velocity of 14 knots. It can be observed that there is a strong effect on the longitudinal force from waves with a period around 15 s. In head waves the ship can encounter added resistance of up to 400 kN/m² whereas in following seas the resistance can decrease by up to 200 kN/m².

The most significant transverse forces are experienced in transverse waves with small periods and are in the order of 4000 kN/m². The lateral force diminishes quickly with increasing wave period with practically no influence from waves with periods above 20 s.

The maximum and minimum yaw moments are also exerted on the ship at small wave periods. This

indicates that the yaw moment mostly depends on the transverse force. This observation seems plausible since the maximum transverse force is one order of magnitude larger than the maximum longitudinal force.

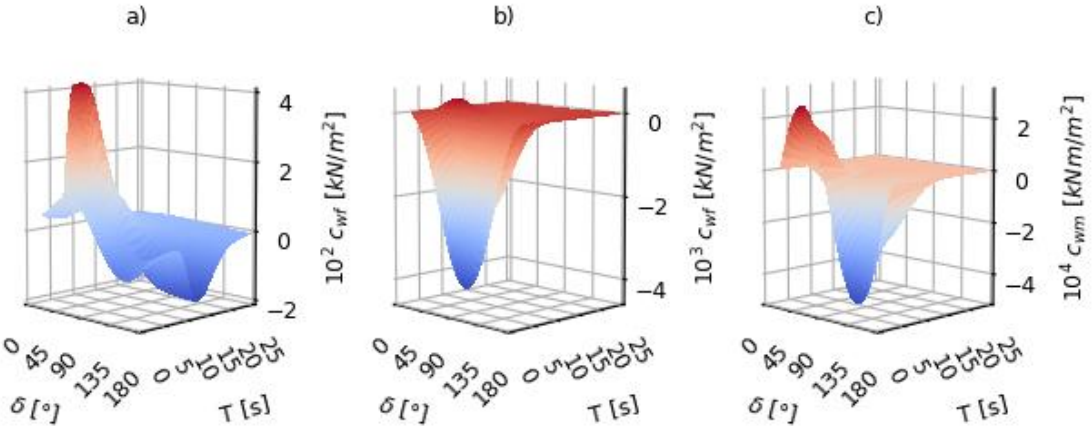

Fig.6: Second-order wave a) longitudinal force coefficient c_{wfx}, b) transverse force coefficient c_{wfy} and c) yaw moment coefficient c_{wmz} as functions of wave encounter angle δ and wave period T for a velocity of 14 knots

To derive the actual added forces, an artificial seaway is created based on the Pierson-Moskowitz wave spectrum for fully developed sea, *DNVGL (2018)*. Wave elevations are determined by superposition of wave frequencies and their associated amplitudes from the spectrum with random phase shifts for discrete points in time. An example of such a wave spectrum for a significant wave period T_s of 10 s and a significant wave height H_s of 1 m as well as the resulting wave elevations are given in Fig.7.

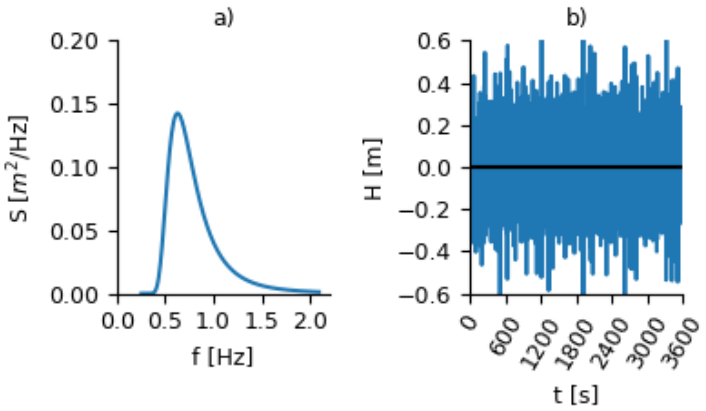

Fig.7: a) Pierson-Moskowitz wave spectral density S over wave frequency f for significant wave period of 10 s and significant wave height of 1 m; b) associated wave elevations H over time t

The seaway envelope is defined as the sum of the square of the instantaneous wave elevations and the square of their rate of change divided by the square of the significant frequency.

$$a(t)^2 = H(t)^2 + \frac{\left(\frac{dH}{dt}\right)^2}{\omega_0^2}$$

Mean force and moment coefficients for a given spectrum are calculated as weighted average based on the contribution of each frequency to the energy of the spectrum.

$$c_{wf} = \frac{\sum c_{wf_i}(\omega) * S_i(\omega)}{\sum S_i(\omega)}$$

Instantaneous forces are then derived by multiplying the mean force coefficient c_{wf} with the seaway envelope $\alpha(t)^2$ and a mean force is derived that can be used in the performance prediction. An example of the seaway envelope and the corresponding instantaneous forces and the resulting mean force is shown in Fig.8.

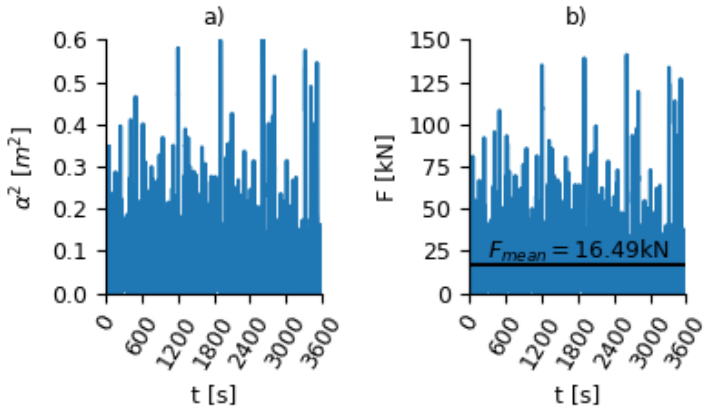

Fig.8: a) Seaway envelope $\alpha(t)^2$ and b) example of resulting instantaneous forces F over time

3. Performance Prediction approach

3.1. Interaction of forces and moments

As shown above, wind forces do not only act as thrust, i.e. as a force along the centerline of the ship, but also affect the other degrees of freedom. Since any ship automatically assumes a state of force and moment equilibrium, these forces and moments and their mutual interactions need to be considered for an accurate powering prediction. The equilibrium state condition can be expressed as follows.

$$\sum F = \sum M = 0$$

The method at hand considers aerodynamic and hydrodynamic forces and moments for three degrees of freedom, surge, sway and yaw. The total force acting along the ship's centerline is calculated as the sum of the aerodynamic force F_{xaero}, the resistance force on the hull F_{xcwr}, the correction for leeway effects F_{xhydro}, the rudder force F_{xr} and the added resistance force F_{xwave}.

$$F_x = F_{xaero}(AWA, AWS) + F_{xcwr}(u) + F_{xhydro}(u, \beta) + F_{xr}(u, \gamma) + F_{xwave}(u, \delta, T_s, H_s)$$

The transverse force is derived in a similar way with the only difference being that F_{yhydro} represents the total calm water force and not a correction, since the transverse force at 0° of leeway is zero.

$$F_y = F_{yaero}(AWA, AWS) + F_{yhydro}(u, \beta) + F_{yr}(u, \gamma) + F_{ywave}(u, \delta, T_s, H_s)$$

Using the longitudinal position of the rudder x_r to calculate its yaw moment, the total yaw moment can be derived as follows.

$$M_z = M_{zaero}(AWA, AWS) + M_{zhydro}(u, \beta) + F_{yr}(u, \gamma) * x_r + M_{zwave}(u, \delta, T_s, H_s)$$

3.2. Total efficiency and engine characteristics

To determine the fuel consumption for a given effective towing power the total efficiency of the propulsion system and the main engine characteristics need to be considered. The break power P_B is the product of the total longitudinal force F_x and speed u, divided by the total efficiency η_{tot}.

$$P_B = \frac{F_x * u}{\eta_{tot}}$$

The fuel oil consumption (FOC) is then derived from the Specific Fuel Oil Consumption (SFOC), which is a function of the engine output.

$$FOC(P_B) = P_B * SFOC(P_B)$$

Fig.9 shows plots of the total efficiency η_{tot} as a function of ship speed u and SFOC as function of engine rating. It can be observed that the total efficiency at a velocity of 10 knots is about 0.63 and increases steeply to around 0.735 at 12.5 knots. From this point onwards it only increases marginally, peaking out at 0.745 at a velocity of 15 knots. Thereafter the efficiency drops to about 0.72 at the end of the plotted speed range. The total efficiency has been derived for ideal calm water conditions without wind or waves. Hence the effects of leeway and resistance variations for a constant speed are not considered.

The fuel efficiency of the main engine increases with increasing power output. The SFOC drops from about 150.4 g/kWh at an output of 2700 kW to 149.0 g/kWh at its maximum rating of 5500 kW.

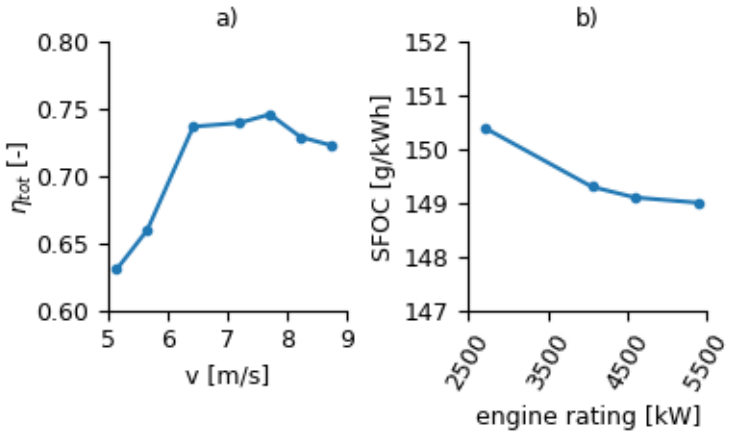

Fig.9: a) Total efficiency η_{tot} over ship velocity u and b) SFOC over engine rating

3.3. Polynomial fitting

The fluid dynamic data shown in chapter 2 is represented through polynomials in the performance prediction module. This has been done for two reasons. Firstly, evaluating a polynomial is a much faster programming operation than for example interpolation. This is an important consideration for a numerical optimization as gradients for each variable usually need to be computed several times for all dependent quantities before an optimum is reached.

Secondly, the polynomials ensure a locally smooth progression of the function values which results in steady functions for the derivatives. Finding an optimum around a discontinuity of a derivative can be troublesome and since many optimizations need to be performed in this application, the optimization process needs to be fast and reliable.

3.4. Constraint optimization

The performance prediction is obtained by applying a constraint optimization procedure. The target function f_{min} to be minimized during the optimization is the total resistance of the ship for the given set of conditions (cruise speed, wind, waves):

$$f = \min\left(F_x(AWA, AWS, u, \beta, \gamma, \delta, T_s, H_s)\right)$$

The constraints are derived from the equilibrium required to sail in a straight line along the specified course:

$$\sum F_y(AWA, AWS, u, \beta, \gamma, \delta, T_s, H_s) = \sum M_z(AWA, AWS, u, \beta, \gamma, \delta, T_s, H_s) = 0$$

The optimization variables are rudder and leeway angles with their respective bounds:

$$-12° \leq \beta \leq 12°$$
$$-45° \leq \gamma \leq 45°$$

The result of this optimization is the minimum total resistance of the ship for the specified velocity under the given conditions from which the required power to propel the ship can be derived. If this power exceeds the Maximum Continuous Rating (MCR) of the main engine, a second optimization is performed, which maximizes the speed for a given engine output. The objective function for the minimization f_{min} then becomes the negative ship speed:

$$f = \min(-u)$$

The power limit is added as an additional constraint:

$$\sum F_y = \sum M_z = P(F_x(AWA, AWS, u, \beta, \gamma, \delta, T_s, H_s), u, \eta_{tot}) - MCR = 0$$

To be able to adjust the power demand, the velocity is turned into an optimization variable, giving a total of three variables to be adjusted.

$$-12° \leq \beta \leq 12°$$
$$-45° \leq \delta \leq 45°$$
$$0 \leq u \leq u_{cruise}$$

The result of this second optimization is the velocity for the given conditions and the specified maximum continuous rating of the engine.

3.5. Performance Prediction results

Fig.10 shows the results of the performance prediction for a cruise speed of 15.0 knots and a true wind velocity of 9 knots, which is thought to be representative of the average conditions experienced during an Atlantic crossing. The effects of waves have been excluded here to focus entirely on the aerodynamic performance.

It can be observed that the power demand in headwinds is just below 5500 kW. It then decreases an at almost constant rate of about 18.5 kW per degree of increase of the True Wind Angle (TWA) up to TWA = 60°. From this point the reduction in power demand continues at a decreasing rate until reaching the minimum of approximately 4300kW at a TWA of about 85°. The power demand then starts to increase again, asymptotically approaching a value of 5000kW at TWA = 180°.

The optimum rudder angle at first starts to decrease with increasing wind angle, reaching a minimum of just below -1° at TWA = 25°. The rudder angle then starts to increase and becomes neutral at TWA = 60°. It continues to increase until reaching the maximum rudder angle of about 2.2° at TWA = 110° before dropping back to zero throughout the remaining TWA range. The leeway angle decreases with increasing TWA to almost -3° at TWA = 70° and then climbs back to 0° at TWA = 180°.

The difference in power demand between the maximum and minimum values is roughly 1200 kW, which corresponds to about 22% of the MCR of the main engine, which is 5400kW. This illustrates the importance of considering the weather during the route planning as the difference in fuel consumption

is directly related to the power of the main engine. Hence, sailing with more favorable wind angles and avoiding unfavorable wind angles can make a difference of the same order of magnitude on the overall fuel consumption of a voyage.

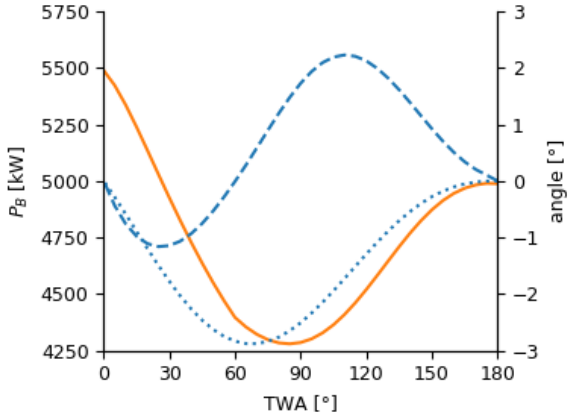

Fig.10: Break power (solid orange), rudder angle (dashed blue) and leeway angle (dotted blue) over True Wind Angle (TWA) for ship speed of 15.0 kn and True Wind Speed (TWS) of 9.0 kn.

Fig.11 shows a comparison of the performance prediction for the presented three degrees of freedom (DOF) model to a one DOF model that only considers longitudinal forces. It can be observed that the one DOF model has a similar progression, but overpredicts the break power at almost all TWAs. The difference between the predictions ranges from 0% in head- and tailwinds up to around 4.5% between TWA = 60° and TWA = 105°.

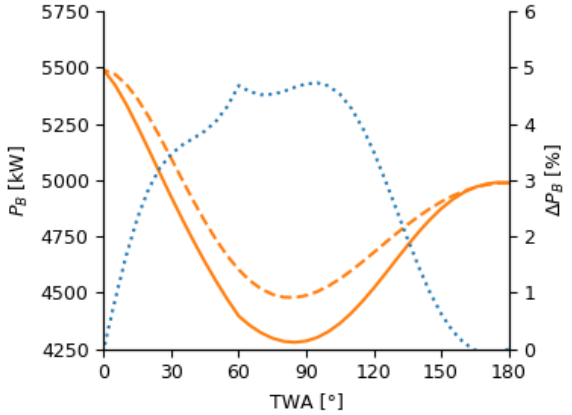

Fig.11: Break power P_B for 3 DOF equilibrium condition (solid orange), break power for single DOF equilibrium (dashed orange) and difference ΔP_B between 3 DOF and 1 DOF models (dotted blue) over TWA for ship speed of 15.0 kn and TWS of 9.0 kn

4. Weather routing

4.1. Routing algorithm

Weather routing is based on the A*-algorithm addressing the problem of finding the shortest path from the departure location to the destination, while avoiding obstacles and minimizing costs. It works on a graph, representing a set of vertices with edges connecting them. A* combines the exact cost of the path from the departure location to any vertex with the heuristic estimated cost from this vertex to the destination.

The principle of the grid generation is illustrated in Fig.12. A set of courses is defined through an angle θ sweep with discrete steps h around the direct course between start and finish. For each of these courses

the velocity and power demand are determined. New node positions are then derived from the velocity along each course and a given time step.

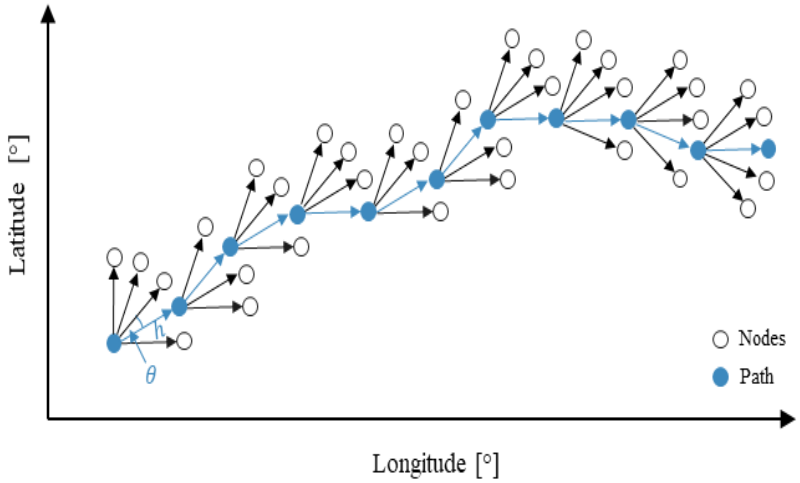

Fig.12: Concept of the dynamic grid generation

4.1.1 Target function and variables

Variables for the optimization are the geographical position (φ_k, λ_k) [°,°] of the next waypoint or vertex k as well as the time t_k [h] and ship's speed v_k between the waypoints. The function value *f(k)* representing the fuel consumption at each vertex k is calculated as the sum of the actual fuel consumption from the start to the current node *g(k)* and the heuristic fuel required to reach the destination on a straight course under calm water conditions *h(k)*. Thus, the optimization problem for every vertex k can be described by the target function

$$f(k) = g(k) + h(k) \leq \min\{g(i) + h(i) \mid i \in B\}$$

With *f(k)* being an estimate of the cost from the starting point to the destination across vertex k. B is a set of vertices, which have not been considered on the path from the starting point to *k, Turau (2009)*. In each loop, the algorithm determines the vertex k that has the lowest estimated costs *f(k)*. In case of the Vindskip® concept, the target function aims to minimize the overall fuel consumption for a chosen route represented by a set of vertexes, describing the route from the departure to the destination with the lowest estimated fuel consumption, and the time t_k, at which the ship passes vertex k considering weather forecasts and restrictions described in the main features as well as safety restrictions according to the International Maritime Organization (IMO).

4.1.2. Restrictions

The algorithm described in section 4.1.1 is subject to a variety of restrictions, which are considered within the optimization routine. Landmasses are considered by initially integrating shape files to dynamically exclude vertexes which are crossing these shape files and thus landmasses. In addition, general operational restrictions are included mainly referring to scheduling and speed control during the routing to reach a destination before a pre-defined given latest possible time of arrival t_{ETA}.

$$t_n \leq t_{ETA}$$

with t_n representing the calculated arrival time. To achieve this, the remaining distance for each course to the destination is estimated based on a given initial velocity and a time step h. The average velocity required to reach the destination on time is calculated using the remaining distance as well as the remaining time in combination with the maximum ship's speed.

For a given position (φ_k, λ_k) and time t_k for a vertex k general weather operational envelopes related to the ship's safety refer to maximum values of the significant wave height $H_{1/3}$ as well as a maximum wind velocity v_w.

$$H_{1/3}(\varphi_k, \lambda_k, t_k) \leq H_{1/3,max} \quad \forall\, k \in [1; n]$$
$$v_w(\varphi_k, \lambda_k, t_k) \leq v_{w,max} \quad \forall\, k \in [1; n]$$

Besides these operational limits, safety restrictions consider the guidance to the Master for avoiding dangerous situations in adverse weather and sea conditions published by the IMO in MSC.1 / Circ. 1228, *IMO (2007)*. Accordingly, adverse weather conditions include wind induced waves and heavy swell. Dangerous phenomena refer to:

- Surf-riding and broaching-to,
- Reduction of intact stability when riding a wave crest amidships,
- Parametric roll motion.

Details for the determination of these phenomena can be found in MSC.1 / Circ. 1228, *IMO (2007)*.

4.2. Results

Weather routing has been performed for nine round trips Atlantic crossing within one year on the route Emden (GER), Jacksonville (USA), Veracruz (MEX), Emden (GER) using a corresponding service speed of 14 kn and hindcast data weather data from 2017. Table II depicts the calculated voyage duration, fuel consumption as well as fuel consumption per day for the nine round trips. As can be observed there is a variation of 3 h regarding the voyage duration and a variation of up to 48.2 t regarding the fuel consumption. The statistical averages for the route segments are given in Table III.

Table II: Route calculations for VINDSKIP® performance tests

Round trip no.	Voyage duration (h)	Fuel consumption (tons)	Fuel consumption per day (tons / day)
1	768	457.7	14.3
2	768	476.4	14.9
3	768	486.9	15.2
4	771	479.2	14.9
5	768	504.9	15.8
6	768	479.9	15.0
7	768	501.6	15.7
8	768	505.9	15.8
9	768	458.2	14.3
Min/ max	771/ 768	505.9/457.7	14.3/ 15.8
Variation	3.0	48.2	1.5

Table III: Statistical averages of VINDSKIP® performance tests

Departure	Destination	Voyage duration	Fuel consumption	Percentage of travel times below service speed
Emden	Jacksonville	294.84 h	187.71 t	0.11 %
Jacksonville	Vera Cruz	95.86 h	60.52 t	0.00 %
Vera Cruz	Emden	377.64 h	235.19 t	0.00 %
Round Trip	768.34 h	483.41 t	0.04 %	768.34 h

Fig.13 shows a plot of an example routing for the round trip mentioned above with date of departure on 23.06.2017 – 10:46.

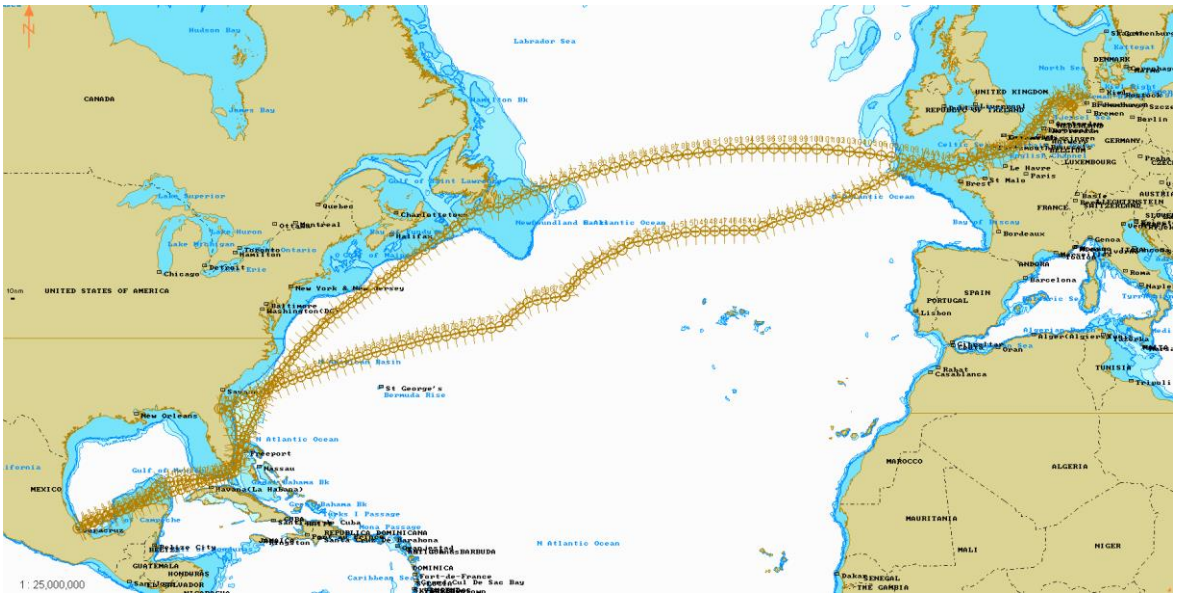

Fig.13: Example routing for a Vindskip® round trip (Emden, Jacksonville, Vera Cruz, Emden)

5. Conclusion

With the Vindskip® performance prediction and weather routing module described in this paper a system has been developed to account for the innovative approach of Vindskip® to use the aerodynamic lift generated by the wind as propulsive force. The results shown in this paper demonstrate the module's ability to find the route with the lowest fuel costs based on optimum wind conditions. In total, the optimization of route waypoints in accordance with the design of Vindskip® benefits an increase in fuel efficiency as well as a safe and comfortable voyage.

References

CLAUSS, G.; LEHMANN, E.; OSTERGAARD, C. (1994), *Strength and Safety for Structural Design and Offshore Structures*, Vol. II, Springer

DNVGL (2018), *Class Guideline – DNVGL-CG-0130 – Wave Loads*, https://rules.dnvgl.com/docs/pdf/DNVGL/CG/2018-01/DNVGL-CG-0130.pdf

IMO (2007), *MSC.1/Circ.1228 - Revised Guidance to the Master for Avoiding Dangerous Situations in Adverse weather and Sea conditions*, Int. Maritime Organization, London

TURAU, V. (2009), *Algorithmische Graphentheorie*, Vol. III, Oldenbourg Wissenschaftsverlag

Innovative Robotic and Performance-based Hull Management Solution

Geir Axel Oftedahl, Jotun A/S, Sandefjord/Norway, geir.axel.oftedahl@jotun.no

Abstract

The paper describes Jotun's Hull Skating Solutions (HSS) for proactive hull cleaning. The solution combines high-performance antifouling, proactive condition monitoring, inspection and proactive cleaning, remote operation from shore as well as, performance and service level guarantees. The paper describes the background for the development of HSS, how it works, its benefits and the partners involved on its' development.

1. Background

The accumulation of fouling over time leads to a significant drop in performance and an increase in the vessel's fuel consumption and environmental footprint. To counter this, ship operators use hull coatings with anti-fouling properties. However, these coatings will not always deliver optimal anti-fouling protection due to changing operational profiles or the operation being so challenging that fouling pressures exceeding coating tolerance.

Many vessels spend time in challenging and complex environments, or are deployed in difficult operational profiles, where hull fouling can have a marked impact on efficiency and raise fuel costs. Various circumstances can prove challenging from a hull performance point of view and require proper attention since the current solutions on the market struggle to address these problems. Also, operational profile factors outside coating tolerance such as speed, activity and temperature can be encountered for a variety of reasons.

Bulk carriers, tankers and general cargo ships can spend long periods in ports being loaded and unloaded. Some of them may also be prevented from berthing for long periods due to neap tides. In such cases, shallow water and temperate environments can lead to accelerated fouling. Many shipowners must deal with these challenging operations on a regular basis.

According to the IMOs 4th GHG emissions study, *IMO (2020)*, International shipping emitted around 919m tons of CO_2 and 21m tons of other GHGs in 2018 (incl. methane, NOx, SOx). According to the same study, 9% of consumption and emissions were caused by biofouling, resulting in a total annual reductions potential of around 83m tons of CO_2 and around 2m tones of other GHGs. The share of consumption and emissions caused by biofouling corresponds with findings from earlier studies including Clean Shipping Coalition submission to the 63rd IMO Marine Environment Protection Committee meeting, *CSC (2015)*.

For the ships the greatest biofouling challenge, the share of fuel consumption caused by biofouling is likely to greatly exceed the 9% average for all ships. The improvement potential is therefore considerable.

Most shipowners and operators accept that anti-fouling coatings and operational measures combine to affect efficiency and they will make choices mostly based on their own experience of different products. There are many solutions in the market today, offering different types of anti-fouling coatings that use different types of technology to ensure that fouling will not settle on the ship's hull. One area, however, where today's solutions for anti-fouling have not fully succeeded is challenging operations, forcing owners and operators to spend a lot of money and effort on inspections and cleaning.

Aside from cleaning or replacing the antifouling during dry-dockings, hulls and propellers may be cleaned occasionally in water while in service. This is normally done on the so-called reactive cleaning basis, which usually takes place during the dry-docking or when heavy fouling is evident. Today,

performance monitoring software tools make it possible to detect varying degrees of fouling based upon the ship's performance and fuel consumption data and allow for cleaning to be arranged. However, at this stage fouling is already a major problem.

Traditionally cleaning would be done manually by teams of divers. This is still a method that is in common use, but which is increasingly coming under scrutiny. Diving teams may be good at clearing the fouling from the hull but there are problems. Firstly, it is a labor intensive and costly process. If there are insufficient divers available, the time needed can be difficult for ship operators to fit into schedules and may lead to off hire time for chartered ships.

Moreover, manual cleaning often leads to the coating becoming damaged and potentially creating an even worse problem in a very short time. The effect on the environment is also an issue as the cleaning process may result in aquatic invasive species and/or eroded coating materials being deposited into the water column. This can have a detrimental effect on local ecosystems and is something that authorities are not keen on permitting.

Finally, and perhaps most importantly, in some situations manual cleaning with divers place the divers at risk. Injuries and deaths are reported each year.

Consequently, manual cleaning by divers is no longer permitted in a number of ports. Many others are considering banning such activities. That does make following the International Maritime Organisation's (IMO) biofouling guidelines difficult and is something that will need to be addressed if controls become mandatory.

Robotic cleaning (with remotely or diver operated equipment) is another way to clean hulls and there are a range of solutions of varying maturity emerging. Some of these solutions even allow for the capture of some or all of the biofouling waste and eroded coating materials removed during the cleaning.

However, the common denominator for all cleaning technologies in use today is that they are used reactively – they are designed for and applied when the fouling has already become a problem.

2. Proactive cleaning and the Jotun Hull Skating Solution

To combat fouling and help address the challenges faced by owners and operators of ships in the most challenging operations, Jotun introduces proactive cleaning through its Hull Skating Solution, a groundbreaking approach engineered to keep the hull free of fouling at all times, Fig.1.

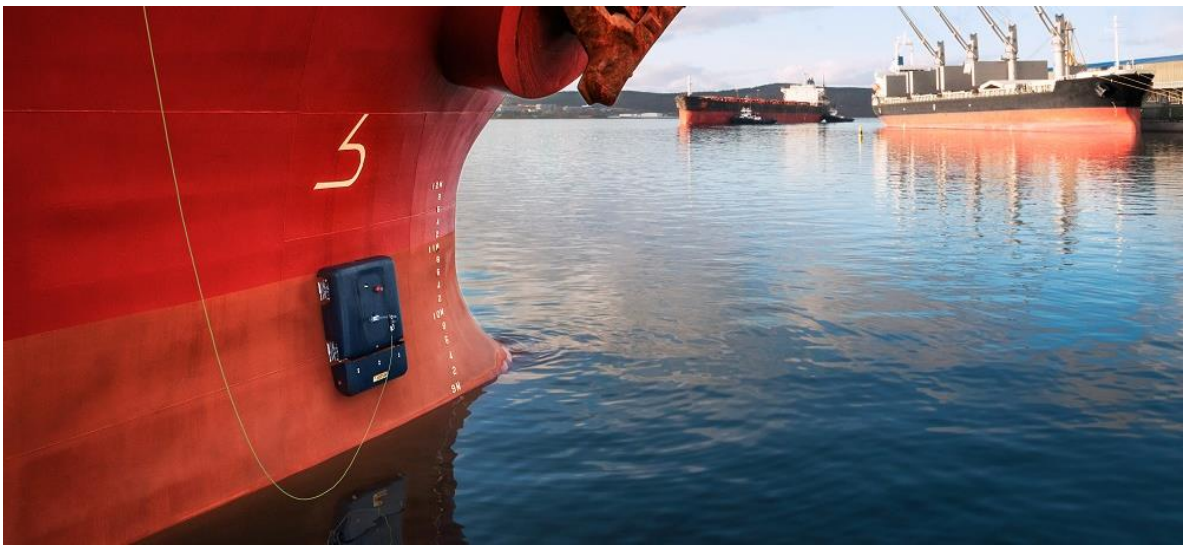

Fig.1: Hull Skater robot in prototype testing

When the biofouling pressure exceeds the antifouling or fouling release capabilities in the coating used, biofouling will begin to settle on the hull. Biofouling progresses in several stages:

Stage 1 (USN FR 0 to 10): Settlement of individual bacteria (within minutes)
Stage 2 (USN FR 20): Biofilm / slime (within 1 day)
Stage 3 (USN FR 30): Algae and single-cell organisms (within 1 week)
Stage 4 (USN FR 40 and up): Macro-fouling (tubeworms, barnacles, etc.) (within 2-3 weeks)

USN FR refers to the US Navy Fouling Rating scale, *US Navy (2006)*.

In the Guideline for Proactive Cleaning of Hull Areas in Port & at Anchorage, *Oftedahl and Enström (2000)*, proactive cleaning is defined as the proactive removal of fouling at Stage 1 and early in Stage 2 - before it reaches Stage 3. Proactive cleaning is achieved by cleaning the hull regularly before fouling takes hold. Fouling is therefore removed before it affects hull performance and before there is biofouling waste to be captured. When fouling is removed at such an early stage, the force needed to remove the fouling is also very limited, with the result that the fouling can be removed without damage to or erosion of the coating.

Put simply, Jotun Hull Skating Solutions keeps ship's hull clean to minimize performance loss with no debris or waste, giving an unmatched environmental footprint and full operational flexibility.

2.1. Solution elements

The solution combines five elements to deliver an always clean hull:

Fig.2: The 5 elements in the Hull Skating Solution

- High performance coatings
  Jotun's 'SeaQuantum Skate' coating has been developed specifically to optimize performance in combination with the HullSkater technology. The new coating builds upon the excellent performance of the SeaQuantum brand, which is the result of over 20 years research and development in silyl acrylate technologies. SeaQuantum Skate is the only coating tailored for Hull Skating.

- Proactive condition monitoring
  This is an essential component of predictive hull maintenance. Jotun's in-house analysts make fouling predictions based on big data trends, algorithms and analyses, and advise customers on when to carry out hull maintenance. This also includes oceanographic assessment for fouling prediction and enabling the Skate Operator to perfectly time the deployment of the system.

- Inspection and proactive cleaning
  The HullSkater is the first robotic device that has been purposed designed for proactive cleaning. It has high inspection and cleaning capacity and removes fouling without damaging the anti-fouling coating. The HullSkater is always kept onboard in a portable station with launch and recovery ramp. This means that it is always available and can be used when the ship

is in harbour or at anchor.

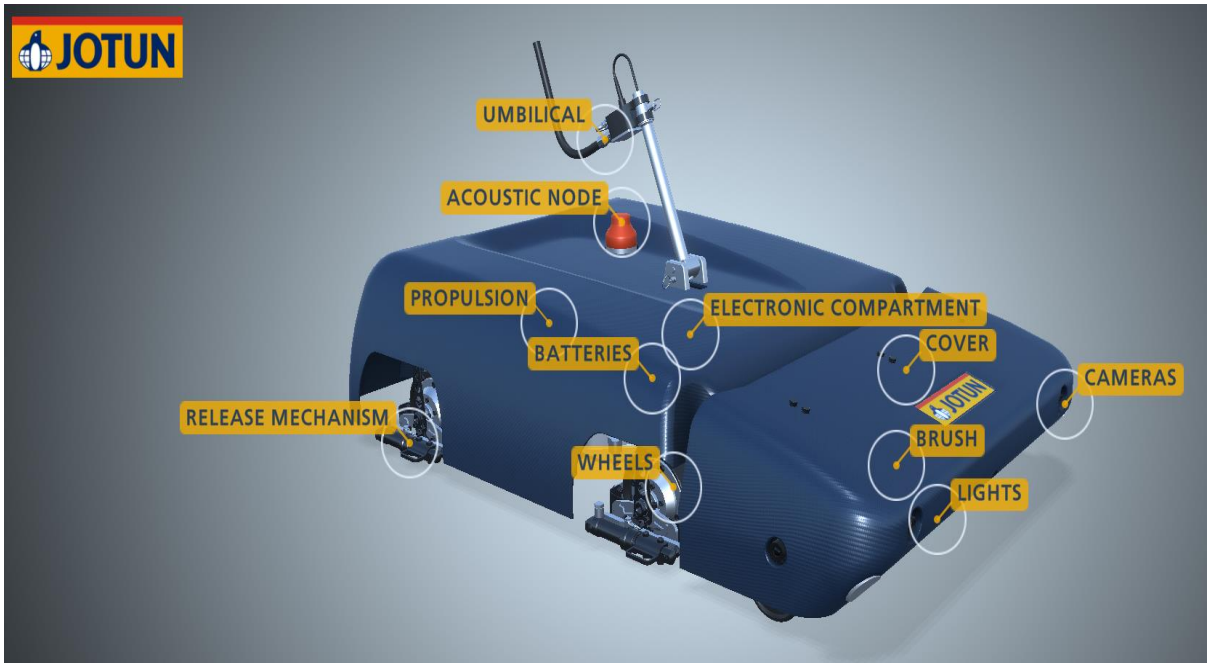

Fig.3: The Hull Skater robot and its key components

- High-end technical service
  The solution includes highly skilled coating advisors who ensure high performance coating application, including a comprehensive regime for measuring and documenting the quality of the application process. Also, every delivery of this solution is supported by a certified project manager, overseeing the application process and ensuring smooth instalment and set-up of the robotics. The HullSkater is remotely operated by Skate Operators working in our "follow the sun" operating hubs, enabling 24/7 support.

- Performance and service level guarantees
  Our confidence in Jotun's Hull Skating Solutions allows us to offer performance and service level guarantees fitting the needs of the most challenging operations.

2.2. How it works

Jotun Hull Skating Solutions is installed on the vessel at the new build or dry dock yard and remains on board and in operation all through the drydocking cycle, Fig.4.

- Drydocking
  During drydocking the painting process is supervised by a certified Jotun Project Manager, who also is responsible for the installation of the Jotun HullSkater and the Skate Station.

- Monitoring
  In Jotun Hull Skating Solutions, big data and advanced algorithms are used to predict the probability of fouling, and to identify when the Skater needs to be deployed for an inspection and potentially proactive cleaning mission.

- Inspection Mission
  When alerted by the fouling prediction algorithm, the Jotun Skate Operator contacts the ship to schedule an inspection mission. The Jotun HullSkater can be operated in port or at anchor, as long as there is sufficient 4G coverage for communication.
- Proactive Cleaning Mission

During the inspection mission, if light fouling is detected, the Skate Operator initiates proactive cleaning. If time does not allow for a proactive cleaning mission, then the Jotun Skate Operator agrees with the ship when the next opportunity will be.

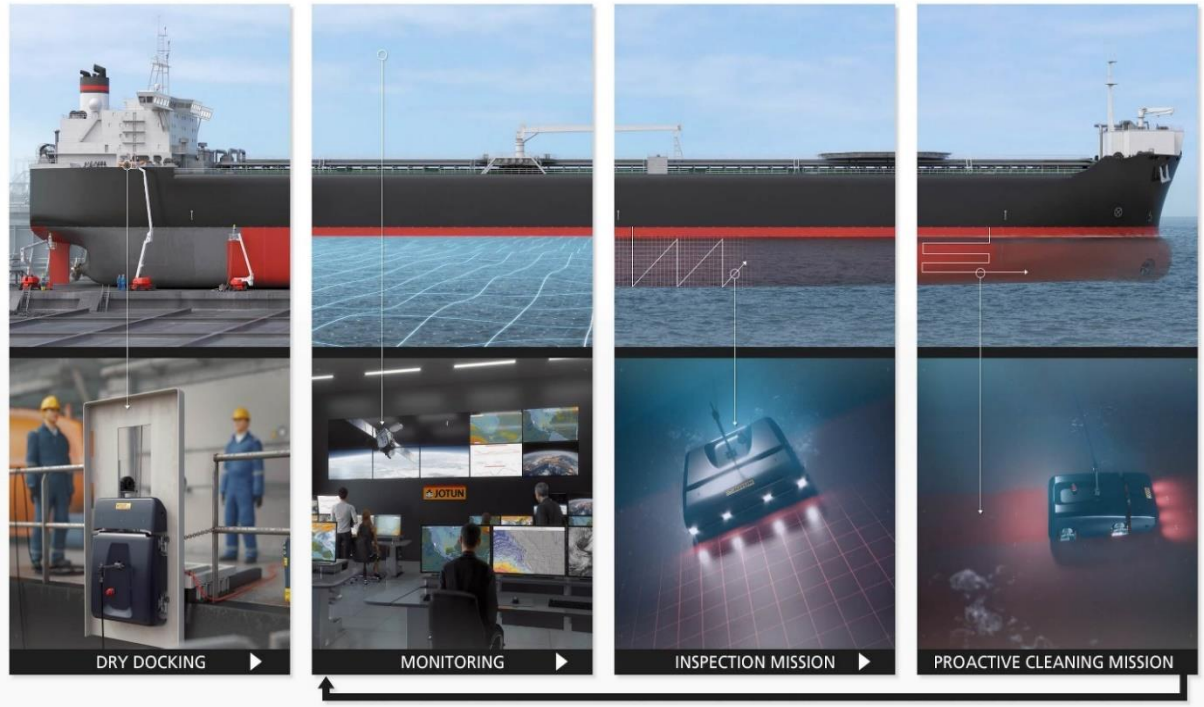

Fig.4: How it works

3. Benefits of proactive cleaning with the Jotun Hull Skating Solutions

Proactive cleaning with Jotun Hull Skating Solutions (HSS) provides market leading hull performance by combining advanced coating systems with proactive, efficient, safe and environmentally friendly inspections and cleaning.

- Full operational flexibility and unlimited idle days
  HSS gives the vessel full operational flexibility with unlimited idle days. This is achieved by combining fouling prediction with the onboard capability to inspect and proactively clean before hard growth takes hold and prior to changing geographical bio-environments. This reduces downtime for unplanned, reactive, inspections and cleaning.

- Reduced fuel costs
  The ability to engage in cleaning the hull proactively allows the hull to be maintained at peak performance, thereby reducing emissions whilst saving fuel costs as compared to market average.

- Reduced environmental footprint
  A continuously clean hull improves fuel consumption resulting in lower greenhouse gas (GHG) emissions.

- Reduced risk of spreading invasive species
  The IMO has published Guidelines for the control and management of ships' biofouling to minimize the transfer of invasive aquatic species. The timely removal of light hull biofouling at its geographical origin reduces the risk of spreading invasive species in the oceans and coastal waters.

- Verification capabilities
  Many incidents at sea trigger the need for underwater hull inspection. HullSkater onboard enables the hull to be inspected at any time, 24/7. HSS also provides documentary evidence of hull cleaning for Port Authorities prior to arrival.

4. Partnerships

The marine business environment is growing increasingly complex and challenging, requiring development of new solutions through partnerships. Developing Jotun Hull Skating Solutions had not been possible without world-class partners, Fig.5.

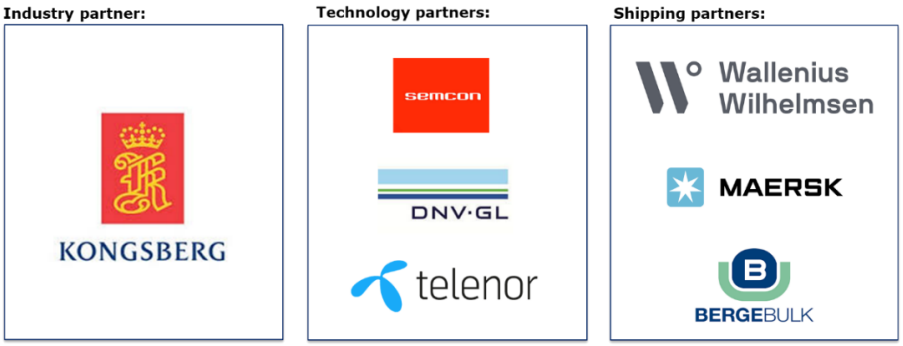

Fig.5: Jotun Hull Skating Solution partners

References

CSC (2015), *A transparent and reliable hull and propeller performance standard*, Clean Shipping Coalition (2015*)* submission to IMO MEPC 63.

IMO (2020), *4th IMO GHG Study – Final Report*, IMO MEPC 75

OFTEDAHL, G.A.; ENSTRÖM, A. (2020), *Proactive Cleaning and the Jotun Hull Skating Solution*, 1st PortPIC Conf., Hamburg, pp.66-70

US NAVY (2006), *Naval Ships' Technical Manual Chapter 081 Waterborne Underwater Hull Cleaning Of Navy Ships*, https://maritime.org/doc/nstm/ch081.pdf

Fuel Cell Systems Applied in Expedition Cruise Ships – A Comparative Impact Analysis

Berend van Veldhuizen, Delft University of Technology, Delft/Netherlands, berendvv96@gmail.com
Robert Hekkenberg, Delft University of Technology, Delft/Netherlands, R.G.hekkenberg@tudelft.nl
Luca Codiglia, Damen Shipyards, Rotterdam/Netherlands, luca.codiglia@damen.com

Abstract

Global endeavors to reduce emissions in the shipping industry are accelerating the interest in fuel cell system. This paper explores the application of different fuel cell types (LT-PEMFC, HT-PEMFC and SOFC) in combination with different fuels (LH_2, LNG, MeOH and NH_3) in expedition cruise ships. The goal of this paper is to evaluate the impact of the combination of fuel cell system implementation and operational profile on the design of expedition cruise vessels. Impact is expressed in ship size, capital cost, operational cost and emissions. The impact model takes into account: fuel storage, onboard fuel processing, fuel cell system characteristics, balance of plant components, fuel cost over operational lifetime and emissions of fuel cell & fuel processing. In the research, 7 different fuel cell systems and 3 different hybridization options are considered.

1. Introduction

Due to the severe possible consequences of climate change, IMO adopted several emission targets and regulations with the goal to reduce global warming, *IMO (2013,2018b)*. Fuel cells are considered as a promising solution to reduce hazardous emissions and to comply to these regulations, *Alkaner and Zhou (2006), Biert et al. (2016), Choi et al. (2016), Boudghene Stambouli and Traversa (2002), Evrin and Dincer (2019), Luckose et al. (2009), Tronstad and Langfeldt (2017)*. They have demonstrated lower heating value efficiencies of 60%, *Payne et al. (2019)*, (even 70% when used with combined generator cycles, *Patel et al. (2012)*) compared with internal combustion engine generators reaching up to 45%, *Biert et al. (2016)*. Cruise tourism is one of the most carbon emitting tourism segments, with an average of 160 kg CO_2 per passenger per day, *Baldi et al. (2018)*. Cruise lines are highly interested in the use of fuel cell systems on their ships. Besides complying to the IMO regulations, cruise lines have an additional interest in sustainable power generation:

i) Several cruise lines report the increasing demand of their customers to reduce their environmental footprint, *CLIA (2019), Alessandro (2019)*. This makes sustainability a competition aspect between cruise lines.
ii) Cruise lines state that continued access to ports is vital for future business operations, *Alessandro (2019)* and local legislators are restricting access for cruise ships with high emissions, for instance in Norwegian Fjords and Port of Amsterdam, *Claus (2019), Kerkhof (2019), WHC (2018)*.

This research focuses on expedition cruise, which is a luxury segment of the cruise industry with a strong focus on (Ant)arctic areas. Fuel cells have several advantages for cruise ships compared to the conventional solution (internal combustion engine generators): reduction in emissions, high efficiency, good part load characteristics, high redundancy, low maintenance and no noise and vibrations, *Biert et al. (2016), Hristovski et al. (2009), Larminie and Dicks (2003), Minnehan and Pratt (2017), Siemens (2013)*. However, fuel cell implementation still struggles with: high capital expenses, size of fuel storage, lack of fuel infrastructure, short lifetime, slow transient behavior and low technological readiness, *Biert et al. (2016), Larminie and Dicks (2003), NN (2004), Tronstad and Langfeldt (2017), Volger (2019)*.

1.1 Current literature

Current research of fuel cell implementation in (cruise) ships was reviewed. *Biert et al. (2016)* did a

very extensive review of fuel cells for marine applications, covering fuel cell types, fuel processing, efficiency, power & energy density, dynamic behavior, environmental impact, safety & reliability and economics. It was concluded that LT-PEMFC fueled with liquefied hydrogen (LH_2) could be a solution for ships with mission requirements up to 12 hours. High temperature fuel cell systems in combination with hydrocarbon fuels can provide high efficiency and low emission solutions for ships with mission requirements of several days, *Biert et al. (2016)*. *Volger (2019)* researched alternative fuels for cruise vessels. He concluded that hydrogen as fuel for fuel cells has most impact on the design of a cruise ships. *Geertsma and Krijgsman (2019)* executed a case study for the application of fuel cells on board of navy support ships. They proposed a methodology to review alternative power system designs based on: mass & volume, capital & operational expenditure, technological readiness, fuel availability and emissions. They concluded that for fuel cells to be commercially used in ships, improvements in technological readiness, efficiency and cost of the fuel cell are necessary. *Minnehan and Pratt (2017)* studied the use of fuel cells on board of various ship types. They concluded that available volume of the vessel is the main technical constraint of the fuel cell system. The following was concluded from reviewing literature:

i) Performance differences for different fuel type and fuel cell type combinations are often not considered.
ii) Little research is performed in cost impact and often not considering fuel cost.
iii) The realized emission reduction is often not provided in the research.

1.2 Research objective

The problem is stated as follows: It is not known which fuel cell systems are most suitable for expedition cruise ships, how they should be applied and what their impact is on ship design, operability, cost and emissions. This information is necessary to successfully apply fuel cell systems. The research objective follows directly out of the problem statement: Evaluate the impact of the combination of different fuel cell systems and operational profiles on the design of expedition cruise vessels, in terms of ship size, ship building cost, fuel cost and emissions.

2. Preliminary selection of fuel cell systems

Based on literature, *Biert et al. (2016), Burel et al. (2013), Das and Gadde (2013), Ellis and Tanneberger (2016), Klerke et al. (2008), Larminie and Dicks (2003), Leites et al. (2012), Pan et al. (2005), Schneider and Dirk (2010), Tronstad and Langfeldt (2017), Semelsberger et al. (2006), Zamfirescu and Dincer (2008),* liquefied hydrogen (LH_2), liquefied natural gas (LNG), methanol (MeOH) and ammonia (NH_3) are selected as potential fuel types. LT-PEMFC, HT-PEMFC, MCFC and SOFC are selected as potential fuel cell types. Every combination of fuel type and fuel cell type represents a different fuel cell system, in terms of equipment and performance. A system decomposition is used to express the performance of these different fuel cell systems, Fig.1.

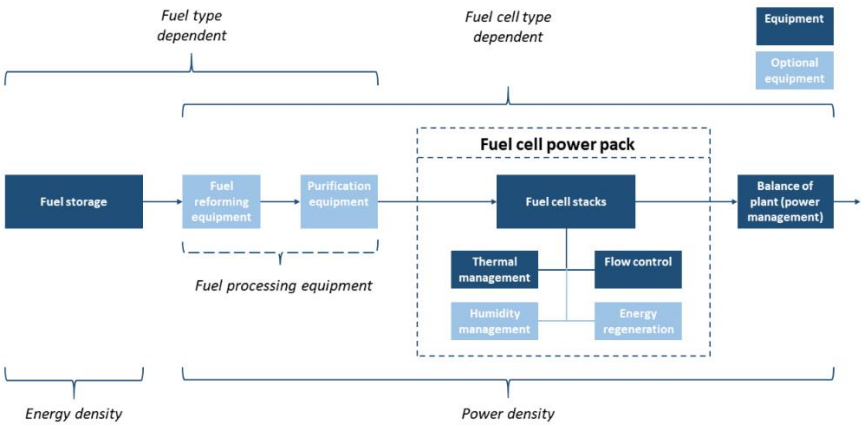

Fig.1: Generic overview of fuel cell system on board of a ship

The fuel cell systems are divided in fuel storage, fuel processing, fuel cell power pack and balance of plant. The performance is expressed by combining the performance of the different components. The performance is expressed in power density, energy density (gravimetric and volumetric) and specific cost of FC system, fuel storage system and generated electricity. Fuel cell lifetime and fuel cell efficiency are included in the performance. Table I quantifies the performance. The options that performed worse than other options on all stated criteria were discarded. E.g., MCFC performs badly on volumetric and gravimetric power density and does not perform better on any areas than all the other fuel cell types. The remaining seven different fuel cell systems are shown in Table II.

Table I: Performance of different fuel cell and fuel combinations on energy density, power density and costs. The performance is based on fuel storage equipment, fuel processing equipment, fuel purification equipment, the fuel cell power pack and electric balance of plant components. The presented data includes fuel cell system efficiency and lifetime of fuel cell stacks in order to compare different options fairly. Derived from *Biert et al. (2016), Chandan et al. (2013), Geertsma and Krijgsman (2019), Ellis and Tanneberger (2016), De-Troya et al. (2016), Fournier et al. (2006), Kee et al. (2005), Klerke et al. (2008), Larminie and Dicks (2003), Lan and Tao (2014), Law et al. (2013), Minnehan and Pratt (2017), Pan et al. (2005), Peters et al. (2016), Thounthong et al. (2009), NN (2004), Søndergaard et al. (2017), Kar Chung Tse et al. (2011), Volger (2019)* and supplier specifications.

Fuel cell system		*Fuel cell plant* **volumetric power density** kW/m^3	*Fuel storage (inc. efficiency)* **volumetric energy density** kWh/m^3	*Fuel cell plant* **gravimetric power density** kW/ton	*Fuel storage (inc. efficiency)* **gravimetric energy density** kWh/ton	*for 15 years* **FC plant** €/kW	*inc. efficiency* **Fuel storage** €/kWh	*inc. efficiency* **Fuel cost** €/MWhe
bunker fuel	*fuel cell*							
LH2	LT-PEMFC	250	604	408	1250	€ 4,213	€ 10.00	€ 898
LH2	HT-PEMFC	99	543	74	1125	€ 6,256	€ 11.11	€ 998
LH2	MCFC	11	604	16	1250	€ 9,532	€ 10.00	€ 898
LH2	SOFC	32	604	119	1250	€ 13,043	€ 10.00	€ 898
LNG	LT-PEMFC	90	1254	272	2931	€ 5,393	€ 3.61	€ 51
LNG	HT-PEMFC	58	1098	74	2565	€ 7,681	€ 4.12	€ 58
LNG	MCFC	11	1411	16	3298	€ 10,735	€ 3.21	€ 45
LNG	SOFC	32	1882	119	4397	€ 14,658	€ 2.41	€ 34
MeOH	LT-PEMFC	41	1575	83	1755	€ 4,929	€ 0.09	€ 159
MeOH	HT-PEMFC	31	1400	74	1560	€ 7,000	€ 0.10	€ 179
MeOH	MCFC	8	1575	16	1755	€ 10,643	€ 0.09	€ 159
MeOH	SOFC	18	1925	119	2145	€ 14,534	€ 0.07	€ 130
NH3	LT-PEMFC	102	1130	155	1620	€ 4,466	€ 0.73	€ 365
NH3	HT-PEMFC	53	1004	74	1440	€ 6,628	€ 0.82	€ 410
NH3	MCFC	10	1256	16	1800	€ 10,087	€ 0.65	€ 328
NH3	SOFC	32	1507	119	2160	€ 13,167	€ 0.54	€ 274
MGO	DG	67	3985	79	3320	€ 425	€ 0.05	€ 121

Table II: Selected fuel cell systems out of performance

Fuel cell system							
LH_2	LT-PEMFC	LNG	LT-PEMFC	$MeOH$	LT-PEMFC	NH_3	LT-PEMFC
LH_2	HT-PEMFC	LNG	HT-PEMFC	$MeOH$	HT-PEMFC	NH_3	HT-PEMFC
LH_2	MCFC	LNG	MCFC	$MeOH$	MCFC	NH_3	MCFC
LH_2	SOFC	LNG	SOFC	$MeOH$	SOFC	NH_3	SOFC

3. Method

It was determined that an impact estimate of the seven selected fuel cell systems is most useful during the first design phase. Consequently, the design method is adjusted to the available information and required accuracy in this design stage. Fig.2 shows the workflow of the impact model, which will be explained in the following sections.

3.1 Input

In the first design phase, the cruise line delivers general requirements (passenger capacity and luxury level), a preliminary design (general arrangement) and the operational profile of the cruise ship. The main dimensions, number of passengers and operational profile are used as input, together with the desired fuel type, fuel cell type and hybridization strategy. Three hybridization strategies are defined:

- Full fuel cell powered ship - All energy is generated by fuel cells. Its main advantage is that no extra engine room is required for diesel generators. However, large fuel storage and an expensive power generation system are expected.
- Hybrid 1: Fuel cell power generation for auxiliaries - All power for auxiliary systems (including hotel) is provided by the fuel cell system. All power for propulsion is provided by the diesel generator set. The advantage of this option is that less balance of plant components are required to ensure the dynamic power capabilities of the power generation system. Fuel cells (especially HT FC) struggle with transient loads, *Biert et al. (2016)*, *Larminie and Dicks (2003)*, and need to be combined with components with good transient behavior, *Choi et al. (2016)*, *Minnehan and Pratt (2017)*, *Welaya et al. (2011)*. From studying the on board power demand, it was concluded that the auxiliary load is much more constant (smaller changes in power demand per time step) than the propulsion load, resulting in lower balance of plant requirements. The disadvantage of this option is that the ship cannot operate solely on fuel cells.
- Hybrid 2: Diesel generators to support in transit - The transit operation, which requires the most stored energy and installed power, is supported with diesel generators. The transit operation is not part of a regular cruise, but executed a few times per year to get the ship to a different cruise location. Since fuel storage is critical for a fuel cell powered ship, this option provides a way to cope with long ranges and huge storage tanks, while still operating mostly on fuel cells. The extra advantage of hybrid option 2 is that the most harmful emissions are mainly emitted outside sensitive areas, which supports in complying to ECA regulations, *IMO (2020a,b)*.

In this paper, model results for different inputs (fuel type, fuel cell type, hybrid strategy) will be compared.

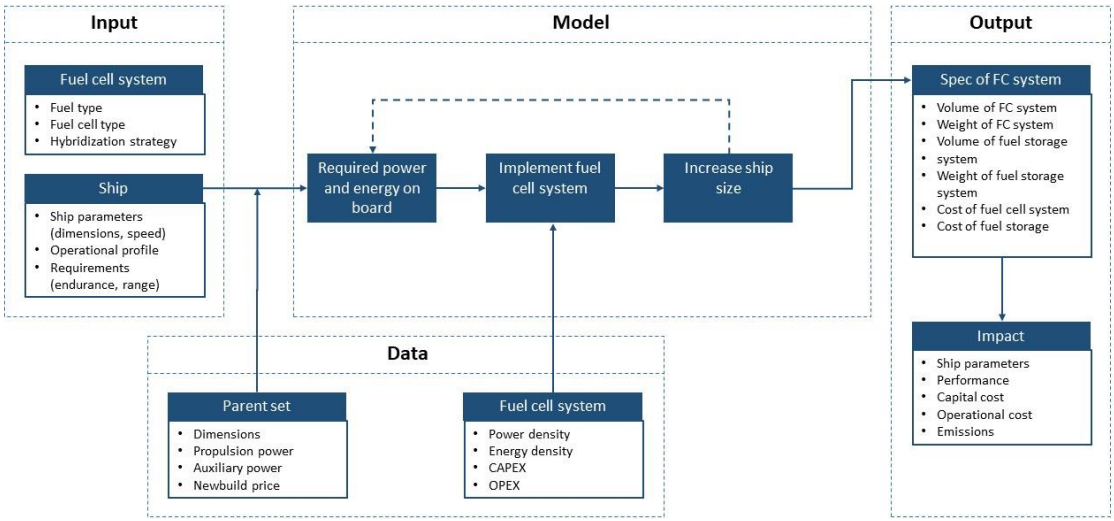

Fig.2: Schematic overview of workflow of impact model

3.2. Data

A parent set of ships is used to give a suitable suggestion for the main ship parameters. 36 expedition cruise reference ships are used which were defined as the luxury segment (>50GT/PAX) from a database of 291 cruise ships. The used reference ships range from 5000 to 70000 GT. The power density, energy density and specific cost for the different fuel cell systems, Table I, is used to determine the volume, weight and cost of the concerned fuel cell system.

3.3. Model

The ship requirements are combined with the parent set to estimate the required propulsion power and auxiliary power. Following, the volume, weight and cost of the fuel cell system can be calculated

from the performance data. The propulsion power is combined with the operational profile and the propeller law to calculate required energy and energy usage. The first defining the weight, size and cost of the fuel storage system and the second defining fuel cost and emissions. This section shortly explains these different steps in the model. For a full understanding of the model refer to the report of *van Veldhuizen (2020)* where the model considerations and the used equations are explained.

3.3.1. Ship parameters

Regression relations retrieved from reference ships are used to suggest a suitable ship. The GT is estimated on the basis of the passenger capacity. The regression relation with GT is used to estimate the displacement. The other ship dimensions are also estimated with use of the GT. To make sure there is no mismatch with the block coefficient C_B and the desired speed, the CB is calculated and compared in the model with the CB of reference ships with a comparable speed.

3.3.2 Installed power estimation

The required power consists of the power required for propulsion and the power required for auxiliaries (including hotel). The required propulsion power is calculated with the admiralty formula and is thus based on the displacement and the ship speed. The admiralty constant is derived from the reference ships. Note that the admiralty constant is only constant for relatively small changes in displacement and ship speed, *Bertram (2012)*. The evaluated ship must not deviate much from the reference ship, so this developed method will not be suitable for evaluating an expedition cruise ship with unique design requirements, like a very high maximum speed.

The auxiliary power is defined in this research as all required power besides the propulsion. For expedition cruise ships, the auxiliary power is dominated by the hotel power. The auxiliary power is defined as function of the number of passengers (PAX). The amount of auxiliary power per passenger is also very dependent on the luxury level. For luxury ships the HVAC needs to cover more volume per passenger and luxury equipment also requires power. Table III shows how much auxiliary power is installed per passenger for different luxury levels on average. Dependent on the hybridization strategy, the required power is divided over the fuel cell plant and the diesel plant.

Table III: Average auxiliary power (including hotel power) per passenger for different luxury classes, based on reference ships (SD=standard deviation)

	Aux. power kW/PAX	SD kW/PAX	Aux. power % of installed
Budget	5.9	1.8	38%
Premium	8.3	2.9	39%
Luxury	16.2	5.7	41%

3.3.3. Energy estimation

Using the operational profile as input, it is possible to determine the required energy on board (defining the fuel storage size) and the energy usage (defining the fuel cost and emissions). The desired speed and propeller law are combined to estimate the required power for every sail mode in every defined operation. Harbour, manoeuvring, slow cruising and cruising are used as sail modes. The defined operations are Atlantic crossing, coastal cruise and (Ant)arctic cruise, which are distinctive itineraries. With the required power and the time for every sail mode, it is estimated how much energy is necessary for all operations.

- Required energy on board - The required energy on board defines the weight, volume and cost for the storage of the different fuels. A fuel margin is defined to make sure delays in the operational profile are possible or to be able to sail a little faster when behind schedule, both increasing the fuel consumption. Consulting Damen engineers, a 10% fuel margin is used for the DG generators. For the FC system a 20% margin is needed, to make sure the range

requirements can still be met at the end of the lifetime of the fuel cell stacks; the efficiency of the stacks decreases over their lifetime.

- Energy usage - The energy usage in every operation is used to determine the fuel cost and emissions. The energy required for an operation is combined with the relative frequency of occurrence of the operations to determine how much energy is used yearly for every operation. The usage rate of the different operations is defined as the percentage time the cruise line executes a certain operation yearly, for instance 10% transit, 50% coastal operation and 40% arctic operation. This especially matters for the yearly fuel consumption of hybrid option 2 where MGO is consumed in transit and alternative fuel is consumed in other operations. The yearly energy usage equals the sum for the different operations.

3.3.4. Fuel cell system implementation

At this point in the model the required power, required energy and energy consumption of the (hybrid) fuel cell system are known. This is combined with the fuel cell system performance, Table I, to calculate the volume, weight, capital cost and fuel cost of the fuel cell system. The required ship volume for the fuel cell system (and of the diesel generator system for a hybrid system) consists of the volume of the power plant (including space for maintenance and other systems) and the ship volume to store the concerning fuel. The power density and energy density data in Table I already include the efficiency of the fuel cell system. The weight of the fuel cell system is determined analogously.

The cost of the fuel cell system (and of the diesel generator system for a hybrid system) is also dependent on the power pack and the fuel storage. The cost of the power pack is equal to the required power times the cost per kW. The cost of the fuel storage is equal to the required energy on board times the cost per kWh for fuel storage.

The fuel cost of the (hybrid) fuel cell system depends on the yearly energy consumption, the operational lifetime and the cost of generated electrical energy, the latter depending on the fuel cost and the efficiency of the system. The efficiency of the fuel cell system decreases linearly with 10% over the lifetime of the fuel cell stacks. This implies a 10% increase of the required energy in the fuel storage and a 5% increase in fuel consumption over the lifetime.

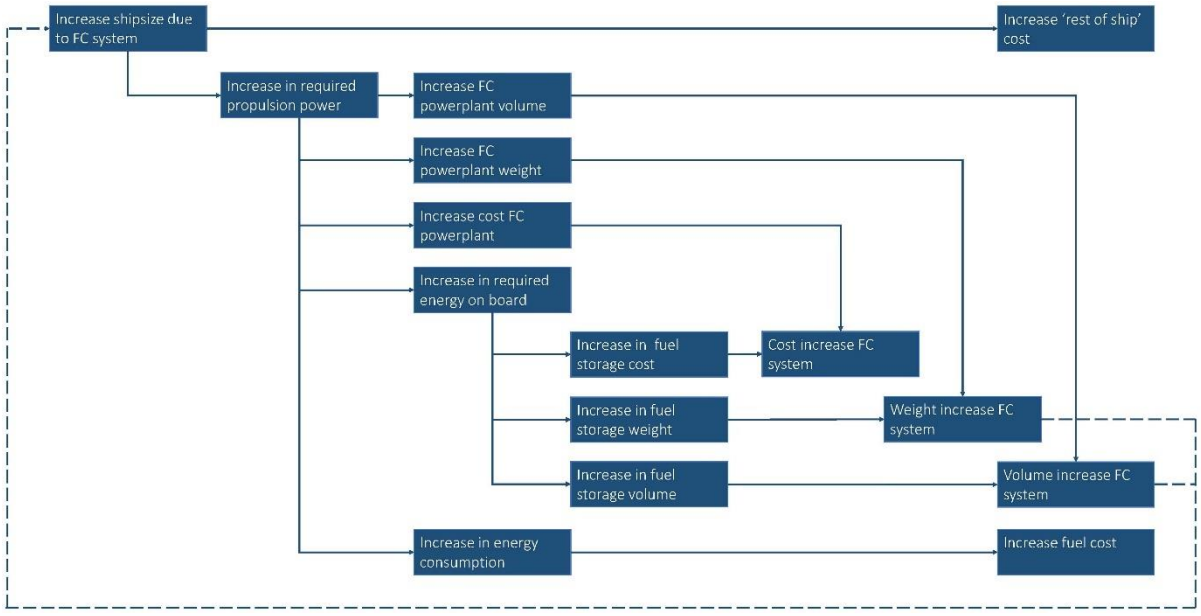

Fig.3: Consequences of increasing ship size to fit fuel cell system. Scheme shows 1 iteration in design

3.3.5. Fit the fuel cell system in the ship

To fit the fuel cell system the ship size is increased, consequently increasing many other ship parameters like installed power and energy consumption. Fig.3 shows on which parameters the increase in ship size has an impact. This impact is iterative: when the ship size increases, the required power increases, increasing the size of the power plant and fuel storage, further increasing the ship size.

- Increase in ship size - While increasing the ship size it is checked whether the increase in ship size is driven by the volume of the fuel cell system or the weight of the fuel cell system. Whether the increase in ship size is volume driven or weight driven was observed to be different per fuel cell system, per hybrid option and dependent on the operational requirements. Following, the actual increase in GT is determined out of the increase in displacement, using regression data. The increase in ship size is defined in GT because an extra cost per GT is defined to take into account extra cost for a larger ship, besides the increase in cost of the fuel cell system, such as cost of: steel weight, systems and cables.
- Increase of power plant - The increase in ship size results in a higher required propulsion power, due to an increase in ship resistance. The increase in propulsion power is again calculated with the admiralty constant of the reference ships via the increase in displacement.
- Increase in required energy - When the required propulsion power increases, the required energy on board increases (when range and speed remain constant). An increase in the required energy consequently increases the volume, weight and cost of the fuel storage system.
- Increase in energy consumption - When the required propulsion power increases, the energy consumption also increases (when operational profile remains constant). This has a direct impact on the fuel cost.
- Iteration process - At the end of one iteration the ship design does not converge: extra volume is calculated for the fuel cell system, but it is not yet fitted into the ship. When iterating infinitely the extra required space approaches zero and thus the increase in ship size approaches zero. This is the case because ΔGT becomes smaller every iteration. Several iterations were performed, and it was found that after one iteration ΔGT is smaller than 0.5% of the total GT for all combinations of fuel cell system and hybridization options. Consequently, one iteration is sufficient to exclude significant mutations from the end result.

Table IV: Specific emissions per generated MWhe for selected FC systems and conventional solution, including system efficiency, *Altmann et al. (2004), Biert et al. (2016), Bloom Energy (2019),* http://convion.fi/products/, *Höhlein et al. (1996), Isaacs et al. (2013), Siemens (2013), Soltani et al. (2014).* The emissions for MGO fueled diesel generator is derived with Damen mechanical engineers. As can be seen in the table, the NO_x, SO_x and PM emissions are not significant compared to those of a conventional system.

		CO kg/MWhe	CO_2 kg/MWhe	NO_x kg/MWhe	SO_x kg/MWhe	PM kg/MWhe
LH2	LT-PEMFC	-	-	-	-	-
LNG	LT-PEMFC	0.0225	514	-	-	-
LNG	SOFC	0.0150	343	0.0008	-	0.0001
MeOH	LT-PEMFC	0.0111	349	0.0005	-	-
MeOH	HT-PEMFC	0.0125	466	0.0006	-	-
MeOH	SOFC	0.0091	524	0.0008	-	0.0001
NH3	SOFC	-	-	0.0031	-	-
MGO	DG	1.56	661	11.99	2	1.60

3.3.6. Emissions

The main purpose of fuel cell implementation in shipping is to reduce emissions. So, it is relevant to indicate the fuel cell system emissions compared with a conventional solution. This shows the

effectiveness of implementing such a system. Although fuel cell emissions are drastically lower than emissions of a conventional solution, *Biert et al. (2016)*, *Larminie and Dicks (2003)*, it should be noted that for some fuel and fuel cell combinations significant emissions remain, *Bloom Energy (2019)*, *Geertsma and Krijgsman (2019)*, http://convion.fi/products/, *Lee et al. (2015)*, *Strazza et al. (2010)*. The emissions over the operational lifetime are calculated with use of Table IV, which shows the specific emissions for CO, CO_2, NO_x, SO_x and particulate matter (PM). This data includes the efficiency of the different fuel cell systems. Fuel cells have very low sulfide tolerance (ppm range), meaning sulfides (in H_2S form) are already extracted from the fuel before reforming, *Larminie and Dicks (2003)*. Zinc oxide is used to subtract the H_2S from the fuel. The absorbent is regenerated and H_2S is stored separately, *NN (2004)*. Consequently, for all considered fuel cell systems the SO_x emissions are zero.

3.4. Model verification

A vast number of calculation steps is implemented in the model, making the chance on typing and programming errors significant. The following verification methods of *Sargent (2010)* are used:

i) Structured walk through.
ii) Balance checks of sums, averages and or combinations of parameters, Table V.
iii) Testing of extreme model conditions.

Table V: Verification of model: balance checks to verify output and intermediate values of the model

Balance check	Description	Max error	Verified
Ship design			
Displacement	Does displacement output match with $L_{wl} \cdot B \cdot T \cdot C_B$	0.0%	✓
GT-GV	Does GT output match with GV output	-0.1%	✓
Cb-speed	Does the block coefficient align with the desired speed	-	✓
Installed power	Is there enough power installed to reach maximum speed	0.0%	✓
Range check	Does total stored fuel satisfy range and endurance requirement	-0.3%	✓
Fuel cell system			
Density of fuel	Does weight and volume of stored fuel match with density	-0.3%	✓
Volumetric power density	Does installed FC power and FC volume match with used $p_{FC,vol}$	0.0%	✓
Gravimetric power density	Does installed FC power and FC weight match with used $p_{FC,grav}$	0.0%	✓
Cost			
Specific cost FC plant	Does cost of FC system and installed FC power match with c_{FC}	0.0%	✓
Cost of FC system	Does cost of FC system match with sum of cost components	0.0%	✓
Shipbuilding cost	Does shipbuilding cost match with sum of cost components	0.0%	✓

3.5. Model validation

After model verification confirmed that the presented model is correctly programmed, the reader should also get the confidence that the programmed model has sufficient accuracy for the model's intended purpose over the application range of the model, *Sargent (2010)*. Full scale validation by comparing the model results with similar models or real-life examples is not possible. Similar models are not found and there are no expedition cruise ships on which fuel cell systems are implemented on a large scale. The validation methods that were executed for this model are, *Sargent (2010)*:

- Data validation - The calculated performance data was presented to fuel cell experts and checked versus their knowledge of these systems.
- Benchmarks - Intermediate results of the model were benchmarked using research results and knowledge of suppliers and fuel cell experts. Examples of executed benchmark validations are:
  i) Size of LNG reforming plant is approximately 3 times the size of the power pack for LNG fueled LT-PEMFC.
  ii) Size of a 2 MW LTPEMFC plant.
- Logical interpretation of results - The results were interpreted and reasoned whether these

model outputs would match expectations from reality. Result interpretation is done in the next section where the results will also be presented.

- Sensitivity analysis - The input and/or internal parameters of the model were systematically changed to determine the impact on the model output. Input is varied in section 5 in terms of range, endurance and GT.

4. Results

This section compares the results of the impact model for different fuel cell systems and hybridization strategies. They are generated for an average ship (compared to the reference ships). The main particulars of this average ship are shown in Table VI. The main requirements and operational profile for the evaluated fuel cell powered ship are shown in Table VII and Fig.4. In all results, the model output is presented. This means for instance, when the volume of the fuel cell system is presented, it already includes the extra volume of the system that is necessary because the required power and required energy increased during the design iteration.

Table VI: Main particulars of average ship (average with respect to reference ships) for which the results are generated. The model uses PAX and luxury level as starting point, of which the other parameters are derived.

Dimension		Unit	Quantity		Unit
Length OA	191	m	Gross Tonnage	31321	GT
Length PP	168	m	Displacement	18858	ton
Beam	26	m	PAX	500	-
Draught	6.3	m	Crew	323	-
Depth	9.8	m	Lifetime	15	years

Table VII: Requirements of evaluated fuel cell powered ship. Derived from operational profiles and requirements of several expedition cruise ships.

Requirement		Unit	Requirement		Unit
Design speed	12	kn	Range	3600	nm
Max speed	14	kn	Endurance	17	days

Operational profile

	Distance	Days	Time	Speed
	nm	-	%	kn
Transit			10%	
Harbour	-	4	23%	-
Manouvring	5	0.5	3%	0.4
Slow cruising	100	1	6%	4.2
Cruising	3500	12	69%	12.2
Total	3,605	18	100%	
Coastal operation			30%	
Harbour	-	2.5	18%	-
Manouvring	5	0.5	4%	0.4
Slow cruising	400	3	21%	5.6
Cruising	2000	8	57%	10.4
Total	2,405	14	100%	
Antarctic operation			60%	
Harbour	-	2	15%	-
Manouvring	5	0.6	4%	0.3
Slow cruising	100	0	0%	-
Cruising	2400	11	81%	9.1
Total	2,505	14	100%	

Fig.4: Used operational profiles for generated results

4.1. Fuel cell system

In this section, the characteristics of the fuel cell implementation are compared with the diesel generator system that would be necessary for a ship with the same requirements. Fuel cell implementation has an influence on the volume, weight and cost with respect to the conventional system.

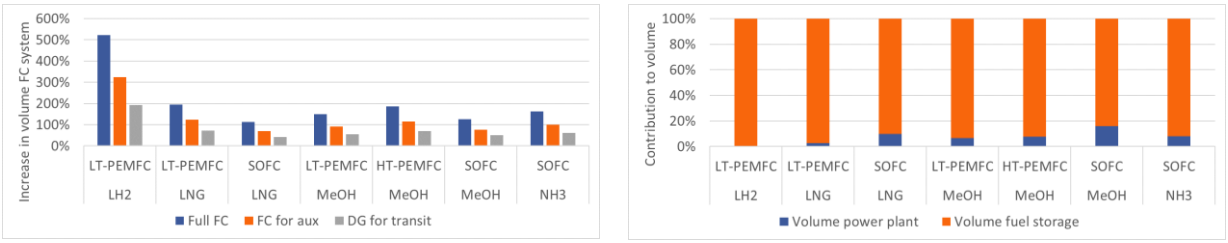

Fig.5: Increase in volume; left: Increase in volume of (hybrid) fuel cell system with respect to the volume of the DG system that would be necessary for a conventional ship. This graph includes power plant and fuel storage; right: Contribution of fuel storage system and power plant to volume increase of (left) for the full FC option (for the hybrid options the graph is similar).

Fig.5 (left) shows the increase in volume of the (hybrid) fuel cell system compared to the conventional system. The volumetric power density and volumetric energy density data of Table I were used to acquire these results. The volume increase is by far the largest for the LH_2 fueled LT-PEMFC system. LNG fueled SOFC offers the lowest increase in volume for all hybrid strategies of which hybrid option 2 (DG for transit) results in the smallest volume increase of all 21 options. The full fuel cell powered ship requires most volume for the fuel cell system; the diesel for transit option requires the lowest volume for all different fuel cell systems. Fig.5 (right) shows the contribution of the fuel storage and the fuel cell power plant to the volume of the FC system. The volume of all considered fuel cell systems is mainly driven by fuel storage.

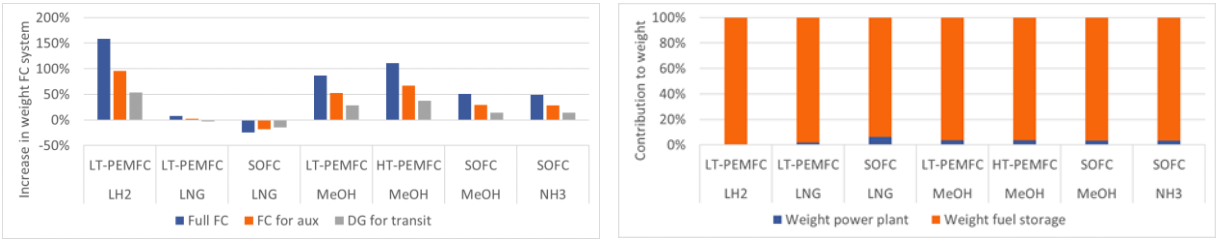

Fig.6: Increase in weight; (left) Increase in weight of (hybrid) fuel cell system with respect to the weight of the DG system for a conventional ship. This graph includes power plant and fuel storage; (right) Contribution of fuel storage system and power plant to weight increase of (right) for the full FC option (for the hybrid options the graph is similar).

Fig.6 (left) shows the increase in weight of the (hybrid) fuel cell system compared to the conventional system. The gravimetric power density and gravimetric energy density data of table 1 were used to acquire these results. The weight increase is the largest for the LH_2 fueled LT-PEMFC system. This can be explained by the high weight of the hydrogen storage tanks. For all considered fuel cell systems, the weight increase is mainly driven by the weight of the fuel storage, Fig.6 (right). For fuel cell systems fueled by LNG, there are options where the required fuel cell system is lighter than the conventional system, due to the low gravimetric energy density of LNG storage. This implies that for these options, the increase in ship size to fit the fuel cell system is purely volume driven.

Fig.7 (left) shows the increase in cost (from the perspective of the ship builder) of the whole fuel cell system compared to the conventional system. The capital cost data of Table I were used to acquire these results. Very large cost increases are found, especially for SOFC systems. Where volume and weight were mostly driven by the fuel storage system, the power generation system dominates in driving the cost (with exception of LH_2 fueled LTPEMFC), Fig.7 (right).

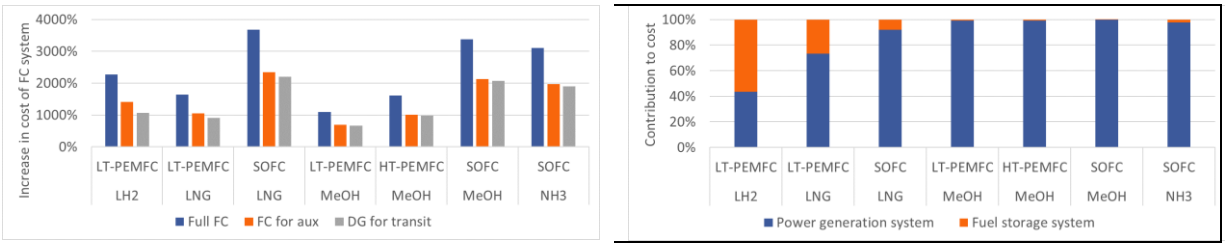

Fig.7: Increase in cost; (left) Increase in cost of (hybrid) fuel cell system with respect to the cost of the DG system for a conventional ship. This graph includes power plant and fuel storage; (right) Contribution of fuel storage system and power plant to increase in cost of (left) for the full FC option (for the hybrid options the graph is similar).

4.2. Increase in ship size

Since the (hybrid) fuel cell system is bigger than the conventional system, the ship size was increased to fit the fuel cell system. Fig.8 shows the increase in GT for the different fuel cell systems and hybrid options. The figure shows that the increase in ship size is very different per fuel cell system and hybrid option. Hybrid option 2 (DG for transit) consistently leads to the lowest increase in ship size. Overall, LNG fueled SOFC in combination with hybrid option 2 leads to the lowest increase in ship size. This was expected due to the high power-density of LNG and high efficiency of SOFC.

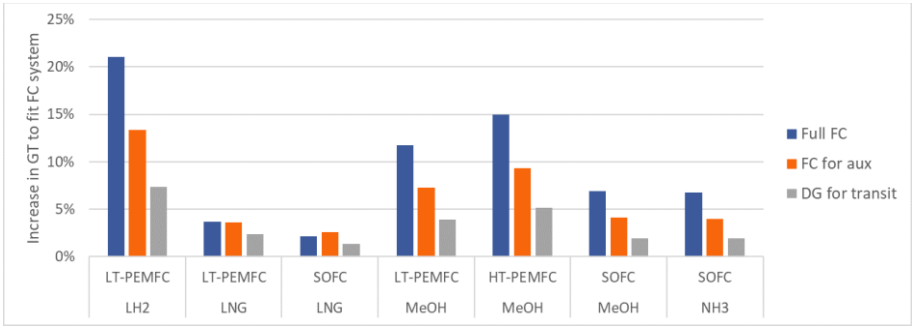

Fig.8: Increase in GT during the design iteration with respect to GT of conventional ship (in order to fit FC system in the ship).

4.3. Increase in cost

Fig.9 shows the increase in newbuild price for the different fuel cell systems and hybrid options compared to the same ship with conventional power generation. As was also reported for Fig. 7, the cost is still dominated by the cost of the power plant (expect for LH_2 fueled LT-PEMFC). The 'rest of ship cost' scales linearly with Fig.8, since a constant cost increase per GT was defined for the design iteration. Fuel cell systems that use SOFC cause the highest increase in newbuild price, due to the high cost of SOFC per kW.

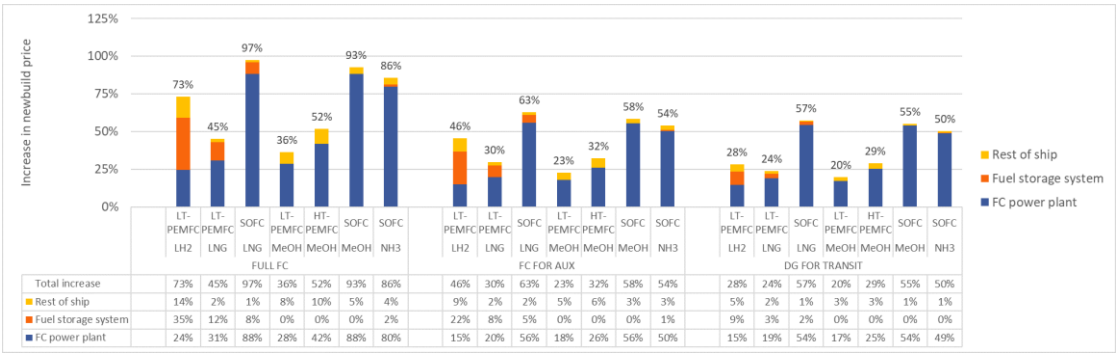

	FULL FC							FC FOR AUX							DG FOR TRANSIT						
	LT-PEMFC LH2	LT-PEMFC LNG	SOFC LNG	LT-PEMFC MeOH	HT-PEMFC MeOH	SOFC MeOH	SOFC NH3	LT-PEMFC LH2	LT-PEMFC LNG	SOFC LNG	LT-PEMFC MeOH	HT-PEMFC MeOH	SOFC MeOH	SOFC NH3	LT-PEMFC LH2	LT-PEMFC LNG	SOFC LNG	LT-PEMFC MeOH	HT-PEMFC MeOH	SOFC MeOH	SOFC NH3
Total increase	73%	45%	97%	36%	52%	93%	86%	46%	30%	63%	23%	32%	58%	54%	28%	24%	57%	20%	29%	55%	50%
Rest of ship	14%	2%	1%	8%	10%	5%	4%	9%	2%	2%	5%	6%	3%	3%	5%	2%	1%	3%	3%	1%	1%
Fuel storage system	35%	12%	8%	0%	0%	0%	2%	22%	8%	5%	0%	0%	0%	1%	9%	3%	2%	0%	0%	0%	0%
FC power plant	24%	31%	88%	28%	42%	88%	80%	15%	20%	56%	18%	26%	56%	50%	15%	19%	54%	17%	25%	54%	49%

Fig.9: Increase in newbuild price with respect to the newbuild price of a conventional ship with equal requirements. The data labels indicate the total increase in newbuild price.

For every hybridization strategy, the MeOH fueled LT-PEMFC results in the lowest increase in newbuild price. LNG fueled LT-PEMFC also offers a low increase in newbuild price for hybrid option 1 (FC for auxiliaries) and hybrid option 2 (DG for transit), followed by LH_2 fueled LT-PEMFC combined with hybrid option 2.

The increase in newbuild price is combined with the increase in fuel cost in order to give a well-founded recommendation on the financial impact of different fuel cell systems and hybrid options. Fig.10 shows the total increase in cost compared to the newbuild price plus the fuel cost of a conventional ship with equal requirements. The total cost is from the perspective of the cruise line. Time value of money and finance cost are not taken into account. As becomes clear from this figure, the fuel cost has a big impact on the economic viability of the option, especially for the LH_2 and NH_3 fueled fuel cell systems. It can be concluded that a ship equipped with LNG fueled LT-PEMFC is the best option for all hybridization strategies from a total cost perspective (perspective of the cruise line). This can be explained by the decrease in fuel cost by LNG. The next best performing options from this perspective are MeOH fueled LT-PEMFC and LNG fueled SOFC for hybrid option 1 and 2. Between the different hybridization strategies, the increase in total cost is slightly lower for hybrid option 2 for most considered fuel cell systems.

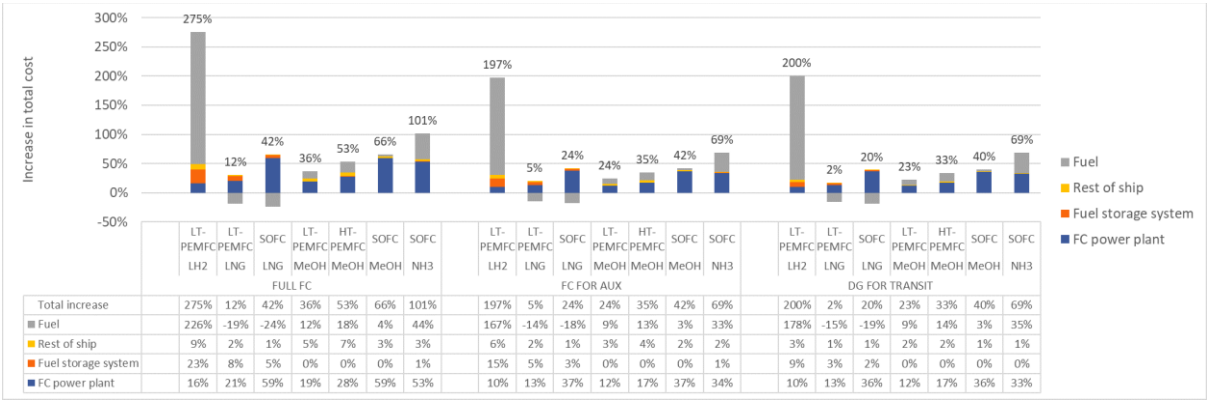

	LT-PEMFC LH2	LT-PEMFC LNG	SOFC LNG	LT-PEMFC MeOH	HT-PEMFC MeOH	SOFC MeOH	SOFC NH3	LT-PEMFC LH2	LT-PEMFC LNG	SOFC LNG	LT-PEMFC MeOH	HT-PEMFC MeOH	SOFC MeOH	SOFC NH3	LT-PEMFC LH2	LT-PEMFC LNG	SOFC LNG	LT-PEMFC MeOH	HT-PEMFC MeOH	SOFC MeOH	SOFC NH3
	FULL FC							FC FOR AUX							DG FOR TRANSIT						
Total increase	275%	12%	42%	36%	53%	66%	101%	197%	5%	24%	24%	35%	42%	69%	200%	2%	20%	23%	33%	40%	69%
Fuel	226%	-19%	-24%	12%	18%	4%	44%	167%	-14%	-18%	9%	13%	3%	33%	178%	-15%	-19%	9%	14%	3%	35%
Rest of ship	9%	2%	1%	5%	7%	3%	3%	6%	2%	1%	3%	4%	2%	2%	3%	1%	1%	2%	2%	1%	1%
Fuel storage system	23%	8%	5%	0%	0%	0%	1%	15%	5%	3%	0%	0%	0%	1%	9%	3%	2%	0%	0%	0%	0%
FC power plant	16%	21%	59%	19%	28%	59%	53%	10%	13%	37%	12%	17%	37%	34%	10%	13%	36%	12%	17%	36%	33%

Fig.10: Increase in total cost over ship lifetime (15 years) with respect to the newbuild price and fuel cost over ship lifetime for a conventional ship with equal requirements. Note that the data label (total increase in cost) does not correspond with the height of the bar, since the bars do not stack for negative values.

4.4. Emissions

While interpreting results, keep in mind that the main driver for implementing fuel cell systems is the reduction of emissions. Fig.11 shows the normalized reduction in emissions compared with the CO_2 targets. The LNG fueled LT-PEMFC, MeOH fueled HT-PEMFC and MeOH fueled SOFC exceed the 2030 CO_2 target for all hybridization strategies. Only the LH_2 fueled LT-PEMFC and NH_3 fueled SOFC do not exceed the 2050 goals (for all hybridization strategies). Fig.12 shows the normalized reduction in emissions compared with NO_x, SO_x, and PM regulations. For the full fuel cell powered solutions, all upcoming regulations (inside and outside ECA zones) are easily met, since NO_x, SO_x, and PM emissions are not significant. For both hybrid options, only the SO_x and PM *S*emissions within ECA zones are not met. For hybrid option 2 this is easily solvable, since the ship can run solely on fuel cells in these zones (although with lower range and maximum speed). Hybrid option 1 cannot comply with the ECA regulations (without consideration of emission abatement).

4.5. Best performing options

The results of the past sections are combined to make a recommendation for the best performing combinations of fuel cell system and hybridization option. The used criteria were the newbuild price, total cost and compliance to the 2030 CO_2 target and ECA regulations.

Table VIII: Recommendation for fuel cell powered ships

Rank	Fuel type	FC type	Hybridization	Ship price	Total cost	Compliance		
						CO2 2030	CO2 2050	ECA
1	LNG	LT-PEMFC	Hybrid 2	++	++			✓
2	LNG	LT-PEMFC	Full FC	-	+			✓
3	MeOH	LT-PEMFC	Hybrid 2	++	+-	✓		✓
4	LNG	SOFC	Hybrid 2	- -	-	✓		✓
5	MeOH	LT-PEMFC	Full FC	+-	-	✓		✓
6	MeOH	HT-PEMFC	Hybrid 2	+-	- -			✓

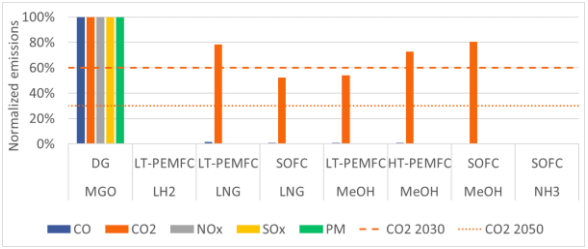

(a) Full FC powered ship

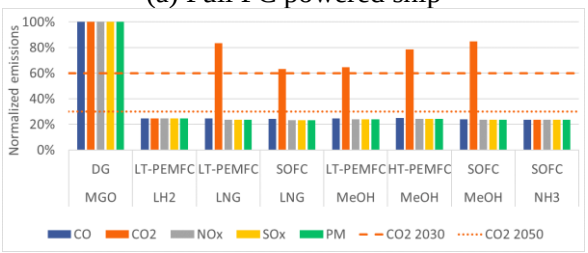

b) Hybrid option 1 (FC for auxiliaries)

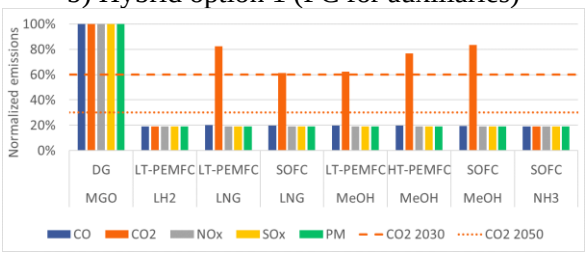

(c) Hybrid option 2 (DG for transit)

Fig.11: Normalized on-board emissions for CO, CO_2, NO_x, SO_x, and PM over lifetime of the average ship with a conventional system and with the selected fuel cell systems. The CO_2 ambition levels for 2030 and 2050 by IMO are also shown in the figures, *IMO (2018a)*.

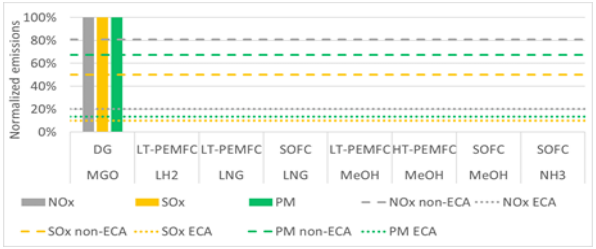

(a) Full FC powered ship

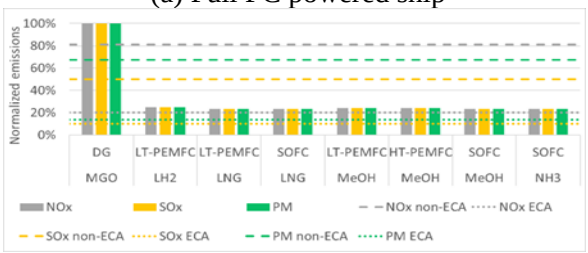

b) Hybrid option 1 (FC for auxiliaries)

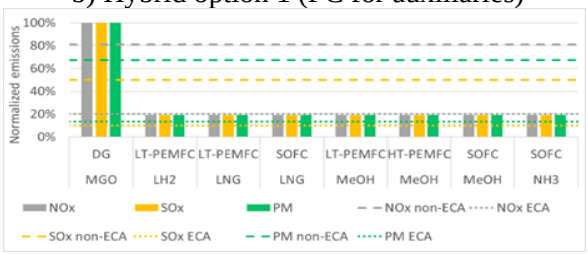

c) Hybrid option 2 (DG for transit)

Fig.12: Normalized on-board emissions for NO_x, SO_x and PM over lifetime of ship for conventional system and selected fuel cell systems. Compared with NO_x, SO_x and PM regulations inside and outside ECA zones, *IMO (2020a,b)*.

All options using hybrid option 1 are discarded since hybrid option 2 always performed slightly better than hybrid option 1. On top of that, hybrid option 2 has the additional advantage that it can operate solely on fuel cells. The six best performing options are selected and stated in Table VII. These will be used for a sensitivity analysis in the next section. Although a ranking is provided, the most recommended option is very case dependent. MeOH fueled LT-PEMFC combined with hybrid option 2 results in the lowest increase in newbuild price. LNG fueled LT-PEMFC in combination with hybrid option 2 results in the lowest increase in total cost (newbuild price and fuel cost.

5. Sensitivity analysis

For the 6 best performing options of Table VIII, a sensitivity analysis method of *Sargent (2010)* was used. The input values are systematically varied to determine the model's behavior.

5.1. Variation of operational requirements

The endurance of the transit operation is varied. It is important to determine the model's behavior for different endurances to see whether the selection of best performing options would be different for other operational requirements. Especially, since some fuel cell systems are more costly per kW installed power and others are more costly per kWh generated energy, which was clearly visible in Table I. The design speed is kept constant, meaning the variation influences the size of the fuel storage but not the size of the power plant, since the latter is related to the required power. The speed during the transit operation is also kept constant. Consequently, the transit range scales proportionally with the endurance.

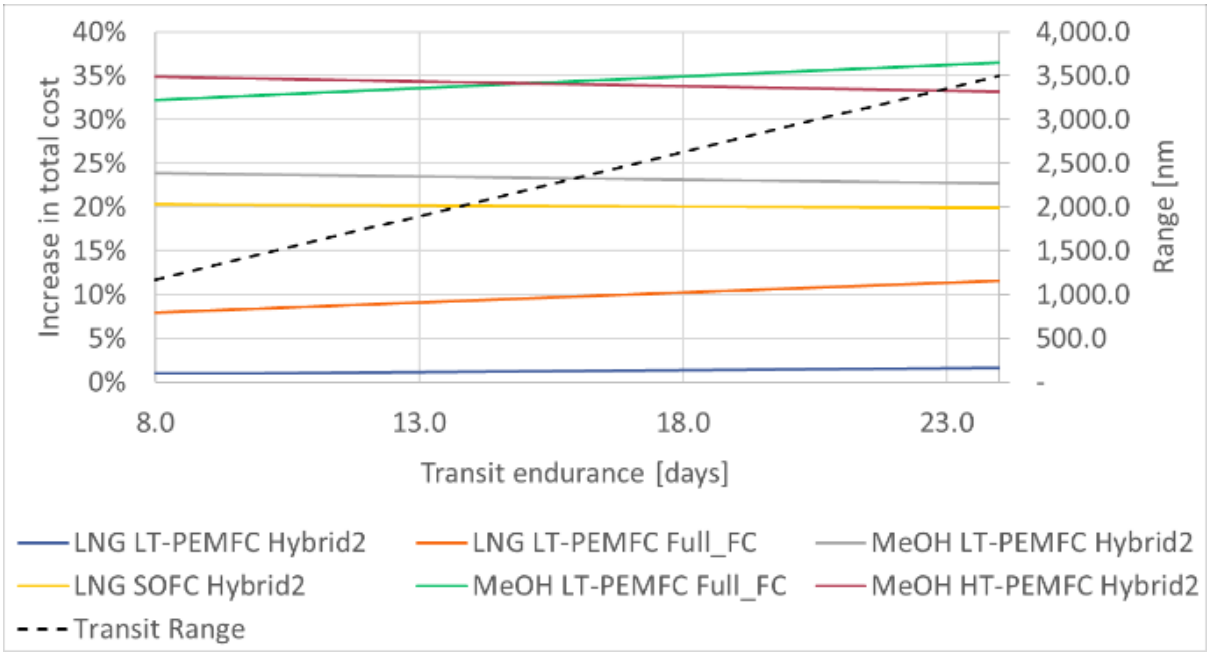

Fig.13: Increase in total cost (compared with a conventional ship with equal requirements) for different endurance requirements of the transit operation.

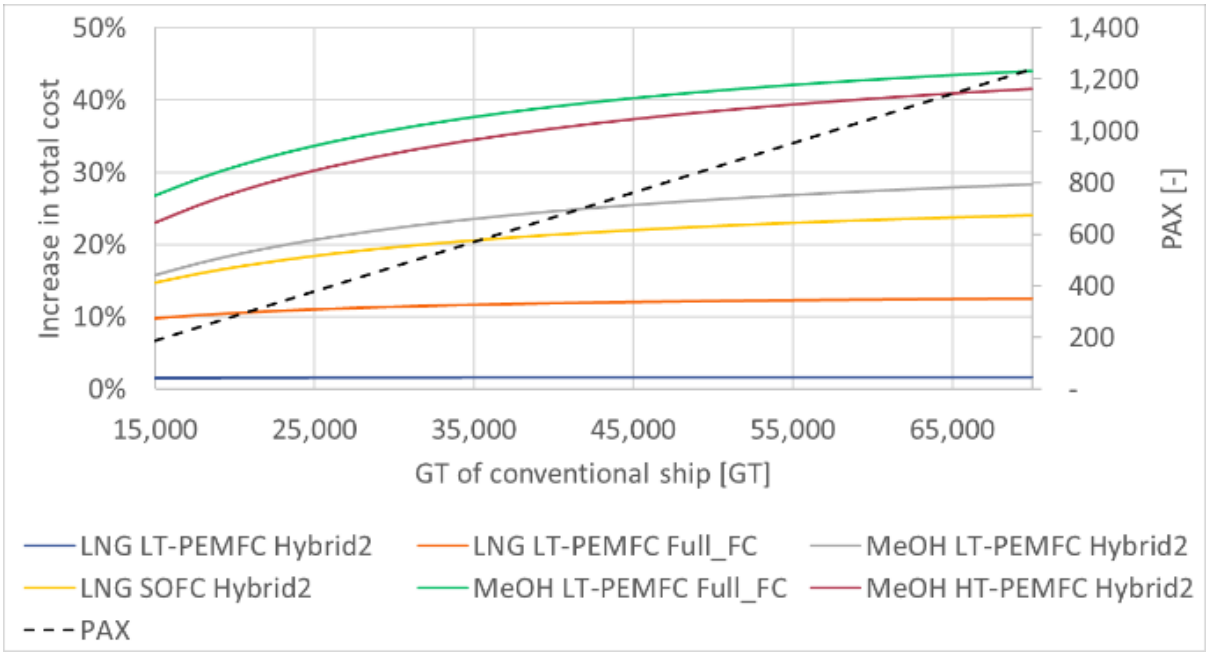

Fig.14: Increase in total cost (compared with a conventional ship with equal requirements) for different capacity requirements

In Fig.13, the total increase in cost is varied over the transit endurance requirement. The total increase in cost consists of the newbuild price of the ship and the fuel cost. Time value of money and finance cost are not taken into account. The green line and purple line cross, meaning between these options, the best performer on total increase in cost is dependent on the transit endurance. For the other options there is no interdependence for different endurance requirements. For all considered endurances, the same conclusion is found regarding the best performing option as was presented in section 4: hybrid option 2 with LNG fueled LT-PEMFC results in the lowest increase in total cost.

5.2. Variation of capacity requirements

In this section the size of the conventional ship (in GT) is varied in order to see whether some fuel cell systems and hybrid options perform differently for different ship sizes. The size of the ship (GT) is driven by the capacity of the ship (PAX) and they were linearly linked in the model since the luxury level is kept constant.

In Fig.14, the resulting total increase in cost is shown for varying GT. In general, the increase in total cost is higher for larger ships. For all considered GT the same order of performance was found as presented in Fig.10. None of the lines cross, meaning the best fuel cell and hybrid strategy for a certain ship in terms of total cost is not dependent on the ship size. For all considered GT, the same conclusion is found regarding the best performing option as was presented in section 4: hybrid option 2 with LNG fueled LT-PEMFC results in the lowest increase in total cost.

6. Conclusion & recommendations

Based on the results of this study it is concluded that:

i) Depending on the fuel cell system and hybridization strategy, the increase in ship size (in GT) ranges from 2% to 21% for an average ship (with respect to the reference ships).

ii) Depending on the fuel cell system, the increase in newbuild price compared to a conventional ship is 36% to 97% for a full fuel cell powered expedition cruise ship and 20% to 63% for the considered hybrid options. Depending on the fuel cell system, the increase in total cost compared to a conventional ship is 12% to 275% for a full fuel cell powered expedition cruise ship and 2% to 200% for the considered hybrid options.

iii) iii) Hybrid option 1 (fuel cell for auxiliaries) is inferior to hybrid option 2 (DG to support in transit) in terms of cost, emissions and complying with ECA regulations.

iv) iv) Hybrid option 2 with $MeOH$ fueled LT-PEMFC offers the lowest percentage increase in newbuild price for expedition cruise ships, which is under 25% for an average ship.

v) Hybrid option 2 with LNG fueled LT-PEMFC offers the lowest percentage increase in total cost over ship the ship lifetime (including fuel cost) for expedition cruise ships, which is under 5% for an average ship. For the six best performing combinations, Table VIII, of fuel cell system and hybridization option, the range, endurance and capacity requirements are systematically varied to determine whether the choice of the best option depends on these requirements.

It was confirmed that conclusion v) still holds for a large range of endurances and ship sizes. Consequently, it was concluded that the choice of the fuel cell system from a total cost perspective should not depend on the range requirements and the size of the ship.

From a newbuild price perspective, hybrid option 2 with MeOH fueled LT-PEMFC is recommended. This does comply with NO_x, SO_x and PM regulations (including ECA zones) and CO_2 goals for 2030. From a total cost (new build price and fuel cost) perspective, hybrid option 2 with LNG fueled LT-PEMFC is recommended. This does comply with NO_x, SO_x and PM regulations (including ECA zones), but does not meet CO_2 goals for 2030. When it is desired to reach this CO_2 target, hybrid option 2 with MeOH fueled LT-PEMFC is also recommended from a total cost perspective.

Finally, it must be noted that no optimal fuel cell system or hybridization strategy can be pointed out. The fuel cell system and hybridization strategy selection are very dependent on the requirements of the customer (cruise line). The cruise line might prefer a ship with a lower newbuild price because it is easier to finance or the customer might even require a full fuel cell powered ship, because the cruise line needs full ship performance in ECA zones. For this reason, the proposed method is very useful, because it can be used to evaluate and compare the different options for different designs requirements.

References

ALESSANDRO, M. (2019), *Imagine - The Future of Cruise Ship Design*, Technical Report, RINA

ALKANER, S.; ZHOU, P. (2006), *A comparative study on life cycle analysis of molten carbon fuel cells and diesel engines for marine application*, J. Power Sources 158, pp.188-199

ALTMANN, M.; WEINDORF, W.; WURSTER, R.; WEINBERGER, M.; FILIP, G. (2004), *FCSHIP: Environmental Impacts and Costs of Hydrogen, Natural Gas and Conventional Fuels for Fuel Cell Ships*, 15th World Hydrogen Energy Conference, Yokohama

BALDI, F.; AHLGREN, F.; NGUYEN, T.V.; THERN, M.; ANDERSSON, K. (2018), *Energy and Exergy Analysis of a Cruise Ship*, Energies 11/10, 2508

BERTRAM, V. (2012), *Practical Ship Hydrodynamics*, Elsevier

BIERT, L.V.; GODJEVAC, M.; VISSER, K.; ARAVIND, P.V. (2016), *A review of fuel cell systems for maritime applications*, J. Power Sources 327, pp.345-364

BLOOM ENERGY (2019), *Energy Server 5 Product Datasheet*, www.bloomenergy.com

BOUDGHENE STAMBOULI, A.; TRAVERSA, E. (2002), *Fuel Cells, An Alternative to Standard Sources of Energy*, Renewable and Sustainable Energy Reviews 6(3), pp.295-304

BUREL, F.; TACCANI, R.; ZULIANI, N. (2013), *Improving sustainability of maritime transport through utilization of Liquefied Natural Gas (LNG) for propulsion*, Energy 57, pp.412-420

CHANDAN, A.; HATTENBERGER, M.; EL-KHAROUF, A.; DU, S.; DHIR, A.; SELF, V.; POLLET, B.G.; INGRAM, A.; BUJALSKI, W. (2013), *High temperature (HT) polymer electrolyte membrane fuel cells (PEMFC) - A review*, J. Power Sources 231, pp.264-278

CHOI, C.H.; YU, S.; HAN, I.S.; KHO, B.K.; KANG, D.G.; LEE, H.Y.; SEO, M.S.; KONG, J.W.; KIM, G.; AHN, J.W.; PARK, S.K.; JANG, D.W.; LEE, J.H.; KIM, M. (2016), *Development and demonstration of PEM fuel-cell-battery hybrid system for propulsion of tourist boat*, Int. J. Hydrogen Energy 41, pp.3591-3599

CLAUS, S. (2019), *Steeds meer cruiseschepen mijden Amsterdam, de sector baalt*, https://www.trouw.nl/economie/steeds-meercruiseschepen-mijden-amsterdam-de-sector-baalt{~}b0fdb7f1/

CLIA (2019), *2019 Cruise Trends & Industry Outlook*, Cruise Line International Association

DAS, S.K.; GADDE, K.K. (2013), *Computational fluid dynamics modelling of a catalytic flat plate fuel reformer for on-board hydrogen generation*, J. Fuel Cell Science and Technology 10

DE-TROYA, J.J.; ÁLVAREZ, C.; FERNÁNDEZ-GARRIDO, C.; CARRAL, L. (2016), *Analysing the possibilities of using fuel cells in ships*, Int. J. Hydrogen Energy 41/4, pp.2853-2866

ELLIS, J.; TANNEBERGER, K. (2016), *Study on the use of ethyl and methyl alcohol as alternative fuels in shipping*, EMSA, http://www.emsa.europa.eu/news-a-press-centre/external-news/item/2726-study-on-the-use-of-ethyl-and-methyl-alcohol-as-alternativefuels-in-shipping.html

EVRIN, R.A.; DINCER, I. (2019), *Thermodynamic analysis and assessment of an integrated hydrogen fuel cell system for ships*, Int. J. Hydrogen Energy 44, pp.6919-6928

FOURNIER, G.G.; CUMMING, I.W.; HELLGARDT, K. (2006), *High performance direct ammonia solid oxide fuel cell*, J. Power Sources 162, pp.198-206

GEERTSMA, R.; KRIJGSMAN, M. (2019), *Alternative fuels and power systems to reduce environmental impact of support vessels*, Marine Electrical and Control Systems Safety Conf.

HÖHLEIN, B.; BOE, M.; BØGILD-HANSEN, J.; BRÖCKERHOFF, P.; COLSMAN, G.; EMONTS, B.; MENZER, R.; RIEDEL, E. (1996), *Hydrogen from methanol for fuel cells in mobile systems: Development of a compact reformer*, J. Power Sources 61, pp.143-147

HRISTOVSKI, K.D.; DHANASEKARAN, B.; TIBAQUIRÁ, J.E.; POSNER, J.D.; WESTERHOFF, P.K. (2009), *Producing drinking water from hydrogen fuel cells*, J. Water Supply: Research and Technology 58, pp.327-335

IMO (2013), *MARPOL Annex VI and NTC 2008 with Guidelines for Implementation*, Int. Mar. Org., London

IMO (2018a), *GHG Emissions*, http://www.imo.org/en/OurWork/Environment/PollutionPrevention/AirPollution/Pages/GHG-Emissions.aspx

IMO (2018b), *UN body adopts climate change strategy for shipping*, http://www.imo.org/en/MediaCentre/PressBriefings/Pages/06GHGinitialstrategy.aspx

IMO (2020a), *Nitrogen oxides (NOx) - Regulation 13*, http://www.imo.org/en/OurWork/Environment/PollutionPrevention/AirPollution/Pages/Nitrogen-oxides-(NOx)-\T1\textendash-Regulation-13.aspx

IMO (2020b), Sulphur oxides (SOx) - Regulation 14, http://www.imo.org/en/OurWork/Environment/PollutionPrevention/AirPollution/Pages/Sulphur-oxides-(SOx)-\T1\textendash-Regulation-14.aspx

ISAACS, R.; PALFREEMAN, N.; ROBERT, R. (2013), *Achieving Ultra-Low NOx Emissions in Methanol Downfired Reformer Applications*, Int. Combustion Symposium, American Flam Research Committee, https://collections.lib.utah.edu/details?id=14363

KAR CHUNG TSE, L.; WILKINS, S.; McGLASHAN, N.; URBAN, B.; MARTINEZ-BOTAS, R. (2011), *Solid oxide fuel cell/gas turbine trigeneration system for marine applications*, J. Power Sources 196, pp.3149-3162

KEE, R.J.; ZHU, H.; GOODWIN, D.G. (2005), *Solid-oxide fuel cells with hydrocarbon fuels*, Proc. Combustion Institute 30 II, pp.2379-2404

KERKHOF, M. v.d. (2019), *Clean Shipping - Vision 2030 and Action Plan until 2021*, Port of Rotterdam

KLERKE, A.; CHRISTENSEN, C.H.; NØRSKOV, J.K.; VEGGE, T. (2008), *Ammonia for hydrogen storage: Challenges and opportunities*, J. Materials Chemistry 18, pp.2304-2310

LAN, R.; TAO, S. (2014), *Ammonia as a Suitable Fuel for Fuel Cells*, Frontiers in Energy Research 2

LARMINIE, J.; DICKS, A. (2003), Fuel Cell Systems Explained, Wiley

LAW, K.; ROSENFELD, J.; HAN, V.; CHAN, M.; CHIANG, H.; LEONARD, J. (2013), *U.S. Department of Energy Hydrogen Storage Cost Analysis*, U.S. Department of Energy, https://www.osti.gov/scitech/servlets/purl/1082754

LEE, Y.D.; AHN, K.Y.; MOROSUK, T.; TSATSARONIS, G. (2015), *Environmental impact assessment of a solid-oxide fuel-cell-based combined-heat-and-power-generation system*, Energy 79, pp.455-466

LEITES, K.; BAUSCHULTE, A.; DRAGON, M.; KRUMMRICH, S.; NEHTER, P. (2012), *Design of different diesel based fuel cell systems for seagoing vessels and their evaluation*, ECS Trans., pp.49-58

LUCKOSE, L.; HESS, H.L.; JOHNSON, B.K. (2009), *Fuel cell propulsion system for marine applications*, IEEE Electric Ship Technologies Symp., pp.574-580

MINNEHAN, J.J.; PRATT, J.W. (2017), *Practical Application Limits of Fuel Cells and Batteries for Zero Emission Vessels*, Sandia National Laboratories, https://classic.ntis.gov/help/order-methods/

NN (2004), Fuel Cell Handbook, EG&G Technical Services

PAN, C.; HE, R.; LI, Q.; JENSEN, J.O.; BJERRUM, N.J.; HJULMAND, H.A.; JENSEN, A.B. (2005), *Integration of high temperature PEM fuel cells with a methanol reformer*, J. Power Sources

PATEL, H.C.; WOUDSTRA, T.; ARAVIND, P.V. (2012), *Thermodynamic analysis of solid oxide fuel cell gas turbine systems operating with various biofuels*, Fuel Cells 12, pp.1115-1128

PAYNE, R.; LOVE, J.; KAH, M. (2019), *Generating Electricity at 60% Electrical Efficiency from 1-2 kWe SOFC Products*, ECS Transactions, The Electrochemical Society, pp.231-239

PETERS, R.; DEJA, R.; ENGELBRACHT, M.; FRANK, M.; NGUYEN, V.N.; BLUM, L.; STOLTEN, D. (2016), *Efficiency analysis of a hydrogen-fueled solid oxide fuel cell system with anode off-gas recirculation*, J. Power Sources 328, pp.105-113

SARGENT, R.G. (2010), *Verification and validation of simulation models*, Winter Simulation Conf., pp.166-183

SCHNEIDER, J.; DIRK, S. (2010), *ZEMShip*, 18th World Hydrogen Energy Conf.

SEMELSBERGER, T.A.; BORUP, R.L.; GREENE, H.L. (2006), *Dimethyl ether (DME) as an alternative fuel*, J. Power Sources 156, pp.497-511

SIEMENS (2013), *SINAVY PEM Fuel Cell*, https://www.industry.siemens.com/verticals/global/de/marine/marineschiffe/energieverteilung/Documents/sinavy-pem-fuel-cellen.pdf

SOLTANI, R.; ROSEN, M.A.; DINCER, I. (2014), *Assessment of CO2 capture options from various points in steam methane reforming for hydrogen production*, Int. J. Hydrogen Energy 39, pp.20266-20275

SØNDERGAARD, T.; JENSEN, J.O.; AILI, D.; HU, Y.; CLEEMANN, L.N.; LI, Q. (2017), *High-Temperature Polymer Electrolyte Membrane Fuel Cells*, Ph.D. thesis, Technical Univ. of Denmark

STRAZZA, C.; DEL BORGHI, A.; COSTAMAGNA, P.; TRAVERSO, A.; SANTIN, M. (2010), *Comparative LCA of methanol-fuelled SOFCs as auxiliary power systems on-board ships*, Applied

Energy 87, pp.1670-1678

THOUNTHONG, P.; RAËL, S.; DAVAT, B. (2009), *Energy management of fuel cell/battery/ supercapacitor hybrid power source for vehicle applications*, J. Power Sources 193, pp.376-385

TRONSTAD, T.; LANGFELDT, L. (2017), *Study on the use of fuel cells in shipping*, EMSA European Maritime Safety

VAN VELDHUIZEN, B. (2020), *Fuel cell systems Applied in Expedition Cruise Ships - A Comparative Impact Analysis*, Delft University of Technology

VOLGER, C. (2019), *Alternative fuels on board of carbon-neutral cruise vessels*, Delft University of Technology

WELAYA, Y.M.; EL GOHARY, M.M.; AMMAR, N.R. (2011), *A comparison between fuel cells and other alternatives for marine electric power generation*, Int. J. Naval Architecture and Ocean Engineering 3, pp.141-149

WHC (2018), *Norwegian parliament adopts zero-emission regulations in World Heritage fjords*, World Heritage Centre, UNESCO, https://whc.unesco.org/en/news/1824

ZAMFIRESCU, C.; DINCER, I. (2008), *Using ammonia as a sustainable fuel*, J. Power Sources 185, pp.459-465

Virtual-Real Interaction Testing for Functions of Intelligent Ships

Fan Yang, Wuhan University of Technology, Wuhan/China, fanyang123@whut.edu.cn
Jialun Liu, Wuhan University of Technology, Wuhan/China, jialunliu@whut.edu.cn
Shijie Li, Wuhan University of Technology, Wuhan/China, lishijie@whut.edu.cn
Feng Ma, Wuhan University of Technology, Wuhan/China, martin7wind@whut.edu.cn

Abstract

This paper proposes and describes a virtual-real interaction testing method for the functional testing of intelligent ships. The method integrates the merits of virtual simulations, model tests, and field tests to make functional testing reliable and affordable. Accordingly, an integration test platform is used with model-scale ships, and designed with systems of real navigation environment perception, testing based on the virtual simulation, and virtual-real interaction testing, etc. Practical applications of the method and platform will be shown.

1. Introduction

As the core carrier of waterway transportation, ship's intelligent, remote and autonomous development has attracted wide attention and continuous investment from all countries in the world, become a hot spot in the current development of the shipbuilding industry and shipping field and will bring innovation and change in shipping mode, *Yan and Liu (2016)*, *Yan (2016)*. For design selection, operation and maintenance, function verification, technology research and development, product inspection, standard formulation, and other technical research and achievement transformation of intelligent ships, it is urgent to form systematic and reliable testing and verification technology.

Although some governments and research institutions have built not a few testbeds dedicated to remote controlling or autonomous navigation, testing for intelligent ships remains time-consuming, inefficient, low-economy, and high-risk. Controllability, customizability, observability, reproducibility, comparability, and quantifiability are important advantages of virtual simulation. However, the modeling and simulation of virtual testing for intelligent ships usually rely on human intrinsic knowledge. How to break the dependence on intrinsic knowledge, establish information association based on real navigation, construct a reliable virtual-real interaction testing method is the crucial difficulty.

2. State-of-the-art research of intelligent ship testing

The International Maritime Organization (IMO) had defined Maritime Autonomous Surface Ship (MASS) as "a ship that can be independent of human intervention to varying degrees" in the 99th Maritime Safety Committee (MSC). And in the 101st MSC, the "Interim Guidelines for MASS Trials" was issued, *IMO (2019)*, approving the MASS Trials need to fulfill the following conditions:

- The trials should be appropriately identified and measures to reduce the risks to as low as reasonably practicable and acceptable.
- Compliance with mandatory instruments should be ensured.
- Remote and onboard personnel involved in MASS trials should be appropriately qualified and experienced to safely conduct MASS trials.
- For the safe, secure, and environmentally sound conduct of MASS trials, the human element should be appropriately addressed.
- Proper infrastructure should be established to provide for the safe, secure, and environmentally sound conduct of MASS trials.
- An appropriate means for communications and data exchange should be provided.
- Appropriate steps should be taken to ensure sufficient cyber-risk management of the systems and infrastructure used when conducting MASS trials.

2.1. Traditional methods for ship testing

Traditional ship testing mainly includes three methods: virtual simulation, model-scale testing, and full-scale testing. Model-scale testing can be subdivided into towing tank testing and field testing. Traditional virtual simulation is usually used in the design process to predict relevant performance. After the design plan is selected, model-scale testing is carried out to evaluate its feasibility to update the construction plan. Finally, the ship's performance is qualitatively judged and quantitatively analyzed through ship delivery by the sea trial experiment, *Liu et al. (2020)*.

Virtual simulation testing is low-cost, risk-free, customizable, accelerated, and repeatable, but it has high R&D costs, doubtful accuracy, and a lack of real feedback. Towing tank testing is more reliable than virtual simulations and can control natural conditions (like wind, waves, currents, etc.) in the tank to a certain extent. But the investment of towing tank testing in the construction of testing conditions is large, high testing costs, scale effects, and less testing scenarios are considerable constraints. The field testing does not require towing tanks or testbeds construction, but the natural conditions are uncontrollable, the testing cost is high and there are still scale effects. The full-scale ship testing is an objective display of the comprehensive performance of the shipborne hardware and software equipment and the ship itself in the real navigation environment. The full-scale testing has high testing costs, long testing time, uncontrollable risks, monotonous testing scenarios, unrepeatable navigation environment, and lack of comparability of testing results. Furthermore, full-scale testing can only be carried out after the construction completed of the full-scale ship, besides shipbuilding and experiments in different places have legal risks. Under the constraints of safety and costs, model-scale and full-scale ship testing are difficult to be used as training and learning platforms for current artificial intelligence decision-making and control methods.

To sum up, how to integrate the advantages of various testing methods, learn from each other and avoid risk, build the simulation platform with physical authenticity, and break the barrier between virtual and real measurement, which is the key to carry out functional testing of intelligent ships with a safe, economic, and efficient way.

2.2. Necessity of interaction testing

In the traditional R&D process of model-scale or full-scale ship testing, it's difficult to completely avoid the potential uncontrollable risks of the ship under test. Due to the increasing complexity of the ship system, the diverse navigation environment, and the changeable natural environment. The efficiency of traditional testing can no longer fulfill the timeliness requirements of the testing for intelligent ships, and cannot cover all the navigation scenarios and working conditions faced by the testing of the intelligent ships. The testing of virtual simulation has the advantages of high efficiency, low cost, and zero risks. Compared with model-scale and full-scale ship testing, the authenticity of pure virtual simulation testing is doubtful, including the authenticity of test scenarios, data sources, and ship dynamics simulation.

Based on the analysis, model-scale or full-scale testing of intelligent ships have problems of safety, efficiency, and coverage. The modeling and simulation of virtual testing usually rely on the intrinsic knowledge of people and lack the random and real impacts of the navigation environment. Therefore, it is necessary to establish a connection between model-scale or full-scale ship testing with virtual simulation. By putting the real data information, environment information, and traffic flow status obtained by model-scale and full-scale ship testing into the virtual simulation as much as possible, reproduces random events that may occur during real navigation to ensure the authenticity of the virtual terminal. Then the testing method of virtual-real interaction that fully integrates the advantages of virtual simulation and real ship testing is proposed. Revolves around the virtual simulation environment and model-scale and full-scale ship testing samples.

The testing method of virtual-real interaction breaking the dependence on inherent knowledge. By establishing the information association between the virtual world and the real world, making full use

of real testing samples to increase the authenticity of virtual simulation, we can design testing methods with low risk, high efficiency, and high coverage, and high reliability.

3. Virtual-real interaction testing scenarios for intelligent ships

In recent years, intelligent connected vehicles (ICV) have achieved certain research results in the construction of virtual testing scenarios. A series of testing tools of the simulation scenarios for automatic driving have been established, including sensor models and interfaces (OSI), environment models (OpenDrive, OpenCRG), and scenario models (OpenScenario). Compared with ICV, there are obvious lags in the standardization research of testing scenarios for intelligent ships. It is urgent to design and develop simulation supporting tools, analyze and construct elements of testing scenarios, and other important core contents of virtual testing. Combining the experience in the construction of ICV scenarios, the testing scenarios for intelligent ships are sorted out.

3.1. Meaning of the testing scenario

The scenario is the description of the system itself usage pattern, requirements, and environment, *Zhu et al. (2019)*. A testing scenario needs to prioritize the type of ship under test, and including the elements of the ship itself, navigation environment, natural environment, and navigation tasks. The testing scenarios of virtual-real integration testing for intelligent ships mainly refers to the overall dynamic description for elements of the digital-twin ship and the surrounding navigation environment over a while. The composition of multiple elements is determined by the expected testing capabilities of intelligent ships.

3.2. Testing scenario library

The advantage of establishing scenario libraries is that it can continuously increase and improve the contents of testing scenarios along with the testing and evaluation indicators are gradually refined. Specific to the typical navigation scenarios that ships may face under actual conditions, a modular testing scenario library is established. The testing scenario library needs to include the sub-libraries of typical ship types, navigation areas, natural environment, and navigation behaviors. The typical ship types mainly include container ships, bulk carriers, oil tankers, and cruise ships, etc. The navigation areas include open waters, restricted waters, curved channels, and continuous bridge areas, etc. The natural environment includes wind, waves, currents, surges, etc. The navigation behaviors include head-on, crossovers, overtaking, following, etc. Through the combination of the above four sub-libraries to form a complete testing scenario, as shown in Fig.1.

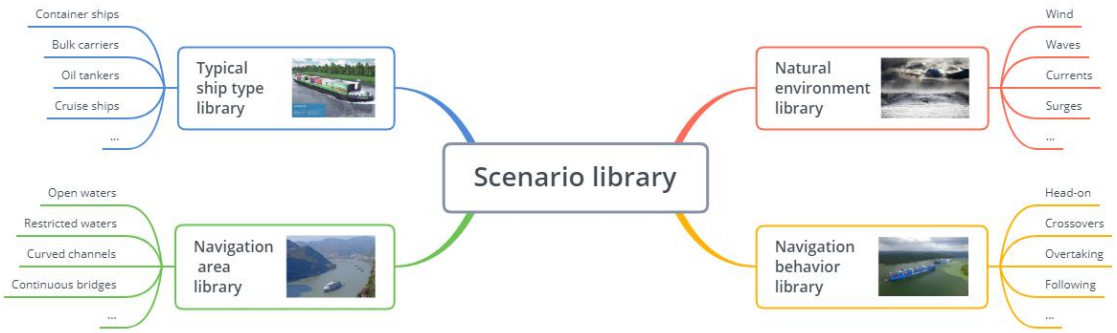

Fig.1: Composition of testing scenarios library

3.3. Elements of testing scenario

Determining the elements of testing scenarios is the core foundation for describing the testing scenario, and is the primary link in the development of virtual-real interaction testing for intelligent

ships. The elements of testing scenarios are analyzed based on the elements of the scenario libraries and the information of the ship itself. Elements of typical ship type are divided into two aspects, geometric characteristics and performance characteristics. Elements of navigation area include navigation information and shore-based information. Elements of natural environment mainly refers to the construction and description of wind field, flow field, and environment field. Elements of navigation behavior include functional elements, navigation systems and navigation behaviors, as shown in Fig.2.

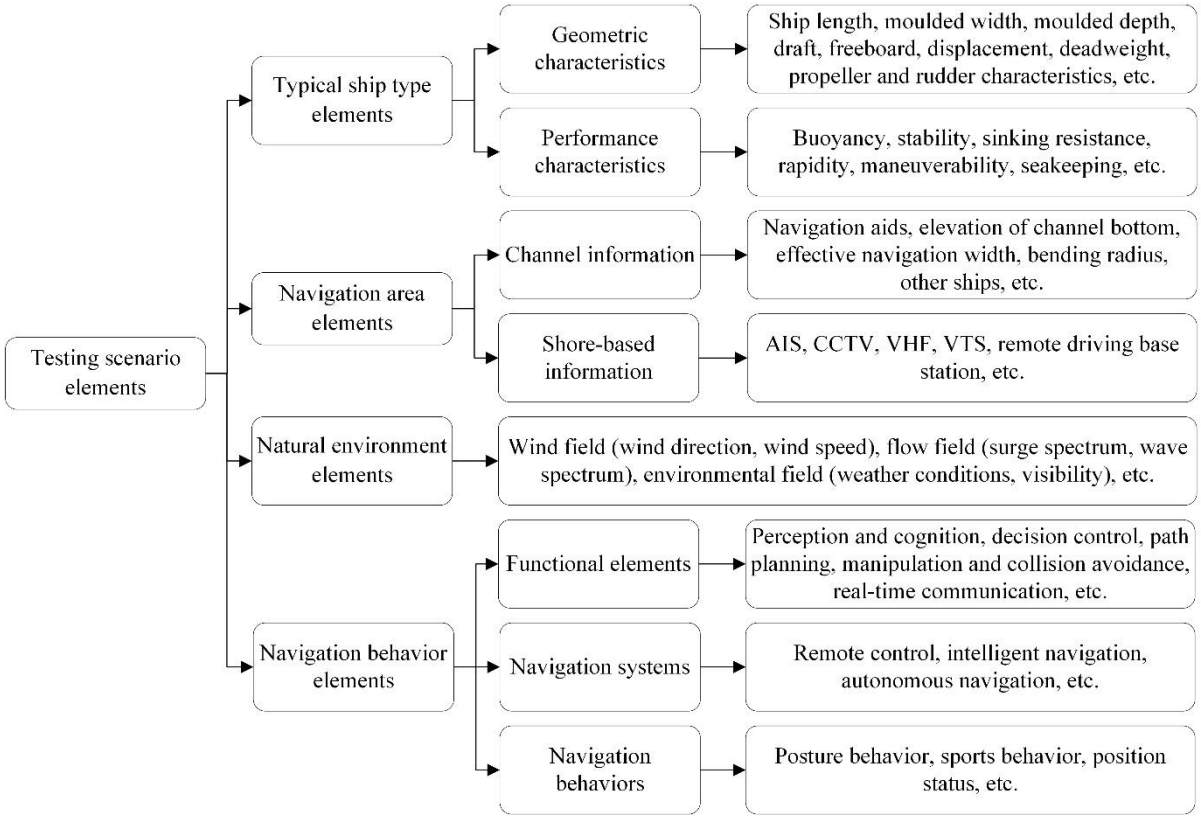

Fig.2: Composition of testing scenarios elements

3.4. Methods of scenario accelerating testing

The virtual-real interaction testing can ensure the coverage, systematic, and completeness of the testing scenario library to a certain extent. However, if the distinguished elements of the testing scenarios are too many, the combination of scenario elements and the adjustment of parameter value will make the generated testing scenarios appear the phenomenon of the exponential explosion. Even the testing speed of virtual simulation will appear obvious efficiency problems in ergodic testing. There is an urgent need to carry out efficient and rapid testing based on ensuring the coverage of scenario elements. By optimizing the combination of scenario elements, adopting single sampling, sub-sampling, multiple sampling, stratified sampling, SPRT, and other methods, *Wang (2014)*, and taking example by the importance sampling theory filter and integrate the testing contents and make the reasonable layout.

4. Virtual-real interaction testing platform for intelligent ships

4.1. Virtual-real interaction testing platform

The R&D and design on the platform of virtual-real interaction testing for intelligent ships is a process of continuous updating and improvement. The platform needs to fulfill the design principles of scalable software and upgradeable hardware. Scalable software facilitates the addition of subsequent submodules and subsystems, improves system functions, and supplements platform

defects. Upgradeable hardware realizes the function enhancement and performance optimization of the system and equipment. The software system of intelligent ships should adopt the overall architecture principles of modularization, hierarchization, encapsulation, high cohesion, and low coupling, while the hardware equipment should adopt the overall design principles of modularization, hierarchization, and standardization.

4.2. Composition of the testing platform

The capabilities that intelligent ships should possess include cognitive capabilities derived from perception, decision-making capabilities derived from cognition, optimization capabilities derived from decision-making, control capabilities derived from optimization, execution capabilities derived from control, and repair capabilities derived from fault. Based on the current research foundation, for the decision-making level of intelligent systems and the execution level of autonomous systems. The testing platform of virtual-real interaction testing for intelligent ships that contains testing based on the virtual simulations, real navigation environment perception, standards of testing scenarios, system in-the-loop testing, virtual-real interaction testing, testing verification and evaluation, benchmark autonomous system, and testing services eight components have been formed, as shown in Fig.3.

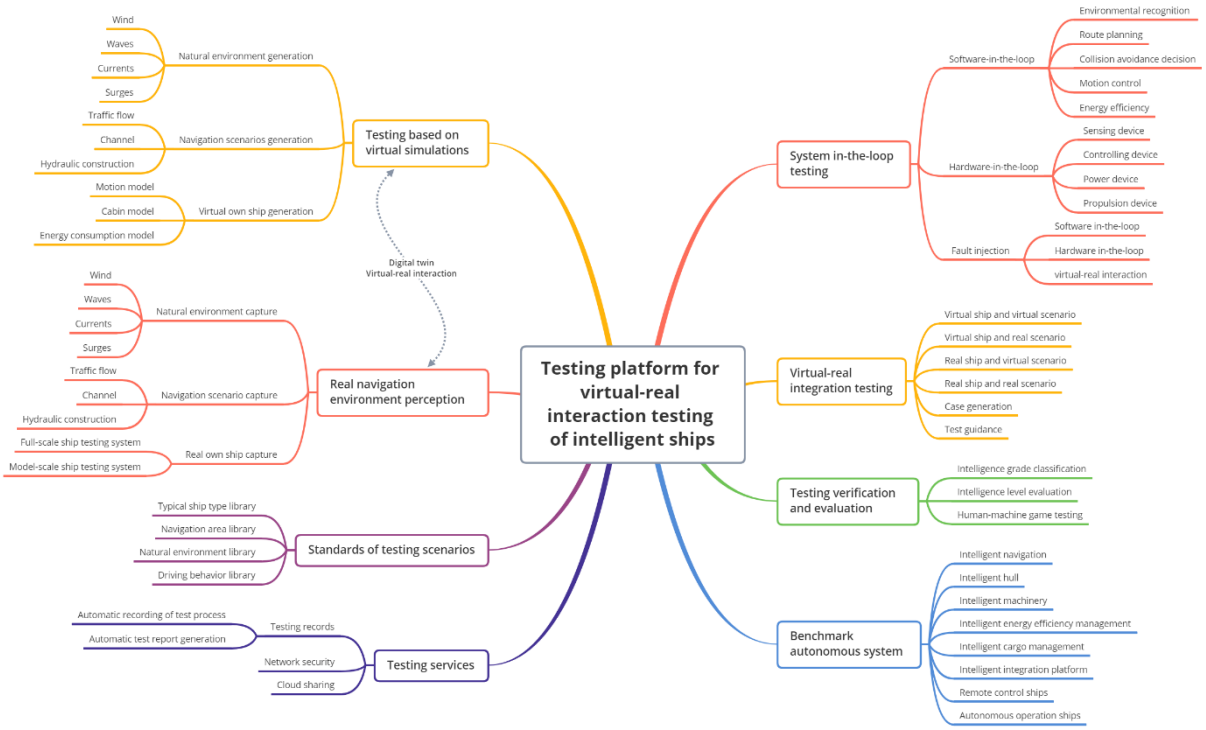

Fig.3: Testing platform of virtual-real interaction testing for intelligent ships

The system of testing based on the virtual simulations is divided into the module of natural environment generation, navigation scenarios generation, and virtual own ship generation. The system of real navigation environment perception is composed of the module of natural environment capture, navigation scenario capture, and real own ship capture. The system of standards of testing scenarios is mainly to standardize the scenario library. In the system in-the-loop testing, the testing of software-in-the-loop, hardware-in-the-loop, and fault injection are the main testing methods. Software-in-the-loop testing is mainly for intelligent algorithms such as environmental perception, route planning, collision avoidance decision-making, motion control, and energy and efficiency management. Hardware-in-the-loop testing is mainly for critical equipment such as perception, control, power, and propulsion. The system of virtual-real integration testing mainly revolves around the layout of the virtual ships & virtual scenarios, the virtual ships & real scenarios, the real ships & virtual scenarios, and the real ships & real scenarios to design case generation and testing guidance. The system of testing verification and evaluation is mainly divided into intelligence grade classification, intelligence level

evaluation, and human-machine game testing. The system of benchmark autonomous refers to the eight detailed functional standards in the 2020 version of the "Rules for Intelligent Ships", *CCS (2020)*. The system of testing services includes important testing auxiliary modules such as testing records, network security, and cloud sharing.

4.3. Application of testing platform

For the optimization and application requirements on the testing platform of virtual-real interaction testing for intelligent ships. The experiments of application testing for core functions of intelligent ships are carried out, including remote control, autonomous navigation, and autonomous berthing and unberthing. The experiment uses the model-scale ship as testing objects, and regard open waters and restricted waters as test fields to design the combination testing of the model-scale ship and real scenario under typical working conditions, *You and Ma et al. (2020)*.

For the capabilities of remote control on the model-scale ship, course control, track control, coordinated control, ship-shore cooperation, and other vital experiments for controlling functions are designed. For the capabilities of autonomous navigation, autonomous perception, autonomous tracking, autonomous obstacle avoidance, and other critical experiments of intelligent functions are designed. For the capabilities of autonomous berthing and unberthing, autonomous unberthing, autonomous U-turn, autonomous berthing, self-stabilization control, and other critical experiments of functional testing are designed. Besides, For the ability of night navigation and power loss and efficiency management of the model-scale ship, corresponding experiments were designed, Fig.4.

Fig.4: Application experiment on the platform of virtual-real interaction testing for intelligent ships

Through the experiments for model-scale ship testing, not only the reliability and stability of the intelligent system control algorithm can be verified, but also various measured data and real scenarios

are collected during the experiments. The data and scenarios are important input of real information on the platform of virtual-real interaction testing for intelligent ships, which are of great value to the optimization and application of the platform.

Acknowledgements

This work was supported by National Key R & D Program of China (2018YFB1601505), National Natural Science Foundation of China (51709217), Research on Intelligent Ship Testing and Verification (2018473).

References

CCS (2020), *Rules for Intelligent Ships*, China Classification Society

IMO (2019), *Interim guidelines for MASS trials*, International Maritime Organization, London

LIU, J.L.; YANG, F.; LI, S.J.; MA, F. (2020), *Functional testing on navigation function of intelligent ships*, Chinese Journal of Ship Research

WANG, C. (2014), *Testability test and integrated evaluation technology with virtual-physical test*, National University of Defense Technology

YAN, X.P. (2016), *Research status and development trend of intelligent ships*, Communication and Shipping 1, pp.23-26

YAN, X.P.; LIU, C.G. (2016), *Review and prospect for intelligent waterway transportation system*, CAAI Transaction on Intelligent Systems 11(6), pp.807-817

YOU, X.; MA, F.; LU, S.L.; LIU J.L.; YAN X.P. (2020), *An integrated platform for the development of autonomous and remote-control ships*, 19th Conference on Computer and IT Applications in the Maritime Industries (COMPIT), Pontignano, pp. 316-327

ZHU, B.; ZHANG, P.X.; ZHAO, J.; CHEN, H.; XU, Z.G.; ZHAO, X.M.; DENG, W.W. (2019), *Review of scenario-based virtual validation methods for automated vehicles*, China Journal of Highway and Transport 32(6)

Modelling Maintenance – Cost Optimised Maintenance in Shipping

Sietske Moussault, Delft University of Technology, Delft/The Netherlands,
s.r.a.moussault@tudelft.nl
Jeroen Pruyn, Delft University of Technology, Delft/The Netherlands,
j.f.j.pruyn@tudelft.nl
Esther van der Voort, Anthony Veder, Rotterdam/The Netherlands,
evdvoort@anthonyveder.com
Geert van IJserloo, Anthony Veder, Rotterdam/The Netherlands,
gvijserloo@anthonyveder.com

Abstract

Most ship management companies base the operational cost calculation on scheduled maintenance jobs. Scheduled maintenance jobs do not take unforeseen maintenance into account. This underestimates the operational budget. The estimation of the operational costs can be improved by including the unforeseen maintenance costs. The amount of unforeseen maintenance costs depends on the implemented maintenance policy, as well as the failure and maintenance intervals. To study this interaction a model is required. A Maintenance Cost Model (MCM) is developed and validated to demonstrate the impact of maintenance policies at Anthony Veder. This model focuses on maintenance cost calculations for different maintenance policies, based on failure behaviour. Anthony Veder will be able to save 60% on average on maintenance costs of mechanical equipment by optimising their maintenance policies. Although applied to Anthony Veder the developed model is generally applicable offering ship management companies' insight in suitable maintenance options.

1. Introduction

Currently, the operational costs of a vessel are estimated in the investment decision-making process, based upon experience and market-information, *van IJserloo (2020)*. A more detailed estimate of the operational costs is made for a short-term period. This estimate is also based on the maintenance jobs scheduled for that short-term time-period. Thus, unscheduled repairs are not taken into account in either of the operational cost estimations. In general, maintenance costs are approximately 40% of the total operational cost of a vessel. Of these maintenance costs, 20% are unscheduled repairs, *van IJserloo (2020)*. Thus, not taking into account the unscheduled repairs when estimating the operational costs, means approximately 8% of the total operational costs are missing.

Especially in the Oil and Gas industry, there is a strong focus on a safe reputation, unforeseen maintenance is therefore not only a cost element, but also impact the reputation of the entire company, far beyond the single vessel. In the tanker business there is an extensive vetting process performed by the cargo-owners, oil majors. These vetting processes consist of Ship Inspection Report Program (SIRE) inspections, which are inspections of individual vessels, as well as Tanker Management and Self-Assessment (TMSA) audits, which examines the whole management of fleet and office, *Bijwaard and Knapp (2009), Hull (2007).* Loss of hire, or even loss of a long-term time-charter can follow an incident. Since TMSA audits examine the whole fleet, this means a defect on a vessel not utilised by the concerning oil major can affect the outcome of an audit by this oil major. Therefor vetting inspections create a strong commercial incentive for ship owners and/or management companies, *Knapp and Franses (2006), Mathur (2018), Cefic (2011).*

This resulting long-term reputation damage, exists more on fleet and company level, as certain clients evaluate the whole fleet and evaluate the management-system and can far exceed the vessel value, *Heijboer (2019), Bijwaard and Knapp (2009), Hull (2007), Knapp and Franses (2006).* Next to the long-term reputation damage, there are also short-term reputation costs. Short-term reputation costs are the reputation costs directly induced by a failure on a particular vessel. This can be loss of hire or also being less flexible at the spot-market as it is not possible to transport all cargo of all clients.

In order to keep costs predictable and thus enhance the competitive advantage, every (ship management) company, with a profit objective, needs to be in complete control of all assets, *Ellram and Siferd (1998), Su et al. (2015), Mathur (2018)*. Therefore, every ship management company needs a valid and accurate estimate of the total operational cost of a vessel. Besides total cost calculations, the trade-off between repair and replacement is crucial for a proactive management strategy, *Handlarski (1980).* For which it is essential to be able to accurately predict the cost associated with unscheduled repair and/or replacement of systems on board a vessel. To be able to make a better substantiated trade-off, information about failure behaviour and the mean-time-to-failure (MTTF) are key. In order to calculate the operational costs, this paper presents an improved cost estimation, based on equipment-specific maintenance costs. Such a method should be able to:

- calculate and compare the maintenance share of the total operational cost;
- consider the lifetime of a vessel;
- looking from an owners' perspective;
- include direct and indirect cost of vessel operation;
- compare different maintenance policies.

1.1. Literature Review

Based on the requirements, the need arises for a method that calculates and evaluates the maintenance share of the operational cost of a vessel from an owners' perspective. Thus, a literature review is presented about, maintenance policies and cost estimation methods.

1.1.1. Maintenance Policies

In recent years different maintenance techniques, have been researched, compared and documented, *Ahmad and Kamaruddin (2012)*. There is an extensive amount of research concerning maintenance policies in capital intensive industries, *Tinga (2013).* Such as the process industry, energy generation industry, manufacturing industry and air, rail, and road transport industry, *Hassanain et al. (2003), Chang and Ni (2007), Cooper and Haltiwanger (1993), Wang (2000), Dekker and Scarf (1998), Callewaert et al. (2018), Chen et al.(2012), Koornneef et al. (2017), Verhagen and Curran (2013), Zorgdrager et al. (2013), Nunez et al. (2014)*. Fig.1 shows a subdivision between the different policies is illustrated, *Tinga (2013)*. As shown in the overview, maintenance is divided in three main branches, namely reactive, proactive and aggressive. In the following sections these maintenance policies are evaluated per branch.

Aggressive maintenance involves adapting the equipment, by redesign or modification, to decrease the amount of failures. An improved system often requires less maintenance, *Tinga (2013)*. Aggressive maintenance can be beneficial in multi-component systems, it is applied in railway, aerospace and shipping amongst others, *Su et al. (2015), Vu et al. (2014), Nicolai and Dekker (2008).* Since the ship design phase is outside the scope of this research, aggressive maintenance is not further elaborated upon, as redesign is considered part of the design phase.

Reactive maintenance is performed after a failure has occurred. The big advantage of reactive maintenance compared to proactive maintenance is therefore, that no remaining lifetime of the (sub)system is wasted. Reactive maintenance is divided in *corrective* and *detective* maintenance *de Jonge et al. (2017), Tinga (2013).*

Corrective maintenance can be more expensive than proactive maintenance because failures often occur unexpected, which then leads to a higher chance of more severe consequences and longer down-time of the (sub)system *de Jonge et al. (2017)*. However, when a failure does not directly lead to down-time of the (sub)system corrective maintenance can be a very profitable maintenance policy, since no useful life of the (sub)system is wasted and no data collection or prediction model is required to predict the optimal maintenance moment.

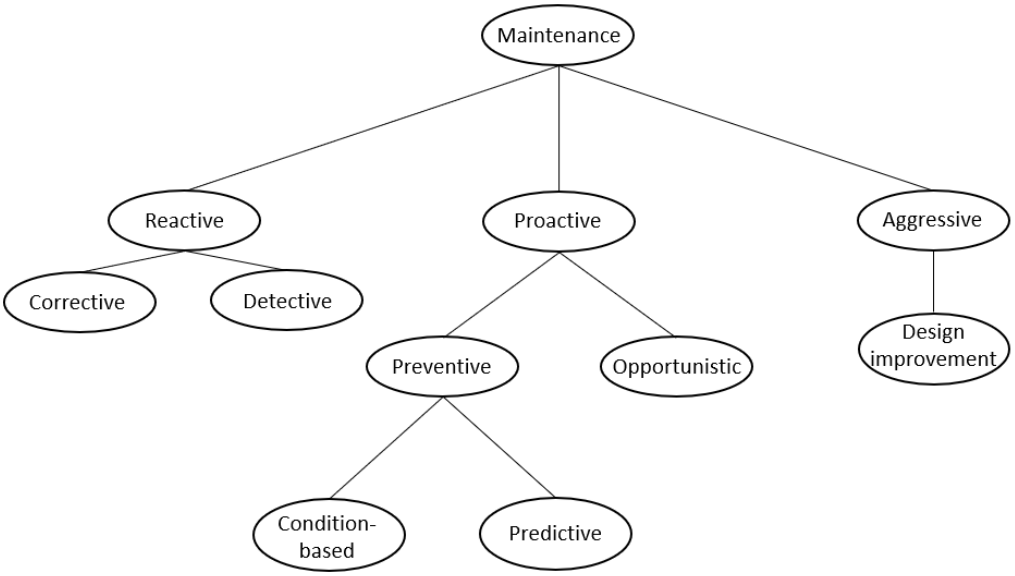

Fig.1: Classification of Maintenance Policies

Detective maintenance only applies to thus-far unrevealed failures. Normally unrevealed failures can only appear on protective devices, for instance sensors and alarms. The failure is only detected when a test reveals that the device has failed, *Tinga (2013)*. Thus, this policy is very limited in the choice of systems. Therefore, detective maintenance is not included in this research. Both corrective and detective maintenance are costless policies, since no data needs to be collected, stored and/or monitored. Furthermore, no remaining useful life of the system is wasted.

Proactive maintenance is performed before a system fails. The proactive maintenance policies are divided into preventive and opportunistic.

Opportunistic maintenance is about clustering maintenance tasks to obtain time and/or cost benefits. An opportunity is any moment in time at which a system can be maintained preventively without obtaining extra cost for the downtime of the system, *Dekker and Dijkstra (1992), Dekker and Smeitink (1991), Zhang and Zeng (2015).*

Preventive maintenance can be condition-based or predictive, *Budai et al. (2006), Barlow and Hunter (1960)*.

In condition-based maintenance the condition of the (sub)system is monitored to determine the optimal moment of maintenance. In this policy the maintenance is performed when it is necessary.

In predictive maintenance, other methods (e.g. operating hours or loads) are used to determine the optimal interval for maintenance, *Tinga (2010)*.

Condition-based maintenance requires several years of data, *Veldman et al. (2011), Verhagen et al. (2017), Tinga (2013)*. Furthermore, condition-based maintenance is a more expensive policy, of which the relative benefit decreases when the uncertainty of the failure threshold increases, *de Jonge et al. (2017)*. Therefore, it is logical to first, determine with a cheaper preventive method, for which system condition monitoring could be beneficial. This becomes clearer when examining Fig.2. If a predictive policy results in a failure prediction with a low standard deviation ($\sigma = 0.5$), it is superfluous to apply the more expensive condition-monitoring. A failure prediction resulting in a high standard deviation ($\sigma = 3$), condition-monitoring of this (sub)system could result in a more accurate prediction and then be a worthwhile investment.

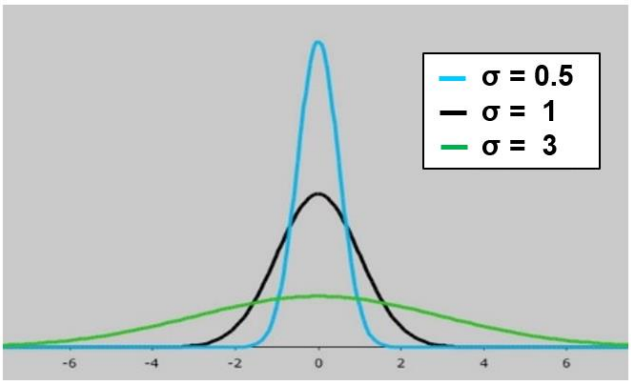

Fig.2: Normal Distribution with Same Mean and Different Standard Deviation

Much research has gone into comparing maintenance policies in clearly defined situations. To do this a cost model is required, however none have focused on shipping, so a suitable cost model needs to be identified as well.

1.1.2. Cost Estimation Methods

Both total costs of ownership (TCO) and Life Cycle Costing (LCC) are extensively used in literature. However no consistent difference can be deduced from literature and in this area the terms seem to be interchangeable as far as the literature goes, *Ellram (1993, 1994, 1995, 1996, 1999), Ellram and Siferd (1993, 1998), Jackson and Ostrom (1980), Fabrycky (1987), Fabrycky and Blanchard (1991), Ferrin and Plank (2002), Hanson (2011), Silva and Fernandes (2006), Barringer and Weber (1996), Wolters (2015)*. The following elements are found to be important for the considered cost model: Direct costs, indirect costs, split into capital costs and operational costs, *Chiadamrong (2003), Parra and Crespo (2012), Roda and Garetti (2015), Shields and Young (1991)*. Finally, a time value of money is to be considered, often the Weighted Average Costs of Capital (WACC) is used for this, though other measures exist, *Barreneche et al. (2015), Fernandez (2010)*. In this paper WACC will be used as it includes the time aspect and can be directly related to the company under investigation.

1.2. Problem Definition

The estimation of the maintenance costs can be improved by including the unforeseen/unscheduled maintenance in this calculation. Determining the optimal maintenance policy is required for the calculation of the corresponding costs. Calculating the cost of a maintenance policy requires the prediction of failure behaviour of a system, *Tinga (2013), Duffuaa and Raouf (1999), Dhillon (2002), Zaal (2011), OREDA (2015)*. To predict or estimate failure behaviour of a system, performance data from the planned maintenance system (PMS), utilised by ship management companies, is required. The previous section illustrated that current approaches to determine total cost of an asset are diverse. No domain-specific TCO or LCC model was found in literature. Furthermore, section 1.1.1 illustrated that the amount of maintenance policies available is incredibly diverse.

Concluding, optimal maintenance is equipment specific and depends on a number of factors. To correctly assess the benefits of changing a maintenance regime a Total Cost Model is required. No such model is available tailored to shipping. For a ship management company maintenance cost estimates can be vital information, that enable a better substantiated total operational cost calculation. Herewith reducing financial risk and therefore contributing to a future proof and healthy company.

2. Method

Different maintenance policies are the basis of the Maintenance Cost Model (MCM) to allow a substantiated maintenance cost calculation.

2.1. Scope

This research covers the unforeseen maintenance cost of the operational cost. It only addresses maintenance-related cost, induced by unforeseen maintenance and does not include routine maintenance jobs, such as greasing, lubrication, painting, etc. The method is developed to make a better-informed maintenance policy decision and not to substantiate design decisions. The model calculates the maintenance cost, with the focus on the systems and engines. Over the entire lifetime of one vessel, and does not consider multiple vessels in a fleet. In this research when a system or component is "no longer capable to fulfil its required function(s)" this is considered a failure, *OREDA (2015)*. This means that when a component of a system has failed, this does not necessarily mean the whole system has failed. As discussed in the literature part, the following maintenance policies are considered relevant, corrective, opportunistic and predictive, this is further elaborated upon below. Furthermore, the scope of the indirect costs as described in the introduction will be limited to the short term, vessel related costs. The measurable effect of the vetting risk is the requirement of a "Condition of Class" (CoC). When a CoC is the result of a failure, the vessel is allowed to sail according to class. There are, however, clients that do impose consequences. It is obvious that no sailing, in whichever form, has a direct negative impact on possibility to generate income for a vessel.

2.2. Maintenance Policies

The literature review describes the general maintenance techniques and policies as described in academic literature. This paragraph analyses the suitability of the different polices to the defined problem.

Different maintenance policies require different data as input, dependent on, for example the level of monitoring. In Table I the different policies are ranked based upon the required input data per policy, as explained in the previous section. Starting with the policy that requires the least data. In the second column of Table I, the cost, represent the (implementation) cost of the policies. This is not the cost of the maintenance itself. In the third column, useful life, yes means that the maintenance is performed before failure and thus useful life of the (sub)system is wasted, and no means, no useful life is wasted. Finally, in the last column the source of this information is presented.

Table I: Maintenance Policies Categorised

Maintenance Policy	Required Data	Cost	Useful Life	Based Upon Research
Corrective	none	zero	no	*Tinga (2013, 2010), de Jonge et al. (2017)*
Opportunistic	none	zero	yes	*Budai et al. (2006), Barlow and Hunter (1960), Dekker and Dijkstra (1992), Dekker and Smeitink (1991)*
Predictive	recommendations from manufacturer	low/ medium	yes	*Zaal (2011), Verhagen and de Boer (2018), Handlarski (1980)*

All maintenance discussed approaches are relevant for this research with the exception of aggressive maintenance, as explained. Detective maintenance is limited in the choice of systems. Therefore, detective maintenance is not included in the model. Condition-based maintenance is more expensive than predictive maintenance and at the moment of this research there is not several years of data available, therefore condition-based maintenance policies are not included in the method. Based on the performed analysis, corrective, opportunistic and predictive maintenance are deemed the most suitable and relevant maintenance policies for this research, these three policies are included in the method.

2.3. Maintenance Cost Model

Calculating the cost of a maintenance policy requires the prediction of failure behaviour of a system *Tinga (2013), Duffuaa and Raouf (1999), Dhillon (2002), Zaal (2011), OREDA (2015).* To predict or

estimate failure behaviour of a system, performance data from the planned maintenance system (PMS), utilised by ship management companies, is required. Making calculations based on practical data, with a range of parameters over a vast range of possible scenarios, involves solving several equations and considering interactions between the different systems. A mathematical model calculating the maintenance cost of a system, for different scenario's and incorporation uncertainties is developed. The gap in the existing knowledge is, an accurate maintenance cost model for vessels, based upon/comparing several maintenance policies.

The goal of the Maintenance Cost Model (MCM) is to be able to compare different maintenance policies, on the basis of the total cost of a policy over the (remaining) lifetime of a vessel. An abstract representation of the MCM is presented in Fig.3. Based on operational input data, the mean-time-to-failure (MTTF) of a system is calculated. Where after, for each maintenance policy, the total costs are calculated. Finally, the calculated total costs per policy are compared. A ranking of maintenance policies is outcome of the model.

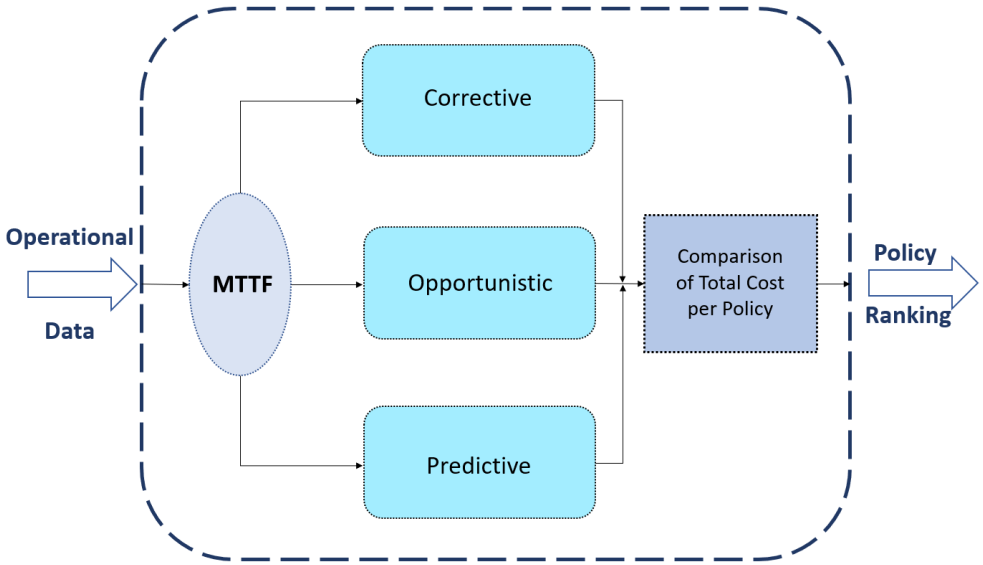

Fig.3: Abstract Representation of Maintenance Cost Model

As illustrated in Fig.3 the cost calculations are performed separately for each maintenance policy. The same three main costs items are calculated for every policy, which together form the total cost per policy. The three main cost items are:

- Replacement cost
- Off-hire cost
- Reputation cost

The sum of these three cost items is the total cost of maintenance of that system/component, per failure. To avoid repetition the explanation of the model is given per main cost item. First explaining the general cost calculation, then highlighting the (potential) differences between the policies.

The delivery time of systems can be substantial, *Zaal (2011), Tinga (2013).* When ordered at the moment of breakdown, this can result in long off-hire time. This often directly results in a proactive policy being optimal. Therefore, two separate tracks within the corrective maintenance policy are investigated. Namely, a corrective policy where the system or component is ordered after breakdown and a corrective policy with one spare system or component stored, and thus directly available. The MCM effectively compares four different policies:

- Corrective Maintenance - order on breakdown
- Corrective Maintenance - store 1 spare
- Opportunistic Maintenance
- Predictive Maintenance

In this research, for both opportunistic and predictive maintenance, an optimisation is performed to find the optimal moment to perform maintenance before failure, based on failure probability from 10% to 90%, with 10% increments. Based on, *Chang and Ni (2007), Dekker (1995), Dekker and Dijkstra (1992), Dhanisetty et al.(2015), Handlarski (1980), OREDA (2015), Zaal (2011)*, a 90% failure probability is utilised to determine the time-to-failure, for the two corrective maintenance policy calculations.

2.3.1. Mean-Time-To-Failure Calculation

As seen in Fig.3 the mean-time-to-failure calculation is the first step in the model. Based upon historic performance data from the PMS, the MCM calculates the MTTF of every system. The two-parameter Weibull distribution is a failure rate description commonly used in reliability engineering, *Khatab et al. (2012), Wang (2000), Dekker and Dijkstra (1992), Dekker and Smeitink (1991), Dekker and van Rijn (1996), Tinga (2013), Grall et al. (2002), Zaal (2011).* This distribution is often used, because it has a correlation between the failure rate and time, and it allows a varying shape parameter. This varying shape parameter means that it is possible to describe both a decreasing, constant and increasing failure rate, *Tinga (2013), Dekker and van Rijn (1996).*

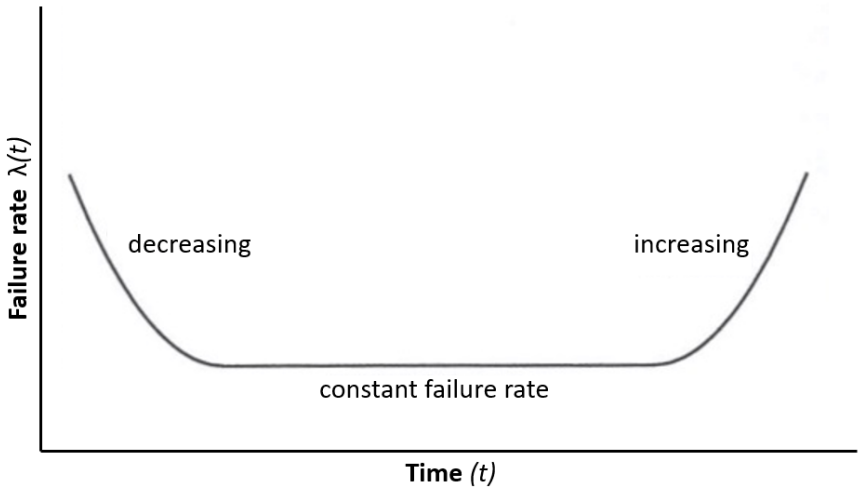

Fig.4: Bathtub Curve

Illustrated in Fig.4 is the bathtub curve, the combination (superposition) of a decreasing, constant and increasing failure rate. Since systems on board a vessel are numerous and diverse, it best suits this research to work with a theory that supports all three failure rates. The Weibull distribution, as presented in Eq.(1), is applied in the model.

$$F(t) = \frac{\beta}{\eta} \left(\frac{t}{\eta}\right)^{\beta-1} e^{-\left(\frac{t}{\eta}\right)^{\beta}} \quad (1)$$

In the probability density function of the Weibull distribution, η is the scale parameter, which represents the characteristic life of the system or component. β is the shape parameter, which indicates the failure behaviour. The value of β indicates in which phase of its operational life a system or component is, see also Fig.4 for further clarification.

- β < 1; means a decreasing failure rate, and this is phenomenon is often the result of infant mortality or the burn-in phase
- β = 1; means a constant failure rate, and describes normal operational life or useful life phase
- β > 1; means an increasing failure rate, and represents ageing systems or the wear-out phase

From the Weibull distribution, the equation for the MTTF is derived, *Tinga (2013), OREDA (2015), Zaal (2011)*. Equation 2 presents the MTTF equation.

$$MTTF = \eta * \Gamma\left(1 + \frac{1}{\beta}\right) \qquad (2)$$

Based on the two equations, and with the historic failure data, it is possible to determine, the MTTF and the failure probabilities.

2.3.2. Replacement Cost Calculation

The replacement costs are the direct costs induced by maintenance. Replacement cost in this research refer to direct costs belonging to the replacement of a system or component. These costs consist of the six elements as presented in Fig.5.

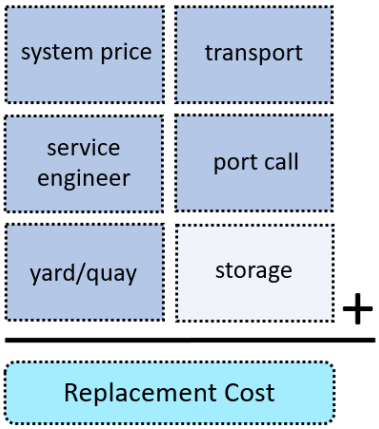

Fig.5: Abstract Representation Replacement Cost Calculation

There is a difference in the replacement cost calculation between the policies. E.g., when applying the corrective maintenance - order on breakdown, there are no spares stored, thus no storage cost.

Opportunistic maintenance is a proactive maintenance policy. Meaning that action is taken before a failure occurs. In the shipping industry a very apparent opportunity presents itself with the compulsory 2.5-year class survey. In this maintenance policy calculation, the yard/quay cost and the port call cost are excluded, as these costs are a result of the class survey and are not evoked by the repair or replacement of this system or component.

Predictive maintenance is also a proactive maintenance policy. Predictive replacement costs do include yard/quay and port call cost, as these costs are a direct result of the repair. However, storage costs are not included as scheduled maintenance provides an excellent opportunity for ordering the systems or components just in time, eliminating the requirement for storage.

2.3.3. Probability Difference Corrective versus Proactive

There is a difference in the probability of a failure occurring, between the corrective and proactive policies. When applying a corrective policy, action is taken after a failure occurs; thus, the probability of failure is 100%.

The calculation of a proactive policy must include the failure probability. Including the failure probability, does not mean simply multiplying the costs with the different probabilities. As, even with a 10% failure probability, there always remains the change of an unforeseen break-down, before the scheduled maintenance.

A small calculation example: With a 10% failure probability, there is a 10% chance of a failure occurring before the scheduled maintenance, and there with a 90% chance that no failure occurs before the scheduled maintenance. So, whenever there is a chance of a failure happening, there is also always the reversed chance of that failure not occurring. More explicit:

10% chance Failure < = > 90% chance No Failure

When maintenance is performed before the failure occurs it is considered proactive, however when a failure happens before the scheduled maintenance, it falls in the corrective maintenance policy. Meaning that, in the 10% calculation example, there is a 90% chance of the calculated cost of the proactive maintenance policy happening, and a 10% chance of the cost of the corrective - order on breakdown maintenance policy happening. Thus, in equation-form this results in the replacement cost per failure probability, being calculated as illustrated in Eq.(3).

$$cost_{probability\ n} = \big((1 - n) * \ cost_{proactive\ policy} \big) + (n * cost_{corrective\ policy}) \quad (3)$$

Where *n* stands for the nine different probabilities. Resulting in the following replacement cost calculation, of a fictive system, for the 10% example:

Corrective Replacement Cost = €3000,-
Proactive Replacement Cost = €1500,-

((1-0.1) * €1500,-) + (0.1 * €3000,-)
(0.9 * €1500,-) + (0.1 * €3000,-)
$Replacement\ Cost_{probability\ 0.1} = €1650,-$

Thus, with Eq.(3) for both opportunistic and predictive maintenance, nine separate replacement costs are calculated. The time-to-failure and therewith the number of replacements of the corrective policy are assumed at the 90% failure rate, as explained. Calculating with this percentage, may lead to a relatively low number of replacements. This assumption is a simplification to obtain a first estimate. This concludes the replacement cost, moving to the off-hire cost calculation.

2.3.4. Off-hire Cost Calculation

Off-hire costs are part of the indirect cost induced by maintenance. Off-hire cost in this research refer to cost induced by the downtime of the vessel. Which means downtime of the system has a direct operational impact on the vessel. Off-hire cost refer to loss of income due to the vessel not being 100% operational, due to the replacement of a system or component. The off-hire costs are based upon downtime [hours] of the vessel times the income/hour [€/hour] times the percentage of the cargo that the vessel cannot transport due to the downtime, as illustrated in Fig.6.

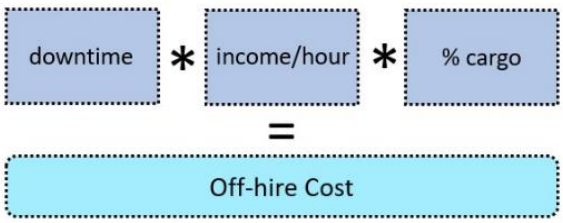

Fig.6: Abstract Representation Off-hire Cost Calculation

Downtime (in hours) is the time the vessel is not fully operational due to the failure.

Income/hour (€/hour) is the income per hour that is lost due to the failure

% cargo, some failures cause a vessel to carry less cargo (e.g. when a cargo cooling compressor fails, the total cooling capacity decreases, thus the tanks of a gas carrier are only allowed to be filled for 85% with ethylene, thus there is a 15% cargo loss, due to this failure)

The off-hire cost calculation is the same for all policies. The difference in outcome between the policies comes from a difference in the length of downtime.

In a corrective policy, downtime is the repair time added to the delivery time of the system or the time the vessel takes to sail to the repair location. In opportunistic maintenance there is only downtime, when the repair time of a system, exceeds the time required for the class survey. As the initial ”downtime” is a result of the class survey and not evoked by the repair or replacement of the system. Thus, in opportunistic maintenance the downtime is determined by a comparison of the time required for the class survey and the repair time only. In predictive maintenance, the downtime equals the repair time. When a repair is known in advance, the system can be ordered in time, eliminating delivery time.

The last aspect of the off-hire calculation is the calculation of the probabilities, as explained in section 2.3.2. For both opportunistic and predictive maintenance policies, nine different off-hire costs are calculated, based on Eq.(3). This concludes the off-hire cost calculation, next, the reputation cost calculation is explained.

2.3.5. Reputation Cost Calculation

Reputation cost in this research refer to the second indirect cost, resulting from the short-term effect of a failure of a system or component. As explained, loss of reputation, loss of hire, loss of a long-term time-charter and even rejection from an oil major are risks of unforeseen maintenance. The difference between long term reputation damage and short-term reputation costs is already explained. As also that only short-term reputation costs are included in the MCM. Short-term reputation costs are the reputation costs directly induced by a failure on that vessel.

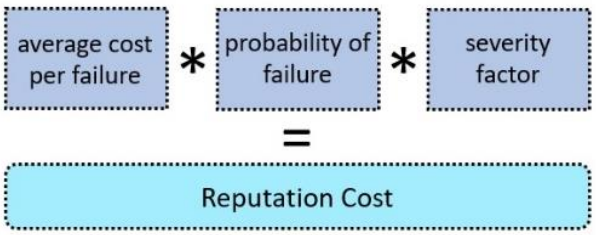

Fig.7: Abstract Representation Reputation Cost Calculation

In the reputation cost calculation, the average cost per failure is multiplied with the probability this failure occurs and a severity factor. Fig.7 shows a representation of the reputation cost calculation.

The probability of a failure has been discussed in section 2.3.1. The average cost per failure is quantified based upon company-specific historic data. The severity factor varies between 0 and 1. It allows for a distinction in the impact of the vetting risk on the reputation cost. The severity factors are company specific and depend on the vetting risk and the type of contract in combination with the type of client.

2.3.6. Total Cost Calculation

Now, the total cost per policy can be determined. The sum of the replacement cost, off-hire cost, and reputation cost per failure results in the total cost per failure, as illustrated in Fig.8.

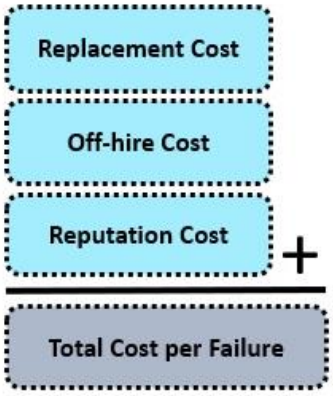

Fig.8: Total Cost per Failure

These total costs per failure have to be multiplied with the amount of failures. The final part of the calculation is determining the amount of failures (and their moment in time) over the remaining lifetime of a vessel.

The calculated MTTF combined with the downtime, results in a meantime-between-failures (MTBF). With the MTBF and the remaining lifetime of the vessel, it is possible to determine how many failures, thus replacements, there will be and when. This is illustrated in Eq.(4). With the amount of replacements determined, the amount of replacement times the total cost per failure, results in the total maintenance cost of that system over the lifetime of the vessel (see Eq.(5)).

$$Number\ of\ Replacement = \frac{Remaining\ Lifetime\ of\ Vessel}{MTBF} \tag{4}$$

$$Total\ Cost = Number\ of\ Replacement * Total\ Cost\ per\ Failure \tag{5}$$

Finally, these total costs are corrected, calculating the current value of future cost. For this calculation the company-specific weighted average cost of capital (WACC) and the inflation rate are utilised. This calculation is presented in Eq.(6).

$$Present\ Value\ Total\ Cost = \frac{Total\ Cost * Inflation\ Rate^{years}}{WACC^{years}} \tag{6}$$

When calculating the total cost of opportunistic and predictive maintenance policies, the complete set of failure probabilities is utilised. A comparison of the cost belonging to the different probabilities performed to find the optimal (lowest cost) maintenance policy. Therewith determining, the optimal coinciding failure rate, and the best time-to-failure. Therewith the MTTF, corrective, opportunistic and predictive maintenance calculations have been completed. The only part that remains is to compare these total costs and determine the optimal policy.

2.3.7. Comparison of Total Cost per Maintenance Policy

The result of the previous calculations is four total cost figures, two for corrective, one for opportunistic and one for preventive. The last part of the MCM is to compare and rank the four calculated total cost figures, from lowest to highest. Lower costs are desirable for any commercial company. This ranking, showing the four policies, as illustrated in Table II, is output of the MCM.

Table II: Maintenance Policies Ranking - Example

Policy	Cost
Opportunistic Maintenance	€ 200.000,-
Predictive Maintenance	€ 400.000,-
Corrective Maintenance – *o.o.b.d.*	€ 600.000,-
Corrective maintenance – *s.1.s.*	€ 800.000,-

Based on the ranking of the four maintenance policies, shipping companies can make a better-substantiated maintenance policy decision per individual system or component, based on the total cost per policy. Concluding with an overview of the entire model, in Fig.9.

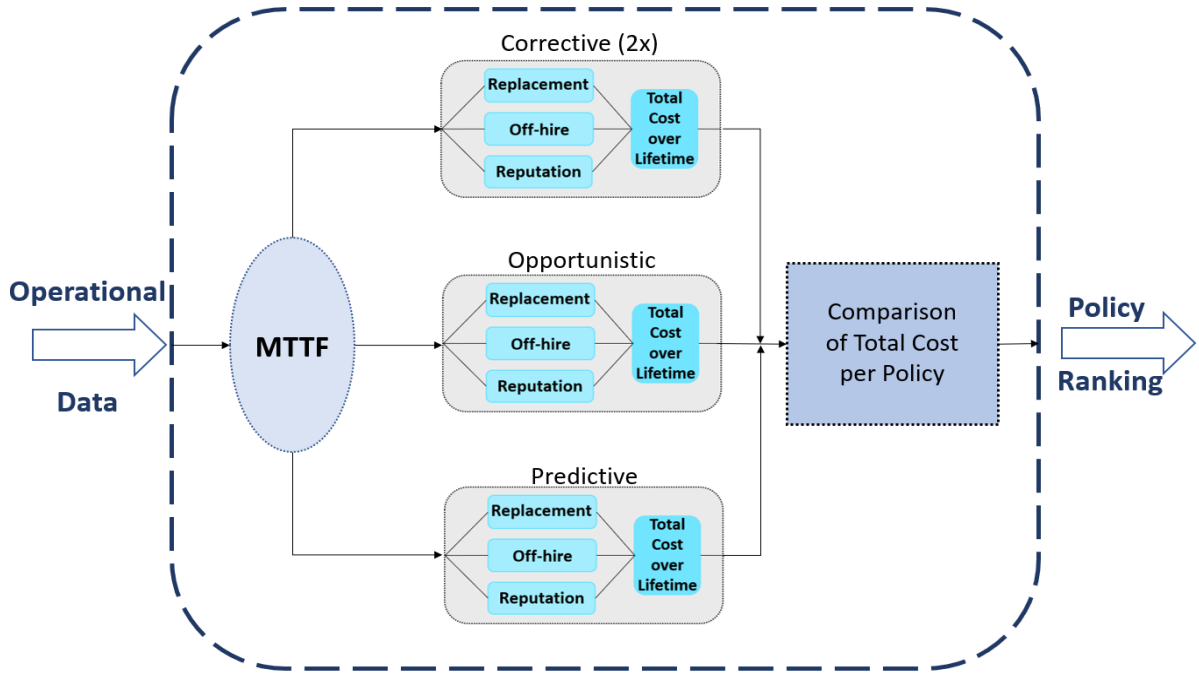

Fig.9: Overview Maintenance Cost Model

3. Case Study: Anthony Veder

3.1. Systems Used for Validation

The MCM is applied to calculate the maintenance cost for systems on board gas tankers of Anthony Veder. In this case study, systems are divided into balanced test-groups, representing systems onboard. The division is made based on system price, operational effect and mechanical or electric, Table III. In collaboration with maintenance experts of Anthony Veder, a system belonging in each group is selected.

Table III: Group Division

Group #	Electric	Mechanical	Effect on Operation	No Effect on Operation	Price < €5000,-	Price > €5000,-
Group 1	•		•		•	
Group 2	•		•			•
Group 3	•			•		•
Group 4	•			•	•	
Group 5		•	•			•
Group 6		•	•		•	
Group 7		•		•	•	
Group 8		•		•		•

3.2. Results Case Study

The failure behaviour is calculated based on the historic data from BASSnet, the vessel PMS Database utilised by Anthony Veder. To allow comparison of the results of the eight groups, all vessel-specific input information is kept the same, only the system specific input is varied between the eight groups. The lifetime of the vessel has been determined at 25 years, the economic lifetime of a gas tanker. The operational area is Europe and the delivery and storage location of the system are set in Rotterdam. All this input can be varied, in next applications of the MCM, however for the comparison in this case study only system specific variations are made.

Table 4 gives the outcome of the application of the MCM is presented and the recommended policy and corresponding financial improvement. This financial improvement is based on comparing the recommended policy with the policy currently applied by Anthony Veder. When the recommended policy is the currently applied policy, there is no cost improvement, shown with n/a.

Table IV: Maintenance Policy Comparison

Group #	Recommended Policy	Cost Improvement %
Group 1	Predictive	1%
Group 2	Proactive	0%
Group 3	Predictive	3%
Group 4	Corrective – o.o.b.d.	n/a
Group 5	Corrective – s.1.s.	70%
Group 6	Predictive	49%
Group 7	Corrective – o.o.b.d.	n/a
Group 8	Corrective – o.o.b.d.	n/a

When evaluating the recommended policies and the improvement percentage. In four groups the recommended policy leads to a cost improvement. The impact per system may vary between 0 and 70%. The average improvement over the 8 groups is, 16%. This is per component on board, so using the MCM to substantiate the maintenance policy for all systems on board, all vessels of a fleet, could lead to a substantial financial benefit. Based on the results of group 5 and 6, it seems that for mechanical systems that influence the operation, cost savings of 60% on average are possible. However, further investigation is required to further validate this claim.

In group 1-3 it can be seen there is (almost) 0% cost improvement. This means that the recommended policy is different from the currently applied policy, but does not lead to cost reduction. Apart from cost reductions there are several other reasons why another policy can be beneficial. For instance, reliability, maintenance frequency or a different level of uncertainties. In this particular case it has been determined that a proactive policy is an improvement compared to the currently applied policy, despite the lack of cost reductions. This illustrates the MCM is not developed to make a decision, only to help substantiate the decision-making process.

4. Discussion of Results

4.1. Novel Approach

This research opens the door for a new way of estimating maintenance cost in shipping. It breaks with the current manner in which the operational costs of a vessel are estimated based on scheduled maintenance jobs, it does not include unforeseen repairs. This novel approach concerns the costs of corrective, opportunistic and predictive maintenance, based on system specific failure data. The model generates a, system specific cost-based ranking of these maintenance policies. The ranking can be used by ship management companies, to obtain a better substantiated system specific maintenance policy.

4.2. Model Usability

The model is suited for all components, systems and engines of a vessel. Depending on the Planned Maintenance System a company uses, the failure behaviour can be calculated real-time. The calculations are based on system-specific and company-specific variables. The company-specific variables can be adjusted once, in first application of the model. Concluding, the developed model is usable for different systems and companies.

4.3. Validity

During the research there were several assumptions and limitations to the developed model. This paragraph will highlight the most critical points of discussion with regards to the assumptions and limitations.

- The MCM is not developed to make a decision, only to help substantiate the decision-making process. It is imperative to critically evaluate the results of the MCM, as there is still a substantial level of uncertainty (depending on the uncertainty of the input values, the error bands). Thus, the policy ranking outcome should not be leading, there is another level of decision-making required, that looks at more than just the numbers.
- The time-to-failure and therewith the number of replacements of the corrective policy are assumed at the 90% failure rate. Calculating with this high percentage, leads to a relatively low number of replacements. As it is likely there are more replacements, it is likely that systems break down earlier. This means the obtained results, especially as the failure probability increases, are optimistic. The (corrective) total costs are optimistically determined, based on a relatively low number of replacements, with a high likelihood of more replacements, thus assuming a best-case scenario.
- The 60% improvement shown in the results of the mechanical equipment emphasizes the validity of the 90% failure probability assumption. A suggestion for further research could be to simulate (e.g. Monte Carlo Simulation) for a certain time-period the values, based upon the reciprocal distribution that has been estimated. When simulating, the observed variation can be better quantified and several scenarios can be tested, and labelled as optimistic and pessimistic. When the simulation is run often enough for several different cases, the boundaries of the different cases can be established.

5. Conclusion

The goal of this research is to present a way to improve the maintenance cost calculation of ship management companies, especially for those with a profit objective. The Maintenance Cost Model is presented and integrates actual operational data from a vessel in the maintenance cost estimation. The operational data from vessels is used to determine the failure behaviour of the systems on board. This failure behaviour is used to calculate the actual failure rate and mean-time-to-failure. Based on this actual data, the replacement-, off-hire, and reputation cost are calculated. Combined resulting in different total cost per maintenance policy per system. The Maintenance Cost Model generates a ranking of the maintenance policies, which can be used by ship management companies, to obtain a better-substantiated system-specific maintenance policy.

This novel approach for the maintenance cost calculation, offers a quick and substantiated total cost per maintenance policy over the lifetime of a vessel. For a ship management company this is important information, that ensures improved true operating costs due to an adapted maintenance approach. The developed model in this research is generally applicable and proves the concept.

Next to these improved operating costs, the successful implementation and application of the MCM also provided valuable novel insights in the general maintenance policy decision-making. Therewith, contributing to the body of knowledge of maintenance decision-making in general.

Recommendations for further research comprise the expansion of the Maintenance Cost Model by means of; increasing the likelihood of replacements, including business cycle predictions, expanding from one vessel to a fleet and including other maintenance policies.

References

AHMAD, R.; KAMRUDDIN, S. (2012), *An overview of time-based and condition-based maintenance in industrial application*, Computers & Industrial Engineering, 63(1), pp.135-149

BARLOW, R.; HUNTER, L. (1960), *Optimum Preventive Maintenance Policies*, Operations Research, 8(1), pp.90-100

BARRENECHE, J.; HERNANDEZ, A.; GARCIA, J. (2015), *Analysis of total cost of ownership (TCO) applied to processes of biomedical technology acquisition competitive intelligence*, Pan American Health Care Exchanges (PAHCE)

BARRINGER, H.; WEBER, D. (1996), *Life-cycle cost tutorial*, 5th Int. Conf. Process Plant Reliability, pp.1-58

BIJWAARD, G.; KNAPP, S. (2009), *Analysis of ship life cycles - the impact of economic cycles and ship inspections*, Marine Policy, 33(1), pp.350-369

BUDAI, G.; HUISMAN, D.; DEKKER, R. (2006), *Scheduling preventive railway maintenance activities*, J. Operational Research Society, 57(1), pp.1035-1044

CALLEWAERT, P.; VERHAGEN, W.; CURRAN, R. (2018), *Integrating maintenance work progress monitoring into aircraft maintenance planning decision support*, Transportation Research Procedia 29, pp.58-69

CEFIC (2011), *Responsible Care Programme and Cefic*, Guidance on good practises for ship vetting

CHANG, Q.; NI, J. (2009), *Maintenance Opportunity Planning System*, J. Manufacturing Science and Engineering 129(1), pp.661-668

CHEN, D.; WANG, X.; ZHAO, J. (2012), *Aircraft Maintenance Decision System Based on Real-time Condition Monitoring*, Procedia Engineering - 2012 Int. Workshop on Information and Electronics Engineering (IWIEE) 29, pp.765-769

COOPER, R.; HALTIWANGER, J. (1993), *The aggregate implications of machine replacement: theory and evidence*. American Economic Review 83(3), pp.360-382

DE JONGE, B.; TEUNTER, R.; TINGA, T. (2017), *The influence of practical factors on the benefits of condition-based maintenance over time-based maintenance*, Reliability Engineering and System Safety 158(1), pp.21-30

DEKKER, R. (1995), *Integrating optimisation, priority setting, planning and combining of maintenance activities*, European J. Operational Research 82(1), pp.225–240

DEKKER, R.; DIJKSTRA, M. (1992), *Opportunity-Based Age Replacement: Exponentially Distributed Times Between Opportunities*, Naval Research Logistics, 39(1), pp.175-190

DEKKER, R.; SCARF, P. (1998), *On the impact of optimisation models in maintenance decision making: the state of the art*, Reliability Engineering and System Safety 60(1), pp.111-119

DEKKER, R.; SMEITINK, E. (1991), *Preventive Maintenance at Opportunities of Restricted Duration*, Research Memorandum 38

DEKKER, R.; VAN RIJN, C. (1996), *PROMPT, A decision support system for opportunity-based preventive maintenance,* Reliability and Maintenance of Complex Systems, NATO ASI Series (Series F: Computer and Systems Sciences) Vol. 154, Springer

DHANISETTY, V.; VERHAGEN, W.; CURRAN, R. (2002), *Optimising maintenance intervals for multiple maintenance policies: a cross-industrial study*, Int. J. Agile Systems and Management 8(3/4), pp.219-242

DHILLON, B. (2002), *Engineering maintenance – A modern approach,* CRC Press

DUFFUAA, S.; RAOUF, J.; CAMPBELL, A. (1999), *Planning and control of maintenance systems: Modeling and analysis*, John Wiley & Sons

ELLRAM, L. (1993), *Total cost of ownership: Elements and implementation*, Int. J. Purchasing and Materials Management 29(4), pp.3-10

ELLRAM, L. (1994), *A taxonomy of total cost of ownership models*, J. Business Logistics 15(1), pp.171-191

ELLRAM, L. (1995), *Total cost of ownership - an analysis approach for purchasing*, Int. J. Physical Distribution & Logistics 25(8), pp.4-22

ELLRAM, L. (1996), *The use of the case study method in logistics research*, J. Business Logistics 17(2), pp.93-138

ELLRAM, L. (1999), *Total Cost of Ownership*, Handbuch Industrielles Beschaffungsmanagement, Gabler Verlag

ELLRAM, L.; SIFERD, S. (1993), *Purchasing: The cornerstone of the total cost of ownership concept*, J. Business Logistics 14(1), pp.163-185

ELLRAM, L.; SIFERD, S. (1998), *Total cost of ownership: a key concept in strategic cost management decisions,* J. 19(1), pp.55-84

FABRYCKY, W.; BLANCHARD, B. (1991), *Life Cycle Cost and Economic Analysis*, Prentice Hall

FABRYCKY, W. (1987), *Designing for the life cycle*, Mechanical Engineering, (January), pp.72-74

FERNANDEZ, P. (2010), *Wacc: Definition, misconceptions, and errors*, Business Valuation Review 29(4), pp.138-144

FERRIN, B.; PLANK, R. (2002), *Total cost of ownership models: An exploratory study*, J. Supply Chain Management 38(3), pp.18-29

GRALL, A.; BERENGUER, C.; DIEULLE, A. (2002), *A condition-based maintenance policy for stochastically deteriorating systems*, Reliability Engineering and System Safety 76(1), pp.167-180

HANDLARSKI, J. (1980), *Mathematical Analysis of Preventive Maintenance Schemes*, J. Operational Research Society 31(3), pp.227-237

HANSON, J. (2011), *Differential method for TCO modelling: An analysis and tutorial*, Int. J. Procurement Management, 4(6), pp.627-641

HASSANAIN, M.; FROESE, T.; VANIER, D. (2003), *Framework model for asset maintenance management*. Journal of performance of constructed facilities 17(1), pp.51-64

HEIJBOER, P. (2019), *Expert Interview*, Vetting Team Leader, Anthony Veder Rederijzaken BV

HULL, S. (2007), *Lessons from LNG Trading - Challenges in the evolution of an LNG spot market*, "Exploration & Production Technology Group", BP

JACKSON, D.; OSTROM, L. (1980), *Life cycle costing in industrial purchasing*, J. Purchasing and Materials Management 16(1), pp.8-12

KHATAB, A.; AIT-KADI, D.; REZG, N. (2012), *A condition-based maintenance model for availability optimization for stochastic degrading systems*, 9th Int. Conf. Modeling, Optimization & SIMulation, Bordeaux

KNAPP, S.; FRANSES, P. (2006), *Analysis of the Maritime Inspections Regimes - Are ships over-inspected?*, Economic Institute Report 30(1), pp.1-39

KOORNNEEF, H.; VERHAGEN, W.; CURRAN, R. (2017), *Contextualising aircraft maintenance documentation*, Int. J. Agile Systems and Management 10(2), pp.160-179

MATHUR, R. (2018), *Best practice guide for vessel operators*, https://www.slc.ca.gov/wp-content/uploads/2018/08/PF2008-PrevPartnering-Responsible.pdf

NICOLAI, R.; DEKKER, R. (2008), *Optimal Maintenance of Multi-component Systems: A Review*, Complex System Maintenance Handbook, Springer

NUNEZ, A.; HENDRIKS, J.; LI, Z.; DE SCHUTTER, B.; DOLLEVOET, R. (2014), *Facilitating Maintenance Decisions on the Dutch Railways Using Big Data: The ABA Case Study*, 2014 IEEE Int. Conf. Big Data, pp.48–53

PARRA, C.; CRESPO, A. (2012), *Stochastic model of reliability for use in the evaluation of the economic impact of a failure using life cycle cost analysis- case studies on the rail freight and oil*, J. Risk & Reliability 226(4), pp.392–405

RODA, I.; GARETTI, M. (2015), *Application of a performance-driven total cost of ownership (tco) evaluation model for physical asset management*, 9th WCEAM Research Papers, pp.11-23

SHIELDS, M.; YOUNG, S. (1991), *Managing product life cycle costs: an organizational model*, J. Cost Management, pp.16-30

SILVA, A.; FERNANDES, A. (2006), *Integrating life cycle costing analysis into the decision making process in new product development*, Int. Design Conf., pp.1419-1425

OREDA, (2015), *SINTEF Technology and Society Department of Safety Research and NTNU*, OREDA - Offshore and Onshore Reliability Data Handbook, OREDA Participants - DNV GL

SU, Z.; NUNEZ, A.; JAMSHIDI, A.; BALDI, S.; LI, Z.; DOLLEVOET, R.; DE SCHUTTER, B. (2015), *Model predictive control for maintenance operations planning of railway infrastructures. in Computational Logistics*, 6th Int. Conf. Computational Logistics (ICCL'15), Delft, pp.673-668

TINGA, T. (2010), *Application of physical failure models to enable usage and load based maintenance*, Reliability Engineering and System Safety 95(1), pp.1061-1075

TINGA, T. (2013), *Principles of Loads and Failure Mechanisms: Applications in Maintenance, Reliability and Design,* Springer Series in Reliability Engineering

VAN IJSERLOO, G. (2020), *personal communication*, February

VELDMAN, J.; WORTMANN, H.; KLINGENBERG, W. (2011), *Typology of condition based maintenance,* J. Quality in Maintenance Engineering 17(2), pp.183-202

VERHAGEN, W.; CURRAN, R. (2013), *An Ontology-based Approach for Aircraft Maintenance Task Support*, 20th ISPE Int. Conf. Concurrent Engineering, pp.494-506

VERHAGEN, W.; DE BOER, L. (2018), *Predictive maintenance for aircraft components using proportional hazard models,* J. Industrial Information Integration 12(1), pp.23-30

VERHAGEN, W.; DE BOER, L.; CURRAN, R. (2017), *Component-based data-driven predictive maintenance to reduce unscheduled maintenance events*, 24th ISPE Inc. Int. Conf. Transdisciplinary Engineering 5(1), pp.3-10

VU, H.; DO, P.; BARROS, A.; BERENGUER, C. (2014), *Maintenance grouping strategy for multi-component systems with dynamic contexts*, Reliability Eng. and System Safety 132(1), pp.233-249

WANG, W. (2000), *A model to determine the optimal critical level and the monitoring intervals in condition-based maintenance,* Int. J. Production Research 38(6), pp.425-1436

WOLTERS, N. (2015), *Controlling contract cost: Introducing total cost of usage to support the management accounting system,* Master thesis, University of Twente

ZAAL, T. (2011), *Profit-driven Maintenance for Physical Assets*, Maj Engineering Publ.

ZHANG, X.; ZENG, J. (2015), *A general modeling method for opportunistic maintenance modeling of multi-unit systems*, Reliability Engineering and System Safety 140(1), pp.176–190,

ZORGDRAGER, M.; CURRAN, R.; VERHAGEN, W.; BOESTEN, B.; WATER, C. (2013), *A Predictive Method for the Estimation of Material Demand for Aircraft Non-Routine Maintenance*. 20th ISPE Int. Conf. Concurrent Engineering, pp.507-516

Improved Prediction of the Energy Demand of Fuel Cell Driven Expedition Cruise Ships

Clemens Boertz, Delft University of Technology, Delft/The Netherlands,
clemens.boertz@outlook.com
Robert Hekkenberg, Delft University of Technology, Delft/The Netherlands,
r.g.hekkenberg@tudelft.nl
Richard van der Kolk, Damen Shipyards Group, Rotterdam/The Netherlands,
Richard.van.der.Kolk@damen.com mailto:email@address.com

Abstract

Fuel cell systems require a better early-stage prediction of the energy consumption of a ship because they are more expensive, more voluminous and less able to deal with rapid load changes than conventional diesel-powered systems. This paper discusses a model for such an improved prediction of the total energy demand of an expedition cruise vessel. The focus is on identifying the peak loads and load changes under consideration of the passenger behaviour, environmental and operational conditions. The used bottom-up approach builds up a parametric model for the early design stages with limited required input data by using typical operational conditions for this type of vessel. The paper concludes that the method provides more insights into the dynamic power and substantially lower predicted energy use.

1. Introduction

The shipping industry contributes significantly to the global greenhouse gas emissions due to the use of cheap fossil fuels. As a response to the Paris Agreement on climate change, the IMO Marine Environment Protection Committee (MEPC) defined the strategy on the reduction of emitted greenhouse gases and emission of carbon dioxide from ships in April 2018. Following this, the carbon dioxide (CO_2) emission per transport work should be reduced across international shipping by at least 40% on average by 2030 with further efforts towards 70% in 2050 in comparison to 2008. The greenhouse gas emissions should peak soon, together with a reduction by at least 50% in 2050 compared to 2018, as stated in the resolution of the MEPC, *IMO (2018)*.

Meanwhile, the cruise ship industry is forced to reduce the carbon footprint to be able to access remote areas with higher restrictions and as part of their marketing strategy towards more sustainability. The majority of ships under construction, including smaller expedition vessels, still use the combination of conventional fuels and scrubbers or SCR systems in order to eliminate harmful exhaust gases. Alternatively, the additional use of batteries can let the engines constantly run at their optimal condition by providing additional electric power in peak loads, as applied in the latest Hurtigruten expedition cruise vessels, *Silk Bidco AS (2017)*.

Research projects by universities, shipyards and other stakeholders address the use of fuel cells with the purpose of eliminating all greenhouse gases, while reducing the high development costs, *Van Biert et al. (2016)*. The storage of pure liquid hydrogen, at a temperature of -253°C is an important challenge to overcome. Other fuels have to be reformed or pressurized. In general, the volumetric and gravimetric energy densities are lower than those of conventional fuels, which results in larger tanks on board when keeping the same operating range and speed. Next to the physical implementation, fuel cells have additional operational limiting factors, which have to be matched with the power demand. Compared to conventional combustion engines, longer start-up times can be expected as well as a lower dynamic response ability. This conflicts with the dynamic power demand of cruise ships in various operational condition, *Baldi (2018)*. Furthermore, fuel cell systems and the associated fuel storage are significantly more expensive than conventional diesel-based solutions. Therefore, a detailed analysis of the ship's energy use is required, to keep the size and cost of the fuel cell system as low as possible and to prevent undesirable mismatches between the dynamics of energy supply and demand.

Typically, in the conceptual design phase at a shipyard the energy demand is estimated for all electric power consumers with the load balance approach. All systems are designed for the maximum operational power demand. The actual power demand is calculated based on the absorbed power from the net and additional predefined factors for several different operational conditions. The ‘number in service’ describes the number of running components in the defined operational condition. In addition, the load factor is defined as relative load of the maximum electric power of the component to be absorbed in the actual situation. The third factor, the simultaneity factor, varies between 0 and 1 as well, and describes the mean operational time of the component. Thus, a factor lower than one considers not continuously operating consumers. The last two factors are often combined as utilization factor. The product results in the actual absorbed power per component, which can be summed up to obtain the total power for the given operational condition, as shown in the simplified load balance sheet in Table I, *Klein Woud and Stapersma (2015)*.

In general, specific conditions like harbor mode and sailing mode at maximum and design speed are predicted, but without any dynamically changing situations. This method provides a relatively crude overview of the power and energy demand of a ship and lacks details about their dynamics. For the early design stage of classic diesel-powered ships, this is acceptable but as discussed before, it is not for a fuel cell-based solution, especially in hybrid configurations.

Table I: Simplified format of load balance sheet

Consumer name	Absorbed electric power	In port				At Sea				…
	[kW]	Number in service	Load factor	Sim. factor	Average absorbed power	Number in service	Load factor	Sim. factor	Average absorbed power	…
Component 1										…
…										…
Total	∑				∑				∑	

Previous studies distinguish between the different operational modes and the consequences for the propulsion load while keeping the energy demand of the hotel systems constant, e.g. *Simonsen (2018)*. For hotel systems for cruise ships, usually part of auxiliary systems, this approach is not defendable due to the high contribution to the total power demand. The focus is mostly on improving the energy efficiency by assessing sea monitoring data in a top-down approach in order to lower the fuel consumption, *Howitt (2010)*. Even if *Simonsen et al. (2018)* state that the "bottom-up" approach is more complex, such a systematic approach is necessary to study the dynamic energy behavior of every system. Thus, the operational behavior has to be considered more detailed already in the predictions within the first design phase, *Guangrong (2017)*.

As a consequence, the required power and energy demand of the different systems on board must be further examined under varying operational conditions over time. Considering the starting and transient load response time, the understanding of the load changes is just as important as the total power demand at a certain condition, as normally investigated statically in the load balance approach.

This paper presents a detailed breakdown of the different electrical consumers and subsystems, grouped in propulsion, auxiliary systems and hotel systems. On the basis of predefined typical days of operations (TDO), the operational conditions and passenger behavior are described. The impact of the different environmental conditions is assessed by applying weather profiles for hot, cold and medium conditions. The resulting power prediction for every system focuses on the individual load behavior. The combined energy demand of the typical operational days finally leads to the total energy demand of the entire

operational profile. Driving factors of the actual load and additional peak loads can be assessed. The results of the power and energy analysis are finally related to the fuel cell characteristics by identifying more favorable systems to be powered by a reliable fuel cell system.

2. Dynamic Prediction Model

First of all, the varying operational conditions have to be defined. Based on these influencing factors, the dynamic power demand is predicted for the different systems, as identified and grouped in the system breakdown. The varying load is the basis for the following energy prediction of the expedition cruise vessel.

2.1. Operational Conditions

Before predicting the power demand, the operational profile, passenger behavior and environmental conditions over the day have to be defined in the first step. They are also referred to as the three main influencing factors of the load behavior. Although users of the method can define their own settings for these aspects, thus making it suitable for their specific application, the cases as described below are used in a case study to demonstrate the way the approach works.

Cruise ships usually have a very diverse operational profile including a long time spent in part load condition. In contrast to cargo vessels, they do not follow a repetitive daily or weekly schedule. Sailing the whole day might be followed by a harbor day in order to offer land excursions. Alternatively, the ships might also travel at low speeds in scenic areas.

In order to define the operational profile, an activity-based approach is applied to obtain typical speed profiles of expedition cruise vessels. The voyage timeline of several reference vessels could be analyzed, where the actual position and corresponding speed is logged over time by using the Automatic Identification System (AIS). In order to model now the power demand for varying conditions, the obtained speed profile is transferred into five typical days of operations (TDO), similar to the used simplification method in the systematic procedure by *Fazlollahi at al. (2014)*. It considers maneuvering, being moored in a harbor or at anchor and sailing at low, medium, design and high speed, as defined in Table II. The energy demand over a week or the whole year can be estimated in a later step by adding up different days similar to the planned schedule or typical speed profile as obtained by the available AIS data as shown in the table as well.

The first defined typical day represents a port day. In the second day the ship would constantly sail at design speed. The remaining three days describe the mixed operational conditions, considering the varying speed profile and a port call during the day.

Table II: Proportion of operations in certain speed ranges as obtained out of AIS data and defined five typical days of operation (TDO)

Speed Range	Defined range (% max speed)	Typical profile (based on AIS)	TDO1	TDO2	TDO3	TDO4	TDO5
Port/Anchor & Maneuvering	<1kn	42%	24h	0h	12h	17.5h	0h
Low Speed	1kn-40%	8%	0h	0h	2h	1.5h	12.5h
Medium Speed	40-70%	27%	0h	0h	6.5h	2h	10.5h
Design Speed	70-85%	25%	0h	24h	3.5h	3h	0h
High Speed	85-100%	4%	0h	0h	0h	0h	1h

The occupancy of a certain area influences the power demand in terms of used facilities and electrical components at a certain time. Thus, the passenger and crew behavior are defined in order to consider this in the predictions later on. The definition is in accordance with the TDOs described above. All spaces are grouped into the main types of areas, like passenger cabins, restaurants, outdoor areas, leisure

and public spaces. Additional areas for the crew are defined by the laundry, galleys, crew public spaces and cabins. The occupancy rate of these spaces is formulated as the ratio between actual number of people per zone divided by the maximum number of people on board. For example, the rate of 50% in the cabins would mean, that half of the passengers are allocated in the cabins in the actual time. Every type of area is related to an occupancy rate per specific time step. Fig.1 shows the distribution of passengers exemplary for the third TDO including a port call (8am-8pm).

The distribution per time step of passenger and crew is based on logical assumptions for typical passenger movements and crew working hours. For example, in the night, most of the passengers are sleeping in the cabins. The main mealtimes are in the morning and in the evening. Lastly, while moored in port, most of the passengers are not on board due to excursions or other individual trips.

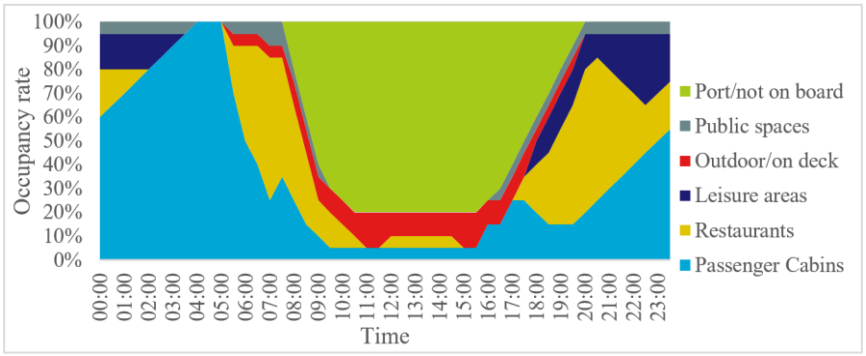

Fig.1: Defined occupancy rate for passengers; TDO3 incl. port call 8am-8pm

Instead of considering only different seasons, varying weather profiles are applied to demonstrate the impact of the environmental conditions on the power demand behavior. The extreme conditions in winter (throughout the day constant at -20°C) and summer (+35°C) are defined by ISO regulations, *ISO (2002)*, as commonly used as design parameter for the HVAC system. For these warm and cold conditions, an example weather profile is considered for Singapore (25-31°C) and Resolute Bay (-16--21°C). The profile of Amsterdam is the third condition as medium weather condition (Amsterdam summer profile used, with varying temperature 17-28°C). In addition, the corresponding hours of sunlight are defined next to a different sea water temperature per location.

2.2. System Breakdown

Before the energy consumption can be predicted, the whole system cruise ship has to be subdivided into the main electrical consumers and subsystems. First of all, the three main groups of systems can be defined. The propulsion systems are the systems which are directly related to the generated thrust to propel the ship. The auxiliary systems are all non-propulsion systems which assist and ensure normal operations. This involves for example the survival systems, including any hazard prevention, detection and fighting systems, like bilge or firefighting system.

Finally, the hotel systems are kept separate from the auxiliary systems due to their high power demand on cruise ships. These systems are more related to the passenger comfort and specific hotel facilities on board. In order to model the different operating subsystems, further grouping of the electrical components is applied resulting in the division as shown in Fig.2.

The subdivision is made on the basis of the belief that if a specific system or component contributes a higher proportion to the overall power demand, temporarily or constantly over time, then it should be modelled with a higher degree of detail, Fig.3. For example, the bow thrusters need a significant amount of electric power while maneuvering. Thus, a more detailed investigation can point out the temporarily high loads.

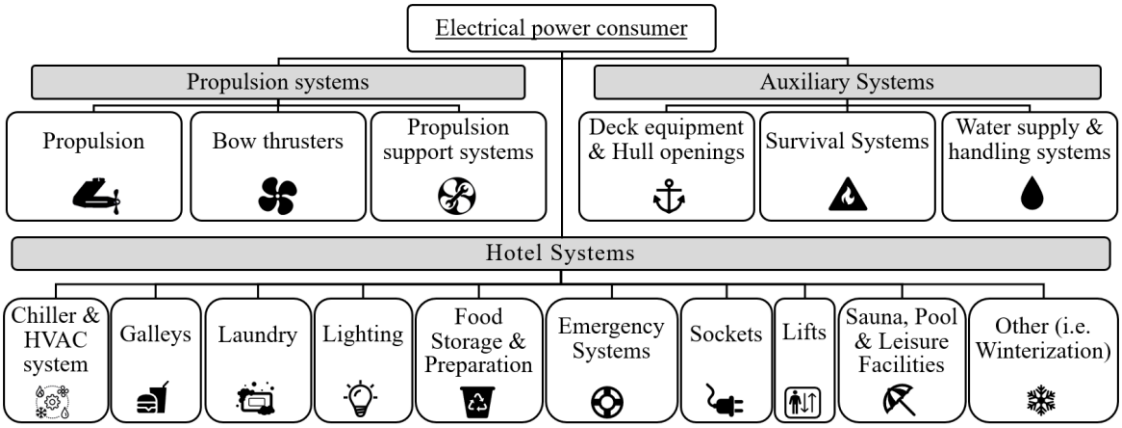

Fig.2: System breakdown of electrical components and systems

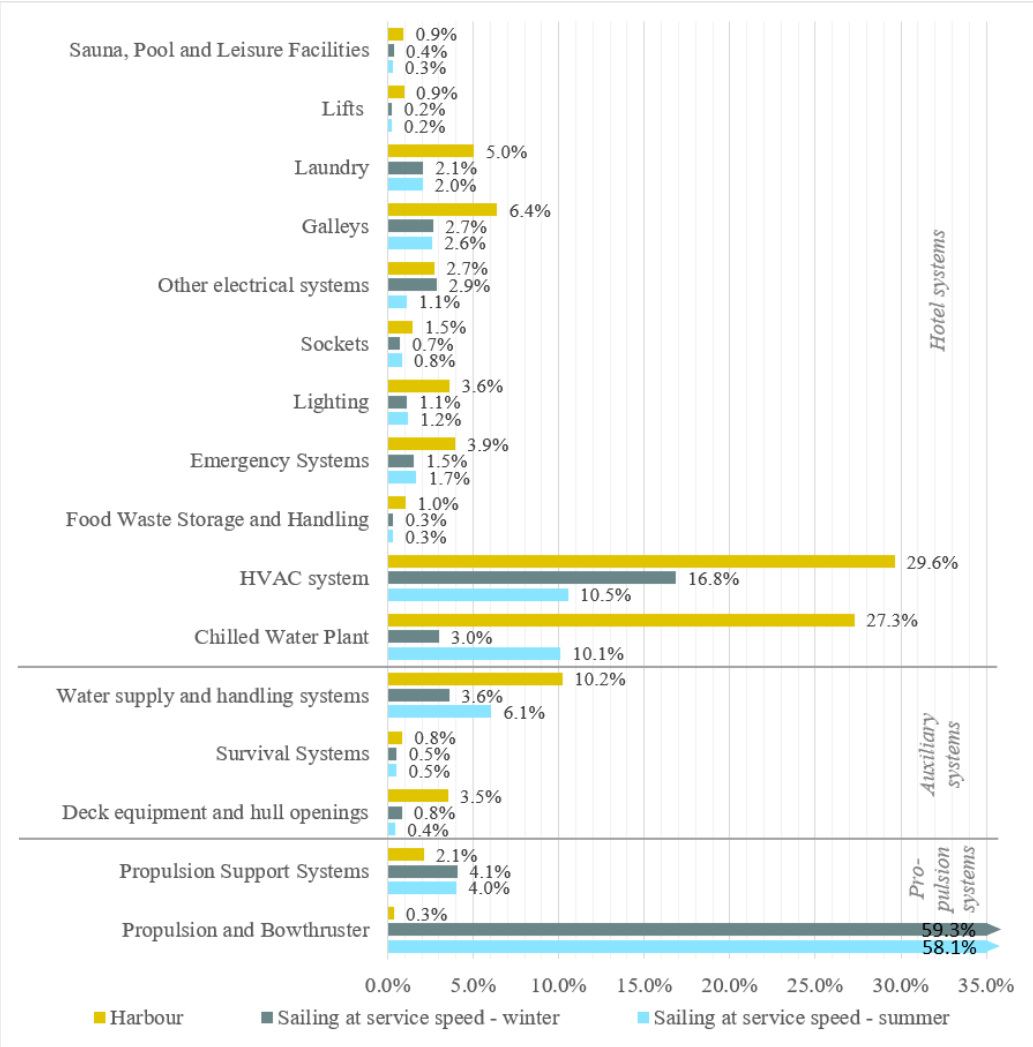

Fig.3: Grouped systems and its proportion of overall power in chosen operational conditions in load balance approach for used reference vessel

Furthermore, some components or systems can be modelled together if they are highly dependent on each other. For example, the HVAC system is modelled together with the chilled water plant even if both systems consume a significant amount of energy. The cooling demand by the HVAC system is directly supplied by the chilled water plant (compare contrary power contribution of HVAC system and chillers in summer and winter in Fig.3). Thus, the systems are directly related and are modelled together under varying conditions.

The third consideration of grouping the components is to take the operating conditions into account. If systems are operating in different conditions, then they should be modelled separately, even if the overall power contribution is low. For example, the emergency systems are only running on stand-by mode in normal operation, while having the higher load in emergency situations.

2.3. Power prediction

In order to estimate the energy consumption, the power demand has to be understood under the operational conditions. This is done by using separate prediction models for the defined groups of systems and electrical components. The focus is on identifying the maximum power demand to assess the power plant (or fuel cell) size. Additional power fluctuations can be analyzed as well, which are critical for fuel cell systems. If an additional peak load cannot be considered within the used time step size of 30 minutes, then it is listed as immediate peak load manually. The prediction models are briefly described and are included more detailed in the master thesis report 'Energy demand of a fuel cell driven cruise ship'.

The power that is required by the main propulsion system is predicted based on the empirical method of Holtrop and Mennen, *Holtrop and Mennen (1982)*. The main dimensions and gross tonnage are used for the vessel as input data, next to defined form factors for a conventional cruise ship hull. The same holds true for using typical efficiencies to obtain the required brake power at design speed. The propeller law can now be used to predict the required propulsion power for speeds unequal to the design speed. The bow thruster is predicted under consideration of the crabbing criteria and the expected side forces. In general, the passenger behavior and weather condition are not considered in the propulsion power predictions.

The power demand of the auxiliary systems is independent of the speed of the ship and only impacted gradually by changing the operational mode (i.e. port to sailing mode). The number of passengers does play a role in predicting the actual load (mainly water supply system), whereas the daily behavior on board is less influencing this group of systems. Lastly, a different sea water temperature per season affects the heating demand within the water supply system, while the varying ambient air temperature does not influence the load behavior of the auxiliary systems.

Except for the water supply system, the auxiliary power demand is widely constant per operational condition. Thus, next to the predicted installed power, constant utilization factors are applied per operational conditions (sailing or port) as well as for the different seasons (summer or winter). The water systems consider the varying demand of potable water and cooling water for the HVAC and propulsion systems.

Lastly, the hotel systems are discussed. The individual configuration of systems and components depends on the owner requirements. However, within the scope of an expedition cruise ship, the limited number of outfitting, leisure and entertainment facilities can be grouped to enable a rough prediction of the electric energy demand in the first design stage.

The HVAC system is one of the most dynamic energy systems on board of a cruise ship. Separate estimations are performed for every area on board. The passenger cabins are supplied by local fan coil units (FCU) and the public and crew areas by centralized air conditioning units (AHU). They include the electrical components of fans, cooler, heater and humidifier. The automated prediction considers the passenger behavior, as defined for the typical operational days, and the different weather profiles for the ambient air in order to get a power demand different for every time step.

The galleys and laundries are related to typical working schedules to consider the varying load. Lighting is reduced in unoccupied areas and cabins and results in varying load depending on the passenger behavior. Minor systems can be linked to a utilization factor for full operation in sailing condition and lower load in port condition due to less people on board.

2.4. Energy prediction

The time-dependent load behavior during the different operational days is the basis for the daily energy demand per typical operational day. It is the basis for sizing the fuel tanks. The required energy per day is calculated directly from a time-domain integration of the power prediction. The demand for a whole operational profile is obtained by adding different typical operational days. For example, the commonly used three-week transit condition is described by using the second operational day, constantly sailing at design speed. Alternatively, a typical coastal profile can be assembled with the different defined days in mixed operational modes considering a varying speed profile of the vessel.

3. Results

The prediction of the power demand is the basis for sizing the fuel cell on board. Using an estimation under dynamic operational conditions provides insight in the demand of the whole cruise vessel after calculating the load of the individual systems. As a potential design point for the different power plant components, it is important to differentiate between the maximum power load and the base load. The base load describes the minimum amount of power needed over the day and is significantly lower than the maximum load, which occurs only temporarily.

Conventional predictions in the design process, like the load balance approach, focus on the maximum loads to size the main engines.

In order to implement fuel cells, most likely within hybrid configurations, the dynamic power prediction identifies the base load and additional power fluctuations up to the temporary maximum load. This provides more well-founded decisions, how to match the operational points of the different power plant components with the individual load more efficiently.

The highest power is required by the main propulsion in sailing mode, Fig.4 (left). However, expedition cruise ships often operate at lower speeds below the design conditions (see obtained speed profile in Table II), which results in a considerably lower demand most of the time, Fig.4 (right). The highest load changes result from adjusting the speed. In addition, high peak loads are shown in maneuvering condition, Fig.4 (right), e.g. before mooring. The operating bow and azimuth thrusters need high electric power within a short period of time.

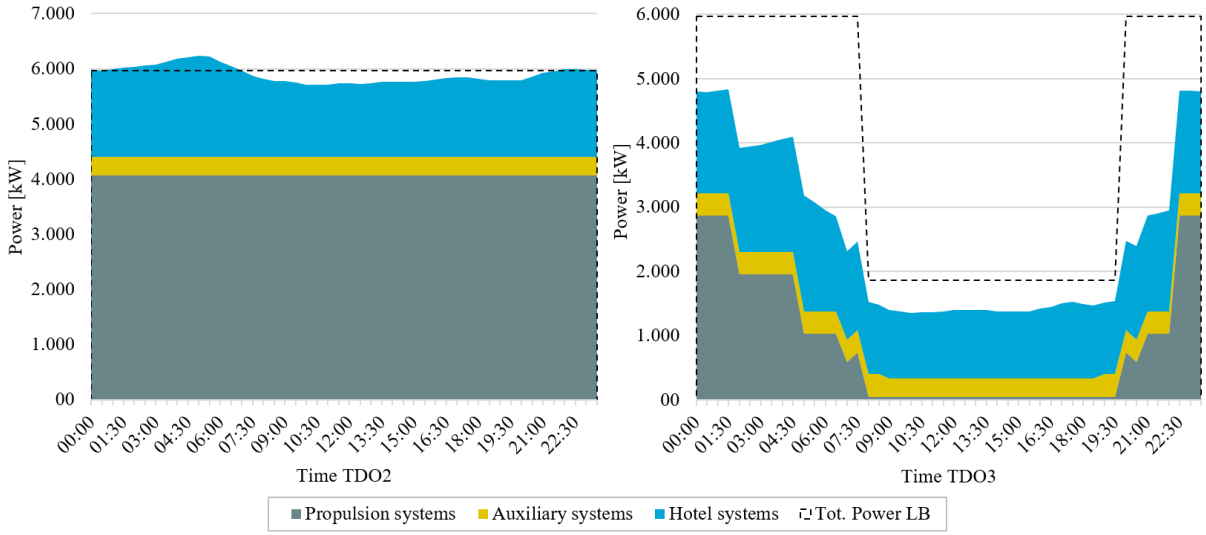

Fig.4: Electric demand of propulsion, auxiliary and hotel systems in winter season, for sailing day constantly at design speed (TDO2) and day including port call, 8am-8pm (TDO3)

In contrast, the power demand of the auxiliary systems is relatively constant close to its maximum load in sailing condition. Only gradual load changes occur by changing the operational mode for example

from sailing to port condition. The maximum load of the hotel systems always appears in the morning, when all passengers are on board and several components ramp up from the lower night mode. In general, the power demand is higher in summer, followed by winter condition. This is due to high heat loads or cooling resulting in a higher electrical load within the HVAC system and chilled water plant. The medium weather condition results in the lowest hotel power demand since no extreme cooling or heating is required. Galleys demand the highest amount of electrical energy in their working hours during the day in mealtimes, while the laundry is often running during the night. The remaining and smaller systems are negligibly impacted by the environmental conditions.

Fig.5 shows the power fluctuations for the hotel systems for the used reference vessel. The power fluctuations are mainly influenced by the passenger behavior. Disembarking in port (see right graph in Fig.5, e.g. arriving in port in the morning) causes the highest changes due to a lower actual utilization in port condition, of several systems that normally ensure the high passenger comfort. Thus, they can run on lower design conditions. For example, the galley provides fewer meals and the running HVAC system can be reduced in unoccupied areas.

Fig.5 shows also the predicted power for the hotel systems out of the load balance approach. The demand has its constant value for sailing and port condition and differs significantly from the dynamic approach. The maximum demand is reached only temporarily, while most of the time the load is lower. As a consequence, the static approach in the load balance analysis results in an overprediction of the electric power demand of the hotel systems under consideration of the passenger behavior and environmental conditions.

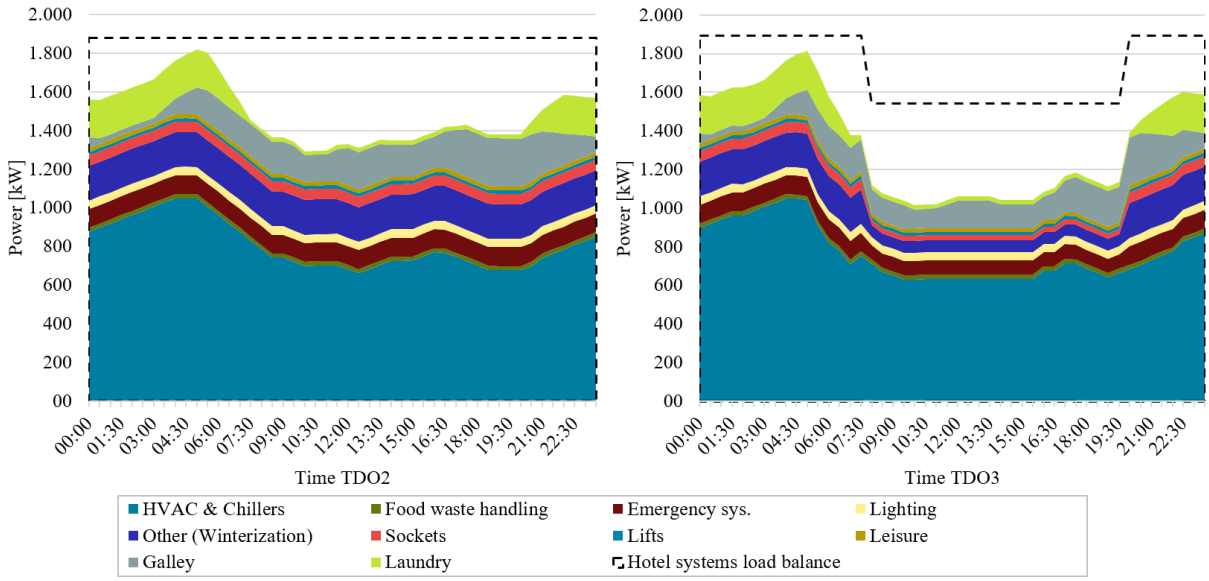

Fig.5: Electric demand of hotel systems in winter season, for sailing day constantly at design speed (TDO2) and day including port call, 8am-8pm (TDO3)

Comparing the total power demand shows that the load changes caused by the hotel systems gets smaller in relation to the changes within the propulsion system as soon as the speed varies, Fig.4 (right), in mixed operational conditions. In port condition, the auxiliary load, including the hotel systems, remains and describes the baseload throughout the day, Fig.4 (right), during the day. Furthermore, comparing the varying load with the load balance approach, the dynamic prediction clearly shows the usually oversized power plant components. In typical costal operations with a varying speed profile, the average load is mostly lower than 50% of the predicted load at design speed (compare sailing day at design speed, TDO2, with mixed operational condition in coastal profile, TDO3, in Fig.4).

The energy demand of the different operational days is predicted for the different considered seasons. Due to the widely constant power demand of the auxiliary systems, the daily energy demand does not vary significantly as well. Different seasons have an impact on the hotel systems due to a different

heating or cooling demand of the HVAC system. However, the driving factor for the overall load is the varying speed, which impacts the propulsion system and lowers the energy demand significantly compared to the demand predicted using the load balance approach. The power fluctuations within the hotel and auxiliary systems, as discussed earlier, have a lower impact on the energy demand. They are averaged out due to partly higher and partly lower loads during the day.

The defined operational days are now used to predict the energy demand of a typically used transit profile and an alternative coastal profile of the same endurance of 3 weeks under dynamic operational conditions. An example 21-day cruise is used as case study based on a planned trip by a cruise line. The total energy demand prediction is reduced by around 40% for the reference vessel, mainly driven by the speed reduction and lowering the corresponding propulsion energy by 60%. The energy demand of the auxiliary and hotel systems is only reduced by around 10% in the coastal profile.

Generally, the dynamic prediction clearly shows the potential to better estimate the required power and energy, if varying operational conditions are considered. Optional fuel cells could be designed more efficiently for specific part loads, like the auxiliary and hotel systems. The varying load with its expected gradual load changes can be quantified and covered by fuel cells, rather than the propulsion systems. Conventional combustion engines or balance of plant components, like batteries, can be designed and optimized for the remaining systems with their high loads and temporarily high power fluctuations. A multi-criteria decision analysis on the power supply side can build up on the required energy and power demand of a certain part load to design a hybrid concept. Especially the impact on weight, volume and costs has to be considered. The required fuel cell size can be quantified based on the estimated maximal load and the fuel tanks by considering the predicted energy demand of the specific group of systems or operations.

4. Conclusion

The electrical consumers could be grouped to analyze the individual power demand behavior in varying operational conditions, under consideration of the dependencies and operating time windows. The situations are modelled in five typical days of operations, which present all usual operational modes of an expedition cruise ship.

The following dynamic prediction shows the varying power demand of the individual systems under varying operational conditions, while the total energy demand is still mainly driven by the variation of speed. Looking only into the auxiliary systems including the hotel functions, the fluctuating load is influenced by the passenger behavior and the operating mode, like port or sailing condition. The different weather season impacts the level of the actual electric load, while the daily varying temperature has a lower influence.

The method supports a well-founded decision on the power supply configuration, if it comes to hybrid systems including different power supply components and their operational characteristics. The individual load of systems can be quantified including expectable power fluctuations, which limits the serviceability of fuel cells for certain loads. In addition, the corresponding fuel tanks can be sized for an energy demand of certain systems and operating time windows considering different operational profiles such as ocean-crossing or coastal operations in more sensitive areas.

The commonly used approaches with its static utilization factors for specific operational modes lead to an overprediction of the power plant components. This gets intensified for fuel cells considering lower volumetric and gravimetric energy densities in relation to conventional diesel-based solutions. The maximum condition is only reached temporarily. Especially cruise vessels are mostly running in part load conditions, for which a hybrid system can be optimized by using the proposed dynamic prediction method.

4.1. Recommendations for further research

Simplifications are made within the power prediction, which leads to further room of improvements. Predefined design parameters (e.g. air changes within HVAC system) simplified the load prediction based on common configurations for an expedition cruise ship. However, further investigations into demand-controlled systems (e.g. using sensors) could further lower the energy demand. The dynamic prediction could be also used to assess energy saving strategies (e.g. varying air recirculation rate in HVAC system). The total power demand could be lowered and load changes further reduced.

In addition, the study focused on the electrical demand of a cruise ship as a basis for a sufficient power supply. Fuel cells could replace the commonly used diesel-powered systems. At this point, it is important to consider further thermomechanical consequences as well. The heat in the exhaust, produced by the combustion process, is normally used by the exhaust gas boiler, heating up water directly or any other heat recovery system. The required heat in the other systems has to be balanced by fuel cells or potentially additional electric heaters or boilers.

Lower exhaust temperatures are expected for some fuel cell types, while additional heat could be taken out of the produced water after the chemical process in the stacks. On the other hand, the liquefied chilled fuels in the tanks (e.g. hydrogen and LNG) have to be preheated as well, before bringing them into the fuel cell membrane. This requires additional heat in relation to the commonly used MGO in liquid phase in ambient condition. Meanwhile, the fuel cell modules require less cooling while operating. The reduction of cooling water and additional ventilation can further be optimized.

Overall, a thermal load balance under dynamic condition should be performed as well to prove the heat balance on board. Alternatively, additional heat has to be produced, for example electrically impacting the electric power prediction.

After having studied the power demand side, the supply side has to be designed under varying conditions as well. As briefly mentioned earlier, different options are available for a hybrid configuration. Next to the conventional combustion engines, batteries are already in use in the maritime industry to balance immediate peak loads on smaller ferries. A reliable power plant can be optimized in terms of different parameters like volume, weight or costs. The different power sources have to be considered with their different advantages. For example, batteries are comparably heavy and expensive, which limits the application. Next to the initial investment costs, the expected operational costs over its lifetime have to be considered as well. Thus, the right combination has to be analyzed for the specific ship in a multiple-criteria decision analysis supported by the proposed dynamic prediction method of the energy demand.

References

BALDI, F.; AHLGREN, F.; VAN NGUYEN, T.; THERN, M.; ANDERSSON, K. (2018), *Energy and exergy analysis of a cruise ship*, Energies 11(10)

FAZLOLLAHI, S.; BUNGENER, S.L.; MANDEL, P.; BECKER, G.; MARÉCHAL, F. (2014), *Multi-objectives, multi-period optimization of district energy systems: I. Selection of typical operating periods*, Computers and Chemical Engineering 65, pp.54-66

GUANGRONG, Z. (2017), *Ship energy efficiency technologies − now and the future*, VTT Technical Research Centre of Finland Ltd., Tampere, pp.47

HOLTROP, J.; MENNEN, G.G.J. (1982), *An approximate power prediction method*, Int. Shipbuilding Progress 29(335), pp.166-170

HOWITT, O.J.A.; REVOL, V.G.N.; SMITH, I.J.; RODGER, C.J. (2010), *Carbon emissions from international cruise ship passengers' travel to and from New Zealand*, Energy Policy 38(5), pp.2552-

IMO (2018), *Initial IMO strategy on reduction of GHG emissions from ships*, Res. MEPC.304(72) - Annex 11, International Maritime Organization, London

ISO (2002), *Ships and marine technology -Airconditioning and ventilation of accommodation spaces - Design conditions and basis of calculations*, ISO 7547:2002(E), International Organization for Standardization, Geneva

KLEIN WOUD, H.; STAPERSMA, D. (2015), *Design of Propulsion and Electric Power Generation Systems*, The Institute of Marine Engineering, Science and Technology, London, pp.66-68

SILK BIDCO AS (2017), *Annual Bond report 2016 Hurtigruten*, Tromso, pp.2-4

SIMONSEN, M.; WALNUM, H.J.; GÖSSLING, S. (2018), *Model for estimation of fuel consumption of cruise ships*, Energies 11, pp.26

VAN BIERT, L.; GODJEVAC, M.; VISSER, K.; ARAVIND, P.V. (2016), *A review of fuel cell systems for maritime applications*, J. Power Sources 327, pp.345-364

A Highly Controllable ASV For Extremely Shallow Waters

Angelo Odetti, CNR-INM, Genova/Italy, angelo.odetti@inm.cnr.it
Marco Altosole, UNINA, Napoli/Italy, marco.altosole@unina.it
Marco Bibuli, CNR-INM, Genova/Italy, marco.bibuli@cnr.it
Gabriele Bruzzone, CNR-INM, Genova/Italy, gabriele.bruzzone@cnr.it
Massimo Caccia, CNR-INM, Genova/Italy, massimo.caccia@cnr.it
Roberta Ferretti, CNR-INM, Genova/Italy, roberta.ferretti@inm.cnr.it
Enrica Zereik, CNR-INM, Genova/Italy, enrica.zereik@cnr.it
Michele Viviani, UNIGE-DITEN, Genova/Italy, michele.viviani@unige.it

Abstract

This paper presents the hydrodynamics aspects of an innovative Autonomous Surface Vehicle, designed to meet the requirement of accessing the extremely shallow waters peculiar of wetlands. SWAMP (Shallow Water Autonomous Multipurpose Platform) is a fully electric, modular, portable, lightweight, and highly controllable ASV. It is a catamaran, equipped with ad-hoc designed azimuth Pump-Jet actuators, and characterized by small draft soft-foam, unsinkable hull structure with high modularity and a flexible hardware/software architecture. SWAMP is double-ended to enhance manoeuvrability in narrow space. The SWAMP prototype has been tested in a towing tank, verifying its expected performance.

1. Introduction

Robotics applied to environmental sciences is intended to help human beings to improve the precision and the quality of the surveys and to perform tasks in those areas where the access is dangerous or difficult. For this reason, the main concept behind the design and development of a robot expressly addressed for a peculiar environment should be its adaptability and compliance to the specific operating conditions in order to extend the operations to the largest possible area.

The research presented in this article is related to the development of a robotic solution targeted to answer the practical needs of monitoring the extremely shallow waters characteristic of Wetlands for a better acquisition of the environmental parameters.

Wetlands are marshes, peat bogs, natural or artificial permanent or temporary basins, with stagnant, running, fresh, brackish, or salty water, including stretches of sea water whose depth, at low tide, does not exceed six meters.

The importance of monitoring wetlands is widely known, but, as reported in *Odetti et al. (2018)*, the surveys of these areas are quite difficult due to the use of technical and operational solutions not always suitable for the peculiar environment. Water sampling, limnological surveys, bathymetric analysis and water quality monitoring are complicated due to the difficulties in accessing the uneven underwater terrains and the extremely shallow waters that characterise ponds, rivers, lakes and coastal areas. Hard access to these areas with traditional means results in approximate and inefficient surveys. Most of research results are finding out that the lack of hydrographic vessel capable of carrying out measurements for shallow waters at depths less than 1 m.

A new class of reliable, modular, reconfigurable, and lightweight Autonomous Surface Vehicles (ASVs) for extremely shallow water and remote areas applications named SWAMP (Shallow Water Autonomous Multipurpose Platform) was built in a collaboration between CNR-INM and DITEN-Unige. SWAMP is a fully electric, modular, portable, lightweight, and highly controllable ASV. It is a catamaran, equipped with four azimuth Pump-Jet thrusters specifically designed for this vehicle, and characterized by small draft soft-foam, unsinkable hull structure with high modularity and a flexible hardware/software WiFi-based architecture.

In order to combine the ability of working in a few centimetres of water, together with satisfactory control abilities the SWAMP ASV design is based on the use of a prototype of a modular azimuth thruster based on Pump-Jet concept. The Pump-Jet solution has previously been adopted in ships and boats working in shallow waters, but never adopted before in robotic vehicles. Only a scaled model of ASV presented by *Peeters et al (2020a,b)* adopted a steerable grid model of Pump-Jet for a new fleet of self-propelled inland cargo barges.

Vehicles expressly designed to work in shallow and confined waters and in harsh environments can minimize the effects of possible (and probable) impact with the waterway ground by combining a flat bottom with the use of a Pump-Jet-based propulsion unit. Since ASVs must be able to access narrow areas for sampling, even in the presence of external disturbances, they should be fully controllable both in station keeping and in path following. For this reason, a propulsion layout based on four azimuth thrusters (like the Pump-Jet Module) was considered a suitable approach for SWAMP.

In order to increase the controllability of the vehicle a series of tests were performed in towing tank both on the hull, both on the vehicle with the propulsion units in self- propelling condition and in bollard pull. This was useful to increase the knowledge related the vehicle behaviour in deep and shallow water and of the propulsion system constituted by four Pump-Jet. The results allow to model and identify SWAMP for a better controlling strategy in a way never done before on this kind of vehicles. And the adoption of sensors like IMU, sonars and cameras can allow to increase the actual prediction of vehicle behaviour in a specific environment.

2. Requirements and Related Works

Wetlands are often remote areas that to be monitored and surveyed require robotic solutions characterised by minimal logistics, low weight, small dimensions and modularity. Moreover, in order to maximize the vessel operative area, its structure, propulsion and steering system require not to be susceptible to possible damages from the very probable grounding that may occur in shallow waters. The operative profiles require vehicles with good controllability that can provide path following and station keeping ability also in narrow space, a good stability for sensors management and open hardware and software architecture for easy adaptability and re-configurability.

As shown in *Bertram (2008)* and *Schiaretti et al. (2017a,b)* a great number of Autonomous Surface Vessels (ASV) with different capabilities and functionalities was developed, mostly in the last twenty years, arising from academic and research institutions. Moreover, the last decade a relevant number of commercial vessels was introduced in the market to answer the operational needs of environmental surveys and protection, demonstrating that ASVs are now a reliable and affordable technology.

Many recent projects include vehicles defined "suitable for shallow waters" such as *Wang et al. (2009)* and *Seto and Crawford (2015)*, i.e. catamarans with big dimensions and low logistics. Some of these catamarans are highly automated as in *Ferri et al. (2015)* but have a structure, a propulsion and a steering system prone to possible breaking due to grounding in extremely shallow waters making these solutions not really flexible enough. Vehicles as described in *Hitz et al. (2012)* and *Raimondi et al. (2015)* are propelled by waterjets (enclosed in a protected part of the hull), but present big dimensions and weights. Also, smaller vehicles as described in *Carlson et al. (2019), Bertram et al. (2016)* are propelled with classical propellers resulting not suitable for extremely shallow waters or lowly controllable and fragile like that of *Grenestedt et al. (2015)*. All these projects have either a structure, or a propulsion or a steering system prone to possible breaking due to grounding in extremely shallow waters making these solutions not really flexible enough. Other solutions like *Idris et al. (2016)* take into consideration low weight simple concepts and an aerial propulsion which is suitable for shallow water. By the way most of the proposed solutions have a simple actuation system that makes difficult to provide high controllability in narrow spaces. With this none of the above-mentioned vehicles responds to all the requirements we have identified. SWAMP was conceived to try to respond to the above-mentioned list of specific technical exigencies.

3. SWAMP ASV

The design of SWAMP was driven by the application (a specific need) that led to research (new concepts to be applied) and can bring to innovation (an appealing system). This means that a novel design technique was applied. And, as a consequence, the classical ship design spiral which is a traditional way of describing the design project, resulted inapplicable. In case of a novel design, the smoothness of the process is not the same, in the case of SWAMP a balanced solution had to be found to search for a compromise between conflicting requirements. The design output, namely the perfect balance between these requirements, does not lead to the optimised solution but to optimum reachable.

This means that every step has to take simultaneously into consideration a variety of parameters that have to be continuously balance at the same time. This brings to a final design without need of iterative processes. In the SWAMP design the conflicting requirements have led to solutions that seemed to be inconvenient if watched from their perspective (e.g. higher wave resistance) but that resulted to be the correct if watched from the global project perspective.

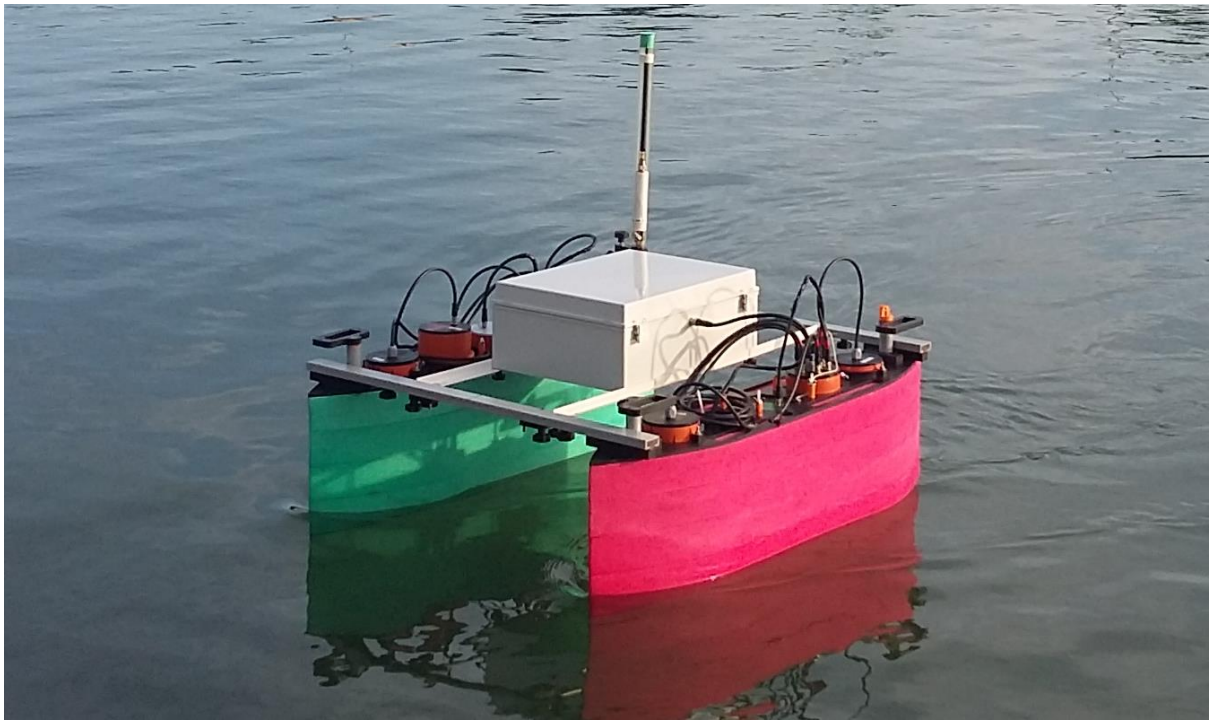

Fig.1: SWAMP vehicle with a payload box on the deck

SWAMP is a full-electric Catamaran 1.23 m long with a design breadth of 1.1 m (variable between 0.7 m and 1.25 m). The hull height is 0.4 m and the vehicle with the structure and the antennas is 1.1 m high. SWAMP lightweight is 38 kg with a draft of 0.1 m, the standard maximum payload is 20 kg with a consequent maximum design draft of 0.14 m but the reserve of buoyancy of SWAMP allows to embark up to 60 kg with a draft of 0.22 m. The small dimensions of the vehicle comply with the idea of a reduced logistics. The vehicle is man-portable and transportable by car or in a small boat. A double ended Wigley-based hull shape was chosen both for hosting four Pump-Jet Module azimuth thrusters expressly designed and studied for this project and to create an innovative structure. Indeed, one of the main peculiar aspects of SWAMP is the use of light, soft and impact-survival flexible structure made with a sandwich of soft closed-cell foam, HDPE plates and pultruded bars. This flexible design allows to host various types of tools, thrusters, control systems, samplers and sensors. Also, for this reason for the propulsion the choice has fallen on the design of a modular propulsion unit that can be easily installed on the vehicle. The propulsion, as already mentioned, is based on Pump-Jet. Using four azimuth thrusters gives SWAMP the controllability that is required for high quality surveys. As shown in Fig.10 the thrusters were positioned in symmetrical positions on the vehicle two fore and two aft.

The Pump-Jet thrusters were built in the CNR-INM labs and tested at various angles and with different configurations. For what concerns the Hardware and Software systems of SWAMP, they consist of a Wi-Fi-based architecture. The hardware architecture of SWAMP is based on COTS components. The basic Navigation Guidance and Control (NGC) package of each hull is composed by an IMU and a GPS. The communication is created by one communication module each hull that provides a communication framework for both its same hull and for the other hull's modules when its work is required.

The SWAMP hulls were tested, also in shallow water, in the DITEN-UNIGE towing tank at various depth, payload and breadth. Maximum speed of SWAMP in infinite depth waters is 1.6 m/s, while the speed in extremely shallow waters down to 200 mm (i.e. 60 mm of under-keel water) is reduced to 1 m/s due to the change in hydrodynamic characteristics occurring in shallow waters.

4. SWAMP Hull

The hull shape is inspired by the double-ended Wigley series. A hard balance between conflicting requirements was necessary in the design phase. Among these requirements, good stability, the length to be contained within 1.25 m with a small draft and a high payload of 25/20 kg, the need of fitting Pump-Jets and easiness of prototyping. The catamaran hull was chosen for its good stability. The Wigley hull is cut at a certain waterline in order to create a flat bottom suitable to host the Pump-Jet thrusters. The Wigley double-ended hull form and the propulsion layout is characterised by equally efficient sailing ahead and astern with the possibility of manoeuvring in narrow spaces. The Wigley hull was chosen also for an easiness to prototype by using expanded foam. In this hull shape the longitudinal centre of buoyancy LCB is centered mid-hull and the hull has large B/T ratios.

As a result the hull values of B/T = 1.7, L/B = 5.1 and $L/\nabla^{1/3}$ = 4.1 of SWAMP result to be small and the bow (and stern) results to be bluff, with a CB = 0.67, if compared to commonly adopted catamarans where, usually, when CB is high the L/B ratio is high too. As a consequence, the resistance coefficients of SWAMP is high due to an increased wave resistance.

DATA	**SWAMP**	**Literature Catamarans**
L/B	5.167	7 - 20
$L/\nabla^{1/3}$	4.06	6.2 - 12
B/T	1.714	1.5 - 2.3
C_B	0.67	0.4 - 0.65

Fig.2: Difference between SWAMP hull and literature Catamarans

The operative profile of SWAMP comprises the presence of shallow waters where, sinkage, trim and wave pattern formation around the hull are modified as shown in *Sahoo and Doctors (2003)*. This depends on water depth h, and in particular on the ratio between water depth and vessel draft: h/T ratio. A substantial reduction in the performances of the vessel in terms of manoeuvrability and resistance is faced. If the h/T ratio is low, then grounding due to excessive squat could occur at the bow or at the stern.

To assess the resistance of SWAMP, towing tank tests were conducted both in deep, and in shallow water. Towing Tank Tests in deep and shallow waters were performed in DITEN Hydrodynamic Laboratories at the University of Genova. Dimensions are about 60 x 2.5 x 3 m with a running distance of 45 m and maximum speed of 3 m/s with capability of measurement of trim and resistance. For the tests in shallow water the carriage was modified and the water in the tank was removed down to the wanted value. When towing a catamaran like SWAMP, the towing point is placed above the waterline and above the Vertical Centre of Buoyancy VCB. In this case an induced trimming moment is generated and a correction was applied. This was done by using a mobile mass for the correction of the vehicle's initial trim so that the dynamic attitude could be the exact one. Tests were performed at h/T = [1.5, 2.0,

2.5, 4.0, 9.0]. At maximum depth the tests were done at 3 different widths: B = [820, 1100, 1250] mm resulting in S/L = [0.46, 0.68, 0.8]. Tests used the standard load condition of 58 kg and T = 140 mm. A test was done at the design width of 1100 mm with load condition of 48 kg and T = 115 mm. In order to evaluate the possible occurrence of channel effect some CFD tests have been conducted during the deep-water tests and no occurrence has been recorded. No CFD test was done for shallow water.

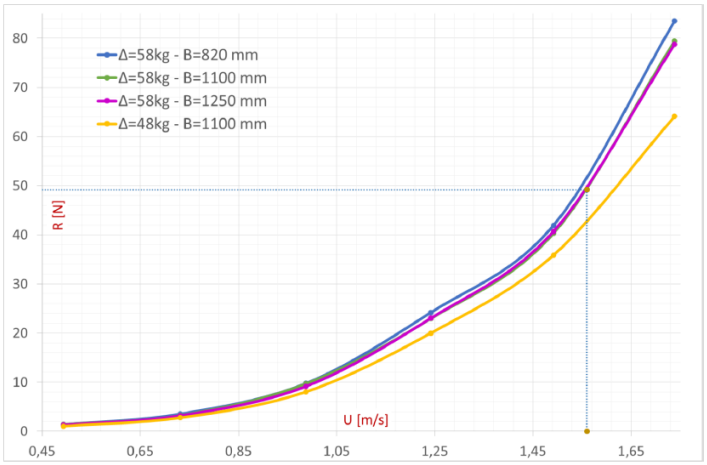

Fig.3: Tests at different B and at different Immersion

A low variability on the resistance depending on the width can be seen with a small interference between the two hulls, Fig.3. Tests at different immersions showed a rough dependence on the wetted surface that allows to foresee the resistance at intermediate immersions.

The SWAMP hulls were tested, also in shallow water, in the DITEN-UNIGE towing tank at various depth, payload and breadth. Maximum speed of SWAMP in infinite depth waters is 1.6 m/s, while the speed in extremely shallow waters down to 200 mm is reduced to 1 m/s due to the peculiar hydrodynamic effects occurring in shallow waters as shown in *Bertram (2011)* and *Briggs (2006).*

Tests were performed at four different water depth at the maximum loading condition. The minimum water depth H = 210 mm with a clearance of 60 mm. From tests results it was possible to see how the resistance gradually increases with the decreasing of water depth and of the H/T ratio. Fig.4 shows the resistance vs depth Froude number. At higher Depth Froude numbers the curves almost collapse.

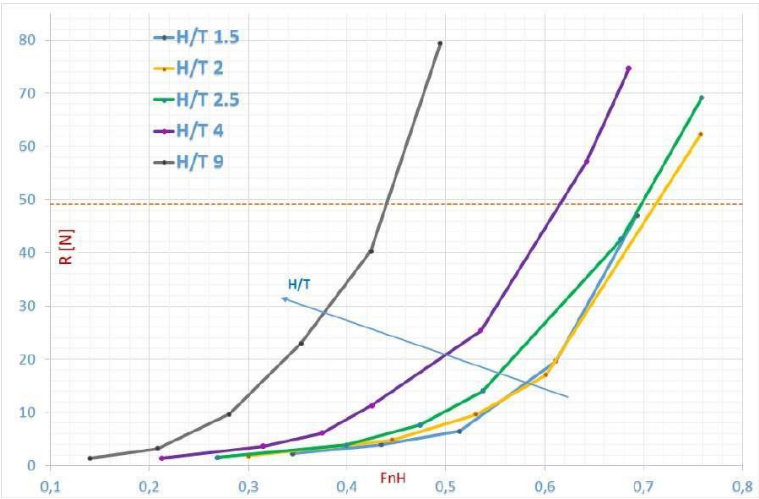

Fig.4: Resistance curves at different H/T in function of Depth Froude Number FnH

This effect is more evident in the Ct vs Fn_H curves. The resistance curves from h/T ≤ 4 are quite superimposable showing the effective relation between resistance increase and the value of Fn_H . This

increase is larger for the smaller water depth and is strictly related to the smaller under keel clearance. The resistance showed a distinct increase near the critical depth Froude Number (Fn_H=1.0) that, anyway, was never reached in the tests.

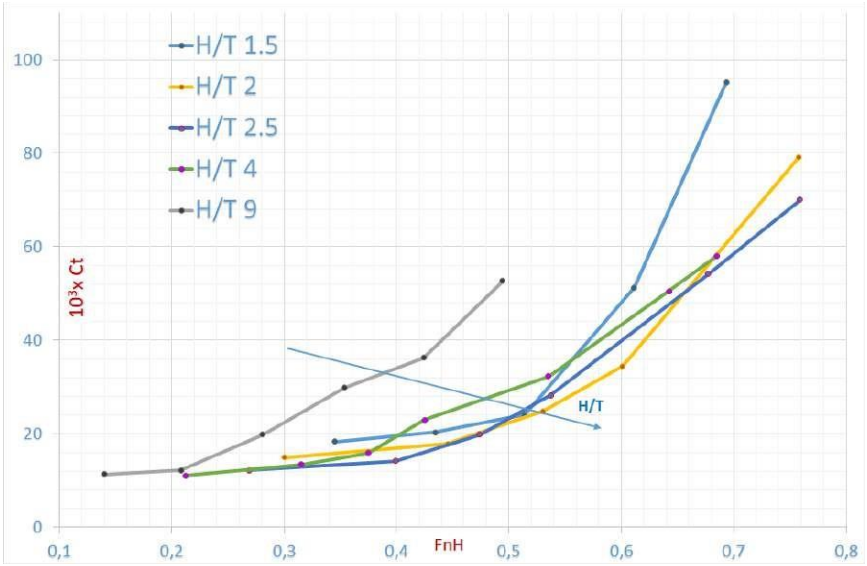

Fig.5: Resistance Coefficients at different H/T in function of Depth Froude Number Fn_H

This may imply that below a certain H/T = 4.0 the resistance can be foreseen by using the signal given by a single beam altimeter.

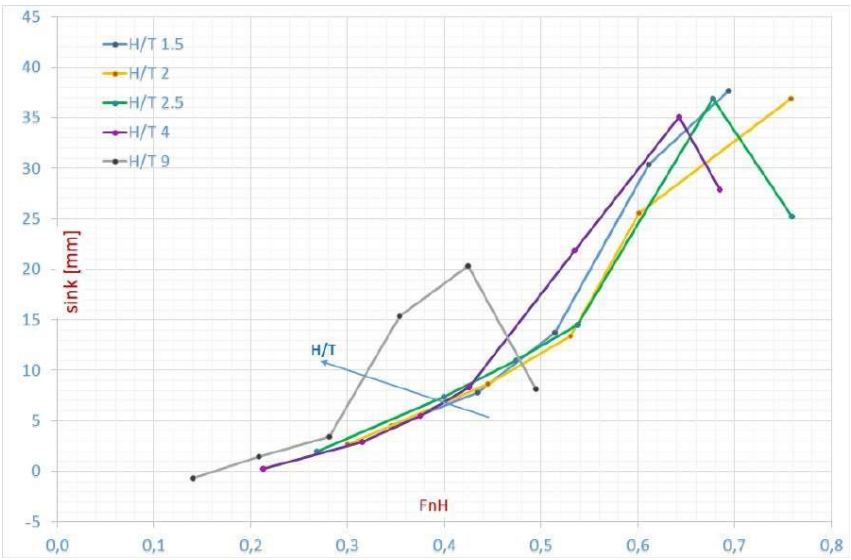

Fig.6: The midship sinkage curves at different H/T vs Fn_H

Fig.6 shows that the increase in resistance is strictly related to an increase in the sinking of the vehicle due to the Venturi effect with the tank bottom. The consequence is the presence of an evident squat effect. This effect is important even at lower speed. The mid-ship sinking in deep water is lower also at the small speed and this difference increases as the water depth decreases. It is important to see that also in the case of sinkage the curves almost collapse in one curve as the Fn_H is increased and regardless of the H/T ratio.

The squat is the maximum reduction in underkeel clearance (bow or stern) between the vessel at-rest and water bottom. From the tests on SWAMP hull, the sinkage at stern is higher than the sinkage at bow when U > 1 m/s. Above this value the sinkage substantially increases up to a value of 80mm for H/T = 2 and U = 1.25 m/s

The squat effect shows the possibility of grounding when going at speed in shallow water supporting the need of an impact resistance hull and propulsion. This can be calculated by knowing the trim of the vessel. Fig.7 shows the trim modification. The trimming of the vessel occurs at lower speed as the water depth decreases. For h/T ≤ 1.5 the trim is never negative, while in the other cases the vehicle passes from a minimum of negative trim to a maximum of positive trim. In shallow water as the depth is decreased, the vessel trim passes to be trimmed by bow to be trimmed by stern at a smaller speed with almost no negative trim in case of H/T = 1.5. Also, in the case of trim, almost all the curves vs Fn_H can be super-imposed.

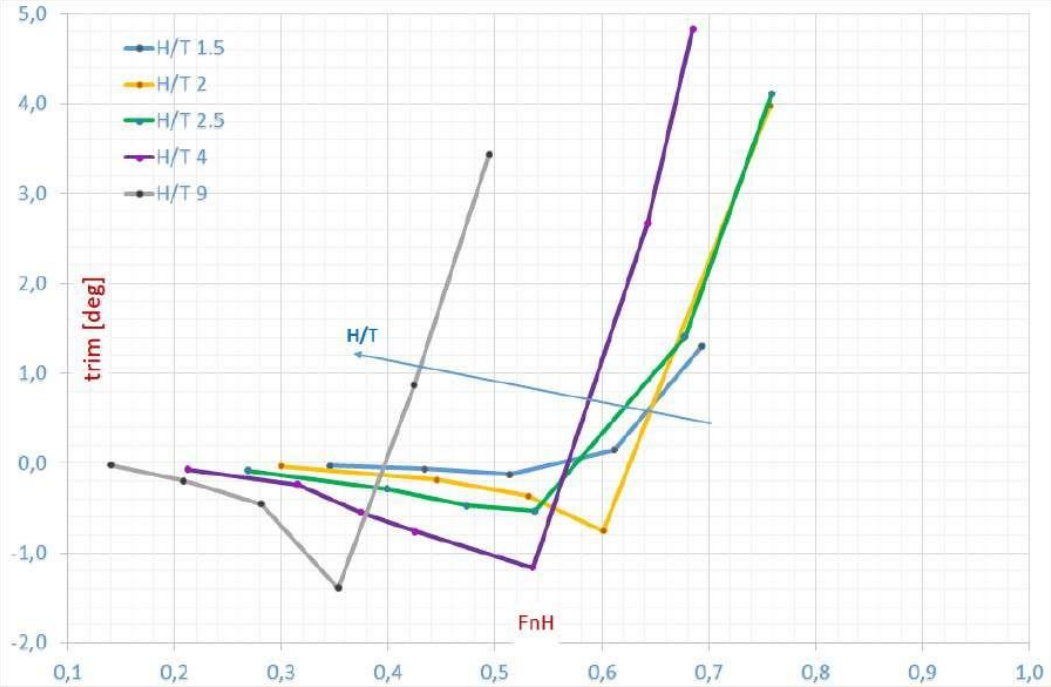

Fig.7: The trim curves vs Fn_H at different H/T

The vessel sinks significantly as the critical region is approached. In this direction significant running sinkage might be an important operational consideration if keel to ground clearances become really small.

By taking these results into consideration is possible to foresee the effective hydrodynamic resistance of the vessel in presence of shallow water thus knowing the thrust that the thrusters have to impress and which is the maximum reachable speed with the thrusters.

The data derived from these tests are interesting also to increase the number of available catamaran geometries, also in shallow water.

From the towing tests it was possible to extract the resistance R = 49 N at a maximum design speed of 1.5 m/s at the maximum loading of the vehicle. The value of 1.5 m/s was considered the reference value to match with the Pump-Jet Module design.

5. Pump-Jet Module and tests

SWAMP was designed around and together the possibility of installing the Pump-Jet Module described in *Odetti et al. (2019)*. The commonly used propulsion systems for shallow waters monitoring ASVs are Free-propeller or Ducted-propeller propulsion modules, Waterjet systems, and aerial systems. Screw propelled solutions are subject to damages caused by impacts with obstacles at low depth and therefore not recommended, aerial propulsion, perfect for shallow water, has the disadvantage of having large dimensions that are not suitable for SWAMP design criteria. On the other hand, the use of Waterjet

propulsion can be considered a suitable choice, but it was difficult to couple such a system to the needs of a highly manoeuvrable vessel. The solution adopted was integrating the Waterjet propulsion with a highly steerable solution and the Pump-Jet geometry was chosen. With respect to classical Waterjet propulsion the Pump-Jet is characterised by lower operative speeds, higher structural integrity given by the total integration in the hull and higher manoeuvrability thanks to 360° steering ability. This kind of system was never adopted before in ASVs.

The main advantage of using PJMs is maximum thrust at minimum draft. It can be used as main thruster and as manoeuvring thruster. The PJM can work in minimum water depths as low as 50 mm without risking damage.

The main idea behind the Pump-Jet Module was to design a watertight module that can easily be dismounted from the ASV for easy transportation and can be employed on different vehicles. For compactness, the control unit is embedded and contained inside the module. The azimuth motor provides continuous feedback on position, guaranteeing high maneuverability with high rotating nozzle speed. The entire casing is designed to be 360° steerable.

The Pump-Jet operates on the principle of a vertical axis pump. A mixed-flow or centrifugal pump sucks in water from beneath the hull, and through the blades, the water is whirled tangentially and radially outward into the casing chamber. The fluid gains both velocity and pressure while passing through the impeller. The outlet nozzles in the steer- able casing accelerate the flow, and a jet of water produces thrust horizontally beneath the flat-bottomed hull. Since thrust is the product of water flow by water velocity then the Pump-Jet requires a very low volume flow to generate a propulsion force. The outlet angle of the water is approximately 15° from horizontal: almost the entire jet thrust is converted effectively into forward thrust.

Concerning the construction, the pump impeller was 3D printed for ease of manufacturing. For the same reason, the module itself was constituted by a 3D-printed element hosting both the inlet duct and the outlet nozzle.

The design based on the theory governing mixed-flow pumps was constrained by geometrical factors (draught, payload, main dimensions), thrust required (giving Pump Head Hp) and RPMs of the chosen brushless motor.

The value of the design thrust for the PJM was obtained from the resistance of SWAMP small-/medium-sized ASVs.

The module may be considered as a free-running propeller studied for bollard pull and low speed. The exact amount of thrust was validated during moving tests where advance speed influences the exact amount of thrust produced by the module resulting into a thrust deduction factor and/or a wake fraction. The thrust produced by the Pump-Jet system can roughly be expressed as $T\alpha = (\rho_w A_n V^2)/\cos\alpha_{out}$ with A_n discharge area, V outlet flow speed, α_{out} the outlet angle. The design thrust of the Pump-Jet Module was identified as T = 12.3 [N].

Bollard thrust tests were performed on the 4 Pump-Jet of SWAMP to measure the delivered thrust and power of the impeller using a test rig. This allowed to characterise the propulsion units by defining the thrust vs RPM and the consequent power vs RPM curves that, as far as the control is concerned, results into a driving reference voltage [V] to be applied to the main motor. The four PJM test results at the maximum thrust angle are reported in Fig.8. These tests show a very good matching between all the thrusters results for what regards thrust vs RPM.

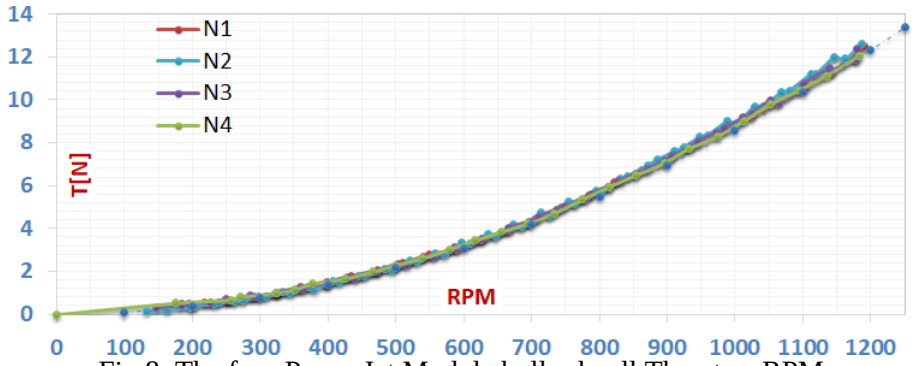

Fig.8: The four Pump-Jet Module bollard pull Thrust vs RPM

Since no existing result is present in literature then self-propelling tests were conducted in the DITEN towing tank with the vehicle at maximum weight 58 kg and T = 140 mm. The results obtained allowed to produce the characteristic thrust vs advance speed at various motor rotations, as reported in Fig.6 in analogy to the well-known performance charts adopted by all waterjet manufacturers. In Fig. 9 the graphic of advance speed vs RPM for the various (1-t) is reported. It is interesting to notice that at low advance speed of 0.5 m/s the (1-t) value is low at lower RPMs while increases as the RPM is increased. This factor is relevant for the controlling strategies since at low advance speed it worth to use two thrusters at higher RPMs instead of four thrusters at lower RPMs. Since a significant increase in the power consumption is recorded. This is true up to when the two thrusters cannot compensate the resistance. In this case a gradual change in the control strategy is required passing from two to four thrusters.

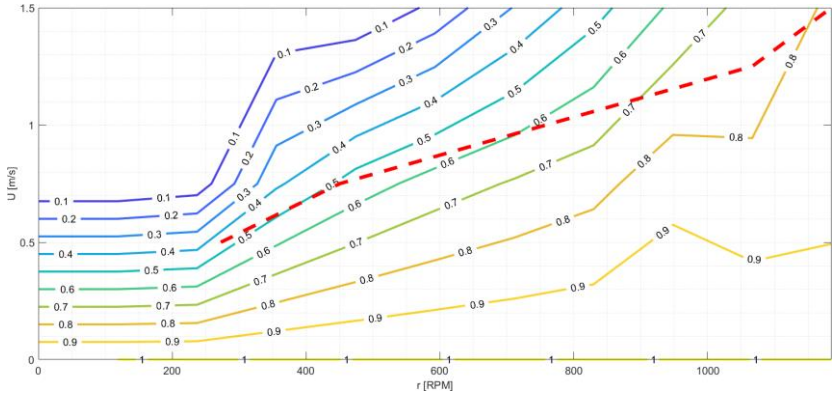

Fig.9**:** Thrust [N] vs Speed [m/s] with the level curves representing the various RPMs of the single Pump-Jet Module. The red line is the actual curve with 4 working PJMs at maximum draft.

Another interesting point is that the maximum value of (1-t) is obtained at the maximum speed of 1.5 m/s at maximum RPMs of 1185. This (1-t) is around 0.85 which, indeed, is a high value that can be compared to screw propellers. It can be assumed that the Pump- Jet can work well also at higher speeds. These assumptions are more related to the Pump-Jet. Another assumption is related to the use of the Pump-Jet Module under the SWAMP hull. Tests were conducted with just a couple of two thrusters working in fore configuration and in aft configuration. This was done to see whether the position on the hull could influence the thrust value. Tests were performed from 0.5 to 0.85 m/s and no significant difference was recorded. The difference was at the same scale of the error that was recorded in single test on the single couple of thrusters.

6. Thrust Configuration

The forces and moments produced by the Pump-Jet Module are referred to the vehicle's coordinate system. The four Pump-Jet Module thrusters are positioned on SWAMP inside holes machined in HDPE foam plates. Each hole centre is placed on the longitudinal axis (x) at a distance of 0.350 m from mid-ship. Through the structure the forces are transmitted to the hull.

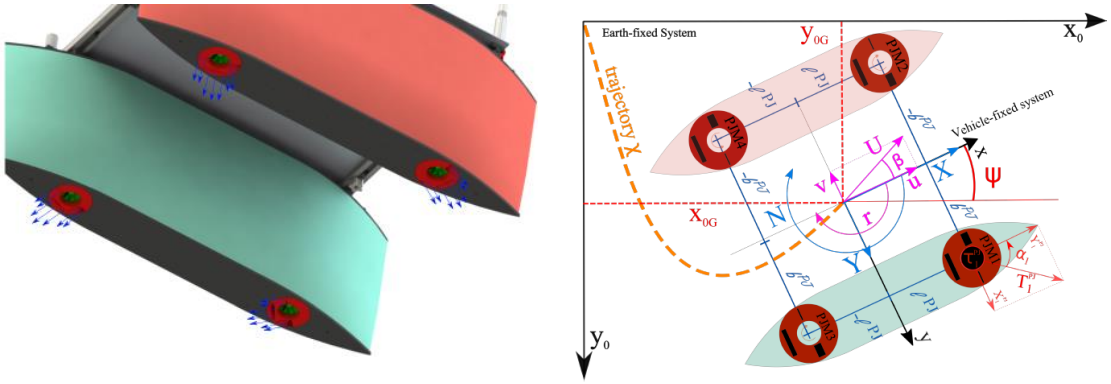

Fig.10: Thrust configuration and system

The adoption of four Pump-Jet Module high degree of controllability with the possibility of providing highly accurate dynamic positioning and path following. Considering the vehicle as a rigid body with three degrees of freedom: two translations, the forward motion along the longitudinal axis x_{0G} and the drift motion along the transverse axis y_{0G}, and the rotation ψ about the vertical axis (Yaw). The rigid body equations in earth fixed and body fixed system are:

$$\begin{cases} X_0 = \Delta \ddot{x}_{0G} \\ Y_0 = \Delta \ddot{y}_{0G} \\ N_0 = I_{zz} \ddot{\psi} \end{cases} \quad \begin{cases} X = \Delta(\dot{u} - vr - x_G r^2) \\ Y = \Delta(\dot{v} + ur + x_G r^2) \\ N = I_{zz} \dot{r} + \Delta(\dot{v} + ru) \end{cases}$$

Being u,v and r the forward, drift and rotational speeds of the body in the body fixed coordinates system and Δ and I_{zz} the mass constants.

In the equilibrium equation the global forces and moments acting on SWAMP are a sum of external disturbances: wind , current, internal forces of the hull and a sum of forces XT , YT and moments NT produced by the thrusters.

Each Pump-Jet Module is constituted by two motors:

- Azimuth motor controlling the orientation α_i of the thrust exerted by the i-th jet, assumed equal to 0 when the thruster pushes along the surge direction. For simulation purposes, the controlled motor is assumed to have a first-order dynamics with time constant tα, i.e. 1
- Pump motor controlling the thrust T_i^{PJ} exerted by the i-th jet. The pump motor is assumed to have time constant equal to zero. Each Pump-Jet is positioned $\underline{p}_i^{PJ} = [l_i^{PJ}, b_i^{PJ}, 0]^T$ with a rotation matrix that is $R_{PJ_i,b} = I$ with respect to the body fixed reference system.

The resulting rotation matrix between the Pump-Jet thrust and the body fixed reference system is:

$$\begin{pmatrix} \cos\alpha_i & -\sin\alpha_i & 0 \\ \sin\alpha_i & \cos\alpha_i & 0 \\ 0 & 0 & 0 \end{pmatrix}$$

Given T_i^{PJ} as the generic thrust always positive and $\alpha_i = (0, 2\pi]$ the generic angle and thrust.
The contribution to the external force and torque given by each Pump-Jet is:

$$\underline{\tau}_i^{PJ} = \begin{pmatrix} X_i^{PJ} \\ Y_i^{PJ} \\ N_i^{PJ} \end{pmatrix} = \begin{pmatrix} \cos\alpha_i \\ \sin\alpha_i \\ -b_i^{PJ}\cos\alpha_i + l_i^{PJ}\sin\alpha_i \end{pmatrix} T_i^{PJ}$$

The thruster forces acting on SWAMP are then the forces and moment produced by the Pump-Jet Module. The thrust configurations on the local coordinates system of the vehicle is summarized:

$$\begin{pmatrix} X_T \\ Y_T \\ N_T \end{pmatrix} = \begin{pmatrix} X_T^{PJ} \\ Y_T^{PJ} \\ N_T^{PJ} \end{pmatrix} = \begin{pmatrix} X_1^{PJ} + X_2^{PJ} + X_3^{PJ} + X_4^{PJ} \\ Y_1^{PJ} + Y_2^{PJ} + Y_3^{PJ} + Y_4^{PJ} \\ N_1^{PJ} + N_2^{PJ} + N_3^{PJ} + N_4^{PJ} \end{pmatrix}$$

From the above equation it is possible to see that there are infinite configurations of the thruster position for every task being station keeping, path following or vehicle cooperation. Whit this configuration the system results redundant respect to a complete failure of one or more thrusters.

Referring to *Veksler et al. (2014)*, in the case of SWAMP, denoting with:

$$\begin{aligned} X_i^{PJ} &= T_i \cos \alpha_i \\ Y_i^{PJ} &= T_i \sin \alpha_i \\ i &= 1..4 \end{aligned}$$

the extended thrust vector χ^{PJ} is defined as

$$\underline{\chi}^{PJ} = \left[X_1^{PJ}\, Y_1^{PJ}\, X_2^{PJ}\, Y_2^{PJ}\, X_3^{PJ}\, Y_3^{PJ}\, X_4^{PJ}\, Y_4^{PJ}\right]^T$$

and the generalised force for the Pump-Jet system is computed as:

$$\underline{\tau}^{PJ} = B\underline{\chi}^{PJ}$$

where

$$B = \begin{pmatrix} 1 & 0 & 1 & 0 & 1 & 0 & 1 & 0 \\ 0 & 1 & 0 & 1 & 0 & 1 & 0 & 1 \\ b^{PJ} & l^{PJ} & b^{PJ} & -l^{PJ} & -b^{PJ} & l^{PJ} & -b^{PJ} & -l^{PJ} \end{pmatrix}$$

Each Pump-Jet thrust is assumed to be positive and lower than a maximum value as it follows:

$$\begin{aligned} X_i^{PJ} \cos \alpha_i + Y_i^{PJ} \sin \alpha_i &\leqslant T_i^{MAX} \\ X_i^{PJ} \cos \alpha_i + Y_i^{PJ} \sin \alpha_i &\geqslant T_i^{min} \\ \alpha_i = atan2\left(Y_i^{PJ}, X_i^{PJ}\right) & \\ i = 1..4 & \end{aligned}$$

Being $\alpha_{i,0}$ the current orientation of the i-th Pump-Jet and $\Delta\alpha$ the maximal angle variation in the sampling period, the following constraints hold

$$\begin{cases} X_i^{PJ} \sin\left(\alpha_{i,0} - \Delta\alpha\right) - Y_i^{PJ} \cos\left(\alpha_{i,0} - \Delta\alpha\right) \leqslant 0 \\ -X_i^{PJ} \sin\left(\alpha_{i,0} + \Delta\alpha\right) + Y_i^{PJ} \cos\left(\alpha_{i,0} + \Delta\alpha\right) \geqslant 0 \end{cases}$$
$$i = 1..4$$

Specific Pump-Jet configurations are selected corresponding to typical working modes such as, for instance, station-keeping and forward/backward surge transfer. In these cases, the Pump-Jet orientation angles are constrained in pre-defined sectors and, according to the positive thrust physical constraint, suitable sub-sets of actuators are allocated to generate the desired directional force and torque. In the research of an equilibrium, in case of station keeping the sum of forces and moment should be 0.

We denote by X_R, Y_R, N_R the resulting external forces and moment acting on the vehicle. Four equilibrium equations are present:

$$F_R = \begin{pmatrix} X_R + X_T \\ Y_R + Y_T \\ N_R + N_T \end{pmatrix} = \begin{pmatrix} 0 \\ 0 \\ 0 \end{pmatrix}$$

The thrust allocation matrix, i.e. the mapping of the required forces on the thrusters present on-board, is then:

$$F_R = B\underline{\chi}^{PJ} : \begin{cases} g_1(\underline{\chi}) : X_R + X_1 + X_2 + X_3 + X_4 = 0 \\ g_2(\underline{\chi}) : Y_R + Y_1 + Y_2 + Y_3 + Y_4 = 0 \\ g_3(\underline{\chi}) : \begin{array}{l} N_R + X_1^{PJ} b^{PJ} + Y_1^{PJ} l^{PJ} + X_2^{PJ} b^{PJ} + Y_2^{PJ}(-l^{PJ}) + \\ X_3^{PJ}(-b^{PJ}) + Y_3^{PJ}(l^{PJ}) + X_4^{PJ}(-b^{PJ}) + Y_4^{PJ}(-l^{PJ}) = 0 \end{array} \\ g_4(\underline{\chi}) : X_1^2 + Y_1^2 - (\tau_1^{PJ})^2 = 0 \\ g_5(\underline{\chi}) : X_2^2 + Y_2^2 - (\tau_2^{PJ})^2 = 0 \\ g_6(\underline{\chi}) : X_3^2 + Y_3^2 - (\tau_3^{PJ})^2 = 0 \\ g_7(\underline{\chi}) : X_4^2 + Y_4^2 - (\tau_4^{PJ})^2 = 0 \end{cases}$$

The equations $g_{4:7}(\chi)$ are used, to remove trigonometric functions from the problem.

The problem has more incognitos than equations. To find a solution and to minimise the required parameters (e.g. thrust or power consumption) an optimum problem has to be solved. An objective function has to be found and the minimum of the surface of possible solutions has to be identified. To do this the method of Lagrangian multiplier can be used.

The Lagrange multiplier method allows to reduce the stationary points of a function in n variables and m boundary constraints $g(\chi) = 0$, said objective, to those of a third function in n + m variables not bound, called Lagrangian:

$$\Lambda(\underline{\chi}, \lambda) = f(\underline{\chi}) + \lambda \cdot g(\underline{\chi}) = f(\underline{\chi}) + \sum_{j=1}^{m} \lambda_j g_j(\underline{\chi}),$$

that is, introducing as many new scalar variables λ as there are the constraints that are called multipliers. That means that, given the above defined g(χ)j:

$$\nabla f(\underline{\chi}) + \sum_{j=1:7}^{m} \lambda_j * \nabla g(\underline{\chi})_j$$

As an example, the function to be optimised can be:

$$f(\underline{\chi}) = \sum_{i=1:4}^{n} \frac{X_i^2 + Y_i^2}{(T^{MAX})^2}$$

Where, to reduce the thrust, T^{MAX} is the sum of the maximum allowable thrust of the four Pump-Jet. The general DP-Thrust allocation problem can be summarised as minimising a cost function including a quadratic approximation of the power consumption as well as a penalty for variations in the extended thrust vector that is intended to reduce wear-and-tear in the thrusters.

7. Conclusions

This article reported the description of the SWAMP vehicle with a special focus on the hydrodynamic tests and on the propulsion layout. SWAMP is an innovative Autonomous Surface Vehicle that was especially studied for extremely shallow waters down to 200 mm. SWAMP installs four new azimuth Pump-Jet thrusters designed for this vehicle. Since the Pump-Jet is installed flush with the hull, it does not produce a significant increase in resistance if compared to other systems, and moreover there is less risk of collision between propulsion unit and underwater obstacles.

The knowledge of the hydrodynamic characteristics of the thruster and of the vessel allows to partly or fully identifying the vessel for a better controllability. With this aim a series of tests have been conducted in the DITEN towing tank. In particular, the advance resistance on the SWAMP hull in deep and shallow water, bollard pull and self-propelling tests with the PJM working have been carried out. These showed that in order to comply with stringent requirements it is necessary to partly scarify hydrodynamic performances. In fact, the resistance coefficients of SWAMP are quite high if compared to existing catamaran hull. This can be foreseen for a good number of small size-high payload ASVs.

But a good knowledge of the hydrodynamic characteristics of a vessel allows to identify the hull more quickly. In the case of SWAMP, for the first time in an ASV, this was done also in shallow waters with a recording of squat effect, of modified trim effect and of the increasing in resistance. This happens as the H/T ratio approaches the value of 5. This is important for this kind of small vessels that work in coastal areas and that need an automatic controlling strategy.

The self-propelling tests allowed to identify the behavior of the PJM at speed. Thrust deduction factor curves where produced allowing to see that at higher speeds and RPMs the Pump-Jet thrust deduction is similar to the one obtained with screw propellers.

Acknowledgments

We want to thank the technical staff composed by Giorgio Bruzzone, Edoardo Spirandelli and Mauri Giacopelli from CNR-INM for their contribution in the design, construction and testing of the

mechanical and electrical systems of the robotic platform. The towing tank tests were possible thanks to the precious help of Alberto Ferrari and Sergio Talocchi of DITEN Unige.

References

BERTRAM, S.; KITTS, C.; AZEVEDO, D.; DEL VECCHIO, G.; HOPNER, B.; WHEAT, G.; KIRKWOOD, W. (2016), *A portable ASV prototype for shallow-water science operations*, OCEANS 2016, Monterey, pp.1-6.

BERTRAM, V. (2006), *Unmanned surface vehicles – A survey*, Singapore Maritime and Port Journal

BERTRAM, V. (2011), *Practical ship hydrodynamics*, Elsevier

BRIGGS, M.J. (2006), *Ship squat predictions for ship/tow simulator*, Tech. Rep., Engineer Research and Development Center, Vicksburg

CARLSON, D.F.; FÜRSTERLING, A.; VESTERLED, L.; SKOVBY, M.; PEDERSEN, S.S.; MELVAD, C.; RYSGAARD, S. (2019), *An affordable and portable autonomous surface vehicle with obstacle avoidance for coastal ocean monitorin*g, Hardwarex, e00059

FERRI, G.; MANZI, A.; FORNAI, F.; CIUCHI, F.; LASCHI, C. (2015), *The Hydronet ASV, a small-sized autonomous catamaran for real-time monitoring of water quality: From design to missions at sea*, IEEE J. Oceanic Engineering 40, pp.710-726

GRENESTEDT, J.; KELLER, J.; LARSON, S.; PATTERSON, J.; SPLETZER, J.; TREPHAN, T.; (2015), *Lorca: A high performance USV with applications to surveillance and monitoring*, IEEE Int. Symp. Safety, Security, and Rescue Robotics (SSRR), IEEE. pp.1-6

HITZ, G.; POMERLEAU, F.; GARNEAU, M.E.; PRADALIER, C.; POSCH, T.; PERNTHALER, J.; SIEGWART, R. (2012), *Design and application of a surface vessel for autonomous inland water monitoring*, IEEE Robotics & Automation Magazine 19

IDRIS, M.H.B.M.; KAMARUDIN, M.A.A.B.C.; SAHALAN, M.I.; ABIDIN, Z.B.Z.; RASHID, M.M. (2016), *Design and development of an autonomous surface vessel for inland water depth monitoring*, Int. Conf. Computer and Communication Engineering (ICCCE), pp.177-182

ODETTI, A.; ALTOSOLE, M.; CACCIA, M.; VIVIANI M.; BRUZZONE, G. (2018), *Wetlands monitoring: Hints for innovative autonomous surface vehicles design*, 19th Int. Conf. Ship and Maritime Research 1, pp.1014-1021

ODETTI, A.; ALTOSOLE, M. ; BRUZZONE, G.; CACCIA, M.; VIVIANI M. (2019), *Design and construction of a modular pump-jet thruster for autonomous surface vehicle operations in extremely shallow water*, J. Marine Science and Engineering 7/7, p.222

PEETERS, G.; AFZAL, M.R.; VANIERSCHOT, M.; BOONEN R.; SLAETS, P. (2020a), *Model Structures and Identification for Fully Embedded Thrusters: 360-Degrees-Steerable Steering-Grid and Four-Channel Thrusters*, J. Marine Science and Engineering 8(3)

PEETERS, P.; KOTZE, M.; AFZAL, M.R.; CATOOR, T.; VAN BAELEN, S.; GEENEN, P.; VANIERSCHOT, M.; BOONEN, R.; SLAETS, P. (2020b), *An unmanned inland cargo vessel: Design, build, and experiments*, Ocean Engineering 201, 107056

RAIMONDI, F.; TRAPANESE, M.; FRANZITTA, V.; VIOLA, A.; COLUCCI, A.; (2015), *A innovative semi-immersible USV (SI-USV) drone for marine and lakes operations with instrumental telemetry and acoustic data acquisition capability*, OCEANS 2015, Genova, pp.1-10

RAYGOSA-BARAHONA, R.; GARCIA-TERÁN, M.Á.; ENRIQUEZ, C.; OLGUÍN-DÍAZ, E. (2017), *Experimental evaluation of an autonomous surface craft for shallow-water bathymetry*, Marine Technology Society Journal 51, pp.59-67

SAHOO, O.; DOCTORS, L. (2003), *A study on wave resistance of high-speed displacement hull forms in restricted depth*, 7th Int. Conf. Fast Sea Transportation (FAST 2003), Ischia

SCHIARETTI, M.; CHEN, L.; NEGENBORN, R.R. (2017a), *Survey on autonomous surface vessels: Part I - a new detailed definition of autonomy levels*, Int. Conf. Computational Logistics. Springer, pp.219-233

SCHIARETTI, M.; CHEN, L.; NEGENBORN, R.R. (2017b), *Survey on autonomous surface vessels: Part II - categorization of 60 prototypes and future applications*, Int. Conf. Computational Logistics, Springer, pp. 234-252

SETO, M.L.; CRAWFORD, A.; (2015), *Autonomous shallow water bathymetric measurements for environmental assessment and safe navigation using USVs*, OCEANS 2015-MTS/IEEE Washington, pp.1-5

VEKSLER, A.; JOHANSEN, T.A.; BORRELLI, F.; REALFSEN, B. (2014), *Cartesian thrust allocation algorithm with variable direction thrusters, turn rate limits and singularity avoidance*, IEEE Conf. Control Applications (CCA), pp.917-922

WANG, J.; GU, W.; ZHU, J. (2009), *Design of an autonomous surface vehicle used for marine environment monitoring*, 2009 Int. Conf. on Advanced Computer Control, IEEE. pp.405-409

WHITTAKER, T. (2002), *A physical study of fast ferry wash characteristics in shallow water*, MCA Research Project Vol. 457

Edge-based Vibration Monitoring of Marine Vessel Engines

Andrei-Raoul Morariu, Åbo Akademi University, Turku/Finland, andrei-raoul.morariu@abo.fi
Wictor Lund, Åbo Akademi University, Turku/Finland, wictor.lund@abo.fi
Andreas Lundell, Åbo Akademi University, Turku/Finland, andreas.lundell@abo.fi
Jerker Björkqvist, Åbo Akademi University, Turku/Finland, jerker.bjorkqvist@abo.fi
Öster Anders, Wärtsilä Finland Oy, Vaasa/Finland, anders.oster@wartsila.com

Abstract

The strive for autonomous operation of machines, vehicles and ships requires a leap in the level of self-diagnostics and situation awareness. This self-diagnostic does not directly add value in form of increased performance but is however necessary for safe operations. Hence, there is a need for implementing self-diagnostics systems using non-expensive equipment. In this paper, we present the design, implementation and installation of a vibration sensing system in a machine room of a cruise ferry. The objective of this installation was to validate our assumption that machine room monitoring can be achieved using non-expensive components and reach consistency and reliability of data output from this system. The reliability would be reached by redundancy of sensors, and intelligent data fusion close to the sensor nodes using edge computing. The emphasis in this paper is on the practical design and implementation of the system including sensors, cabling, edge computing nodes and on ship storage of data. The implementation of the analytics and sensor fusion will be presented in a later paper. As a result, we present how the system has worked and generated data for the just under 6 months' time the system has been running in the cruise ferry.

1. Introduction

An increased value of the new products and components on the market comes from the digitalization of the market where Industry 4.0 plays a major role. Automation is a major advantage for most of the industries where tools as Internet of Things (IoT), big data and cloud-based analytics help achieve better functionalities of the devices. Yet, all the technologies mentioned generate large amounts of data, which needs to pass through several stages of processing after collection. These include data gathering, data transmission, storage, sending the data to cloud, analysing the data into the cloud or on site, generating reports, reducing or removing redundant data etc. The data that needs to be processed can sometimes reach the limit of storage of the local devices and needs to be either transferred to another platform or reduced. In addition to this, by having so many procedures, there may be a noticeable increase in energy consumption from the system.

Edge analytics describes a computing topology in which information, processing and content collection and delivery are placed closer to the source of this information. Edge analytics can give a major push forward to the current technologies by performing the analytics close to the sensor, *Nastic (2017)*. In this way, the data bandwidth and energy consumption are reduced, improving the overall functionality of the system.

Edge analytics was discussed in several articles or white papers for a long time. Drivers supporting edge application use are deemed to be cost efficient, have low latency, low bandwidth and improved operational efficiency. This marked the beginning of a new era of technology where most of the computations execute locally on edge devices, so that the high load from central servers will reduce. In this way, the central servers will be capable of executing high-level processing such as pattern extraction and content analysis, etc., *Qi (2018)*.

Edge technology using an Industrial IoT solution where a smart sensor is sending data through backhaul communication networks via technologies as Corporate Lan, LoRA, 4G LTE or 5G networks securely to an IoT platform was described in *Asalapuram (2019)*.

Smart condition monitoring applied at "the edge" can help vessels into day-to-day operations by an additional assist to the engines' behaviour.

This paper presents an edge setup, implemented on a cruise ferry travelling in the Baltic Sea between Finland and Sweden, that aims to facilitate the functionality of the ship's main engines. This aim is achieved by observing several factors coming up from analysing the main engine such as running time, vibration etc. The setup was implemented using vibration sensors (accelerometers) attached to four Wärtsilä 12V32 4SA diesel engines and their stands in order to analyse the vibration generated. Our main purpose is to create a system capable of creating diagnostics from the functionality of the main engines of the vessels. This way, during the time when the vessel is on voyage, engine raw data is analysed on site, and important insights are provided to the vessel crew in real time. Other plans include gathering the data from the engines in order to do long-term analysis and performance monitoring of the engines (e.g. anomaly detection).

2. Background and related work

The purpose of our experiment is to improve the situational awareness in the engine room by applying a sensor system using edge analytics for monitoring the main engines of a cruise ferry. Throughout the research we made, the number of related papers to the experiment were on machinery health monitoring, situation awareness, and maintenance solutions. Relevant related work is how the systems are being used and next is an overview of how sensors and sensing systems are working in their environments.

2.1. Situation awareness and anomaly detection of sensor data analysis

Situational and threat awareness are usually achieved from fusing information of the current system from sensors with signatures of threatening and normal processes, *Van den Broeck (2011)*. Users can predefine lists of normal procedures and abnormal procedures when conclusions are being generated from the raw data analysis so that unnecessary alarms will be avoided.

Information fusion is a key feature in providing decision support, *Roy (2001)*. It includes many components such as theory, techniques, tools for analysing the information from different sensors that help on different purposes such as predicting future behaviour, *Dasarathy (2001)*.

Sensor data acquisition can generate large amounts of data that sometimes needs to be analysed by a decision maker. Raw data can be transposed into graphical interface by doing several calculations (e.g. Fast Fourier transformation). In this way, specialists can act into the situation awareness making valuable decisions. Nowadays, there is still an important need of human interaction in decision making of processes. Adequate visualisation of the data can bring new possibilities to the users other than decision allowing them to interact with the data by getting insights and conclusions in order to come to better decisions, *Riviero (2008)*. Authors claim that the approach produces satisfactory outcomes as single attribute anomalies can be discovered. Hence, there were no user tests performed for proving the effectiveness of the methodology.

2.2. Condition-based health monitoring of machinery

Condition-based health monitoring of machinery on cruise vessels implies collecting data from sensors and creating analytics from anomaly detection algorithms. The data collected is usually sent to some central servers located onshore for analysis. Sending large quantities of sensor data readings to shore is often challenging. Machinery Health Monitoring (MHM) can be conducted using deep learning in order to solve the problems related to bandwidth. *Asalapuram (2019)* implemented Convolutional Neural Networks in order to make predictions on Smart Health Monitoring of the electric induction motors. Their approach is using data-driven deep learning in order to classify whether a motor is running in healthy or faulty condition. After the raw data is being collected and analysed, on the vessel, important insights are being provided to the engineers of the vessel and in

case there are some serious issues, the Vessel Alarm Monitoring System can be activated in order to prevent other incoming problems. The authors claim that their approach can be implemented to any scenario where equipment is in remote locations, or where is poor connectivity.

Rao (2019) have examined other approaches related to the MHM in terms of power quality problems. They use an industrial internet of things (IIOT) framework, which assists in monitoring, fault detection and harmonic mitigation of the electric power systems on board of the vessel. Their experiment involves collecting electrical sensor data on the vessel, using FFT analysis for decomposing signals into the frequency components, and then calculating the positive, negative and zero-sequence components of the three phases. The generated information helps on fault diagnosis and reduction of total harmonic distortion to the load.

2.3. Maintenance methods for monitoring engine related components

Predictive maintenance is implemented depending on the methodology of the domain that the experiment will be used. It usually has different formats depending where is being installed. The aim of maintenance is to reduce the number of anomalies or failures of the equipment and to help avoiding breakdowns, which can result in larger issues during the equipment runtime. According to *Jimenez (2020)*, the shipping sector will undergo an accelerated development by 2030 since the industry is pushing forward into complex predictive maintenance approaches.

Corrective maintenance or "run-to-failure", *Wilson (2013), Zaal (2014)*, is about fixing the equipment when it breaks. It also means the maintenance that is carried out after the fault recognition and aims in bringing back the equipment to the initial state where it can execute in normal conditions. Corrective maintenance is usually accepted when the failure is not affecting the overall system, *Jimenez (2020).*

Condition-based maintenance (CBM) activities include a sequence of monitoring, inspection, testing, analysis, and related maintaining actions. CBM comes from physical inspections where experts report if there are changes in the engine related equipment attributes such as vibration or sound. Other anomalies can appear from the real-time analysing sensors attached to engines or other systems. Despite the increasing popularity in smart sensors, *Okoh (2013)*, the focus is related to applying smart sensors only on the equipment which has a critical impact on the overall system. CBM can help increase the situation awareness of the overall system being monitored reducing the risk of other related events that can appear (e.g. engines breakdown).

3. Hardware implementation of our edge solution

The experiment started with the search for suitable sensors for measuring vibration of the main engines of the vessel. There were some attempts using Bosch XDK sensor, *Hesser (2019)*. This is an embedded programmable sensor device, and a prototype platform developed to enable IoT for different processes and purposes. The experiment is still on place at "Vaasa Energy Business Innovation Centre" (VEBIC) testing facility from Vaasa/Finland. VEBIC is a platform, which includes laboratories in fuel development and an internal combustion engine laboratory, https://www.univaasa.fi/en/sites/vebic/.

The above-mentioned equipment was not suitable for a cruise ferry due to the design requirement of not relying on wireless communications or battery powered devices. The plan was then updated from using Bosch XDK sensors, into using cable-attached sensors (Texas Instruments Sensor Booster Pack, SBP) for the experiment.

Our experiment on the cruise ferry started in the beginning of March 2020 with the mounting of the SBP sensors, from now on called sensor units (SU, Fig.1), on the main engines (ME), Fig.4. The SUs were connected to Raspberry Pi 4 computers, acting as power units (PU). PUs were placed in control unit (CU) boxes, with two PUs in each CU box, together with SUs connected externally to each PU. There are in total ten SUs with three SUs to the upper PU and two SUs to the lower PU, Fig.4.

The CU boxes were connected to an equipment rack in the control room. The rack holds an industrial Adlink computer, and other components such as a network router and network switch. SBP was used for temperature, accelerometer and gyroscope readings. SBP was placed in a metallic box in order to be protected from several factors such as temperature or humidity. Altogether, they were named sensor units, Fig.1.

Fig.1: Sensor Unit (SU)

The temperature sensor (TEMP007) inside the SUs is used for checking the temperature inside the CU boxes, and the temperature from the sensors attached to the four main engines and their holding structures. The BMI160 inertial measurement unit from the SBP board is a 6-axis digital accelerometer and gyroscope sensor that measures the sensor orientation, and acceleration. Gyroscope readings are used for establishing whether the orientation of the SU has changed. In the same time, accelerometer readings from the 3-axis are extracted for internal calculations in establishing the vibration measurements.

Eight of the SUs have been placed in the following order: two on each main engine of the vessel (one is attached directly to the engine block, and the other is attached close to the first one, on the engine frameset). The two sensors placed on the engine are connecting to different processing units, providing redundancy. The SUs arrangement scheme is visualised in Fig.2, where the I2C connection is shown.

The I2C bus was chosen because it was supported by both the chosen SUs and the PUs. The clock signal (SCL) and the data signal (SDA) use open-drain output drivers with single-ended signalling. Each SU is connected separately to a PU using a separate I2C bus. At the beginning, we made use of the hardware implemented I2C interface present in the Raspberry Pi for one of the connected busses and software implemented bit banging I2C interfaces to connect the rest of the busses (Software buss switching at fixed output time). However, it seems that the I2C hardware interface on the Raspberry Pi has an internal error, which prevents it from doing clock stretching properly. Therefore, we decided not to use the hardware-implemented interface at all.

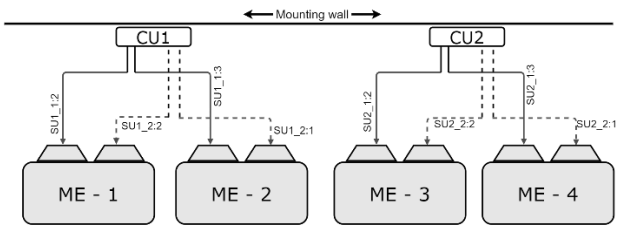

Fig.2: Montage scheme of the sensor units to the main engines of the vessel

Raspberry Pi 4 were used as the processing units (PU), were some of the calculations are being made. Four PU were used with two in each CU. Each PU connects to either two or three SUs depending on the case. The upper placed PU had three SUs connected, where two are mounted on the engine and the engine's frame, and one is used as reference for checking the temperature inside the CU, together with the reference measurements of acceleration and gyro coming from the vessel's movement.

Each CU contains two PUs, an SU, a network switch, a circuit breaker, and a switching mode power supply (CU-ZYXEL), as in Fig.3.

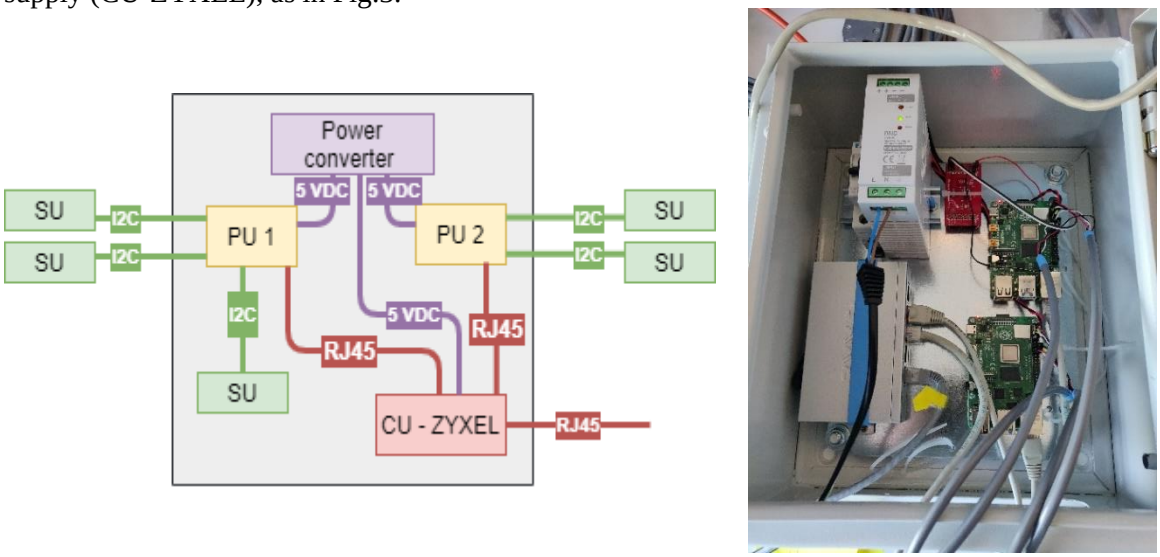

Fig.3: Edge Control Unit (CU) and electric schematic

The CUs were connected to the Adlink industrial computer used for data transmission, processing, and storage. Attached to the industrial computer is a network switch in turn connected to a router used for data transmission to the shore.

Daily reports and status information are sent over 4G mobile network when available, or HF radio otherwise, i.e., on open sea. The data is sent from the ship to KNL networks, https://knlnetworks.com/knl-features/radio/, cloud system using the KNL radio's Python API. The data is then polled at regular intervals to a cloud-based server where the reports and other messages are stored and forwarded as emails. This transmission is file-based, so we also have a two-way connection over a VPN through the ship's own internet connection for development and monitoring purposes.

In Fig.4, we visualise the overall schematic of our experiment together with the cable lines between the engines, control room, and deck area. Here you can see the two CUs previously visualised in Fig.3 from where the connection lines leave towards ME 1 to 4. We decided to connect two different sensors on different engines in order to reduce the impact of PU failure. This way we will continue having data coming up from all the engines.

Cables with RJ45 connectors were used for communication using TCP/IP protocols, Fig.4, between PUs and CU-ZYXEL switches, placed in the engine room. The connection continues from the CU-ZYXEL towards the control room, connecting it to the network switch.

Connection between the switch inside each CU (from the engine room) and network switch inside the equipment rack has been created using cable routing towards the deck where the control room is situated. Inside the equipment rack, a network router and an industrial PC (Adlink) are connected to the switch. The KNL radio is placed closer to the deck and is connected to the switch in the rack using a VLAN over the ship's ethernet network. The router is connected to the vessel's internet connection. Using a VPN tunnel, we can then access the system for maintenance, monitoring and configuration. From the KNL radio system we also get GPS coordinates, course and speed of the ship. Those can be used for determining when the ship is moving or when it is situated in the port.

4. Edge software implementation

The software running on the PUs is implemented as three different processes. The sensor data flows through these as a pipeline and is sent over the ethernet network to the Adlink computer. The Adlink computer stores the data. Our software pipeline schematic can be visualised in Fig.5.

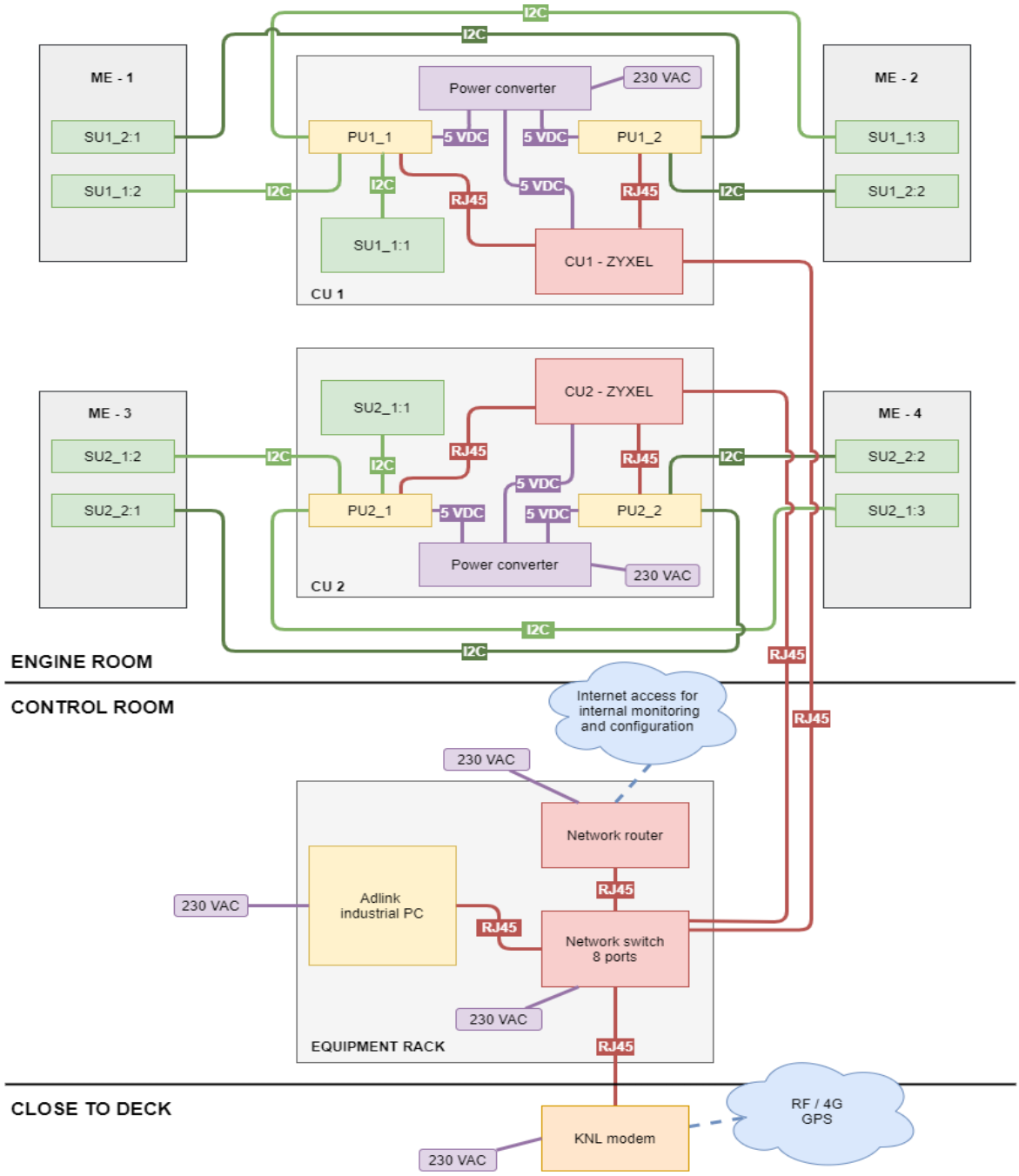

Fig.4: Cruise ferry installation setup

Telegraf, https://www.influxdata.com/time-series-platform/telegraf/, is used for collecting sensor measurements as well as metrics and events generated by the attached sensors. Telegraf has the advantage of compiling into single binary with no external dependencies, and it only requires a minimal memory usage.

Influx database, https://www.influxdata.com/, is a high-speed read and write database where data is written in real-time, and where measurements and results are processed. Tracking and monitoring of real-time and historical data from sensors allow users to get insights of the current situation. The Influx database accepts data points from Telegraf in a so-called line protocol format. This format contains measurement name, tags and field values as well as a timestamp.

First, a reading software initializes the sensor device on a specific I2C bus. After, the initialization the

software reads measurements from the accelerometer at a frequency of 400 Hz. The reading software is implemented as a loop, which in each iteration reads one measurement and sends it out on a socket to Telegraf in the Influx line protocol format. The reading software process is implemented in-house using C and C++.

The Telegraf process receives the data sent from the reading software and sends it via the network to the Influx database on the Adlink computer. Some of the sensor data is diverted, and a data processing and augmentation script - FFT.py is regularly called on a batch of accelerometer measurements to calculate the frequency of the vibrations using FFT, mean, max, min, variance etc. The FFT.py process feeds the calculated frequency components back to Telegraf, which sends it to another Telegraf instance on the Adlink.

On the Adlink, a Telegraf process forwards some of the input data to an Influx database. Since it was not practical to log all the raw data to Influx because of performance reasons, we decided to log the raw data using "s6-log". We configured "s6-log" to split the input into files based on the source of the measurement. On log rotation, the logs are compressed using Z standard, https://en.wikipedia.org/wiki/Zstandard.

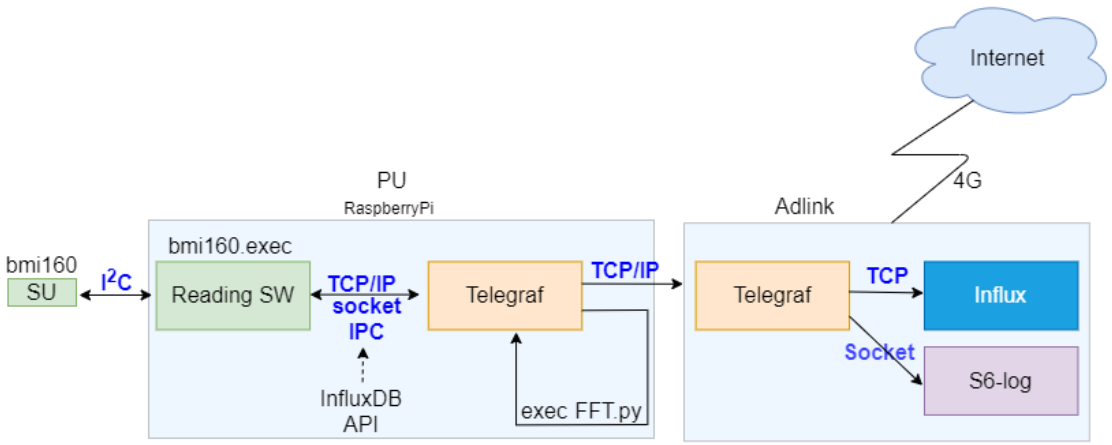

Fig.5 Edge software pipeline

5. Results

The experiment is up and running since mid-April 2020. We had some constraints on installing our equipment due to the time restrictions as the cruise ferry had a tight schedule for when it is in harbour. The entire installation took approximately three weeks because there was only enough time one day per week due to the ferry's timetable.

Fig.6 is a part of a daily report. The report contains data related to the ship location, and analytics about main engines such as vibration energy on three axes, histograms, temperature readings, and spectrograms from the sensors attached to the main engines, and control unit. The report is generated on the Adlink PC as a Jupyter notebook, https://jupyter.org/ and then converted into HTML format. The report is then compressed and sent to a cloud server using the KNL radio, from where it is distributed by e-mail.

Since we mounted the SUs on the engines, we have also recorded data in terms of temperature. A concern was the high temperatures in the places situated on the engines for placing the sensors. However, there have not been any problems related to the temperature. Fig.6 displays the temperature readings during a 24h cycle from September 2, 2020 for each engine. The grey marks indicate the time when each engine has been active. It can be observed that the engine number one was not running on that day. BME280 sensor located inside each SU is used for temperature readings of the main engines. The average maximum running temperature that the engines usually run is 64-68 °C.

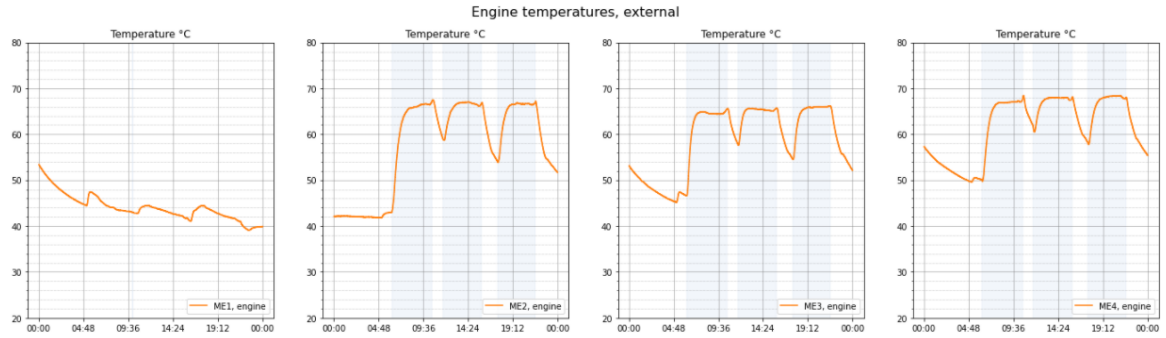

Fig.6: SU temperatures from main engines 1 - 4 engines

The SUs mounted on each main engine help us better understand also the vibration energy (variance of the vibration measurement) of each engine. It can be observed that not all the engines run the same amount of time when the vessel ferry is during the operation time. The ship engines can for example be turned on in order to improve the speed (in case of delays), or for some other reasons such as weather or wave conditions. This can be concluded from Fig.7 where ME 3 has been turned on for a shorter duration compared to the other main engines. Data related to the speed and the course of the cruise ferry is being generated by the KNL radio system, Fig.4.

Fig.7: Runtime visualisation of the main engines using the Influx database UI

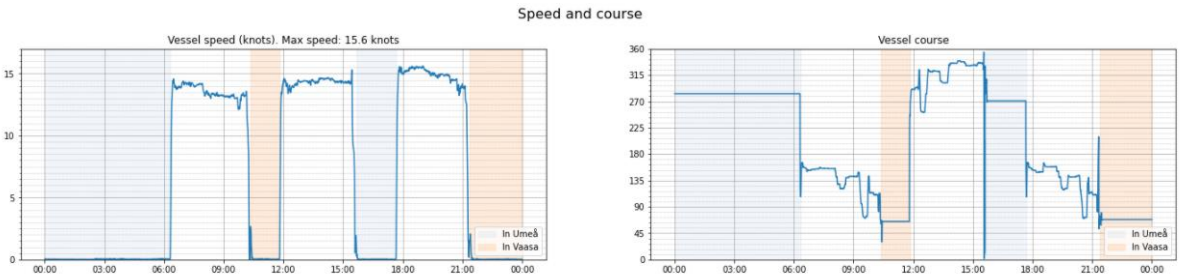

Fig.8: Speed, course and location of the cruise ferry

Fig.8 represents measurements data from KNL radio system in terms of speed and course of the cruise ferry. The vessel speed is between 12 and 17 kn. The course of the vessel varies according to its

position and local conditions. In addition to the speed and course, the KNL radio system offers information about the ferry's location. It can be noted that the cruise ferry had three voyages during that day, and that it has been for two times at the ports in Vaasa/Finland and Umeå/Sweden.

Figs.6, 8, 9 and 10 are part of an engine usage report generated daily for the previous day. From analysing the first plot of the Fig.11, it can be observed that the cruise ferry is having an increased vibration on three axes at the beginning and end of each trip; this is typical behaviour. In addition, there are significant changes in the vibration energy when comparing the three times when the cruise ferry operated that day. The three spectrograms in Fig.12 show the main frequencies of the vibrations of the engine. These are calculated automatically on the PUs and stored in the database. Note that the time scale does not represent the entire day as the other plots do. The frequency with the most intensity is caused by the ignitions in the engine.

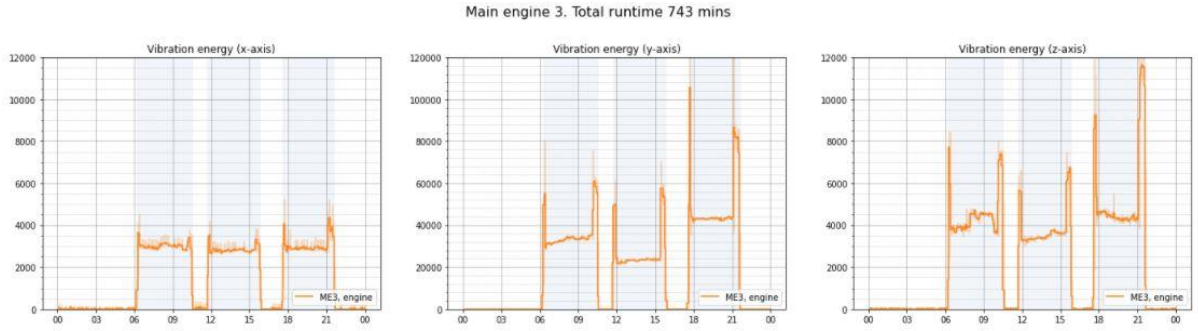

Fig.9: Main engine 3 vibration energy and runtime

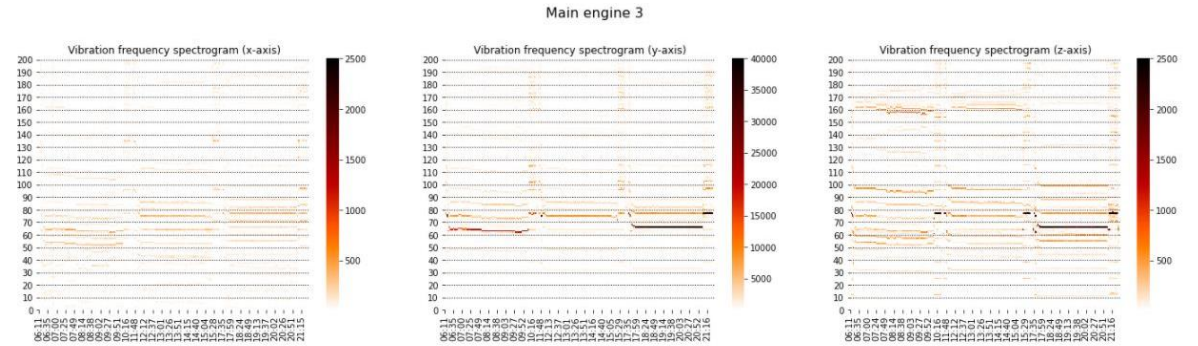

Fig.10: Main engine 3 vibration frequency spectrogram

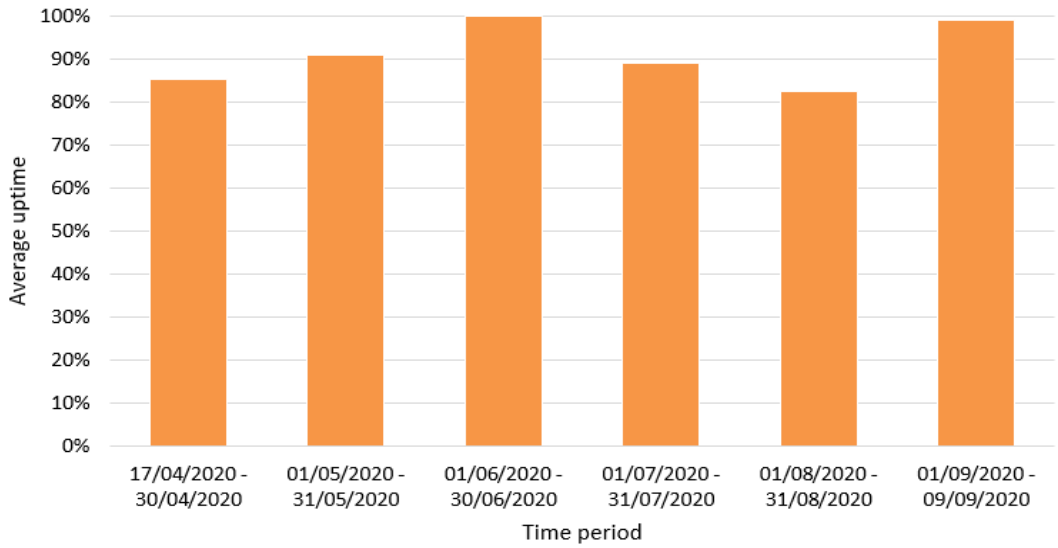

Fig.11 Average uptime of the sensors during each month

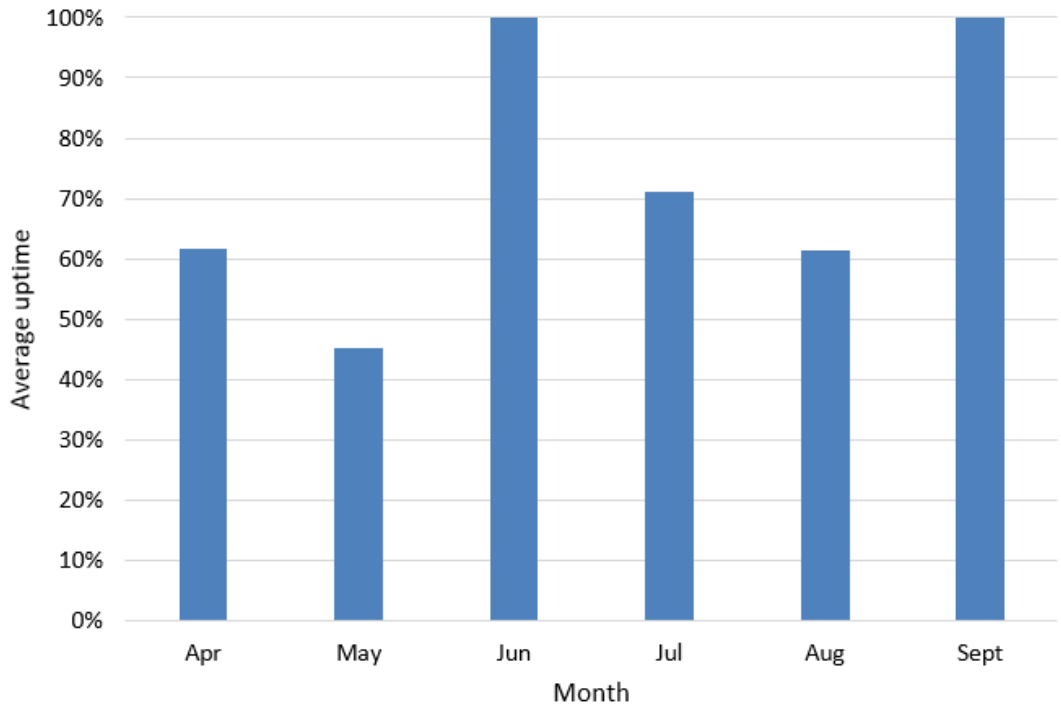

Fig.12 Average working days of the edge system per month

As shown in Fig.11, the total average runtime of the sensors on each month is above 80%, showing a good reliability of the edge-based system. The sensors started recording on 17th of April 2020, when the installation was finalized on the cruise ferry. On the month of September 2020, there have been only nine days of recordings as it has been decided to count the results until that day in order to have enough time for the scientific research on the data.

Fig.12 shows the uptime of the system for the calendar months between April and September. The uptime during the whole test period was is 73%. There were several reasons for why the system did not run so well during April, May, July or August, including further development of the system's software. Those activities were also related to system maintenance, having the sensors shut down for a specific duration of time. Other reasons include restarting the system and performing other optimisation procedures that caused some interferences on the sensor readings.

Table I: KPI on the experiment setup

Maximum temperature recorded on main engines	ME1: 69.1°C	ME2: 69.2 °C	ME3: 67.4 °C	ME4: 71.0 °C
Data generated / day	3.67 GB (compressed text)			
Total data generated	375 GB			
Total running time	102 days			
Uptimes during the total experiment	73%			
Length of cables installed	130 m – I2C connection		100 m – Ethernet	
Estimated man hours to install the system	40 h			
Costs				
Sensor Unit (SU)	Sensor enclosure, cable			40 €
Control Unit (CU)	2 Raspberry Pi 4, network switch, supported electronics, enclosure			250 €
Equipment rack	Adlink Industrial PC, network switch and network router, rack			3.000 €

Some key performance indicators (KPI) of our experiment have been listen in Table I. First, the temperatures on each of the four engines has been listed. In addition, specifications of system performance such as amount of data gathered, running time or total uptime, are shown. Details about the attached equipment have also been provided, together with their approximate costs.

6. Conclusions and next steps

This paper described the design, installation and analysis of an edge-based vibration monitoring system installed on the four main engines of a cruise ferry travelling in the Baltic Sea between Finland and Sweden. The objective was to analyse the reliability of non-expensive sensor and computing system, with the capability of perform data analysis close to the sensors. The use case of this system is to enable unmanned monitoring and increases situation awareness in the engine room.

The first phase of the experiment was the installation of the sensors and computing system, and the collection of information from the system. During the five months of the system has been operational, an uptime of 73% was recorded. However, this includes planned stops and maintenance, where the system was tuned and settings were altered. In fact, during the time the system has been in operation, the hardware has worked as planned, without any major setbacks. The main data recorded is 3-axis vibration data from ten sensors with a sampling frequency of 400 Hz. Additionally, temperature, as well as location, speed and course of the ferry has been recorded.

The long-time objective is to use this edge sensor and edge sensor system in order to achieve increased situational awareness, including anomaly detection and automated system diagnostics. This enables predictive maintenance based on machine learning and AI, driven by edge computing equipment installed close to the sensors themselves.

References

ASALAPURAM, V.I. (2019), *A novel architecture for condition based machinery health monitoring on marine vessels using deep learning and edge computing*, IEEE Int. Symp. Measurement and Control in Robotics (ISMCR)

DASARATHY, B. V. (2001), *Information fusion-what, where, why, when, and how?*, Information Fusion 2/2

HESSER, D.F. (2019), *Tool wear monitoring of a retrofitted CNC milling machine using artificial neural networks*, Manufacturing Letters

JIMENEZ, V. J. (2020), *Developing a predictive maintenance model for vessel machinery*, J. Ocean Engineering and Science

NASTIC, S.E. (2017), *A Serverless Real-Time Data Analytics Platform for Edge Computing*, IEEE Internet Computing

OKOH, P.A. (2013), *Maintenance-related major accidents: classification of causes and case study*, J. Loss Prevention in the Process industries 26/6

QI, X.A. (2018), *Enabling deep learning on IoT edge: Approaches and evaluation*, IEEE/ACM Symp. Edge Computing (SEC)

RAO, K.I. (2019), *Fault Detection and Harmonics Mitigation in Diesel Electric Ships Using IIOT Edge Devices*, IEEE Int. Symp. Measurement and Control in Robotics (ISMCR)

RIVEIRO, M.G. (2008), *Improving maritime anomaly detection and situation awareness through interactive visualization*, 11th Int. Conf. Information Fusion

ROY, J.R. (2001), *Human-computer interface for the study of information fusion concepts in situation analysis and command decision support systems*, Signal Processing, Sensor Fusion, and Target Recognition X. Vol. 4380

VAN DEN BROEK, A.C. (2011), *Improving maritime situational awareness by fusing sensor information and intelligence*, 14th Int. Conf. Information Fusion

WILSON, A. (2013), *Asset management: focusing on developing maintenance strategies and improving performance*, Conference Communication

ZAAL, T. (2014), *Profit-driven maintenance for physical assets*, Maj Engineering Publ.

On Future Strategy and Technology Roadmap of Maritime Industry

Kohei Matsuo, National Maritime Research Institute, Tokyo/Japan, kohei@m.mpat.go.jp
Fumiaki Tanigawa, ASAKAWA Shipbuilding Co., Ltd., Imabari/Japan, f-tanigawa@asazo.com

Abstract

The future strategy and the technology roadmap are organized for the maritime industry in 2016. Some future strategies are taken up in this paper, and an overview of the future strategy, the technology necessary for its realization, and future scenarios according to the strategy are introduced for each future strategy. Future strategic to be taken up are; open shipyards (how to work in future shipyards), ultra-short delivery in shipbuilding, and construction of new marine container transportation. Through future strategies, the paper organizes technology trends of simulation technology, robot technology, ICT technology, etc. for shipbuilding.

1. Introduction

Innovations in social structures and business models in recent years have been born out of seemingly unrealistic ideas and goal setting. On the other hand, rapidly evolving information technology makes them feasible. In this research, we have organized future scenarios and strategic hypotheses of the maritime industry that can be triggered by innovative future technology from the perspective of "how to transform customer value and business models in the maritime industry". Looking ahead to the future direction (20-30 years ahead), we examined the issues that the maritime industry should tackle in the next 10 years.

2. Draft of a strategic hypothesis

2.1. Conditions for drafting strategic hypothesis

We formulated future strategic hypotheses based on the perspective of "how to reform customer value, business models, and social structures in the maritime sector" and "how to strengthen maritime industry and differentiate it from other countries". Future strategic hypotheses were proposed to cover all aspects of the maritime industry, including shipping, shipbuilding, and the marine industry.

First, the conditions for drafting a future strategic hypothesis are discussed as follows. The strategic hypothesis in this study was conceived as a bold and idealistic one to pursue a prospective maritime industry in the future. Rather than developing a deductive vision of the future as an extension of current social and technological trends, we focused on fundamental problems and ideal images, and formulated a strategic hypothesis based on the attitude of the future image we wanted to create. After that, we focused on how to implement the strategic hypothesis, and organized the technology to achieve the hypothesis.

2.2. Analysis of social trends surrounding the maritime industry

In drafting the strategic hypothesis, we first set out the premised social trends. Then, we organized the image of the future society according to the social trend and extracted the cases where it was applied to the maritime industry.

First, we have summarized the current major trends in society as follows: In general, the society of the future is likely to move toward the importance of the existence and values of the "individual" such as diversification, borderlessness, and personalization. Also, with the development of IoT technology, everything will be computerized. We also anticipate that environmental awareness will become stronger and that environmental activities will be taken for granted.

Table I: Summary of major social trends

Major social trends	Specific social movements (keywords)
Diversification	Diversification of society, diversification of way of life and sense of value, society from vertical integration type to horizontal development type. Diversification of lifestyle (increased dual-income work and single-person households), diversification of work styles Understanding of minorities, rise of NPO
Borderlessness	Changes in the concept of nations and borders Mixed industries, the rise of collaborative commons, open communities
Personalization	User experience, experience sharing, equal opportunity. Dissemination of SNS, sending from individuals, commercialization of individuals, prosumers, cloud founding A society that aims to improve quality of life and spiritual wealth from a society of mass production and consumption Mass customization and servicing, From tangible goods consumption to intangible goods consumption
Optimisation	Eliminate waste, make smart Zero marginal cost, “own” to “use”, sharing economy Break away from simplification, continuity, centralization, large scale, specialization
Visualization and digitization	Always-on connection, real-time connection. You can see what you couldn't see before. Data centric, open source, open & close strategy, cloud computing
Expansion of human ability	Fusion of human, computers and machines Evolution of brain science, communication without language
Energy saving and greening	Use of natural energy, zero energy, local production for local consumption, decentralized and autonomous society Natural regression, a society where people and nature coexist in harmony

The direction of the progress of science and technology that causes the above social trends is summarized as follows: These science and technology fields can be fundamental and important drivers of development in maritime technology.

Table II: Summary of major science and technology and impact on social trends

Major science and technology	Impact on social trends
ICT technology	Various services such as smart phones, tablet PCs, google, etc. realize an individual's constant connection to the Internet. In addition, new interface technology represented by VR/AR technology promotes fusion of human and computers. ICT technology renders the concept of distance meaningless. As internationalization progresses, people who have been unable to connect until now are connecting with each other. The SNS service enables the dissemination of information from anyone, anywhere, and the rise of individuals. Inter-personal transactions and marketization of individuals are progressing. It is changing people's values and their views of life.
Big data technology, Artificial intelligence (AI) technology	With the spread of mobile terminals and the Internet of Things connection via the IoT, various things will be converted into data, creating a world where we can see what we could not see before. Large-scale data analysis technology and artificial intelligence technology produce interpretations that exceed human capabilities. The way of thinking about knowledge changes. Personal

	computers with artificial intelligence will enable computers to support every corner of human life. People's lives will coexist with prediction technology and artificial intelligence technology.
Robot technology	Robot technology, together with ICT technology, promotes expansion of human capabilities. Drones and nanorobots expand the active areas and roles of robots.
New materials/nanotechnology	Carbon fiber materials promote weight saving and promote energy conservation. New materials not only promote weight reduction, but also add new functions for ships. This not only gives the product a completely new function, but also has the potential to fundamentally change the form and structure of the product.
Environment/energy technology	Utilization of natural energy promotes energy saving and greening of society. Hydrogen technology promotes the hydrogenation of society. When hydrogen becomes the energy medium of the future, the use of natural energy will be promoted.

Based on these social and technological trends, the future trends in the maritime industry can be summarized as follows: Business players are becoming borderless and it is expected that industries in land will enter the maritime market. On the other hand, the maritime industry is also expanding to land. The way of service is going to be more detailed and optimized overall for “individuals”. In terms of environment, extremely high levels of environmental protection and energy saving performance are required. In addition, the sea becomes familiar to people all over the world. On the other hand, there will be conflicts, as individuals and nations are required to enjoy the benefits equally.

Table III: Summary of future trends in maritime industry

Future maritime industry trends	Overview
Diversification and borderlessness of the maritime industry	The existing division of roles will change and will be operated by various players. The borderlessness of land and sea is progressing, and there may be competition with land transporters and courier companies. The role that ships play in society will also be diversified. It is necessary to think of a new type of ship.
Visualization, optimization and personalization of the maritime industry, Servitization of the maritime industry	In the future, it is expected that there will be increasing demands for the refinement and optimization of logistics, such as dealing with individual transactions and small-lot transportation. It is important to optimize the production of shipyards, including complex marine transportation networks and suppliers. The importance of people's work worth and respect for life is emphasized, and the maritime industry is required to respond to that.
Energy saving and greening of the maritime industry	It seems that the ultimate such as zero energy and non-negative that has no effect on the environment will be aimed at.
The openness of the sea	The borderlessness of the ocean and the maritime industry's response to personalization will make the ocean and the maritime industry more accessible to the general public. At the same time, there will be a stronger demand for fair and comfortable access to and use of the ocean (including marine resources). The sea is more of a place of life and relaxation, as well as a stage for industry and settlement.

In this research, the future strategic hypothesis of the maritime industry is envisioned based on the social trends and maritime industry trends summarized in this section.

3. Strategic hypothesis

Seven strategic hypotheses were formulated in this study. Three strategic hypotheses are introduced in this paper.

- A Concept of future shipyard by ICT and Robot technology (in section 3.1) - Strategic hypothesis to create a new way of working and make shipbuilding a community-based industry.
- Innovation of industrial structure by ultra-short delivery of shipbuilding (in section 3.2) - Why is shipbuilding vulnerable to the external environment? A strategic hypothesis to make a ship that is not easily affected by the market price.
- B-to-C and value-added shipping business model (in section 3.3) - A strategic hypothesis that proposes new ways to use ships and how to carry things.

3.1. A Concept of future shipyard by ICT and Robot technology

To envision a future shipyard that fully utilizes ICT and robotics technologies and the way people work there. Not only to optimize the production of the shipyard, but also to envision how the shipyard can make the work worthwhile, and how the shipyard can create various ways of working and the people who work there, so that the shipyard can shine as a symbol of the region in a new way.

Viewpoint:

- In the future, young human resources will become the seller's market. It is expected that the frequency of employee turnover and job changes will increase. If companies cannot provide attractive workplaces for young people, it will be difficult to attract excellent personnel, or the people who have been trained will leave for other industries.
- Shipbuilding is human-supported manufacturing, but sometimes people are still doing simple or heavy labor that can be replaced by machines. Workers focus on partial tasks and do not know the whole construction process. If we can recognize that we are involved in the whole construction process, we will be able to use our true abilities and be more motivated.
- Shipbuilding work is largely dependent on professionalism, and there is a lack of systematic training methods based on scientific theory. Objective assessment of skill levels is not available, and the contribution to production is not properly linked to the assessment.
- The shipbuilding process depends on human factors, which makes it difficult to optimize production. Many ad hoc solutions are provided, and work procedures are not properly recorded, which does not lead to improvements.
- There is room for improvement at shipyards in terms of working conditions. The workers on-site are in poor work conditions and, unfortunately, there is a possibility of industrial accidents.
- The operation is not fully standardized, and it is difficult to recruit new workers. It is difficult for women and disabled people to work in this industry due to the poor working environment.

Future vision created:

- The shipbuilding process can be drastically reviewed and innovated through the introduction of IoT, artificial intelligence (AI), robotics, 3D printers, and other technologies. By integrating and analyzing information spread across all processes, the entire process of shipbuilding will be optimized. Also, by standardizing shipbuilding operations, the operations will be opened to non-experienced workers and variety of human resources.
- Shipbuilding will employ advanced production management and automation, with the introduction of AI-based construction plans and the use of construction robots and power-assist suits to ensure efficient and safe operations.
- With the use of IoT with wearable devices and sensors, the entire construction process will be

recorded, and traceability and quality will be improved. All equipment in the shipyard will be connected to the workers' mobile devices, enabling them to work and collaborate remotely.

- Shipyard workers will see the whole process rather than a part of the construction, leaving simple tasks to robots and engaging in tasks that utilize their knowledge and creativity. Workers will also be assessed on a quantitative basis and will be paid a fair wage in exchange for their skills, making them feel more rewarded for their work.
- In shipyards with advanced automation and efficiency, there will be minimal noise and vibration problems and a comfortable working environment. The shipyard will be a place where all kinds of people, young and old, men and women, will be able to work in various ways.
- In addition, the use of remote work will also enable various people from remote areas to participate in the shipbuilding process.

Technical issues and mechanism for success:

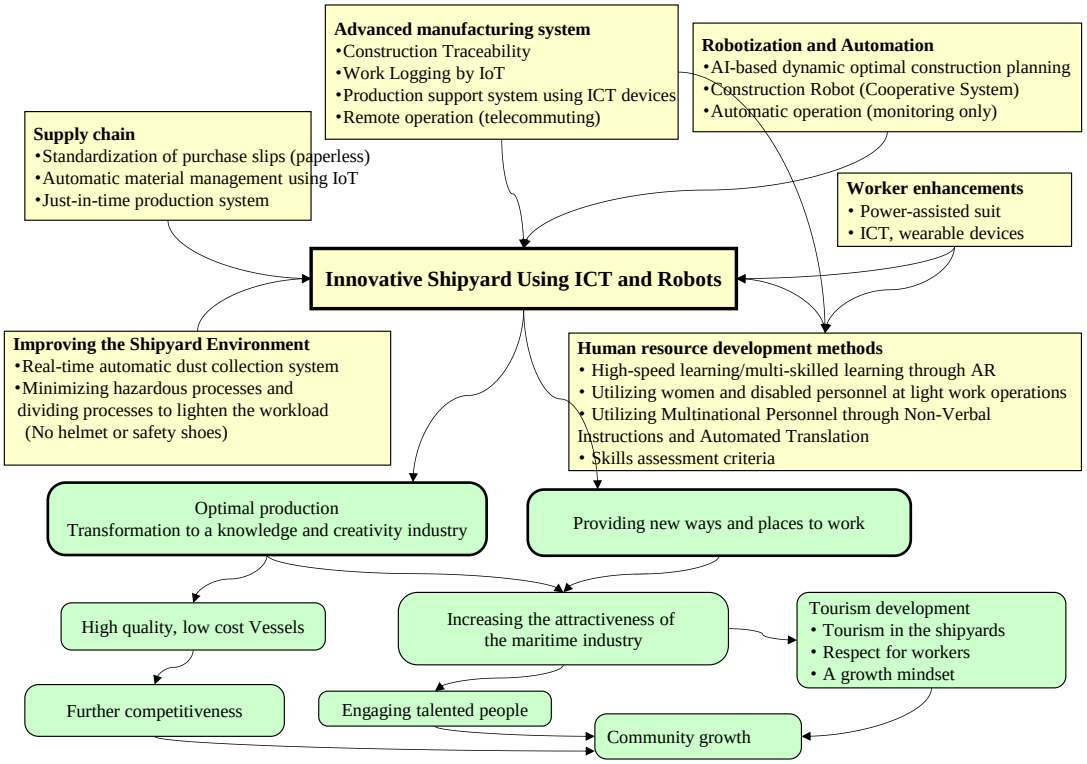

Fig.1: Technical issues and mechanism for success

Technology for realization:

Key technology	Outlines
ICT technology	Use ICT technology to effectively support the work of workers. This will encourage a diverse group of people to work in shipyards. This includes optimization of production planning and production management of shipbuilding processes through IoT and big data analysis technologies.
Technology for advanced robotics and construction	Introduce automation and robots into shipyards to improve productivity and quality in the shipbuilding process and to provide better workplaces and working styles.
Technology for advanced shipbuilding process	This strategic hypothesis suggests to arrange new production processes according to the skill level. It is also important to create a system to accurately record and measure the skill level and job content of workers.

Technology roadmap:

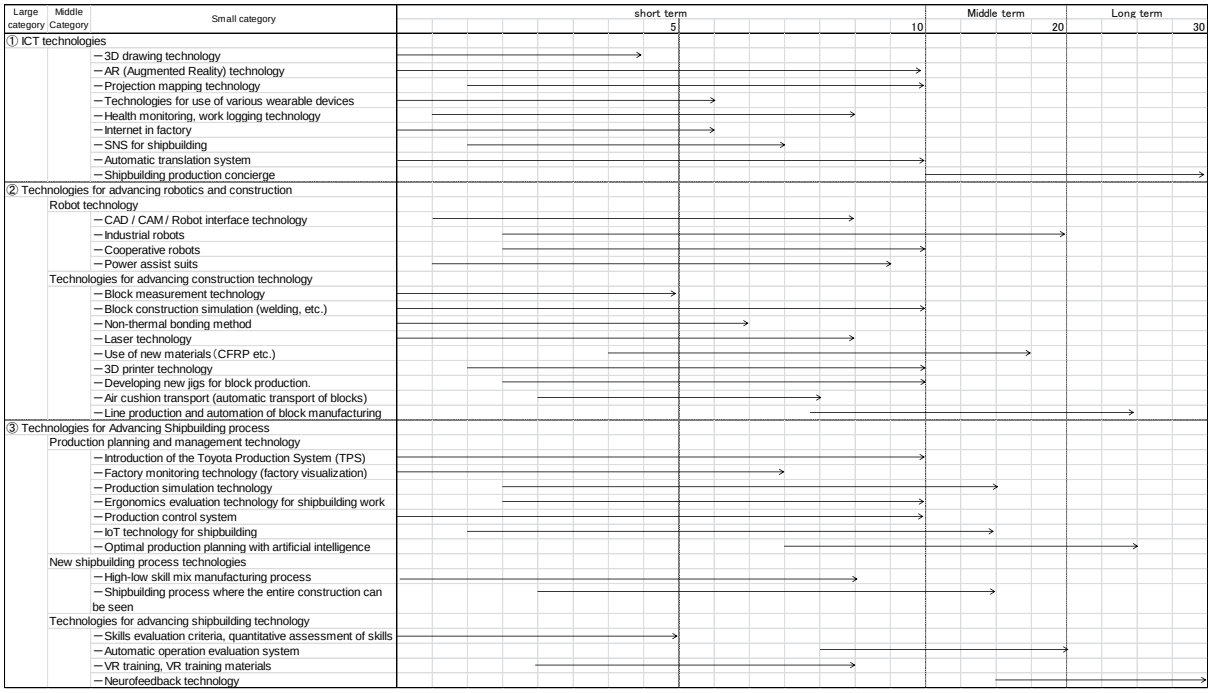

Short-term future image:

- Parts of the shipbuilding process will be visualized and standardized through the introduction of IoT etc. Shipyards will restructure their shipbuilding processes and build a separate work building for part-time workers, where part-time workers can work on simple task such as material installation and processing of outfitting parts in a comfortable environment without wearing a helmet or safety shoes. Shipyards provide the same work environment and conditions similar to those of supermarket, and the shipyard becomes a place of further diverse employment in the community.
- In such shipyards, a system of production planning and production control will be well organized. Precise and detailed production planning and control are essential to allow different people to work in different ways. Work instructions and manuals using ICT devices will also be developed.

Medium-term future image:

- Standardization of shipbuilding work is progressing, and robots are replacing shipbuilding work. Workers will work in cooperation with robots. Simple and heavy tasks are exclusively done by robots, and many shipbuilding tasks are automated using artificial intelligence.
- Shipyards are moving forward with the adoption of IoT and open platforms Workers will have their own wearable devices with shipbuilding-specific apps to receive operational supports and to operate equipment and robots. Personal devices and the equipment in the factory will work seamlessly on the same platform.
- The IoT of the shipyard will record the entire construction process. Workers will have an accurate record of their work, and this information will help to ensure the quality of the ship.
- Workers will be evaluated for the added value they create rather than the hours spent on the job. This not only encourages workers to be more motivated, but also leads to more diverse work styles. People express their appreciation of the fairness and richness of work through social networking sites, and a network of shipbuilding jobs is established in the local community.

Long-term future image:

- These days, most of the design and construction work in shipbuilding is automated due to the accumulated data and AI. Only advanced production control and some special skills will be performed by people. Everyone working in the shipyard will be involved in the entire construction process.
- Ships can be proposed and designed by the ship owners. The client, together with the shipyard, will be able to draw a 3D model of the ship in their minds in a virtual space. Ideally, the person who wants to use the ship should be able to design it freely.
- The shipyard is connected to the head office and the factory, and construction plans are shared and constantly optimized by the head office and shipyard staff. The environment will be safe and comfortable in all weather conditions and there will be no work at high places. Workers work with artificial intelligence (Shipbuilding Concierge) installed on wearable devices. The artificial intelligence will also predict and inform workers of the dangers ahead.
- These future shipyards will become a symbol of the community, with a variety of people participating in shipbuilding. The business of shipbuilding is expected to play a leading role in the community, and it will become important for the shipyards to propose new ship concepts that solve social problems. The industry is also engaged in a variety of non-ship businesses using shipbuilding technology.

3.2. Innovation of industrial structure by ultra-short delivery of shipbuilding

By establishing ultra-short delivery construction technology, the structure of the shipbuilding market will be changed from “orders based on anticipation and speculation” to “orders based on actual demand”. New shipbuilding orders based on actual demand through ultra-short lead-time construction will reduce risks and opportunity losses, which will benefit the management of the customer. The de-factoring of ultra-short delivery will weed out excessive supply capacity of ships and make speculative entry irrelevant.

Viewpoint:

- The global upheaval in the shipping and shipbuilding market has had an unfortunate effect on the shipbuilding industry. For example, shipbuilders tend to take orders for unfamiliar vessels because of the availability of docks or spread out their engineering resources during a recession, while during a boom period, they build new vessels without making special improvements because of high prices.
- The shipbuilding industry is a build-to-order industry, but the reality is that the orders are prospective and speculative. If we look at shipping and shipbuilding from a higher level, the shipbuilding industry is not based on actual demand, but on predictions of the logistics industry. This prospective and speculative market has led to wild price swings in the market.
- As a principle of manufacturing, if there are no constraints, it is ideal to build to order rather than to build on a prospective basis. The automotive industry, for example, has transformed itself over the years from a prospective production model to a make-to-order model to get rid of the risk of prospective production.
- The shipbuilding market becomes speculative because the waiting time for new shipbuilding orders (i.e., from order to delivery) is two or three years, which is far from the normal decision-making cycle of economic activity.

Future vision created:

- Ultra-short construction will transform the new shipbuilding market from one of prospective and speculative construction to one of true build-to-order production based on actual demand. New ship orders based on actual demand will benefit customer management. By encouraging the de-facto construction of ultra-short delivery, excess supply capacity will be weeded out. It

will make speculative entry by emerging nations meaningless, and competitive shipbuilding companies will continue to demonstrate its capabilities in a stable market.

Technical issues and mechanism for success:

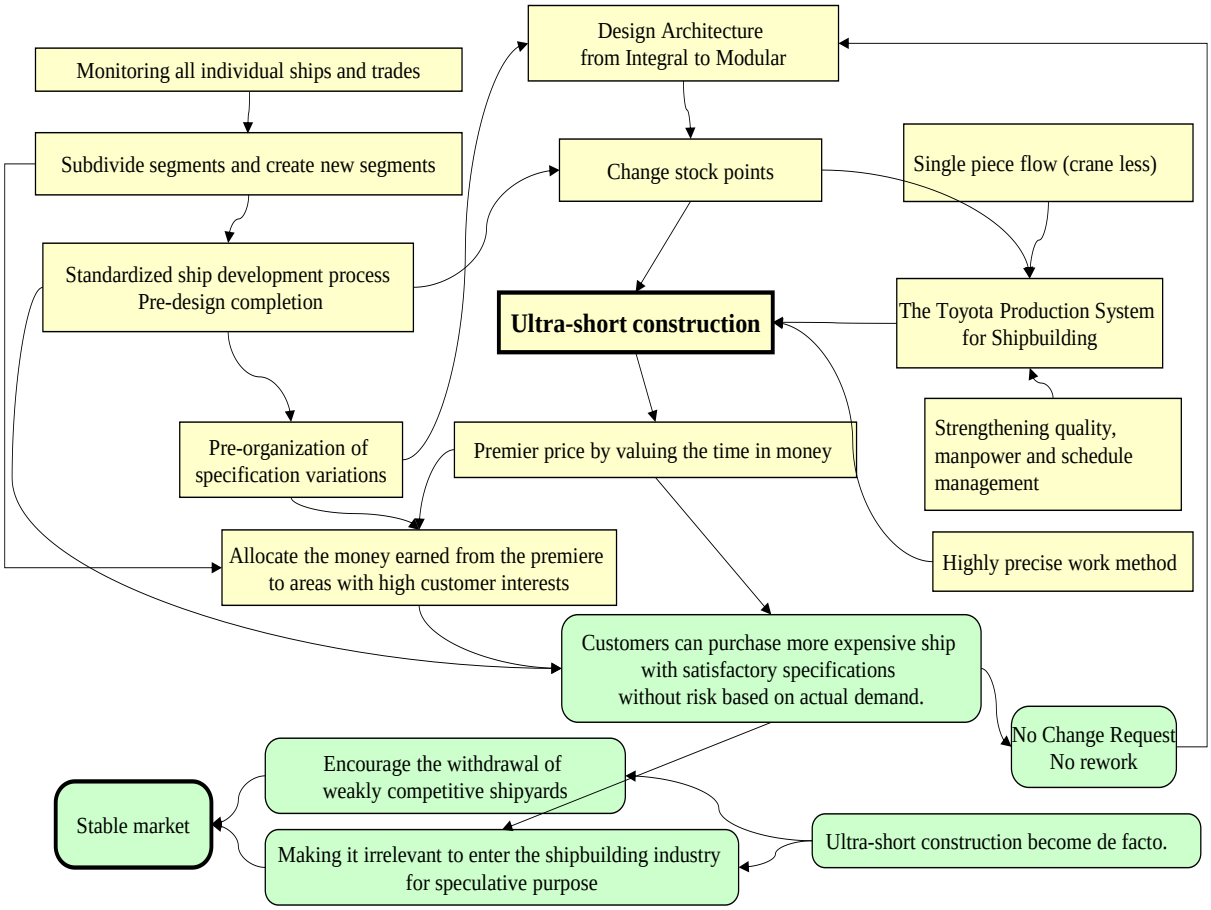

Fig.2: Technical issues and mechanism for success

Technology for realization:

Key technology	Outlines
Technology for a strategic product development	To develop ultra-short construction, it is necessary to select a standardized ship. In order to concentrate management resources, a mistake in the selection of a standard ship must be avoided. It is necessary to analyze the operating conditions of ships around the world and information on cargo traffic on land and at sea to develop strategic products.
Technology for the standard ship development	The ultra-short construction ships will be built on the basis of the standard ships. This is to enable us to allocate design resources and perform design front-loading. In construction, the blocks will be converted to modules and the optimal combination of modules will be used to build ships.
Ultra-short construction technology	Technology for building ships with ultra-short delivery
Advanced supply chain management technology	Ultra-short construction requires an efficient connection between shipyards and suppliers.

Technology roadmap:

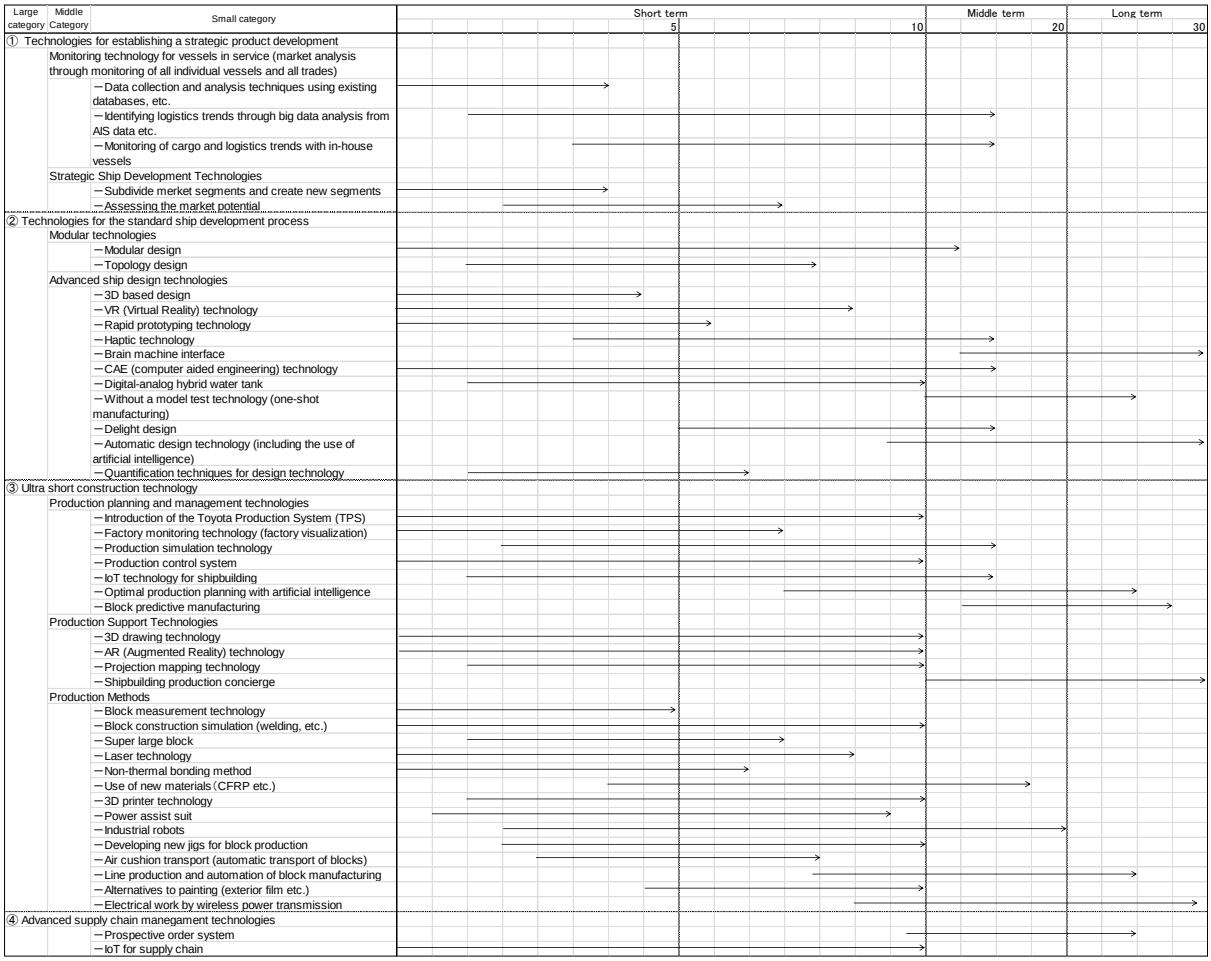

Short-term future image:

- Strategic product developments in shipyards are established and strategic new ships are brought to market by shipbuilders. Strategic product development and standard ship development have enabled shipbuilders to concentrate their design resources, leading to front-loading and pre-design of ships as a standard. This pre-design process enables efficient and scientific control of the manufacturing process. The production plan is optimized, and the construction system is lean and efficient.

Medium-term future image:

- In these days, shipyards can bring new ship models to market at the best time based on the analysis of a vast amount of data from ships in service, satellites and AIS, etc. Some shipyards are launching small satellites for their own use to get exclusive satellite data. As a result, ultra-short construction have become an essential requirement. As construction technologies are innovated, efforts to optimize constructions by automation, robots, artificial intelligence, etc. are becoming more and more significant. Ultra-short construction are achieved, shipbuilding orders will be mostly shifted to a build-to-order system. Shipbuilding is no longer an industry that emerging countries can enter, as it has become a combination of advanced information and a highly efficient manufacturing system.

Long-term future image:

- The process from order to delivery can be done in some month. Sometimes, the construction of ships can even start before the orders are received, as decided by artificial intelligence. The advanced design and construction technologies free us from standardized or modular designs at this stage, and a production system is established which allows us to build any type of ships appropriately. Shipyards propose new ships that solve social problems by utilizing information such as logistics. And, utilizing the obtained information, the shipbuilding industry is also working on businesses other than ships.

3.3. B-to-C and value-added shipping business model

In view of the trend toward smart society, we propose new container transportation service. Specifically, we propose to build a marine container transportation system using smaller containers than the current ones, to improve convenience and efficiency of door-to-door transportation, and to add value of marine transportation.

Viewpoint:

- Current ocean container transportation is standardized in 20- and 40-ft container sizes, but they are too big considering the future trends. It is necessary to build a container transportation system that can handle smaller lots of shipping containers.
- Problems with current container transportation (from the viewpoint of container size);
- There is a growing need for the transportation of small lots of packages that are smaller than the container size. If it is less than the container size, the transportation cost will be high, and in some cases, the transportation opportunity will be lost.
- In the case of small lots of luggage, it is mixed with other cargo. Sorting work is required at ports and warehouses, which not only costs money but also increases the lead time for transportation.
- If small lot container transportation becomes established, it will encourage momentum for individual parcel transportation, and diversification of container transportation and development of various new services can be expected.
- New technologies that make this possible are becoming more and more practical. It is high time to review the container transportation system.
- Along with the introduction of autonomous ships, we can expect the maritime industry to respond to B-to-C and C-to-C shipping and to transform itself into a value-added maritime industry. This will enable the maritime industry to contribute more directly to the society. The maritime industry may create new social innovations.

Future vision created:

- Envision the next generation of container transport and container ships. To develop a transportation system that can flexibly handle small-lot cargoes, in particular, develop smaller containers than the current containers.
- A small container can be mounted in the current container. For example, by specifying the size as 5ft x 4ft x 4ft, it can be mounted in the current container without any gaps.
- Develop a new container ship that directly carries a new type of small containers.
- This will make it possible for ocean container transportation to handle small lots of small sized containers. Small lots will be handled per container, which will increase the convenience for customers. It will be handled in container units up to the end of distribution. Door-to-door transportation by containers and self-contained containers occur.
- Small lot sizes and the handling in individual containers eliminate the need for co-packing and simplify the sorting and cargo handling process at ports. Shorten logistics lead time.
- It will also encourage diverse and efficient transportation. There will be various types of transport services (slow, local, ultra-high quality, etc.) depending on the cargo status.
- Container transportation of small lot cargo enables individual cargo handling. Contribute to

the realization of the concept of adding value during marine transportation. Since it is a small container, it is easy to handle the container on board. In the future, container sorting, transshipment of luggage, customs clearance, and distribution processing during inboard transportation may be realized.

Technical issues and mechanism for success:

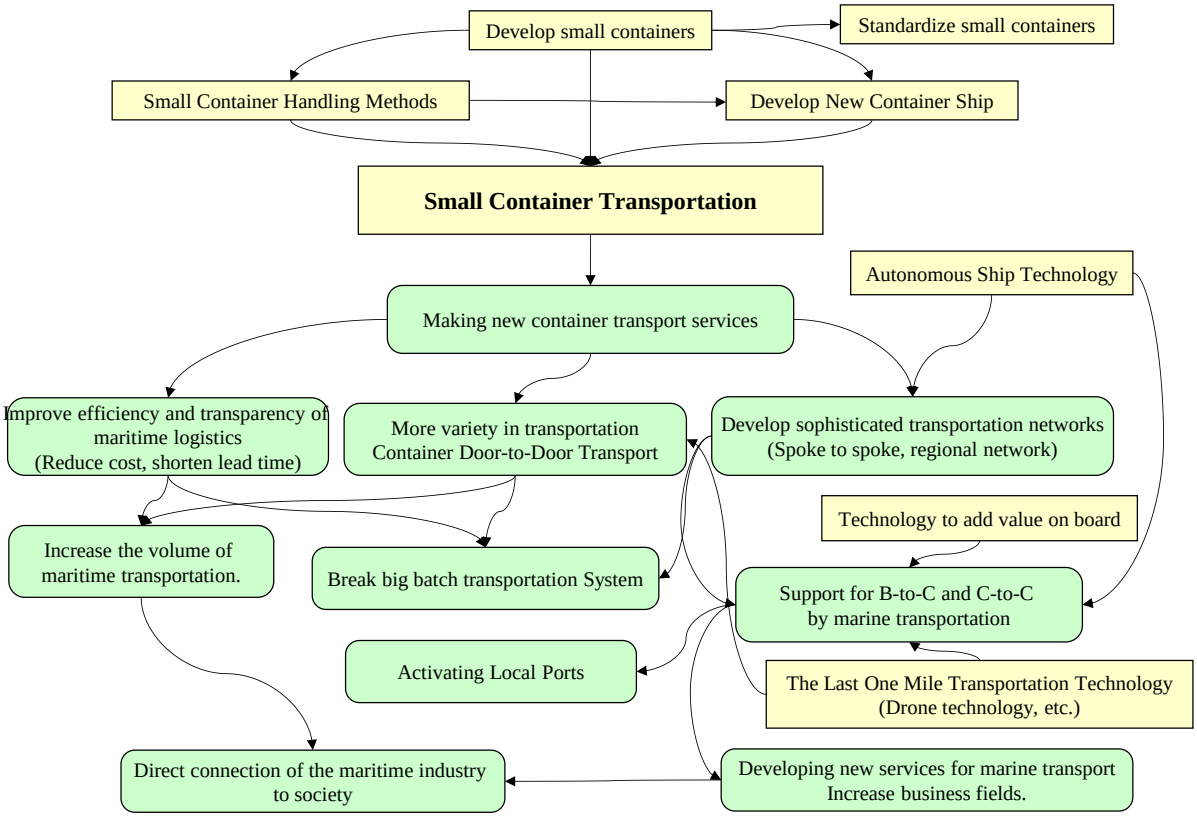

Fig.3: Technical issues and mechanism for success

Technology for realization:

Key technology	Outlines
New container transportation technology	Develop and standardize containers smaller than 20 or 40 ft. and implement new container transportation systems. Develop a small container and consider how to handle it on board and in the port. Consider a new container ship that can directly load small containers.
Expanding marine transportation services with new containers	Construct new marine container transportation networks using new containers. Considering the emergence of autonomous ships in the future, we will review the current hub and spoke transportation system and consider BtoC and CtoC business for marine logistics. In addition, we will consider interface technology with land using drone technology.
Adding value technology	Increase the value of marine logistics by sorting cargo, customs clearance, distribution processing and production on board of new container ships.

Technology roadmap:

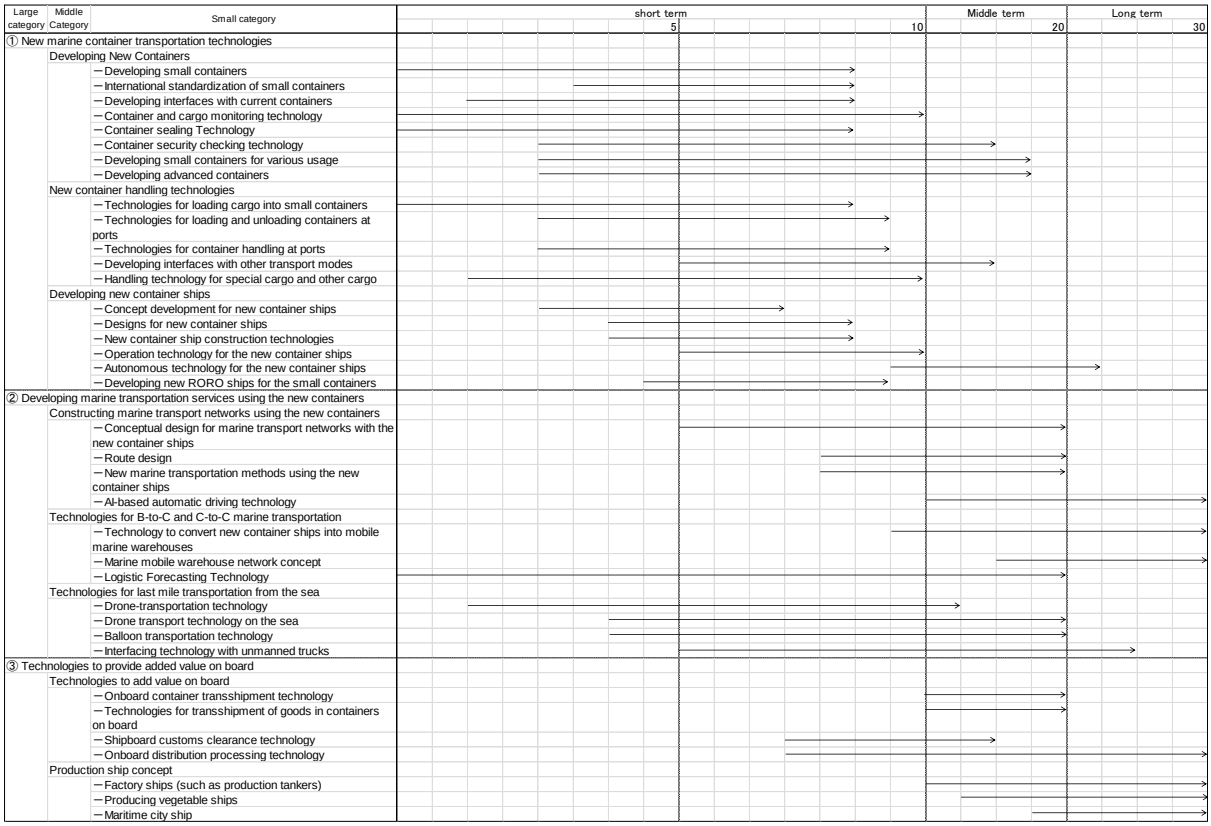

Short-term future image:

- Smaller containers proposed will become more popular, and smaller lot sizes will be handled more flexibly and efficiently. This will increase the convenience for shippers and increase the volume of marine container transportation. New types of container ships which can carry small containers directly on board will be developed.
- As small container transports become more popular, a variety of marine container transport will be available. There will be ships that carry slower but at lower prices, ships that carry at very fast speeds, ships that operate in niche locations, and ships that offer special shipping arrangements. The focus of business for shipping and shipbuilding companies is shifting to providing new transportation services.
- Customers (shippers) will load and unload cargo into and out of containers by themselves as small containers are becoming their own. Door-to-door transportation by container becomes widespread. When sending packages, customers search the WEB for a transportation service that suits their tastes. Customers will be able to check the availability of ships in real time and load packages directly on container ships (a world where shipping companies and shippers are directly connected). Sea transportation will be visualized, and cost transparency and optimization will be realized. Visualization of containers and packages in transit will be put to practical use using IoT technology.

Medium-term future image:

- Next-generation feeder container ships will become autonomous ships using autonomous technology, which will advance maritime transport. Next generation autonomous feeder container networks will cover all of Japan and the Asian regions (construct regional container transport networks).

- For each small container, the logistics work that was previously carried out on land will now be carried out on board (the type of service can be handled on a container-by-container basis. The small container makes it easier to handle on board). Specifically, container sorting work, container baggage sorting work, customs clearance work, distribution processing work (inspection, labeling, picking, etc.) will be performed on board.

Long-term future image:

- More precise marine container transportation and adding value on board will promote not only BtoB transport, but also BtoC and CtoC.
- The next generation of autonomous feeder Container Network will develop not only for transportation between destinations, but also as a mobile warehouse for daily commodities, etc., which will patrol all around the coastline to build a supply network for society. Unmanned trucks, drones, and logistics marketplaces will be used to deliver goods directly from the maritime warehouses to consumers on land.
- Logistics at this time are so advanced that it has become commonplace for people to get everything from all over the world in the shortest time. Even in the cities, we can enjoy local foods in almost the same conditions as they are available at their origin. We can enjoy the latest products and hottest sweets even in rural areas. Everyone will have access to the authentic stuff. Logistics will carry not only goods but also things. In a world where distance constraints have been significantly lifted by logistics, the problem of disparity between cities and regions is a thing of the past. Universal services will be realized, and people will live wherever they like according to their tastes and lifestyles.
- All services will be optimized for the individual. In such a society, the purchase of goods is also ultimately customized for individuals. Products are customized onboard and delivered for the final consumer. Ships will evolve into a social platform that not only transports and stores, but also manufactures and processes goods. When production activities at sea become active, the idea of moving the place of life not only on land but also at sea may come out.

4. Conclusion

In this paper, three strategic hypotheses are introduced. It is necessary to conduct interviews and other researches on each of the strategic hypotheses to further examine their validity, usefulness, priority, and feasibility. Technology development is often preceded by technological seeds. On the other hand, it is increasingly important to conceptualize a strategy based on a higher-level view and a larger vision, and to develop business and research and development in accordance with that strategy.

Acknowledgements

This work was supported and funded from Japan Ship Technology Research Association (JSTRA). I would like to thank the members of JSTRA.

An Electrified RIVA Powerboat – Optimised

Sven Albert, NUMECA Ingenieurbüro, Altdorf/Germany, sven.albert@numeca.de
Rodrigo Corrêa, NUMECA Ingenieurbüro, Altdorf/Germany, rodrigo.correa@numeca.de
Thomas Hildebrandt, NUMECA Ingenieurbüro, Altdorf/Germany, thomas.hildebrandt@numeca.de
Stefan Harries, FRIENDSHIP SYSTEMS, Potsdam/Germany, harries@friendship-systems.com

Abstract

This paper investigates the hydrodynamic performance of a classic wooden powerboat, the RIVA Junior, using CFD and driven by an environmentally friendly electric motor. The original hull shape is parametrised for variation in an optimisation chain: several operating points and various objectives are considered, aiming to model different operational profiles of an electric propulsion. The goal is to derive hull design trends for both highest speeds for a given power, but also maximised range using the limited electric energy, and of course the trade-offs in between.

1. Introduction

Tackling climate change is one of the key challenges in the upcoming years, and likely even decades. The need to switch from fossil energy to renewable ones is a fact that all industries feel, through all branches. One of the most promising players in greener energy is the electric drive, slowly starting to replace combustion engines in a lot of applications, ranging from cars to even aircraft. In the ship building industry this trend seems to be picking up also, and that is especially true for smaller vessel, like private pleasure boats. Also, regulations on inland waters are continuously increasing in terms of pollution, noise and maximum number of allowed (conventional) craft. Here electric propulsion is often the only option to get the pleasure of a motorboat.

The main challenge here is obviously the battery: energy density is increasing each year with development of new types and materials, but there is still a huge gap compared to fossil fuels (far more than one order magnitude). On the other side, electric propulsion has huge advantages in aspects like everyday use (e.g. greatly reduced maintenance needs) or even operation (large torque at low RPM is often very favourable). Hence in all electric propulsion systems the key trade-off is always the battery capacity against its weight, which in the end often leads to power versus range.

Speaking of trade-offs, optimisation instantly comes to mind. Exploring possible designs options and strategies, for example the variation of a vessel hull shape, or the variation of motor power and battery size directly during the design process will in the end lead to a better understanding of the boundaries and to a better product, when executed correctly that is. And speaking of the design process, modern numerical methods like CFD can give very accurate results for even complex flow problems and a deep insight into the physics, while allowing a close-to-real-world modelling.

These ingredients form the basis of this work: optimisation of a small pleasure craft utilising electric propulsion. We presented a first optimisation at the HIPER 2016 (Powerboat in the Cloud), but of course there have been major changes and improvements in the meantime. However, we picked again Carlo Riva's Riva Junior from the 1960s, a time-less design cut out of wood. Also, it is a planing boat, which increases the challenge for CFD when compared to a typical displacement ship.

2. A short description of the key ingredients

2.1 RIVA Junior and operating conditions

Object of interest is the RIVA Junior hull, a hard-chine motorboat with a single propeller and rudder. The Junior was considered the entry level design of the Riva powerboats, and the total length of the base geometry is close to 6 m. A key goal of this study is to investigate a large design space, meaning

both a great variability in hull shapes, but also in terms of operating conditions. With the electric drive and its battery challenge in mind, two displacements are investigated (1 m^3 and 1.2 m^3). The idea is to model two powertrain versions (motor, controller, battery) and find the best-possible in terms of speed and range. Furthermore, a large range of speeds is considered, covering the full operating regime:

1) 5 m/s: A slow full-displacement mode which might be used near the marina, when aiming for a relaxed ride only, or to save battery to come home safely.
2) 20 m/s: A high-speed ride for maximum pleasure and adrenaline.
3) 12.5 m/s: A moderate speed mode in between for the rational driver.

This leads to six operating points per design, which is quite an effort for a high-fidelity CFD simulation with motion coupling and free surface modelling. Some strategies to speed up will be given in the following chapters.

2.2 Parametric modelling and simulation ready CAD

A complex geometry like a planing hull requires a powerful modelling tool, which is CAESES® from FRIENDSHIP SYSTEMS GmbH, https://www.caeses.com. The full description of the parametric model can be taken from our 2016 HIPER paper, since the parametrisation showed very good results it was unchanged. This time the overall boat length is also subject to change, albeit in a small range (±0.35m). Still we wanted to investigate the impact of this presumably strong parameter. This leads to a total of 10 free parameters, which is a quite low number for the geometric variability it provides, as can be taken from Fig.1. This is a key point, as an increased number of free parameters largely increases the optimisation costs.

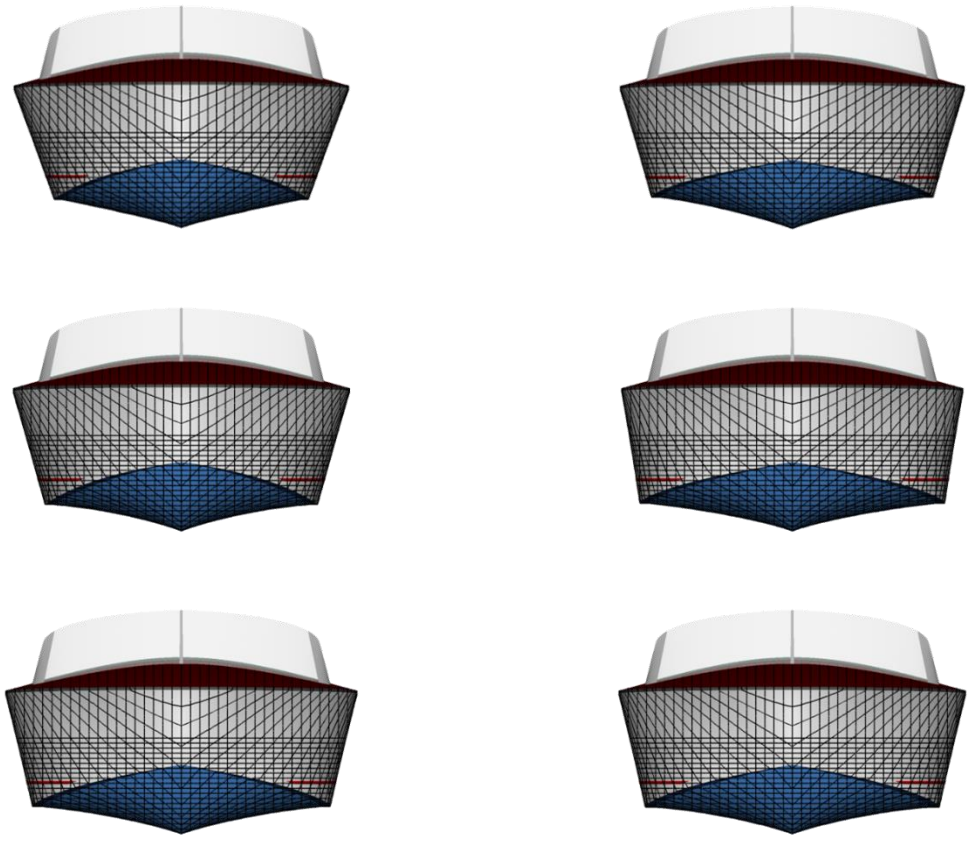

Fig.1: Variants generated by changing a sub-set of ten parameters

To maximise workflow stability several very useful features of CAESES® are utilised. First, the

surface model of the Riva hull is triangulated, with the accuracy easily adaptable locally and globally. The CFD domain (a box surrounding the hull) is also created in the parametric modeller and the Boolean operation is performed on the STL level. Finally, stitching of all surfaces ensures a fully conformal and watertight representation of the domain. An indication of the step from surface to final STL tri-mesh is given in Fig.2. Using a so-called coloured STL all relevant features like the spray rail, transom, upper and lower hull or the bounding box faces can be exported via a defined name, which is important for the meshing and pre-processing of such automated workflows.

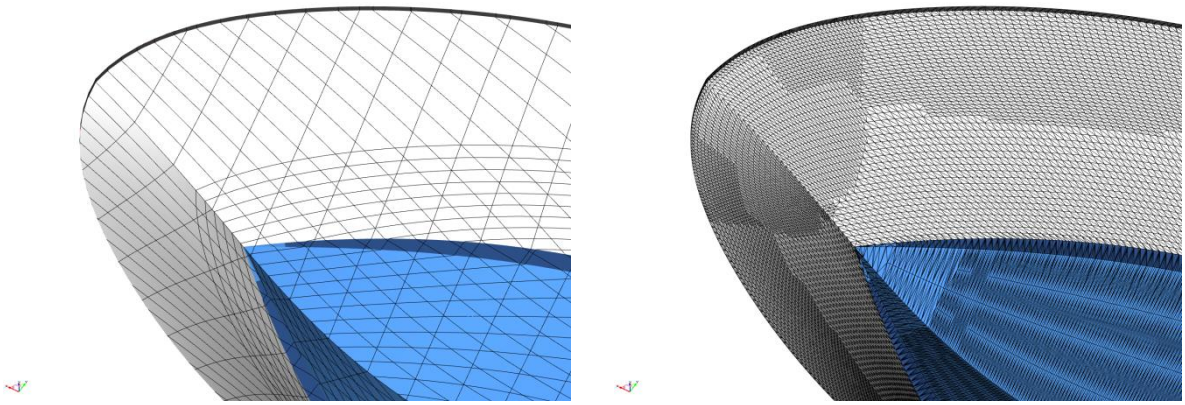

Fig.2: Surfaces and watertight tri-mesh approximating the surfaces

2.3 Meshing

The meshing is done in NUMECA's HEXPRESS™, http://www.numeca.de, which generates a fully hexahedral unstructured grid with hanging nodes. It allows granular control over the cells distribution to achieve the necessary numerical accuracy where needed. Prominent regions are e.g. the spray rail or the transom, which is completely dry in high-speed operation and hence requires a fine spatial discretisation. Using an inflation technique, the Euler mesh is moved from the solid boundaries to increase space in this so-called buffer layer. Then viscous layers are inserted with a defined first cell size and stretching ratio, ensuring an adequate y+. Some impressions of the mesh are given in Figs.3 and 4. The CFD-experienced reader will directly stumble over the missing discretisation along the free surface. For accurate free-surface modelling a fine layer of cells is required perpendicular to the water surface, but in our case these cells will be generated directly in the flow solver using an adaptive grid refinement strategy, see the chapters below.

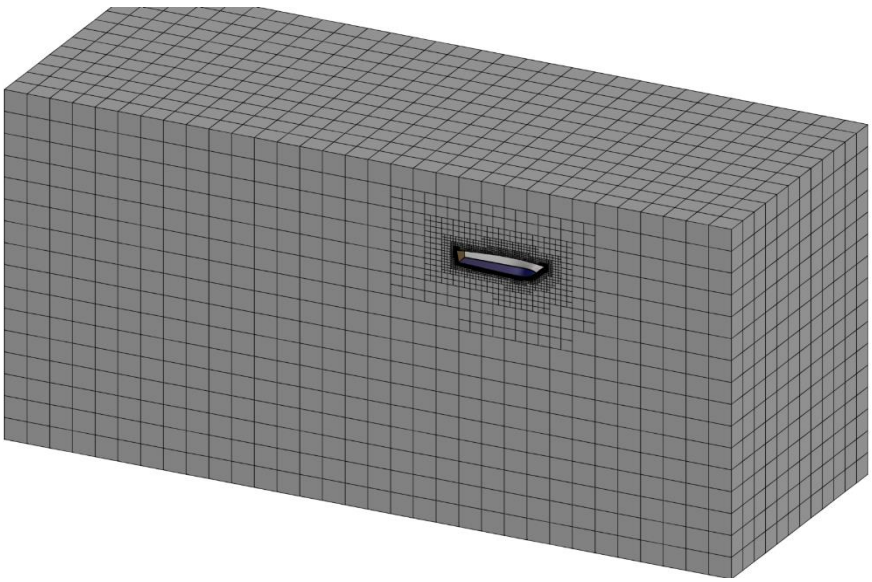

Fig.3: CFD Mesh: high-quality hexahedral grid with suitable regions of refinement near the vessel

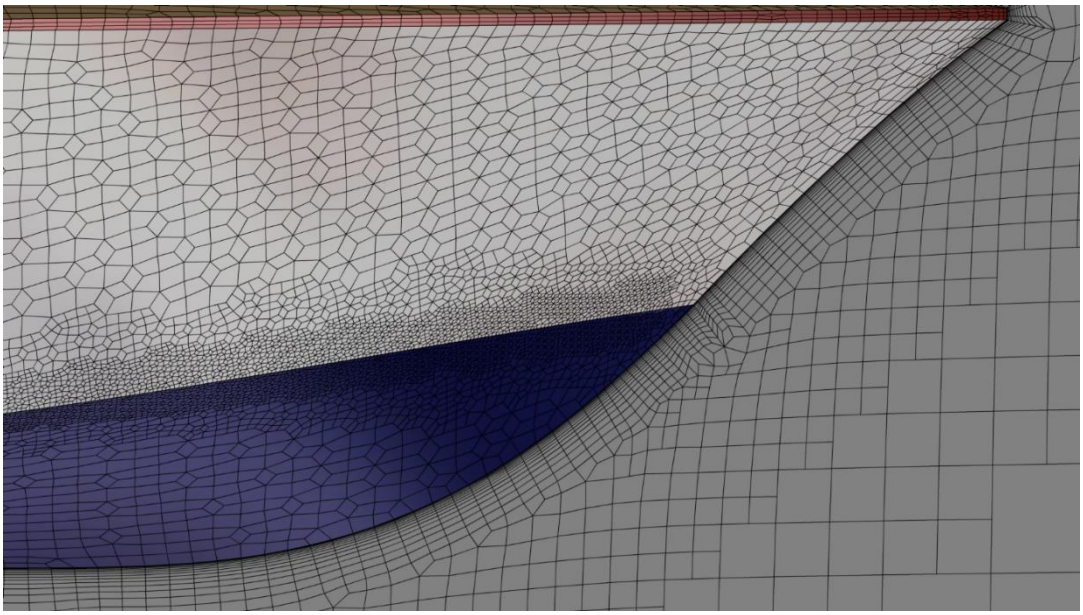

Fig.4: Close-up of the viscous layer along the hull with fixed first cell size, large number of layers and a smooth transition into the Euler mesh

Mesh dependency is investigated using the base design. Since quite a few designs are foreseen in the optimisation, and on 6 operating points, each extra cell will sum up to a quite large difference in total turnaround time. The final mesh without free surface grid refinement consists of 420k cells, including the high-Reynolds viscous layer. Overall, the geometry is not very complicated (from a meshing point of view), hence a quite coarse Euler mesh (around 160k cells) suffices to capture important features like spray rail, bottom surface and transom edge. The remaining cells (260K) are then placed in the boundary layer. On top of this comes the adaptive grid for the free surface and its bow and stern patterns as well as some spray. Strongly dependent on the vessel speed and the design this then leads to a final average mesh size of 700k cells.

A comparison with higher Euler mesh discretisation and a finer (still high-Re) viscous layer, up to 1M cells without the free surface, shows an acceptable difference in terms of the total resistance and its pressure and viscous components. And as always with numerical optimisation, all design variations are treated equally, and the trends are most important, and absolute accuracy comes only second.

Finally, all NUMECA software can be run in batch mode and controlled via a Python API, which is mandatory for automatization. A dedicated yet flexible class module is used to handle all the meshing steps, from geometry import to mesh resolution definition depending on geometrical features, viscous layer insertion and mesh export.

2.4 Pre-processing and some solver details

NUMECA's FINE™/Marine is used as flow solver, developed at ECN in Nantes, France. A detailed explanation of the solver can be taken from the references, following are just a few key features. It is a dedicated CFD system for the marine engineer, allowing highly accurate free-surface modelling and featuring a 6-DoF body motion solver. FSI-capabilities, cavitation and transitions modules capture even more physics if required.

An adaptive grid refinement technique (AGR) is fully integrated, which adapts (that means refines or de-refines) the mesh during runtime, both in space and time. Several criteria are available, e.g. gradient and overset grid continuity ones, but the widest used are multi-surface ones (free surface or cavitation bubbles). A dynamic CPU load balancing ensures an efficient CPU usage, so this itself is already a very dynamic system.

Solver setup is quite standard for a resistance CFD simulation: the mirror plane is utilised, a ramp accelerates the vessel to final speed and the trim and sinkage motions are solved. K-omega-SST is used for turbulence closure, here in a high-Reynolds formulation. The propulsion is modelled via a so-called drag-based wrench as indicated in Fig.5, meaning that the current drag is balanced via a virtual force, affecting in turn the vessel motions. For a high-speed vessel location and angle of the propeller are of course very impacting parameters, this was investigated and confirmed on the base hull prior to start of the optimisation. Although possible, these parameters were not changed in the work shown here, mainly due to time constraints.

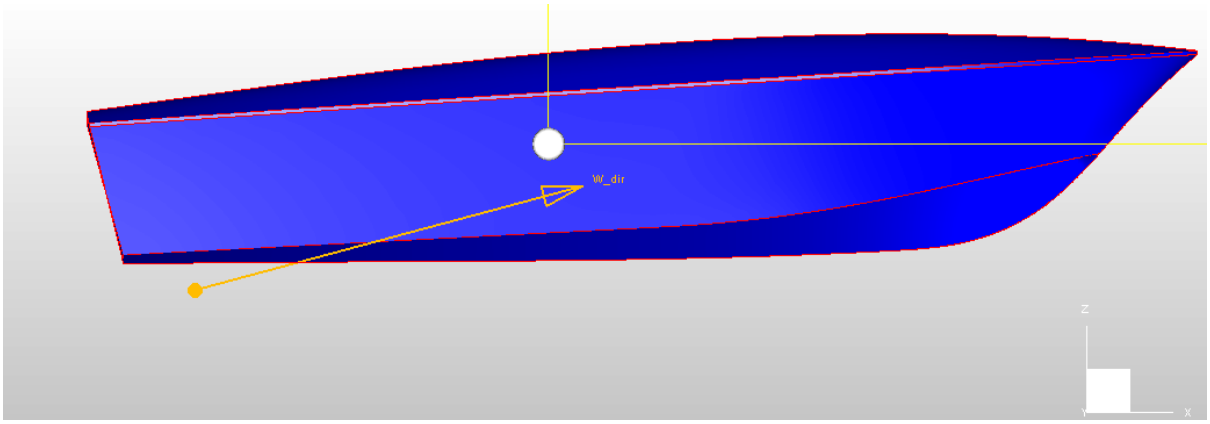

Fig.5: Centre of gravity (grey dot) and propulsion point and direction (orange vector)

An integrated tool called domhydro is run on all the geometries to estimate the free surface location, depending on the geometry itself and the displacement. Also, the inertia matrix is calculated. For this work the displacements were kept constant at 1 m³ and 1.2 m³, which is of course an approximation when changing strong parameters like length and beam. The parameter ranges were moderate on the other side, and assuming e.g. a bare hull weight of 500 kg one could easily calculate a surface density for the base hull and use this as a scale factor for the modified geometries with modified total hull area. CAESES® totally allows this, again the time constraint did not allow it for this work.

Again, the Python API and a class module takes care of all the pre-processing steps: vessel speeds, initial location of the free surface, AGR parameters, body motions, solver settings.

2.5 Optimisation strategy

The optimisation toolkit is NUMECA's FINE™/Design3D, which uses Cenaero's MINAMO package. FINE™/Design3D encloses all the workflows steps, meaning it first calls the parametric modeller and updates the design parameters. Result of this step is the triangulated geometry, which is passed to the meshing process. After mesh generation the pre-processor is called and the 6 simulations per design are defined. The solver is started, and the results are gathered in the post-processor afterwards. The design variables are passed back to FINE™/Design3D and processed further.

The whole optimisation workflow is depicted in Fig.6 and can be separated into three parts:

1) A database containing random samples is generated (the exact method used is called Latinised Centroidal Voronoi Tessellations). The goal is to gain a large diversity and little clustering of design parameters with as little samples as possible.

2) Then an online surrogate-based strategy is used: RANS-CFD simulations are still comparably expensive. Thus, the discrete input-output parameters defining a specific design are approximated via a surrogate model to deliver a continuous description. On this the actual optimiser, a genetic algorithm, is applied, calling the surrogate model thousands of times. Several versions of genetic algorithms exist, in this work a Pareto-type multi-objective one is used.

3) Interesting candidates are then passed to the CFD chain to get an accurate evaluation of the new designs, and these are then fed back to the database. This is what online stands for in the strategy.

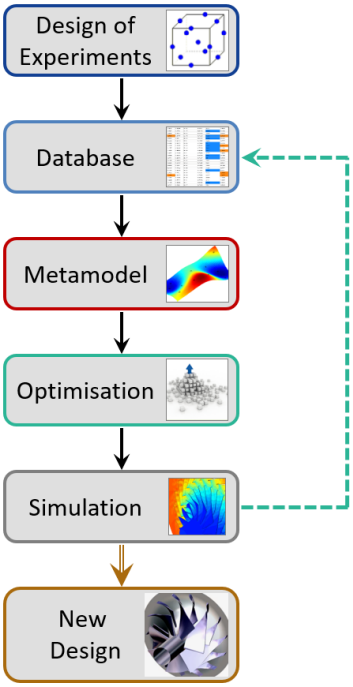

Fig.6: Optimisation strategy using a surrogate model

The main advantage over e.g. gradient based methods is the diversity achieved in the design space. Ideally, the optimiser samples are distributed evenly along the physical feasibility boundary, called Pareto front. All these samples are optimal in at least one of the objectives, and it is the designer's final choice how to weight the contradictory objectives and find the best trade-off, the most fitting solution. When compared to brute-force methods like Monte Carlo, this strategy is still feasible even with high-fidelity RANS simulations.

2.6 Efficient CFD chain challenges

The first simulations on even only slightly modified geometries already showed a huge impact on hull resistance and trim angles, but also on the solver runtimes and convergence behaviour. A planing hull is a complex and very dynamic system, and especially the database with random samples can deliver unfavourable geometries. This requires a detailed analysis of such geometries to correctly handle the outputs of interest, find quantities that clearly define such undesired behaviour and, in the end, control the optimisation process and deliver reasonable and consistent data to the optimiser. The latter is of utmost importance, since the surrogate models will of course pick up incorrect data and then mislead the optimiser.

Two extremes are depicted here:

1) Fig.7 shows a random design at 20 m/s and fully in the air at the final time step. In this time step the final drag value is of course very low, which is why all the quantities of interest need to be averaged, a window of 30% of the last time steps is used for the final runs. The time-dependant drag also shows a huge oscillation due to the periodic slamming of the hull, and it is visible in the motion variables as well. While the averaged resistance might not be that bad, passenger comfort likely suffers. Hence, calculating the relative standard deviation gives a very good impression of the behaviour and can be used to drive the optimiser. For the optimised samples in this work we use an arbitrary limit of 20% as a constraint.

2) Fig.8 gives an immense bow wave and spray at 5m/s, the total resistance is more than doubled compared to the base geometry. Since the free surface is captured via the AGR algorithm this also leads to largely increased mesh sizes and hence longer simulation times. On the other hand, resistance values will be far more accurate when compared to a static mesh approach, when not using a very conservative (large refinement zone around the free surface) mesh. Hence, over the course of all designs, displacements and speeds the AGR approach surely delivers the most efficient turnaround time.

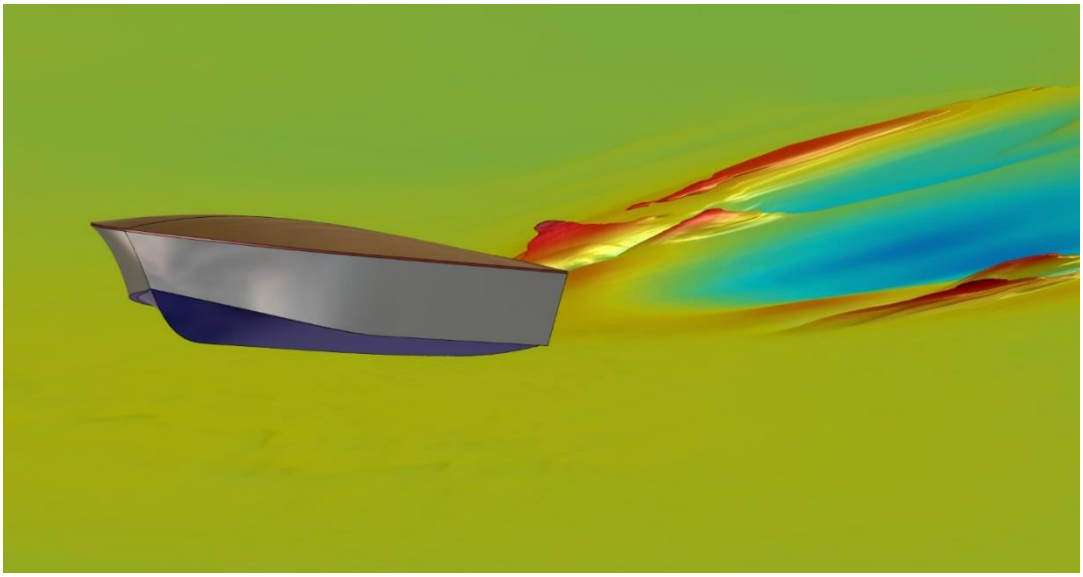

Fig.7: A sample from the database at 20 m/s, flying at the last time step (and slamming before)

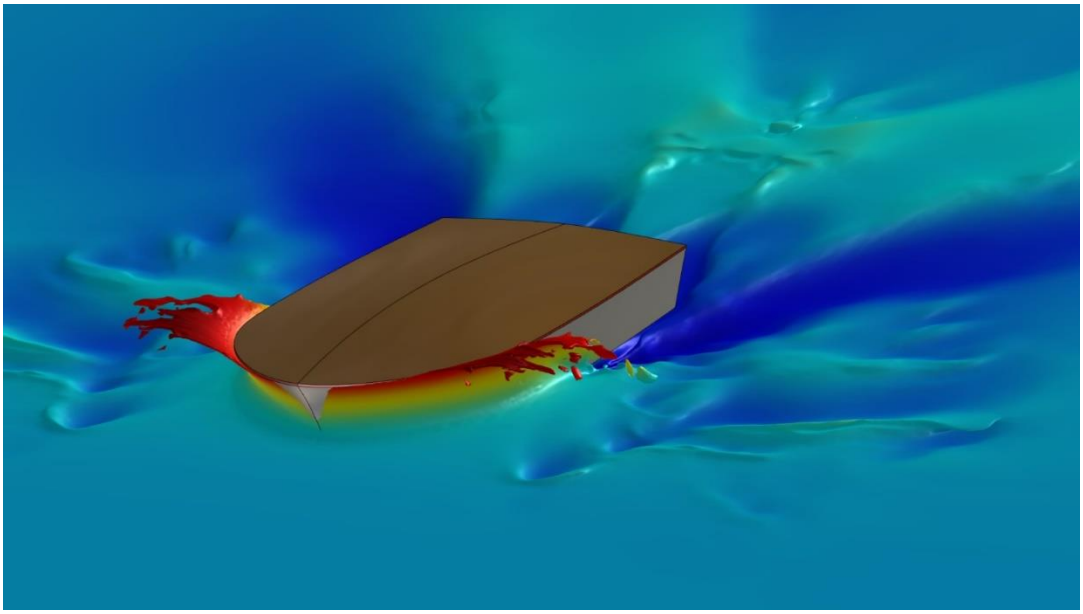

Fig.8: Worst database sample at 5 m/s, producing huge bow waves and drag

Another physical property of the hulls is the time to reach a stable hydrodynamic position, if reached at all, and this translates directly into solver convergence and time dependent drag. A convergence checking tool, directly integrated into FINE™/Marine, allows to monitor time histories and stops the process when a given tolerance for e.g. the drag is reached.

Altogether, all those dynamic systems (physics, mesh, convergence) lead to a huge variation in solving time (say 20 minutes to 2 hours per OP on 14 cores), but an efficient trade-off between accuracy and time is found for all those challenges.

3. Results

After the whole workflow is established, using some preliminary results to doublecheck all inputs and outputs and find the ideal setup according to 2.6, the final database and optimisation is started. As stated above, ten free parameters are included, and six operating points per design are evaluated. The ranges of those free parameters are one of the key impacts on the overall success, and must be selected carefully.

Most of the plots in this chapter are directly derived from the Data Mining tools provided by MINAMO and are accessible to the user during runtime. This allows a continuous monitoring of the process and can give important feedback in case adaptions are required (prominent example: change of constraints and objectives) or if convergence is obtained, and the process can be stopped.

3.1 Database

The database step is a quite simple one, samples are generated using the defined bounds and the sampling scheme. Depending on maturity of the base design there might already be interesting (equals better) samples in the database, and a key point to check is the accuracy of the surrogate model used later in the optimiser. MINAMO provides this by means of a leave-on-out analysis, which gives the correlation (factor and distribution). Since the genetic algorithm purely relies on the surrogate model, a good correlation is important for a successful optimisation. Also, it can indicate when enough samples are generated to continue to the optimisation step.

A total of 32 samples have been generated in the database, which is on the safe side on most cases in terms of accuracy for ten free parameters. Fig.9 shows the correlation graphs for the averaged total resistance for 5 m/s and 1000 kg (left) and 20 m/s and 1200 kg (right). The correlation coefficient for all six drag values are in the range between 0.7 and 0.9, which is very good.

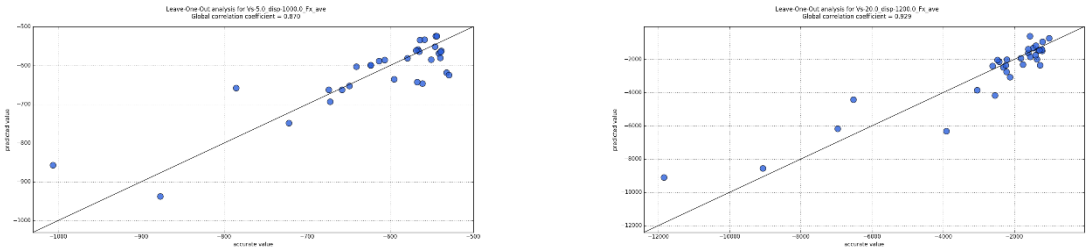

Fig.9: Leave-one-out analysis (LOO): correlation between accurate values and approximated values from the surrogate

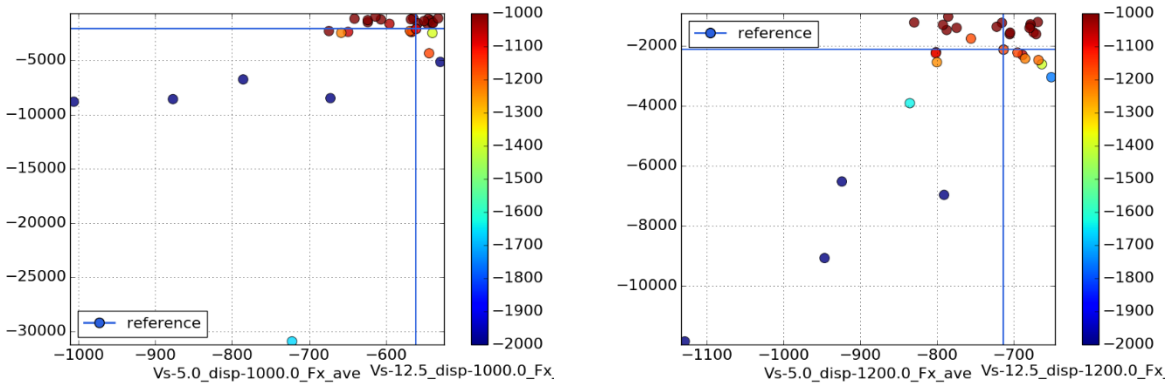

Fig.10: Total resistance of database samples (left: 1000kg; right: 1200kg)

As is expected with the challenges explained above, scattering of the total resistance is quite high. Fig.10 shows the averaged drag at 20 m/s over 5 m/s, coloured by the value at 12.5 m/s. Due to the axis definition all values are negative, and hence the closer to 0 (that is in the top right side) the better

the design. The blue cross gives the starting point, that is the Riva Junior base design. Aside from the extreme designs there are already some good designs, which show substantial less drag.

Fig.11 is a zoom on the interesting designs, and the sample number is also displayed. It is interesting to see that there is a correlation between the two drafts, but it is by far not absolute. The scattering of the points is not identical, and for example the really good performance of design 9 at 1200 kg is not fully kept at 1000 kg, there are other samples which are superior at that load condition. Hence, as expected there does not seem to be a one-hull-does-it-all design, this might be confirmed by the optimiser run, and using the more advanced data mining tools shown later.

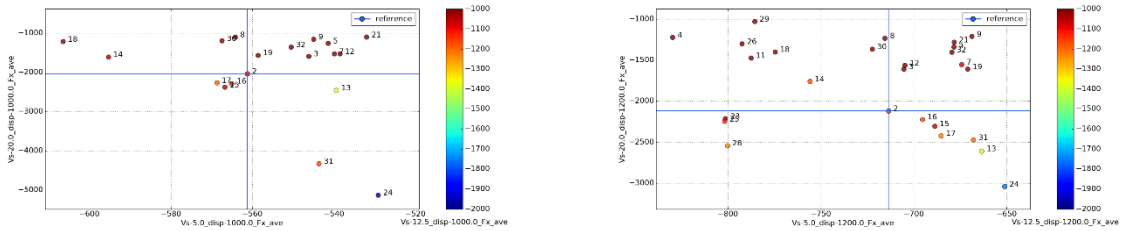

Fig.11: Zoom into the interesting region

3.2 Optimisation

In this work only one set of multi-objective optimisation run is shown: the Pareto type optimiser uses all six averaged drag values as objectives (to be defined as maximise due to the negative sign) and the relative standard deviation of the drag is specified as constraint to be less than 20%, for all six operating points. Of course, there would be room for many more sets of objectives and constraints, but the following results already show quite good results overall. Vessel motion variables are also evaluated, but except from the flying/slamming hull type these values are not excessive and hence not deemed necessary as objectives. Also, the overall physical behaviour of the hull is well represented by just the time evolution of the drag, and its standard deviation.

Figs.12 and 13 show the total resistance values, this time without a colormap for the values 12.5 m/s. Blue dots indicate database samples, orange ones are coming from the optimiser, while small dots indicate non-feasibility (here: drag deviation constraint of 20% not met). Again, the results seem very good and indicate a successful optimiser run. There are no samples in the completely un-usable region, showing a very good prediction from the surrogate model – high scattering here would point in that direction. There is also only a small amount of non-feasible designs. To complete the picture, Fig.14 shows the drag for both displacements at 12.5 m/s.

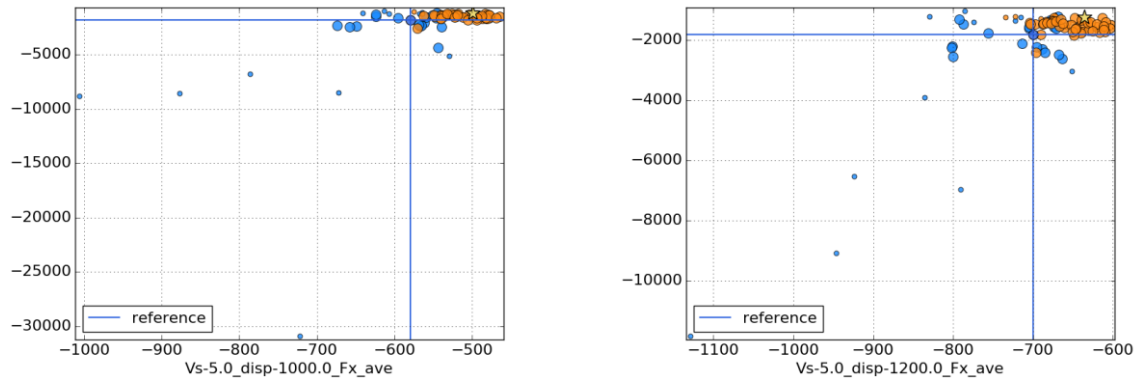

Fig.12: Total resistance of optimised samples (left: 1000 kg; right: 1200 kg)

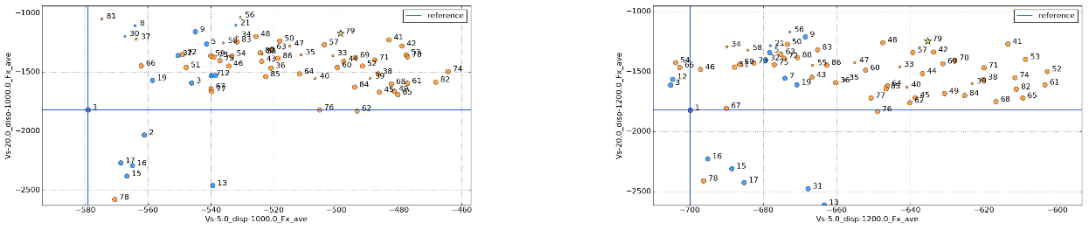

Fig.13: Zoom into the interesting region

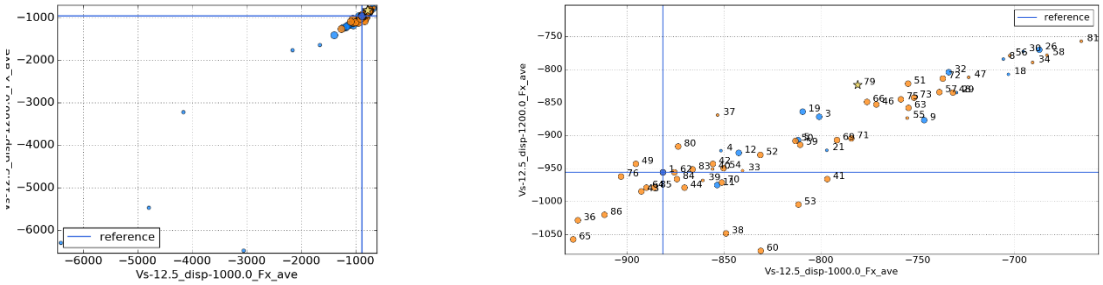

Fig.14: Total resistance values at 12.5 m/s

Figs.15 and 16 show again a zoom and giving all resistance values per displacements. In total 56 samples were generated during the optimisation run, which is not that much regarding the complexity of the problem. Still there are already many samples that indicate the Pareto front, and by just judging from the penalties design number 79 (marked with a star) shows a very good overall performance. At a displacement of 1 m³, resistance at 5 m/s is reduced from 1160 N (all values shown in the plots are for half ship models) to around 1000 N, which is around 13%. At 12.5 m/s, there is an 11% reduction is from 1760 N to 1560 N. The highest speed of 20 m/s shows the greatest improvements, total resistance is decreased from 3630 N to 2340 N, hence 35%. This design can also keep these improvements at 1.2 m³ and is hence seen as optimal in respect to all six objectives.

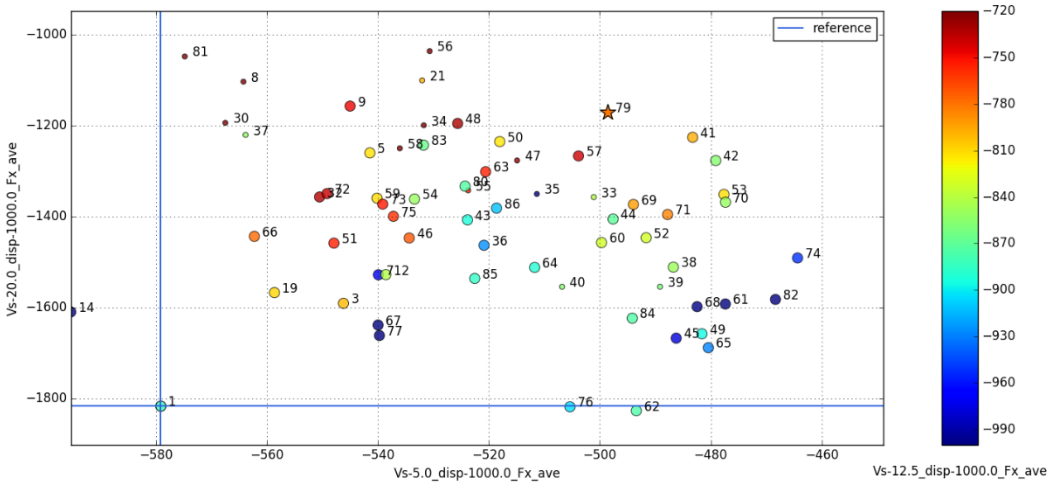

Fig.15: Total resistance values at 1000kg

These figures also show another important advantage of the Pareto-type optimisation: there are several other candidates found which are probably not as balanced as design 79, but favour objectives in respect to others: this is the strength of a true multi-objective algorithm with a wide range of very good potential designs. Looking at 1m³: design 48 is slightly worse at 5m/s compared to number 79 and can almost keep the performance at 20 m/s, but it shows another 6.5% decrease at 12.5 m/s, hence this could be a hull shape for a light battery configuration with great endurance at already planing conditions (water-skiing comes into mind), and still has the potential for thrilling high-speed driving.

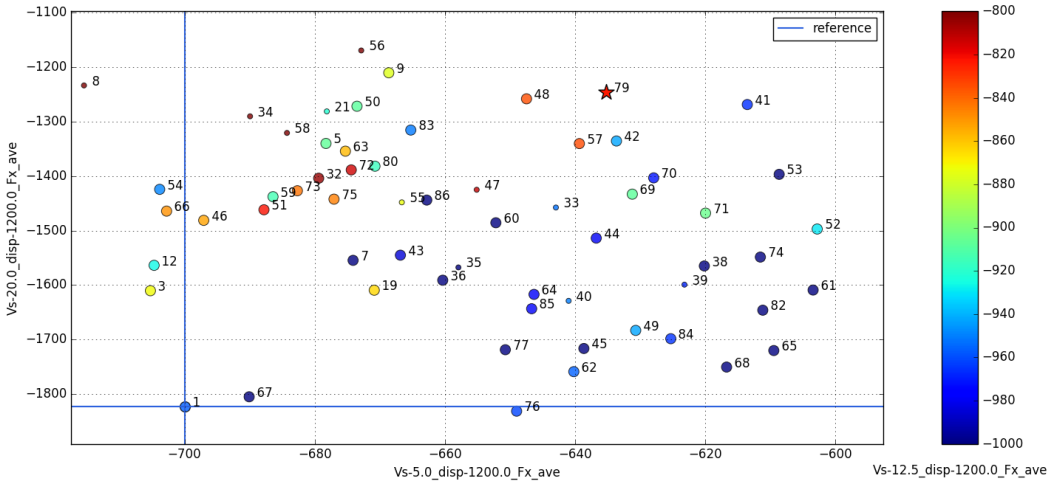

Fig.16: Total resistance values at 1200kg

A final word on the overall turnaround time: a 28-core machine is used for the database and optimisation, running two operating points in parallel on 14 cores. The database took only a couple of days, and the optimisation was completed in around a week (pure CPU time), which is very fast considering the complexity and the small machine used.

3.3 Data Mining

The procedure shown here produces a lot of data, and so far only new designs and their performance improvements are discussed. But, using this data and applying so called data-mining tools can greatly increase the understanding of physics and the correlation to input parameters. Fig.17 shows one of those tools, the self-organising maps (SOM). They are also based on a surrogate model, and project high-order data (here a problem with ten input parameters and six objectives) into 2D space. Each point indicates a design of the database and optimisation loop, and it is fixed in space. The colour contours display the total resistance values for all three speeds (rows) and the two draughts (columns). Note that red means low resistance and blue a high one. There is a strong correlation between all six performance values on the top left side of the SOMs, and a very favourable area at full displacement speed (5 m/s) on the bottom right. The planing modes are strongly focusing on the top right side, especially for 12.5 m/s, while at 20 m/s the bottom part is also attractive.

These plots clearly show that trade-offs must be made when aiming for a Jack of all trades design, and number 79 (marked by a star) is very good overall. There are samples which favour either of the operating modes, but at the cost of others. Again, the designer or engineer needs to decide what he or she wants.

Of course, these plots can also be created in the same way for the input parameters, see Fig.18. When comparing these to Fig.17, each parameter can easily be correlated to the performance at a given operating condition. Taking for example the beam parameter, a smaller value correlates quite closely to all resistance values.

Another useful tool is the analysis of variance (ANOVA). It is also based on the surrogate model and allows to calculate the sensitivity of all input parameters in respect to the output, here resistance values. Fig.19 gives the ANOVA plots for all six operating conditions in this study. The rocker parameter, which impacts the keel line towards the transom, is quite dominant for all planing conditions (12.5 m/s and 20 m/s), although a bit dependent on the displacement: it is far more impacting on the light version than on the heavier one. Total boat length on the other hand is a strong factor for the displacement speed, while completely irrelevant for high speeds.

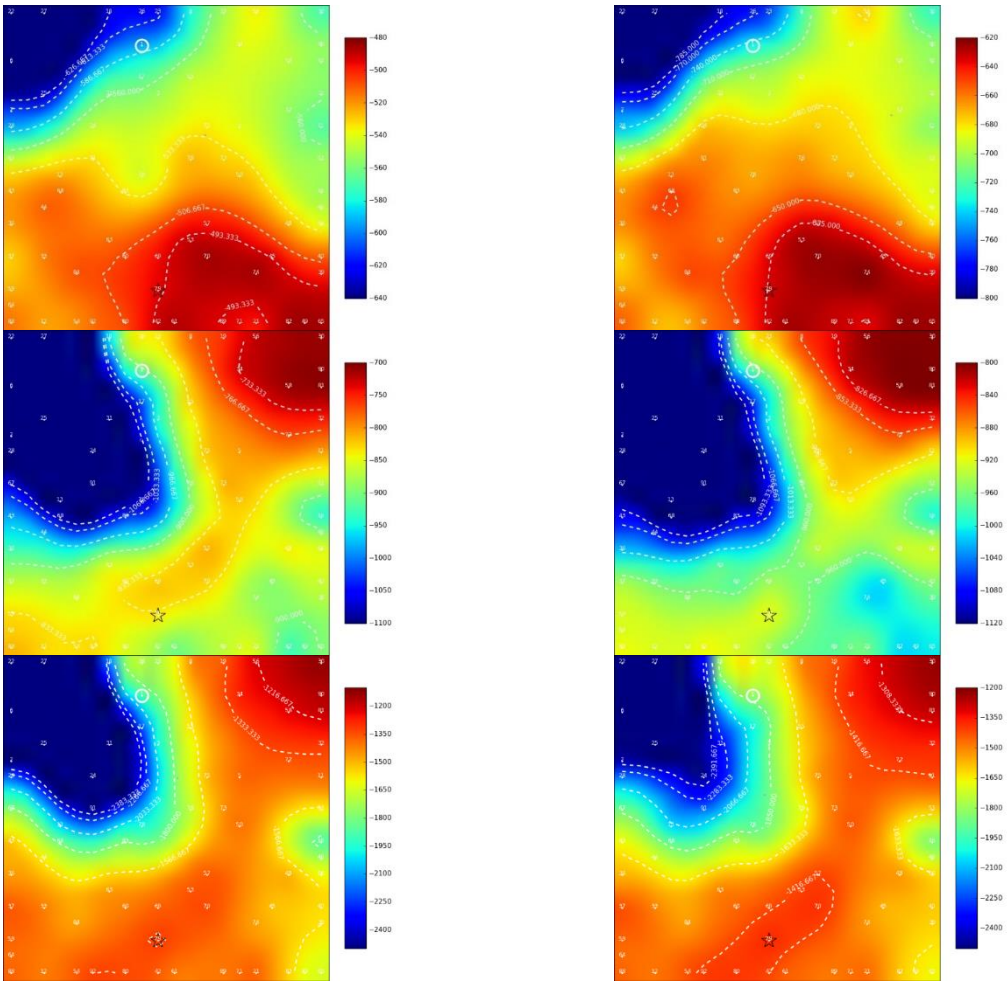

Fig.17: SOM of resistance values: left 1000 kg, right 1200 kg, top to bottom: 5 m/s, 12.5 m/s, 20 m/s

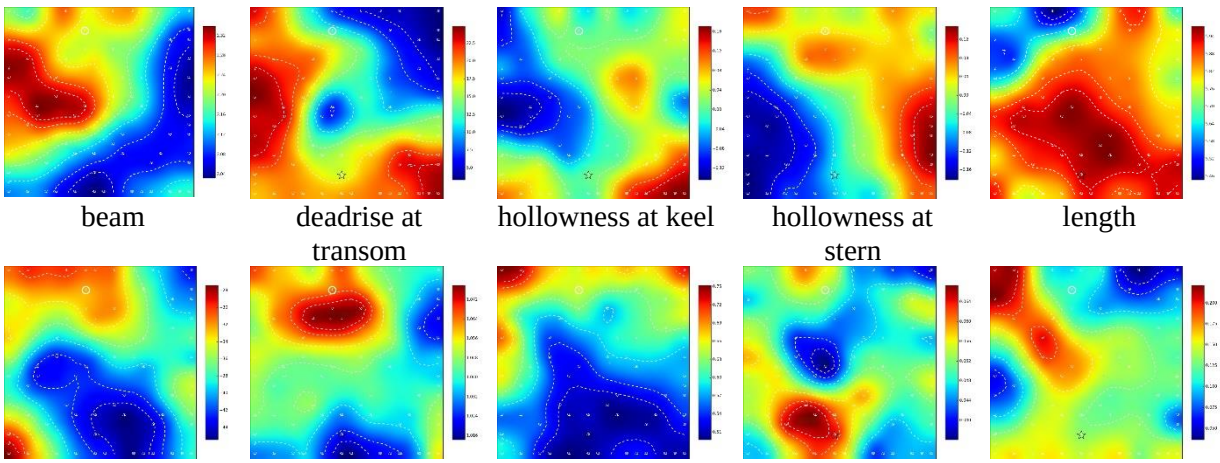

Fig.18: SOM of all geometrical input parameters

For each parameter in the pie diagram a local variance can be calculated, Figs.20 and 21. This variance is coupled to defined designs (shown here are 1 and 79) and it will give the local correlation of an input parameter to an output parameter. A change of the rocker feature has a much larger impact on the base design 1 than on the balanced optimised design 79. Obviously, these designs differ in all parameters, and hence a (local) variation of one specific parameter is likely to give different effects.

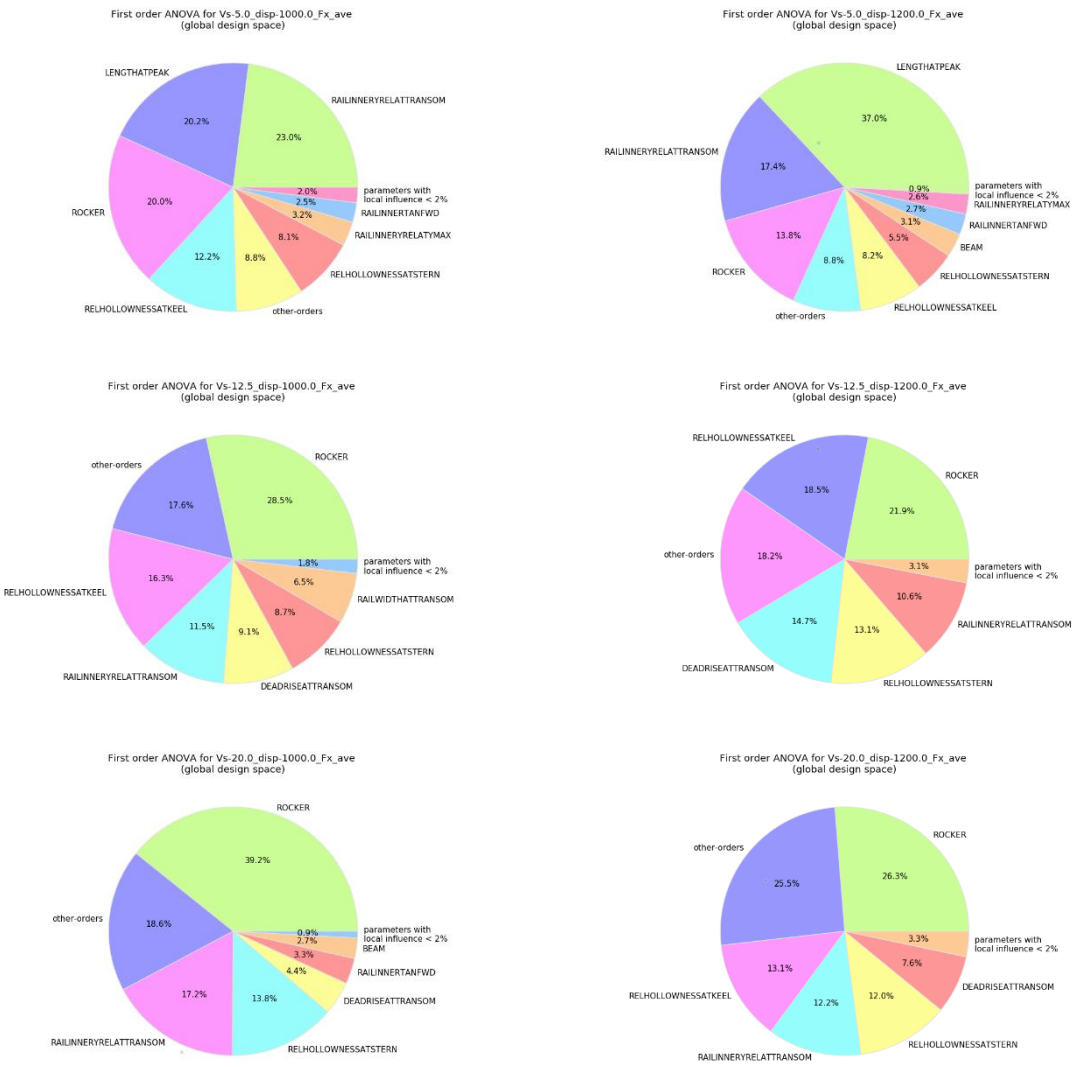

Fig.19: ANOVA: left 1000 kg, right 1200 kg, top to bottom: 5 m/s, 12.5 m/s, 20 m/s

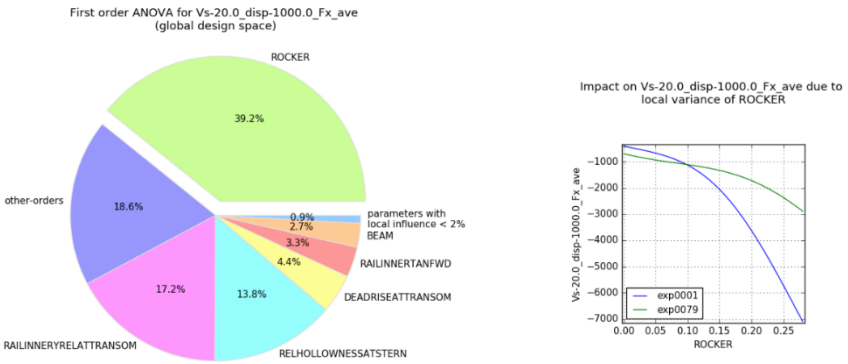

Fig.20: Rocker parameter as important feature at 20 m/s and 1000 kg, plus the local variance

ANOVA can hence guide a designer in a lot of ways: for example, it can show sensitivities which were probably not known before and need to be considered much more in the next project. This can be a change of parametrisation for finer control over important features and paving the way for even better designs. And the opposite might be true as well: less important features can be neglected, which in a workflow similar to the one presented here will save CPU time, or in the real world could also save material or costs in general.

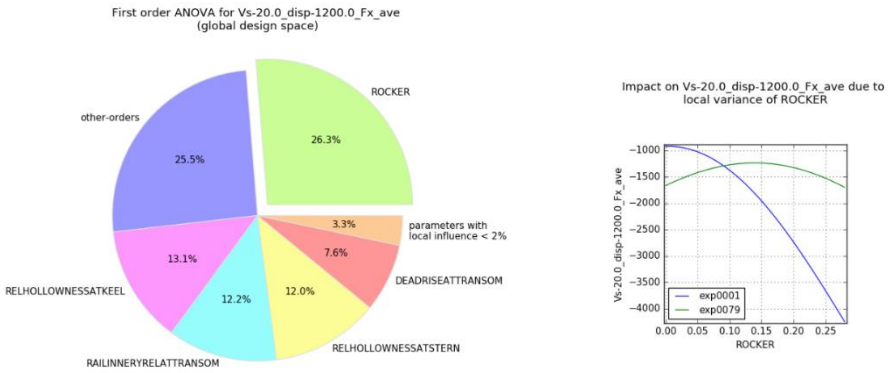

Fig.21: Rocker parameter as important feature at 20 m/s and 1200 kg, plus the local variance

4. Conclusions

An optimisation of a small powerboat has been presented, using numerical simulations. One focus lied on the application of electric propulsion instead of a combustion engine, which brought a few extra challenges with it: battery size is a crucial parameter and was respected using two different displacements. The full operating range, from low to high speeds was considered, to allow for a complete picture of such a powerboat. A powerful combination of efficient parametric modelling using CAESES® and state-of-the-art CFD solutions from NUMECA led to a very stable, yet cost-effective design process. The results of the optimisation run were quite promising, showing some major gains in terms of total boat resistance. A few designs were discussed in more detail, showing some trade-offs between the six operating conditions. A deeper look into the results and the vast amount of data was given via data-mining tools, that can easily show trends, correlations and anti-correlations in the design space. Also, sensitivity analysis methods were applied to highlight a few of the important geometrical features of such a boat.

References

HARRIES, S.; ABT, C.; BRENNER, M. (2015), *Upfront CAD – Parametric Modeling Techniques for Shape Optimization*, Int. Conference on Evolutionary and Deterministic Methods for Design, Optimization and Control with Applications to Industrial and Societal Problems (EUROGEN 2015)

HARRIES, S.; ALBERT, S; HILDEBRANDT, T; REYER, M., *Hydrodynamic Optimization of a Power Boat in the Cloud*, HIPER Conference 2016, Cortona

LEROYER, A.; VISONNEAU, M. (2005), *Numerical methods for RANSE simulations of a self-propelled fish-like body*, J. Fluid & Structures, 20/3, pp.975-991

MALLOL, B. (2012), *Computation of Free-Surface Viscous Flows around Self-propelled Ships with the Help of Sliding Grids*, Conf. Computer and IT Appl. Maritime Ind., Liege

QUEUTEY, P.; VISONNEAU, M. (2007), *An interface capturing method for free-surface hydrodynamic flows*, Computers & Fluids, 36/9, pp.1481-1510

VISONNEAU, M; QUEUTEY, P; DENG, G.B; WACKERS, J; GUILMINEAU, E; LEROYER, A; MALLOL, B. (2012), *Computation of Free-Surface Viscous Flows around Self-propelled Ships with the Help of Sliding Grids*, Conf. Computer and IT Appl. Maritime Ind., Liege

WACKERS, J.; AIT SAID, K.; DENG, G.B.; MIZINE, I.; QUEUTEY, P.; VISONNEAU, M. (2010), *Adaptive grid refinement applied to RANS ship flow computation*, 28th ONR Workshop on Naval Hydrodynamics, Pasadena, California

Wind Assisted Propulsion Systems as Key to Ultra Energy Efficient Ships

Uwe Hollenbach, Heikki Hansen, Ole Hympendahl, Martina Reche, Esperanza Ruiz Carrio,
DNV GL, Hamburg/Germany, uwe.hollenbach@dnvgl.com

Abstract

This paper looks at wind assisted propulsion systems (WAPS) from a design and efficiency point of view. WAPS can become a significant measure to meet IMO targets for energy efficiency in the next decade. The paper explains technical options, and how WAPS affect energy efficiency. A performance prediction program for early stage assessment of different WAPS is presented, which only requires ship main particulars and dimensions of the WAPS. Energy savings beyond the current EEDI assessment can be harvested if WAPS are combined with dedicated routing systems. A route optimization model is implemented which finds pareto-optimal *routes with respect to voyage time and fuel consumption based on the performance prediction results for a vessel. Case studies employing these tools illustrate the savings potential of different WAPS and how route optimization can harvest more of this potential. The performance prediction program together with the route optimization model provide insight into the key role that WAPS may take towards low-carbon shipping within the next decade.*

1. Introduction

DNV GL has been offering services around energy efficiency and sailing technology for a long time, in certification, consultancy, engineering services and software. These fields now come together in the efforts to meet the zero-emission shipping by 2050 vision of IMO.

The idea of wind-assisted propulsion systems (WAPS) as a powerful lever for saving energy and lowering emissions is not new. *Bertholdt and Riesch (1988)* prophesied already: "Using the wind means using the most environmentally friendly energy source. Saving (fossil) fuel means emitting fewer pollutants. Time will come, in which this aspect will be considered more valuable than pure commercial interest." *Schenzle (2010)* summarizes current concepts for wind propulsion of ships. He argues that sea transportation particularly lends itself for first steps away from carbon combustion, for three reasons:

- Its uniquely low energy demand could be largely covered from solar sources;
- Wind is easily available at sea and can directly drive ships without transformation losses;
- Weather routing and energy management can largely compensate for the variable input.

The ambitious IMO targets are asking for just this. Cutting greenhouse gas emissions with mandatory targets has driven ship owners and operators to re-think their propulsion systems. One possible solution to cope with IMO's requirements is to install a WAPS to supply part of the propulsive power. As we perceive an increasing interest about the chances and possibilities of WAPS technology among ship owners, this paper will discuss various option from a design and operational perspective.

In addition, the realizable fuel savings are of course of great interest. To calculate these, this paper presents a performance prediction program for vessels with WAPS to predict power and fuel savings during the feasibly study of a WAPS project. These results are combined with a weather routing model to ensure that the effect of optimizing the route for the WAPS is considered adequately in the fuel savings.

2. Technical options and effect on efficiency

The following discussion is largely taken from a master's thesis in cooperation between Danish Technical University and DNV GL, *Reche (2020)*. Three typical, but fundamentally different WAPS are compared: Rotor Sails (a.k.a. Flettner rotors), Rigid Wingsails and DynaRigs, Fig.1. These systems were chosen for three main reasons:

1. These devices are proven to be feasible. E.g., Rotor Sails are installed in presently operating commercial vessels; Rigid Wingsails are nothing else than vertical, fully studied airplane wings; and DynaRigs are successfully used in several large sailing yachts.
2. These devices are the most likely ones to be adopted by the shipping industry due to their market availability and reference installations. Also, most of the technical papers on WAPSs in recent years have focused on the development, implementation, analysis and validation of these three devices.
3. Our limited time for this assessment. In the future, we may also extend our analyses and assessment to other WAPS, including kites and turbosails.

The following subchapters will cover each of the selected WAPS devices, presenting the state-of-the-art and a bit of history, available configurations and further references.

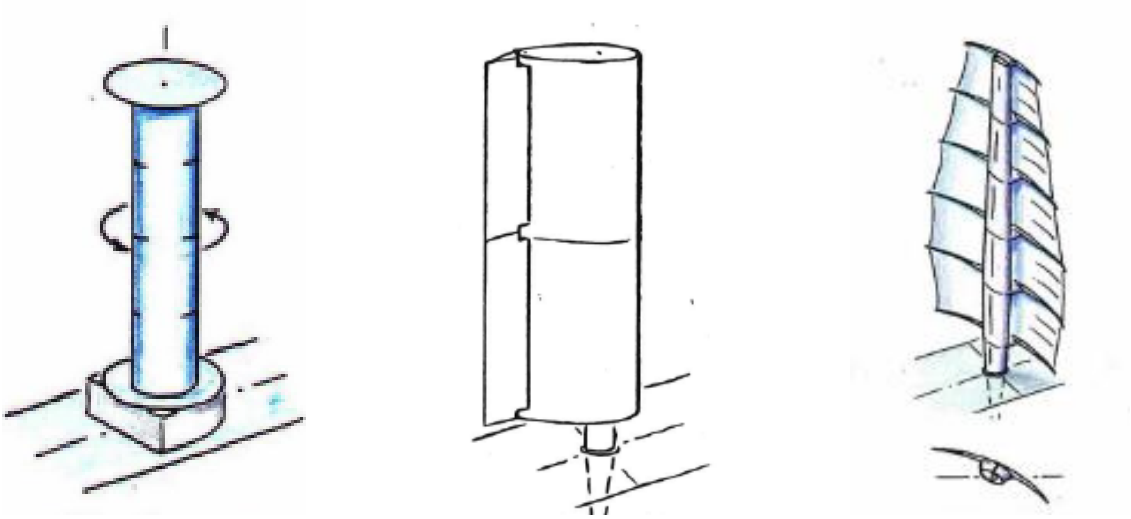

Fig.1: Rotor Sail (left), Rigid Wingsail (center) and DynaRig (right), *Schenzle (1983)*

2.1. Rotor sails (Flettner rotors)

The Rotor Sail is an active rotating cylinder that generates aerodynamic loads due to the Magnus effect. It is commonly called a Flettner Rotor, named after the German inventor Anton Flettner, who designed and built an experimental rotor vessel named 'Buckau' in 1924, Fig.2. Two 15.6 x 2.8 m Rotor Sails were installed with a total rotor area of 87.4 m^2, as an additional source for propulsion to reduce fuel consumption. A few more ships were equipped with Rotor Sails in the decades to follow, but due to low the oil prices, Rotor Sails had no convincing business case and remained an exotic side note until the beginning of the new millennium when interest in WAPS revived with energy efficiency and reduced carbon footprints coming on the agenda. In 2008, E-Ship 1 was launched, Fig.2. Four 27 x 4 m Rotor Sails were installed. Enercon, the owner and operator of the E-Ship 1, claimed operational fuel savings of up to 25% compared to same-sized conventional freight vessels. In 2018, the 'Maersk Pelican' was fitted with two 30 x 5 m Norsepower Rotor Sails, Fig.4. Through measurements before and after installation Norsepower determined fuel savings of 8.2% during the trial period, *Paakkari et al. (2020)*.

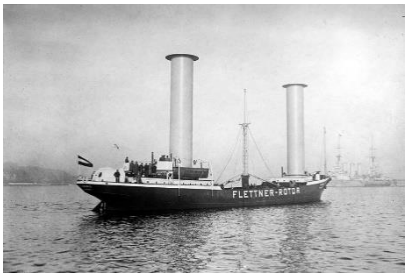

Fig.2: 'Buckau' (1924)

Fig.3: E-Ship 1 (2008)

Fig.4: 'Maersk Pelican' (2018)

Advantages of Rotor Sail systems for cargo ships are:

- As for all WAPS, fuel savings and thus lower operational cost
- Easy handling, not requiring extra crew or even much training
- Lower cost for installation and maintenance per thrust force than other WAPS, *Borg (1985)*
- Very good maneuverability for ship
- Passive load limitation: Since all rotating cylinders have a maximum operating spinning velocity, if they encounter high wind speeds, their velocity ratio drops and, consequently, their aerodynamic loads follow the same trend. Thus, Rotor Sails depower themselves which makes them a hurricane proof device, an advantage not inherent in other type of WAPS.

Disadvantages of Rotor Sails are:

- Vibrations induced from the rotors my cause crew discomfort or even structural damage.
- Rotor Sails are active rotating devices, requiring some electrical power to spin.
- Rotor Sails have a relatively small lift-to-drag ratio, thus they are less effective for fast vessels where the apparent wind angles are generally smaller.

2.2. Rigid Wingsails

Rigid Wingsails are airfoils, similar to airplane wings. Their main differences are their vertical orientation and their ability to generate lift on either side. This last characteristic is vital for a vessel since, unlike airplanes, they must tack while following the wind. For this reason, Rigid Wingsails have generally symmetric NACA profile cross sections. Also, they may feature flaps:

- Leading-edge flaps increase the maximum lift of an airfoil by delaying its stall angle but are rarely implemented.
- Trailing-edge flaps generate additional lift through an increase in the effective camber of the airfoil, but also induce earlier stall. Plain flaps and slotted flaps are the most common in the maritime sector.

While the idea of Rigid Wingsails dates back at least to the 1920s, it was only in late 1960s when John G. Walker designed a 10 m long Rigid Wingsail propelled cruiser, Fig.5, *Walker (1985)*. Popularly called Walker Wings, they were the first successful maritime implementation of Rigid Wingsails. In the 1980s, the U.S. government commissioned a study with Walker on the economic feasibility of wind assisted propulsion in response to soaring fuel prices.

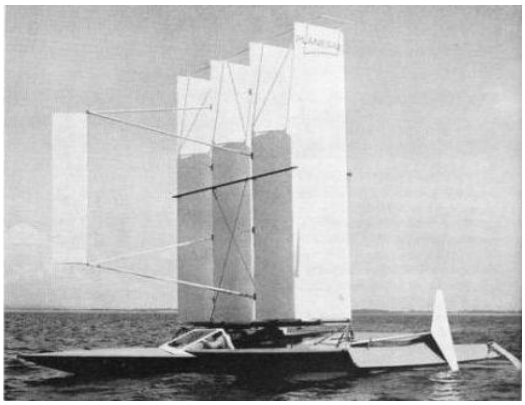

Fig.5: Planesail of John G. Walker

Fig.6: Maribot VANE

While Rigid Wingsails fitted aboard commercial vessels demonstrated 15-25% fuel savings, they failed to be widely implemented due to the low oil prices at the time. In the early 21st Century, Rigid Wingsails entered high-performance sailing yielding unprecedented speeds e.g. in America's Cup regattas. They also saw applications in maritime drones, Fig.6, *Reche and Ruiz (2018)*.

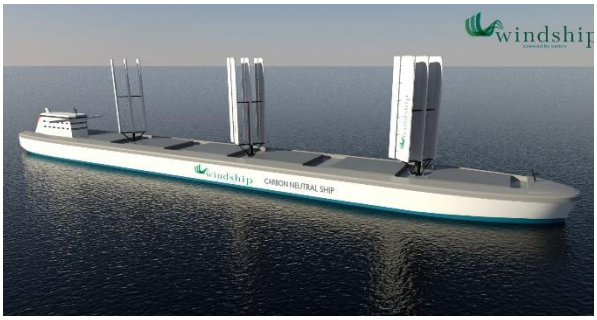

Fig.7: Windship Technology project

Fig.8: wPCC

Rigid Wingsails have featured in several high-profile design projects, such as the British Windship Technology project, Fig.7, and the Swedish Wind-Powered Car Carrier, wPCC, Fig.8. However, so far these projects have remained in the design stage.

Advantages of Rigid Wingsails are:

- Easy handling requiring no extra crew
- Easy installation and maintenance
- Most of them are retractable (reducing risk of overload in storms and facilitating cargo handling)

Disadvantages are:

- Relatively expensive (compared to traditional sails)
- Larger deck-space requirements (possible interference with cargo handling and other deck operations)

2.3. DynaRig

The DynaRig is a square rig developed in the late 1960s by Wilhelm Prölss. The main characteristic of this WAPS is its free-standing mast with the yards connected rigidly to it. The sails are trimmed to the wind by rotating the mast. Prölss designed the DynaRig for cargo ships. He carried out wind tunnel tests for a 6-masted bulk carrier of 16,000 dwt at the Hamburg University in the 1960s and the 1970s, Fig.9. The DynaRig proved to be about twice as efficient as traditional square rig sails.

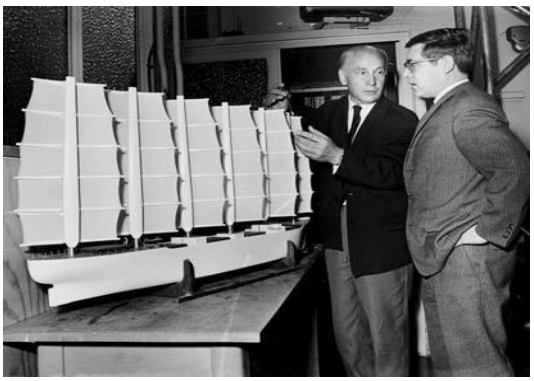
Fig.9: Wilhelm Prölss with DynaRig


Fig.10: WASP EcoLiner

Prölss took patents of his design in all shipbuilding countries worldwide, but due to low fuel prices and the difficulty to build a full-scale mast with sufficient stiffness, the idea did not take off until the beginning of the new millennium. The DynaRig saw the light on the mega-yacht "Maltese Falcon" in 2006, *Dijkstra et al. (2004)*. Ten years later, the DynaRig sailing yacht "Black Pearl" was released. Also some design concepts for commercial vessels involve this technology like the WASP EcoLiner Project, Fig.10.

Advantages of the DynaRig are:

- Fully automated requiring no extra crew
- Same as Rigid Wingsails, DynaRigs are highly controllable
- Aesthetic design appealing also to the yacht market

The main disadvantage is:

- Higher lifecycle cost than for Rigid Wingsails

3. Power prediction of WAPS

We developed a 6 degrees of freedom (DoF) Performance Prediction Program (PPP) for wind-assisted cargo ships to contribute to the knowledge on WAPS performance utilizing DNV GL's modular performance prediction workbench FS-Equilibrium. It is a fast and easy tool able to predict reasonably accurately the performance of any commercial ship equipped with one of three different WAPS: Rotor Sails, Rigid Wingsails and DynaRigs. The tool requires only ship main particulars and general dimensions as input data and is based on semi-empirical methods and a WAPS aerodynamic database created from published data on lift and drag coefficients. All WAPS data can be interpolated to scale to different sizes and configurations.

3.1. Hull model

The forces acting on the hull and superstructure of the vessel are described by so-called forces modules, which account for the different force components:

- The gravity module allows to calculate the forces due to a point mass located at a point in the body fixed coordinates, in this case, the centre of gravity of the cargo ship. This mass module is used here to model the non-movable mass of the vessel. It is based on Newton's Second Law of Motion.

- The buoyant module is used to model the forces due to the hydrostatic pressure acting on the hull, i.e. buoyancy and hydrostatic stability. Normally, this force and their respective rolling and pitching moments caused by perpendicular distance between the lines of buoyancy and weight are calculated thanks to a set of offset points of the geometry of the ship hull. In this hull model, since any cargo ship must be modelled with few input data and as an early stage design tool, the set of offset points will be normally not available. Thus, the buoyant force is modelled from basic ship theory equations and approximations according to *Rawson and Tupper (2001)*.

- The hull resistance is predicted with the Holtrop module, which calculates the resistance of single screw ships, especially tankers, bulk carriers, general cargo, fishing vessels, container ships and frigates in the preliminary design stage. This method was developed by a regression analysis of a collection of model experiments and full-scale data, available at the Netherlands Ship Model Basin, *Holtrop (1977,1984)* and *Holtrop and Mennen (1978,1982)*. The target of

the Holtrop and Mennen study was to develop a numerical description of the ship's resistance, the propulsion properties and the scale effects between the model and the full size. Since the Holtrop and Mennen semi-empirical method is based on towing tank tests, a roughness allowance needs to be computed and added. This force is based on the wetted area of the hull (also approximated following *Holtrop and Mennen (1978)*) and the roughness coefficient according to *ITTC (1978)*.

- Wind-assisted ships experience a significant lateral force compared to conventional motor ships in response to the aerodynamic loads from the sailing devices such as Rotor Sails, Rigid Wingsails and Soft Sails, for instance. The side force is computed with the approach by *Schenzle (1989)* for sailing ships without long fin keels as suitable for wind-assisted cargo ships.

- The rudder hydrodynamic force module calculates lift and drag of the rudder based on *Whicker and Fehlner (1958)*. Due to the side force and yawing moment generated by the WAPS, the vessel adopts a leeway angle and a rudder angle is required to balance the yawing moment.

- The parasitic aerodynamic resistance of the superstructure is calculated based on the drag coefficient and the frontal area of the superstructure, which is taken as the beam multiplied by the accommodation height above deck. For tankers and bulk-carriers, it can be assumed that each floor height is 3 m and an additional height of 2 m is added counting for equipment at the top of the vessel.

- The propeller thrust, in combined and pure motor configuration, is calculated assuming a Wageningen B-Screw series propeller following *Kuiper (1992)*. Typical values for wake fraction, thrust deduction and relative rotative efficiency, η_R, are assumed to account for the effect of the hull on the propeller. The force module returns the delivered power, PD, and the propeller revolutions per minutes, RPM.

- The added resistance in waves is calculated by the AddRT force module based on an in-house semi-empirical method used at DNV GL for high-level assessment of the added resistance in a seaway. The sea spectrum is modelled according to JONSWAP spectrum, taking significant wave height and wave period as user-specified input data.

3.2. Rotor sails (Flettner rotors) model

The forces on a rotating cylinder can be described as superposition of two simple flows: the parallel flow and the circulatory flow. The resulting flow pattern is based on the resultant velocity vectors, sum of both the free-stream parallel flow velocity, V_{free}, and the circulatory flow, $V_{rotating}$. The streamlines moving in the direction of the flow created by the Rotor, V_{favour}, have a total velocity of,

$$V_{favour} = V_{rotating} + V_{free} \tag{3.1}$$

while, the streamlines moving against have a total velocity, $V_{against}$,

$$V_{against} = V_{free} - V_{rotating} \tag{3.2}$$

Due to this velocity difference between rotating cylinder sides, a pressure distribution over the device appears, creating a side force (Magnus force in Fig.11). The total aerodynamic force acting on the Rotor Sail can be calculated from lift and drag. The total aerodynamic moment acting on it is the torque. The lift is the force perpendicular to the incoming flow, defined as:

$$Lift = \frac{1}{2}\,\rho_{air} \cdot AWS^2 \cdot Area \cdot C_L \tag{3.3}$$

The drag is the force parallel to the incoming flow, defined as:

$$Drag = \frac{1}{2}\,\rho_{air} \cdot AWS^2 \cdot Area \cdot C_D \tag{3.4}$$

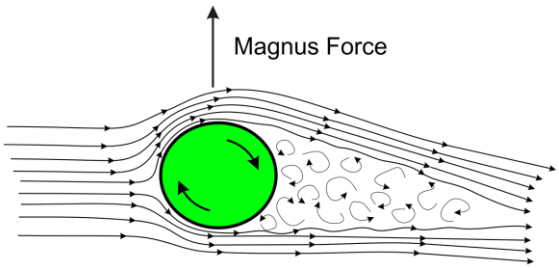

Fig.11: Magnus effect seen in a rotating cylinder. The vertical arrow represents the resulting lift force, *Rdurkacz (2013)*

Neglecting energy dissipation, a theoretical lift coefficient value can be derived by substituting the expression of lift for the dimensionless lift coefficient into the Kutta-Joukowski theorem of lift equation defined as:

$$F_L = \rho \cdot \Gamma \cdot AWS \cdot Radius \tag{3.5}$$

Thus, the lift coefficient of a rotating cylinder in an ideal fluid is:

$$C_L = 2\pi \cdot \frac{U}{V} \tag{3.6}$$

U/V is the velocity ratio of the Rotor Sail defined as:

$$\frac{U}{V} = \frac{\omega \cdot R}{AWS} \tag{3.7}$$

This theoretical value does not consider viscosity. Empirical coefficients in real fluids are much lower, typically 25-50% of the theoretical value. The drag coefficient cannot be derived from ideal fluid theory. It can only be established empirically.

However, what it is clear is the relation between lift and drag coefficients with the Rotor Sail velocity ratio. This is responsible for its inherent load limit. According to Eqs.(3.6) and (3.7), at increasing apparent wind speed, the velocity ratio diminishes due to its maximum spinning RPM and the lift coefficient follows the same trend. Thus, the total force tends to a maximum total cylinder load limit, Fig.12. Rotor Sails are stormproof systems thanks to this characteristic.

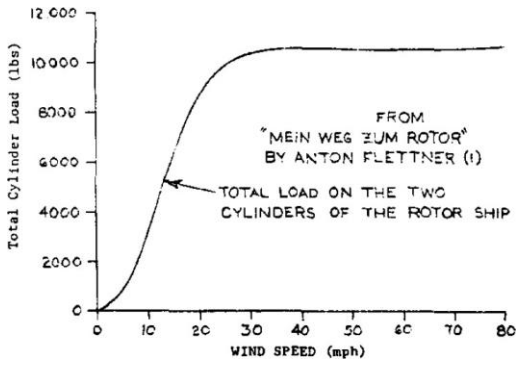

Fig.12: Total cylinder aerodynamic force for TWS range, *Bergeson and Greenwald (1985)*

We use historical results from *Prandtl and Betz (1932)* for two reasons: its wide acceptance as high-quality data inside the scientific community and its high velocity ratio range (up to 8 when most of the sources are up to 4). The results are based on the measurement of lift and drag coefficients as function of velocity ratio for two cylinders, one with aspect ratio of 1.68 and the other with aspect ratio 12. Also, endplate size was varied with diameter endplate/diameter rotor sail ratios De/D = 1.1, 3 and 5.2.

3.3. Rigid Wingsails model

The Rigid Wingsails model allows choosing between three different Rigid Wingsails configurations: a plain symmetric profile, a symmetric profile with a trailing edge plain flap and a symmetric profile with a trailing edge slotted flap, Fig.13. The performance of these three Rigid Wingsails can be predicted with this model. The user can specify the size of the flap (expressed relative to the chord length of the symmetric profile) and the maximum flap angle.

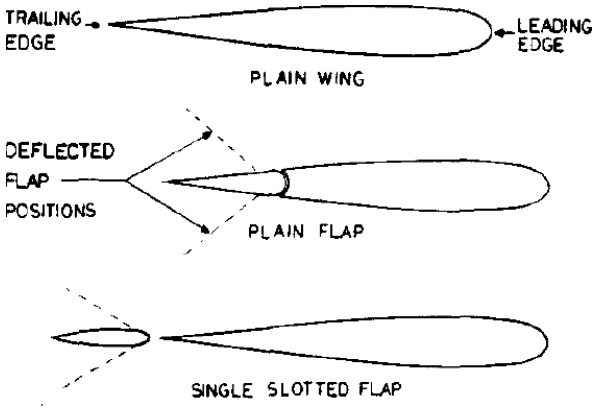

Fig.13: Rigid Wingsails configurations included in this Performance Prediction Program, *Bergeson and Greenwald (1985)*

The lift and drag prediction model for Rigid Wingsails is divided into two main parts: 2D prediction and 3D prediction. The 2D approximation accounts for the profile shape and the camber effect while the 3D approximation modifies the 2D results to account for the effects of aspect ratio and tip vortices. The assumptions of this model are:

- No wing-ship interference is considered.
- No profile thickness effects are considered due to their negligible effects on lift coefficient.

The 2D profile data (lift and drag coefficients as function of angle of attack) is obtained from the NACA 0012 symmetric profile.

The effect of camber on lift and drag coefficients for profiles with flaps is determined using the DA-TCOM 1978 methods by *Finck (1977)* and *Young (1953)*. With this method, lift increase due to trailing-edge plain and slotted flap implementation is modelled. These sorts of high-lift devices increase lift for 0° angle of attack while reaching a higher maximum lift coefficient but a lower stalling angle.

The 3D model accounts for downwash reducing lift and induced drag due to spillage around wing tips. It also accounts for different aspect ratios. These effects are modelled according to Prandtl's lifting line theory, *Abbott and von Doenhoff (1959), Newman (2017)*. 3D lift and drag coefficients are derived as:

$$C_L = \frac{C_{L2D}}{1 + \frac{C_{L2D}}{AR \cdot \pi}} \tag{3.8}$$

$$C_D = C_{D2D} + C_{Di} = C_{D2D} + \frac{C_L^2}{AR \cdot \pi \cdot e} \tag{3.9}$$

C_{L2D} and C_{D2D} are the 2D lift and drag coefficients which account for angle of attack and camber. C_L is reduced from C_{L2D} value as function of aspect ratio *AR*. If aspect ratio tends to infinity, C_L approaches C_{L2D}. C_{D2D} is the 2D drag coefficient at zero lift due to skin friction and wing section shape. C_{Di} is the induced drag coefficient produced at the wing tips due to lift. C_D adds induced drag to the ideal 2D drag coefficient. If the aspect ratio tends to infinity, C_D approaches C_{D2D}. *e* is the Oswald efficiency which depends on the lift distribution. For an elliptic lift distribution, it gets its maximum value of 1.

All data is loaded into the developed model in the Performance Prediction Program. It is fitted to find the right values for each given input condition, such as flap dimensions, following a multi-dimensional cubic spline interpolation of the discrete input data.

The Performance Prediction Program constantly trims the angle of attack and the flap deflection (if applicable) of the Rigid Wingsails to optimize the trim objective (minimum total power or maximum speed). The angle of attack valid range is up to 90° - downwind condition is also modelled according to plain airfoil wind tunnel tests data, *Schenzle (1980)*.

3.4. DynaRig model

The DynaRig generates aerodynamic loads following the same principles explained in section 3.3. DynaRigs are cambered sails. The potential of the DynaRig is evident as soon as the AWA becomes large. As this angle becomes larger, a higher camber performs better, *Perkins et al. (2004)*. However, for several DynaRigs interacting, it is not always the same mast which needs the deepest camber. For this reason, an average camber of 10% - 12% is most common for this technology. The centre of pressure of these sails sits just forward of and near the centreline of the mast for an optimum performance trimming.

As Rigid Wingsails, the DynaRig does not require any active power to generate aerodynamic forces such as the Rotor Sail. Little power (assumed negligible in this model) is required for trimming them.

Several wind tunnel tests have been carried out for this device since Prölss invented the DynaRig, including *Perkins et al. (2004)*, *Smith (2013)* and *Bordogna (2020)*. We used the data of *Bordogna (2020)*. The DynaRig was virtually trimmed via a computer program which optimizes the maximum thrust for each AWA. The DynaRig model of these wind tunnel tests is a 1.85 aspect ratio sail with a camber of 10%. Bordogna studied the aerodynamic performance of a single DynaRig, two DynaRigs with GD = 2.5 (horizontal distance between the two masts relative to sail chord) and two DynaRigs with GD = 4.

The Reynolds number effect is assumed negligible. The aspect ratio effect is also negligible since the model just accepts DynaRig configurations of the average commercial aspect ratio of 2. In the DynaRig model of the Performance Prediction Program the data is fitted following a sequential linear interpolation. This computes sequentially an interpolation for each parameter.

4. Route optimization

The Route Optimization Model (ROM) consists of several components, Fig.14, *Ruiz Carrio (2020)*. The key components of the ROM are the optimizer, the route evaluation algorithm and the multi-objective optimization algorithm.

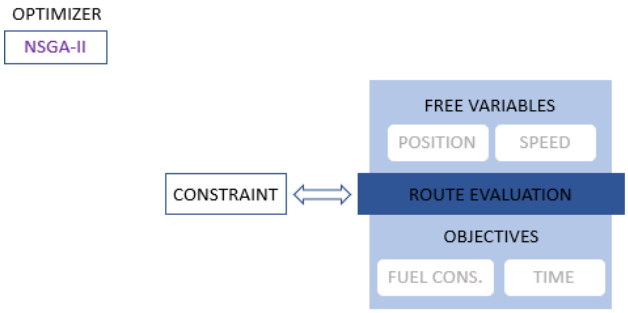

Fig.14: Functional structure of ROM

The optimizer randomly selects a set of free variables. The route evaluation algorithm builds the route with these free variables. The optimizer checks if the route is violating the constraints at any point of the route. If it does, the route becomes invalid and, thus, discarded right away. If the constraints are satisfied, the algorithm calculates the objectives according to the free variables selected. These objectives are feedback for the optimizer and the Non-dominated Sorting Genetic Algorithm II (NSGA-II) optimization algorithm. A new selection of free variables is based on this feedback. This process is repeated until the Pareto-optimal set is found.

4.1. Route Evaluation Algorithm

The concept behind the route evaluation algorithm consists of perturbing the Orthodromic route in benefit of the weather pattern to take maximum advantage of the sailing devices. The Orthodromic route represents the shortest distance between two points on the Earth surface, also known as Great Circle line. The perturbation approach is based on the deviation of the vessel from the Orthodromic route, i.e. from the shortest route, in order to find a different route with lower fuel consumption and sailing time. The approach considers non-constant speed profiles for the vessel. The methodology the route evaluation algorithm can be explained as:

- Orthodromic route definition - The shortest route in distance between the departure and arrival points is computed. This route is the one that aims to be perturbed in order to find the optimal one. Supposing departure and destination points are given by Cartesian Coordinates, (φ_1, $\lambda 1$) and (φ_2, λ_2) where φ represents the latitude of the coordinate and λ, the longitude, the Great Circle distance can be expressed using the Haversine equation:

$$Haversine = 2 \cdot R \cdot arcsin(\sqrt{sin(\Delta\varphi/2)^2 + cos(\varphi_1)cos(\varphi_2) * sin(\Delta\lambda/2)^2}) \quad (4.1)$$

  where $\Delta\varphi$ and $\Delta\lambda$ are the latitude and longitude variations respectively and R represents the Earth radius.

- Orthodromic route discretization - The Orthodromic route is discretized with a fixed number of equally spaced waypoints. The number of waypoints is a trade-off between the accuracy needed to find the optimal route and quantify savings and the computational effort of the model. For each control point considered, many interpolations are required regarding ship performance and weather patterns, which is costly in computational terms. Moreover, the number of free variables that the optimization faces is increased by two for each waypoint considered.

- Orthogonal shifts - The route to be evaluated is created by perturbing the Orthodromic route. This model consists of an orthogonal deviation on each waypoint, changing in this way the course of the vessel as shown in Fig.15. The orthogonal shifts together with the ship speed for each leg will later be used as free variables for the optimization process. The model differs from *Hinnenthal and Saetro (2005)*, who used spline curves in order to get a smooth course line. Contrarily to that approach (for motor-ships), the orthogonal shifts allow sharp turns at

the waypoints and thus tacking into the wind. The pronounced course changes allow the vessel to set a sail configuration for each leg. The orthogonal deviation in each way point allows the Course Over Ground to vary. The maximum orthogonal deviation is also a variable that can be adjusted depending on how distant the vessel should be from the Orthodromic route.

Fig.15: Sketch of the orthogonal shifts concept. The blue dots represent some of the potential orthogonal deviations from the Orthodromic route (represented by a non-continuous curve).

Course Over Ground plays a key role in route modeling for wind assisted vessels since it determines the True Wind Angle. The True Wind Angle (TWA) is the relation between True Wind Direction (TWD) and Course Over Ground (COG). TWD and COG are relative to the North direction. The Course Over Ground (COG) can be expressed as the heading in addition to the leeway which is the side-way drift of the desired course. As the Performance Prediction Program already studies the leeway, thus, the Course Over Ground is the input into the ROM.

The rhumb line equations are used to determine the course and distance between waypoints:

$$course = arctan\left(\frac{\Delta\lambda \cdot cos\left(\frac{\varphi_1 + \varphi_2}{2}\right)}{\Delta\varphi}\right) \tag{4.2}$$

$$distance = \frac{60 \cdot \Delta\varphi}{\cos(course)} \tag{4.3}$$

$\Delta\varphi$ and $\Delta\lambda$ are the latitude and longitude variations, respectively.

- Compute the new positions - Given the orthogonal deviation in relation to the Great Circle Line (GCL) at each waypoint, the new locations at each control point can be computed. There are unlimited numbers of route combinations by changing the position of the control points. At this stage, the exact position of the way points for each route will be known by using the orthogonal deviation in relation to the GCL. With known positions of the waypoints, the distance between and the course between them can be determined. The distance is used to determine the time of arrival at each waypoint as well as the total sailing time. Course and time are key to compute the fuel consumption.

- Weather interpolation (wind, waves and currents) - The weather data relevant for the development of the model needs to be known in order to evaluate the route. The weather data set is interpolated at ten waypoint positions plus five intermediate positions for each leg at the time that the vessel reaches each position, using multivariate interpolation with a uniformly spaced regular grid. The true wind speed, true wind direction, significant wave height and surface type will be known for the control points at a specific time. By the wind components, the true wind angle is extracted from the course of the vessel between two waypoints. The true wind angle together with the true wind speed and the significant wave height are the parameters extracted from the weather data for the Performance Prediction Program at the control points.

- Performance Prediction Program application - The vessel characteristics are introduced in the ROM by using the results of the Performance Prediction Program (PPP) run for this vessel. The ROM is a broad model that can host any cargo vessel importing vessel-specific Performance Prediction Program results.

Again, a multivariate interpolation is used to apply the Performance Prediction Program results to the route. The input information for the PPP is ship speed, true wind speed, true wind angle, and significant wave height. With these input values at each control point, the model interpolates the corresponding delivered power. Then the fuel consumption for a leg of the route is:

$$fuel\ consumption = SFC \cdot PD \cdot time \tag{4.4}$$

SFC denotes the Specific Fuel Consumption and PD the Delivered Power.

- Time and Fuel Consumption computation - Sailing time and fuel consumption are summed over all legs of the route to find the total time and fuel consumption invested for each route evaluated.

5. Energy savings for WAPS

The aim of this case study is to show the energy savings potentials and the main differences in the performance between the several WAPS available in the model: Rotor Sails, Rigid Wingsails and DynaRigs. The cargo ship used to perform these calculations is the 'Maersk Pelican' shown in Fig.4. Thanks to their available deck space, tankers and bulk-carriers are especially suitable for wind propulsion. Also, due to their low design speed, for tankers and bulk-carriers it is more challenging to fulfill the requirements of the Energy Efficiency Design Index (EEDI).

The first challenge when comparing the performance of each WAPS is selecting their total sail areas. An area for each WAPS that gives a total similar forward thrust for given wind and sailing conditions is needed. Otherwise, the results are difficult to interpret. The required difference in size will also give us the efficiency of each WAPS in terms of forward thrust per square meter of projected sail area. To do so, a performance prediction calculation is conducted for one 30x5 m Rotor Sail with De/D = 2 installed mid-ship for the reference sailing condition. The true wind speed (TWS) is defined as 10 m/s, a typical average TWS in the North Atlantic Ocean. The ship speed is taken as *Vs* =12.5 kn, the mean real service speed of the 'Maersk Pelican' *Paakkari et al. (2020)*.

Its maximum forward thrust, experienced at a true wind angle TWA = 110°, is used to get the Rotor Sail lift coefficient at this wind condition. Assuming that all Rigid Wingsails have the same aspect ratio as the DynaRig, namely 2, their maximum lift coefficient is obtained from the model data source. Then, the area needed to equalize the Rotor Sail lift at maximum forward thrust for each WAPS is computed. The performance efficiency of each wind-assisted device is given as a factor of lift force generated per projected sail area. The results, normalized to the least efficient device, are shown in Table I.

Table I: WAPS efficiency comparison

WAPS	3D C_L	Area m^2	N/m^2	Normalized
Rotor Sail (AR=6 & DeD=2)	9.15	150	650.37	7.76
Rigid Wingsail No Flap (AR=2)	1.18	1163.47	83.45	1
Rigid Wingsail 30% Plain Flap (AR=2)	1.70	807.59	120.8	1.44
Rigid Wingsail 30% Slotted Flap (AR=2)	1.73	793.58	122.93	1.47
DynaRig (AR=2)	1.48	927.63	105.17	1.25

These findings show the relation in area between WAPS to generate the same maximum lift. Thus, their efficiency in creating a lift force per projected sail area. The Rotor Sails are most efficient, ~8 times more efficient than a Rigid Wingsail plain airfoil without flaps. Thus, a Rigid Wingsail with aspect ratio of 2 must be nearly 8 times bigger in size than a Rotor Sail to produce the same forces. However, the Rotor Sail's trade-off is its required power to spin which does not allow it to always rotate as fast as it should to maximize lift. Fig.16 visualizes this efficiency.

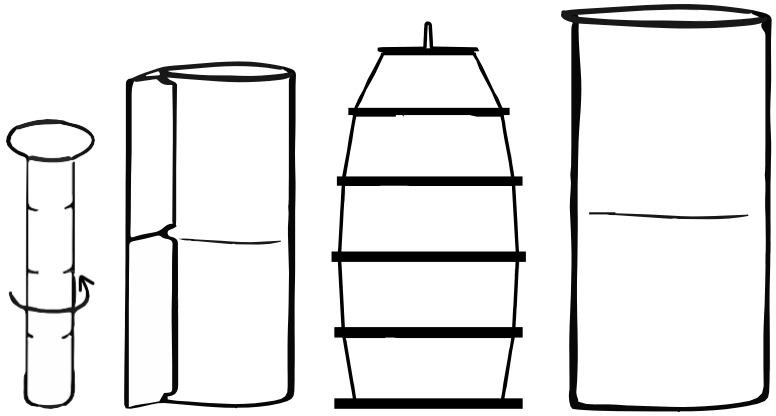

Fig.16: WAPS area proportions according to Table I

The WAPS efficiency comparison is used to design the Rigid Wingsails and the DynaRig aiming at similar savings as a single 30x5 m rotor sail. We use the WAPS configurations presented in previous Table I with a total projected sail area of 800 m^2 for all Rigid Wingsails and the DynaRig. All WAPS are installed at mid-ship, but the vertical centre of effort differs due to different mast heights (Rigid Wingsails and DynaRig have the same vertical centre of effort because of their equal aspect ratio).

To compute power savings, the delivered power of the traditional pure motor 'Maersk Pelican' (without any WAPS installed) is first predicted for the same wind conditions and sailing speed. Then, all WAPS performance predictions are run independently. The power savings compared to the pure motor configurations are determined for each simulation point. Rotor Sails' RPMs and Rigid Wingsails' angle of attack (AoA) and flap deflection are trimmed constantly to maximize total power savings. Windage for DynaRig and Rotor Sails is also included. Rigid Wingsails are assumed retractable. These windage forces are active when the WAPS produces a higher negative forward thrust than its own windage component. In those conditions, WAPS's aerodynamic forces are deactivated. The total Rotor Sail spinning power required as function of its RPMs is also accounted in the calculation of total power savings. It is added to the delivered power of the wind-assisted cargo ship. Fig.17 shows the power savings for all five different WAPS for the reference condition at 10 m/s TWS and 12.5 kn ship speed.

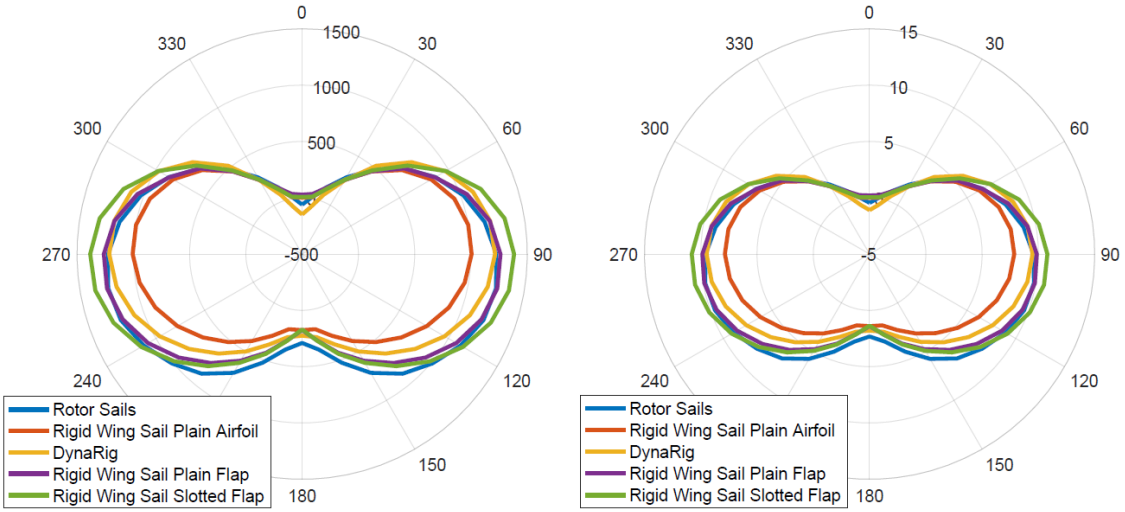

Fig.17: Power savings polar diagrams for all WAPS for 'Maersk Pelican' (12.5 kn and 10 m/s TWS) for TWA relative to bow. Left: absolute power savings [kW]. Right: power savings [%]

Maximum savings for all WAPS are very similar as intended by selecting the sail area of 800 m^2. Rotor Sails perform undoubtedly better than the other WAPS in downwind and broad reach sailing courses. Trailing edge slotted and plain flaps can generate much higher forward thrust than the plain airfoil which leads to overall higher power savings for all TWAs. In pure downwind (TWA=180°), all Rigid Wing Sails perform equally since the AOA is set at 90° and the major component of the total aerodynamic force is drag. The DynaRig stands out in upwind sailing courses where it outperforms the other configurations. For the non-retractable devices such as the DynaRig and the Rotor Sail, windage is accounted for in the overall power savings calculations. This is clearly seen at pure upwind condition (TWA=0°) where savings are negative. The vessel must deliver higher power to overcome this air resistance than without WAPS installed. For Rotor Sails, for pure upwind course it is better to have the Rotor Sail rotating at a velocity ratio $U/V \approx 1$ than turning it off and having only its windage component. At this low velocity ratio, the drag force is lower than its non-rotating windage thanks to flow circulation.

The percentage of savings are for one WAPS of each type installed at mid-ship of the 'Maersk Pelican'. As a first order approximation, the results can be scaled to predict the savings when more devices are installed. However, interaction effects in the overall aerodynamic performance and the non-linear hydrodynamic effects such as propeller efficiency, drag due to side force and rudder hydrodynamic side force play a key role and should be considered by conducting the performance predictions explicit with all installed WAPS.

6. Energy savings for specific route and optimized route

For the specific route analysis and optimization, the performance prediction results for the 'Maersk Pelican' without Rotor Sails and with two Rotor Sails as installed on the vessel, see Fig.4, are used as input. PPP results are generated for a full set of realistic operating speeds, true wind speeds and significant waves heights for all true wind angles. As the exemplary route a North Atlantic passage from Europe to North America is selected. The route analysis and optimization are conducted for 3 return voyages in 2020, one each in January, April and July. For each trip a specific departure date is selected, and the hindsight weather data is obtained at ten positions between each waypoint at the specific time. The weather data is not averaged.

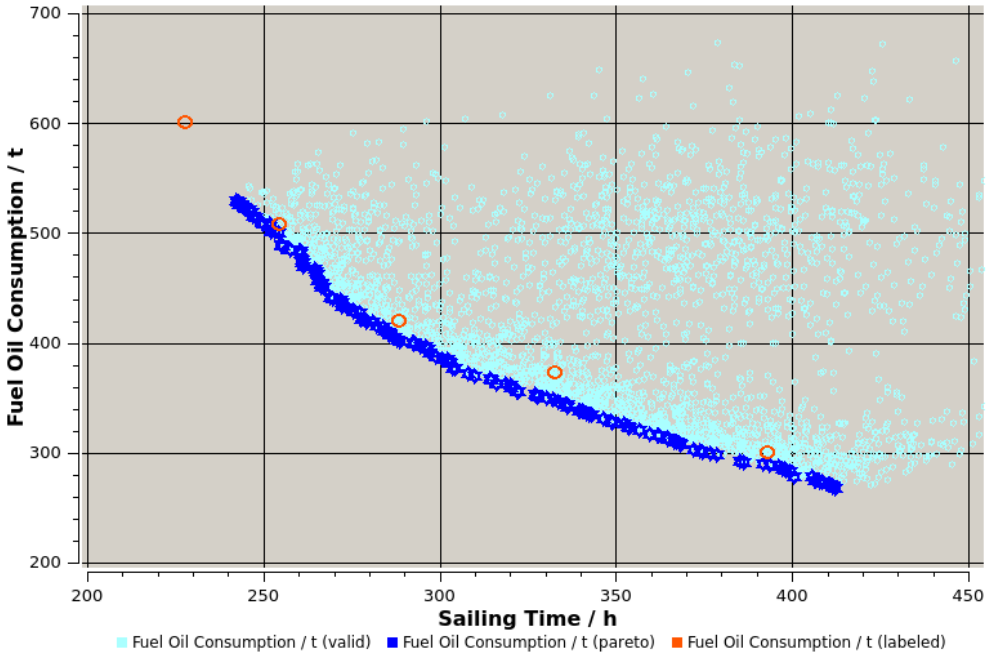

Fig.18: Fuel oil consumption versus voyage time for eastbound passage in April 2020, with Rotor Sails. Cyan: All valid route candidates, blue: pareto-optimal route candidates, orange: passages on great circle line with constant speed

For each passage two route optimizations are conducted, one assuming the Rotor Sails are used where possible, and one assuming no Rotor Sails are installed. The total time for the voyage is not constrained in the optimizations, leading to a set of pareto-optimal route candidates. Fig.18 shows, for the eastbound passage with Rotor Sails in April 2020, all evaluated route candidates in cyan, the pareto-optimal route candidates in blue, and for reference in orange passages on the great circle line with five different constant speed.

As an example, for a pareto optimal route, Fig.19 shows the vessel's position (red dot) and the wind pattern for four stages of the optimized eastbound passage with Rotor Sails in April 2020, with a total voyage time of 332 hours (13.8 days). It is visible how the course takes advantage of areas of favorable wind and avoids areas of strong adverse wind.

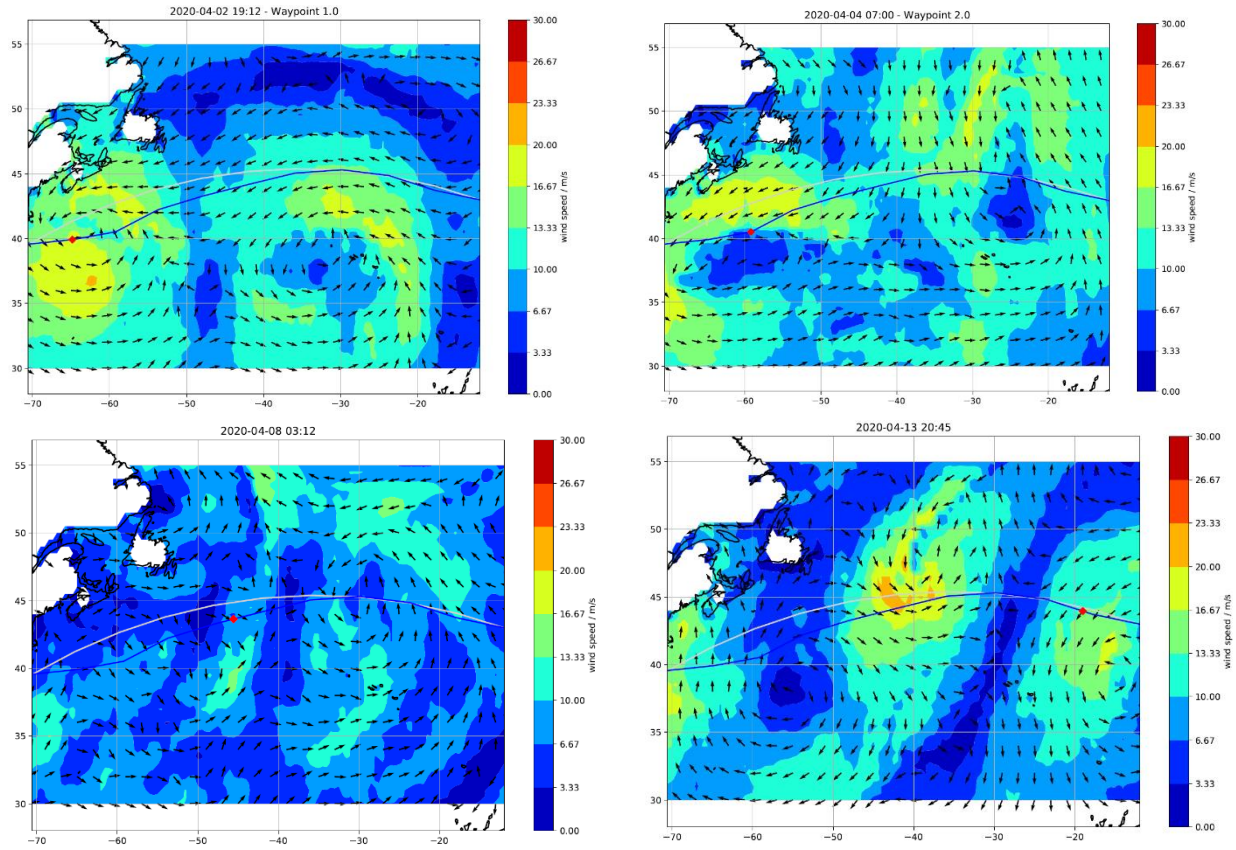

Fig.19: Optimized route for eastbound passage using Rotor Sails in April 2020. Ship position marked in red. Blue: optimized route. Grey: Great circle line (shortest distance)

In order to quantify the savings potential for a certain voyage time, the optimized route is compared against the constant speed crossing on a great circle line with the same voyage time. The fuel savings are averaged over the three round trips (six voyages/passages). Fig.20 shows the obtained average fuel savings through weather routing as a function of voyage time for the vessel without and with Rotor Sails. The average fuel savings from weather routing are 0.8-2.6% for the motor ship and 2.5-4.1% for the vessel with Rotor Sails. The percentage savings tend to increase with voyage time. The absolute fuel savings show no clear dependency on voyage time.

For reference, Fig.21 shows the average speed required to reach the voyage times when travelling on the great circle line.

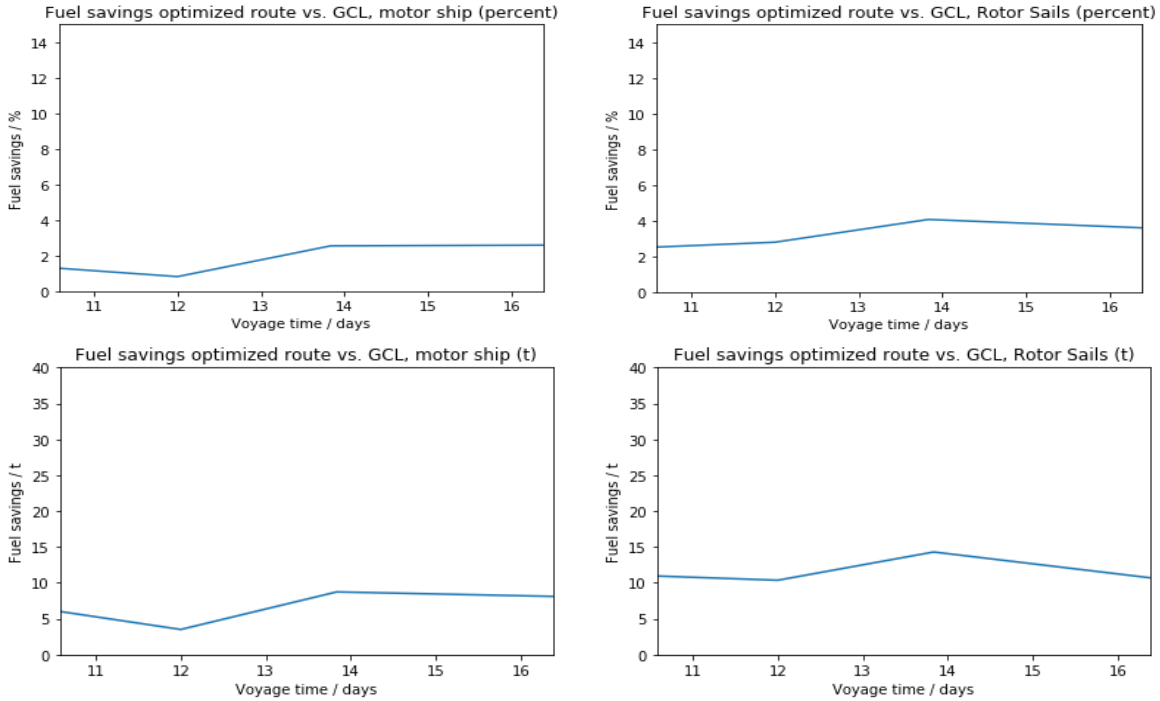

Fig.20: Average fuel savings by using weather routing. Left: Vessel without Rotor Sails. Right: Rotor Sails used wherever possible. Top: Fuel savings in percent, bottom: Fuel savings in metric tons

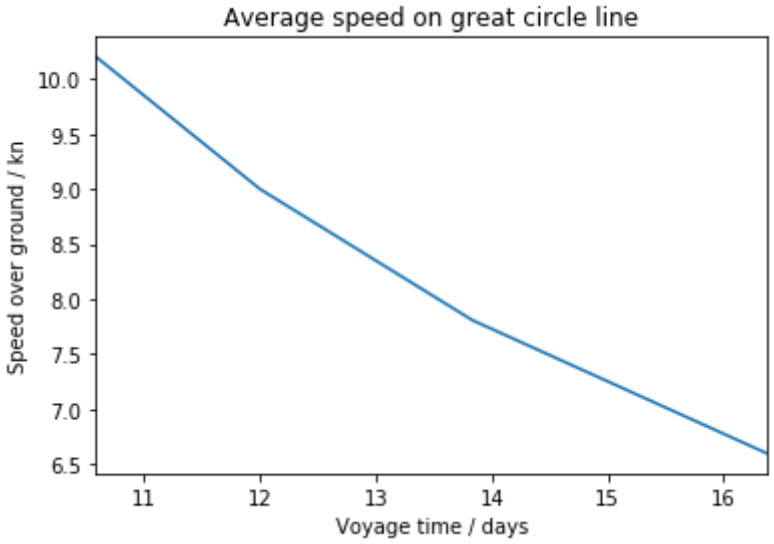

Fig.21: Average speeds on great circle line corresponding to the voyage time

Fig.22 shows the average fuel savings which can be achieved by the Rotor Sails. The average fuel savings due to the Rotor Sails on the great circle route are 5.8-10.0%, on the optimized route 7.3-10.5%. As before the percentage fuel savings tend to increase with voyage time. The reduced ship speed increases the relative contribution from the Rotor Sails and the increased voyage time broadens the range of feasible optimized routes. Again, the absolute fuel savings show no clear dependency on voyage time. They remain at a similar level across the range of voyage times.

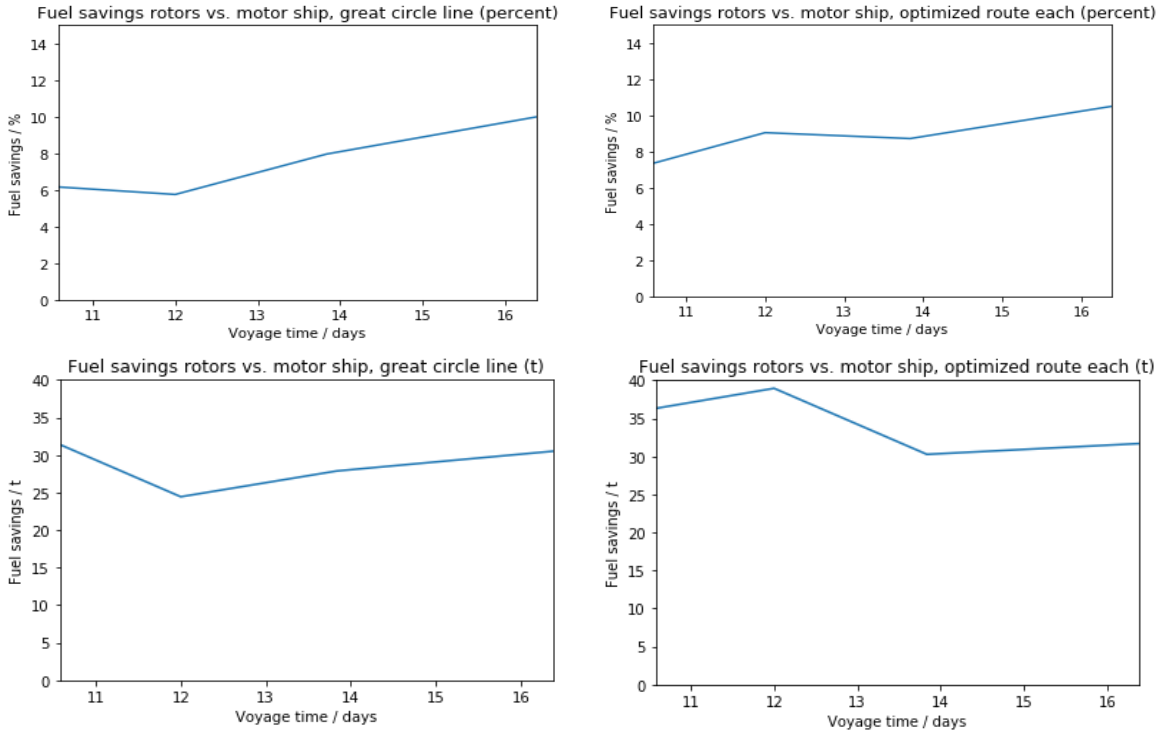

Fig.22: Average fuel savings for vessel with Rotor Sails. Left: Sailing on great circle line with constant speed. Right: Optimized route. Top: Fuel savings in percent, bottom: Fuel savings in tons

7. Conclusions

The performance prediction program together with the route optimization model presented in the paper allow for the realistic assessment of the fuel savings for different WAPS, which can currently be retrofitted on existing vessels and designed for new builds. Only the main particulars of the vessel and the dimensions of the WAPS are required so that the approach can be utilized during early stage feasible studies.

Utilization of a detailed ship model where the individual force components are modelled and where equilibrium is found in all six degrees of freedom means that this method is also suitable to study wind ships which are predominantly propelled by the wind.

The exemplary route analysis and optimization shows moderate average savings potentials of weather routing of up to 4.1% for the vessel with Rotor Sails and up to 2.6% for the vessel without Rotor Sails. The results are obtained from 6 sample voyages with hind-sight weather data. A larger number of voyages can be investigated to ensure that a sufficiently large number of weather conditions is considered to obtain statistically relevant average fuel savings. It can also be expected that the savings from weather routing increase with thrust contribution from WAPS. Wind ships, which are predominantly propelled by the wind, benefit more from weather routing than motor ships.

In the presented example, the fuel savings due to the Rotor Sails are significant, even if the vessel simply follows the great circle route at constant speed. In case additionally weather routing is applied, the savings can be further increased, ranging from 7.3 % to 10.5%.

This type of analysis can provide valuable insight into the key role that WAPS may take towards low-carbon shipping within the next decade.

Acknowledgements

The authors sincerely thank the project partners at the Technical University of Denmark, especially Professor Harry B. Bingham, and at KTH Royal Institute of Technology for their support and contribution to this work.

References

ABBOTT, I.H.; VON DOENHOFF, A.E. (1959), *Theory of Wing Sections*, Dover Publications

BERGESON, L.; GREENWALD, C.K. (1985), *Sail Assist Developments 1979-1985*, J. Wind Engineering and Industrial Aerodynamics 19

BERTHOLDT, J.; RIESCH, H. (1988), *Windschiffe*, VEB Verlag Technik

BORDOGNA, G. (2020), *Aerodynamics of Wind-assisted ships. Interaction effects on the aero-dynamic performance of multiple wind-propulsion systems*, PhD Thesis, Delft University of Technology

BORG, J. (1985), *Magnus effect: An overview of its past and future practical applications*, Naval Sea Systems Command, Department of the Navy

DIJKSTRA, G.; PERKINS, T.; ROBERTS, D. (2004), *The Maltese Falcon: The realization*, Int. HISWA Symp. Yacht Design and Yacht Construction

FINCK, R.D. (1977), *USAF Stability and Control DATCOM*, McDonnell Douglas Corporation, Douglas Aircraft Division

HINNENTHAL, J.; SAETRA, O. (2005), *Robust Pareto-Optimal Routing of Ships utilizing Ensemble Weather Forecasts*, 4th COMPIT Conf., Hamburg, pp.17-24, http://data.hiper-conf.info/compit2005_hamburg.pdf

HOLTROP, J. (1977), *A statistical analysis of performance test results*, Int. Shipb. Progress 24, pp.23-28

HOLTROP, J. (1984), *A statistical re-analysis of resistance and propulsion data*, Int. Shipb. Progress 31, pp.272-276

HOLTROP, J.; MENNEN, G.G.J. (1978), *A statistical power prediction method*, Int. Shipb. Progress 25, pp.253-256

HOLTROP, J.; MENNEN, G.G.J. (1982), *An approximate power prediction method*, Int. Shipb. Progress 29, pp.166-170

ITTC (1957), *Skin Friction and Turbulence Stimulation*, 8th ITTC

KUIPER, G. (1992), *The Wageningen Propeller Series*, MARIN publication 92-001

NEWMAN, J.N. (2017), *Marine Hydrodynamics*, MIT Press

PAAKKARI, V.; HURFORD, A.; CARDDOCK, C. (2020), *Rotor Sail GHG Reduction Potential, Modelling and Sea Trila Validation*, 5th Innov'Sail Conf.

PERKINS, T.; DIJKSTRA, G.; PERINI-NAVI; ROBERTS, D. (2004), *The Maltese Falcon: the realization*, Int. HISWA Symp.on Yacht Design and Yacht Construction

PRANDTL, L.; BETZ, A. (1932), *Ergebnisse der Aerodynamischen Versuchsanstalt zu Göttingen*, Kaiser Wilhelm Institute for Fluid Dynamics

RAWSON, K.; TUPPER, E. (2001), *Basic Ship Theory: Hydrostatics and Strength*, Butterworth-Heinemann

RDURKACZ (2013), *Sketch of Magnus effect with streamlines and turbulent wake*, Wikimedia Commons

RECHE, M. (2020), *Performance Prediction Program for Wind-Assisted Cargo Ships*, Master Thesis, Danish Technical University, Lyngby, https://findit.dtu.dk/en/catalog/2596915357

RECHE, M.; RUIZ CARRIO, E. (2018), *Optimization of the rig for an autonomous sailing vessel*, Bachelor Thesis, Univ. Politecnica Catalunya, Barcelona, https://upcommons.upc.edu/handle/2117/119322

RUIZ CARRIO, E. (2020), *Route Optimization for Cargo Vessels with Wind Assisted Propulsion Systems*, Master Thesis, Danish Technical University, Lyngby, http://www.nor-mar-eng.org//-/media/Sites/NOR-MAR-ENG/education/thesis_examples/MSc_thesis_Esperanca_Ruiz_Carrio.ashx

SCHENZLE, P. (1980), *Standardised Speed Prediction for Wind Propelled Merchant Ships*, Symposium on wind propulsion of commercial ships, The Royal Institution of Naval Architects

SCHENZLE, P. (1983), *Wind as an aid for ship propulsion*, 8th WEGEMT Summer School 'Ship Design for Fuel Economy'

SCHENZLE, P. (1989), *Sailing without finkeel - Towing tests with sailing ship hulls*, STG-Sommertagung, HSVA

SCHENZLE, P. (2010), *Wind Ships in the 21st Century? - Current concepts for wind propulsion of ships*, STG Jahrbuch, Springer

SMITH, T. (2013), *Analysis techniques for evaluating the fuel savings associated with wind assistance*, Low Carbon Shipping Conf.

WALKER, J. (1985), *High Performance Automatic Wingsail Auxiliary Propulsion System for Commercial Ships*, J. Wind Engineering and Industrial Aerodynamics 20

WHICKER, L.; FEHLNER, L. (1958), *Free-stream characteristics of a family of low-aspect ratio, all movable control surfaces for application to ship design*, David Taylor Model Basin Report No. 933.

YOUNG, A. D. (1953), *The Aerodynamic Characteristics of Flaps*, Aeronautical Research Council Report and Memoranda, London

Numerical Analysis of Flettner Rotors Performances on the MARIN Hybrid Transition Coaster

Maxime Garenaux, MARIN, Wageningen/The Netherlands, M.Garenaux@marin.nl
Joost Schot, MARIN, Wageningen/The Netherlands, J.J.A.Schot@marin.nl
Rogier Eggers, MARIN, Wageningen/The Netherlands, R.Eggers@marin.nl

Abstract

This paper presents a numerical study of the aerodynamic performances of Flettner rotors on the MARIN Hybrid Transition Coaster (MHTC) at full scale Reynolds numbers. The effects of the interaction between the MARIN Hybrid Transition Coaster (MHTC) and its three Flettner rotors are investigated. Large interaction effects are found to depend on both the spin ratio and the apparent wind angle. It is therefore concluded that these interactions cannot be omitted. A model based on the thrust identity approach together with a correction for the effective apparent wind angle is proposed to correct the performance of free standing Flettner rotor to the performance of a rotor on the deck of the vessel.

1. Introduction

The Flettner rotor is the dominant device in the recent market introductions of Wind Assisted Ship Propulsion (WASP). Flettner rotors provide ship owners with a low operational impact wind propulsion concept with reported power saving reaching up to 15%. Even though Flettner rotors are often applied as retrofit, recent new-built projects are incorporating Flettner rotors in the ship design phase, which enables them to be fully integrated and to reach larger savings.

In the literature, the performance of wind propulsors is generally derived from wind tunnel tests data or CFD, considering undisturbed incoming flow, *Li et al. (2012), De Marco et al. (2106)*. Even though these studies give valuable insights on Flettner rotor performances, they often omit the interactions between multiple wind propulsors, and the interactions with the ship and its superstructures. Omitting these interactions may lead to an erroneous assessment of the wind propulsion performance once positioned on the deck of a vessel.

In *Bordogna (2020)* interaction effects between multiple wind propulsors are largely discussed. It is concluded that the interactions between two Flettner rotors can affect the lift and drag forces of the rotors. These interactions are found to depend on the distance between the rotors and the apparent wind angle. To a lesser extent, similar findings are reported in *Jones et al. (2019)* which concluded that positioning the Flettner rotor as far apart as possible and in a staggered pattern should reduce rotor-rotor interaction effects.

Besides rotor-rotor interactions, ship-rotor interactions should also be accounted for. In the same study by *Jones et al. (2019)*, ship-rotor interactions are reported. To the writer's knowledge this is the only publicly available study reporting interaction effects between a Flettner rotor and a ship. *Jones et al. (2019)* conducted CFD calculations for multiple Flettner configurations under uniform wind profile conditions. Changes up to 50% in lift are reported for a rotor mounted on a generic ship when compared to a rotor in isolation. These interaction effects are reported largest under beam wind condition. With beam wind condition, the blockage induced by the hull creates a region of decelerated flow with can encompass the Flettner rotor leading to a decrease in rotor efficiency.

Contrary to previously reported study, *Li et al. (2012), De Marco et al (2106)* or *Jones et al. (2019)*, an atmospheric boundary layer profile (ABL) is used in this study as opposed to a uniform wind profile. At sea the wind is generally following an atmospheric boundary layer profile which results in a twisted apparent wind profile. The twist in apparent wind angle (AWA) and apparent wind speed (AWS) originates from the change in true wind speed over the height of the rotor while the ship speed and ship heading remain constant. For the atmospheric boundary layer profile, the wind reference is defined

using the reference wind at 10 m above mean sea level (MSL). A power law profile is used to approximate the atmospheric boundary layer. The power law is defined as follows:

$$V(z) = V_{ref} * \left(\frac{Z}{Z_{ref}}\right)^{exponent} \quad (1)$$

Where V_{ref} is the reference wind speed at the reference height Z_{ref} of 10 m above MSL. In Eq.(1) the choice of the exponent, also known as Hellmann exponent, is affecting the type of wind profile. This exponent is determined by the mean wind speed, the atmospheric stability and the surface roughness, *Counihan (1975)* and *Bañuelos-Ruedas (2010)*. In the literature, an exponent equal to 0.11 is often used. This value of 0.11 is however sometimes associated with wind profiles under extreme weather conditions as indicated by *IEC (2009)* and as recommended by *ABS (2014)*. According to *Hsu et al. (1994)*, this value can also be used for the near neutral atmospheric stability conditions on basis of measurements in the Gulf of Mexico. For normal weather conditions, a value of 0.14 or 0.12 is usually recommended as indicated by *ABS (2014)* and *DNV (2010)*. Recent wind speed measurements of the atmospheric boundary layer above the Atlantic Ocean indicates that even lower values of the Hellmann exponent can occur *Dhome (2020)*. It is reported that a value of 0.045 is estimated to be the most likely to occur with a probability of 25% of the measurements. Choosing the correct Hellmann exponent can become a dedicated study on its own. For the present study, an exponent equal to $\frac{1}{7} \approx 0.14$ has been selected as it will reflect the differences with a constant speed wind profile.

The main objective of the present study was to further understand the ship-rotor interactions under realistic sailing conditions. Therefore, MARIN decided to evaluate the performance of three Flettner rotors mounted on the MARIN Hybrid Transition Coaster (MHTC) subjected to an atmospheric wind profile. To this end, a numerical approach using RANS simulations has been developed to estimate the effects of the interaction between the MHTC and its three Flettner rotors. Additionally, the performance of the Flettner rotors positioned on the deck of the vessel is compared to the performance of a free standing Flettner rotor. Finally, a model to determine the effective wind velocity similar to the thrust identity method of propellers combined with a correction for the effective flow angle is proposed. This model is used to quantify the interactions ship-rotor. In this paper, the results of this research conducted at MARIN are presented.

2. Numerical methods

2.1. Geometry

In this study both the Flettner rotors and the vessel are included in the simulations. Multiple geometry configurations have been evaluated throughout the study. Initially, simulations with a standalone Flettner rotor have been conducted to compare the data with reference experimental data. Simulations with one Flettner rotor on the deck of the MHTC have then been performed to evaluate the influence of spin ratio and apparent wind angle on the ship-rotor interactions. Finally, simulations with three rotors on the MHTC have been conducted to assess the ship-rotors and rotor-rotor interactions.

For all geometry configurations, the same Flettner rotor geometry has been used. The rotor used has a diameter *D* of 3 m and a height *H* of 18 m. The rotor is fitted with a top end disk rotating with the rotor. The top end disk has a diameter *De* of 5.5 m and a thickness *Te* of 0.1 m. The rotor is mounted on a planar surface (simplified deck or deck of the vessel) which is not rotating with the rotor. The dimensions of the rotor are detailed in Table I.

For the simulations with ship, the geometry of the MHTC is used. The MHTC is a coaster with Lpp=86.76 m, beam 13.99 m and freeboard 7.0 m. The superstructures of the vessel are not considered in the simulations. The MHTC is fitted with three Flettner rotors, Fig.1. The rotors are separated by 28.27 m and the aft rotor is positioned 26.69 m ahead of the transom.

Table I: Dimensions of full scale Flettner rotor

Quantity	Symbol	Value	Unit
Rotor height	Hrotor	18.0	[m]
Rotor diameter	Drotor	3.0	[m]
Disc thickness	Tdisc	0.1	[m]
Disc diameter	Ddisc	5.5	[m]
Lateral area	Arotor	54.0	[m2]
Aspect ratio	AR	6.0	[-]

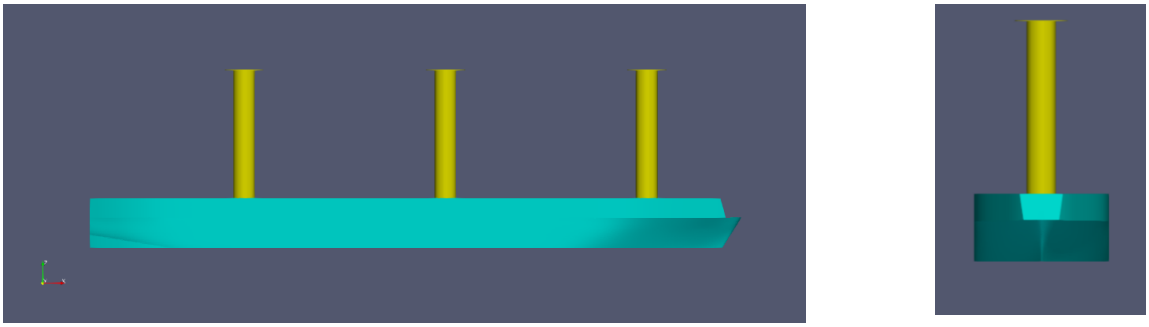

Fig.1: Flettner rotor configurations on MHTC

2.2. Computational domain and grid

Hybrid computational grids coupling different unstructured meshes generated by Hexpress have been used for all simulations. For each simulation a cylindrical unstructured grid is used around each Flettner rotor. Even though initially a Cartesian grid was used for the Flettner rotor, it is concluded that using cylindrical grids results into a significantly smaller numerical error compared to a Cartesian grid of similar cell size. For the region away from the rotor, ship domain and/or background domain, a Cartesian unstructured grid generated by Hexpress is used. The subdomains are coupled via interfaces. A second order interpolation scheme is used at the interfaces to ensure that the information is correctly transmitted at the interfaces. A representation of the subdomains for a standalone Flettner rotor and Flettner rotors on the MHTC is shown in Fig.2.

For the standalone Flettner rotor simulations, a rectangular background domain is used. The dimension of the domain is defined so that the domain is 300 D long, 200 D wide and 100 D high. For the simulations with MHTC, a circular background domain around the vessel is used. The diameter of the domain is then defined to be equal to 170 D. The wall distance to the ship and Flettner rotor(s) is defined to resolve the near wall boundary layer ($y^+ < 1$).

2.2. Grid sensitivity

A grid sensitivity study has been carried out for a standalone Flettner rotor and for a case with a single Flettner rotor on the vessel. For the standalone rotor, the grid is successively refined by increasing the number of cells over the diameter of the rotor. This sensitivity study is conducted at both model and full-scale Reynolds number. For the single Flettner on the deck of the vessel, the grid around the vessel is successively refined while retaining geometrical similarity. This sensitivity study is conducted at full scale Reynolds number. The lift and drag coefficients are found to exhibit a good convergence behaviour with successive grid refinements. The results of the grid sensitivity study are presented in Fig.3 and Table II. The intermediate grid for the standalone rotor (2,631,176 cells) is selected for the rest of this study, including the simulations with ship. For the single rotor on the ship, grid number 2 (18,814,696 cells) is selected for the rest of this study.

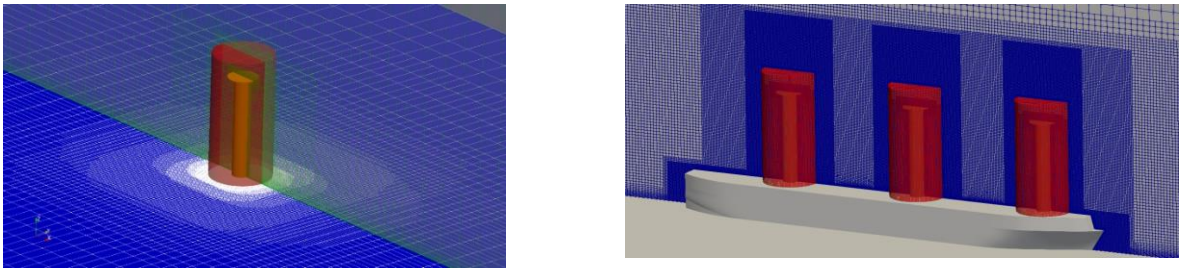

Fig.2: Left: Interfaces of Flettner rotor domain and empty background domain. Right: Interfaces ship domain with Flettner rotor domains. Red surfaces represent the interfaces.

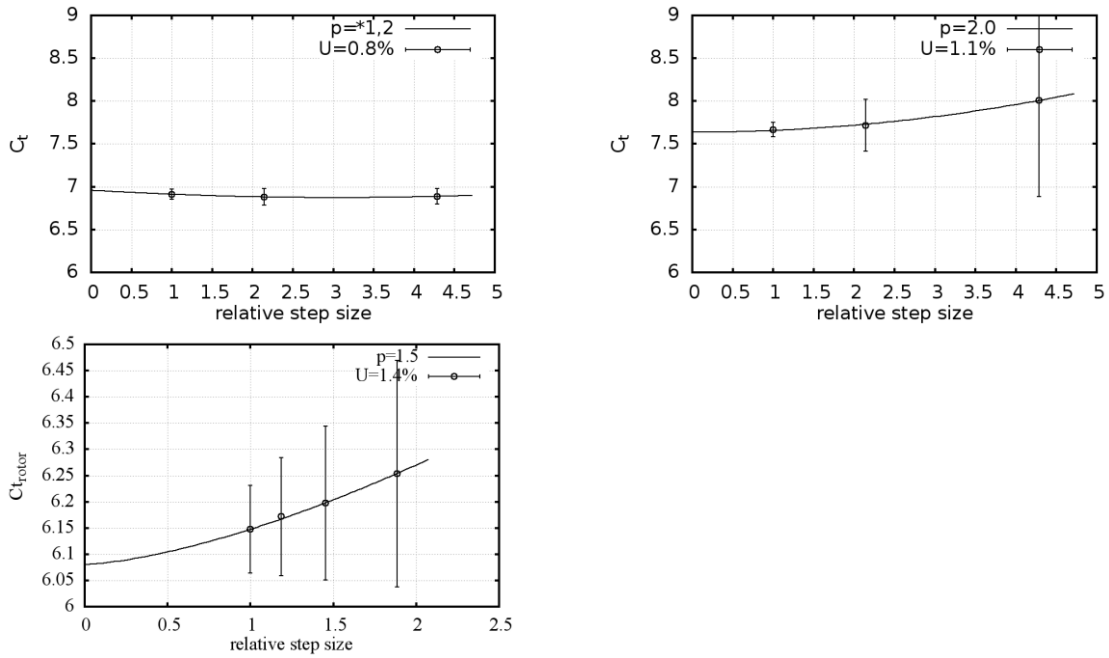

Fig.3: Results of grid refinement study. The total force coefficient C_t is used as metric. Top left: standalone rotor at a low Reynolds number. Top right: standalone rotor at a high Reynolds number. Bottom left: single rotor on the MHTC at a high Reynolds number.

Table II: Results of grid sensitivity study. The estimated numerical error δd in the total force coefficient Ct is given together with the estimate of the 95% confidence interval Ud95 also in terms of Ct. Results for spin ratio of 2.5

Low Re (standalone rotor)				High Re (standalone rotor)				High Re (single rotor on ship)			
Ncells	Ct	δd	Ud95	Ncells	Ct	δd	Ud95	Ncells	Ct	δd	Ud95
[-]	[-]	[-]	[-]	[-]	[-]	[-]	[-]	8,642,946	6.25	0.17	0.21
511,250	6.89	0.07	0.09	999,144	8,01	0.36	1.12	18,814,696	6.19	0.11	0.14
1,427,722	6.88	0.08	0.10	2,631,176	7.72	0.09	0.30	34,658,220	6.17	0.08	0.11
7,441,574	6.91	0.05	0.06	13,576,576	7.67	0.02	0.08	57,854,818	6.08	0.06	0.08

2.3. Flow conditions

For all simulations, a no slip boundary condition is used on the surface of the vessel. A no slip rotating wall boundary condition is set on the surfaces of the Flettner rotor to account for the rotation. For the simulation with standalone Flettner rotor, a velocity inlet boundary condition is used at the front of the CFD domain. A pressure boundary condition is set at the sides, outlet and top of the domain. At the bottom of the CFD domain two boundary conditions are used: a free slip wall is set for the background

part of the domain and a no slip wall boundary condition is defined near the foot of the rotor. For the simulations with ships and rotors, four inflow boundary conditions are set on the sides of the circular domain. This is a functionality available within ReFRESCO, www.refresco.org. Moreover, it allows to compute wind conditions from all directions. At the bottom of the CFD domain, a no slip wall is defined.

Unless specified otherwise, i.e. for benchmark between CFD with experimental tests and sensitivity to the type of wind profile, an atmospheric boundary layer profile is specified at the inflow boundary conditions of the simulations.

A comparison between the atmospheric wind profile (ABL) and a uniform wind profile is proposed in Fig.4 (left). Both wind profiles have the same speed at 10 m above MSL. The definition of the atmospheric wind profile accounts for the ship speed and drift angle meaning that a twisted wind profile is generated. Fig.4 (right) presents a typical atmospheric wind profile (upper) with varying apparent wind angle (lower).

In addition to the speed profile at the inflow, a free stream turbulence condition is specified based on the work described in *Spalart et al. (2007)*. It is mandatory that the turbulence values associated with the ABL profile are not used in the CFD simulations. This is discussed in detail in *Spalart et al. (2007)*. The length scale of the turbulent eddies associated with the ABL are very large compared to the ship and rotor, these scales would not interact with the small boundary layer forming on the vessel. If included in the RANS simulations these turbulent values will cause artificially high turbulent viscosity instead of large-scale unsteady inflow velocities.

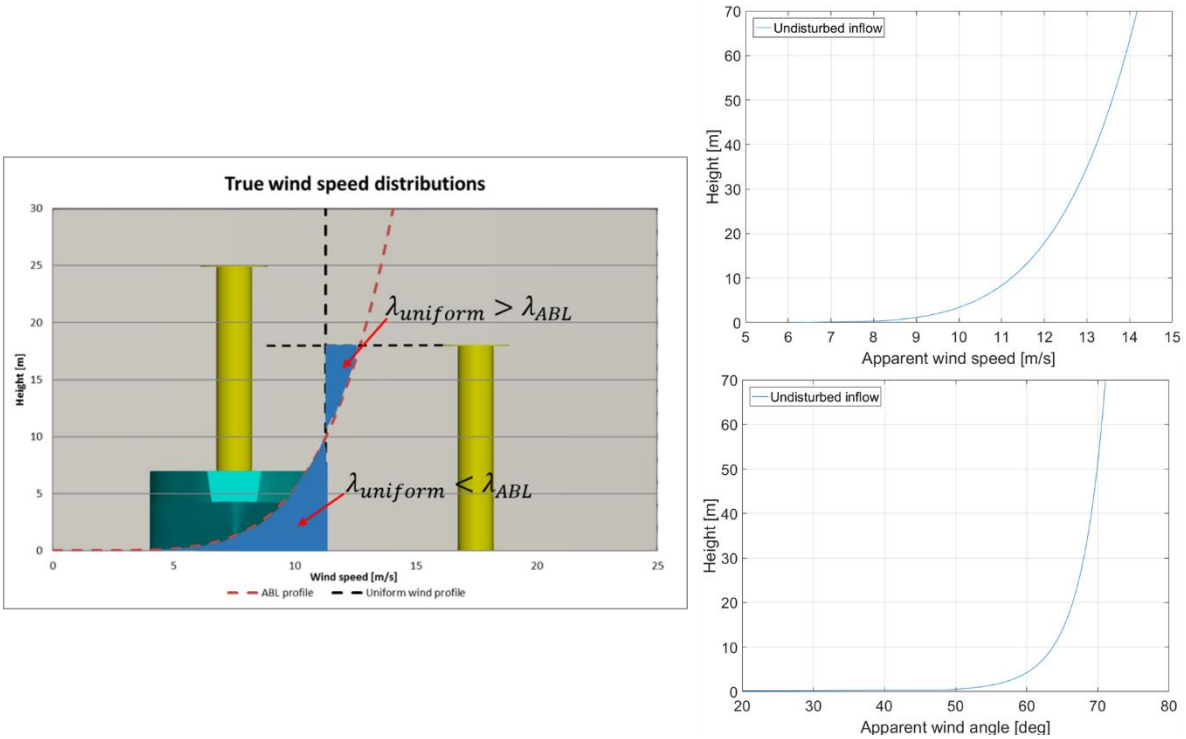

Fig.4: Left: Comparison between uniform wind profile and atmospheric wind profile. Lambda indicates the spin ratio of the Flettner rotor for both wind profiles assuming equal rotation rate. Right: Illustration of resulting apparent wind speed and apparent wind angle.

2.4. Solver

The CFD simulations are performed using the RANS code *ReFRESCO (2020)*. A finite volume approach with cell-centred collocated variables is used to discretise the equations. Mass conservation is ensured using a pressure correction equation based on the SIMPLE algorithm. For the momentum equations, a total variation diminishing scheme (TVD), using the Van Leer's Harmonic scheme, is used for convection. The effects of turbulence are modelled using the Explicit Algebraic Reynolds Stress

Model (EARSM) model developed by *Hellsten (2004)*. The model has been developed for high-lift aerodynamic applications, using a non-linear constitutive model for the Reynolds stresses instead of the Boussinesq assumption. It aims at resolving complex flows with adverse pressure gradients, wakes, mixing layers and curvature effects. The model aims to accurately predict the onset of separation. Massive flow separation is more difficult to capture with the Reynolds stresses model. Scale resolving turbulence models are likely more accurate for these conditions but also more computationally demanding. A second-order scheme is chosen for the convective flux discretisation in the turbulence equations. Except for the sensitivity study with unsteady simulations, all simulations are performed using a steady state approach. The steady state approach gave results in agreement with model scale experiment for a standalone rotor. The results appeared to be in good agreement with the findings reported in *Li et al. (2012).* The validity of the steady state approach was further verified for some simulations with rotors and ship.

3. Comparison with experimental data and scale effects

3.1. Comparison with experimental results

Experimental tests in a collaboration between MARIN and Peutz BV are used to validate the CFD approach for low Reynolds number. In particular, the choice of the turbulence model and the steady state approach were validated.

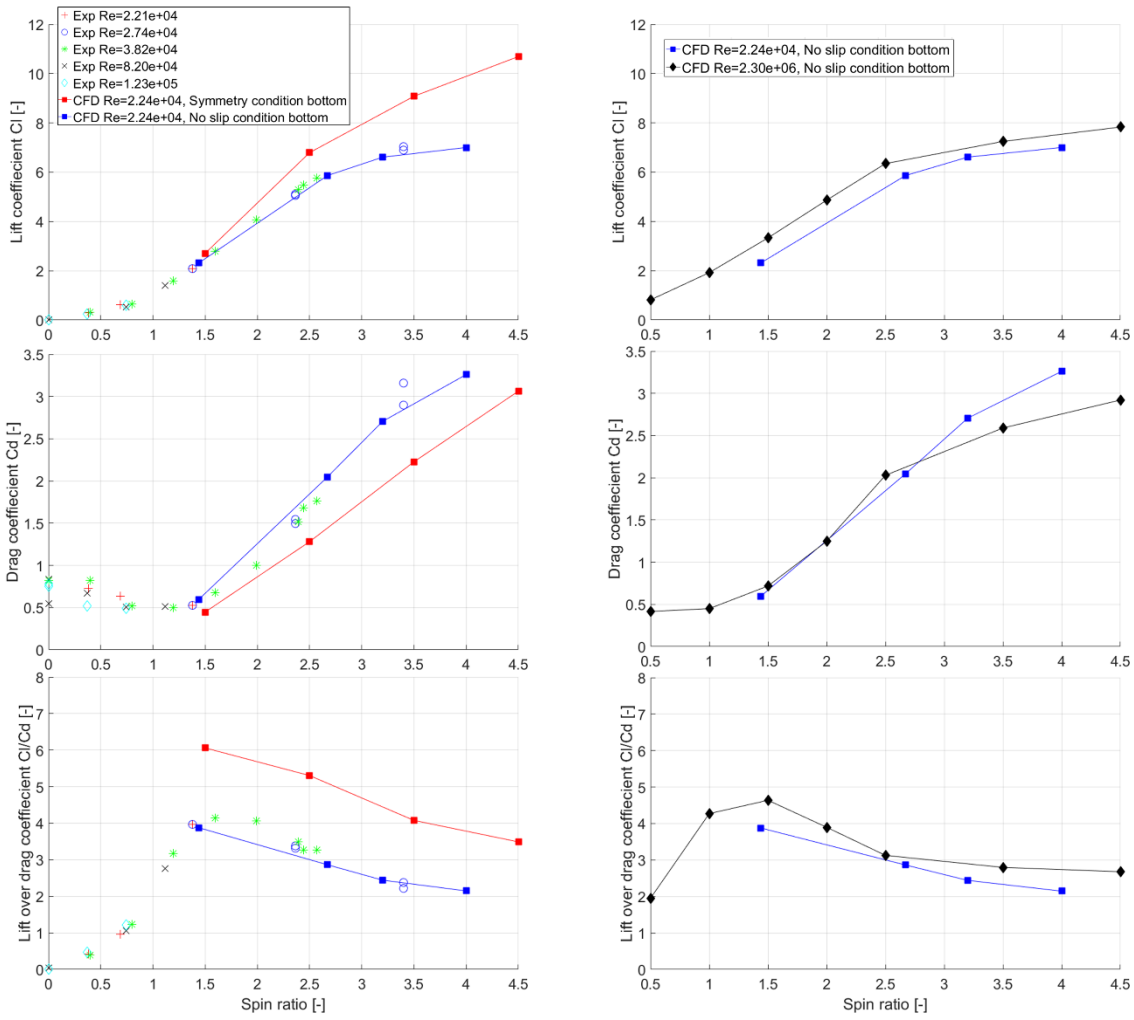

Fig. 5: Comparison lift, drag and lift over drag coefficient function of the spin ratio. Experimental data from Peutz BV are compared to CFD simulations at Re=2.24e+04 (left). Scale effects from CFD simulations at Re=2.24e+04 and Re=2.30e+06 (right).

The Flettner rotor used for the CFD simulations is identical to the geometry used in the wind tunnel tests. The geometry is scaled with a factor 19 compared to the full-scale geometry of the rotor. The CFD domain is modified to match the tunnel geometry. A constant wind speed is applied at the inflow. The velocity used to make the results dimensionless is corrected for the blockage of the rotor lateral area relative to the tunnel area.

Two type of boundary conditions at the bottom of the CFD domain are investigated: a symmetry boundary condition and a no-slip boundary conditions for all tunnel walls. The results with the symmetry boundary condition are shown in red in Fig.5 (left)and observed to be higher than the experimental values. The results with the no-slip boundary conditions are shown in blue in Fig.5 (left). The correlation with the wind tunnel data is much better once the no-slip boundary conditions are used. As visible in Fig.6, the decrease in rotor efficiency obtained with the no slip boundary condition is due to the creation of flow separation at the foot of the rotor.

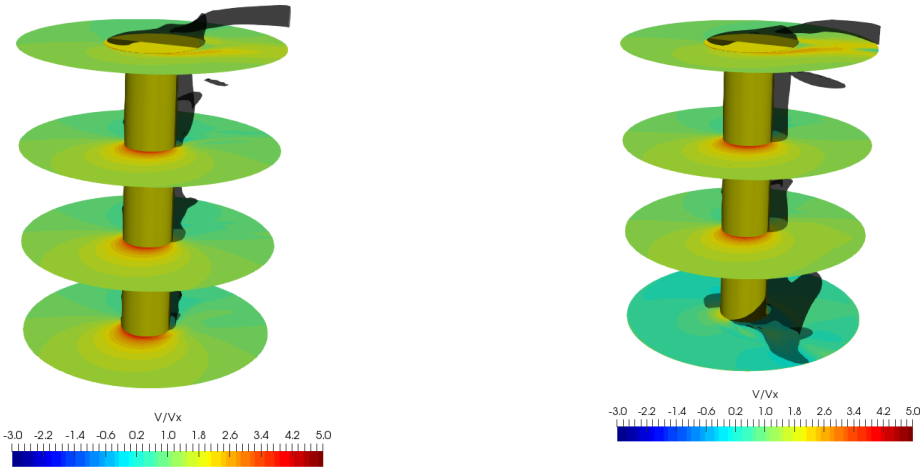

Fig. 6: Relative velocity around the rotor and flow separation region between the results with symmetry boundary condition (left) and with no-slip boundary condition and inflow boundary layer (right)

Additional calculations are also conducted to investigate the influence of the bottom boundary layer profile and the boundary layer at the tunnel walls. No noticeable influences on the results are found suggesting that the effect is therefore mainly caused by the no-slip bottom boundary at the foot of the Flettner rotor.

3.2. Scaling effects

The numerical approach is also applied at full scale Reynolds number (Re=2.20e+06). The results are presented in Fig.5 (right). Generally, an increase in lift coefficient is found from model to full scale results. This is visible throughout the whole range of spin ratios. For the drag coefficient, an increase is predicted from model scale to full scale Reynolds number for spin ratio around 2.5. For spin ratios between 0.5-1.0 the drag is lower in full scale compared to the model scale experimental results. For spin ratio above 2.5, a decrease in drag coefficient is found from model scale to full scale Reynolds number. The observations made on the scale effects matches to a certain extent the findings reported in *Bordogna (2019)*.

Larger flow reversal regions are predicted at model scale compared to full scale. The extend of this region reduces for increasing spin ratios. Over the height of the rotor there are variations in the shape and size of the separation region. The pressure distributions have been compared at various vertical positions along the rotor for both the model and full-scale Reynolds number and for various spin ratios. The differences between the scales seem similar as observed in 2D CFD simulations. Some minor variations in the pressure distribution are observed over the height of the rotor.

4. Influence wind profile on results

The influence of the wind profile on the Flettner rotor is investigated for a single rotor positioned on the deck of the vessel. First the vessel is simulated standing still to prevent the twist in apparent wind angle. The simulations are conducted under beam wind conditions with a fixed wind speed. The rotation rate of the rotor is adjusted to simulate multiple spin ratios. The results are presented in Fig.7. The total force coefficient is used as it is independent from the apparent wind angle. The results obtained from a standalone Flettner rotor are also shown in the graph. The reference speed at the centre of effort (COE) is used to make the results dimensionless. Large reduction in total force coefficient are found once the rotor is positioned on the deck of the vessel compared to the standalone rotor. These reductions in total force coefficient are in particular large for the rotor in uniform wind profile, green curve compared to red curve. For the rotor in atmospheric wind profile condition, the differences are noticeable for spin ratio higher than 2, black curve compared to blue curve.

Under beam wind conditions the influence of the vessel plays an important role in the performance of the rotor. This can be explained by the fact that the transversal area of the vessel is maximum under beam winds. As presented in Fig.8, the flow obstruction created by the vessel results into a wake extending over the deck and part of the Flettner rotor. A loss of lift generation is observed at the lower half of the rotor as visible in Fig.9. Combining the data presented in Fig.7 with the observations from Fig.9 suggests that the interactions between the ship and the rotor results into a reduction of the lift at constant RPM of the Flettner rotor once positioned on the vessel. These findings are in keeping with the results reported in *Jones et al. (2019)* suggesting that the rotation rate of the rotor positioned on the deck of a vessel should be adapted, compared to a standalone rotor, in order to maintain efficient rotor operation. It is also concluded that using a uniform wind profile is not recommended for this type of study as it artificially increases the blockage of the vessel compared to the ABL profile.

To investigate how the performance of the rotor can be influenced by the blockage of the vessel, additional calculations with ship speed are conducted. The combinations of sailing speed with wind speed are selected so that the apparent wind angle is reduced to 48 and 64° at 10 m height. The targeted spin ratios are chosen around 2.5 to stay close to the results obtained with the ship standing still. The results are presented in magenta in Fig.7. The results are found to be closer to the standalone Flettner rotor results. It is suspected that the reduction of the blockage of the vessel largely influenced the performance of the rotor and deserves further investigation which will be presented in the next section.

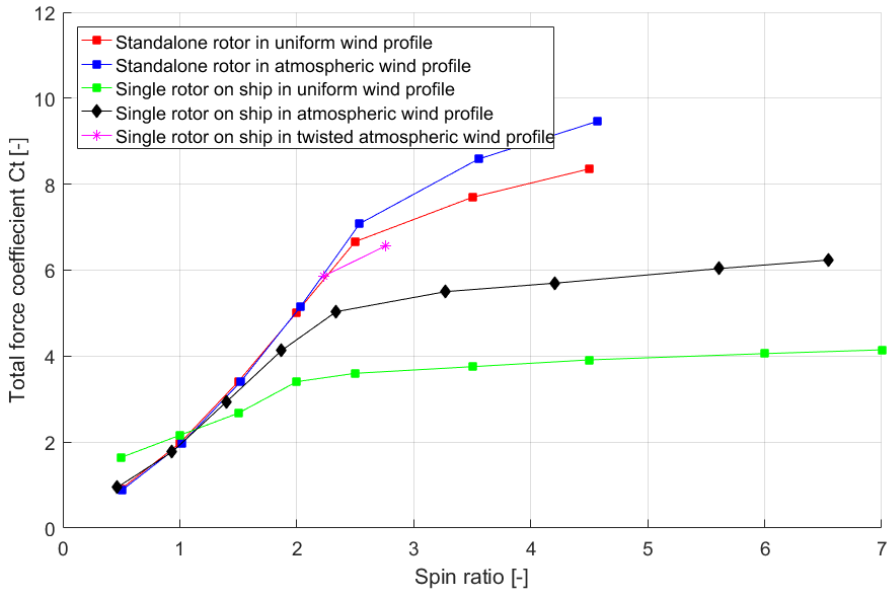

Fig.7: Influence of wind profiles and ship on total force coefficient of Flettner rotor function of the spin ratio. Results are made dimensionless using velocity at centre of effort of the rotor (COE). Results obtained under beam wind conditions.

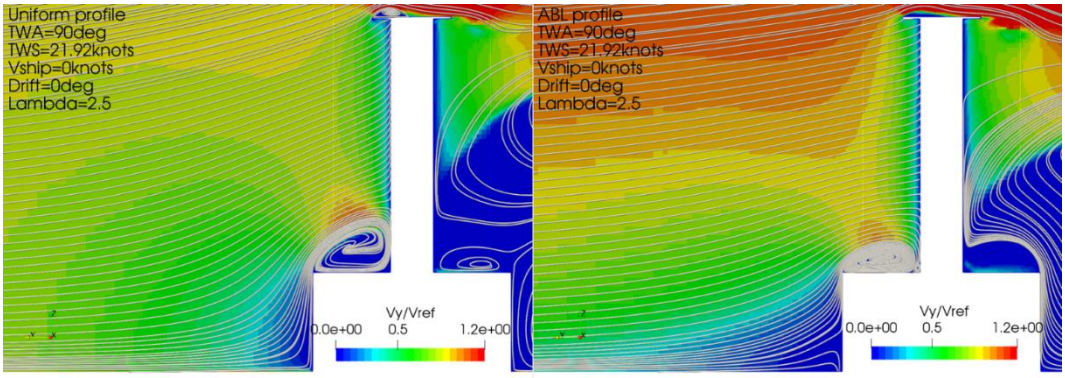

Fig.8: Dimensionless transversal velocity distribution around vessel and Flettner rotor. The flow is from left to right. Left: atmospheric wind profile condition. Right: uniform wind profile condition

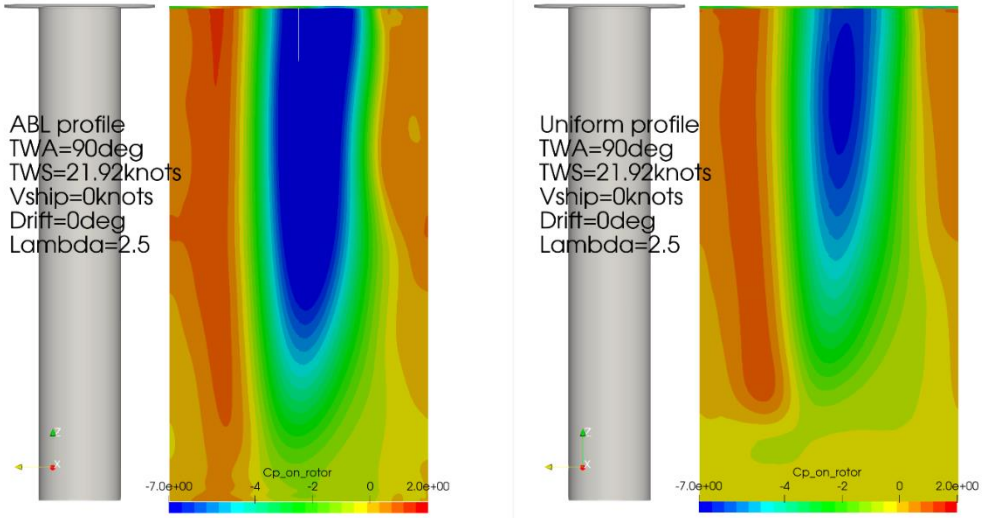

Fig.9: Distribution of the pressure coefficient around the Flettner rotor positioned on the deck of the vessel. The surface of the rotor is unfolded for visualization purpose. Left: atmospheric wind profile condition. Right: uniform wind profile condition.

4. Interaction effects between MHTC and Flettner rotors

4.1. Ship-rotor interaction

In this section the interaction rotor-ship are investigated. The calculations are first performed with one single Flettner rotor on the deck of the vessel. Conducting the simulations with one rotor suppresses the possible rotor-rotor interactions. In order to distinguish the influence of the wind direction from the influence of the spin ratio, a systematic variation of the apparent wind angle and spin ratio is conducted. For the simulation with one single rotor on the MHTC, the ship is kept still. The wind direction is varied from 20 to 160°. The wind speed is kept constant which implies that different spin ratios are obtained by varying the rotation rate of the rotor. The results are presented in Fig.10. The dotted lines in Fig.10 represents the results obtained for a standalone Flettner rotor. The circles represent the averaged results obtained from 3 rotors on the deck of the vessel. It is concluded that the lift and drag of the Flettner rotor on the vessel is influenced by both the apparent wind angle and the spin ratio. The changes relative to the standalone rotor increases with increasing spin ratio. Around beam wind conditions the losses in terms of lift coefficient are maximum. An increase in lift to drag ratio is predicted in bow quartering wind conditions compared to the standalone rotor. For stern quartering wind conditions, the drag coefficients of the rotor on the ship is increased leading to a decrease of the lift to drag ratio.

The spin ratio of the rotor is defined by the rotor diameter, the apparent wind speed and the rotation rate of the rotor. In order to understand if the apparent wind speed influences the performance of the rotor

on the deck of the vessel additional simulations are conducted. In these additional simulations, the wind speed is reduced by a factor 2 while maintaining the spin ratio of the rotor meaning that the rotation rate is adjusted accordingly. The results are presented in Fig.10. Hardly any differences are found if the apparent wind speed is reduced by half. It is concluded that the lift and drag coefficients of the rotor on the deck of the vessel can be fully described by the apparent wind angle and the spin ratio no matter how the spin ratio is reached.

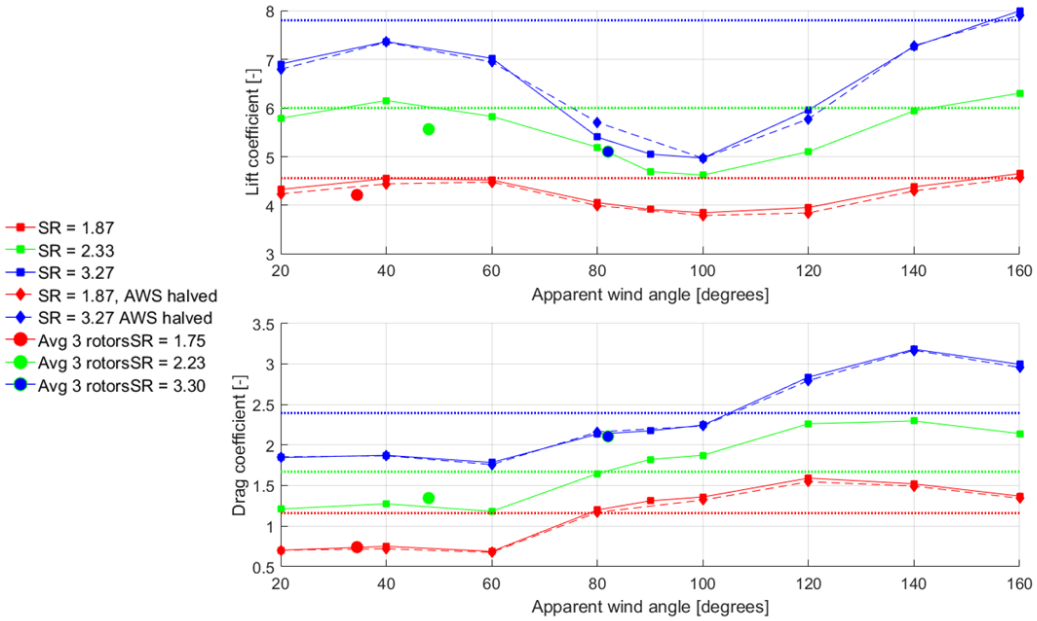

Fig.10: Lift and drag coefficients from single Flettner rotor positioned on the deck of the MHTC function of the apparent wind speed and spin ratio. Results under atmospheric boundary layer profile (ABL) at full scale Reynolds number with ship standing still. The dotted lines are the results from a standalone Flettner rotor. The circles are the averaged results from the simulations with 3 Flettner rotors on the MHTC. The results are made dimensionless using velocity at centre of effort of the rotor (COE).

4.2. Model to capture ship-rotor interaction

The results from the previous section indicate that interaction effects between a vessel and its wind propulsors cannot be omitted. The interaction effects discussed in the previous section cause an issue as the changes in drag and lift forces of the Flettner rotor on the deck of the vessel show a dependency to both the spin ratio and the apparent wind angle. In order to circumvent the need for dedicated CFD simulations for each sailing conditions, an interaction model is proposed. Note that the model is developed for this particular study case and it needs further validation for different ship and deck configurations. Nonetheless, the model proposes as a new way to describe the ship-rotor interactions which can be useful for future study.

The idea of the model is to find the effective wind velocity explaining the observed thrust and the effective apparent wind angle explaining the lift over drag ratio change from the standalone rotor. This approach uses a similar method as the thrust identity method used for propellers combined with a correction for the effective apparent wind angle. The unknowns in the Flettner rotor case are the effective wind speed and the effective apparent wind angle at the rotor location. The rotation rate of the rotor and the diameter of the rotor are known. A new term, $\frac{C_T}{SR^2}$, is introduced in Eq.(2). The term presented in Eq.(2) has the advantage of being independent from the effective apparent wind speed which is unknown.

$$\frac{Ct}{SR^2} = \frac{Total\ force}{0.5 * \rho * V^2 * A} * \frac{V^2}{\left(\pi * D * \frac{N}{60}\right)^2} = \frac{Total\ force}{0.5 * \rho * \left(\pi * D * \frac{N}{60}\right)^2 * A} \quad (2)$$

The relation between $\frac{C_T}{SR^2}$ and SR can be determined from the standalone rotor simulations. This relation is presented in Fig.11.

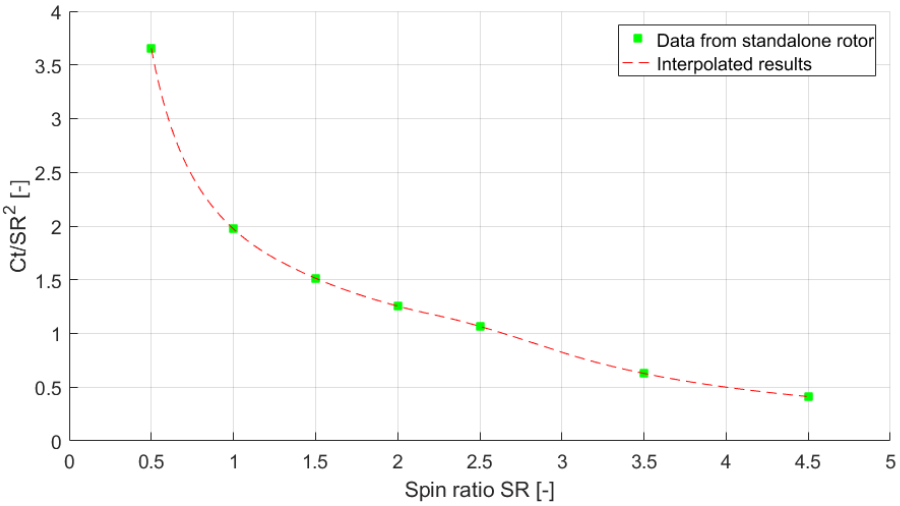

Fig.11: $\frac{C_T}{SR^2}$ function of the spin ratio. The relation is derived from results obtained with a standalone Flettner rotor in ABL profile at full-scale Reynolds number

Similarly, the term $\frac{C_T}{SR^2}$ can be computed for the simulation with one rotor on the deck of the vessel meaning that the associated effective spin ratio SR_{eff} can be found. The SR_{eff} can in turn be used to determine the corresponding "Taylor" wake fraction w using Eq.(3). The term "Taylor" refers to the analogy with the method used in propeller modelling.

$$w = 1 - \frac{SR}{SR_{eff}} \quad (3)$$

The resulting wake fractions are presented in Fig.12. Good agreement is found between the results obtained from three different rotation rates of the Flettner rotor. An acceleration of the effective apparent wind speed, w<0, is found for bow and stern quartering winds. This can be explained by the relative low blockage of the vessel resulting into a flow contraction above the deck. The flow acceleration is more important in stern quartering winds. In beam wind conditions however, the effective apparent wind speed is reduced. The large flow blockage of the vessel results into a region of flow separation over the deck which reduces the effective apparent wind speed.

In addition to the wake fraction, a correction to the effective apparent wind angle is derived from the effective spin ratio. This correction, $\theta_{correction}$, is obtained by the difference in angle of the total force of a standalone rotor at a spin ratio SR_{eff} compared to the angle of the total force of the rotor on the deck of the vessel. This correction is presented in equation (4) and visualized in Fig.13. Similarly to the wake fractions, a good agreement is found between the results obtained from three different rotation rates of the Flettner rotor. In bow quartering winds, the effective apparent wind angle is increased. This is beneficial for the driving force generated by the Flettner rotor. In beam and stern quartering winds, a reduction of the effective AWA is found. In beam wind this is disadvantageous, because the effective force factor rotates toward the stern. In stern quartering winds the effect is dependent on the initial direction of the total force vector w.r.t. the centre line. In any case the impact is less pronounced.

$$\theta_{correction} = tan^{-1}\left(\frac{Cl_{standalone\ rotor\ at\ SR_{eff}}}{Cd_{standalone\ rotor\ at\ SR_{eff}}}\right) - tan^{-1}\left(\frac{Cl_{rotor\ on\ deck\ at\ SR}}{Cd_{rotor\ on\ deck\ at\ SR}}\right) \quad (4)$$

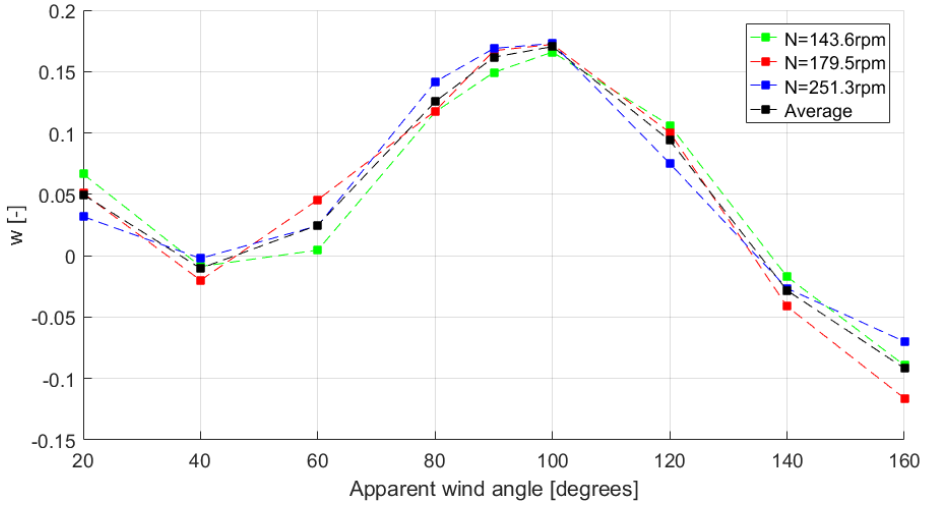

Fig.12: Wake fraction as function of the apparent wind angle. Results for ABL profile at full-scale Reynolds number with ship standing still fitted with one single Flettner rotor.

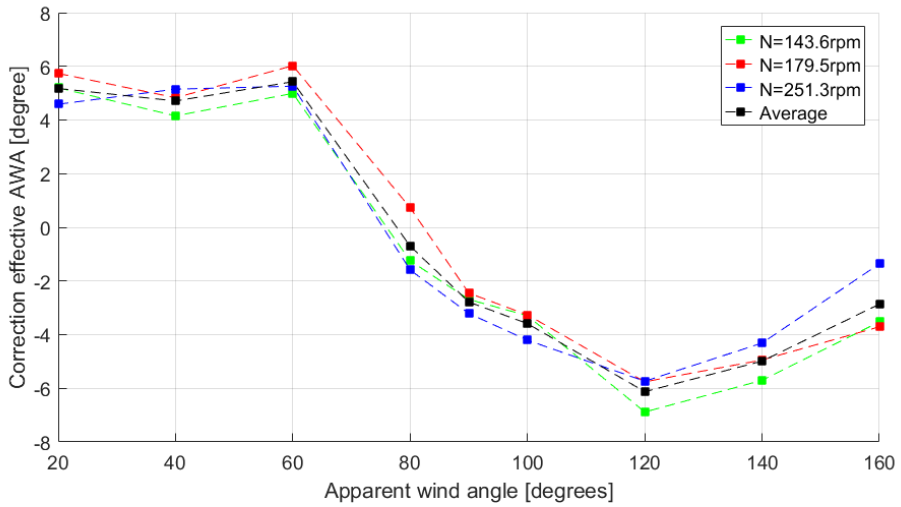

Fig.13: Correction to the effective apparent wind angle. Results for ABL profile at full-scale Reynolds number with ship standing still fitted with one single Flettner rotor.

The corrections for the wake fraction and for the effective apparent wind angle are used to correct the performance of the standalone Flettner rotor towards the performance of the rotor on the deck of the vessel. The model is also used to compute the performance of the rotor at different spin ratios. A comparison of the driving force Cx obtained from the interaction model and computed by CFD is shown in Fig.14. Model and the CFD results agree well suggesting that the model is valid for this case.

In order to judge the influence of the ship-rotor interaction, a comparison of the driving force is shown in Fig.15 for three scenarios: no interaction accounted for, interaction derived by the effective apparent wind speed, interactions derived by the effective apparent wind speed and effective apparent wind angle. Thus, accounting for the ship-rotor interactions increases the driving force in bow and stern quartering winds. In beam winds however, the interactions reduce the driving force produced by the Flettner rotor. It is concluded that the interactions ship-rotor are well driven by the change in apparent wind speed in beam wind conditions. In bow and stern quartering winds however, the changes in effective AWA affect the most the results and should therefore be accounted for.

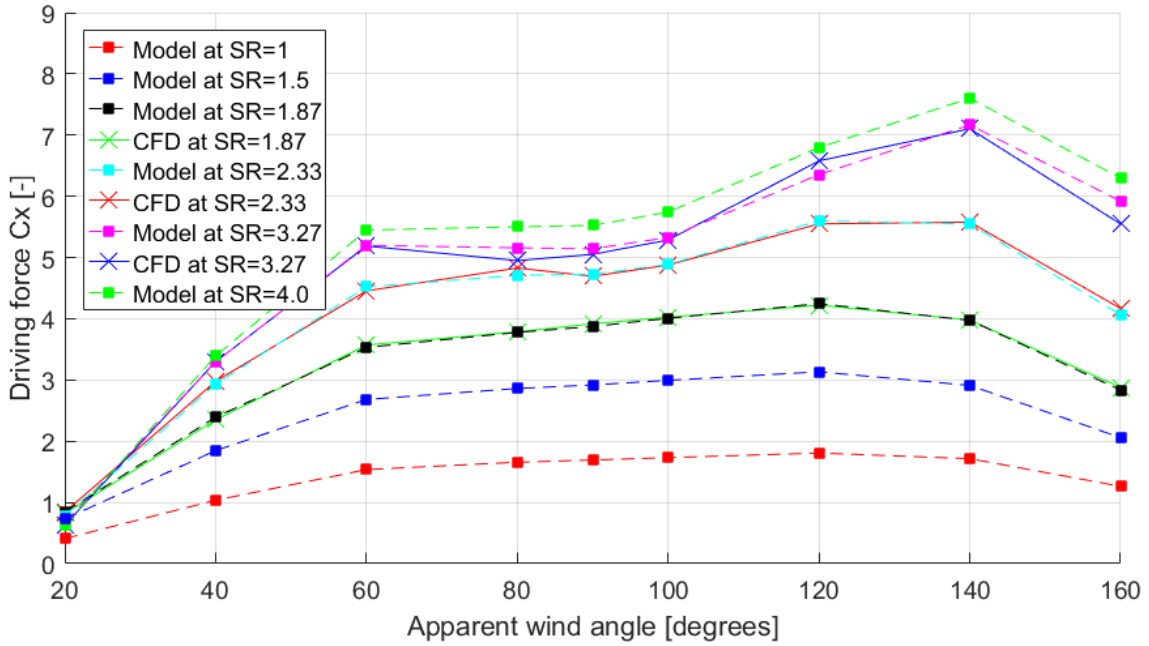

Fig.14: Driving force Cx function of the apparent wind angle. The CFD results are compare to the results obtained with the ship-rotor interaction model. Results under ABL profile at full-scale Reynolds number without ship speed fitted with one single Flettner rotor.

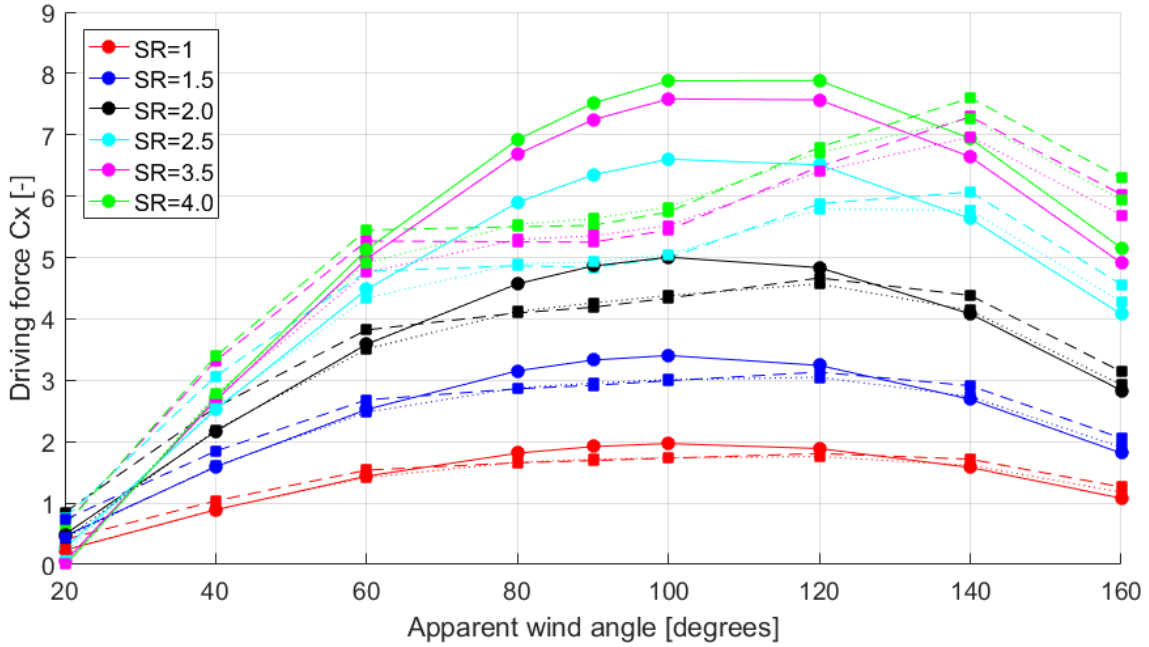

Fig.15: Driving force Cx function of the apparent wind angle. All results are derived from a standalone rotor. Continuous lines: results obtained without interaction. Dotted lines: results obtained with interactions derived from the effective apparent wind speed. Dashed lines: results obtained with interactions derived from effective apparent wind speed and wind angle. Results under ABL profile at full-scale Reynolds number.

4.3. Results with three Flettner rotors on MHTC

The interaction effects between the MHTC and multiple Flettner rotors are investigated by simulating multiple sailing conditions with three rotors on the deck of the vessel. The results are compared to the performance of a standalone Flettner rotor at equal spin ratio. The spin ratio is defined based on the undisturbed apparent wind speed at the centre of effort of the rotor. The atmospheric wind profile is

used for the simulations. Each sailing condition is based on a VPP prediction and corresponds to a unique combination of ship speed, wind speed, ship heading, wind direction and rotation rate on the rotors. Sailing conditions with apparent wind angle from 0 to 180° are computed. The individual rotors are operated at the same rotation rate.

The results are presented in Fig.16 in terms of relative changes with respect to the results obtained with a standalone Flettner rotor. The results indicate that the rotors do not perform equally. Following the findings reported in *Bordogna (2020)*, rotor-rotor interactions should not be dominant as the distance between the rotors is large. Nonetheless, no calculation on rotor-rotor interaction without ship have been conducted in this study. Therefore, rotor-rotor interaction cannot be differentiated from the ship-rotor interaction and it cannot be concluded to what extent rotor-rotor interactions affect the results. Additionally, it is also suspected that the interaction between the ship and an upstream rotor can affect the performance of a rotor positioned downstream. Such interactions are also not easily quantified. Further quantification of the rotor-rotor interactions should therefore be conducted in the future study by making use of a model such as described in *Bordogna (2020)*. The ship-rotor interaction may also vary as a function of the position of the rotor on the vessel. In the absence of a rotor-rotor interaction model, it can only be concluded that the position of the rotors relative to the vessel and/or to the others rotors have an influence on the results.

Independently from the differences between the three rotors, a general increase of the lift for AWA lower than 50° and a large decrease of the lift for AWA larger than 60° is found. The blockage of the vessel is, at least partially, responsible for the loss in lift generation. The drag forces, on average, decrease for the rotors on the vessel for AWA between 50 and 140°. For bow and stern quartering winds (AWA<20° and AWA=180°) large increases in drag forces are found. The lift to drag ratios of the rotors on the deck are largely reduced compared to the standalone rotor, up to 50% reduction is predicted. In stern quartering wind, the fore rotor appears to have a large increase in lift to drag ratio. The results presented in Fig.16 are in keeping with the results reported in *Jones et al. (2019)* for a single rotor on a deck of a simple ship geometry. Fig.17 shows the resulting driving force.

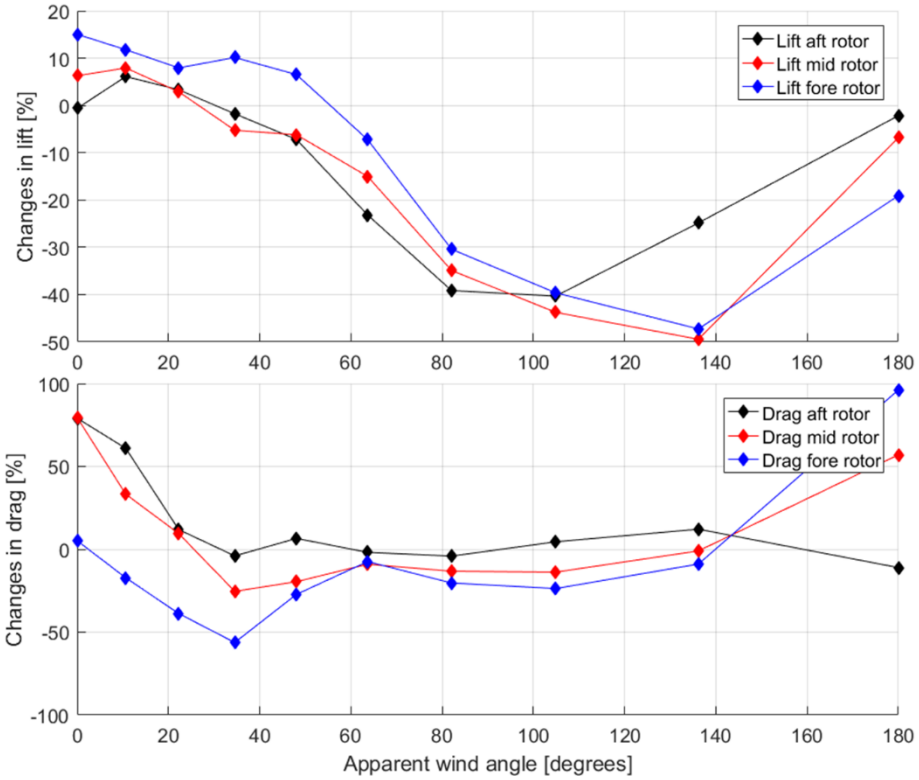

Fig.16: Lift, drag changes for Flettner rotors positioned on the deck of the MHTC relative to a standalone rotor. Results under atmospheric boundary layer profile (ABL) at full-scale Reynolds number.

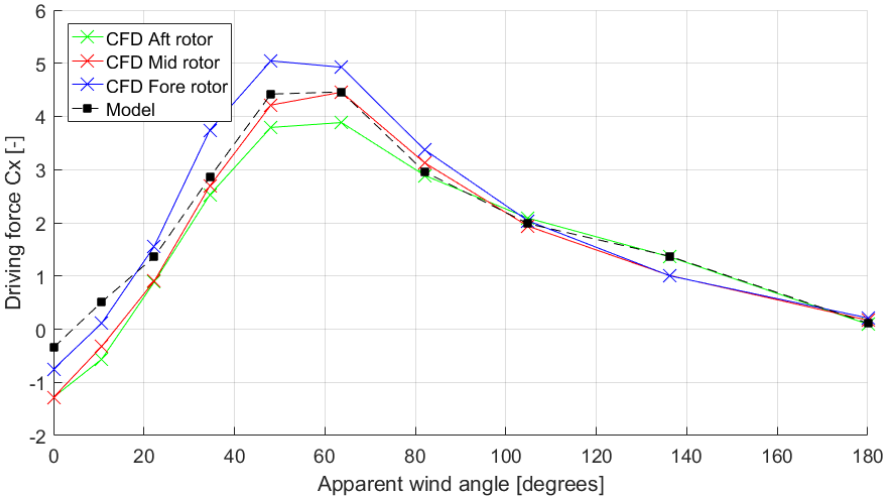

Fig.17: Driving force Cx function of the apparent wind angle. CFD results with 3 Flettner rotors on the deck are presented and compared to the results obtained from the ship-rotor interaction model

As for the results presented in section 4.2, the ship-rotor interaction model can be used to predict the performance of the Flettner rotor on the deck of the vessel. Note that the ship-rotor interaction model presented in section 4.2 omits the rotor-rotor interactions. Thus, wake fraction and angle correction should in principle be determined anew, accounting for the rotor-rotor interaction. In principle, this can be done with the same type of CFD calculations as conducted. However, independent variation of Spin Ratio per rotor was not included in the calculation program. The induced flow at one rotor will depend on the loading (SR) at the other Spin Ratio. In order to capture this effect, additional work is required. To save cost, it is attractive to conduct this type of calculations (partially) with simplified methods. Considering the limited rotor-rotor interaction effects that were expected in this case, such calculations were not conducted. Fig.17 shows a comparison between the model (without rotor-rotor interaction) and the direct CFD results. The good agreement between the model and the CFD results for the rotor at mid deck suggests that rotor-rotor interactions are not dominant around beam wind conditions. In stern and bow quartering winds, the model deviates slightly from the CFD results which is likely mostly due to the wake of upstream rotor and upwash and downwash effects. The results presented in Fig.17 covers a range of spin ratios between 0 and 4.5.

5. Conclusions

A CFD approach has been developed for a Flettner rotor in isolation and on the deck of a vessel. The results are found to be in good agreement with the experimental results for a standalone Flettner rotor. The results are however sensitive to the type of boundary condition used at the foot of the Flettner rotor. A no-slip condition is recommended. Scaling effects have been investigated for a standalone rotor; from model to full scale Reynolds numbers changes in lift and drag coefficients are observed. These changes are found to depend on the spin ratio and on the type of boundary condition used at the foot of the rotor.

A sensitivity study to the type of wind profile has been conducted for a single rotor on the deck of the MHTC. Large differences are found depending on the type of wind profile. The uniform wind profile artificially increases the blockage of the vessel and should therefore be avoided. An atmospheric wind profile is recommended instead.

Interactions between a single rotor and the vessel have been analysed. The results show large differences in lift and drag forces between a rotor on the vessel and a standalone rotor. These differences are dependent on both the spin ratio and apparent wind angle. With respect to the spin ratio, it can be said that the differences relative to the standalone rotor increase with increasing spin ratio. With respect to the apparent wind angle, it has been found that the losses in terms of lift are maximum for around beam wind conditions. In terms of driving force, a decrease is also found in beam winds. Additionally,

an increase in lift to drag ratio is observed in bow quartering winds for the rotor on deck when compared to the standalone rotor. For stern quartering winds, both the lift and the drag of the rotor are increased. In bow and stern quartering winds, the driving forces generated by rotor on the deck increase compared to the standalone rotor.

It is concluded that interaction effects cannot be omitted in the evaluation of WASP. A simplified model leading to an effective wind speed and effective apparent wind angle explaining the differences between a standalone rotor and a rotor on the deck of the vessel is proposed. This model corrects the lift and drag of a standalone rotor towards the lift and drag of a rotor on the deck of the vessel. A good agreement between the model and the computed CFD results is found suggesting that such model can be a valuable tool within a prediction program used for the evaluation of WASP.

Finally, the interactions between the vessel and three rotors are investigated. Differences in the performance of the rotors are found at equal rotational velocity and equal wind conditions. Since, no calculation on rotor-rotor interaction without ship have been conducted in this study, rotor-rotor interaction cannot be differentiated from the ship-rotor interaction. Thus, the position of the rotors relative to the vessel and/or to the other rotors affect the results. Despite the differences between the rotors, general trends can be derived from the data. The trends appeared to be relatively well captured with the ship-rotor interaction model developed from simulations with one single rotor on the deck of the vessel. Further refinement of this interaction model to account for rotor-rotor interaction and ship-rotor interactions with different positions of the rotor on the deck should improve the quality of the model.

Acknowledgements

This research is partly funded by the Dutch Ministry of Economic Affairs. The collaboration with Peutz BV is also highly appreciated.

References

ABS (2014), *Guide for Building and Classing Offshore Wind Turbine Installation*, American Bureau of Shipping

BAÑUELOS-RUEDAS, F.; ANGELES-CAMACHO, C.; RIOS-MARCUELLO, S. (210), *Analysis and validation of the methodology used in the extrapolation of wind speed data at different heights*, Renew. Sustain. Energy Rev. 14, pp.2383-2381

BORDOGNA, G. (2020), *Aerodynamics of wind-assisted ships: Interaction effects on the aerodynamic performance of multiple wind-propulsion systems,* PhD thesis, TU Delft

BORDOGNA, G.; MUGGIASCA, S.; GIAPPINO, S.; BELLOLI, M.; KEUNING, J.A.; HUIJSMANS, R.H.M.; VAN'T VEER, A.P. (2019), *Experiments on a Flettner rotor at critical and supercritical Reynolds numbers,* J. Wind Engineering and Industrial Aerodynamics

COUNIHAN, J. (1975), *Adiabatic atmospheric boundary layers: A review and analysis of data from the period 1880-1972,* Atmos. Environ., pp.871-905

DHOME, U.; KUTTENKEULER, J.; M. RAZOLA, A. SEGALINI (2020), *Preliminary results on measurements of the atmospheric boundary layer over the Atlantic*, 5th InnovSail Conf., Gothenburg

DNV (2010), *Environmental Conditions and Environmental Loads*, DNV-RP-C205, Det Norske Veritas, Høvik

HELLSTEN, A. (2004), *New two-equation turbulence model for aerodynamics applications,* Helsinki University of Technology

HSU, S.A.; MEINDL, E.A.; GILHOUSEN, D.B. (1994), *Determining the Power-Law Wind-Profile Exponent under Near-Neutral Stability Conditions at Sea*, J. Appl. Meteorol. 33, pp.757-765

IEC (2009), *Wind Turbines Part 3: Design Requirements for Offshore Wind Turbines*, No. IEC61400-3, Int. Energy Comm., Geneva

SPALART, P.R.; RUMSEY, C.L. (2007), *Effective inflow conditions for turbulence models in aerodynamic calculations*, AIAA 45/10, pp. 2544-2553

New Oil Spill Response & Recovery Technologies

Jesús Cisneros-Aguirre, Univ. Las Palmas de GC, Las Palmas/Spain, jesus.cisneros@ulpgc.es
Maria Afonso-Correa, Pontho Engineering Srl,Valsequillo/Spain, mdafonso@pontho.com

Abstract

This paper presents three new technologies for Oil Spill Response. The first one is a reusable foam which absorbs oil from water, the oil recovery capacity for a kilogram of foam is around 6 tonnes. The second technology is a new granulates with a high oleophilic and hydrophobic capacities. Particularly useful for a Response action, because it cleans all the tools and reduce the hard oil smell improving the quality of work. The third technology is a bioremediation with allogenic bacteria, selected for its capacity to degrade oil, and for its tested innocuity for the human health and environment.

1. Introduction

The Oil Spill accident occurred in Gran Tarajal Harbor could change the Response Decision Making for the rest of similar accidents over the world. In this accident we used three new developments that reduced to almost zero, the environmental impact and the odor disturbances to the population. The three new technologies are: Reusable sponges absorbents with very high Hydrophobic and Oleophilic properties, granulates with same capacities, and bacteria inoculums with very high and quickly capacity to degrade the different hydrocarbons.

The Gran Tarajal harbor is in Fuerteventura Island, in the Archipelago of Canary Islands. The tropical storm EMMA, sinking 5 pontoons plenty of machinery and 3 tug ships, producing an important Oil Spill taking account the small dimension of the harbor, around 100 tons of different oils were spilled.

Using the foam reusable absorbent, we have recovered 57 tons of hydrocarbon with around the 5% of water in three days, and in those 6 months we have recovered from water surface around 80 tons of Oil. The foam has a simple design/use with hand squeezed system, with very high Hydrophobic and Oleophilic capacities, 1 kg removes up to 30 kg of oil in every use and with more than 200 uses without losing these properties, 1kg of sponge can remove more than 5 tons of oil.

The second development was the bacteria, Pseudomona putida, which degrades the oil quickly. Specially the light hydrocarbon like Diesel, but as well as the light fuel. It reduces the hydrocarbon viscosity and surface tension, that means a reduction of its adherence to sand, rocks, concrete, ropes and others surfaces. This property allows to increase the lixiviation process from the sand, gravel, and mud to surface (Intertidal areas), and a constant degradation of the Oil attached to surfaces (Cleaning the harbour). The bacteria residues finally dissolved in water or sinking as organic matter.

The third technology is a granulate with a great hydrophobic and oleophilic capacities, that allows to clean surfaces, tools, globes, boots, floor, and avoid the spills from the harbor again to the water when the machinery plenty of oil were recover. We also filtered the oiled water before spill back to the sea.
These technologies applied avoid a relevant environmental impact, nevertheless the big amount of oil spilled in a short space, and the environmental recuperation of the harbor was completely. All analytical results: hydrocarbon concentration in water, sediment, organisms, and three ecological indexes of sediment`s infauna and macro-fauna population show a clear recovery of the initial environmental conditions in short time.

2. Overview of Current technologies

Despite the apparent media movement, marine environmental care is not enough developed, that retrograde mentality gives an extremely poor environmental protection technology development in

many sectors, including sea protection. The clearest consequence of this is that Current Oil Spill Response and Recovery Technologies are weak developed, centred in hide the pollution and remove from water surface the oil as soon as possible, without taking account the consequences.

A quickly oversee of the current technologies shows this negative approach and give us a good idea about the existing state of mentality:

2.1. Dispersion Strategies

2.1.1. Chemical Dispersants

Still considered as the main strategy to Oil Spill Response in open seas. The main purpose is to remove the oil from water surface breaking the oil surface in small stains improving oil sedimentation process. This strategy translates pollution from water surface to water column and sea bottom, increasing the amount of pollutants creating a negative synergy between oil and chemical products. The pollution becomes more difficult to degrade because bottom conditions are less effective, and the mixture between chemical dispersant and oil becomes more resistant to bacteria, increasing environmental impact more than the oil pollution itself.

2.1.2. Mechanical Dispersion

In countries where the Dispersant are banned there is a strategy called mechanical dispersion. That "system" consist on cross the oil slick with any kind of boats back and forward producing a maximum turbulence with the propellers, breaking down the slick in smallest slicks, inducing a great dispersion, the consequence is to translate the oil from water surface to water column increasing the environmental impact.

2.1.3. Burning

Still considered an Oil Spill Response procedure in many places, oil burning, in this condition, produces a huge pollution (furanes, dioxines, etc). Wind moves the black cloud to other parts and deposits these harmful products, again at sea surface, or inland. That produces noxious impact not only in environment but in human health. This "response" moves oil from water surface to other parts depending on the wind direction and strength.

2.2. Recovering Strategies

For a harbour spill, Skimeer is the only one system included in the current protocols, combined with boomers or surface barriers and absorbent are the only technology to try to reduce pollution at sea. These three systems have a very reduced performance, skimmers are very difficult and hard to use, it is necessary trained people with experience to use it, it has a very low capacity to recovery oil, with a big percentage of water. In those three firsts days of the response one skimmer used with experts from Official Spanish Savage Team get half cubic meter of oiled water with more than 50% of water.

Floating barriers do not retain the oil very well, it passes upward and downward depending on the wind, waves, and currents, and even inside the harbour they have serious problems to retain oil.

Standard absorbents are awfully expensive, and it is a solution for small spills, the final product, absorbent plus oil, needs a specific management as harmful product and it becomes expensive as well as, the management of this residues.

3. Conclusion

It is necessary a change of mentality in Oil Spill Response and Recovery responsible, there are available new technology that far exceeds current technologies includes in European contingency

plans. In this presentation we want to demonstrate the efficiency of just three new technologies, that can allow to clean a harbour affected by a great oil spill taking account harbour dimensions.

Reusable sponges can give you an extra possible capability to remove oil from surface, with a low percentage of water (less than 5% in working conditions), that means a directly reusable oil. At it finish life, more than 200 or 300 uses the sponges can be recycled by the manufacturer as new sponge. Then this absorbent does not produce residues at all, and combinations between barriers and sponges increase the capacity to block oil in surface. We are developing new systems combining with bacteria, AUV's (Autonomous Underwater Vehicles), granulates, ultrasonic probes, etc.

Granulate Absorbents increases work conditions for workers in an extremely aggressive ambience, cleaning all the surfaces, removing odour, but as well as retain oil on inland spills. They act as inland barriers and can filter oiled water retaining oil, and together with sponges can increase this capacity.

Our experience in Gran Tarajal harbour show another strategy to use oleolithic Bacteria. Due to the number and complexity of ships rescue, the harbour suffered several minor spills after the initial big spill from March to October, that constrain us to use almost continuous inoculation of bacteria cultures. The standard approach for bioremediation is first able remove as much as possible oil from water and then use bacteria. The new approach is to use bacteria at the very initial moment at the same time the recovery works. Bacteria start to degrade oil immediately changing its properties, reducing its viscosity and surface tension, reducing its harmful capacity to attach to the surfaces, algae, ropes, rocks, sand, fish, boats, that is the consequence of its environmental impact; this change of oil properties facilitate the removing process, specially the absorption capacity of the sponges.

We are developing and improving other Oil Spill Response & Recovery technologies like soft cleaners' products, ultrasonic probes, catalytic process, and including these technologies, washing machine systems for oiled sediments, new cleaner ships, new barriers, etc…

But the great question is: Are they, Oil Spill Response & Recovery Managers and Responsible, ready and open to introduce quickly new technologies in Contingency Plans?

References

ANDERSON C. M.M.; MAYES M.; LABELLE R. (2012), *Update of Occurrence Rates for Offshore Oil Spills*, BOEM, https://www.boem.gov/sites/default/files/uploadedFiles/BOEM/Environmental_Stewardship/Environmental_Assessment/Oil_Spill_Modeling/AndersonMayesLabelle2012.pdf

ETKIN, D.S. (2001), *Comparative Methodologies for Estimating On-Water Response Costs for Marine Oil Spills*, Int. Oil Spill Conf.

GESAMP (2007), *Estimates of oil entering the marine environment from sea-based activities*, IMO, http://www.gesamp.org/publications/estimates-of-oil-entering-the-marine-environment-from-sea-based-activities

NN (2012), *Oil Spill Cost Study*, The UK Offshore Oil and Gas Industry Association Ltd (Oil & Gas UK) and Offshore Pollution Liability Association Ltd (OPOL), http://oilandgasuk.co.uk/wp-content/uploads/2015/04/Oil-spill-cost-study-120531.pdf

Unique Information Data & Information Models: Out-Of-The-Box Integrated, Collaborative, Multi-Authoring, Managed Environment for Ship Design and Construction

Nick Danese, NDAR, Antibes/France, nick@ndar.com

Abstract

Modern computational technologies and tools available to ship designers and builders span all disciplines but rarely are they connected, let alone integrated. This paper discusses the unique, heterogeneous, Out-Of-The-Box Integrated, Collaborative, Multi-Authoring Environment for the Design and Construction environment spanning 3D modelling, weight engineering, CFD, FE, fatigue, seakeeping, stability, etc. A practical non-linear workflow is clearly defined in real-world terms along LEAN and AGILE business strategies. From a PLM perspective, a focused information management process is implemented thanks to the innovative "unique data & information models" tailored to each stakeholder, managed by active notification of Work-In-Progress and Release deliverable archives status.

1. Introduction

For a High-Performance Marine Vehicle to enter service and serve as such a plethora of successful initiatives, actions and events must play to a tune under the sharp metronome of creative management. Much research addresses individual aspect of High-Performance, from applying Artificial Intelligence to design strategies, to hull shapes, to propulsion plants, to (finally) aerodynamic resistance and propulsion to automation, etc. and deservedly so. On the other hand, the topic of how "does it all actually come together" remains relatively unexplored. Most processes and procedures underlying the orchestration of all that it takes to bring a High-Performance vehicle to perform still belong to the domains of habit and common practice, regardless of whether an added value is actually contributed to the effort.

High-Performance does not necessarily mean high-speed - think of a not-so-fast vessel which on the other hand does not have to slow down in heavy seas - and efficiency does not necessarily mean high power-to-weight ratios or super-efficient propellers. High-Performance is clearly found in its own right in other aspect of the existence of a marine vehicle. For example, ecological anti-fouling and high-yield project management bring as intangible as vital and positive contribution to the existence, life and impact-reduction on the planet of the marine vehicle.

This paper will explore and discuss High-Performance within the realm of design and construction from a process stand-point.

2. The Status Quo

There is value in understanding how the present was arrived at and even more so when it entails discussing what can be considered the apparently out-of-synch fast-forward and ever-accelerating technological post-World War II evolution versus the innate human resistance to change. A number of milestones, *Danese and Pagliuca* (2019), exemplify the availability of technology and highlight the limitation of its application to apparently non-disruptive areas of society, business and industry at large:

- the colour TV set was patented in 1897, prototyped in 1928, and colour broadcasting started in 1951. Yet, colour-tv fabrication became affordable for the middle-class in different countries decades apart
- T-Square and SketchPad, the first CAD programs, saw the light in 1961
- ARPANET became operational in the early 1960s, adopted TCP/IP to become the internet as we know it in 1983 and the World Wide Web was invented in 1990

- the mouse was invented in 1961 and unsuccessfully commercialized in 1964 (20 years before Apple eventually shipped it with the first MacIntosh)
- PLM was invented in 1965 at American Motor Corporation
- Olivetti's Programma 101 desktop computer included a keyboard and a printer in 1965. Screen, mouse and WYSYWIG software were introduced with Xerox Alto, in 1973,
- man landed on the moon in 1969, with no protection from the yet-unknown extremely radioactive solar storms and using computers less powerful than a modern kitchen appliance's
- email was first used in 1972
- Motorola first produced a cell phone in 1973 but finally commercialized it only in 1983
- the first computer graphical interface was seen on the Xerox Alto in 1973
- the MITS Altair 8800, the first PC, was introduced in 1975 and commercialized it in 1983
- GSM was born in 1975, GSM 2 appeared in 1991, 3G (GSM 3rd generation) in 2003, 4G (LTE technology) in 2009 and deployment of 5G started in 2018, https://www.brainbridge.be/news/from-1g-to-5g-a-brief-history-of-the-evolution-of-mobile-standards
- derived from a 1977 commercial software, AutoCAD was first released in 1982, already a 3D CAD program and supporting plug-ins
- Amazon was founded in 1994, Yahoo was created in 1995, Google was created in 1998
- Facebook was launched in 2004
- Nano technology was industrialized in 1999-2000 (intriguingly, it was unknowingly invented and used since the 4th Century AD, the first example thereof being the Lycurgus Cup created in Rome, https://www.nano.gov/timeline

It can be argued that yet inexistent infrastructure and the cost of industrial production at the time of invention also contributed to it taking decades for many brilliant ideas to become the common place they are today in everyone's life. In some cases, however, culture and aversion to change were possibly even greater hindrances. (IBM was advertising "taking the computer out of the back room" in the late 1970s.)

It is interesting to see that while implementation and adoption of new technology takes place sooner and sooner since its development, said new technology is more often than not embedded in existing applications (example: domotics): whether this is a conscious subterfuge to counteract resistance to change or whether this is dictated by financial and time-to-market constraints is almost irrelevant when compared to the fact that nowadays something new enters everyday life rather smoothly, sometimes even with acclamation. However, while the benefits of the "new" are reaped where it is applied, the same "new" is often not available to produce compound benefits elsewhere.

Moreover, much as in the marine world, there remains a distinct separation between the providers of this or that new feature or service as opposed to the collective embracing of a collaborative and shared information and service ecosystem.

Almost in contradicting fashion, 5G communication technology is intended to turn any and every electrically operated device into an IoT component. To be noted, 5G research & development work started in 2008 when NASA and its funded Machine-to-Machine Intelligence Corp created M2M, machine-to-machine communications, and 5G in parallel, efforts matched immediately by South Korea and in 2012 by the New York University founded 5G-focused NYU WIRELESS.

Why such future-looking efforts and commercial technology permeate only certain and well-delimited portions of society and areas of industry is discussed elsewhere by this author, this paper remains focused on how remedy and constructive solutions are immediately available to everyone in order to move the design and production processes in the marine industry to High-Performance.

3. Underlying paradigms

Recent years have seen the acceptance of concepts fundamental to efficient processes, such as LEAN

and AGILE. LEAN and AGILE are well known business strategies, as easy to apply as they are not, yet anyway, applied. Rooted in the 1950s and fundamentally based on common sense and good practice, the two are fully complementary in that LEAN was spawned by the post-WWII transformation of mass-production in the reborn but not yet computerized automotive industrial landscape while AGILE's roots are found in the early research on iterative & incremental development methods aimed at uninterrupted adding of value to the product, *Danese and Morais (2016)*, and assorted contributions in Morais' blog https://www.ssi-corporate.com/blog/waveform/.

In other words, the aim is to share data and information in a way that adds value to the end-product. As the end-product's making includes the corresponding human effort it becomes evident that effective and efficient communications are key to the achievement of the best end-product possible.

In turn, this entails a structured and targeted communication strategy and an effective supporting data and information distribution system. The corollary is that the well-known single-source-of-truth paradigm is the inherent backbone of any Agile and Lean process and that the available-vs-accessible paradigm coined by SSI's Denis Morais represents its ubiquitous conjunctive tissue. Moreover, a true distributed, collaborative workspace calls for different applications, apparently but even possibly somewhat redundant to share the same data set and that the underlying data is used as-is, modifications are not allowed. From a high-level perspective, the above can be represented very simply, for example in Fig.1.

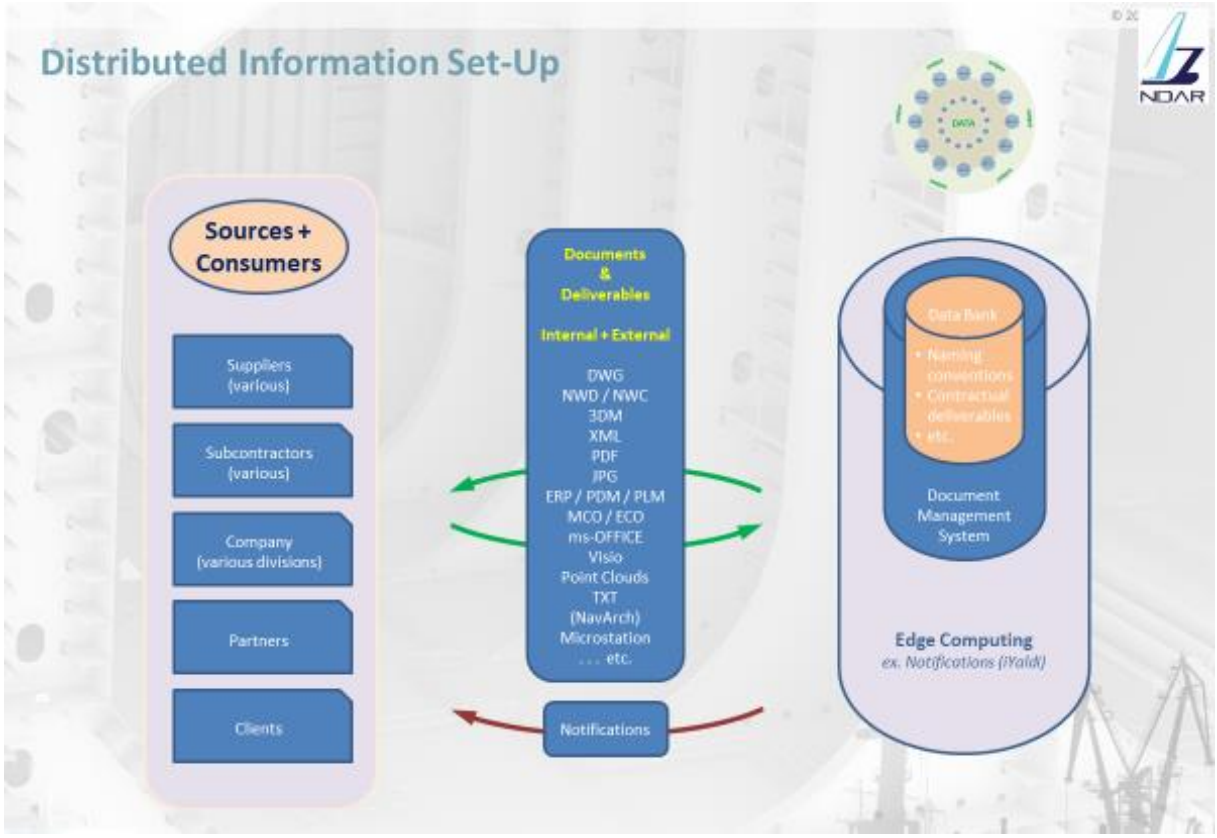

Fig.1: The same data and information sets produced by various authors compose the project space and are shared in various formats tailored to the recipients' requirements, supported by a managed repository strategy and a notification policy.

4. The Project Space

A Project Space is the ensemble of all data, information, processes, authors, etc. relating to a given project, however directly or indirectly, however insignificant this or that component of the Space appears to be. Obviously, any given Project space is not isolated from other Spaces, be they Project Spaces

or of another nature - for example the Company / Enterprise Space - and this overall "Great Space" is what Product Lifecycle Management (PLM) is generally slated to manage. Any Space, Project Space included, is made up of tangible and intangible components.

4.1 Intangible components

“Change is the unrecognized birthplace of every initiative” goes a proverb. Change is the intangible, disruptive component of any Space and, if taken as an opportunity (see the AGILE paradigm), it will be the fertile ground so important for the seed of opportunity to germinate and grow.

However, most feel that change is at best a nuisance, if not a problem or even a showstopper, feelings which are intangible yet potentially lethal component of every Space. It can be argued that the unwanted effects of change, such as rejection, are generally due to poor planning and inadequate preparation, and both can be remedied by improved communications (ref. the LEAN and AGILE paradigms).

Tracking, review, evaluation and planning what to do next are more intangible components of any Space, easily supported by careful and thought-out planning, clearer and more granular goal definition, more waypoints and closer milestones, purpose-defined assignment of people and tools to tasks, etc.

4.2 Tangible components

Tangible components of every Space include people, tools, processes, etc., all somewhat visible, qualifiable and measurable. It is important to say that intangible components have intentionally been considered before tangible components in this discussion of because the former pervade the latter like conjunctive tissue and will influence the Space and the results of the work being carried out therein in ways that are anywhere from not evident to fully unintelligible.

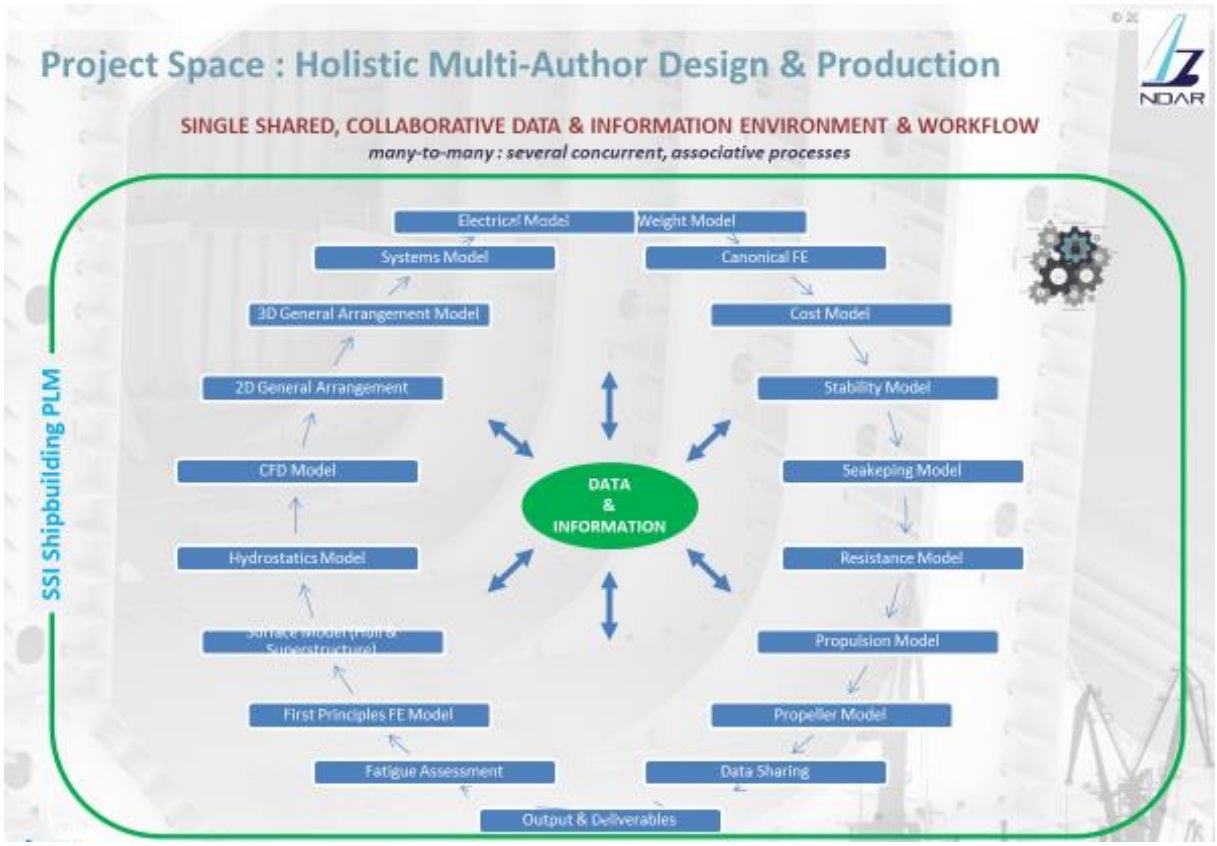

Fig.2: The same data and information sets are shared throughout the Project Space by tangible components - people, processes, tools, software, etc. - and subject to the influence of intangible components - change, fear, resistance, etc.

Therefore, tangible components require identification, qualification, pursing and goal-focused application.

5. Performance

The Project Space, or any Space for that matter, is in itself a platform of platforms, *Danese and Morais (2020)*. In other words, a collection of disparate, autonomous authors interacts in an asynchronous manner throughout a distributes, collaborative ecosystem. Then, Performance can be defined in terms of how effectively the overall, all-encompassing macro-process achieves the completion of the end-product. In marine terms, that is the delivery of a vessel perfectly matching the design brief, perfectly accomplishing the defined mission, at the lowest possible cost and in the shortest time.

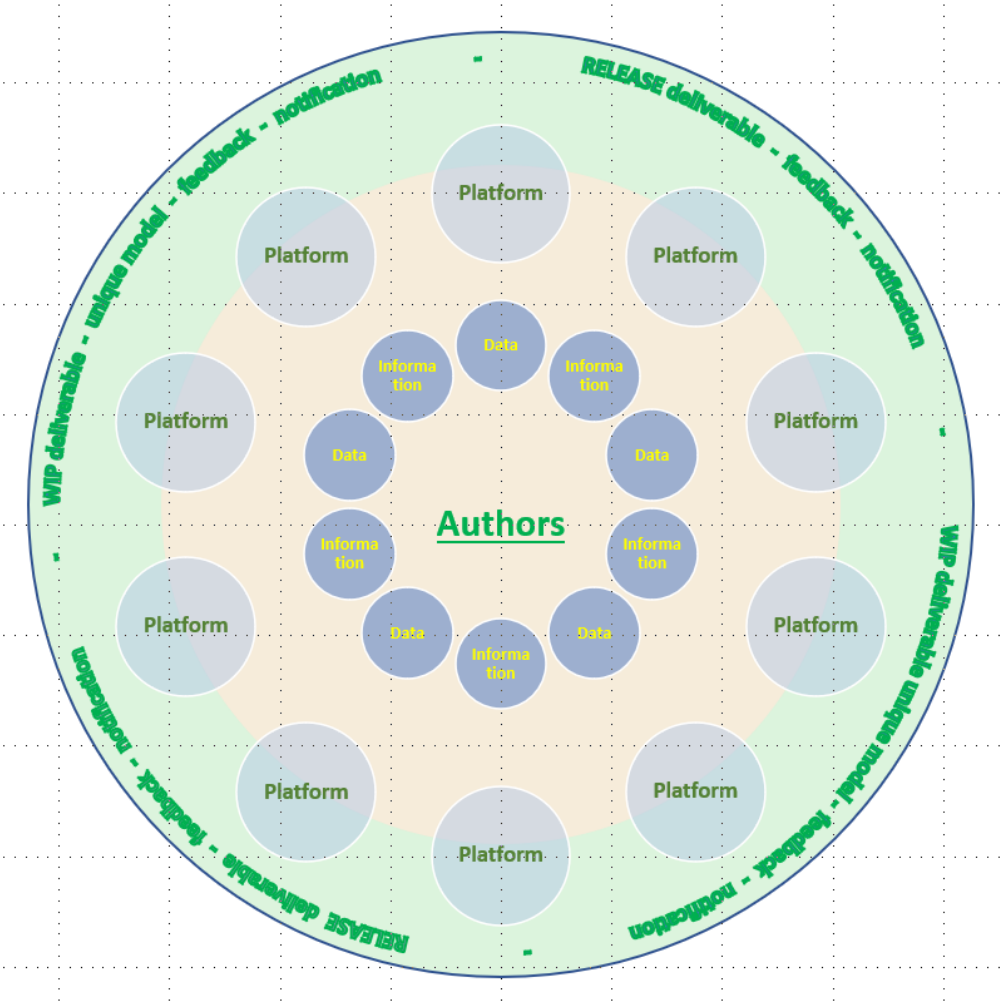

Fig.3: In a Space, for example the project Space, every component, be it people, machine, tool, process, data, information, etc. of every process in an Author.

5.1 Authors

Somewhat a departure from common culture, practice and understanding it is important to accept that even in the most ineffective work environments the concept of "consuming" data and information should and can safely be relegated to the past. Newton's Third law states the most evident example of the inexistence of passiveness in that "the force exerted by object 1 upon object 2 is equal in magnitude and opposite in direction to the force exerted by object 2 upon object 1." Going to the esoteric opposite end of the spectrum "the flap of a butterfly's wings will cause a storm on the opposite side of the world" is a philosophical way of saying that every action will cause a reaction. Very interestingly, the opposite ends meet in the idea that small things can have non-linear impacts on a complex system.

To stress the importance and seminal relevance of the "Author" and absence-of-passiveness concepts one can refer back to Prof. Lorenz (Meteorology, Massachusetts Institute of Technology) and his challenging of Isaac Newton's view, expressed thought the laws he stated, that nature is a probabilistic mechanical system, “a clockwork universe" and of Pierre-Simon Laplace's argument that "unpredictability has no place in the universe". Using the butterfly' wings flapping as an analogy, Prof. Lorentz proposes that "complex dynamical systems exhibit unpredictable behaviors such that small variances in the initial conditions could have profound and widely divergent effects on the system’s outcomes ... [to the point of] ... becoming unpredictable". This idea became the basis for a branch of mathematics known as chaos theory, which has been applied in countless scenarios since its introduction - https://www.americanscientist.org/article/understanding-the-butterfly-effect.

A more common place example of action-reaction and of the fact that an action influencing itself as well as the reaction is that of Schrodinger's Cat. All this reinforces the fact that the tangible and intangible components of a Space are inherently inextricable and that even doing nothing following an event is a reaction which bears its own set of consequences. Then it can be said that every component of every process is an Author and that dead-end "consumers" simply do not exist. This is important because it highlights the importance of managing communications, of the available vs accessible paradigm and of the feedback loop, *Danese and Pagliuca (2019), Danese and Morais (2020).*

5.2 The distributed, collaborative ecosystem

Having established that every component of every Space is an Author it is now possible to identify the nature of a distributed, collaborative ecosystem. Much as the definition per-se is simple, its implementation remains a conundrum for, still, far too many.

A distributed system is just one where different components perform different or slightly redundant work in different ways, by people in separate groups, perhaps in different places and with different tools and cultural outlooks on the job being performed (therefore attributing different value to it than others), etc.

However, the result of distributed work must come together to compose a wholesome product. Sadly, still too often it does not. "NASA lost its $125-million, 638 kg Mars Climate Orbiter because spacecraft engineers failed to convert from English to metric measurements when exchanging vital data before the craft was launched" – Los Angeles Times, October 1st, 1999. "As it entered the water, the vessel started to lean to the port side, and then quickly capsized", CNBC Wednesday, June 4th, https://www.cnbc.com/2014/06/04/10-million-yacht-sinks-after-launch.html. More common and less dramatic, although not always less costly mistakes are routine in the marine industry and, not so far-fetched, pretty much all could have been avoided.

"Collaborative", used here as an adjective, is actually a requirement if the distributed environment is to function successfully. Collaboration is very much a member of the intangible components group. Tainted by irrationality, it is difficult to define, code and enforce collaboration, thereby leaving the distributed environment destabilized by the volatile human framework.

5.3 Asynchronous Synchronisation

One might conclude at this point that the making of an Integrated, Collaborative, Multi-Authoring, Managed Environment for Ship Design and Construction is pretty straightforward, but impossible to achieve.

While true at the macroscopic level – 42 is after all not the answer to all questions in the Universe – it is not so at the microscopic, less ambitious, and more every-day level. Applying LEAN and AGILE concepts it is surprisingly easy to collect common-place components of the ship design and ship production macro-processes into high-yield, smaller Spaces and orchestrate their operation to a successful end.

An asynchronous process sees events take place without automatically triggering a direct reaction. For example, one might complete a stability report and publish it to his company's project folder. At some point someone, or another software tool, will consider and review the stability report and decide whether further action is called for, or not.

A synchronous process is one where a reaction immediately follows an action. For example, the stability report indicates that the VCG exceeds a upper limit value and the stability software itself sends a message to predefined recipients.

A similar example could be that of the weight estimation process acquiring data showing a new rare marble swimming pool beach on the top deck of a large yacht, heavy and expensive, and producing its report. The VCG is now higher but still 1mm below the limit, the tag price of the yacht just jumped up by a couple hundred thousand but is still just undern the established budget upper limit. All the spare room left for the VCG and the cost is now used up, but no warning is sent.

Now let us consider the case when the most interested party in knowing that VCG height or cost limits have been approached or exceeded is located at the antipodes and that, let us say a person, she or he just left the office for the day. The person will not be informed util 12 hours later: should all work stop while waiting for further instructions?

Or it is a software program that takes action automatically following the publication of the report, identifies the marble beach as the culprit and deletes it from the yacht's layout specification, thereby cancelling the order, etc. The yacht's future owner will likely be unhappy and would have been ready to pay for the price increase the and a technical solution could probably have been found.

Many if not most of the individual software tools commonly used today support both the asynchronous and synchronous processes, being able to produce bespoke output and, possibly fewer, capable of wait-state operation.

Moving to practice, there is not one rule for all Spaces and humans will play the key role in selecting the instruments to compose the Space's orchestra, tune them and conduct it.

It is just as clear that in the case of limited and well defined Spaces the combination of synchronous and asynchronous processes is at everyone's reach today, using common place software tools (tangible components of the Space) and common sense (intangible component of the Space).

Then, each Author will perform when solicited, appropriately and according to defined rules (synchronous) and produce a result that will be made available to other Authors (asynchronous) for these other components' action if and when this is called for, all under the supervision of informed humans.

6. Information streams: Work-In-Progress-Real-Time vs Release

Two information streams already exist in every Space: Work in Progress (WIP) and Release, *Danese and Morais (2020)*. While inherently present in the distributed environment sense they are generally unstructured, unmanaged, and ineffective from a collaborative standpoint.

It is interesting to consider these information stream under the synchronous / asynchronous spotlight as this allows to better define what Authors should do in High-Performance pursuit of the end-product goal and within the ecosystem's constraints.

6.1 Work in Progress Real Time

WIP is a relatively asynchronous process, in that all Authors contribute to the WIP "version" of the Space at the same time and to some extent in a somewhat disconnected fashion. For example, a General Layout might be undergoing significant changes to evaluate alternative: this need not result into action,

yet, by the structural layout engineers who must just be aware of the process of change and check from time to time that a significant change to the structural layout is not required after all. It might be a different story for the weight manager or for the cost estimating purchasing officer.

Not all numerical limit violations or representations of this or that portion of the project taking place at a given moment in time during the design phases demand immediate or drastic reactions, and adjustments and corrections derive from collegial reviews. What is most important here is that the project as a whole, e.g. the Project Space, is available to the Authors at every moment in time, and even more so that it is available in the format suited for its use by each Author. Then, every Author can be aware of the contents of the Project Space in wholesome unity – but not forcibly as one "model" - and elect to review, study and provide feedback on whichever part thereof she or he chooses or is programmed to. When considering software and processes as Authors, action will be triggered following human-made rules and will remain fully available to be executed by whoever decides to do so.

For example, everyone will have access to a author-agnostic rich CAD model that can be viewed on screen and in Virtual Reality (VR), navigated, sectioned, interrogated, will include hyperlinks to related documents, pre-set views and labels, allows red-lining and locked-saving.

Such a model is available today with common-place programs like Autodesk's Navisworks, capable of all the above (and more) and able to read a large number of native file formats, from CAD to Excel to SQL, 2D drawings, point clouds, etc. Additionally, following a minimum of set-up, the data and information coming from different Authors is associated with the corresponding, common-ground CAD object and available as properties. Moreover, Navisworks exports grouped collections of objects' metadata in reports, CAD model to VR, etc.

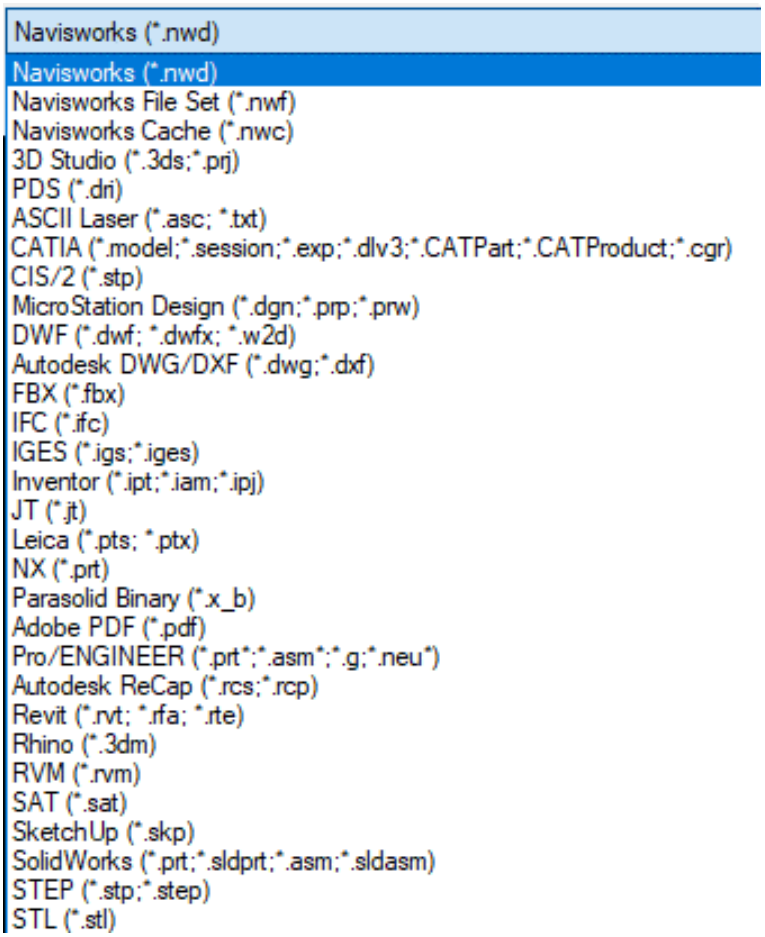

Fig.4: Navisworks supports several CAD and non-CAD data formats

Unlike other similar programs, for example Solibri®, Navisworks also imports logical models, for example from ShipWeight®, etc.

Navisworks is available packaged with AutoCAD, even comes in a free version (Freedom) therefore being commonplace already today in just about every company that uses AutoCAD, but not only. This is one example of how all Authors could exploit the WIP information stream, today.

The issue then shifts to making the "input" easily available, in a managed fashion and in, for example, Navisworks compatible formats. Alongside reading input is the need to notify of changes in the Project Space, for example the appearance and disappearance of components, in other words a managed information environment.

6.2 Release

The Release information stream is more synchronous in that it involves formal data and information that will constitute a milestone and therefore requires a timely, collegial and individual scrutiny, possibly approval. Likewise, the absence of a planned publishing also requires collegial and individual scrutiny, possibly a change of plans.

One significant advantage of a well-organized distributed and collaborative environment is that the release information stream will use the same tools, formats, and channels as the WIP information stream, only producing unmodifiable documents and placing them in dedicated repositories.

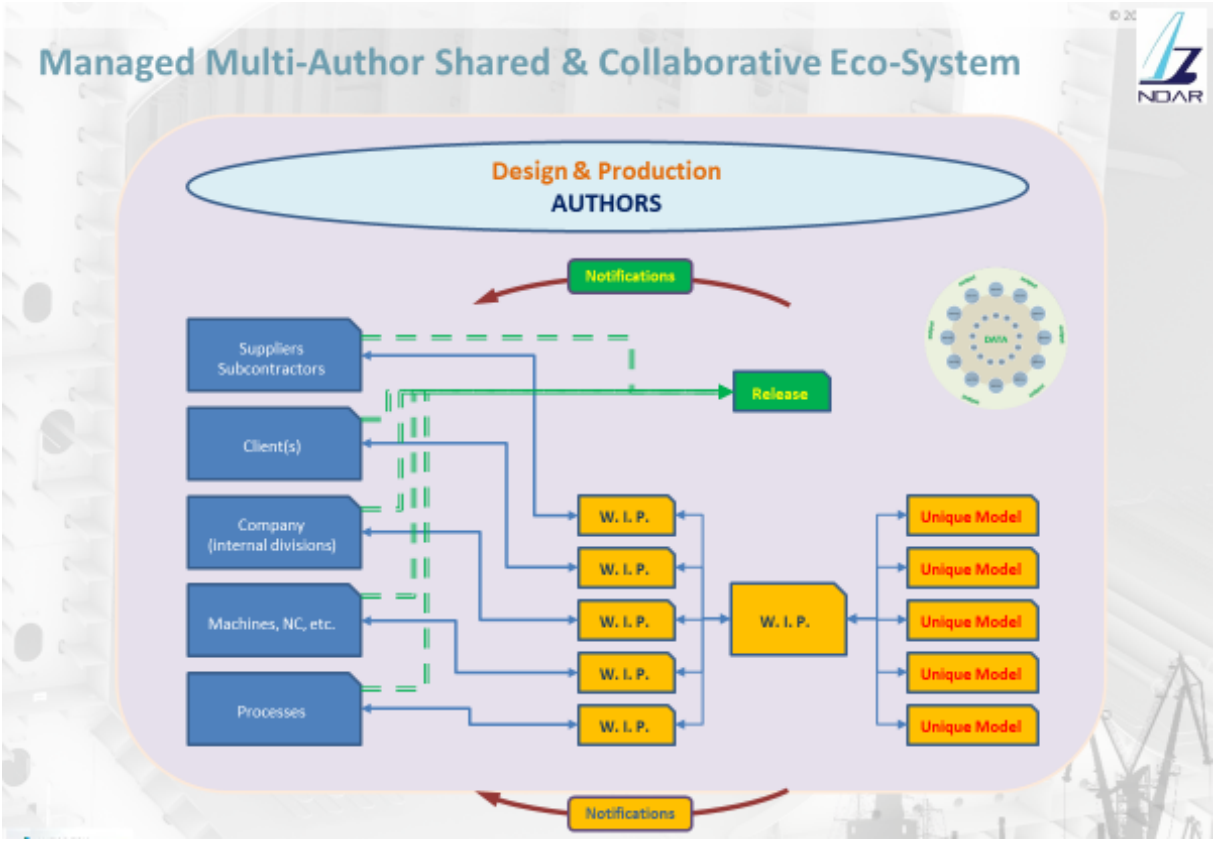

Fig.5: Work in Progress Real Time and Release information streams represented in simplified schematic.

8. Which Author at which post

Essentially, the question is which Author should do what, when and how, *Danese and Pagliuca (2019),*

Danese and Morais (2016,2020). The underlying, seminal requirement is the ability to create Unique Information Data & Information Models which are in fact data & information sets: these are none other than the large number of Digital Twins that make up the Project Space, *Danese and Morais (2020)*.

In direct support of the following discussion a short aside on Digital Twins deserves its place in that then, interestingly, Digital Twins evolve yet a little more from the legacy stigma of being the tiles of a generally CAD-based mosaic (or puzzle) - even performance-emulation Digital Twins are still too often associated with "physical, CAD" objects - and take their rightful place as purpose-focused digital representations of anything requiring it. For example, the output of a manufacturing process like painting will be affected by climatic conditions, neither being a CAD object and both being representable digitally with photographs and weather maps.

8.1 When and how

When and how take precedence over who and what because when and how will define who is eligible to do what. Taking stock of the research conducted in the world of PLM for some 65 years, the conclusion coming from the research work and field testing underlying this paper is actually very simple:

- whatever can be automated should be automated
- whatever requires judgement, evaluation, consideration should be left to humas to take care of
- whatever data and information relevant to a given stage of any process active in the Project Space which can be gathered, formatted to suite the receiving Author and made available to that / those receiver(s) deserves the resource investment required to gather and process it
- whatever data and information relevant to a given stage of any process active in the Project Space which cannot be gathered should be known and its absence documented and made known to all as part of the WIP information stream
- the contents of the Project Space must be collected and packaged for this or that Author by the authoring tools, not people, in a managed, organized fashion and in a structured archive architecture

8.1 What and who

What is essentially which data, information and results are required to achieve the prescribed end-product. Who, on the other hand, will include people, software programs, processes, machines, etc. thereby possibly requiring a little more effort to determine. Within the context of an Out-Of-The-Box Integrated, Collaborative, Multi-Authoring, Managed Environment for Ship Design and Construction resting on common-place software, tools and people's expertise, fundamental and general requirements placed on who will include (all Authors):

- to be able to exploit a common format (software), language (people), etc.
- to be able to publish relevant, bespoke output (software and people using that software)
- to be commonly available (software tools and people's expertise)
- etc.

When considering software tools in general they should:

- run on commonly found platforms (hardware and software)
- ideally already be present in or at least available to be included in the Project Space
- be easy to learn and use
- produce immediate results and ROI
- etc.

When considering people, desirable traits include:

- common sense
- ability to analyse and reduce queries to first principles
- creativity
- expertise in use of software tools
- good relational attitude
- flexibility
- etc.

Processes are generally the tough component, not least because very few people are able to analyse processes objectively and apply LEAN and AGILE considerations during that work. Anyway, requirements placed on processes include:

- flexibility
- possibility to define and configure simple procedures
- ease of configuration and reconfiguration
- extensibility
- etc.

Machines are typically the weak link when it comes to common place components of the Project Space which they are an integral part of. They should be capable of at least:

- electronic connectivity (IoT)
- a measurable level of automation
- flexibility (ex. can cut steel and aluminium)
- etc.
- (robots are not considered commonplace at this point in time)

Looking back to *how* and keeping in mind the caveats of change it is worth highlighting certain of the above mentioned "desirables":

- software: be easy to learn, be easy to use, produce immediate results and ROI
- processes: define and configure simple procedures, ease of configuration and reconfiguration
- people: common sense, good relational attitude, flexibility

9. Unique Information Data & Information Models: The Bespoke Digital Twins

It follows from the above that the very blood of the Out-Of-The-Box Integrated, Collaborative, Multi-Authoring, Managed Environment for Ship Design and Construction is made of the Unique Information Data & Information Models, identified hereafter as Bespoke Digital Twins. As has been seen, each of the software programs operating in and around any given Space should be capable of authoring several different deliverables (sets of results) in parallel and deliver these to predetermined destination Authors or to a system that will do that.

In its simplest form this is achieved by saving files to predetermined locations. This is what is generally done by most, but despite folders providing some level of collection it is a rather unstructured and unmanaged process with little control on "write" and no control whatsoever on "read".

One step up, management of the read and write traffic can be implemented rather easily. Sticking to the out-of-the-box paradigm and to that keeping track of "read" is a less common feature than keeping track of "write" it will be noted that, despite the use thereof still being rare pretty much across the marine industry several document management systems are available on the market at entry-level prices and can very easily be integrated in an out-of-the-box environment.

Bespoke Digital Twins authored by individual software applications have been the focus of other papers, *Danese and Pagliuca (2019), Danese and Morais (2016,2020)*, where the cross-use thereof has been documented with real life examples. However, these can be considered "simple" information entities in that they are the fruit of a single Author's work. (The simplest of Bespoke Digital Twin would be the pure CAD (just geometry) or pure data (a simple Bill of Materials table) ones. They are intentionally not considered here as they contribution to the Out-Of-The-Box Integrated, Collaborative, Multi-Authoring, Managed Environment for Ship Design and Construction is rather poor).

It is at this point important to recognize the relevance and compound role and impact on High-Performance Spaces of Bespoke Digital Twins that are made up of bespoke collections of other Bespoke Digital Twins, or portions thereof. These will be referred to as "complex" information entities, will be briefly discussed here and the on-going work on the subject will be the focus of future papers.

9.1 Complex Bespoke Digital Twins

Different Authors will require different type of Complex Bespoke Digital Twins, several of which are easily identifiable.

9.1.1 Meta-CAD Complex Bespoke Digital Twins

The Meta prefix is in order here as these Complex Bespoke Digital Twins rest upon CAD entities and objects but include of non-CAD metadata (properties attributes, relations, associations, etc.). (Meta comes from the Greek prefix and preposition meta, which means “after” or “beyond”.)

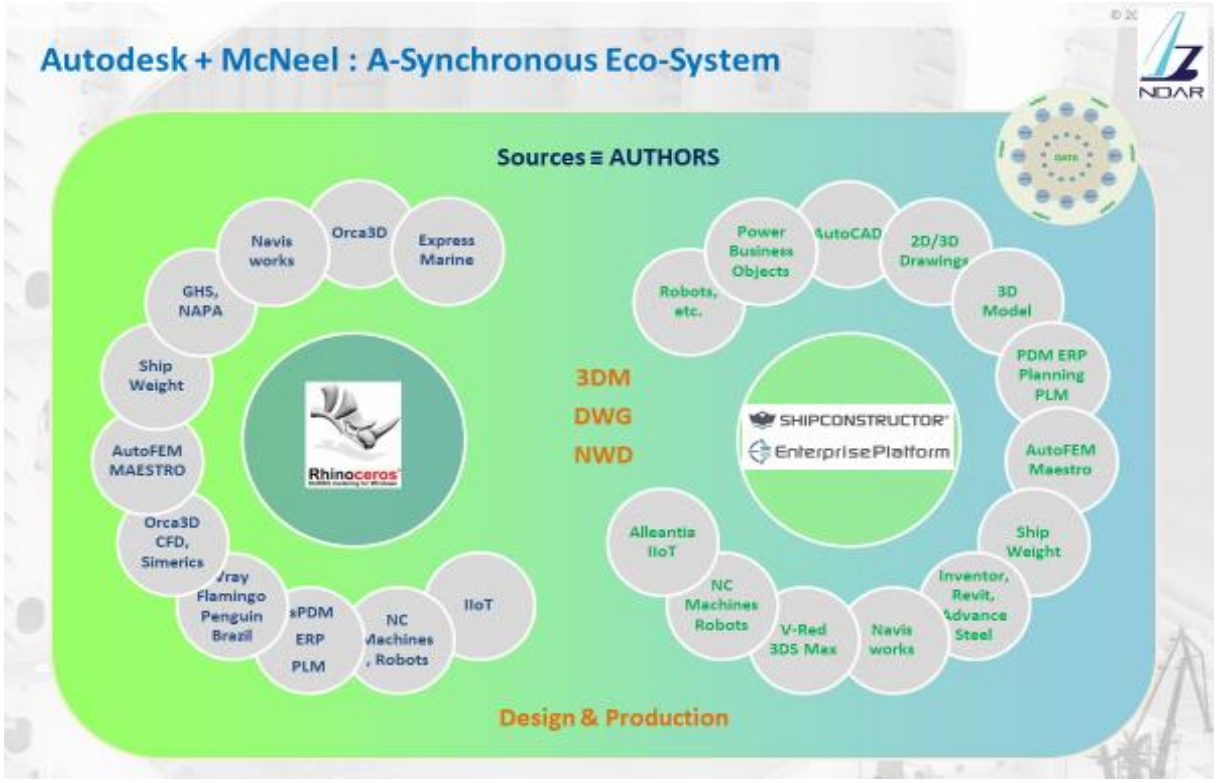

Fig.6: Out-of-the-box: the combined McNeel and Autodesk platforms constitute per-se a Complex Bespoke Digital Twin capable of generating all types of Complex Bespoke Digital Twins. Other platforms fit the mould just as well, too, and can be added to an existing Space (redundance and overlap are overlooked assets) or replace some of a given Spaces' components.

One example of a meta-CAD complex Bespoke Digital Twin has already been discussed, although not yet identified as such at that stage, that is the Navisworks collaborative review environment. Navisworks offers far more than meets the eye because not only can it read several native CAD and other

data formats (text, csv, tsv, SQL, etc.) but it allows development of plug-ins. (A plug-in is a third-party application which run inside the hosting software's environment.) SSI, Canada, one of the six major software houses in the marine industry has already taken advantage of this and in bi-directional fashion with its ShipExplorer. The SSI ShipExplorer exploits a 2-way channel allowing the Navisworks user full access to the ShipConstructor Space and allowing the ShipConstructor user access to the Navisworks Space. (ShipConstructor is SSI's CAD-centric Space for marine design and production. It is fully embedded in the SSI DigitalHub and SSI ShipBuildingPLM dematerialized Space.) In addition, Navisworks is an Author in its own right as not only does it allow human interaction that would otherwise not be possible, but it also produces deliverables, from Excel reports to VR-ready models.

AERYS' Smart Shape offers much of what is by Autodesk's Navisworks within a concurrent, multi-user environment running as a cloud collaborative platform, https://aerys.in/.

9.1.2 No-CAD Complex Bespoke Digital Twins

No-CAD means just that, there are no CAD entities or objects contained in this Complex Bespoke Digital Twin, although it might refer to some or to Meta-CAD Bespoke Digital Twins. Another example of a sadly underutilized Complex Bespoke Digital Twin is the ubiquitous MS-Excel®, which virtually everyone uses at the simple level but few do in complex fashion despite the fact that it really easy to connect an Excel workbook to several other Excel workbooks, CSV files, SQL sources, etc. and run updates on a regular or on-event basis. Still in the no-CAD category other programs like SAP's Crystal Reports® are very accessible and very easy to use in composing No-CAD Complex Bespoke Digital Twins.

9.1.3 Hybrid Complex Bespoke Digital Twins

The hybrid Complex Bespoke Digital Twins includes a combination of entities, objects, data, information, relations, associations, consultation records, archives of deliverables, etc. DigitalHub and PLM-type environments are the most recognizable hybrid Digital Twins. Some *out-of-the-box* solutions exist, for example SSI's DigitalHub and ShipBuildingPLM. Despite the fact that these applications become easier to implement as time goes their adoption remains limited, one common constraint being that there remains a misconception in the industry as to the scope of application that should be pursued when implementing such systems. In other words, the human approach to implementation is under-informed and unrealistic, leading to quasi-systematic failure.

10 The delivery system

Once the payload known it is left to consider how it will be delivered. One crucial aspect of the delivery system is that it must support active notification and a feedback loop. In the out-of-the-box category and not including the less common document management systems the spotlight would be trained on the combination of Microsoft TEAMS and Flow. A detailed discussion of this platform is left for future papers but, in short, it fulfills a number of requirements:

- transparently based on SharePoint, allows ubiquitous and fully managed document sharing via every-day Windows folders
- TEAMS provides managed access to deliverables and bespoke notification streams
- Flow permits extensive customization of data sets, processes and actions, very powerful in building Complex Bespoke Digital Twins
- These (and a lot more) applications are included in a single software package (Microsoft 365)

11. Management

With the orchestra at its best and ready to play, enter the conductor. The topic of Management is virtually unlimited. In this forum only the aspects pertaining to the available vs accessible paradigm applied

to the information flows have been considered, and intentionally so. In fact, the application of the available vs accessible paradigm transforms "management" in an evolving concept.

A fundamental paradigm shift takes place when considering a pervasive, informative "Space" as opposed to silos and isolated tasks and accepting that all components of all Spaces are Authors: responsibility for the contents and quality of deliverables moves from the checking station upstream to the Author, *Danese and Pagliuca (2019)*. The paradigm shift is more cultural than technological but the very presence of Simple and Complex Bespoke Digital Twins makes it possible for every Author to be informed appropriately in support to that Autor's work and to receive feedback even from previously disconnected Authors.

This is certainly not to say that a chain of command and a hierarchical management structure should not exist, quite the contrary. On the other hand, the advocated shift in responsibility allows a better informed and more streamlined decision-making process thanks to a higher quality contribution by each Author to the Space via Simple and Complex Bespoke Digital Twins.

12. The future

It is easy to imagine such a solution based on just the software, people and processes currently present in one's office or one's company - for example the already ubiquitous McNeel and Autodesk platforms that everyone knows and knows how to use - but this would deprive the Space of valuable contribution and components.

It is more and more recognised that a Space is not composed of imposed components but rather it includes all available components capable of contributing to its High-Performance.

This of course clashes with the business model and commercial agenda of monolithic "solution" vendors but fortunately some white knights exist, and virtuous examples of collaboration can be found, *Morais et al. (2016)*, *Perez et al. (2020)*. It can only be hoped that more will follow suite, soon.

13. Conclusion

This paper focused on implementing an Out-Of-The-Box Integrated, Collaborative, Multi-Authoring, Managed Environment for Ship Design and Construction based on Unique Information Data & Information Models (Bespoke Digital Twins) via the application of the available vs accessible paradigm in LEAN and AGILE fashion with asynchronous and synchronous processes.

The concept of a "Space" adaptable and adapted to specific realities allows the Environment to be scaled accordingly and the Bespoke Digital Twins to be defined as a function of that.

Then, there remain one intangible component to dompt: the human factor. However, daunting as this might seem, significant advances are very easily achieved by automating whatever can be and shifting the responsibility of deliverables' contents and quality upstream.

Building Bespoke Digital Twins in Navisworks and Excel and using the notification-capable MS-TEAMS ® application is well within everyone's reach. And, once these easy wins achieved, one may turn to expanding the hybrid environment of any given Space as more software vendors support the initiative.

Acknowledgments

As usual, the research & development work underlying this paper benefits from the contribution of many, each and every one of whom deserves the Author's sincere thanks and appreciation. On this occasion, Denis Morais provided an almost daily sparring and was a patient companion during the many hours of fertile brain storming. Thank you, Denis.

References

DANESE, N.; PAGLIUCA, P. (2019), *Available vs Accessible Data and Information: The Strategic Role of Adaptive Communication the Ship Design and Ship Building Processes*, CNM/ATENA Conf., Napoli

DANESE, N.; MORAIS, D. (2016), *The Synchronised Shipyard*, Proceedings, ICCAS Conf., Bremen

DANESE, N.; MORAIS, D. (2020), *The Platform-of-Platforms and Symbiotic Digital Twins: Real Life Practical Examples and a Vision for the Future*, COMPIT Conf., Pontignano

MORAIS, D.; WALDIE, M.; LARKINS, D. (2016), *Innovative Methods for Leveraging a 3D Model*, ICCAS Conf., Bremen

PEREZ FERNANDEZ, R.; MUÑOZ HERRERO, J. (2020), *How to Achieve Smart Ship Design through the Industry 4.0*, COMPIT Conf., Pontignano, pp.263-270

Fully Electric Work Boat: Design and tests

Ermina Begovic, University of Naples Federico II, Napoli/Italia, begovic@unina.it
Carlo Bertorello, University of Naples Federico II, Napoli/Italia, bertorel@unina.it

Abstract

This paper presents design development, tests and lessons learned after one season service of ELECTRA, a zero emission luxury 12 passengers boat working on the Como Lake. She represents a successful example of a fully electric boat to get performances and mission profile comparable to a sistership with conventional propulsion. This result has been achieved by a concurrent design approach considering hull form, propulsion system and energy storage, on board as well as ashore. Technical aspects have been integrated with modern classic design and wooden construction. Safety issues and regulatory frame are highlighted. Performance data are reported and critical aspects are discussed.

1. Introduction

Full electric propulsion, due to its unique potential of emission absence is very interesting when low noise and reduced environmental impact are requested. Such specific features are most interesting for small passenger craft operating in sheltered or internal waters. While characteristics and advantages of hybrid electric marine propulsion - although influencing ship design - can be achieved with standard layouts and mission profiles, a full zero emission behaviour is generally connected to strong limitations in performances and range mainly due to technical limitations and high cost of on board energy storage provided by batteries. Fuel cells with much better potential are still far from small craft application due to on board space and weight limitations and lacking distribution net ashore.

Como Lake is one of the most fascinating inland water scenarios of Europe, due to natural and historical reasons. On its shores, there are the most famous luxury residences and hotels crowded by tourists from all over the world.

Since early years of 20th century, Como Lake was plenty of high class European and English people who liked the milder climate and imported some small craft from their own countries, so that “Inglesina” and “Vaporina” are commonly used words by people of the Lake. The first refers to an English clinker planked rowboat while the second generally refers to a slender powerboat with a box shaped superstructure and two cockpits, one forward for the driver, and one aft for passengers. Both craft were built in wood by very clever artisans.

The luxury touristic offer of the Lake is based on highest level hotels which consider a must to provide their clients the possibility of cruising the Lake in a wooden Vaporina as aristocrats of early 900 did. Ernesto Riva Shipyards in Laglio (Como) operates since 1771 and has been the leader in building successful Vaporinas as CABIRIA shown in the following Fig.2. She combines cosy wooden and leather interiors, traditional look and 26 knots cruising speed very useful for fast commuting hotel clients to typical restaurants spread all around the Lake.

Over the last years, a general interest for environment and sustainability has grown up. This has been felt very much in closed environments as internal waters. Power limits are set in many European lakes. Lakes of Como is characterised by a long and successful racing powerboat tradition and its administration has chosen not to limit speed or allowed powering on board, but to encourage zero emission electric propulsion co-funding “Electric Lake of Europe” project that considers 15 electric charging stations for small craft, spread along the lake shores.

The luxury market is also very keen about the sustainability of the products so that the hotel operating CABIRIA considered the purchase of a zero-emission electric sister-ship provided hydrodynamic performances, range and operability would have been comparable.

From these premises, in 2018 the ELECTRA project has been commenced. Main characteristics are reported together with CABIRIA's ones in the following Table I. Although ELECTRA has been designed considering the ultimate state of the art electrical components, a quick comparison of the values reported in the table allows to immediately focus the differences that full electric propulsion implies in respect to a diesel engine.

Table I: CABIRIA and ELECTRA main characteristics

	ELECTRA			CABIRIA	
Length over all (LOA)	m	9.975		m	9.975
Length of hull (Lh)	m	9.963		m	9.963
Length waterline	m	9.435		m	8.930
Beam	m	2.752		m	2.752
Depth (f.l.)	m	0.478		m	0.404
Lightship	kg	2685		kg	2045
Full Load Displacement	kg	3615		kg	3225
Max Load	kg	930		kg	1180
Brake Horsepower	kW	2x80		kW	124
Engine Weight	kg	2x100		kg	354
Battery weight	kg	960		/	/
Fuel	/	/		kg	250
Passengers and crew	n	12		n	12
Deadrise angle at transom	deg	16		deg	17
Deadrise angle at midship	deg	20		deg	22
Max speed	kn	24.2		kn	28.0
Cruising speed	kn	16.2		kn	22.0
Range at 24.3 kn	nm	24.3		nm	170
Construction	Wood/epoxy			Wood/epoxy	
Design Category EU 13/53				C	

Fig.1: ELECTRA cruising at 10.4 kn

Fig.2: CABIRIA at full speed (28 kn)

2. Zero emission small craft design

Within the present general attention to ship and navigation sustainability, the design of small working craft is very interesting due to several options of hybrid and full-electric propulsions that suggest challenging targets. The final result in terms of ship environmental sustainability will result from the optimization of sea-hull interaction, the reduction of installed horsepower, and the peculiar choices of engine type and propulsion. Hull forms generally used for small planing craft do not allow the full exploitation of the concept as they can benefit of engines with large horsepower at a reduced weight.

Reduced environmental impact got by present craft is generally connected to low cruising speed and more in general too poor hydrodynamic performances, not practical either adequate for any type of commercial activity. That's why a successful full zero emission sustainable design needs dedicated and

optimized hull forms as well as the full exploitation of available resources concerning electric propulsion. The interaction between the hull and surrounding environment as well as Life Cycle Assessment (LCA) have to be considered also.

2.1. Hull form

The environmental impact of a ship is mainly related to hull hydrodynamic interactions, - waves and wake wash - and to motion resistance that is related to installed horsepower. The viscous interactions do not influence the environment although the resulting forces will contribute to motion resistance and to consequent brake horsepower. The reduction of the wave pattern is related to wake wash also and is the most important issue within this context. It is a consequence of the hull form's geometrical and dynamic characteristics. The geometrical features influencing wave resistance components are: hull slenderness $V/0.01L^3$, waterline angle at bow and Block Coefficient C_B. Each of them has to be minimized as much as possible. Geometric slenderness ratio L/B has to be the highest possible, although limited by stability and layout issues. The optimal longitudinal position of Center of Buoyancy (LCB) is also important. More in general wave pattern is related to relative speed and to waterplane slenderness. Relative speed is a fundamental concept in naval architecture and is represented by Froude number (Fr) that identifies the hydrodynamic regime in which the hull is operating and puts in direct relation waterline length LWL with cruising speed v. In case of small size craft, a practical cruising speed lead to inevitably medium high relative speed. Hull and waterplane slenderness effects on wave pattern are known since ancient ages of navigation as the proportions of Greek and Persian oar propelled battleship attest. In case of a very small passenger craft adequate transversal stability limit slenderness ratio. This and requested cruising speed lead to consider planing hull forms able to get planing condition at lowest possible speed.

Since 2005 intensive work has been done at University of Naples towing tank for design and development of non-monohedral hull forms, with better hydrodynamic performances in respect to standard monohedral ones and in the last years the research has been focused on low drag hull forms able to get strong hydrodynamic lift at low relative speed. Such hull forms are suitable for use in internal and sheltered waters considered in this paper. The typical hump present in resistance trend of any planing craft is faired by the high lift provided by low deadrise stern sections and a small bow down trim at rest. Interceptors or stern flaps can be useful to get the best running trim and to fit load conditions and passenger position. In this frame, a light structural weight is most important to get hydrodynamic equilibrium at the lowest possible speed.

2.2. Main Engine(s)

The electric engine is one of the most diffused and diversified machinery all over the world. Even limiting to the field of marine propulsion the types are numerous and the power ranges from few kW to MW.

Zero emission small craft at first used DC (Direct Current) engines that are very simple to install and to control; they work with low voltage but have small power and are relatively heavy. At present DC engine applications for small craft marine propulsion are limited to 20-40 kW at 48-96 V.

To get higher power and better Power/Weight ratio it is necessary to shift to a higher voltage and to AC (Alternating Current). Among different types, a very interesting recent proposal is the Permanent Magnet Synchronous Motor (PMSM). It is an AC synchronous motor, the field excitation of which is provided by permanent magnets. PMSM is a cross between an induction motor and a brushless DC motor. As a brushless DC motor, it features a permanent magnet rotor and stator windings. However, the winding structure of the stator, constructed to produce a sinusoidal flux density in the machine air gap, resembles that of an induction motor. The power density is higher than induction motors with the same ratings, since there is no stator power supply dedicated to the production of the magnetic field.

With permanent magnets, the PMSM can generate driving torque at zero speed. They require the use of digitally controlled inverter for operations. PMSM motors are generally used when high performance and high efficiency motors are needed. Motor control features smooth rotation over the entire motor speed range, full torque control at zero speed and rapid acceleration and deceleration.

The performance of PMSM is most interesting. Power/Weight ratio is about 1-1.2 kW/kg; dimensions are extremely reduced. Careful engine design leads to rpm value that can be compatible with small diameter propeller regime allowing direct shaft connection without a gearbox.

Very often electric engines, due to their reduced dimensions are housed into pods directly connected to the propeller. This setup has benefits as no engine inside the hull and very easy cooling, but any leak into the pod or any engine maintenance force to hauling the vessel ashore. For this reason - in the present project internal engines with the standard propeller shaft and thrust bearing have been chosen. Twin engine installation is due to several reasons: better manoeuvrability, safety, higher margin in respect to engine max horsepower, easier installation of two smaller engines than a big one.

2.3. Energy Storage on Board

Energy storage on board zero emission marine vehicles can be provided by fuel cells and or batteries. Technical characteristics and reciprocal advantages of the two means are very well presented and evaluated in *Minnehan and Pratt (2017)*. The conclusion is that fuel cells are more suitable for large ship and Lithium based batteries better fit small craft with high relative speed. The present and predicted future trends confirm this conclusion.

The high energy storage density of liquid hydrogen tanks (1.3 kWh/L) compared to gaseous hydrogen tanks (0.36 kWh/L) and battery systems (~0.09 kWh/L) make liquid hydrogen-based systems the most capable in terms of its ability to meet a wide variety of vessel sizes and mission requirements. Longer endurance missions favour hydrogen fuel cell systems because of this. As endurance increases the energy component of the system increases. For fuel cell systems this is just the fuel tank; the fuel cell itself remains constant at the level needed for the power. For battery systems, the entire battery system size must increase even though the power level is constant. Since the energy density of battery systems is less than 1/10 that of liquid hydrogen, battery systems quickly become much larger than hydrogen systems as stored energy demand increases.

For small vessels requiring high power for short durations: the fuel cell systems generally are not able to meet the volume requirements while the battery system is. This is due to the size of the fuel cell system. For a high-power system that does not require a lot of stored energy, a battery-only system can meet both the power and energy requirements with just the batteries.

Fuel cells require a hydrogen fuel tank and the possibility of refuelling. While electric energy is easily available from shore almost everywhere Hydrogen option is at the very beginning. For the considered project and for the most of small craft full electric designs, the energy storage by batteries is chosen and in practice is the only possible option.

Battery technology is improving rapidly and is predicted to become more mass and volume efficient in the coming years. Currently, for shipboard propulsion, Li-ion batteries offer the highest energy density, a suitable power density, high efficiency and an acceptable lifetime.

The family of Lithium batteries is vast and the electro-chemistry can be tailored for the specific need. Some types offer high energy density or high power density, some others like Lithium Titanium Oxide (LTO) have superior thermal stability for fast charging and discharging but offer lower capacity typically 50-70 Wh/kg. Research continues into electro-chemistry and new battery technologies, advanced Lithium-ion, Lithium-Sulphur and Lithium-air being types that seem to offer significant advantage and are currently preferred. Essentially, the demand for higher energy density (driven by

demand from the road vehicle industry) is spurring on development, potentially offering higher energy densities, fast recharge times, and enhanced lifecycle. Cost still remains very high.

Current batteries are limited in the lifecycle (maximum is 10 years but typically 5 years) which means they may have to be replaced several times throughout the ship lifetime. The battery replacement cost together with the cost of electricity consumed from the local grid are the major operating cost of the propulsion plant, but that there is no longer any need for bunkering diesel fuel and regular maintenance of diesel engines.

Energy storage that means type, size and technical characteristics of the accumulators is strictly linked to propulsion engine characteristics and to the required range.

While the AC high power electric motor has proven quite successful the difficulties in managing energy storage and conversion with DC voltage in the order of 400V on a small boat affected negatively the final result. High voltage batteries present several problems from high working temperature to preheating and too complex charge management, but are the only choice if performance is requested. Inverters are heavy and bulky. A general trend is to use DC current with low voltage generally 48V sometimes 96V for small horsepower. At present, there are several available options of plug and play packages of electric asynchronous brushless engines complete with controls and BUSes designed for marine applications on small craft. Horsepower is up to 30 kW. Power transmission to propellers is available through standard shaft or pod.

In the ELECTRA project, the requested performances inevitably lead to higher horsepower and higher AC voltage.

When zero emission propulsion became a realistic option for small craft and several engine manufacturers proposed electric engines set for marine use, many expectations for wider exploitation of the concept were based on the predicted cost decrement of high-performance batteries. This, in spite of the larger number of different vehicles using electric or hybrid propulsion, did not happen to batteries suitable for marine applications. The different types of Lithium batteries are still very expensive and limited in their working life. The most of research and development for the best performing batteries is focused on automotive where the battery is generally set below the passenger accommodation area and has a flat rectangular shape almost two-dimensional, with main dimension in the range of 1.5-1-8 m. This shape is very unpractical for small craft unless the whole designed layout is conceived around the battery(ies). In case of an existing layout, as in the case of ELECTRA, compact parallelepiped batteries with the main dimension below 1 m are preferable.

In conclusion, energy storage on board is, at present, the weak point of the chain. In the case of Lithium batteries, the most interesting for the presented project, there are several factors of influence:

- density of energy for weight unit (kWh/kg);
- density of energy for volume (kWh/l);
- life of the battery (number of cycles);
- disposal at the end of the working life;
- intrinsic efficiency of the charge-discharge (%);
- depth of discharge DOD (%).

These two last characteristics lead to a significant difference between the quantity of energy that the battery can deliver and the energy that has to be stored. This means that about 20-25% of battery weight is carried on board without any direct benefit for the performance.

2.4. Recharging and ashore energy

This aspect is, at present, very critical. Performance and size of full electric marine vessels have increased and consequently, the quantity of electric energy to be stored on board from ashore has

increased too. Moreover, the time of battery charge has become shorter so that a large amount of energy in a short time is needed; the order of magnitude is quite larger in respect to domestic and automotive applications, and the availability of such energy in a single point has become a critical issue for the exploitation of full electric marine vessels. A very interesting solution has been developed by the Norwegian shipping company The Fjords that manages a purely electric ferry the 'Future of the Fjords' since 2018. As the local grid does not have the capacity to charge the ship at the dock a new charging solution called the PowerDock has been made. This is 40 m long, 5 m wide floating glass fibre dock set in the water at Gudvangen, housing a 2.4 MWh battery pack. This charges steadily throughout the day via connection to the local grid network. The innovative solution allows the vessel to stably, efficiently and cost effectively 'refill' in just 20 minutes. The similar, smaller solution is considered to recycle Li-ion batteries of older type or too heavy to be used on board.

Electra can benefit of "Electric Lake of Europe" ashore installations of standard automotive charging columns, (400 V three-phase with power up to 40 kW) on the docking piers.

2.5. Safety

Safety critical issues peculiar to zero emission small craft are basically two: the presence on board a small craft of relatively high electric voltage and the behaviour of Lithium batteries in case of damage or sinking. The emergency stop is mandatory according to ISO 16315, *ISO (2016)*. This Regulation considers safety according to standards of electrical systems, but a peculiar approach focused on the consequences of collisions and on Lithium battery hazards seems appropriate. In case of fire, the battery may catch fire and explode.

2.6. Regulatory frame

In the case of electric propulsion and more in general of electricity on board peculiar aspects are considered by Classification Societies, and by ISO Rules that have general validity. Pertinent ISO Rules are:

- ISO 10133 for direct current system installations, which operate at a rated voltage not exceeding 50 V;
- ISO13297 for single-phase alternating current installations, which operate at a rated voltage not exceeding 250 V;
- IEC 60092- 507 (Ed. 2000) for three-phase alternating current systems, which operate at a rated voltage not exceeding 500 V.

The favourable consideration of 48V DC choice is enhanced by the application of the less stringent ISO normative. Recently in the frame of European Directive for Pleasure Craft 2013/53 the ISO 16315 Small craft - Electric Propulsion Systems, has been issued. This Regulation clarifies most of design and installation aspects related to full electric propulsion on small craft.

2.7. Sustainability

Although both batteries and fuel cells are zero emission on the ship, the energy used to recharge the batteries or make the hydrogen may not be zero emission. Full emissions analysis with comparison to conventional diesel technology is needed to understand the true global impact of converting vessels to zero emission.

Lithium Ion batteries contain elements that may pose health risks to individuals if they are allowed to leach into the ground water supply. In some countries, it may be illegal to dispose of these batteries in standard household waste. Recycling facilities exist that process Lithium ion batteries, in part due to the value of the materials contained within the individual cells.

2.8. Electrical system and propulsion total efficiency

Besides the mentioned benefits in term of emissions, full electric propulsion has several disadvantages in comparison with diesel engines of the same horsepower:

- Weight of batteries is much higher than the corresponding weight of fuel;
- Weight of batteries has to be carried on the boat always, while fuel weight is going to be consumed along the trip and in many cases, fuel tanks can be partially filled;
- Batteries have a working life shorter than diesel engines;
- Electric engine together with inverter and controls has an intrinsic efficiency of about 0.9; this value affects the total propulsion efficiency of the boat;
- Batteries have a charge/discharge process efficiency (about 0,9) and the stored energy can be used up to a certain extent that is given by DOD (Depth of Discharge), in the best cases =0.9.

This means that the standard efficiency chain that connects Effective Power PE to Brake Horsepower PB, in case of electric propulsion is handicapped by three new members smaller than 1. On the other hand, electric engines do not need exhaust system, are smaller and lighter. In many cases, they do not need a gearbox.

2.9 Suitable mission profiles

From the previous considerations, it is evident that a suitable mission profile has to be established to get successful results. The present available technical resources and high budgets can allow acceptable performances but the same value in terms of max cruising speed and range cannot be achieved. Nevertheless, the fascinating silent navigation, as well as the compliance to present and future trends in terms of sustainability, has led to start the construction of a very competitive small commercial craft as reported in the following paragraphs.

3. Electra

In the following the peculiar features of ELECTRA project are reported.

3.1. Hull form and resistance predictions

ELECTRA hull forms are derived from the successfully tested non monohedral planing hull form developed at Naples towing tank by MArine HYdrodynamic Research Group (MAHY). ELECTRA has slightly smaller deadrise angle at stern and fuller afterbody to get lower planing speed than CABIRIA and to counteract the heavier displacement due to battery weight reported in Table I. Forebody remains deep V, this is due for better damping pitch and heave in case of encountering the short and deep waves produced by ferries operating on the lake. Tank testing which results are summarized in Figs.5-6 is very useful for preliminary powering assessment and when full scale results are available as in this case to better identify propulsion efficiencies for future projects as detailed in the following Par 3.5.

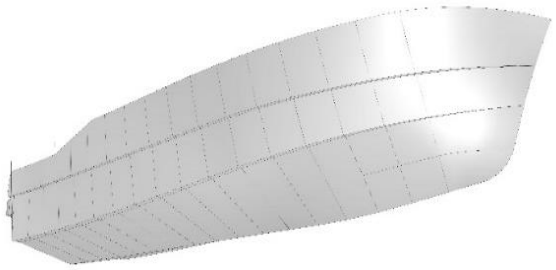

Fig.3: ELECTRA hull form

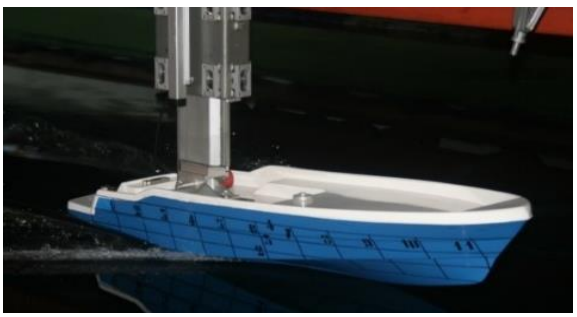

Fig.4: Towing tests at DII tank of parent non monohedral hull form

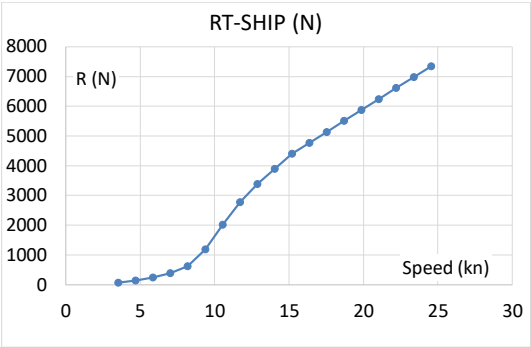

Fig.5: Ship bare hull resistance from tank tests

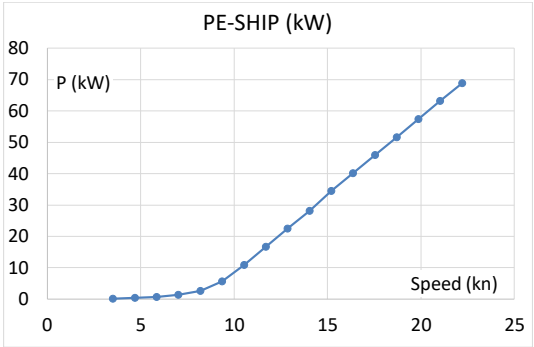

Fig.6: Effective power from tank tests

Effective power from tank testing is relative to bare hull augmented of 7% for the appendix and 3% for aerodynamic resistance. From towing tank results powering assessment has been done considering a total propulsion efficiency (mechanical, electrical and hydrodynamic) of 0.45 leading to the predicted Brake Power curve reported in Fig.11. On this basis, the propulsion engines have been chosen as reported in the following par 3.2.

3.2. Powering and propulsion

Electric engines are Permanent Magnet Synchronous Motor (PMSM). Their main characteristics are reported in the following Table II. Weight and dimensions are small and the installation very easy. The hollow rotor shown in Fig.7 allows very easy shaft connection.

In the case of electric engines max rated power is a builder choice and small increase in rpm can increase delivered power. Max potential power of the chosen engines is about 100 kW at 2250 rpm. The chosen value of 80 kW would allow a 23.2 kn speed, with a very good safety margin. Each engine has a water cooling system and a thrust bearing.

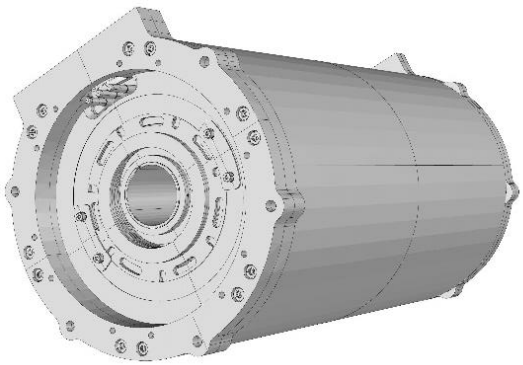

Fig.7: Synchronous PMSM engine by ATS

Table II: Main engine - Technical features

Manufacturer	ATS Antriebstechnik GmbH	
Type of engine	Synchronous PMSM	
RPM	n/min	2000
Max rated power	kWh	80
Operating voltage	V AC	440
Frequency	Hz	130
Max Torque	N m	400
Length	mm	500
Diameter	mm	280
Weight	kg	100
Height		
Cooling system	Water (double)	
Efficiency		0.95
IP protection		67

3.3. Energy storage on board and ashore recharging

Electric energy is stored in 12 batteries described in the following Figs.8-9 and Table III. They are standardized Li-ion traction battery with specific characteristics at the top of the range. Specific energy is 0.19 kWh/kg and 1.59 kWh/l.

Fig.8: Ecovolta EvoTB 96V 15kW Battery

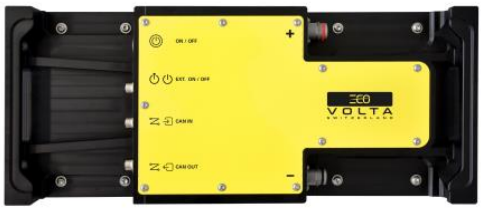

Fig.9: EvoTB 96V 15kW Battery top view

Table III: Battery Technical Features

Manufacturer	Ecovolta	
Model	EvoTB 96V 15kW	
Type of battery	Lithium NMC	
Number of batteries		6 for each bank
Capacity for single battery	KWh	15
Operating voltage	V	650
DOD (Depth of Discharge)	%	90
Charge/Discharge efficiency	%	90
Charging Time	h	4.5 @40kW
Length	mm	520 for each modulus
Width	mm	220 for each modulus
Height	mm	440 for each modulus
Cooling system		Air
Weight (each)	kg	80
IP protection		67

The configuration of the chargers used on ELECTRA is as follows, with reference to following Fig.10: the boat has two independent 650V 90kWh battery banks. Each bank is recharged by a group of three single-phase battery chargers 220V AC 6.6kW, the DC side of the chargers is put in parallel, while the AC of each charger is connected between a phase and neutral, forming in this way a system that works with three-phase 400 Vac and power of 22 kW. In this way, the total usable charging power is 44 kW. The two groups of chargers are shown in Fig.10 as CHRG1-2-3 and CHRG4-5-6.

Ashore on the docking piers standard automotive charging columns, (400V three-phase with power up to 40 kW) have been arranged.

3.4. Electrical layout, controls and systems integration

Fig.10 shows the electrical layout of the propulsion plant and energy storage. Each main engine has its own battery pack, inverter and control system. The motor is driven through the use of a vector controlled MAC inverter and configured for operation with torque control, a resolver is used as a feedback sensor on the motor. The system is managed and piloted by an accelerator throttle with communication via CANBUS (Control Area Network BUS).

650 V voltage is used for propulsion and 12 V voltage is used for controls and auxiliaries. CT1, CT2, CT3 are components used to insulate and if necessary add termination on the CANBUS lines that are connected between the various batteries; essentially, for safety reasons, they increase the degree of galvanic insulation between the 650V traction voltage and the 12V voltage used in control and visualization systems and everything else of the boat Batteries and charging details have been already given in previous Par. 3.3 controlled and GW are gateway devices used as Master interface for the data collection from the six slave batteries connected in series and from chargers.

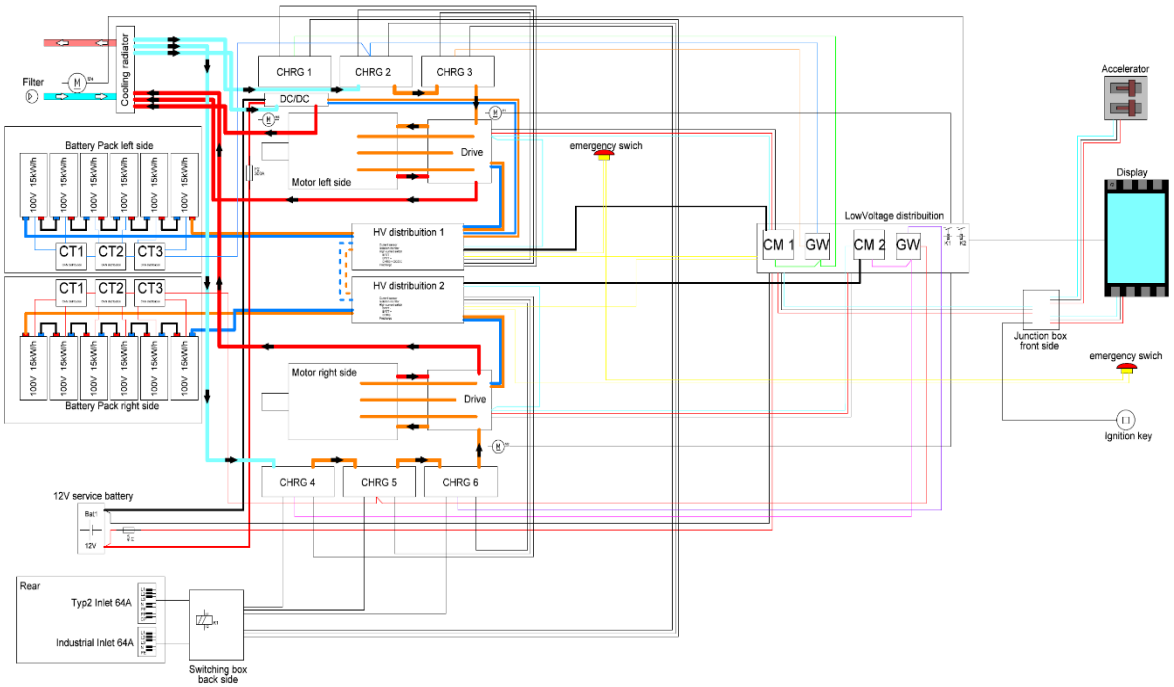

Fig.10: Electrical layout and cooling system of the propulsion plant

This data is processed and sent to car managers. CM1 and CM2 indicate Car Manager, these are two electronic control units they collect the command and safety signals, the CANBUS serials among other devices and PWM communication with the charging stations and deal with system management. For the cooling system at the beginning, a heat exchanger with a main pump connected to seacock for cooling the fresh water exchanger has been set. Then from the side of the closed circuit, three standard automotive pumps for circulation in the various devices have been used, as reported in Fig.10. In the current ELECTRA, some changes have been made by eliminating the exchanger and using only the master pump with the seacock and direct circulation of lake water. 12V auxiliary battery is intended for starting the system and for auxiliary services, the recharge of this battery is provided by 650V battery pack and through 12V 200A DC/DC converter.

This layout derives from previous experience of a full electric successful powerboat “Ernesto” (Small boat of the year at 2019 Genoa Boat Show) built by the same team. The cooling system is still neglected by the electric engine manufacturer and a driven pump as used in the thermic marine engine could be simpler and better. Nevertheless, inverter and charger need cooling also when the engine is stopped and this requires some independent pump.

The DC 12V battery is a weak point as it takes energy from the propulsion battery and failure in them would cause a blackout stop of the whole system. It has been considered the option of a completely independent 12V DC source.

The battery management in general and first start, in particular, is demanding and requires skilled personnel.

3.5. Full-scale performances and electric efficiency assessment

In the case of electric propulsion, the electric power absorbed by the engine(s) can be easily read on the control panel where electrical current and voltage are measured. The absorbed power can be related to the delivered Brake Power considering the engine-inverter combined efficiency provided by the manufacturer (=0,92). In Fig.11 both Predicted (from tank tests) and Measured Brake Horsepower values are reported.

All data are relative to boat completely equipped with six passengers and two crew. At first trials, the boat got a maximum speed of 24,3 kn with engines delivering a PB of 142,5 kW. This value is slightly better than the predicted one, as shown in Fig.11, leading to a total propulsion efficiency of 0.506. This value is consistent with the proposed values of 0,92 for inverter/engine and a realistic total efficiency (hydrodynamic and mechanical) of 0,55 already observed in sistership CABIRIA.

The Brake Horsepower value can be reported to possible mission profiles with the used battery pack of 2 x 90kW considering the energy requested by the engines (PB/0,92) and the higher value of energy to be stored into batteries due to charge/discharge efficiency and DOD values reported in Table III.

In the following Fig.12, speed (kn) and range (nm) are reported. It is interesting to appreciate that the-very low planing speed and the trend of the resistance curve provide very similar range values at a higher speed. This is very consistent with the lake mission profiles where the maximum range in miles is about 25. Obviously when the speed drops significantly the range increases accordingly. Fig.12 show graphically these observations.

ELECTRA standard half day mission profile considers a cruising speed of 16,2 knots allowing 1 h and 35' cruise for a range of 25,6 nm. This leaves a 10% margin of energy into the batteries due to the considered DOD. Recharge time is about three hours.

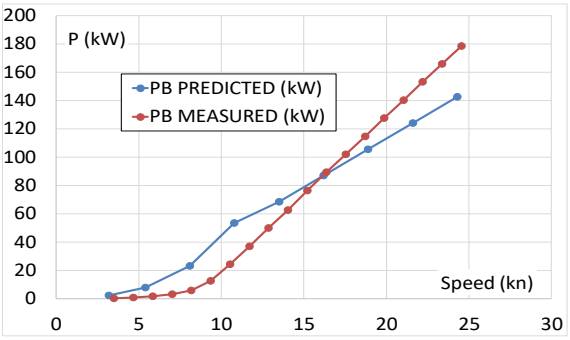

Fig.11: ELECTRA Brake Horsepower predicted and measured in full-scale trials

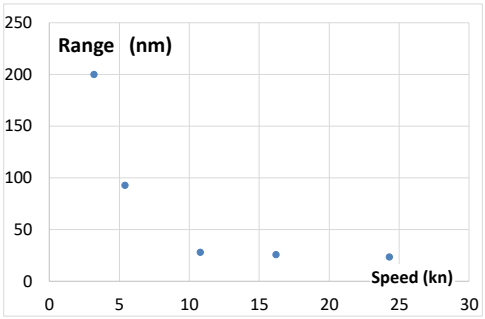

Fig.12: ELECTRA range vs speed

4. Conclusions and Future Developments

The availability of full-scale data together with accurate performance prediction for hull form, electrical propulsion and storage system allowed a realistic evaluation of electric efficiencies and effective battery performances. This is a critical issue for the evaluation of limits and potential of full electric propulsion. The target of ELECTRA project has been achieved. After one successful working season and a few months of the present one, the boat has proven reliable and complying the given requirements. Small details have been optimized and new construction had been already started if touristic business had not been heavily affected by Covid-19.

The future developments are focused on easy installation and maintenance as well as on safety. It is difficult to forecast in the present scenario new significant progress or cost decrease for energy storage on board of such craft. In the long term future, radical changes to hydrogen fuel (liquid or high pressure) have to be considered also for small craft according to the trend began on cruising ship.

Acknowledgements

The Authors thank Ernesto Riva Boatyard and MAC engineering S.r.l. A special thanks to Mr Andrea Giurato for his kindest cooperation. This work has been financially supported by Department of Industrial Engineering, University of Naples Federico II.

References

BERTORELLO, C.; BEGOVIC, E. (2016), *Zero Emission Sustainable Craft for Coastal Marine Protected Areas,* Int. Annual Conf. AEIT 2016, Capri

BIGERNA, S.; MICHELI, S.; POLINORI P. (2019), *Willingness to pay for electric boats in a protected area in Italy: A sustainable tourism perspective,* J. Cleaner Production 224, pp.603-613

ISO (2016), *ISO 16315 Small craft - Electric Propulsion Systems,* Int. Standard. Org., Geneva

LEE, D.K.; JEONG, Y.; SHIN, J.G.; OH, D. (2014), *Optimized Design of Electric Propulsion System for Small Crafts using the Differential Evolution Algorithm,* Int. J. Precision Engineering and Manufacturing-Green Technology 1/3, pp.229-240

LETAFAT, A.; RAFEI, M.; ARDESHIRI, M.; SHEIKH, M.; MOHSEN BANAEI, M.; BOUDJADAR, J.; HASSAN KHOOBAN, M. (2020); *An Efficient and Cost-Effective Power Scheduling in Zero-Emission Ferry Ships,* Complexity Volume 2020, Article ID 6487873

MINNEHAN, J.J.; PRATT, J.W. (2017), *Practical Application Limits of Fuel Cells and Batteries for Zero Emission Vessels*, SAND2017-12665, Sandia National Laboratories

MUTARRAF, M.U.; TERRICHE, Y.; NIAZI, K.; VASQUEZ, J.C.; GUERRERO, J.M. (2018), *Energy Storage Systems for Shipboard Microgrids—A Review*, Energies 11, p.3492

RATTHAKRIT, R.; YODCHAI, T.; SATHIT, P; TEWARAT, N.; PHANSAK, I. (2015), *The Possibility of using Electrical Motor for Boat Propulsion System*, Energy Procedia 79, pp.1008-1014

WUA, P.; BUCKNALLA, R. (2016), *Marine propulsion using battery power*, Shipping in Changing Climates Conf.

Innovative 3 DoF Wind-Assisted Propulsion System

Amnon Asscher, Nayam Wings, Hilla/Israel, amnon.asscher@gmail.com

Abstract

Nayam Wings is developing wind propulsion system composed of unique wings that produce high propulsive forces. Each wing has 3 degree of freedom (yaw, pitch and roll). The wing is constructed of multi element asymmetric airfoils. Its unique design allows controlling the heeling moment created by all wind propulsion systems. The highly efficient wing design leads to low drift forces and induced ship drag. The masts can be telescopically lowered to reduce air draft and passive wind resistance when necessary.

1. Technology description

NAYAM WINGS's wing sail technology is a category by itself with the highest propulsive, stability and energy efficiency performances.

NAYAM WINGS technology is the unique system that utilizes a wing with 2 degrees of freedom manoeuvrability: yaw and roll.

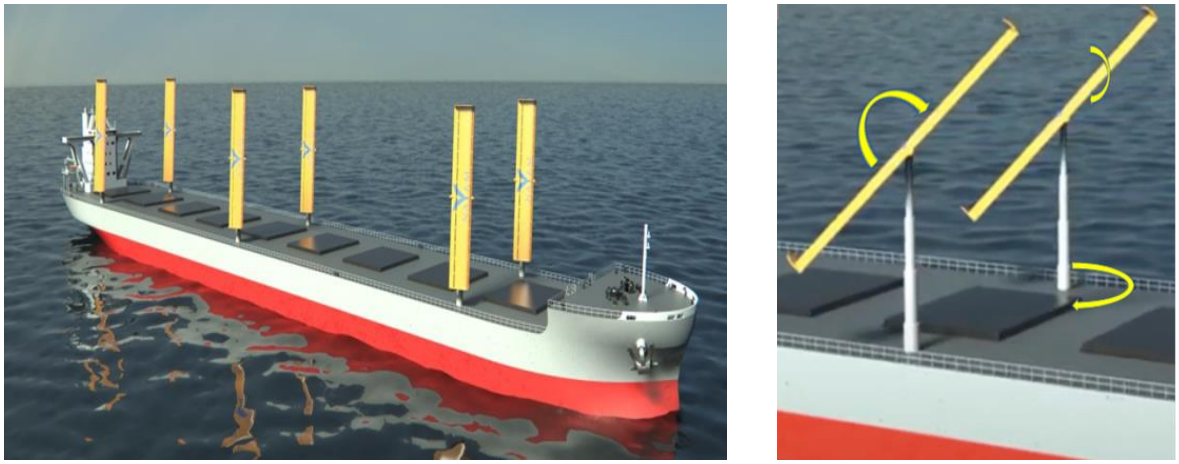

Fig 1: Yaw and roll of the wing

This unique manoeuvrability enables the wing to be constructed of multi element asymmetric airfoil and control the heeling moment created by all wind propulsion systems while sailing in front apparent winds.

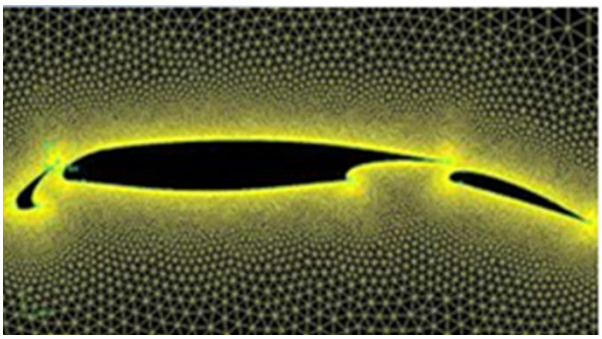

Fig.2: Asymmetric three-element wing

These two fundamental abilities deliver the big advantages of NAYAM WINGS technology:

1. Utilizing multi-element asymmetric airfoils, Fig.2, with much higher lift coefficient than any other wing sail technology: $C_{L,\,max} > 4$. The three-element airfoil is designed to highest lift force in very low speed compared to aircrafts. The wings have very precise DOG (Degree, Overlap, Gap between the three elements) with flap and slat to maintain highest lift force constantly, Figs.3 and 4.
2. Controlling and reducing heeling moment, Figs.5 and 6.

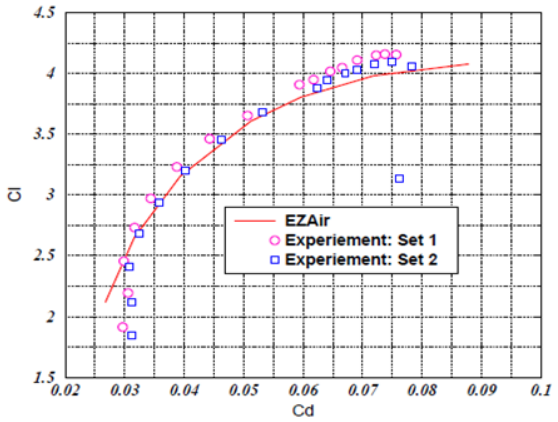

Fig.3: Lift vs drag coefficients

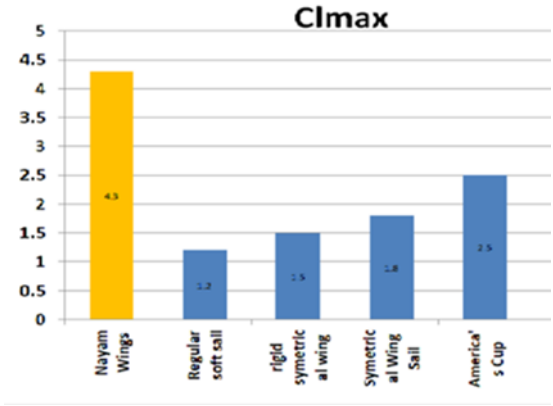

Fig.4: Lift coefficient comparison

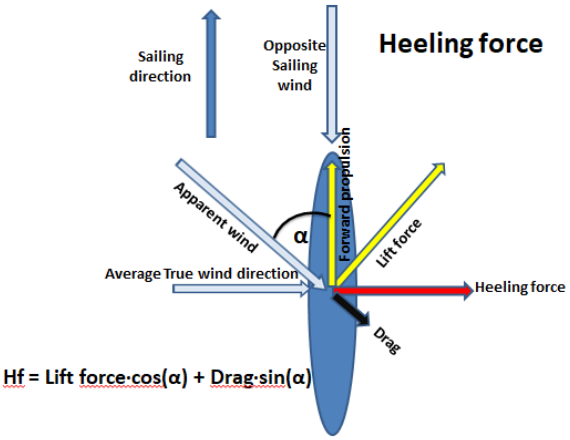

Fig.5: Lift, drag and heeling forces and average wind directions

Fig.6: Heeling moment

Due to the roll manoeuvrability of the wing NAYAM WINGS can control and reduce the dangerous heeling moment, Fig.7.

NAYAM WINGS have very low drag to lift ratio:

$C_{Dmax} / C_{Lmax} = 0.075 / 4.2 = 0.018$

The lower the drag force, the lower the heeling force and the higher the forward efficient thrust force in average apparent wind directions, Fig.5.

2. Overall forward propulsion and drift force

$$\text{Drift force} = \text{Lift force} \cdot \cos(\alpha) + \text{drag} \cdot \sin(\alpha)$$

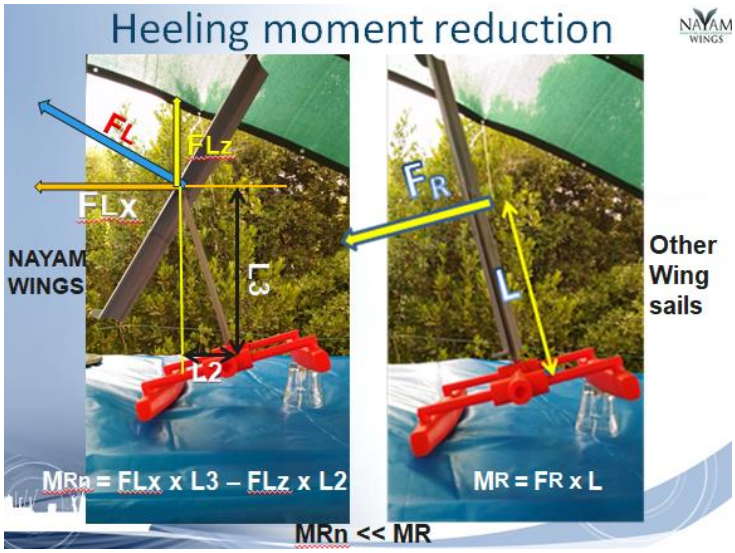

Fig.7: NAYAM WING's solution for controlling and reducing the heeling moment

Forward efficient thrust force = Lift force · sin(α) - drag · cos(α)

α = angle between apparent wind and sailing direction

$$\text{Lift force} = \frac{\rho}{2} \cdot V_A^2 \cdot S \cdot C_{L3D}$$

ρ = air density in sea level = 1.3
V_A = Apparent wind speed
S = Wing projected area (chord x span)
C_L = Lift Coefficient

NAYAM WING's 2D C_{Lmax} = 4.2 at AOA 20°
NAYAM WING's 3D C_{Lmax} = 3.5 at AOA 20°
3D $C_L = C_{L3D} = C_{L2D}/(1+C_{L2D}/\pi e A_R)$
e = Oswald Efficiency Factor = 0.95±
A_R = Aspect Ratio = span/cord = 6

Example of NAYAM WING's lift force at true wind speed of 7 m/s from beam (90°) and sailing speed of 7 m/s. Wing dimensions: 5 x 30 m

Apparent wind direction – 45°

Apparent wind speed: 7/cos(45°) = 9.9 m/s

Lift force = $\rho/2 \cdot V_A^2 \cdot S \cdot C_{L3D}$ = 33.5 kN

NAYAM WING's drag force = 0.018 x 33.5 = 0.6 kN

Forward efficient thrust force = Lift force · sin(α) - drag · cos(α) = 23.26 kN

1 NAYAM WING (5 x 30m) power at 7 m/s sailing speed = 163 kW

When apparent wind directions are 90° - 270° the drag force contributes to forward thrust but also to heeling force. Such wind directions are limited and are close to back winds where most wing sails will position themselves vertical to the wind (AOA = 90°) and benefit the highest drag force for obtaining high forward thrust in case the back wind speed is higher than the sailing speed, Fig.8.

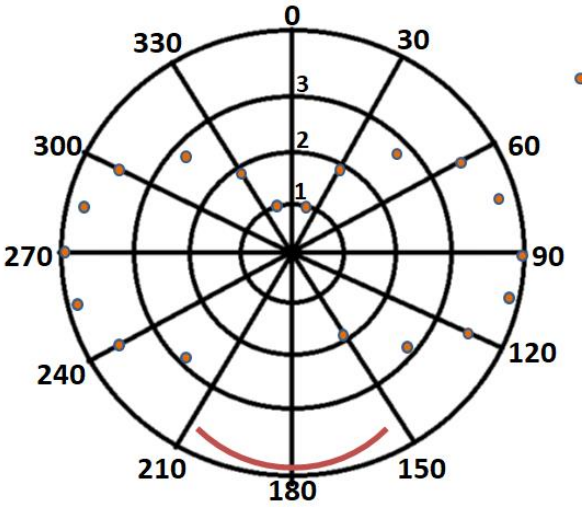

Fig.8: Polar diagram showing overall forward propulsion: Thrust coefficient (C_T) vs. apparent wind direction (assuming constant apparent wind speed). 2D C_{Lmax} = 4.2, C_{Dmax} = 0.075

The most important element in Energy Efficiency Design Index (EEDI) is the ratio between the lift and the drag coefficients. As shown before, NAYAM WINGS have very low drag-to-lift ratio:

$C_{Dmax} / C_{Lmax} = 0.075 / 4.2 = 0.018$

3. Heeling control vs forward propulsion

Calculating the forward propulsion while rolling and yawing the wing in order to reduce the heeling angle of the ship is quite complicated and is depended on 5 variables: Wing roll angle, wing yaw angle, apparent wind angle, wing's angle of attack, ship heeling angle.

In Fig.7, we can see the catamaran / ship heeling angle and the wing roll angle. In Fig.5 we can see the apparent wind angle.

The desired 3D angle of the wing is such that maintains the angle of attack (AOA) to the apparent wind (20°) that creates the highest lift force, position the wing in vertical angle to the wind, and limits the heeling angle of the ship's deck. This 3D angle is dependent on all 4 other variables mentioned above.

$$3D\ wing\ angle = f(\alpha, \beta, \gamma, \delta)$$

4. Wind Drift/heeling force, ship's drag and overall fuel consumption reduction

One of the most important influences on the overall fuel consumption is the water drag created on the ship's hull due to the drift force created on the wings (or any other wind propulsion system).

$$Drift\ force = Lift\ force \cdot \cos(\alpha) + drag \cdot \sin(\alpha)$$

As long as the apparent wind direction is bigger than 45° the wing's lift force contributes more to the efficient forward propulsion and less to the drift force. At the same time the wing's drag force contributes more to the drift force. The bigger the wing's drag-to-lift ratio, the bigger the water drag on the ship's hull and the higher the fuel consumption, Fig.5.

Calculating the influence of the wing's drift force on the ship's hull drag is complicated and made by CFD analysis.

In order to maintain cruising speed while enlarging the ship's drag, it is needed to enlarge the engine's power and consume more fuel.

Except for the rolling wing and yawing the mast there are no moving parts in NAYAM WING's system. Rolling the wing happens only when wind direction relative to vessel's sailing direction changes side (from star board to port side and vice versa) and that is slow motion. Besides there is constant adjustment of the wing's angle of attack to the wind and to the ship's heeling angle. These are small and slow motions. This makes the wings maintenance friendly.

The wing can be lowered in extreme wind conditions or entering harbours. First the wing levels itself and then the mast can be reduced telescopically lowering the wing to the desired height above deck.

Considerations for a Novel Augmented Reality Display on the Ship's Bridge

Stephan Procee, NHL Stenden University of Applied Science, Leeuwarden /The Netherlands,
stephan.procee @nhlstenden.com

Abstract

The use of a Head Mounted Display (HMD) for the Augmented Reality (AR) interface has practical issues. An alternative, Platform Mounted Display (PMD), might help the user to perceive the synthetic layer as overlay to the world, adapt to AR. The decision-making process is supported by an Ecological Interface. One aspect of the proposed AR interface visualizes targets and their associated conflict space in a novel rectangular scheme, the Velocity Obstacle Diagram. In a realistic scenario it is illustrated that the use of this VOD provides the user with potential solutions for the resolution of close quarter situations with multiple targets and a platform dependent escape potential as well.

1. Introduction

From a recent user test, *Procee et al. (2020)*, it became clear that the concept of Augmented Reality (AR), i.e. providing reliable directional information about the real-world features around the ship, is viable. The candidates, who were trained and tested in the use of AR in a realistic simulated environment, were all positive about the potential of this novel approach.

However, it also became clear that the involved hardware, a bi-ocular Head Mounted Display (HMD), has its user dependent issues. The test group, exclusively experienced professional navigators, not only varied in age and experience but also varied in their capability of their visual receptor system. This mainly affected their learning curve, i.e. adapting to the interface and wearing an HMD, but in some cases candidates were unable to focus on the displayed synthetic image and combine this with the world. Yet, these candidates do work with displays like RADAR and ECDIS apparently without a problem. Hence, an alternative is proposed for the display of the visual overlay, i.e. the AR Cocoon.

1.1 Sketch for a next step AR display in conventional bridge operation

There are many variations in how the physical layout of an AR display can be realized. They can be grouped in displays worn by the user, e.g. helmet- or head mounted displays, and displays mounted on the vehicle, e.g. head up display in the cockpit of an airplane or inside a car. The growing interest in AR in many fields of application results in an ongoing development of displays. Although for that reason the issue of hardware might seem irrelevant, testing an experimental interface design with real users in a realistic working environment needs an instance for visualizing AR. It cannot be disregarded that the chosen instance influences the experiment. The mentioned issue with combining the AR overlay with the world is an example. The limited movement over the bridge when wearing an HMD connected to fixed computing hardware is another example that influences an experiment.

Except for demanding environments like ice or harbors, berths and locks, the navigator usually works from a central position at the bridge. The contemporary bridge layout is T-shaped with one watch chair for the navigator and the other for the captain or pilot. Both positions are in reach of the conning console in the center and each have their RADAR/ARPA ECDIS display and associated controls.

Where it seems suitable to wear an HMD when moving over the bridge, e.g. to observe the situation from the bridge wing, the discomfort of wearing such a device for the full duration of the watch may be unacceptable. Therefore, an alternative is sought in a fixed head up display. This consists of one or more transparent monitors or windows in which the AR image is visualized. The vessel's attitude, heading heel and trim, is derived from a motion sensor and used to line up the artificial, i.e. AR, horizon providing an inside-out view of the world. These monitors are situated in front of and around the navigator's watch chair creating the AR-Cocoon.

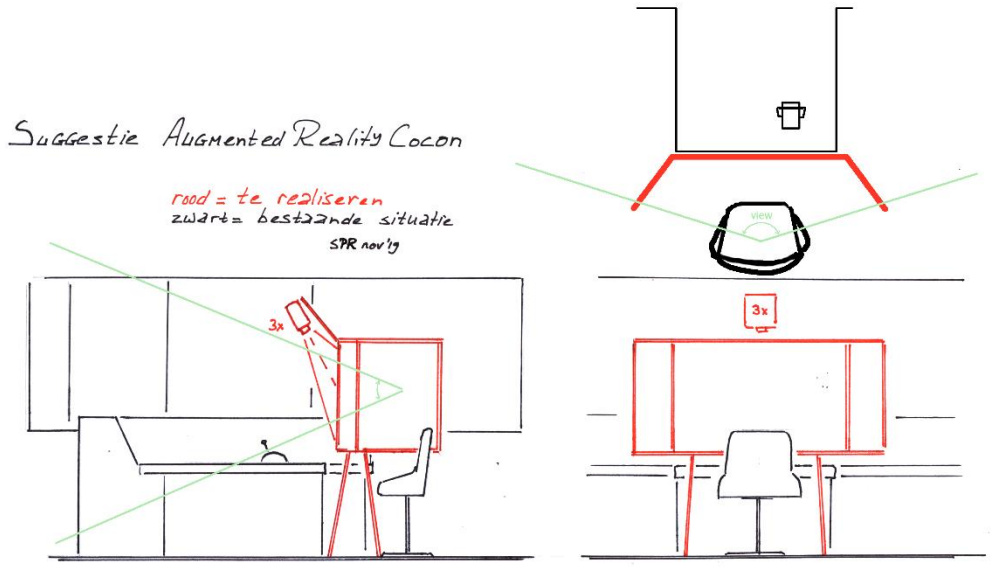

Fig.1: Suggested Configuration of the AR-Cocoon

The proposed idea for the next experiment using the AR-Cocoon is sketched in Fig.1. The sketch shows a single watch chair at the head of the T-shaped console. This configuration is driven by the dimension of the bridge simulator where the experiment will be held. The previous experiment showed that the relatively short distance to the simulator's monitors introduced artefacts like parallax errors. This sketched experimental configuration tries to mitigate these effects by locating the observer in the optical center, i.e. the physical origin of the circular sector where the simulator's monitors are mounted. Presumably, in a following realistic experiment, the cocoon will be constructed around each of the watch chairs of the bridge providing a shared information base for both workers.

It is not known whether the use of a conventional RADAR/ARPA ECDIS display (panels) in conjunction with an AR overlay is advantageous over the potential of displaying these panels as part of the AR interface. It can also be hypothesized that the conventional layout of these panels will evolve in time to a layout suited for both perspective and orthogonal hybrid presentation in AR. Synthesizing the hardware controls of the vessel, e.g. rudder and telegraph, is considered outside the scope of the AR interface design.

Hardware suitable for use as cocoon window varies. Transparent monitors of sufficient dimension, e.g. 55 inch, using OLED technique are currently available. OLED technique offers synthetic imaging without the need for back light. Alternatively, a construction can be made using a semi-transparent foil at which an image is projected through a projector. Different foils, each with their unique opaqueness, can be used as a trade-off between transparency and the displayed brightness in order to adapt to the environmental luminescence. A third alternative is to use the reflected image of a rear located monitor in a glass surface in front of the observer (info Kjetil Nordby).

All three options provide an image that needs to be aligned with the world. Therefore, the image must be corrected for the movement of the vessel in the first place. The position in 3D space of the observer must also be monitored in order to correct for misalignment. These requirements are, however, not different from the requirement when AR in an HMD is used and can be realized with a tracker device for the observer's head and a ship's motion sensor.

2. Sailing safely in the Solution Space, Velocity Obstacles revised.

2.1 Ecological Interface and MNARS

There is a general understanding that a worker uses a mental model as basis for decision making. The quality of this mental model depends on a number of factors like experience, but also the effort that

can be, or has been, spent on it. Besides that, the mental model can be too limited for decision making in a complex situation, or it lacks meaningful information. In the latter case a human-machine interface can be used to provide this information for the worker to improve her mental model. *Flach and Bennet (2011)*, page 25, a.o. argue that the meaningfulness of information is not created in the mind of the worker but discovered by the mind of the worker. *Rasmussen (1983)* and *Flach et al. (1998)* argued that the solution for a problem or situation that is new to the worker requires analytic and creative skills, also known as problem solving skills.

From this it can be inferred that an interface needs to reflect the affordance, or limitations, of the environment, i.e. the ecology, and be rich in cues in order to support analysis of the situation and the refinement of the worker's mental model. It should also provide the worker with timely feedback on the effect of her actions. Augmented Reality as information layer 'on' the world is inherently visually linked to the environment. Enriching the AR layer with the ship's mission, i.e. the intended track, its limits and the safety margin to a nearby danger, contributes to the worker's awareness of her affordance. In addition, cues referring to progress, i.e. course and speed, ground and water track, rate of turn, propulsion and steering provide the worker with a second element of affordance. Thirdly, cues related to the position of targets and objects, their speed and dimension of their protected zone as well as the dimension of the worker's own ship's protected zone complete the ecological interface.

2.2 decision making

RADAR/ARPA and ECDIS in combination with visual observations are conventionally the sources of information for the navigator to build a mental picture of her situation in the world. However, this simplified ideal picture suggests that she is isolated from all other processes that take place on the bridge, and that she has only one task at hand at the time. *Procee et al. (2017)* analyzed the tasks of the watch keeper and visualized the work domain showing that the navigator has to work with many constraints in varying intensities depending among others on location, type of vessel, weather and traffic. This means that the plethora of signals have to be scanned constantly and prioritized in order to select meaningful information from it. A visualization of an information processing model of decision making is shown in Fig.2.

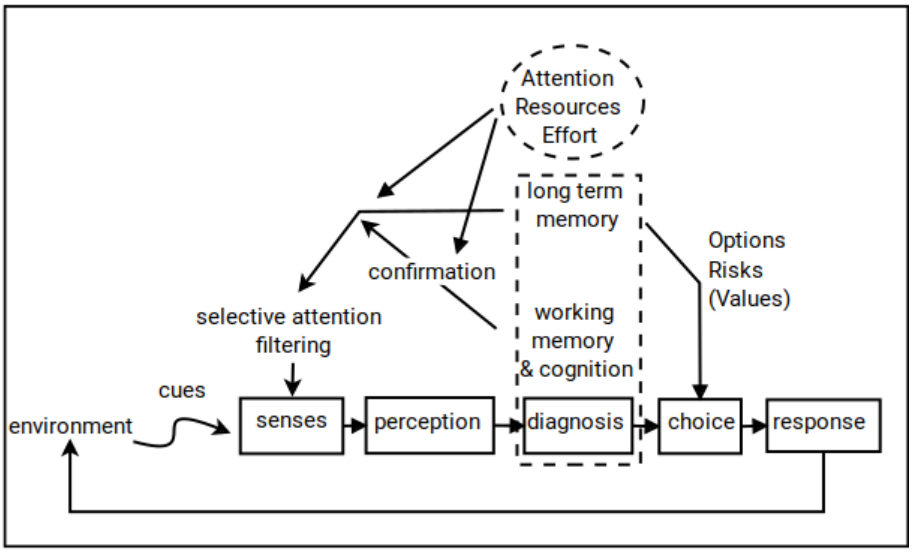

Fig.2: Information processing model of decision making (adapted from *Wickens and Holland (2000)*

The model shows that cues from the environment have to be selected and processed to meaningful information, i.e. the front-end of decision making, leading to a response selection and execution, i.e. the back end of decision making. The feedback loop points to the iterative nature of decision making, i.e. the effect of a response can be used for diagnosis testing and refining and can be used to build decision making skills. The model also shows that the, mostly front-end, processes involved in

decision making, require resources. The consequence is that a trade-off between effort and the chosen diagnostic strategy can be expected.

An information processing model of decision making helps in understanding the need for certain types of information in relation to interface design. It can be inferred, among others, that a high quality and direct feedback will enhance the quality of decision making. But also, e.g., will a relatively low-effort attention filtering help in freeing the limited resources that can in turn be paid to the diagnostics process possibly leading to a higher frequency confirmation loop or more exploitation of the long-term memory.

The MNARS-2 prototype interface design, *Procee et al. (2018)*, aims at providing cues that help the navigator in her decision-making process. Augmented Reality is used to immerse the navigator in her environment, that is, providing cues in a visual synthetic overlay *on* the world rather than distract the navigator with different and simplified or generalized constructs *of* the world like RADAR/ARPA and ECDIS.

2.3 Motivation for a Velocity Obstacles Diagram

An often phrased and stereotypical task of the navigator is to keep safe navigation. Although the term safe seems to comprise a rather obvious meaning. When a definition is needed, e.g. to derive design criteria for a process description, it turns out that the term safe is only vaguely defined or might even be unmeasurable, *Hollnagel (2014)*. For this reason, working procedures, guidelines and rules of the road among others aiming to support safe navigation, are deliberately kept vague, i.e. not instructional specific, leaving the decision to the navigator. Therefore, an information system aiming at safety that provides the navigator with a solution might not easily be foreseen, hence, a more realistic expectation might be that enhancing safety by expert support can be found in a review of interface design. That is, develop an interface that supports the navigator better in her decision-making process than the existing interfaces do.

The Protected Zone (PZ) is a safety enhancing measure that was already standard in aviation. For shipping it was introduced by *Degré and Lefèbre (1981)*. Although a formal approach of such a zone is, to the authors knowledge, not part of curricula or fleet operation manuals, the existence of and an appreciation of its dimension is intuitively in the mind of the navigator. This can be part of the long-term memory, Fig.2, but might also be part of the private or shared values of the ship's navigators.

Taking the suggested use of a PZ for safe navigation as a start-point, we might be tempted to visualize this zone as a video overlay in the AR interface. However, this will not be of much help to the navigator because the notion of entering someone's PZ doesn't solve the problem what to do about it.

More effective is to visualize the prediction of the PZ in time and derive a conflict zone from that. The conflict zone can be seen as the area in which one ultimately enters the PZ of the other. Hence, all space outside the conflict zone can be seen as Solution Space. Visualizing the predicted conflict space is also known as Velocity Obstacles, its principle working is covered in numerous papers starting with *Degré and Lefèbre (1981)*.

In their contribution on the perception of layout and knowing distances, *Cutting and Vishton (1995)*, pp.69-117, found that the effectiveness of depth cues decreases with increasing distance except for Interposition and Aerial perspective. Of these two cues, only Interposition, also referred to as occlusion, was found to have a relative strong effect and seemed independent of distance. The effectiveness of aerial perspective, though weaker than Interposition, was found to increase with distance but diminishes again and drops below the assumed utility threshold towards the horizon. From this it can be concluded that human observers at sea, where there's a lack of objects that can provide the Interposition cue, are not good at discriminating distances in the far field. Moreover, the perspective projection of a (2D) velocity obstacle in an AR overlay is not effective because its synthetic representation lacks any depth cue. To overcome this problem the Velocity Obstacles

Diagram (VOD) is introduced. In this diagram both the target's position and its PZ and associated conflict zone is projected in rectangular space as well as the predicted position of the own ship. From this it becomes immediately clear to the navigator whether her present course and speed will lead to intrusion in the target's PZ or that the target will intrude in her PZ. It also immediately shows alternative combinations of course and speed that will avoid the conflict zone, i.e. it shows the Solution Space.

A relatively simple encounter, e.g. one conflicting target in open sea, is not illustrative for the power of this novel approach. Encountering multiple conflicting targets in a limited sea space, however, will be far more demanding to the human navigator. The following example of an ordinary traffic situation consisting of only three ships in open sea demonstrates the effectiveness of using the VOD.

3. Example of a traffic situations

3.1. Situation

Fig.3 shows a situation in the southern North Sea where the Own Ship (OS) sails on a north easterly course with a speed of 12 knots. From the west target-A is approaching, sailing 14 knots on an easterly course. From the north, target-B approaches on a south westerly course, sailing 10 knots. The respective tracks are depicted in the figure as black lines and the positions are shown at six-minutes intervals. Each vessel has required a PZ of one mile in diameter, shown in Grey. Outside territorial waters the Collision Regulations 1972 apply, all three vessels are underway and show no special status, like restricted maneuverability. About time t=18', target-A is predicted to pass OS at the stern at a critically small distance (CPA).

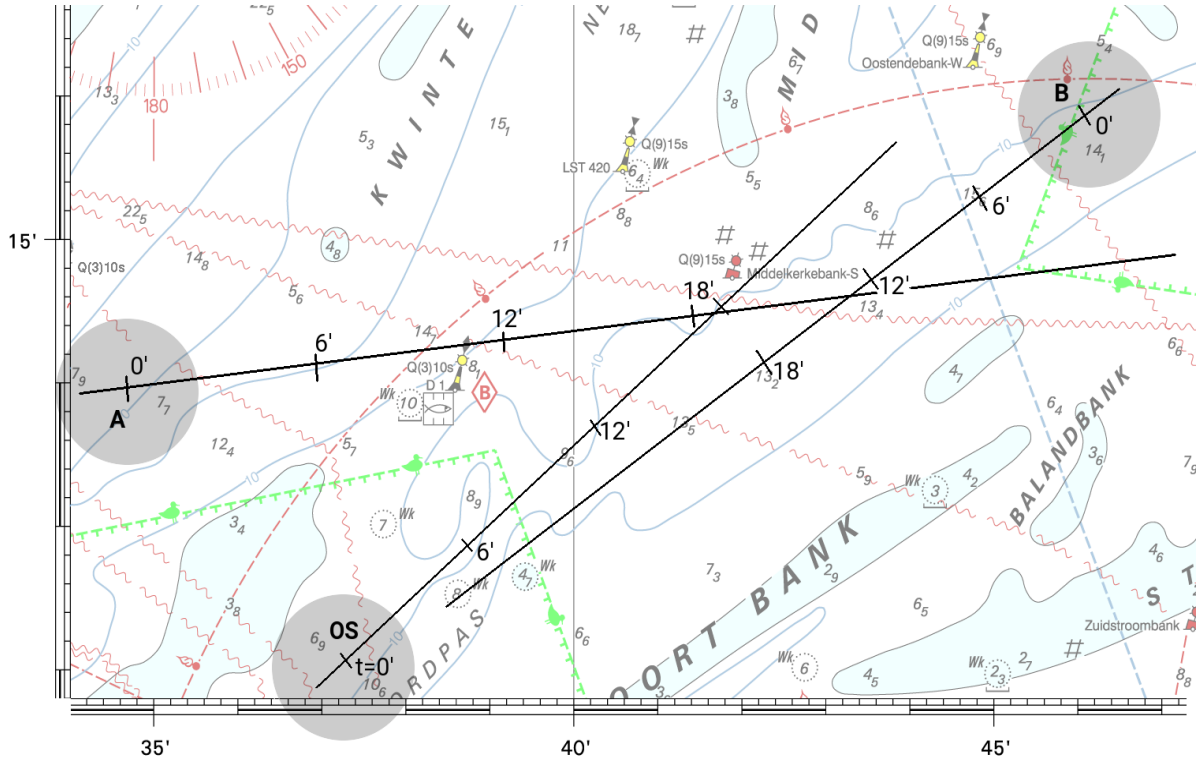

Fig.3: Traffic Situation in the Southern North Sea

Based on the rules, target-A is the give way vessel and OS is required to keep course and speed as the stand-on vessel. The rules apply straight forward for two ships in this situation. The encounter of OS with target-B, however, is not clearly defined in the rules. The encounter might be regarded a head-on situation, requiring both vessels to change course to starboard, it might as well be regarded safe passing at an uncritical CPA, which leaves both OS and target-B unengaged with each other. Target-

B, however, might regard target-A as a vessel crossing at a critical CPA. Meaning that for these two vessels target-B is the give way vessel, leaving target-A the stand-on vessel, i.e. obliged to keep its course and speed.

The seabed complicates the situation even further. The nautical chart illustrating the traffic situation shows shallow areas that can be regarded as No-Go zones depending on the draught of the respective vessels. The charted buoys mark the limitations of these shallows and are also to be passed at a safe distance. The situation in this example does not take wind and tidal stream into consideration. The effect of these is that a ship will sail at a correcting off-set course in order to stay on its intended track, which is perceived by surrounding traffic as a direction different from the track it appears to sail.

From the perspective of the OS the situation is not at all clear. The engagement with target-A requires OS to keep course and speed and wait for A to act, engagement with target-B is not clearly defined, the solution however would be to change course to starboard to mitigate the CPA. This results however in a bow crossing situation with B and a closer encounter with the shoals located eastwards. From the perspective of target-A, the encounter with OS is at a critically small CPA, changing course to starboard is not possible due to shoals southward of its position and changing course to port gives a complication with target-B that in its turn might want to change course to starboard in order to increase its CPA with target-A. The perspective of target-B is equally complicated, changing course to starboard in order to give way to target-A is limited due to shoals located northward of its position and also will it result in bow crossing with OS. Changing course to port, however, is limited due to shoals located southward.

From this, the navigator of OS might conclude that keeping course and speed and waiting for the situation to resolve is not the best alternative. She might also reason that, given the traffic situation and the natural limitations, target-A might not be able to resolve the situation and avoid a collision, by its own, and decides that she wants to take action. What will be her options, and how will these options be visualized in the VOD?

3.2. Visualizing Solution Space and predicted target trajectory in a rectangular frame

The egocentric view of the navigator can be based on two relevant dimensions in 2D space, bearing and distance. The third dimension, height or depth, conventionally reflects in projected, i.e. charted, contourlines (depth) or obstructions (height) and is not shown in the VOD as a separate dimension.

Distance is omnidirectional and relative to the OS, expressed in nautical miles starting from zero at the OS position. Bearing has also its origin at the OS's position and is expressed in degrees relative to the OS's ground vector (COG), starting with zero at COG and ranging 180° on either side. This reflects in the inside-out display of the VOD, Fig.4. The direction of the bow, referred to as heading, and the direction of the ground vector (COG) can be different due to wind drift and current. These two angles are usually known by the navigator and are used to correct the vessel's heading in order to keep the intended track. The MNARS interface displays and visualizes both heading and COG.

The OS's Protected Zone, which in this example is defined as a circular area of one nautical mile in diameter, projects as a rectangle, because its range is half a mile in any direction. It is shown in Fig.4 by the blue tinted area. At a specific moment in time, t0, the position of target-A relative to OS is expressed in a bearing, about 90° on the port side, and a distance, about 2.2 nm. The target's ground vector, COG and speed, are received trough AIS and are used in combination with OS's ground vector to project the trajectory of target-A in time relative to OS. This is shown in Figure 4 as a black curve with ticks at six minutes interval. For the situation in this example it can be seen that target-A will intrude in the OS's PZ about 15 minutes later than t0. This also shows the closest point of approach is about 0.2 nm from the OS and will happen about 18 minutes after t0. The latter is usually referred to as Time-CPA (TCPA). The predicted trajectory of target-B in the given example is also shown. From this it can be concluded that OS and target-B will pass at about 0.5 nm. distance about 18 minutes after t0. Target-B will not intrude in the OS's PZ. In both cases, the shape of the predicted trajectory

shows that the targets will cross at the stern of OS. A bow crossing would result in decreasing relative bearings, and an unchanged bearing points to collision danger.

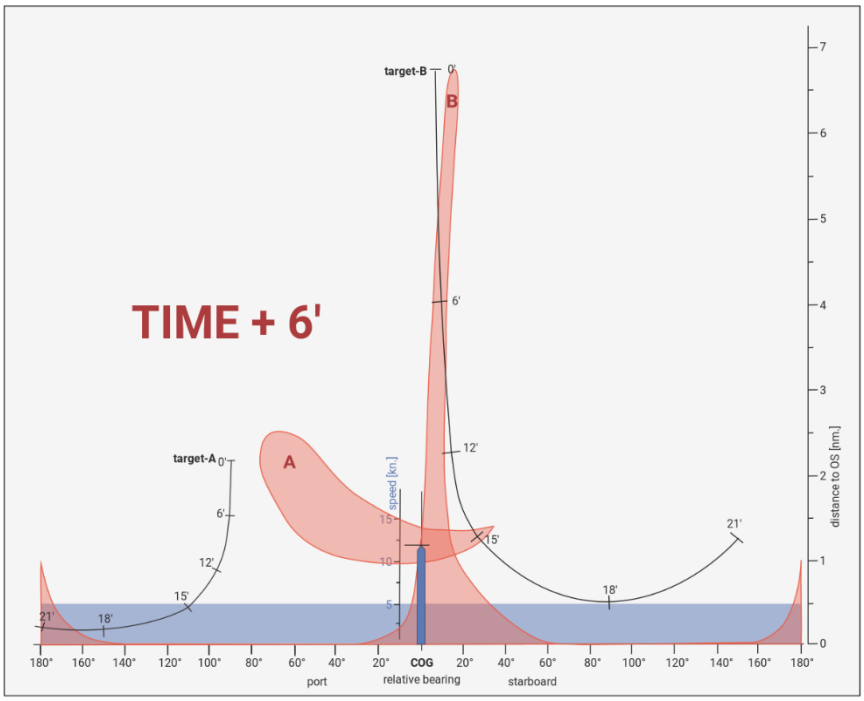

Fig.4: Velocity Obstacles Diagram for time zero plus six minutes

The position of the Conflict Zone of target-A predicted 6 minutes ahead in time is visualized by the brownish colored polygon containing the letter A. The area of it represents all combinations of OS's course and speed, i.e. all ground vectors, that will result in an intrusion in the PZ of target-A. The predicted position of target-B's Conflict Zone is also shown. The predicted position of OS is shown by the dark blue vertical bar. From this it can be seen that 6 minutes from now (t0) OS's ground vector points to a position inside the Conflict Zone of target-A and to the border of the Conflict Zone of target-B. From this it can be concluded that when OS wants to resolve the future conflict on he own, she has either the choice to keep the speed constant and at the same time change course to port side at least 55°, or to starboard for about 30° or more. Another possibility is to keep the course constant and accelerate to at least 14 knots. Slowing down, however, will not resolve imminent intrusion in target-B's PZ because the respective tracks, Fig.3, are not parallel. Hence, OS's Solution Space is found in the combinations of course and speed that are not covered by target-A and -B's respective Conflict zones. It will be possible, although not shown here, to visualize the maneuvering freedom, or envelope, of OS in the VOD, e.g. by a box representing the maximum speed and maximum course change to either side.

Instead of taking immediate action, OS might reason that the TCPA is still sufficient to wait for target-A's compulsory reaction to solve the imminent conflict between OS and A, and also to wait for target-B's reaction who might react to target-A. In that case OS's navigator can use a prediction further in time. This is illustrated in Fig.5.

Fig.5 shows that the Solution Space has decreased when OS postpones action for six minutes. The position of the predicted Conflict Zones changed, and their horizontal dimension became wider. OS's navigator can still choose to resolve the situation, hence, based on the time6' plus 6minutes prediction she analyzes that resolution can be found in an acceleration to 15 knots or a course change of either 55° to port or 42° to starboard. Reduction in speed will result in an intrusion in target-B's PZ.

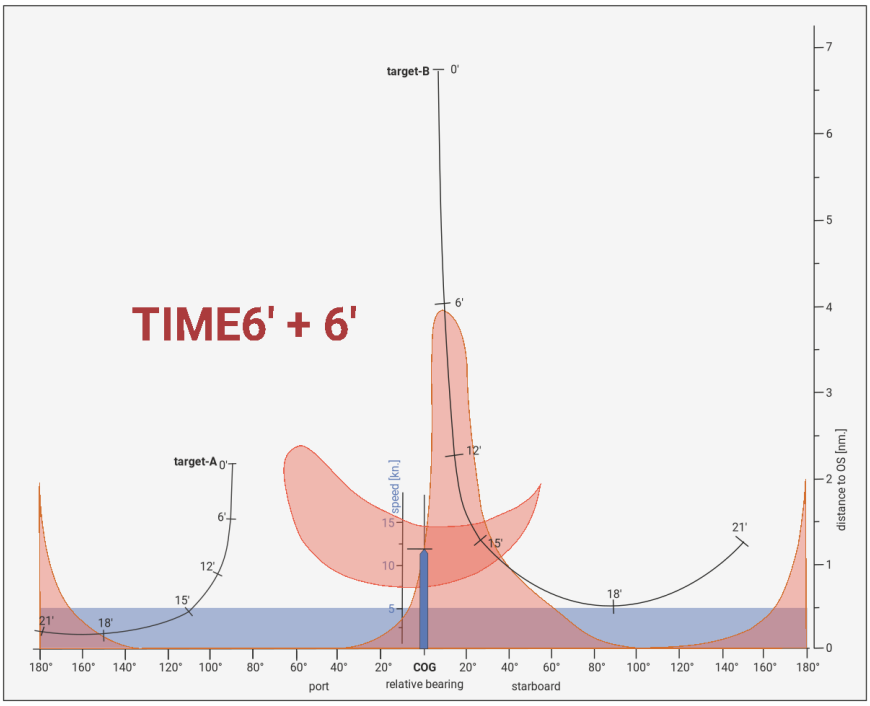

Fig.5: Velocity Obstacles Diagram for time 6 minutes plus six minutes

Again, suppose OS's navigator might want to wait another 6 minutes for target-A to act. She analyses from Fig.5 that in 12 minutes time her Solution Space has decreased further to a course change either 55° to starboard or 35° to port or an acceleration to at least 15 knots. However, the predicted trajectory of target-A shows that in 12 minutes time (t12) the proximity will be less than a mile, and intrusion into OS's PZ is imminent, i.e. within three minutes from t12.

Apart from that, the necessary action must not only be part of the maneuvering envelope, it should also result in the required course change or acceleration within the time left. The latter depends on the maneuverability of the ship.

3.3 Showing Escape Potential

A standard for the exchange of maneuvering information is the Pilot Card, compulsory for all ships under SOLAS 1974 requirements (IMO's Resolution A.601(15) 1987). This information comprises among othres the dimension of turning circles at full rudder, emergency manoeuvres, and stopping and accelerating characteristics. Although more refined modeling is preferable, the basic information from the Pilot Card can be used to predict the turn rate as function of time when hard rudder is applied. From this the ship's Escape Potential is derived in terms of maximum course change during the minimal time left before intrusion in the target's PZ.

For the given example, Fig.6, the point of the predicted trajectory at t12 is 0.9 nm. distant from the base, i.e. from OS, the PZ of target-A has radius 0.5 nm. and from these it can be inferred that at t15 OS will intrude the PZ of A, this leaves three minutes to manoeuvre. If e.g. the Pilot Card states that in three minutes time the ship is able to perform a 50° course change to either side, then this will be shown by the green horizontal bar, Fig.6. And when the acceleration performance shows that in three minutes time the speed has increased from 12 kn. to 14 kn., and the deceleration curve, i.e. giving full astern, shows that speed is decreased from 12 kn. to 4 kn., this is shown by a vertical green bar. Providing the navigator with this Escape Potential, or affordance, it becomes immediately clear that a measure in speed will not resolve the emerging conflict with either one of the targets, nor will a course change to starboard resolve it. Changing course to port by giving hard rudder has the biggest chance to avoid intrusion in target-A's PZ. Although the Solution Space for target-B can be reached

with a less drastic manoeuvre, the conflict is only solved when both targets stay out of OS's PZ and OS intrudes in their respective PZ's neither.

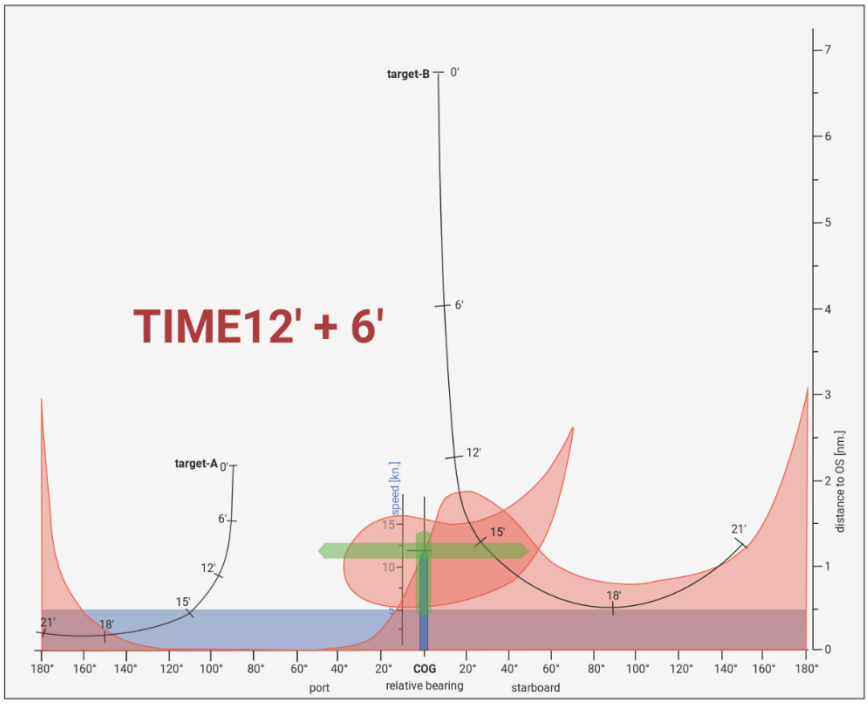

Fig.6: Velocity Obstacles Diagram for time 12 minutes plus six minutes

Visualizing the Escape Potential must be seen as a last line of defense. Not incorporated in this model is e.g. the potential action of target-A who might change course to starboard at the last possible moment, which ultimately results in a head on close quarters situation of OS and A. More research is needed to define when and how this Escape Potential should be shown to the navigator in order to avoid misconceived suggestions how to act in a critical situation. It can further be argued that in the first place an interface should support the avoidance of such critical situations in order to be effective for safe navigation.

4. Conclusion

The introduction of new hardware and interfaces involves functional, ergonomic and physical aspects. User acceptance is likely to depend all aspects. Practical watch keeping involves being in a static position, a watch chair, for most of the time. Therefore, wearing a head mounted display during watch has unarguable not the support of navigators. Functional and physical problems with the adaption to observing the world and an augmented overlay in a HMD adds to that lack of support. A vehicle mounted display, like the AR-Cocoon, is an alternative solution that might overcome the mentioned problems. Further research on this is needed and planned at the Academy Willem Barentsz Terschelling part of the NHL-Stenden University of Applied Science.

The Velocity Obstacles Diagram is an adaption of the orthogonal visualization of Velocity Obstacles suited for use in an AR interface. Refinement and enriching with relevant variables are ongoing. Extending the VOD with a visualization of the escape potential seems to suit the Ecological character of the interface. Providing the user with possibilities for evading action within the envelope of maneuverability of the ship is a novel approach. Further experiments are needed to understand the effectiveness of the current interface design and its implications with the Collision Regulations.

References

BENNETT, K.B.; FLACH, J.M. (2011), *Display and Interface Design*, CRC Press

CUTTING, J.E.; VISHTON, P.M. (1995), *Perception of space and motion,* Academic Press

DEGRE T.; LEFEVRE, X. (2012), *A Collision Avoidance System*, J. Navigation 34(2), pp.294-302

FLACH, J.M.; VICENTE, K.J.; TANABE, F.; MONTA, K.; RASMUSSEN, J. (1998), *An Ecological Approach to Interface Design*, Human Factors and Ergonomics Society 42nd Annual Meeting

HOLLNAGEL, E. (2014), *Safety-I and Safety-II*, CRC Press

PROCEE, S.; BORST, C.; PAASSEN, R.v.; MULDER, M. (2017), *Toward Functional Augmented Reality in Marine Navigation: A Cognitive Work Analysis*, 16th Int. Conf. Computer and IT Applications in the Maritime Industries (COMPIT), Cardiff

PROCEE, S.; BORST, C.; PAASSEN, R.v.; MULDER, M. (2018), *Using Augmented Reality to Improve Collision Avoidance and Resolution,* 17th Int. Conf. Computer and IT Applications in the Maritime Industries (COMPIT), Pavone, pp.298-312

PROCEE, S.; BORST, C.; PAASSEN, R.v.; MULDER, M. (2020), *Measuring the Effect of Augmented Reality on Situational Awareness,* 19th Int. Conf. Computer and IT Applications in the Maritime Industries (COMPIT), Pontignano, pp.292-304

RASMUSSEN, J. (1983), *Skills, rules, and knowledge; signals, signs, and symbols, and other distinctions in human performance models*, IEEE Trans. on Systems, Man, and Cybernetics, SMC-13(3)

WICKENS, C.D.; HOLLANDS, J.G. (2000), *Engineering Psychology and Human Performance*, Psychology Press

Intelligent Industrial Internet of Things & Services (IIIoT&S): An Innovative, Plug & Play, High-ROI Approach for The Extended Enterprise

Nick Danese, SYRRKLE, Antibes/France, nd@syrrkle.com
Alexander Vannas, ALLEANTIA, Pisa/Italy, alexander.vannas@alleantia.com

Abstract

Electronics are the undisputed backbone and are becoming the DNA of data and information collecting, sharing and processing. IIIoT&S is a fundamental, yet intangible component of "everything", the "everything connected" Industry 4.0 chart being one corollary. The innovative plug & play strategy discussed hereafter underpins the necessary consumer-oriented implementation required to fulfil the 4.0 mandate – digital twin, monitored /controlled / assisted / autonomous ships – and effortlessly prepares the field for the 5.0 effort – full monitoring & control. Importantly, the Unique Business Values of the plug & play strategy reviewed herein benefit the industry overall: design, construction, repair, maintenance, operation refit, commercial and Navy.

1. Introduction

From a mechanical standpoint, HIPERformance is inherently reliant on the performance of all components of a given system. The fastest hull will not make speed if propulsion components are not performing as intended in the various conditions, they are meant to deliver the prescribed power in and if ship resistance is not quantified, all of that as accurately and exactly as possible.

Manufacturing of the ship, a moving object, must be executed "to a T" down to its smallest component if it is to stand a chance of delivering the prescribed performance. And, once afloat and loaded, it must operate as a perfectly tuned orchestra led by the Captain. The human's role is to make decisions supported by automation, decision which are to ensure the success of automation itself in achieving the required performance. It goes without saying that neither automation nor Captain can do much without accuracy and precision in both the monitoring and control of devices.

IIoT is the solution of the problem from the root up proposed by Industry 4.0. IIoT is more present in other industries than ours: it is once again time to be inspired, forward looking and implement proven technologies. This paper explores the Industry 4.0-type solution offered by Alleantia, Italy, in its ground-breaking approach to supplying a ubiquitous IIoT solution and how this already provides a bridge to Industry 5.0.

2. It all started with electricity

Exploitation of electricity at the industrial level started in earnest at some point during the last quarter of the XIX Century. At that time, humanity crossed a no-way-back threshold and, with no idea of what was awaiting, pushed the fast-forward button on the technological evolution console. As is custom, large industrial conglomerates gobbled up the commercial opportunity and, save for the stifled genial bursts of a few visionaries, electricity and all its consequences were soon corralled by Big Business - in fairness, the financial burden of development could not have been supported by any lesser players. Consumerism and Military became the inexhaustible source of innovation fuel and today, hardly one hundred years later, video is streamed from Mars (well, just about).

In this paper we will explore how, in the age of GAFAM's electronic dominance, a small start-up has become the Gartner-acclaimed 'Erquy' of the electronics industry. (Erquy, the Gallic village that the Romans never managed to conquer as the resident Druid concocted a magic potion making who drank it infinitely strong, from the Asterix The Gallois & Obelix novels by René Goscinny and Albert Uderzo.)

3. Significant industry milestones

The defining traits of the various industrial revolutions have become common-speak since Industry 4.0 was given a Hollywoodian status, but some subtle consideration deserve being made in light of the entwined nature of technological advance and its effects on social weave.

Fig.1: Erquy, the fictional village of Asterix and Obelix

3.1 Industry 2.0

The second industrial revolution is identified with the industrial use of electricity to create mass production. In more ways than one this was the start of modern capitalism. From a technological standpoint, the defining threshold is that of the advent of truly portable energy. Gas was already portable and widely used, but required a significant infrastructure compared to that sufficient for electricity. The ability to move energy to the location where power is required transformed not only industrial production but also, and profoundly so, society. For example, the appearance of electrical lights made it possible to consume goods and services later into the day, in places without natural light, etc. (Alessandro Volta built the first battery in 1800, in 1882 the Edison Electric Illuminating Company brought electric light to parts of Manhattan but only in 1925 did half of all urban homes in the U.S. have electric power. The first electric refrigerator to be commercialized was Red Wolf's DOMestic ELectric Refrigerator in 1913.) Soon after that, the appearance of refrigeration created choice in the consumption of food and other perishable goods. This profound social transformation sealed the immortality of consumerisms and the exponential growth of waste. Consumerism and waste became at this point symbiotic and will reach critical mass at the time of Industry 4.0.

3.2 Industry 3.0

Industry 3.0 was sort of a hybrid stage, during which miniaturization revolutionized the use of electricity thereby allowing somewhat reliable communications and, as a corollary, automation. (It is worth to indulge in a bit of semantics: the Greek ‘auto’ prefix means ‘self’ but the modern word ‘automation’ indicates a "machine which performs a range of functions according to a predetermined set of coded instructions" – The Oxford Dictionary. Therefore, it is perhaps when Artificial Intelligence will be applied in a truly autonomous fashion, one that includes learning and creativity, that ‘auto’ will be used correctly.) Communications, intended as the transmission of electrical (or other energy) signals, has existed since radio was invented, but the very nature of radio would preclude the support of automation until the quantum leaps in signal technology that took place over a century later. Development in communications lagged behind miniaturization for a while but was eventually slowed down for a while by the lesser progress of mechanical machines' performance.

A point of interest during this time was the eventual compounding of advances in technology, miniaturization included, and communications. But a perhaps less-"industrial" factor also played a role in feeding that compounding: object-oriented programming (OOP), first "invented" at MIT in the late 1950s. It is easy to make a parallel between OOP and the Ensemble Theory fathered by Ludwig Boltzmann in 1871, who did not see the appearance of the first OOP language, SIMULA, in 1963. By the way, Artificial Intelligence as we know it today dates back to 1956. (On a historical note, the idea of inanimate objects coming to life as intelligent beings has been around for a long time. The ancient Greeks had myths about robots, and Chinese and Egyptian engineers built automatons. The beginnings of modern AI can be traced to classical philosophers' attempts to describe human thinking as a symbolic system – 'A Brief History of Artificial Intelligence', Tanya Lewis, Live Science, December 04, https://www.livescience.com/49007-history-of-artificial-intelligence.html)

In the end, changes in technology started being driven by very new, ground-breaking evolution in human thought and in how humans thought of the world around them.

The closing stages of Industry 3.0 saw, ironically, a somewhat contradictory situation where the acceleration in the development of ever more powerful computers coupled with the need to be first to market caused inefficiencies and performance losses. Perhaps not a truly-scientifically proven example, but many may recall the 15 floppy disc installation set of a well-known word processor becoming a crammed 600Mb CD one version to the next and not working as well as its predecessor.

And, not an inefficiency but an inescapable performance damper, heat generation became the nemesis of miniaturization, electronics and communications.

Fig.2: IIoT is used in non-marine industries in true Industry 4.0 fashion

3.3 Industry 4.0

Vaibhav Rajkarne notes what Industry 4.0 should be: "The fourth era of industry is the era of Cyber Physical Systems (CPS). CPS comprises of smart machines, storage systems and production facilities capable of autonomously exchange information, triggering actions and control each other independently. This exchange of information is done by the Industrial Internet of things (IIOT) in which thousands of sensors work real time and transfer the data to a local server or a cloud server. Here the analysis of the data is carried out by developing predictive models . . . Predictive Maintenance . . . This data is very huge and termed as Big Data. The data analysis helps the industries not only to maintain the processes but also to improve manufacturing processes, material usage, supply chain and life cycle management of the product", www.quora.com/What-is-the-main-difference-between-Industry-3-0-and-Industry-4-0. The absence of humans is prominent in his take.

Perhaps a little cynically, this author will argue that of the above we have today a lot of official Big Data (on the unofficial front, ever wander how privacy-violating, pre-digital recordings of telephone conversations from the 1980s resurface from time to time?), a lot of cloud computing (favouring Advertising Big Brother with Priority 1), and a lot of military high-tech (some of which admittedly derived from the commercial world). Still a little cynically, perhaps, one might say that Industry 4.0 has not quite yet fulfilled the promise of smart machines, storage systems and production facilities capable of autonomously exchange information, triggering actions and control each other independently. If

some factories and machines are becoming smarter as time goes, most remain in a barely Industry 3.0 state, if not even less developed.

This is due to many factors, one being the longevity of many machines that were designed and built to last, the cost of replacing them, a very scarce communication infrastructure in the industrial sector (incredible but true), the absence of adequate IT infrastructure at the local level and, the inevitable party spoiler, the human factor.

Another factor that deserves singling out is the attempt by large companies to achieve industrial domination by providing totally closed, monolithic systems aimed at forcing the user of their technology to remain umbilically connected to that one supplier. Not only is this uneconomical, but it actually damages the end-user by limiting or even forbidding the possibility of extending the reach of the installed Industry 4.0 ecosystem: that is the big contradiction, one may rightfully use a much stronger word, in the antinomic marketing and sales of locked, non-communicative, non-extensible "Industry 4.0" systems.

Before moving on it is relevant to mention what Industry 5.0 is deemed to be. As Master Control puts it, https://www.mastercontrol.com/gxp-lifeline/3-things-you-need-to-know-about-industry-5.0/: "The term Industry 5.0 refers to people working alongside robots and smart machines. It's about robots helping humans work better and faster by leveraging advanced technologies like the Internet of Things (IoT) and big data. It adds a personal human touch to the Industry 4.0 pillars of automation and efficiency."

It is in the in this time of the ‘Song of Heat and Deceit’ that our story begins.

4 CERN's Large Hadron Collider

From the CERN website: "The Large Hadron Collider consists of a 27-kilometre ring of superconducting magnets with a number of accelerating structures to boost the energy of the particles along the way. Thousands of magnets of different varieties and sizes are used to direct the beams around the accelerator, including 1232 dipole magnets 15 m in length which bend the beams, and 392 quadrupole magnets, each 5-7 m long, which focus the beams. Just prior to collision, another type of magnet is used to "squeeze" the particles closer together to increase the chances of collisions. The particles are so tiny that the task of making them collide is akin to firing two needles 10 km apart with such precision that they meet halfway."

Fig.3: The Large Hadron Collider

It does not take much to imagine who much heat is generated during operation and how critical it is to dissipate it exactly as required. The team tasked with developing and installing the system to monitor

and control heat dissipation included Stefano Linari, a nuclear physics student at the University of Pisa working on his thesis. His job was to make sure the compact solenoid accelerators stayed at the prescribed temperature. Lack of previous programming experience was quickly overcome in order to deal with the embryonic web-type applications used at CERN and to develop the monitoring & control system that would manage the 15000 t, 12 m diameter, 30 m long auxiliary systems for particle acceleration. The cooling systems were operated under Programmable Logic Controllers (PLC). (A Programmable Logic Controller (PLC) is an industrial computer control system that continuously monitors the state of input devices (sensors) and makes decisions based upon a custom program to control the state of output devices (the machine). Crucially, PLCs include process fault diagnosis.) From an IT standpoint PLCs can be considered rather rudimentary but they have the crucial advantage of being robust and remain a very common way of controlling machines.

The "web" in web-applications hardly exceeded using HTML formatted files. (The work at CERN's LHC started in 2008 and eventually resulted in the observation of Higg's Boson in 2012.) It is hard to believe what CERN achieved with relatively limited technology, but mankind is not foreign to such exploits. In terms of achievement, the pre-IIoT world of the Large Hadron Collider is probably comparable to the quasi-IT-free Apollo missions to the moon.

Fig.4: Money: a good reason to adapt IIoT

5. From Fermilab to controlling the water supply of the city of Arezzo

A stint at the Fermilab reinforced a feeling that the world of PLCs and other forms of siloed drivers could be improved. The difficulty of dealing with segregated technology is very evident in ships, where bridges are overcrowded with proprietary displays and control centres crammed into ever too small consoles. Admittedly, system integration has made giant steps in recent years, but in parallel major vendors continue to tighten their grip and there is hardly any hardware interchangeability even in purported integrated systems.

The step to SCADA (Supervisory Control And Data Acquisition) was short but a new approach was required, and it was made possible by the by now ubiquitous internet.

The move to true innovation started here, with the use of the internet to apply the SCADA paradigm. At this time, though, each monitoring & control software remained under its own umbrella, the same yoke as before. The following technologically ground-breaking initiative was to imagine a set-up where one would communicate with the various PLCs and other drivers via a web-based graphical interface and using higher-level software applications resting, amongst other elements, on the results of Big Data analysis.

This prompted the development of the connectivity required to centralize, one could say integrate, just about every device on the market. Some were easy, for example PLCs, others less so, for example proprietary systems allowing little or no access. It was the beginning of a new time, where available technology was being applied from a very different perspective but this time, opposite to what happened during Industry 3.0, with the goal of creating a truly open-architecture, vendor-agnostic eco-system.

4. Efficiency of Industrial Systems

The ability to be vendor-agnostic and to implement a SCADA-type approach at the control station opened the door to eliminating repetitive and redundant processes. Moreover, disparate data collected from separate sources finally allowed taking stock of a distributed environment and elaborating more effective reaction and control strategies.

As the implementations of this early IIoT-SCADA systems multiplied so did the number of "drivers" developed. To be clear, these "drivers" may but generally do not control the device directly at all, rather they interact with the device's own drivers and control systems. A practical example of this is seen in the SmartEngine® application jointly developed by this author and Donald MacPherson of Hydrocomp Inc. in the early 1990s, which computed engine and propeller parameters to attain a used-defined target such as constant speed, maximum speed, speed to ETA, etc. (Interestingly, in field tests SmartEngine® achieved drops in fuel consumption in excess of 25% over manual operation of engine and propeller controls or, more often, in the absence thereof. Hampered by the absence of appropriate technology on the receivers' side (the devices) and the closed-minded culture in the industry the project was eventually mothballed.) The system stored engine and propeller performance maps and the only input required was GPS speed readings. In true IIoT-SCADA fashion, SmartEngine supplied "requests" to the engine and propeller control systems. The input required was limited engine rpm and propeller pitch readings (in case of a variable pitch propeller).

Fig.5: Some of the IIoT "nano" customers

6. A "different" IIoT paradigm

Stefano Linari's vision in the making was that: to source data from any device (monitor) and provide a path back to the device (control) for those requiring it, agnostically. This effectively de-silos devices in true Industry 4.0 fashion within a pristine vertical architecture. In this way, virtually any device can be monitored and, for those devices supporting it, controlled through via its own control system.

The data mined from the various sensors and other measuring devices becomes available to any application, from a simple dashboard, to complex performance evaluation algorithms, to automatic preventive safety action reactions, to preventive maintenance, etc. It is clear that the paradigm embraced in this effort was "different" in that it matched Industry 4.0 precepts, opposite to what other players in the industry were doing.

Around 2011the effort was recognized by a successful round of investment and a formal software development initiative saw the light. The ever-expanding device-agnostic IIoT connectivity was embedded in various commercial energy-management applications supplied by industry vendors. Although somewhat still rudimentary, far-seeking applications of the agnostic approach included the creation of electro-spinning machines used to position nanoparticles to produce man-made materials. This was the commercial spin-off of a research effort conducted in partnership with the University of Pisa. Another application was the production of nanomaterials for the weaving industry and of biodegradable tubes used in creating arterial bridges that guide the growth of cells into restoring the damaged tissue.

Fig.6: The water treatment plant serving the city of Arezzo

7. How about ships?

Neither IIoT nor nano technology are commonplace in the marine industry, yet, and it is easy to construe how the latter would benefit from such technologies, already proven elsewhere, for example in the field of low friction antifouling materials.

Another marine application, patented, is a dry scrubber for ships (and industry at large, too) made of nano-assembled porous ceramic particles. Developed in partnership with the Danish Technical Institute, the filter operates at very high temperatures (hence the ceramic) and comes out at 1/3 to 1/2 the size and weight of wet scrubbers. The 7M€ project developed use of ceramic nanofibers made from liquid heated to 350°C thereby producing a high-efficiency filter about 1000 time smaller than conventional ones thanks to its volume being about 80% empty. The filter is printed on nanometric surfaces made of pure catalyser and serves both conventional and hybrid propulsion plants. IIoT comes into play as it applies to scaled down ovens and quality control systems, electronic microscopes, gas chromatographers, spectral photography, etc. Other notable applications include AI-driven IIoT brain implants to re-train portions of the human brain to perform duties previously carried by now-damaged parts, for example to restore vision.

Other marine applications would follow soon enough.

8. 2012

Around 2012 a number of defining evolutions started taking shape in the world of IIoT, one being the adoption of Alleantia technology by the HiProd cloud platform for the optimization of production processes. Beneficiaries of these advances include Bosch GmbH (monitoring & control of manufacturing machines), Leonardo SpA (predictive maintenance for helicopter blades), Brembo SpA (monitoring & control of manufacturing machines), etc.

In the multiple-site world, co-author Alexander Vannas spearheaded a major project that was to be instrumental in the release of the Alleantia commercial IIoT-SCADA software product. The task was to equip the existing 36 photovoltaic plants supplying electricity to the ensemble of hospitals in Tuscany with remote monitoring & control capabilities despite the considerable variety of devices and vendors involved and, no less, to integrate the lot with the also already-existing Property Management System. One challenge was presented by the closed software/hardware environment of Fronius inverters which required the retro-engineering of programming languages and communication protocols Alleantia had been excelling for years already.

At this time the computer hardware employed was generally commercial-grade but not rugged, which made it necessary to build redundant architecture around the web-based communication channels. The web was further exploited by sending data to cloud-based servers and repositories. It deserves mentioning that remote photovoltaic plants did not enjoy a cable connection to the telecommunications grid, therefore it was necessary to adapt the IIoT-SCADA system to the fragility of data transmission, both in monitoring and in control, of the GSM network.

9. Web applications and GUI

The release of IIoT-SCADA as a commercial product required a web-based GUI, reachable remotely and resident on the local processing device, the gateway. Moreover, the software application was to develop configurable edge-computing capabilities and had to be easily integrated into end-user systems of any architecture.

This definitively identified Alleantia as a software solution provider and its device-agnostic paradigm sealed its ubiquity. It also meant a redoubled effort in creating connectivity to all sorts of languages, protocols, connectors, etc. and, most importantly, in evolving the software architecture to be expandable by design, thereby catering from the onset to the yet unknown developments in communication and data handling technologies to come. The ever-increasing list of supported languages, protocols, connectors, etc. started reading like a Who' Who of data communications.

The net advantage for the user of true, integrated IIoT solution is easily identified in lower cost in general, from reduced energy consumption, reduced down time, preventive maintenance, etc. all made possible by a minimum level of automation supported and driven by the human Captain, be it a ship, a factory or a group of buildings. Already in pre-BIM (Building Information Models) time, 2D and 3D CAD models are easily retrieved and integrated dynamically in monitoring & control applications, for example Safety Management Systems on board ships. The information pertaining to a given CAD object selected by the operator is available and displayed in its raw and/or processed format.

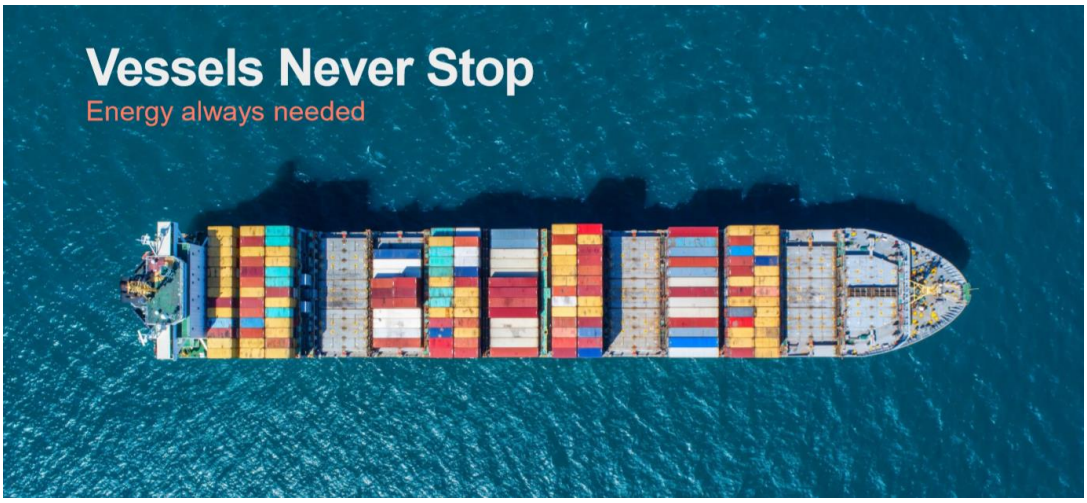

Fig.7: IIoT, the keenest eyes and the sharpest ears in the maritime industries

This is the beauty of the agnostic approach, the ability to serve any and all industries with exactly the same software product.

10. IT Majors and Gartner take notice

Since 2012 a number of strategic alliances were inked in, including with (in no particular order) CISSCO, DELL, Microsoft, TIM, Advantech, Boomi, IBM, Hewlett Packard, etc. These included providing the Alleantia IIoTA-SCADA software solution as an OEM package to be embedded in those vendors' own hardware and software offers such as rugged gateways, routers, etc.

Gartner also took notice of the *true-to-the-Industry 4.0-cause* nature of Alleantia's mission statement and rewarded its agnostic approach with several special mentions every year since 2018. "Disruptive", "visionary", "vendors to watch", etc. are some of the qualifiers used by Gartner to underpin the inclusion of Alleantia's solution in Gartner's Top 10 lists.

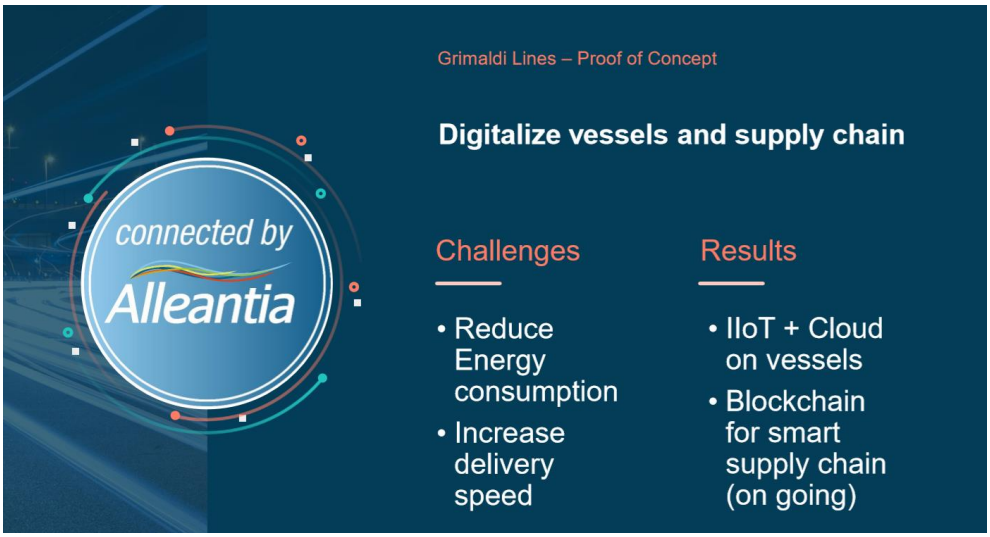

Fig.8: The world of Industry 4.0 IIoT cannot be called so unless it spans the ecosystem.

11. The Internet of Things *aka* a very important Digital Twin

The Digital Twin is made of data and processes, and people use that data to make a decision, take an action, carry out forensic analysis, etc. In this respect, IIoT must fulfil a double role: collector and distributor. Therefore, in its most useful form the Digital Twin is a dynamic entity composed of a variety of input from several sources, collected a combined according to Industry 4.0 precepts.

11.1 XPANGO

The vast collection of "drivers" developed over time by Alleantia was eventually collected under the XPANGO label as the ‘Library of Things’, underlining the agnostic philosophy of the industrial approach implemented by the group. XPANGO offers a huge variety of 5000+ "drivers" receiving from and transmitting to hundreds of devices using dozens of protocols, etc.

11.2 Data Distribution

The data collected has to be distributed, in raw or edge-computed format, to whoever requires it and to wherever the data should be stored. Cloud-type solutions include Microsoft Azure, Yammer, Facebook, but also the various AWS, GE Predix Platform, IBM Watson, Microsoft Azure, PTC ThingWorx, SAP, etc. Alexander Vannas also engineered important industrial partnerships with FMD INFOR, ANTOS / BRAVO MES 4.0, EXTRASYS (GKN Augmented Reality), COMAU (robotics), PWC (Enervit), ODOO, VIMAK and SYNCHRO (industrial machinery), QUINTI (automated / robotics assembly

lines), FC Impianti (Oil & Gas), TIM (telecommunications), Ansaldo (metallurgy, steel industry, marine propulsion), Circumvesuviana (public transport), Marcegaglia (steel industry), Bonfiglioli (automotive), etc.

12. Plug & Play

A very innovative next step was taken deliberately in order to make the agnostic paradigm truly ubiquitous when it was decided to render the end-user virtually autonomous. The Plug & Play initiative lead to a "Universal & zero-coding Industrial IoT Gateway" and makes available the full XPANGO library to every Alleantia customer.

Not only, but to make the end-user even more autonomous, a number of machine simulators are available to all as is a "driver-writer". The latter is most important, as it allows the end-user to effectively create a new "driver" themselves via a reserved, interactive tool available on the Alleantia web site. Let us recall here that Alleantia "drivers" do not physically monitor or control the device in question but rather interacts with the devices own control system.

One more significant advantage of the plug & play evolution is the ability to pre-configure a complete system and then carryout remote installation, final configuration and maintenance.

Fig.9: Ubiquitous connectivity to logical and physical devices is key to being Industry 4.0 compliant.

The combination of Plug & Play and of a "driver writer" is as Industry 4.0 compliant as can be.

13. More industries, more ships

One of the earliest Augmented Reality solutions was presented by Alleantia at the 1st PLM IoT Forum hosted by the University of Cambridge in 2015. This contributed to an increased demand from various industries, including the marine world, namely the Italian ship operator Grimaldi.

Under the impulse of Vannas, subsequent field installations spanned the integration of industry majors the like of Fanuc, Siemens, Heidenhein, ecc. Simultaneous multi-platform connectivity included building systems, Enterprise Resource Planning and Product Lifecycle Management solutions.

More modern machinery finally allowed more control and greater levels of automation and, eventually, a standard product offer materialized the culmination of the Plug & Play paradigm via a "shrink-wrap" software package.

This is important because it was the vehicle that allowed a major ship operator to install and operate the Alleantia IIoT-SCADA solution with a quasi-zero field intervention - limited to minimal training of the customer's IT team - by the software provider.

The now standard, "packaged" software product is called the "Alleantia ISC Software Solution" on which the Marine 4.0 solution was founded.

14. All Things Joined: The Digital Transformation

With a commercial, standard software offer and a number of rugged gateways with WiFi, Bluetooth, LAN and GSM capabilities now available off-the-shelf the attention turned to the web-based GUI to be used for system configuration and operation alike. Arguably, from an IIoT perspective anyway, Digital Transformation was achieved.

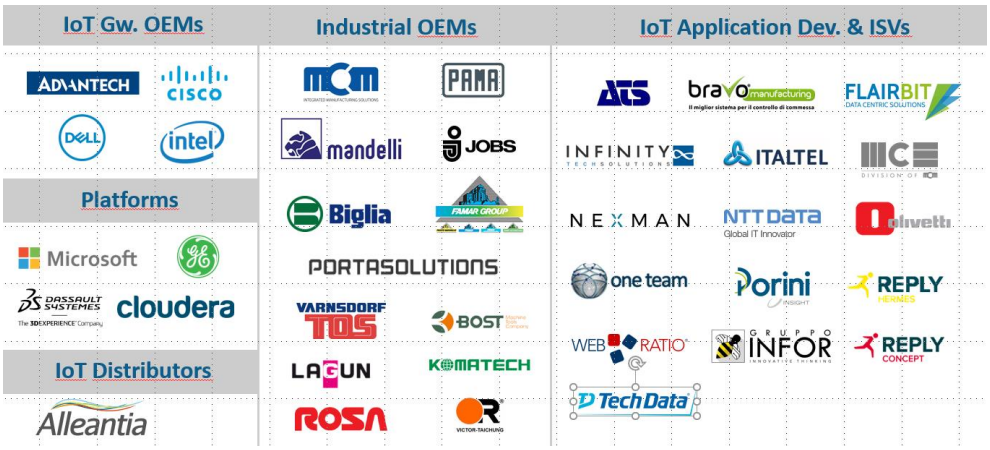

Fig.10: A few examples of Industry 4.0 connectivity

With the evolution of other industrial software and systems, the bridge between Information Technology (IT) and Operational Technology (OT) takes on ever more importance. (Information technology (IT) refers to anything related to computer technology, including hardware and software. The main difference between OT and IT devices is that OT devices control the physical world, while IT systems manage data.) Moreover, this is also when industrial system integrators gain access to a new world, that of a remarkably low-cost, agnostic and ubiquitous connectivity, thus progressing towards a more generalized Industry 4.0 compliant world. Supporting system integrators confirms itself as a significant part of Alleantia's business model, formalized by providing structured Training and Certification programs. More partnership with device vendors followed and a new player popped up: security.

Fig.11: It's all about data.

15. Security

Hacking is available as a service and, with the relative availability of hacking packages, even a commodity. ("According to Kaspersky … just $5 for a five-minute attack and $400 to overwhelm a server … for a whole day. The SecureWorks report quotes ... $5 an hour or $30 per day", www.businessinsider.com/things-hire-hacker-to-do-how-much-it-costs-2018-11) Major players the size of shipping companies MAERKS, MSC, Toll Group, terminal operator APM, etc. have suffered crippling attacks.

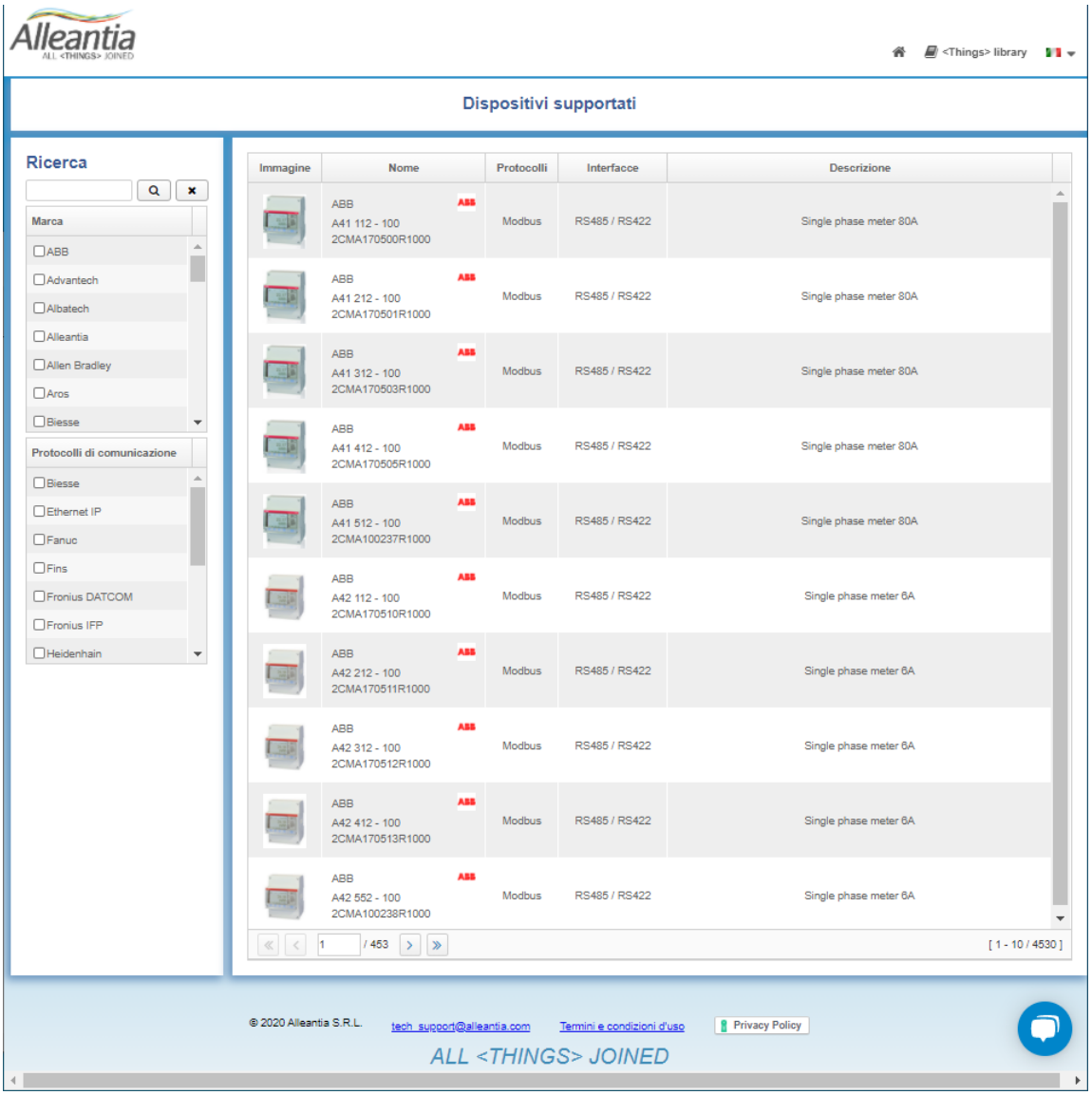

Fig.12: A snapshot of the 5000 strong XPANGO "driver" library

Itai Sela, CEO of Maritime Cyber Defence Solution provider Naval Dome, https://navaldome.com/, resumes the worsened current situation very clearly: "Covid-19 social restrictions and border closures have forced OEMs, technicians, and vendors to connect standalone systems to the internet in order to service them ... The global crisis and social distancing measures are preventing OEM technicians flying out to ships and rigs to upgrade and service critical OT systems, resulting in operators circumventing established security protocols, leaving them open to attack ... As budgets are cut and in the absence of service engineers, we are seeing ship and offshore rig staff connecting their OT systems to shoreside networks, at the behest of OEMs, for brief periods of time to carry out diagnostics and upload software updates and patches themselves . . . This means that their IT and OT systems are no longer segregated and individual endpoints, critical systems and components may be susceptible. Some of these are legacy systems [Windows NT, Windows XP, Windows CE, etc.] which have no security update patches and are even more susceptible to cyber-attack . . . The increase in OEM personnel working remotely on home networks and personal PCs, which are not well protected, adds to the problem".

Naval Dome data shows that during the first three months of 2020, attacks targeting home workers increased tenfold. PC security software provider McAfee has reported that that between January and April 2020 cloud-based cyber-attacks on all businesses increased by 630%. Israeli maritime cyber security experts Naval Dome claim there has been a 400% spike in shipping-targeted hacks since February 2020, https://splash247.com/number-of-shipping-cyber-attacks-leaps-400-since-february/.

Actually, long before the marine industry suddenly woke up to the threat, special attention had been paid to IIoT security in collaboration with IT major partners such as CISSCO and DELL, and *ad-hoc* firewalls and specific security protocols applied to gateways. Segregated IT and OT LANs, dedicated penetration sentinels, automatic shut-down procedures, etc. were built into the gateways and in the connectivity software. Certified Secure Connectors were used in connecting ships to the cloud, for example to AZURE servers, upstream of the operator's own secure environment. Customer Leonardo also contributed with specific penetration tests. The efforts received the stamp of approval by Wallix, https://www.wallix.com/identity-as-a-service, the first "bastion" recognized by Gartner.

The ability to dissociate on-ship IT and off-ship OT means that even if Northbound flow were to be compromised, Southbound flow remains protected and the ship can continue to operate normally, in full segregation and autonomy. (Southbound: data flow on the ship side of the gateway, that is between the gateway and the devices. Northbound: data flow ship-to-shore and shore-to-ship (or ship to/from wherever input might originate). Architecture flexibility allows easy adaptation to rationalizing the system as might be required by specific requirements.

Fig.13: Man & machine make a great team

16. Case studies

Marine applications of true Industry 4.0 IIoT are not common, yet, but two notable cases can be mentioned at this time.

16.1 Commercial shipping

While the ship operator referred to here asked not to be mentioned until the deployment of the shore side systems is complete, the Alleantia IIoT ecosystem that was deployed can be described.

Some 75 of 120 ship now carry secure gateways with on-boards Alleantia's ISC software solution. The task is to collect a large number of operational data, carry out some edge processing and transmit the lot to shore. Notable constraints are the automatic switching between Sat-Com and GSM as soon as the latter becomes available, limited bandwidth, limited transmission time when under Sat-Com, and limited data. All have been satisfied. The data is sent to shore-based cloud, more specifically to MS-AZURE servers.

In the absence of an existing solution, a custom dashboard was developed and implemented at the control centre on shore. Quasi-real time display of vital data is supported by edge-computed values such as averages, spikes, occurrence of spikes, etc.

16.2 Heavy Lift

Aging systems and locked, siloed IT environment prompted the barge operator to add a second, parallel, monitoring system resting on open architecture, extensible and designed to work with any device required to perform the heavy-lift work, that including installing whatever replacement could be found off-the-shelf following a failure during operation, a very time critical condition. The job specification included the development of a customer-designed dashboard.

Adding a system to an existing installation requires retrofitting the software to be installed to the hardware and software already present – a "feature" inbuilt by design in the agnostic ISC software package The choice fell upon a set of Advantech Analog ADAM 6017 input modules connected to an Advantech UTX 3117 dual-LAN gateway, the lot configured to retrieve sensor signals in parallel with the existing monitoring application. A specialized partner, INFOR, Italy, developed the customer-designed dashboard, installed on a dedicated PC.

Fig.14: The 122 m LOA heavy lift barge has a 28000 t lifting capacity

The system was shipped following a succinct training course held for the designated operator and installed autonomously by the customer.

17. An eye to IIIoT&S and Industry 5.0

Industry 4.0 is indeed here but only in very niche portions of a rare few industries, very high-tech manufacturing and advanced aviation being a few. "Robots helping humans work better and faster by

leveraging advanced technologies like the Internet of Things (IoT) and big data" is not such a farfetched idea, a very basic example thereof would the autonomous floor sweepers and a more advanced one the quadruped robots that carry ordnance on the battle field.

Agnostic, portable, autonomous, highly user configurable IIoT solutions provide the backbone of both Industry 4.0 and Industry 5.0, the latter being different from the former essentially in the nature of the devices being connected. Somewhere between the two lies the first "I" and the "S" in IIIoT&S which stand for Intelligent Industrial Internet of Things & Services.

The "intelligent" part is already here, except not in the right place. Decision making, including monitoring tactics and strategies and device control exit today but are mostly relegated to the human-manned control stations. Anything from simple algorithms to Artificial Intelligence applications can and probably should reside on the gateway, thereby providing a closer-to-the-action layer of intelligence. Such a solution would rest on and make easy use of the data channelling ability of agnostic solutions like Alleantia's.

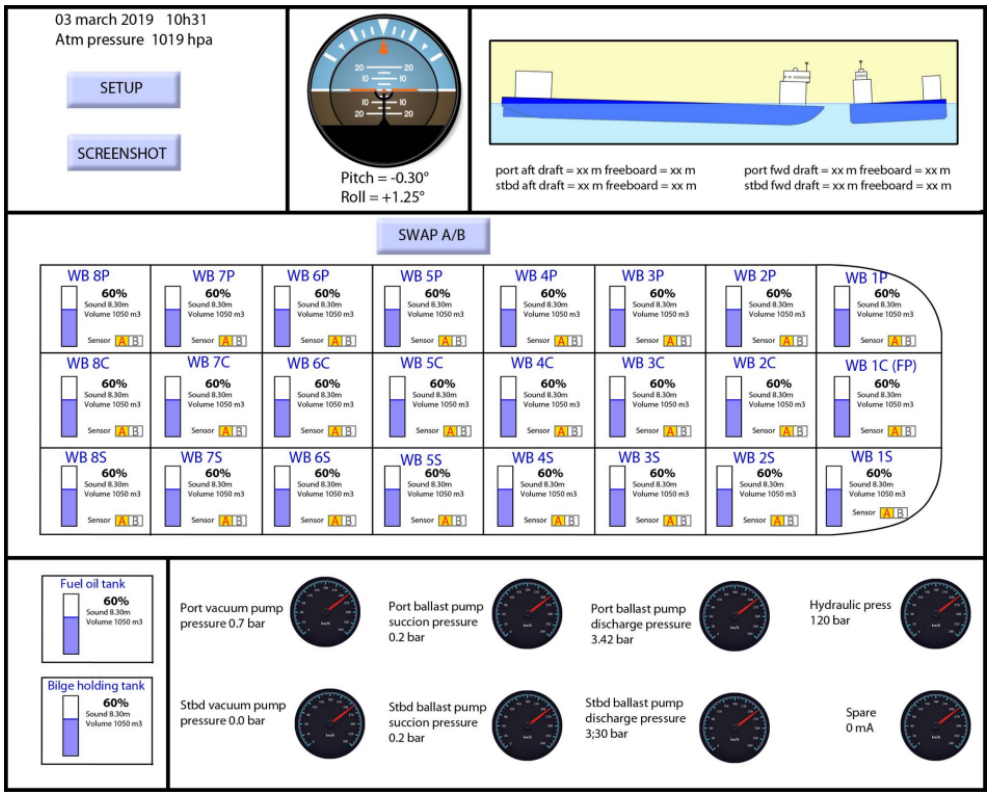

Fig.15: The customer-designed dashboard monitors redundant pressure sensors in 28 tanks as well as trim and heel sensors, etc.

The "S" of Services will require need more than ever before an agnostic IIoT system, in that all sorts of disparate Big Data will be required to fulfil the mission, a true Industry 4.0 performance that major suppliers of siloed IoT simply cannot deliver. One poignant example is the landmark contract signed by Nippon Yusen Kaisha (NYK) and major shipbuilder Japan Marine United Corporation (JMU) to introduce a new shipbuilding contract that guarantees propulsion performance for new box ships in actual sea conditions.

"Shipbuilding contracts typically guarantee ship speed by confirming the relationship between ship speed and horsepower in calm sea conditions without waves ... confirmed during sea trials [conducted] before acceptance of the ship. However, calm voyages without wind and waves are rare during commercial voyages, and stormy weather conditions are often encountered. ... Therefore, it is generally the obligation of shipping companies to identify and procure ships that have good propulsion performance

in actual weather conditions. ... NYK will collect necessary data for a certain period of time, verify the data, and confirm the degree of achievement of the guarantee. This performance guarantee will confirm the relationship between ship speed and horsepower under sea conditions that include wind and waves", https://splash247.com/nyk-seals-landmark-shipbuilding-contract-guaranteeing-propulsion-in-actual-sea-conditions/.

This will require quite a number of data sets to be sourced from various sensors and on-board systems, meteorological data providers and engine and propeller manufacturers. All of it will be delivered to a shared repository for distributed processing, followed by the issue of control instructions aimed at optimizing the ship's performance. Now, if that is not HIPER...

17.1 IIot as a Service

This is major aspect of the IIoT technology described this far, albeit a very simple one. The business model based on plug & play and customer autonomy is based on providing the ability to communicate, as opposed to selling drivers and connectors. Drivers and connectors are supplied free of charge and the customers only pays for the number of channels (effectively number of variables) that will transit through and will be managed by a given gateway. In a larger installation, each gateway can be configured differently and carry different amounts of traffic.

By commercially providing "channels" as opposed the data connectivity itself (drivers and connectors), the supply of IIoT becomes a service that is modulated by the end-user, at will, at any time, an infinitely flexible and customer-driven arrangement.

And, as mentioned above, one more significant advantage of the plug & play evolution is the ability to pre-configure a complete system and then carryout remote installation, final configuration and maintenance, another keystone in the Industry 4.0 paradigm.

18. Conclusion

Industry 4.0 has not materialized in the marine industry, not quite or not yet, some reasons including mistakenly perceived cost, time, difficulty of applying classic connectivity, culture, adequate processes being used, etc. On the other hand, some building blocks of Industry 5.0 are already being used in other industries.

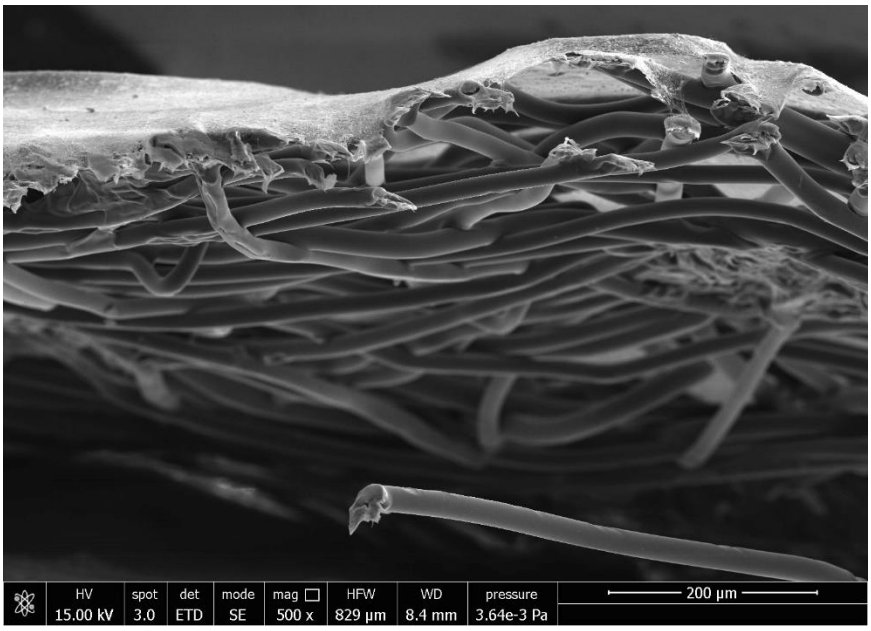

Fig.16: Nano fibers in a weave

Security has proven a major weakness across the board and both ship and shore players have been hit heavily by relatively easy hacks. But, effective and easy to implement, proven, Commercial-Off-The Shelf (COTS) solutions exist.

And, with respect to dematerialization, fully remote configuration, installation, operation and maintenance via GSM, SatCom and internet is a mature, proven strategy. In parallel, full cloud management of Big Data used by client applications in fully and human-controlled automatic modes is also commonly available.

Covid 19 might turn out to be the best friend yet of Industry 4.0: ironically, it is not an increase of the price of fuel but rather a drop in consumer revenue that could spur the marine industry to make better use of available technology in seeking the elusive Grail of efficiency while reducing waste and pollution. For this to happen, though, as co-author Alexander Vannas puts it: "open architecture, end-to-end system integration must become a commonly available service".

Acknowledgements

Alexander Vannas, co-author, took time and proved patient while introducing me (Nick Danese) to IIoT. His teaching and support were fertile ground for my Industry 4.0 and IIIoT&S adventure. Others helped, too, many and in many sectors of IIoT, shipbuilding, ship management, etc., and I thank them all with gratitude.

SWOT Analysis of SWATH Technology – Towards Smarter Vessel Design Solutions?

Ali Ebrahimi, Ulstein International AS, Ulsteinvik/Norway, ali.ebrahimi@ulstein.com
Jose J. Garcia, Ulstein International AS, Ulsteinvik/Norway, jose.jorge.agis@ulstein.com
Per O. Brett, Ulstein International AS, Ulsteinvik/Norway, per.olaf.brett@ulstein.com
Øyvind G. Kamsvåg, Ulstein International AS, Ulsteinvik/Norway, oyvind.kamsvag@ntnu.no

Abstract

When the cargo-carrying capacity of the vessel solution is not a high priority requirement, there is more freedom to choose other hull forms than a monohull. The final required mission(s) of the vessel, traditions, and the willingness to experiment with novel hull configuration ideas will allow or not, such alternatives to come to realization. Over the years, different hull forms including, catamarans, small water plane twin-hull design solutions (SWATHs), trimarans and or pentamarans have been developed to serve different specialized missions. In this article, we explore the strengths, weaknesses, opportunities and threats that a SWATH technology represents. We analyse the applicability of the SWATH concept in three particular vessel segments: (i) service operation vessels for the ocean wind energy generation industry, (ii) exploration cruise vessels and (iii) patrol vessels. Vessel motions and accelerations, and the effect on the operability and comfort of SWATHs are evaluated in more detail. Overall performance yield of the developed SWATH solutions is compared with corresponding monohull concepts with similar size and functional capabilities. Furthermore, the article explores production strategies meant for enhancing the competitiveness of such SWATH designs and their operational attractiveness. Myths and truths of the SWATH concept are being discussed and current wisdom is challenged. The proposed vessel design solutions are performance yield benchmarked with existing peer vessels in their respective markets.

1. Introduction

At present, the shipbuilding industry is facing dramatic changes with respect to technologies being applied, the capacity and capability of big data analyses, knowledge enhancements, and a disruptive market situation. With a historical low vessel newbuilding contracting activity and rising construction costs in many ship segments, even though there is a significant worldwide overcapacity of shipyards compared to the current demand for new buildings, the competitiveness of the European shipbuilding industry is under scrutiny and deterioration and has been like this for quite some time, *Brett et al. (2018)*. Over the past three years, vessel newbuilding prices in Europe have increased by more than 25% for several ship market segments. This somewhat surprising behaviour is traced in almost all the vessel segments of the European market, including offshore and service vessels, fishing vessels, Ropax vessels and cruise-exploration vessels. The offshore wind energy generation (OWEG) market, so far, mostly driven by European needs and interests has, however, opened up a fairly new, but reasonable robust business opportunity for many of the European shipyards. Yet, the above-mentioned price development is challenging the competitiveness of Northern European shipbuilders as suppliers of such service operation vessels (SOVs). In such circumstances, finding alternative solutions that can secure the vessel main required mission performance but at lower capital and operational cost is paramount to retain worldwide competitiveness and thereby represent a realistic alternative for owners looking in particular for expanding their fleets in this buoyant market segment.

The offshore wind energy generation market is under constant pressure to become more competitive and to reduce the 'Levelized cost of energy' (LCOE) to eventually, become subsidy-free. Vessels providing services to these market-segments are expected to contribute to the overall LCOE reduction and not increasing it. Such a development might prove to require a disruptive market change in our ship design approaches, *Brett et al. (2018)*. Exploring new ways to increase the revenue-making capability of vessel design solutions besides reducing their overall costs (CAPEX, OPEX, and VOYEX) are pursued in this article. Thus, we first need to identify critical elements contributing to the revenue-making potential of

the vessel and then eliminate “nice to have” features that do not really contribute to higher revenue but increase the cost of owning or operating the vessel. For a service operation vessel, serving more turbines per unit of time, larger storage area (more spare parts and repair equipment for more turbines) or higher operability (operating a larger proportion of time) are some of the alternatives that can support a higher revenue-making capability of such novel vessel design solutions. However, these features require a larger accommodation area (more technicians onboard), larger vessel (higher damping forces) and a larger propulsion plant (compensating for higher environmental forces). To achieve these improvements following the existing monohull design concepts will, according to our experience, result in a substantial increase in capital and operational costs, challenging the overall competitiveness of such vessel designs. Hence, looking for the application of alternative hull forms is essential in the development of the next-generation SOVs. So, how can we increase the performance of the vessel designs while reducing its size and cost?

When the vessel segment is not cargo-weight sensitive, designers have more freedom to explore alternative hull forms. The SWATH concept is one of them. It has been around for decades, but for different reasons it has really found its application in many market segments – some of them are, however, navy applications, pilotage services, ocean research, and also smaller passenger transportation vehicles. Considering the main needs of the offshore wind farm service market, we propose that among different hull forms, the SWATH technology can represent a more competitive technical and operational capable vessel design solution with respect to improved revenue making, increasing operability, and lowering their costs, than a conventional mono-hull design solution. In this article, we evaluate, discuss and compare the competitiveness of such alternative solutions by the use of three design perspectives of design for effectiveness - vessels doing the right things), design for efficiency - vessels doing the right things right and design for efficacy - vessels doing the right things the right way with the right resources.

2. Design perspectives as a methodology

The development of competitive next-generation vessel designs requires a broad evaluation of the performance of the novel vessel design solutions, its operations and its commercialization. To enable such a complex evaluation, Ulstein has developed and tested out a set of three performance perspectives, *Ulstein and Brett (2015)*. Fig.1 shows schematically how the three different performance perspectives developed at Ulstein can be applied in a new SOV design solution and to evaluate the balance of factors influencing the overall final performance yield of the design solution. In this paper, it is described how one can move from a monohull vessel solution to a SWATH SOV concept applying the design perspectives A, B and C.

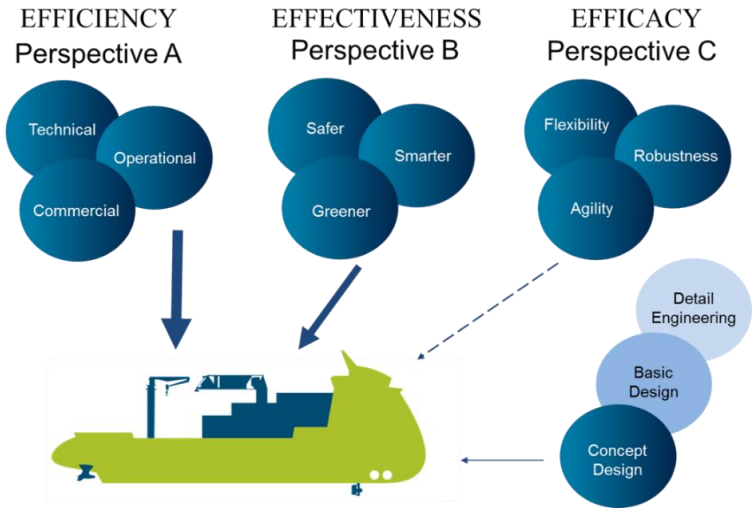

Fig.1: Three different performance perspectives (A, B and C). Adapted from *Ulstein and Brett (2015)*

A ‘Design for Effectiveness’ (perspective B), constitutes the three main constructs: Smarter, Safer and Greener: The Smarter aspect secure a clean, neat, intelligent, fashionable, useable vessel, referring to

the ability of the vessel, or system, to increase the overall effects of the combined technical, operational and commercial performance, achieving more with less- high revenue earning capability and low costs related to CAPEX, OPEX, and VOYEX. The Safer aspect idea is that the vessel design solution should protect people onboard from any danger or harm. Where people onboard are not likely to be hurt or to be lost, referring to the ability of the vessel, or system, to reduce the risk and consequences of failure, damage, error, accident or any other event that could be considered non-desirable – meaning improved safety on board. The Greener aspect is understood as the role of the vessel design to capture the concern for the protection of the environment, referring to the ability of the vessel, or system, to contribute towards a reduction of the environmental footprint and efficient use of energy and resources – connected to environmental friendliness.

A 'Design for Efficiency' (perspective A), constitutes the three main constructs: Technical, Operational and Commercial aspects: With technical aspect, the idea is to connect with the skills needed of the vessels for a particular job, which refers to all factors/articles/systems that influence the intrinsic efficiency of the vessel over its project life-cycle and that affects the design and construction process of the vessel. The Operational aspect covers the vessel's connectivity to how the business, machinery, system, etc. works, referring to all factors/articles/systems that influence the performance of different missions, for which the vessel is designed and set to do, improving operational conditions. The Commercial aspect secures the connection to the attractiveness of buying and selling of the vessel, referring to all factors/articles/systems that influence the valuation, preferences and exploitation of the vessel during its operational lifetime and increases the returns of the investment.

A *'Design for Efficacy'* (perspective C), constitutes the three main constructs: Flexibility, Agility and Robustness of the vessel design solution. The efficacy of a vessel design solution is an indication of being capable of meeting the design expectations and performing the required mission with the right means over time with relevant technology, expertise, skills and tools. From a customer's point of view, those expectations can be vessel cargo-carrying capacity, speed, operational rout, endurance, or onboard mission equipment, *Koutroukis et al. (2013)*. From this perspective, the product itself (vessel design solution) is a means to achieve required outputs and outcomes in a pre-defined maritime operation and future proof for other likely operational situations to occur. The flexibility of such a design solution indicates the ability to change to suit new conditions or situations during the lifetime of the vessel. The ability to move or change quickly form one operational system state or mode to another is covered by through agility and the quality of the final solution to hold up strong and unlikely to fail represents the robustness of the solution. At the design process level, right resources, such as designers, design tools, software, as well as guidelines, procedures, and instructions from the organizations constitute the efficacy perspective. The ability of designers to move away from their comfort zone in designing monohull ships and developing the hull forms like what the SWATH platform represents the flexibility of the process to accept changes. How quickly these changes happen and how successful are the designers to develop a competitive solution represents the agility robustness of the process respectively.

Implementing such design perspectives in the early design stages provide the designers and ship-owners with a scientific decision-making approach to make appropriate balances and compromises in a particular design solution decision-making process. That will lead to meet predefined design needs/ expectations and mandatory rule requirements for a given mission within the lifecycle of a product. Other relevant design performance yields which are important for decision-makers and market competitiveness of a product are also optimized during the process.

3. SWATH technology its history, advantages and disadvantages

Small-waterplane-area-twin-hull vessels are not something new. The first SWATH vessel, an offshore support vessel with name MV Duplus, was built an entered operation in 1969. Since then, SWATH technology has been used in multiple applications. The German yard Abeking & Rasmussen has built more than 30 SWATH-vessels over the years, *A&R (2018)*. Due to its characteristics, SWATH designs have been applied in vessel segments such as pilot, research, passenger, patrol, and pleasure yachts, not so much in other segments and for good reasons, because the physics of the SWATH concept cannot be

explored to its full potential in such other markets. Although in most of the cases the use of SWATH designs has been limited to smaller units (vessels below 50 m length overall), there are also larger applications in the market, such as the cruise vessel MV Radisson Diamond with 131 m of length overall (LOA) or the research vessel MV Planet of 73 m LOA.

All these applications rely on the principle of elevating the marine platform out of the water, to create a more stable and less wet work platform and the waves to reduce the contact between the water surface and the vessel and thus significantly reduce the forces setting up undesirable vessel motions and accelerations. The buoyancy elements of the SWATH design concept are emerged deeper into the sea with fewer wave effects and to make a small waterplane area to reduce the wave generating motions SWATHs are specially recognized by its excellent seaworthiness performance, *Bondarenko et al. (2013)*. Based on a literature review study, *Bondarenko et al. (2013), Chun and McGregor (2012), Collins et al. (2007), Jupp et al. (2014), Papanikolaou et al. (1991)*, we can summarize the advantages and disadvantages of SWATH designs against traditional monohulls as presented in Table I.

Table I: Summary of the advantages and disadvantages of SWATH designs

Advantages	**Disadvantages**
Lower horsepower requirement for high speeds	Large wetter surface
Superior seakeeping	Sensitive to weight changes
Ample stability	Pitch instabilities (fins required)
Good manoeuvrability	Larger drifting forces
Lower resistance in waves	Higher resistance at low speeds in calm water
	Uncertainties around construction costs

The physical properties of a SWATH design represent a set of advantages compared to alternative hull forms. The most remarkable strength relates to its seakeeping behaviour, whether roll, pitch and or heave. In a SWATH design, these motions and related accelerations are significantly reduced compared to similar-sized monohull vessels or catamarans. Most full-scale and tank-test measurements show that roll motions are reduced to a third of a monohull vessel for comparable size and capability, while vertical accelerations are six times lower, *Collins et al. (2007)*. Compared to catamarans, *Jupp et al. (2014)* identify a 50% reduction of the vertical accelerations.

A SWATH design also presents lower wave-making resistance, which is critical when sailing at higher speeds in heavy seas. On the other hand, SWATH designs can require somewhat higher installed power for low-speed operations due to its larger submerged surface, *Jupp et al. (2014), Papanikolaou et al. (1991)*. This might be the reason why SWATH applications have, traditionally, been related to high-speed passenger transportation and not so frequently applied in lower speed application areas.

In addition to the hydrodynamic benefits, the SWATH platform represents in many cases a competitive solution for vessel segments where the deck area is important, in contrast to traditional monohull designs where open workspace is often restricted or confined. This is an advantage, resulted from the non-linear (de-linked) nature of SWATH vessels, *Beena and Subramanian (2003)* – superstructure and mission equipment can be replaced without necessarily changing the marine platform. Contrary to monohulls, the size of the underwater hull is not directly connected to the deck area of the vessel - hence, its stability and partly its overall construction cost. Thus, the naval architect has a higher degree of freedom to increase the deck area of the superstructure without making a major modification to the submerged hulls and not leading to a too large of a vessel with unfavourable hydrodynamic coefficients such as Cb, Cp, and L/B and B/T ratios.

Generally, static stability is not a problem for larger SWATH units. However, at high speeds, and due to the low values of submerged volume per centimetre of immersion, SWATH ships are and can be longitudinally, dynamically unstable and in many cases require the installation of active fins and advanced control systems to maintain heave and pitch stability, *Begovic et al. (2015)*. The loss of longitudinal stability is higher the lower the strut waterplane area is, *Begovic et al. (2015)*. Transverse

stability is generally good at any speed. Weight and weight distribution are critical elements to consider during design, construction, and during operation of these vessels.

So, given all these advantages and some disadvantages, why hasn't SWATH technology been more broadly applied? The lack of knowledge and experience designing, building and operating such vessels can be a stopper for initially interested maritime actors when considering new vessel designs, *Garcia (2020).* Another plausible explanation is the fact that SWATH designs can require higher initial capital investment (CAPEX), because of compensation for uncertainty and risks involved due to the novelty of vessel design solution. Higher operating (OPEX) and voyage (VOYEX) costs can also result, *Jupp et al. (2014).* Despite potentially higher costs, when evaluating the overall economic performance, SWATH vessels can still, present an attractive investment for shipowners, *Papanikolaou et al. (1991).* Thus, SWATH designs can contribute to a higher value creation per unit of investment.

Yet, in the current market situation, higher initial investments can jeopardize newbuilding projects, and despite higher performances, vessel designs need to be competitive CAPEX-wise. The simplification of hull shapes plays a critical role in the attractiveness of SWATH designs concerning its building costs. SWATH designs enable the use of more simplistic forms and structural modules (basically, cylindrical, prismatic, and flat panels) and thus enable standardization, modularization, and automation in production to a larger extent than for a conventional monohull vessel design. It is, therefore, proposed by this article, that this attractive feature of the SWATH can be exploited to achieve very competitive newbuilding prices. Cylindrical underwater hulls reduce construction costs and present low resistance, yet, present limitations as they will typically increase the overall draught of the vessel, *Lamb (2003)*. For areas of shallower waters, designers might explore alternative elliptic or prismatic forms that allow the reduction of total draught while retaining the simplification of its construction. This can also lead to easier and less costly dockings of the vessel.

Further, SWATH designs can be susceptible to mega waves, current and wind drifting forces (surge and sway), *Macedo (2018)*, which are especially critical for zero speed dynamic-positioning operations. Higher drifting forces might require higher propulsive power, affecting negatively the CAPEX and VOYEX investment of the vessel. On the positive side, the shorter length of SWATH designs compared to monohulls for the same functionalities and capacities, and its more pronounced symmetry contribute to lower moments around the z-axis (yaw), which could compensate the need for higher installed power, *Macedo (2018).*

From a commercial and operational perspective, SWATHs can present limitations with regards to the access to operation and maintenance (O&M) ports and shallow water operations. This relates to both, the deeper and wider character of these vessels compared to monohulls. On the other hand, it might offer benefits due to a lower quayside length requirement. Considering Scottish ports, for example, the number of port-sites reduces from 35 units for a monohull (B<18 m, T<5m) down to 17 units for a SWATH (B<25m, T<6m) (Bryan 2020). The operational limitations also relate to docking procedures and other activities that require docking of vessels. Crew members might not be used to operate multi-hull vessels, which can require additional investment in simulation training and adaptation periods.

From a construction perspective, the knowledge and experience from building medium to large size SWATH vessels (over 50 m LOA) are limited. Very few ship designers and yards have, to date, being involved in such type of projects. Except for more experimental projects being carried out in the past in USA, Japan and more recently in Germany by Abeking & Rasmussen, yet, a few more initiatives have recently emerged both, in Europe and Asia, and the first SOV SWATH design is currently under construction at a Turkish yard.

4. SWATH design for cost-efficient offshore wind services

As the offshore wind energy generation industry matures and grows, wind farms are being developed further from shore and becoming larger wrt nos. of turbines per windfarm. The turbines and their nacelles are also becoming bigger and heavier. Following this expansion, the requirements for vessels

used in such operations and maintenance activities are also changing. Hence, the single, most critical aspect for SOV vessels is their operability. The larger the turbines, the larger the opportunity cost of lost energy generated by them when they are down or malfunctioning. Therefore, the more important extended operability becomes to avoid such opportunity losses. The operability of an SOV vessel is defined by its ability to transfer personnel to the wind turbines under different weather- and sea conditions. The transfer of personnel is, typically, limited by the motions and the accelerations set up by wind, waves and currents acting on the vessels at the offshore site. As windfarms move further offshore and into harsher weather conditions, the need for larger vessels has accentuated, making them more expensive to build and operate, which puts pressure on the overall goal for reducing the 'Levelized cost of energy' (LCOE) of a single turbine and the total wind farm site and the overall competitiveness of the OWEG industry.

Table II includes a summary of current design expectations and constraints for service operation vessels (SOVs) in the European market. This excerpt is based on actual expectations and constraints from tenders to which the authors of this article have had access to over the past months and years.

Table II: Summary of current design expectations and constraints for SOV vessels in Europe

Function	**Performance expectation**
Endurance	4 weeks marine crew 2 weeks for technicians
Max speed	14 knots
Service speed	12 knots
Operations	12/24 hours year-round, location Europe
People onboard	80-120 (single cabins for technicians)
Draft limit	Not to exceed 6 m due to port limitations
Draft air (from waterline)	Less than 35 m
Environmental condition for operation	Wave height up to 3,2 m, wind speed up to 21 m/s, current speed up to 1 m/s
Free deck area	350-450m2 to carry 6-8 containers (TEU)
Deck strength	2,5 t/m2
Position keeping capability	DP 2, complying with DNV GL DP capability (8,7,7,5)

Accommodation capacity is also an important design criterion in this vessel segment. To a large extent, an SOV simply functions as a floating hotel for the people carrying out installations and particularly maintenance and repair functions of the wind farm. It gives accommodation and transfer capability to technicians to and from the offshore turbines through a gangway system. The technicians perform maintenance and repair tasks while at the turbine and they also rest and live onboard the vessel as a hospitality function. Typically, 2 to 3 technicians are needed per turbine, on a schedule of 5 to 7 hours. Personnel work only during daylight periods-14 hours in the summer, 12 hours in spring and autumn, and 10 hours during wintertime—except for repairs that require the use of a fixed jack-up vessel, where the technicians do not need to be transferred to the turbine via a flexible and moving gangway. Two shifts of technicians will work 24-hours per day in 12-hours shifts to carry out replacements of large components, *Maples et al. (2013).* In general, offshore wind turbines require in the range of four to five site visits per year, including one regular annual maintenance visit and three to four visits in case of malfunctioning, *Röckmann et al. (2017)*. Thus, the accommodation capacity of the vessel becomes a linear function of the total number of turbines it will service.

Fig.2 shows the layout of a group of wind farms in offshore northern Europe. The arrangement of the wind farms and the turbines composing them give an idea of the importance that manoeuvrability has for these SOV-vessels. One element of manoeuvrability is the capability of transiting between turbines backwards and forwards, which increases the overall vessel utilization, as it reduces the turnaround transit time among the turbines. A second element is the capability of operating the gangway on both

sides of the vessel, port and starboard. The latter will increase the flexibility of the vessel on the wind farm and reduce turnaround time. That also enables the vessels to adjust its heading to the most favourable condition and at the same time stay connected to the turbine even in heavy seas extending the operating window.

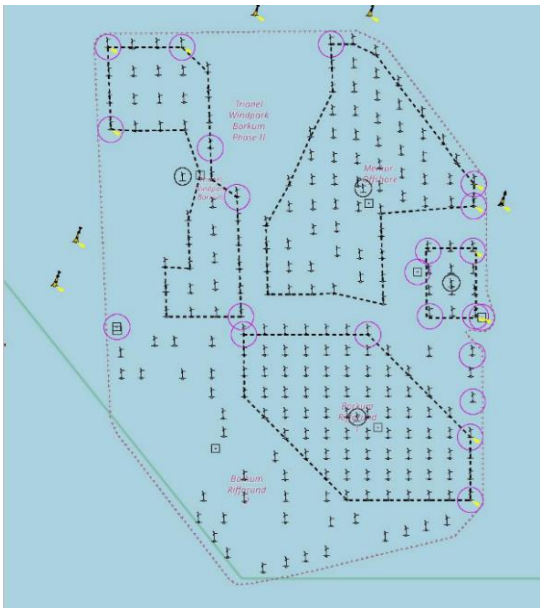

Fig.2: Example of wind farm arrangement and turbine location

With the expectation criteria defined in Table II in mind, Ulstein has initiated the development of alternative vessels design-solution-concepts of higher competitiveness than that of current vessel designs. The development includes asymmetrical vessels, double-ended (X-Bow and X-Stern features) and SWATH hull platforms. The main objective of developing the next generation of service offshore vessels was to enhance vessel seakeeping performance/operability and reduce the cost/price compared to monohull concepts of a similar size range. According to this study, a SWATH concept has a promising potential referring back to most of the literature and research being carried out by Ulstein. Thus, Ulstein initiated the development of a SWATH SOV design in the pursuit of facilitating smarter, safer and greener SOV operations – higher revenue-making performance at lower costs. The initial concept design is presented in Fig.3.

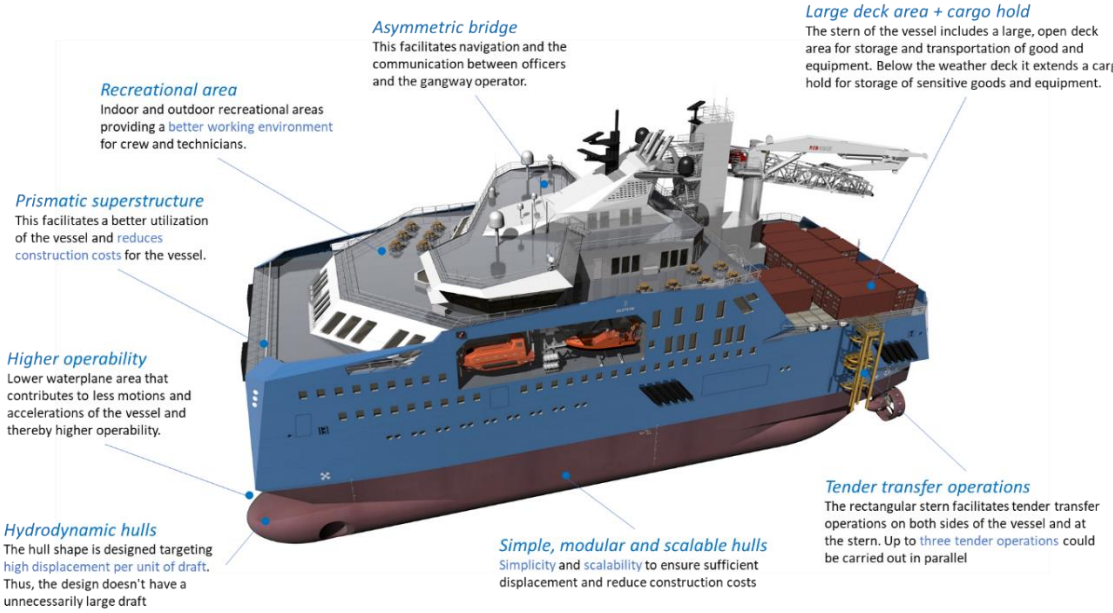

Fig.3: Top view of Ulstein's SWATH SOV concept

A critical factor to consider, while designing a SWATH vessel is its cargo weight and space-carrying capacity and its duration – capacity to stay offshore, in other words, the deadweight required for the vessel. The deadweight requirement for a large SOV is predicted in Table III. Around 700 t deadweight is required to carry out typical and present O&M operations for 15 days with 120 people on board; including margins. This is substantially less than what current mainstream monohull designs are achieving. A monohull vessel design solution, because of its excessive DWT very often will require a fair amount of extra ballast water or even fixed ballast. The reduction and potential elimination of such ballast water or fixed ballast needs is, in itself, an advantage for SWATH designs.

Table III: Deadweight requirement breakdown for a large SOV

Deadweight in tonnes (needed)	
Fuel (MGO)	250
Freshwater	120
Lubricant oil	25
Cargo	190
Other weights	60
Topside	50
Total deadweight	695

One potential limitation of the rather low deadweight provided by SWATHs is the capability to carry heavier spare parts equipment like nacelles or rotors. For the current 8 to 10 MW turbines, the weight of the nacelle is in the range of 300 to 500 tonnes; and up to 600 tonnes for a 12 MW unit. Yet, considering that the reliability of these units is above 99%, *Okedu (2018)*, the actual benefit of a vessel to be able to carry such heavy weights back and to a wind farm is rather limited, because the demand for such operations is minuscule. To demount and lower these components, normally, a larger crane vessel is anyhow required, which can also easily bring the heavy spare parts to the site and back.

The resistance of SWATH vessels is made up, in the same way than for monohulls, of skin friction and residual drag (wave-making resistance), *Begovic et al. (2015)*, *Papanikolaou et al. (1991)*. In a first evaluation, we estimated the propulsion power of our SWATH concepts based on the methodology proposed by *Medakovic (2013)*, and relying on data from existing SWATH vessels, Table IV. Table IV includes length overall (LOA), beam (B), draft (T), displacement (Δ), max. speed, sponsons length (l), sponsons depth (d), the distance between sponsons (b), waterline length (lwl), wet surface (S) and brake power (P).

Table IV: Propulsion power prediction

Vessel name	**LOA (m)**	**B (m)**	**T (m)**	**Δ (tonnes)**	**Speed (knots)**	**l (m)**	**d (m)**	**b(m)**	**Lwl (m)**	**S (m2)**	**S*V2**	**P [kW]**
Skrunda	25,7	13,0	2,7	133	20,0	23,8	2,2	11,0	19,7	300	120 000	1 618
Jakob Prei	26,1	13,0	2,7	133	20,0	23,8	2,1	11,0	20,1	300	120 000	1 618
Perseus	25,2	13,0	2,7	125	18,0	23,6	2,1	11,0	19,5	300	97 200	1 420
AdHoc24m	26,9	9,8	2,0	75	25,0	22,0	1,5	8,3	23,5	220	137 500	1 800
AdHoc41m	48,0	16,9	3,7	375	28,0	41,3	2,7	14,2	41,0	670	525 280	7 200
MC-ASD	20,0	9,6	1,5	60	14,0	18,1	1,5	7,6	17,8	190	37 240	676
FOBSWATH	25,0	10,6	2,5	100	22,9	24,6	2,5	8,0	18,3	310	161 858	1 800
Planet	73,0	25,0	6,8	3 500	15,0	69,4	6,2	20,0	60,5	2 400	540 000	4 160
SWATHOPV	49,4	19,0	4,6	900	20,0	46,0	3,5	15,0	45,9	1 100	440 000	7 600
MVChinaStar	131,0	32,3	8,4	12 880	14,0	122,6	7,0	24,2	117,7	6 000	1 176 000	11 340
SilverCloud	41,0	17,8	4,1	600	14,0	38,0	3,2	14,6	36,0	770	150 920	1 640
Elbe	49,9	22,6	5,9	1 500	14,0	46,5	4,2	18,3	42,8	1 400	274 400	2 000
Dose,Duhnen	25,2	13,0	2,7	125	18,0	23,5	2,0	11,0	19,5	300	97 200	1 420
KiloMoana	57,0	27,0	7,6	2 588	15,0	52,6	6,5	20,5	52,8	1 800	405 000	3 000
SeaFighter	79,9	22,0	3,6	950	55,0	71,5	2,6	19,4	73,0	1 000	3 025 000	44 800
SWATH concept C	67,0	27,0	6,5	3 500	14,0	62,0	4,5	15,0	62,0	2 600	509 600	4 050

Comparing the resistance between a monohull vessel (estimated following the ITTC78 approach) and a SWATH vessel concept in calm water, we can confirm two observations: (i) monohull vessels have

slightly better performance at speeds below 15 knots – grey and blue curves in Fig.4. (ii) above 15 knots, our SWATH concepts outperforming existing SOV monohull designs. At those speeds, the contribution of the residual drag is higher and thereby promotes the strength of the SWATH concept. We have to state here the limitation of our methodology and the neglect of "hump and hollows" effects in the resistance curve of the SWATH design.

The situations are very different when considering other sea states than calm water. As wave height increases, the additional power required by SWATH designs compared to monohull is much less than that of the monohull vessel solution. As long as the pontoons are sufficiently submerged, the wave-making resistance of SWATH designs can be assumed neglectable, *Chun and McGregort (2012)*. For very rough seas (SS6; Hs = 5.3 m and Tp = 3.3) the SWATH concept outperforms the monohull for any speed above 7 knots. In other words, given a Sea State 6, the SWATH design could remain operating at the designed service speed while the monohull design would experience a speed loss of almost 3 knots. Thus, considering the actual operating conditions of SOV's in the North Sea, the SWATH concept will outperform the monohull vessel designs at the desired service speed of 12 knots.

Damping forces are calculated based on the closed-form expression developed by *Jensen et al. (2004)* and added resistance is calculated based on the method explained by *Strom-Tejsen et al. (1973)*.

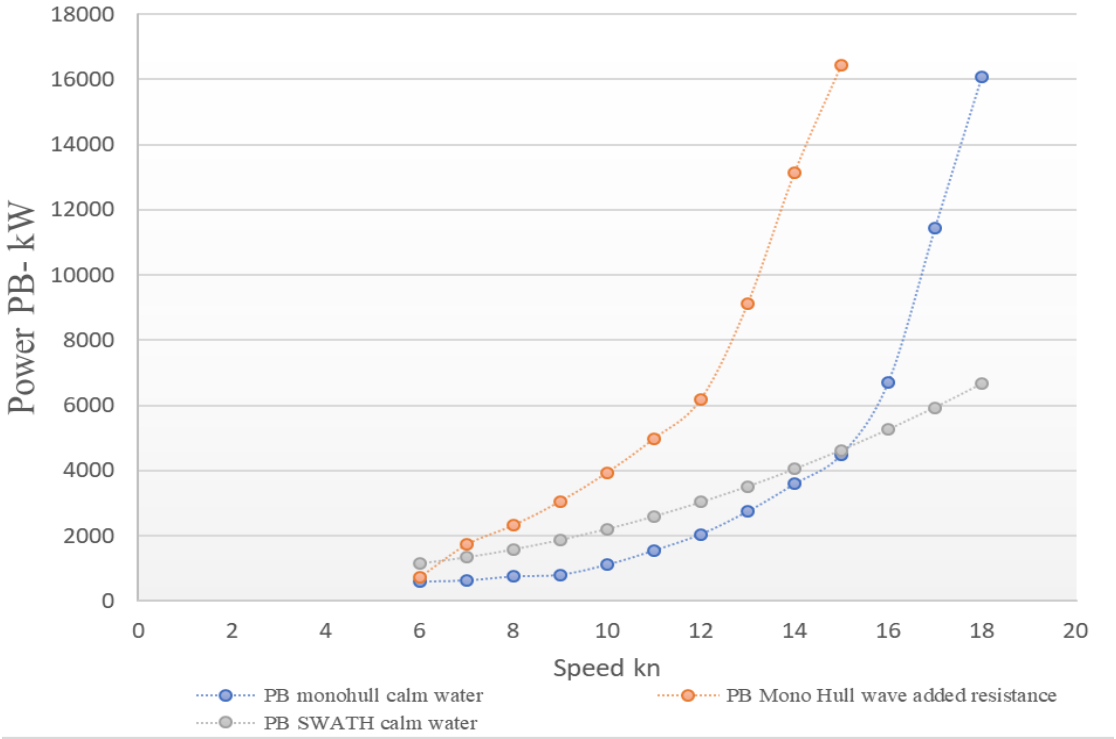

Fig.4: Speed-power comparison for an SOV based on SWATH and monohull concepts

The total installed power is calculated and balanced based on the need for propulsion power, vessel position keeping, mission equipment and hotel load. Based on our estimates a power plant composed of four diesel generators of 1250 kW plus an energy storage system of 1500 kWh would suffice. The propulsion of the vessel would consist of two azimuth thrusters and two bow tunnel thrusters. Therefore, both the power plant and the propulsion plant are similar to those of existing SOV vessels

.

The arrangement of the vessel has been explored based on a functional diagram approach as presented in Fig.5. The engine room (grey) is located in the aft of the vessel. Accommodation (green) is moved forward, to compensate longitudinally for the weight of the engine room. The cargo area (orange and yellow) is located in the centre of the vessel, thus, the trim of the vessel will be less sensitive to different loading conditions and the need for ballast will be reduced.

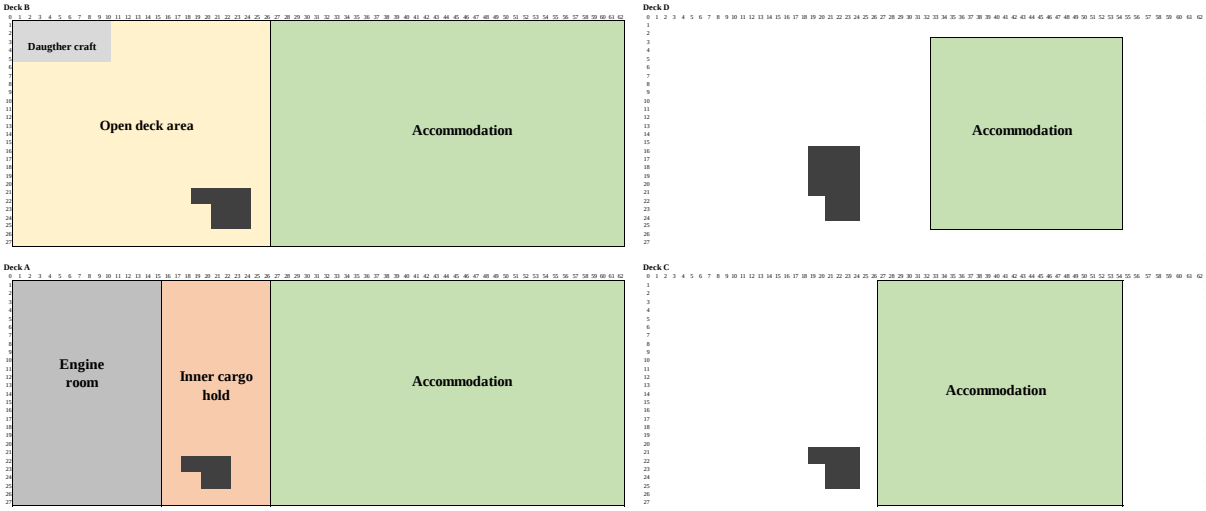

Fig.5: Functional diagram of the SWATH SOV concept studied – plan view

The seakeeping behaviour and operability of the hull forms are other important performance comparison criteria, that needs to be initiated for more robust decision making in this context. It is planned at Ulstein to conduct a separate study based on strip theory to estimate responses amplitude operators (RAOs) and verify the results by model tests. However, due to limitation in time in case of this article, we relied on the results from the reviewed articles, which all confirms the improved seakeeping performance of a SWATH compared to a monohull vessel design at comparable sizes. Among the reviewed articles, *Macedo (2018)* compares SWATH and monohull close to the size range of our study. Based on his findings, heave RAO at sea state 7, for head sea at 0-knot speed is almost 50% lower for SWATH compared to the corresponding monohull at different waves length. Almost similar improvements are achieved for Pitch RAO comparing SWATH and monohull concepts. Based on Macedo's finding, roll motions are almost neglectable for SWATHs compared to a monohull. Surge and sway forces as a consequence of larger projected area and higher shape factors are almost double for a SWATH compared to a monohull in the worst-case encountering angle based on his findings. Such a result means higher power demand for position keeping in the wind farm during site operation. Although *Macedo (2018)* argues the motions are less in SWATHs compared to a monohull. Such a finding can be the consequence of a more symmetric longitudinal geometry of SWATHs compared to a monohull. However, a similar study is planned to be conducted at Ulstein since these results require further validations and verifications.

The last but not least, important element to consider is the construction of the vessel and its resulting cost. Our original proposition was that SWATH designs could be a competitive alternative to monohull vessels given a newbuilding price of equal or lower magnitude. Thus, it was of critical importance to consider the production plan and production process during the conceptualization of the design. Starting from the newbuilding cost of a conventional monohull SOV, the following considerations have been done: (a) hull costs for the SWATH concept are estimated to be 30% lower than the equivalent monohull. This is a direct consequence of a 25% lighter structure and a simpler steel production – more flat surfaces and simpler longitudinal and transverse stiffening and structures. Based on previous projects, the cost of producing double bended plates is almost twice compared to flat structures; (b) main equipment costs are comparable for the two designs, although we expect some cost reductions resulting from a smaller platform with fewer decks – costs relating to fresh water and fuel systems and the electrical installation onboard the vessel are estimated to be reduce by 5%; (c) mission equipment costs are consider to be the same although, due to the lower motions experienced by a SWATH design, simpler and cheaper gangway and crane could be expected; (d) accommodation area is equal for both vessels, we expect a cost reduction in the range of 5% due to a reduced number of decks and simpler interior volumes; (e) production (excl. steel work), outfitting and engineering costs can be reduced for a SWATH design in the range of 5 to 7 % due to a simpler structure with the exception of the struts; (f) project costs are expected to be higher for a SWATH concept to cater for potential risk and uncertainties and lack of

experience from the designer and yard. Overall, the newbuilding cost-price of a SWATH SOV vessel is expected to be in the range of 90 to 94 % of the newbuilding cost-price of an equivalent monohull vessel design. Besides, will the effect of a perceived less expensive walk to work gangway additionally improve the cost-price difference in the favour of the SWATH, See Fig.6 for a detailed breakdown of the newbuilding cost-price of a new SOV and potential savings by application of SWATH technology.

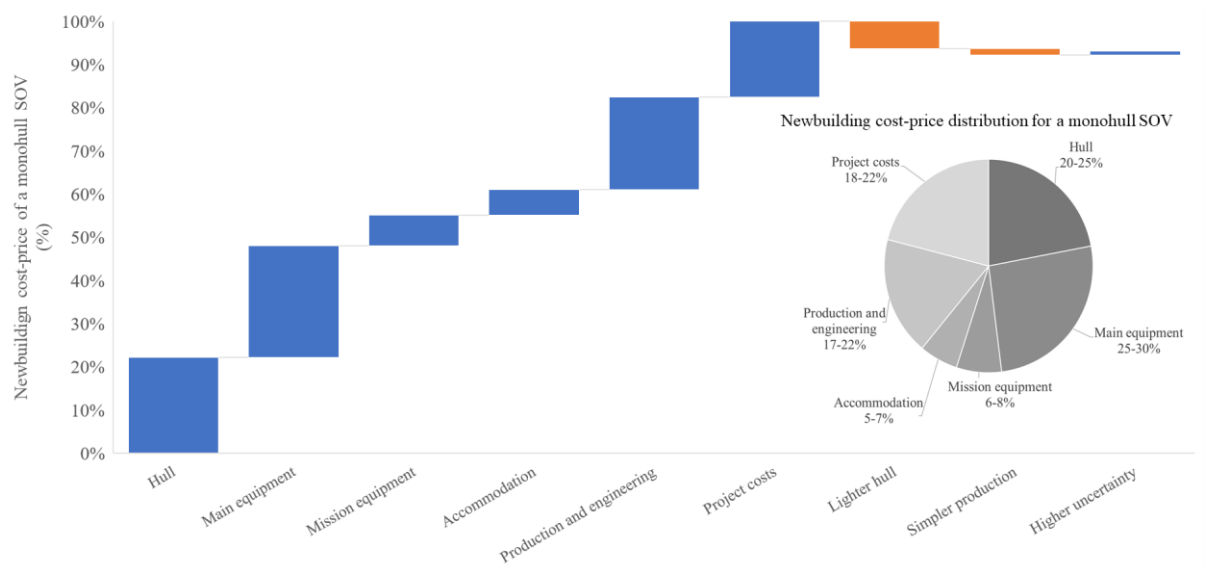

Fig.6: Newbuilding cost-price distribution for an SOV monohull and potential savings by application of SWATH technology

SWATH platforms also provide the potential for standardized modular design and production. In other words, the design can be decomposed into well-defined parts and components that can later be recombined into new designs, *Erikstad (2019).* Modularity will enhance flexibility along the entire lifecycle of the vessel, starting by design, production and during its operation. During the design and construction phase, the SWATH vessel becomes a "building-block". For example, different size and shapes of sponsons and struts can be combined to achieve a range of displacements without modifying the main hull and superstructure of the vessel. Similarly, a given combination of sponsons and struts could be used for multiple applications. Additionally, with a simple adjustment of the distance between the sponsons, the design can provide a larger deck area and improve its intact stability. Modularity and its resulting flexibility could contribute to a further cost reduction that hasn't been quantified really in our analysis.

To sum up, as part of this case investigation we have developed and studied three SWATH concepts (A, B and C). These three concepts, which follow the same design principles as described in Fig.3, have been assessed concerning the original expectations stated in Table II and benchmarked with three comparable existing monohull vessels (I, II, III). The capacities and capabilities of the six designs are listed in Table V.

Table V: Capacities and capabilities of the six vessel designs evaluated

	Length overall (m)	Beam (m)	Draft (m)	Deadweight (tonnes)	Ligthweight (tonnes)	Free deck area (m2)	Max. Speed (knots)	People onboard	Cost price comparison*
Monohull I	74,0	17,0	5,6	2000	2525	225	14,5	60	74%
Monohull II	88,0	18,0	5,9	2900	3400	380	13,5	60	88%
Monohull III	93,4	18,0	6,0	3200	3700	500	13	120	100%
SWATH concept A	70,0	22,0	7,0	630	2535	425	14	90	83%
SWATH concept B	80,0	23,0	7,0	800	2922	525	14	120	94%
SWATH concept C	65,0	27,7	6,0	800	2720	600	14	120	92%

*Taking as reference the cost-price of monohull III.

As previously highlighted, the deadweight of the three SWATH concepts is substantially lower than for the monohull vessels, although sufficient for the operations they are intended for – with exception of SWATH concept A. On the other hand, the deck area available for the SWATH designs outperforms the monohull designs by far, but very often this extra deck capacity can be exchanged for a smaller overall vessel to reduce cost-price if the extra deck area space is not meaningfully utilized. SWATH solutions could provide higher deck space compared to monohull concepts as a consequence of a large beam. That is quite attractive for customers to have a large free deck area to carry deck cargo and have some repair workshops onboard – it normally makes the vessel smarter, and not least, safer.

Accommodation capacity ranges between 60 and 120 people. Larger accommodation is preferred by vessel operators, which makes SWATH designs more attractive – more POB capacity can be achieved in a smaller vessel with fewer decks. The power demand and installed propulsion power are, however, similar for all vessels. Monohull units outperform at typical lower operational speeds in calm seas, while they will be inferior to the SWATH when operating in most sea conditions. Up to 3 knots of speed loss is estimated between monohull and SWATH designs. The SWATH designs require a larger draft compared to a similar monohull vessel. This might be a limitation in some wind farm projects. Overall, the SWATH designs result in higher competitiveness, providing improved seakeeping performance and larger deck area at a lower investment.

5. Other promising SWATH applications

The extraordinary seakeeping performance of SWATH platforms has also triggered interest among stakeholders in the cruise industry. Together with a significant improvement of the comfort onboard the vessel, SWATH vessels facilitate the integration of larger accommodation and recreational areas in relatively smaller units. Thus, achieving more cruise service offerings for less – cost. The distribution of areas and volumes onboard the vessel can be done more effectively, and additional features can be integrated into the superstructure above the water level. An example of a SWATH concept recently developed by Ulstein is presented in Fig.7.

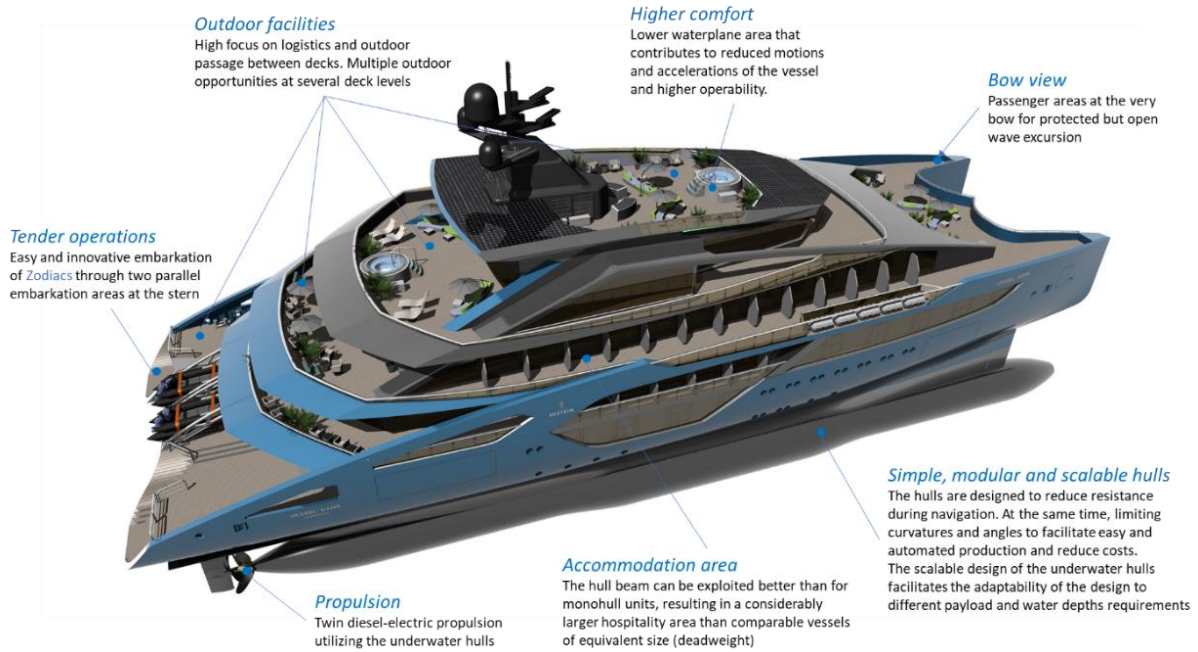

Fig.7: Lateral view of a Swath exploration-cruise vessel for warmer climates

Another segment where alternative hull shapes can provide benefits and improve the overall performance of vessel operations is in research vessels, surveillance vessels and for ocean patrol vessel activities. Vessel units performing such tasks spend a large part of its operating life in standby mode or sailing at low "waiting for something to happen" speeds. Occasionally, the vessels need to perform quick

mobilization and relocations that require higher speeds for shorter periods, even in severe sea conditions. These vessels have a variety of roles, from the control of ocean borders, oversight of fisheries, development of underwater maps, to the inspection of ocean structures at offshore oil & gas fields, subsea structures and offshore wind turbines, and other applications. With the development of drone technology, Ulstein foresees a fast development towards a more intensive use of drones and drone "mother" vessels to perform such tasks. Together with state-of-the-art ship autonomy technology, the combination of drones and autonomous drone-motherships can represent an attractive alternative solution for performing such surveillance and patrol operations at lower costs and for longer periods – by means of higher effective utilization with remote control. Such vessels can be produced both for military and civilian applications.

Fig.8: Drone mother ship (DMS)

The type of operations carried out by these units, the limited need for cargo carrying capacity and the need to perform operations in severe weather conditions require a special vessel platform. SWATHs provide a proper marine platform to outperform existing design solutions in those three application areas.

Ulstein has developed two drone mother ship (DMS) concepts, a smaller unit with a total length of 35m and a larger version of 64 meters. The smaller units can deploy up to four airborne drones of different sizes simultaneously. The drones are carried out in a protected hangar and transferred to the flight deck by autonomous robots. The larger unit can deploy up to six drones. Additionally, both units can deploy underwater unmanned vehicles to subsurface or ocean space operations as indicated in Fig.8. The drone "mother" vessels can be fully onboard manned vessel operations or made fully or partially autonomous for shore operational control centres or from operational control centres onboard other larger commissioned vessels in operation.

6. Discussion of the case studies

Our case studies highlight the applicability of SWATH designs in specialized vessel segments such as the offshore wind energy generation market, research vessels, exploration-cruise vessels and patrol and surveillance vessels, where cargo weight capacity requirements are not particularly high compared to the need for larger and partly protected workspace and extraordinary operability. The overall performance benefits to the SWATH vessel business cases we have studied can be summarized with respect to their effectiveness, efficiency and efficacy.

- SWATH effectiveness – a smarter, safer and greener ship design solution
  The effectiveness of a SWATH solution relates to several aspects. Firstly, the SWATH vessel design solution can achieve a similar accommodation capacity and deck area on a substantially lighter and partly smaller platform, which has in itself very positive effects on the construction and maintenance costs of the vessel – making the vessel smarter. Further, the SWATH enhances the seakeeping capability of the vessel, increasing the operating window (higher revenue at less costs) and the comfort of the crew onboard – a safer working platform. The need for larger amounts of ballast water is eliminated by thinking different, which will contribute to the sustainability of the ocean – greener operations.

- SWATH efficiency – a well-balanced technical, operational and commercial vessel design solution
  Comparing the efficiency of the two different SWATH and monohull design solutions by technical, operational and commercial aspects shows that both design solutions can meet the technical requirements to perform operational needs. However, improved seakeeping performance and subsequent vessel enhanced operability, especially, in harsh weather conditions, are the fortes of the SWATH vessel design solution. Minimizing the roll motions to neglectable levels and reducing heave and pitch motions by almost 50% with comparable monohull vessel design solutions are significant gains. Due to the larger B/A ratio and the symmetric hull shape of a SWATH, the hull provides much better manoeuvrability in the offshore field compared to conventional monohull vessels. In terms of commercial aspects, it is argued that a 10-15% per cent CAPEX reduction is achievable. Vessel fuel consumption and voyage costs (VOYEX) will also be lower in transit modes specifically in real sea-going conditions. Because the needed power for position-keeping will be higher for a SWATH, little or no net gains in the VOYEX are expected. Enhanced manoeuvrability and possibility for both-sided operations of a SWATH vessel represent extra commercial performance yield by reducing the turnaround and transit time working back and forth among the offshore wind turbines. Vessel maintenance costs are also expected to be reduced by making better and easier access to engine room and ship equipment areas in the SWATH design solution.

- SWATH efficacy – a more flexible, robust and agile vessel design solution
  The limited deadweight capacity of a SWATH concept, compared to existing monohull vessel designs, will reduce its flexibility for potential future conversions. This represents a limitation in itself. However, there are still multiple conversion alternative feasible for SWATH designs. Research and rescue vessels, passenger transportation, surveillance or small ROPAX/container vessels. Only minor changes in the propulsion system and cargo containment and handling areas are considered necessary. A similar conversion of a monohull vessel would be hampered by their normally much higher slenderness ratio and prismatic coefficient. The issues around longitudinal stability and vessel trim in a SWATH concept reduce its operational robustness compared to a monohull vessel design solution. However, the SWATH vessel is more robust from a standpoint of performing gangway and crane operations in much tougher weather conditions compared to a monohull, due to its significantly improved seakeeping performance. Comparing the design processes for the two different ship types, we expect to use fewer tools, fewer people, and overall, less time developing the SWATH vessel design concept. However, the general experience, skills and expertise of the design and building community for SWATHs are limited and scattered. A SWATH new building project might, therefore, be associated with higher uncertainty and risks compared to a monohull vessel.

Fig.9 presents the results of our performance comparison between the SWATH vessel design and a corresponding monohull vessel solution. The performance comparison has been carried out based on the methodology being presented in Chapter 2. The green-coloured performance features show where the SWATH has an advantage to the monohull vessel solution. The yellow performance features show where the monohull vessel solution has preference over the SWATH vessel design. The grey-coloured performance features show where both vessel design alternatives perform equally.

Effectiveness			Efficiency			Efficacy		
Smarter	Safer	Greener/sustainable	Technical	Operational	Commercial	Flexibility	Agility	Robustness
Better size utilization	Less motion induced sea-sickness for people onboard	Less resources needed resouces to realize	Deck area	Less roll motions	Less CAPEX	Convertibility	Lower mobilization and demobilization time	Less sensitive to cargo movements on deck
Better power utilization	Better longitudinal stability	Fuel consumption	Accommodation capacity	Less heave motions	Less OPEX	Changeability of cargo carrying capacity at lower costs	Less transit time to the field	More stable operation in harsh weather conditions
Lower power demand in harsh environments	Improved safety in case of collision	Application of alternative/greener fuels	Higher DWT/payload	Less pitch motions	VOYEX	Adaptability to new offshore operations	Easier and faster to apply functional changes	Less sensitive to changes in environmental conditions
Simpler production	No green water on deck	Emissions	Required installed power	Less vertical accelerations	Easier to charter in the market	More flexible to carry different cargo types	Easier to be converted to new market needs	Less sensitive by port draft limitations
Higher adaptability for modular design and construction	Safer deck work environment		Required propulsion power	Less sway motions	Higher market acceptance			Less needs for new design and construction knowledge and skills for vessel realization
Simpler engine and equipment maintenance	Better transvers stability in operation		Capability to perform needed functions	Less surge motions	Easier to contract as a newbuilding			Less influenced by dock sizes
No need for active or passive fin stabilization			Less steel weight to provide needed functionality	Higher comfort for people on board				Less sensitive to cargo weight
Less dependence of functional criteria to main dimensions			Less light weight to provide needed functionality	Higher operability in waves				Less sensitive to trim changes
Higher capability of 360 degrees operation			Higher capability to provide larger onboard spaces and area's	Lower speed loss in waves				
Higher ability for both ended operation			Less need for ballasting	Higher manoeuvrability inside the field				
Potential for operating at higher Froude numbers				Higher design freedom and spaces for vessel arrangement				

Legend (colour represents the alterntive with higher performance): SWATH Monohull Similar

Fig.9: Performance analysis overview of SWATHs vs monohull vessel designs

7. Conclusion

This article reviews the strengths, weaknesses, opportunities and threats of SWATH vessel designs compared to a more traditional monohull vessel solution for servicing relevant, specialized ship market segments. This article reviews, summarizes, and discusses the most particular and unique features – capabilities (functions) and capacities (size) of a SWATH vessel design solution compared to a monohull vessel solution. A newly proposed benchmarking method to perform such comparison analyses is presented. The article has put more emphasis on discussing the holistic aspects of the design than the very details of it. The article has been produced in an effort to collect, collate and make it easier to retrieve relevant and vital information about alternative hull forms to the traditional monohull versions. For different reasons, it has been recognized by the authors of this paper that the previously widespread awareness and knowledge of the SWATH concept technology have deteriorated and partly vanished among "ship design custodians" – the innovative naval architects and marine engineers. One of the purposes of this article is, therefore, to "bring to front" the SWOT features of the SWATH design. This effort has been done to challenge conventional wisdom and current ship design practice, and hopefully, to remind and prepare the maritime community for seriously considering and selecting more novel avenues when next-generation specialized new buildings are ordered in the near future.

The key findings from our analysis are listed in Fig.10.

For many application areas, the SWATH design solution represents a significant advantage over the monohull solutions if and when specialization of the vessel is in question. We have in this study identified a set of such advantages, which can be further applied in ship design projects and thereby produce major performance yield for their owners in the future…

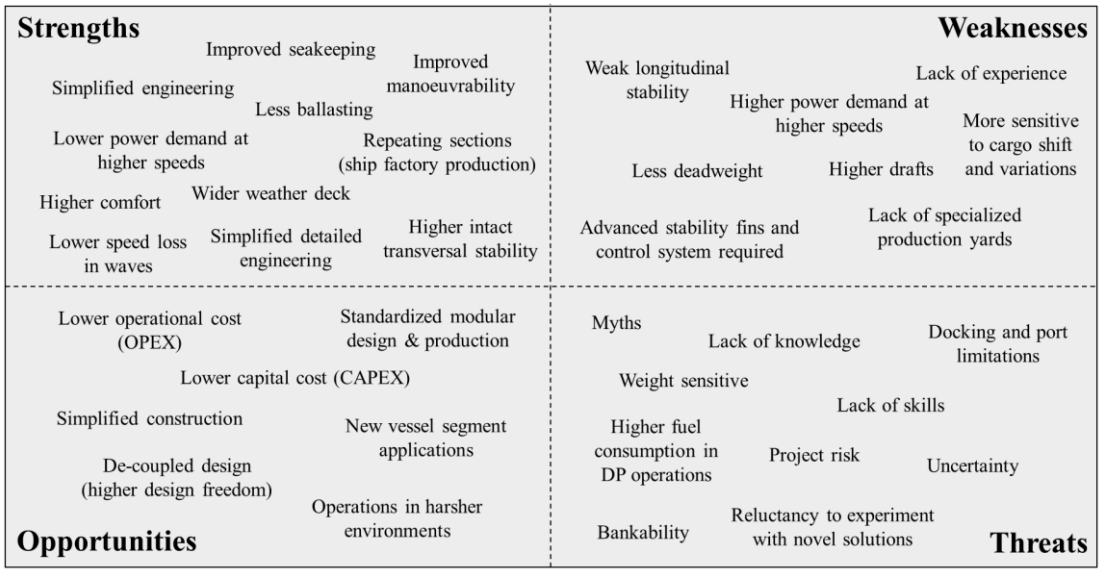

Fig.10: SWOT analysis overview of SWATHs vs monohull vessel designs

References

A&R (2018), *SWATH Technology – The Calm Revolution*, Abeking & Rasmussen, Bremen, https://www.abeking.com/en/swath-technology/

BEENA, V.I.; SUBRAMANIAN, V.A. (2003), *Parametric Studies on Seaworthiness of SWATH Ships*, Ocean Engineering 30(9), pp.1077-1106

BEGOVIC, E.; BERTORELLO, C.; MASCINI, S. (2015), *Hydrodynamic Performances of Small Size SWATH Craft*, Brodogradnja 66(4)

BONDARENKO, O.V.; BOIKO, A.P.; SEROPYAN, I.R. (2013), *Determination of the Main Characteristics of the Small Waterplane Area Twin Hull Ships at the Initial Stage of Design*, Polish Maritime Research 20(77), pp.11-22

BRETT, P.O.; GASPAR, H.M.; EBRAHIMI, A.; GARCIA, J.J. (2018), *Disruptive Market Conditions Require New Direction for Vessel Design Practices and Tools Application*, Int. Marine Design Conference (IMDC), Helsinki

BRYAN, A. (2020), *Ports for Offshore Wind - A Review of the Net-Zero Opportunity for Ports in Scotland*, Glasgow

CHUN, H.H, McGREGOR, R.C. (2012), *Reduced Resistance of SWATH Models in Waves*, AIAA J. 29

COLLINS, C.A.; CLYNCH, J.R.; RAGO, T.A.; MARGOLINA, T. (2007), *Comparison of SWATH and Monohull Vessel Motion for Regional Class Research Vessels*, Marine Technology Society J. 41(2), pp.56-61

ERIKSTAD, S.O. (2019), *Design for Modularity*, A Holistic Approach to Ship Design - Volume 1: Optimisation of Ship Design and Operation for Life Cycle, Springer, pp.329-356

GARCIA, J.J. (2020), *Effectiveness in Decision-Making in Ship Design under Uncertainty*, NTNU, Trondheim

JENSEN, J.J.; MANSOUR, A.E.; OLSEN, A.S. (2004), *Estimation of Ship Motions Using Closed-Form Expressions*, Ocean Engineering 31, pp.61-85

JUPP, M., SIME, R.; DUDSON, E. (2014), *XSS - A Next Generation Windfarm Support Vessel*, Design and Operation of Wind Farm Support Vessels, London, pp.43-51

KOUTROUKIS, G.L.; PAPANIKOLAOU, A.; NIKOLOPOULOS, L.; SAMES, P.; KÖPKE, M. (2013), *Multi-Objective Optimization of Container Ship Design*, Developments in Maritime Transportation and Exploitation of Sea Resources, pp.477-489

LAMB, T. (2003), *Ship Design and Construction*, SNAME

MACEDO, P. (2018), *SWATH SOV Hull Concept and Optimisation for Seakeeping and Comparison to SOV Monohulls*, Chalmers University of Technology

MAPLES, B.; SAUR, G.; HAND, M.; VAN DE PIETERMAN, R.; OBDAM, T. (2013), *Installation, Operation, and Maintenance Strategies to Reduce the Cost of Offshore Wind Energy*, Nat. Renewable Energy Lab., Golden

MEDAKOVIĆ, J.; DARIO, B.; BLAGOJEVIĆ, B. (2013), *A Comparison of Hull Resistances of a Mono-Hull and a SWATH Craft*, Int. J. Engineering Science and Technology 2(4), pp.155-162

OKEDU, K.E. (2018), *Stability Control and Reliable Performance of Wind Turbines*, IntechOpen

PAPANIKOLAOU, A.; ZARAPHONITIS, G.; ANDROULAKAKIS, M. (1991), *Preliminary Design of a High-Speed SWATH Passenger / Car Ferry*, Marine Technology 28(3), pp.129-141

RÖCKMANN, C.; LAGERVELD, S.; STAVENUITER, J. (2017), *Operation and Maintenance Costs of Offshore Wind Farms and Potential Multi-Use Platforms in the Dutch North Sea*, Aquaculture Perspective of Multi-Use Sites in the Open Ocean - The Untapped Potential for Marine Resources in the Anthropocene, Springer, pp.97-113

STROM-TEJSEN, J.; YEH, H.Y.H.; MORAN, D.D. (1973), *Added Resistance in Waves*, SNAME

ULSTEIN, T.; BRETT, P.O. (2015), *What Is a Better Ship? – It All Depends…*, Int. Marine Design Conf. (IMDC), Tokyo

Calculating Kite Performance through Flow Field Prediction

Konrad v. Streit, University of Southampton, Southampton/UK, konrad@streit-kr.de
Bernat Font, University of Southampton, Southampton/UK, b.fontgarcia@soton.ac.uk
Marin Lauber, University of Southampton, Southampton/UK, M.Lauber@soton.ac.uk
Gabriel Weymouth, University of Southampton, Southampton/UK, G.D.Weymouth@soton.ac.uk

Abstract

The design of a kite over a wide range of flow conditions is usually performed with multiple CFD simulations yielding a high computational cost. This work proposes an approach to reduce the cost through a combination of flow field prediction and optimal transport theory. A few CFD runs are used as basis for an interpolation of the flow field. Unlike linear interpolation, optimal transport theory offers a way of interpolating between the known flow fields while maintaining coherent flow structures.

1. Motivation

CFD calculations are currently the most practical method to predict flow features and forces in engineering, but accurate simulations are computationally expensive. Alternatives such as simple analytical models offer ways to calculate a rough estimate but fail to predict many features such as flow separation. And experimental methods can give good estimates, but scaling problems and even higher costs often make them unfeasible, *Tucker (2016).*

Significant research has therefore been focused on reducing the computational cost associated with fluid simulations, and the application of machine learning has showed some promising results. *Raghu and Schmidt (2020)* provide a good overview over basic deep learning methods in a scientific environment. *Guo et al. (2016), Goodfellow et al. (2014), Karpatne et al. (2017), Kim et al. (2019), Raissi et al. (2019)* and *Mao et al. (2020)* trained neural networks using CFD data to predict new flow fields. Different network structures were applied and some introduced physical knowledge into the networks to improve predictions. However, each of these still suffers from a similar problem, as they need training sets of a considerable size, $\mathcal{O}(10^2)$ to $\mathcal{O}(10^5)$. Calculating the CFD data for such a training set would be prohibitively expensive in most cases.

Instead of replacing CFD simulations, *Weymouth and Yue (2015), Weymouth (2019)* have shown ways to efficiently improve surrogate models. By introducing physical information into machine learning methods, the required training data is greatly reduced. An accurate surrogate model can thus be constructed from very sparse data. However, only specific outputs are obtained through this method as opposed to a full flow field obtained from CFD simulations.

A different approach has been proposed by *Bonnard (2019),* by recasting flow field predictions as a machine learning and interpolation problem. As an example, consider the simulations of the flow past a kite at two angles of attacks shown in Fig.1. Given only two simulations such as this, the ML methods discussed above would be impossible to train. However, the two CFD fields can be interpolated to any new angle of attack and the error in this interpolated solution can be established using their governing boundary, continuity and momentum equations. By minimizing this error, the interpolated flow field is brought very close to the correct solution, and using the optimal interpolated flow field as an initial condition was shown to reduce the time necessary for CFD convergence from days to hours compared to a naïve initial condition.

The strength of this approach rests on the fact that the residual error in any candidate interpolated field can be determined quickly using the governing equations, removing the need for any additional training data. However, it relies heavily on the need for an accurate and trainable ML interpolation methodology. *Bonnard (2019)* used inverse distance weighting interpolation, which led to some problems enforcing the boundary conditions. More complex interpolation methods such as polynomial or Kriging models

could potentially improve predictions, however a completely different perspective is proposed in this work.

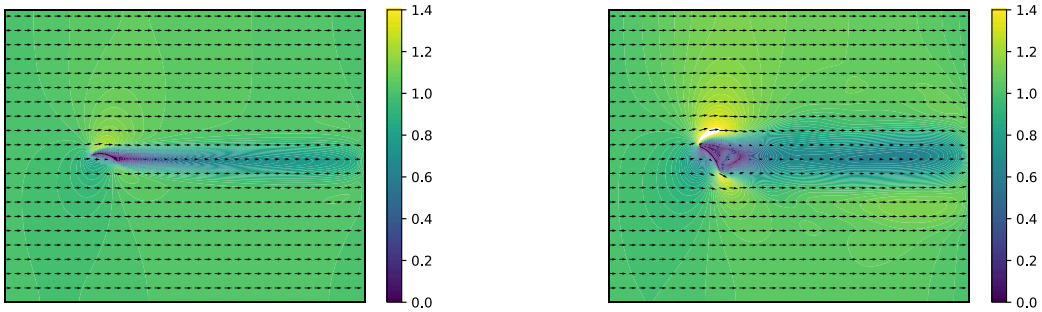

Fig.1a: $\alpha = 10^{\circ}$ Fig.1b: $\alpha = 40^{\circ}$

Fig.1: Velocity Fields

By interpreting vorticity distributions as probability distributions, optimal transport (OT) theory can be applied. An introduction to optimal transport theory and its numerical application can be found in *Peyré and Cuturi (2019)*. It is currently used intensively in image processing, an overview over which can be found in *Papadakis (2015)*. Originally developed by the French mathematician Monge at the end of the 18th century, optimal transport considers both the distance between points in distributions (ground cost) and the mass or density at each point. The optimal transport map between distributions is then the map requiring the least amount of work to move one distribution to the other. The difference between a classic interpolation scheme such as linear interpolation and optimal transport theory is shown in figures 2 and 3. In each figure, a circle is moved from one side of the domain to the other. As can be seen, linear interpolation fades one circle out and the other one in, while optimal transport moves the circle across the domain. Relating this back to the vorticity field around a kite at different angles of attack, the area of high vorticity at the trailing edge would be expected to slowly move through the domain rather than fading in at one position and out at the other.

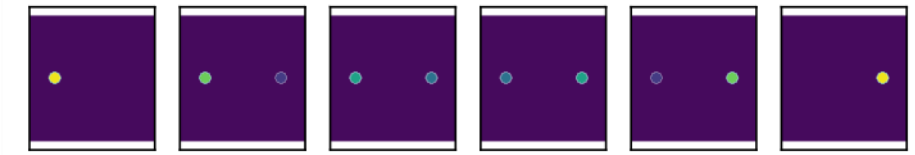

Fig.2: Moving a Circle with Linear Interpolation

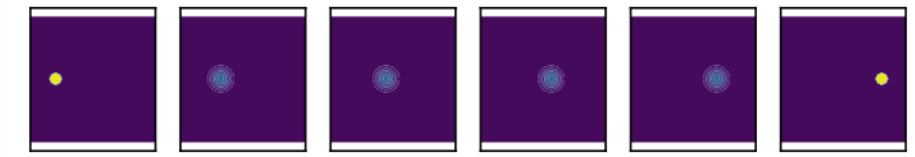

Fig.3: Moving a Circle with Optimal Transport Interpolation

The original OT formulation was extended by the Russian mathematician Kantorovich to allow for mass splitting between distributions. *Wilson (1969)* introduced entropic regularization into optimal transport theory, allowing for the calculation of an approximate solution at a much-reduced cost. *Benamou and Brenier (2000), Cuturi (2013), Benamou et al. (2015)* introduced highly efficient iterative solvers, which was extended by *Solomon et al. (2015)* using a heat kernel approximation of the ground cost. *Bouharguane et al. (2012)* and *Hug et al. (2014)* have applied physical constraints and penalizations such as rigidity to optimal transport theory. With this, they succesfully interpolated shapes and sea surface height charts. It produced good interpolations conserving boundaries very well, however appears to suffer from performance problems.

2. Methodology

This work predicts the flow around a kite at different angles of attack using optimal transport theory to assess its effectiveness as a ML interpolation method. A simplified model of the kite as a 2-dimensional arc segment in a uniform flow is used. CFD simulations at multiple angles of attack α have been carried out. To ensure a steady laminar flow at low angles of attack, the Reynolds number is set to 150, however some unsteadiness in the wake is to be expected at very large α. Two exemplary velocity fields are shown in Fig.1, at $\alpha = 10°$ and $40°$. At $10°$, the flow follows the curvature of the kite, producing only a narrow wake. At $40°$ on the other hand, the flow is seperating at the leading and trailing edges, producing a big area of low velocity flow behind the kite. As the methods implemented are built on equations for steady flow, the following calculations have thus been limited to the range of $\alpha = 0°$ to $20°$.

A flowchart of the proposed method is shown in Fig.4. To start the process, a few flow conditions have to be known, e.g. from CFD. From these training points, the flow field is interpolated to a new condition. The changes between conditions could potentially be anything from inflow velocity to body shapes, in this work different angles of attack are being looked at. Once a new flow field has been calculated, its physical error is considered. If the magnitude of the error is deemed sufficiently small, the field is put out. If it is not, the interpolation parameters are updated and a new flow field is calculated until the error is driven down sufficiently.

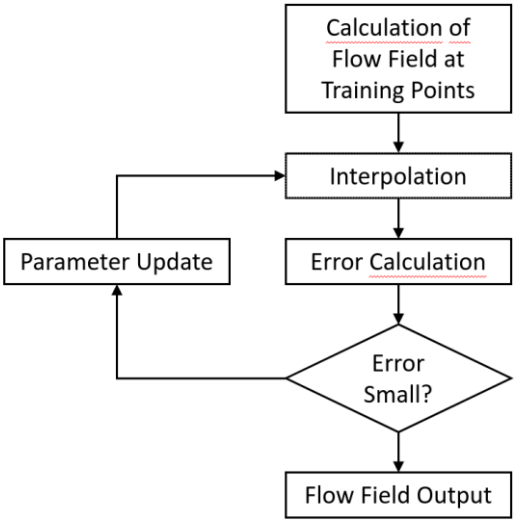

Fig.4: Methodology Flowchart

2.1 Velocity and Vorticity

Full field predictions imply that all of the velocity components and the pressure field are computed. However, independently interpolating these multiple fields would increase the computational cost and can lead to issues with differing levels of accuracy/error in the different fields, *Bonnard (2019)*. We can avoid these issues in an incompressible two-dimensional flow by interpolating the single z-vorticity field and using this to determine all of the other flow variables.

In a 2D steady and incompressible flow, and using the Helmholtz decomposition, the flow can be decomposed into an irrotational (the background flow) and a rotational part.

$$u = u_\infty + u_\omega \tag{2.1}$$

The rotational part of the velocity is purely defined by the vorticity ω and can be re-obtained from the vorticity field using the law of Biot-Savart

$$u_\omega(x) = -\frac{1}{4\pi}\int_{V'} \frac{r\times\omega(x')}{||r||^3} dV' \tag{2.2}$$

where $r = x - x'$ and ω are known and thus the velocity field can be calculated. As one knows the background flow, interpolating the vorticity field gives sufficient information to reconstruct the entire velocity field. The vorticity field will therefore be interpolated in this work.

Figs.5 and 6 show a velocity field obtained from the simulation alongside the corresponding vorticity field. As can be seen, the majority of the flow is in fact still nearly uniform, while the non-uniform flow is found close to the high vorticity areas.

In a discrete numerical setting, Eq.(2.2) becomes a simple summation of the influence of each point on each point. The computational cost therefore goes with $\mathcal{O}(N^2)$. As can be seen in Fig.6, however, the majority of the grid points has a negligible vorticity magnitude. By only calculating the influence of the M points with non-negligible vorticity, the cost can be reduced to $\mathcal{O}(NM)$.

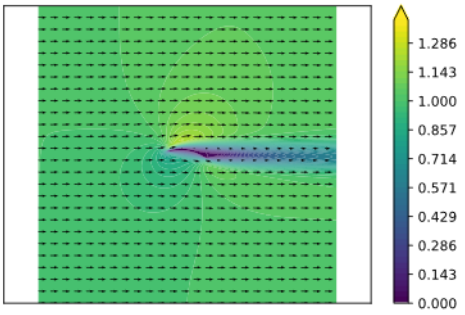

Fig.5: Velocity Field at α=10°

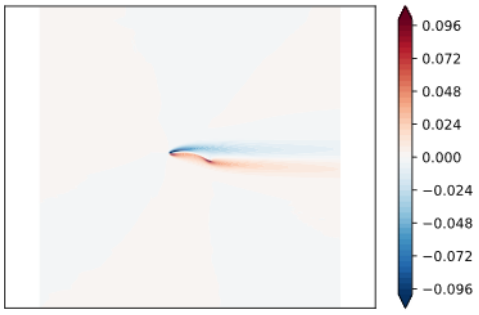

Fig.6: Vorticity Field at $\alpha = 10°$

2.2 Interpolation

The linear interpolation method as used in the previous work on flow field prediction, *Bonnard (2019)*, can produce very unphysical results. In this work, the use of optimal transport is proposed instead.

Optimal transport theory can offer a more intuitive way of interpolation between measures as has been shown in figures 2 and 3. The first mathematical formulation as done by Monge reads

$$\min_{\sigma\in Perm(n)} \frac{1}{n}\Sigma_{i=1}^{n} C_{i,\sigma(i)} \tag{2.3}$$

where $C_{i,\sigma(i)}$ is the ground cost matrix, describing the cost of moving mass between points in the domain, and $\sigma(i)$ the function assigning each point i in one distribution to one point j in the other.

Monge described the problem as a worker trying to move one pile of earth of prescribed shape into a different pile of a prescribed shape. The minimal work necessary for this task depends on the distance walked, called the ground cost, as well as the mass of earth carried on each walk.

While Monge was looking for a map associating each point x_i to a single y_j, this has since been generalized to allow for mass splitting (one point x_i to multiple y_j). Originally introduced by *Wilson (1969)*, entropic regularization can be used to obtain a blurred out, approximate solution at a significantly lower cost. Using the Sinkhorn-Knopp algorithm as introduced by *Cuturi (2013)*, the optimal transport plan between distributions can be calculated significantly faster than with linear programs used before. The algorithm reads

$$u^{(l+1)} = \frac{a}{Kv^l} \tag{2.4}$$

$$v^{(l+1)} = \frac{b}{K^T v^{l+1}} \tag{2.5}$$

where a and b are the original distributions and $K = e^{\frac{C}{\text{reg}}}$ is the Gibbs kernel using the cost or distance matrix C and the regularization factor reg. v^0 is initialized arbitrarily as a vector of ones. The vectors u and v can be used to calculate the transportation matrix $P = \text{diag}(u)K\text{diag}(v)$, in which entry $P_{i,j}$ describes the mass moved from position i in distribution a to point j in distribution b. The regularization factor reg can be adjusted and controls the bluriness of the solution. A more blurred out solution usually relates to a faster calculation.

The calculation of the Sinkhorn-Knopp iterations as above still require the storage of all pairwise distances between the two distributions. This leads to extremely high memory requirements on large domains. *Solomon et al. (2015)* showed that instead of the Gibbs kernel, a heat kernel can be used. This does not require the storage of all pairwise distances, instead it only requires the knowledge of how to apply the kernel.

When $c_{i,j} = d_{i,j}^p$, where d is a distance, the commonly used distance measure for optimal transport is the Wasserstein distance defined as:

$$W_p = \left|\Sigma_{i,j} P_{i,j} C_{i,j}\right|^{\frac{1}{p}} \tag{2.6}$$

Given a set of k distributions α_i and weights w_i, the distributions can be interpolated to a distribution β by taking their weighted average using the wasserstein distance:

$$min_{\beta} \Sigma_{i=1}^{k} w_i W_p(\beta, \alpha_i) \tag{2.7}$$

This barycentric interpolation using convolutional distances is implemented and readily available for python in the python optimal transport package, *Flamary and Courty (2017)* and has been used for this work.

2.3 Boundary Conditions

Once an interpolated flow field has been calculated, flow tangency has to be ensured along the immersed body. Without this step, optimizing any interpolation method would always lead to the same result, no matter what point in the design space is the target, as the physical error in the interpolation would not change depending on the desired boundary conditions.

By enforcing the boundary conditions on the body, the flow fields and therefore the phyiscal error is changed. This creates the potential for an optimization towards the best solution. In this work, the boundary conditions on the body are enforced using a vortex line method. This method introduces multiple small vortices along the body, each inducing velocities according to the law of Biot-Savart (eq. 2.2) on the surrounding flow. By solving for the correct vorticity for each of the introduced vortices, flow tangency can be achieved.

2.4 Combining Interpolation and Enforcing of Boundary Conditions

The substep called 'Interpolation' in Fig.4 consists of three steps, outlined in Fig.7:

1. The optimal transport interpolation calculates a new vorticity field from the input vorticity fields (section 2.2)
2. The application of the law of Biot-Savart recovers the flow velocities from this new vorticity field (section 2.1)
3. The vortex line enforces the boundary conditions along the body, ensuring tangential flow (section 2.3)

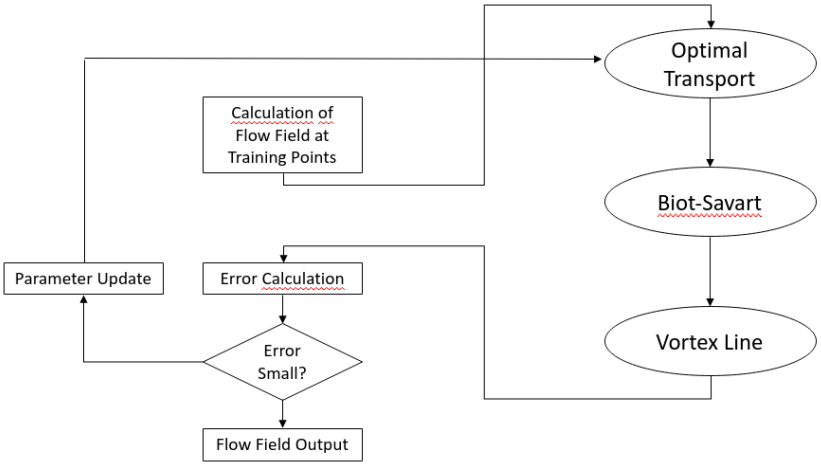

Fig.7: Flowchart of Interpolation sub-steps

These three steps need a total of seven inputs:

1. The training vorticity fields
2. A distance function for the ground cost
3. The interpolation weights
4. The entropic regularization parameter
5. The vorticity threshold for the application of the law of Biot-Savart
6. The definition of the background flow
7. The precise coordinates of the kite at the target condition

The resulting velocity field is used to compute its physical error. Depending on the error, the field is either put out or the interpolation adjusted and started again.

In this work, three cases have been calculated, with the vorticity fields at $\alpha = 0°$, $10°$ and $20°$ as training data. The ground cost is calculated using a heat kernel approximation as outlined by *Solomon et al. (2015)*. The interpolation weights and entropic regularization parameter have been varied, as is shown below in section 3. The background flow is a uniform flow in x-direction of magnitude 1.

2.5 Residual

To optimize the interpolation, a measure is needed to quantify its closeness to the correct solution. If the correct field is known, the difference between the correct answer and the interpolation can be readily calculated. However, the general aim is to develop a method that can predict unknown fields for which such error cannot be calculated.

In this sense, one could construct an arbitrary loss function based on known physics that the predicted field has to adhere to. For example, the continuity error of the interpolated field can be considered as a loss function. Fortunately, continuity is always enforced when obtaining the velocities from the vorticity as described above. The second error commonly calculated for fluid simulations is the momentum error. This can be calculated from the vorticity transport equation as

$$\epsilon = \frac{\partial \omega}{\partial t} + u\frac{\partial \omega}{\partial x} + v\frac{\partial \omega}{\partial y} - \nu\left(\frac{\partial^2 \omega}{\partial x} + \frac{\partial^2 \omega}{\partial y}\right) \tag{3.10}$$

A fully correct solution would show a momentum error of 0 over the entire field, however numerical approximations usually do not reach this. Instead, the simulations are tweaked until the momentum error converges to a reasonably small value. While we know that there is a unique solution at which the momentum error vanishes, merely minimizing it does not necessarily lead to a coherent and correct

flow. The calculation of the momentum error will therefore later be accompanied by calculations of the error in the vorticity and velocity fields.

3. Results

3.1 Comparison with linear interpolation

The new OT method is compared to a linear interpolation scheme to give a first measurement of the proposed method's performance. Fig.8 illustrates the development of the momentum error and the error in the vorticity field.

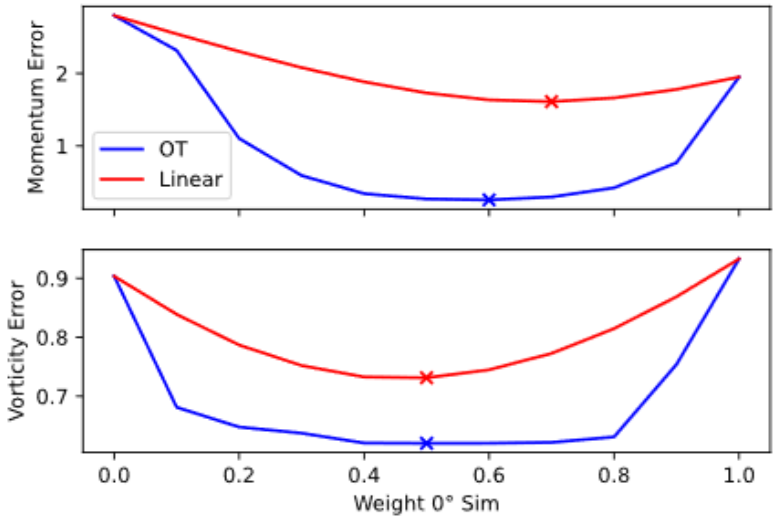

Fig.8: Errors in Linear vs. Optimal Transport Interpolation

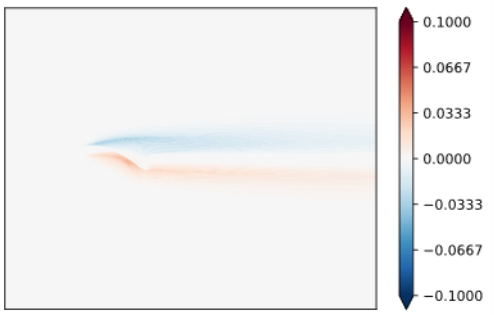

(a): Optimal Transport

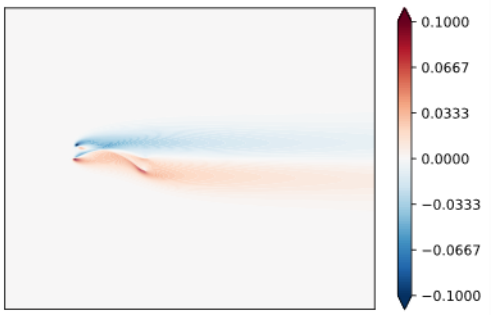

(b) Linear

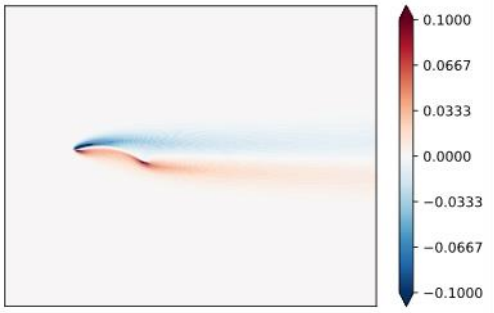

(c) Simulation

Fig.9: Vorticity Fields

The interpolation was done using the $\alpha = 0°$ and $20°$ simulations as bases, trying to obtain the field at $10°$. The x-axis gives the weight of the $0°$ simulation. The momentum error is normalized by the

momentum error in the 10° simulation. The vorticity error is defined as the norm of the difference between the simulated vorticity field and the interpolated vorticity field, normalized by the norm of the vorticity in the simulation.

As can be seen, the proposed method outperforms the linear interpolation significantly, both in the momentum error and the vorticity error calculation. Fig.9 illustrates a further advantage of the optimal transport approach. While the vorticity field obtained through linear interpolation (9b) distinctly shows the two pairs of leading and trailing edges of the two interpolation bases, the optimal transport interpolation shows a much more coherent flow structure, Fig.9a. There is still a significant difference to the simulated vorticity field as shown in Fig.9c, however the performance gain over linear interpolation is significant.

3.2 Weights

For three different cases, the interpolation weights have been systematically altered. The cases are:

1. CFD Data at $\alpha = 0^\circ$ and 10°, interpolated to $\alpha = 5^\circ$
2. CFD Data at $\alpha = 0^\circ$ and 20°, interpolated to $\alpha = 10^\circ$
3. CFD Data at $\alpha = 0^\circ$ and 20°, interpolated to $\alpha = 5^\circ$

As can be seen, cases 1 and 2 are symmetric, while the interpolation is expected to be significantly biased for case 3. The development of the momentum error and vorticity error over the interpolation weights are plotted in Fig.10.

It can be clearly seen, that optimal transport theory produces significantly better predictions. In all three cases, the minimum momentum error is more than twice as big when using linear interpolation. The difference is not quite as drastic when looking at the error in the vorticity field, however the optimal transport theory is still outperforming linear interpolation in all three cases.

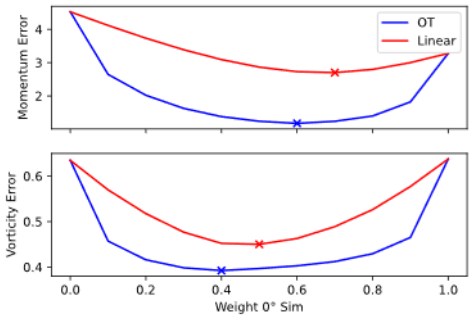

(a) 0° and 10° to 5°

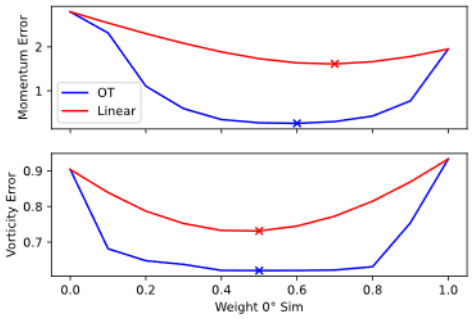

(b) 0° and 20° to 10°

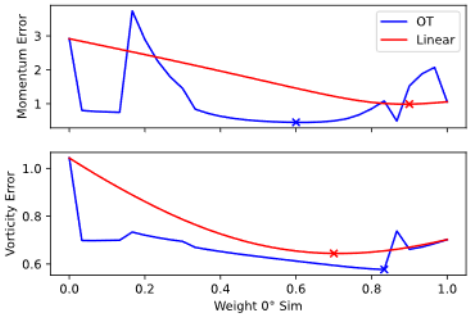

(c) 0° and 20° to 5°

Fig.10: Interpolation Weights and Errors

The calculation of the error in the vorticity field would not be possible in the intended application, however it makes a validation of the results possible. In this case, it shows a significant difference

between the interpolation weight that leads to the minimum momentum error in the predicted field and the interpolation weight leading to the smallest difference in vorticity. Optimizing an interpolation purely on the base of the momentum error would therefore not lead to the optimal result. However, the curve of the momentum error is relatively flat, a shift of the interpolation weights to gain the minimum error in vorticity would not greatly increase the momentum error.

3.3 Regularization

As first introduced by *Wilson (1969)*, entropic regularization can be used to increase calculation speed for optimal transport problems. The higher the regularization factor, the more blurred out results appear. Fig.11 illustrates the differences in the relevant case. Each plot shows the vorticity field obtained from optimal transport using a different setting for the entropic regularization, interpolating from $0°$ and $10°$ to $5°$.

As can be seen, at a very high setting (Fig.11a), only two distinct areas of vorticity are visible. Areas of the same sign vorticity are still visible with lower regularization, however they are much more localized. At a regularization factor of $1e^{-3}$, the location of the kite can already be estimated. At $1e^{-7}$, the high vorticity area can be seen following the curvature of the arc. A further decrease in regularization, however, does not show any more detail in the flow.

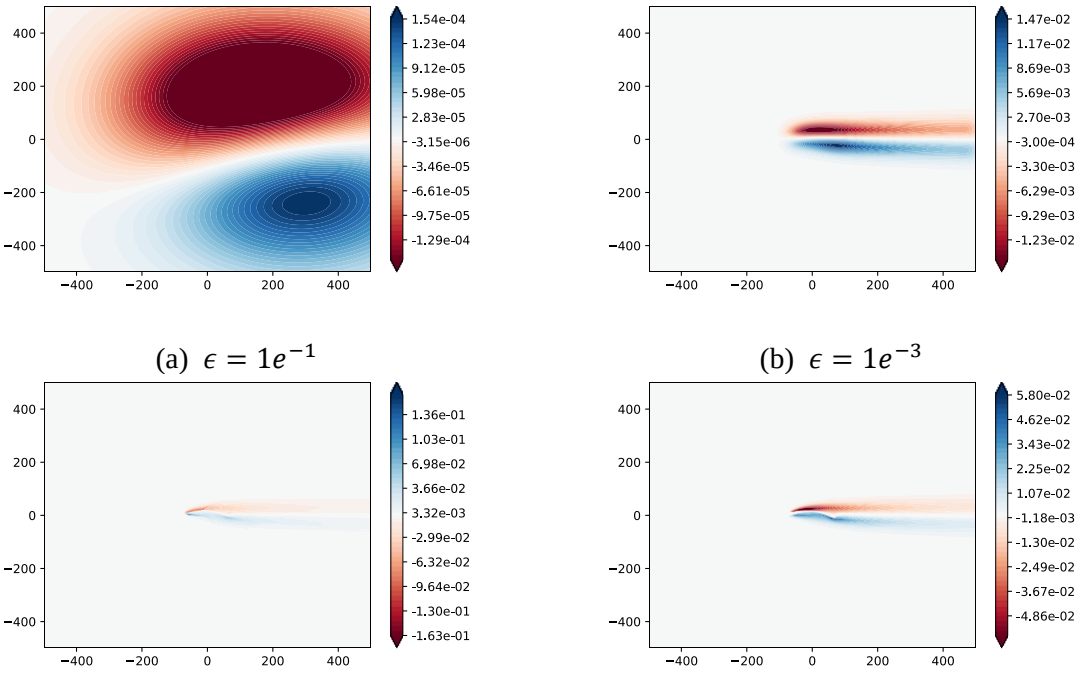

(a) $\epsilon = 1e^{-1}$ (b) $\epsilon = 1e^{-3}$

(c) $\epsilon = 1e^{-5}$ (d) $\epsilon = 1e^{-7}$

Fig.11: Vorticity Fields with different Reguarizations; Note different colorscales due to different value ranges

Fig.12 quantifies the prediction performance depending on the regularization factor. The right half of the plot shows the expected behaviour, a decrease in vorticity error being traded off with an increase in calculation time. The left part of the plot has to be further examined, as an instability is expected at very low regularization factors due to machine precision limits. The numbers obtained here, however, seem to show the most efficient combination of calculation time and accuracy at low regularization.

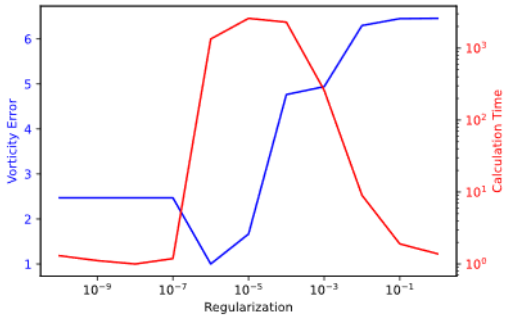

Fig.12: Prediction accuracy and calculation time depending on regularization factor

3.4 Lift & Drag Coefficients

As the ultimate goal of the flow prediction is to obtain the forces acting on the kite, these have been calculated at different angles of attack. First, the induced forces have been calculated from the pressure and velocity fields near the body. As shown in Fig.9, the near-body region of the predicted fields are not in very good agreement with the CFD target fields. This led to poor accuracy of the predicted force. A control volume approach was therefore used to obtain the forces from momentum changes. The results of both methods are illustrated in Fig.13 for one interpolation case. The vertical blue line shows the correct lift and drag coefficients as calculated with the CFD solver. The blue bar indicates the result of the control volume approach on the CFD data, showing reasonable accuracy. While the lift prediction using the pressure approach shows a reasonable result when using linear interpolation, the optimal transport interpolation results in a coefficient outside the range of coefficients in the training simulations (0.1 to 1.2). The control volume predictions show even less accurate results. Looking at the drag coefficients, neither interpolation or force calculation methods predict accurate forces.

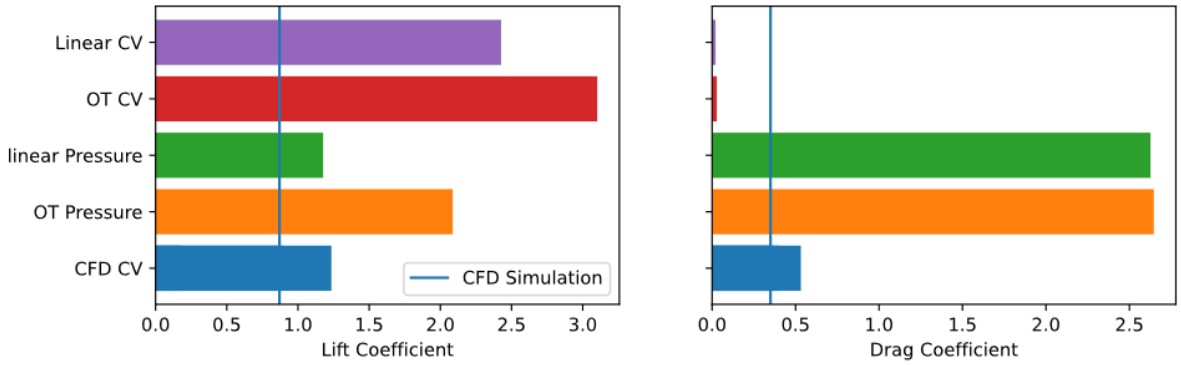

Fig.13: Lift and Drag Coefficients using different calculation methods, $\alpha = 0°$ and $20°$ to $10°$

4. Conclusion

A method using optimal transport (OT) for full flow field prediction has been developed based on the concept of full flow field ML interpolation, leveraging the known governing equations to avoid costly training data. This new approach was applied to a kite simulation test case and the OT interpolatation method was shown to outperform an inverse distance weighting method significantly. Both the momentum error and the error in the interpolated vorticity field were substantially lower. OT predicted fields displayed more coherent structures in comparison to linear interpolation, although some discrepancy to target CFD data was still observed. While the use of convolutional optimal transport was reasonably fast on the large domain, it produced diffused interpolated vorticity fields which limited the accuracy on the calculation of the forces induced to the body. Standard OT interpolation also suffered from relatively few parameters to optimize over (regularization and interpolation weights). These parameters did not offer enough learning capacity to reduce the error in the OT interpolated field to a level matching CFD data. A different approach using an anisotropic ground cost could aid the transportation of the field with the body rotation hence providing more accurate interpolations. An

investigation into OT with physical penalizations, such as introduced by *Bouharguane et al. (2012)*, *Hug et al. (2014),* in combination with efficient algorithms could also improve the current results. Overall, the concept of OT interpolation in combination with physics based machine learning has the potential to greatly speed up generalization of sparse CFD results across a design and operational space, and further research in this direction offers many interesting theoretical and practical problems of interest.

References

BENAMOU, J.; BRENIER, Y. (2000), *A computational fluid mechanics solution to the Monge-Kantorovich mass transfer problem*, Numerische Mathematik 0, pp.375-393

BENAMOU, J.D.; CARLIER, G.; CUTURI, M.; NENNA, L.; PEYRÉ, G. (2015), *Iterative bregman projections for regularized transportation problems*, SIAM J. Scientific Computing 37(2), pp.A1111-A1138

BONNARD, H. (2019), Physics-Based Machine Learning for Flow-Field Prediction Using Small Dataset.

BOUHARGUANE, A.; MAITRE, E.; OUDET, E.; PAPADAKIS, N. (2012), *Multiphysics optimal transportation and image analysis*, https://hal.archives-ouvertes.fr/hal-00740671

CUTURI, M. (2013), *Sinkhorn distances: lightspeed computation of optimal transportation distances*, Advances in Neural Information Processing Systems 26, pp.1-13

FLAMARY, R.; COURTY, N. (2017), *POT Python Optimal Transport library*, https://github.com/rflamary/POT

GOODFELLOW, I.J.; POUGET-ABADIEY, J.; MIRZA, M.; XU, B.; WARDE-FARLEY, D.; OZAIRZ, S.; COURVILLE, A.; BENGI, Y. (2014), *Generative adversarial nets*, Advances in Neural Information Processing Systems 3, pp.2672-2680

GUO, X.; LI, W.; IORIO, F. (2016), *Convolutional neural networks for steady flow approximation*, ACM SIGKDD Int. Conf. Knowledge Discovery and Data Mining, pp.481-490

HUG, R., MAITRE, E.; PAPADAKIS, N. (2014), *Multi-physics Optimal Transportation and Image Interpolation*, ESAIM Mathematical Modelling and Numerical Analysis 49(6)

KARPATNE, A.; ATLURI, G.; FAGHMOUS, J.H.; STEINBACH, M.; BANERJEE, A.; GANGULY, A.; SHEKHAR, S.; SAMATOVA, N.; KUMAR, V. (2017), *Theory-Guided Data Science: A New Paradigm for Scientific Discovery from Data*, IEEE Trans. on Knowledge and Data Engineering 29(10), pp.2318-2331

KIM, B.; AZEVEDO, V.C.; THUEREY, N.; KIM, T.; GROSS, M.; SOLENTHALER, B. (2019), *Deep Fluids: A Generative Network for Parameterized Fluid Simulations*, Computer Graphics Forum 38(2), pp.59-70

MAO, Z.; JAGTAP, A.D.; KARNIADAKIS, G. E. (2020), *Physics-informed neural networks for high-speed flows',* Computer Methods in Applied Mechanics and Engineering 360, p. 112789

PAPADAKIS, N. (2015), *Optimal Transport for Image Processing*, Université de Bordeaux, https://hal.archives-ouvertes.fr/tel-01246096v8.

PEYRÉ, G.; CUTURI, M. (2019), *Computational optimal transport*, Foundations and Trends in Machine Learning 11(5-6), pp.355-206

RAGHU, M.; SCHMIDT, E. (2020), *A Survey of Deep Learning for Scientific Discovery*, pp.1-48, http://arxiv.org/abs/2003.11755

RAISSI, M.; PERDIKARIS, P.; KARNIADAKIS, G. E. (2019), *Physics-informed neural networks: A deep learning framework for solving forward and inverse problems involving nonlinear partial differential equations*, J. Computational Physics 378, pp.686-707

SOLOMON, J.; FERNANDO DE GOES, F.; PEYRE, G.; CUTURI, M.; BUTSCHER, A.; NGUYEN, A.; DU, T.; GUIBAS, L. (2015), *Convolutional Wasserstein distances: Efficient optimal transportation on geometric domains*, ACM Transactions on Graphics 34(4)

TUCKER, P.G. (2016), Advanced computational fluid and aerodynamics, Advanced Computational Fluid and Aerodynamics, pp.1-567

WEYMOUTH, G.D. (2019), *Roll Damping Predictions using Physics-based Machine Learning*, COMPIT Conf., Tullamore

WEYMOUTH, G.D.; YUE, D.K.P. (2015), *Physics-based learning models for ship hydrodynamics*, SNAME Trans. 121(1), pp.772-783

WILSON, A.G. (1969), *The Use of Entropy Maximising Models, in the Theory of Trip Distribution, Mode Split and Route Split*, J. Transport Economics and Policy 3(1), pp.108-126

Reducing Friction with Passive Air Lubrication: Initial Experimental Results and the Numerical Validation Concept of AIRCOAT

Johannes Oeffner, Fraunhofer CML, Hamburg/Germany, johannes.oeffner@cml.fraunhofer.de
Nils Hagemeister, Fraunhofer CML, Hamburg/Germany, nils.hagemeister@cml.fraunhofer.de
Herbert Bretschneider, HSVA, Hamburg/Germany, bretschneider@hsva.de
Thomas Schimmel, KIT, Karlsruhe/Germany, thomas.schimmel@kit.edu
Carlos Jahn, Fraunhofer CML, Hamburg/Germany, carlos.jahn@cml.fraunnhofer.de

Abstract

The EU project AIRCOAT aims to develop a passive air lubrication technology for ships. Using self-adhesive foils instead of paints and inspired by the Salvinia effect, an air coated ship hull is meant to reduce friction, biofouling, corrosion and noise. This paper outlines the validation concept to quantify the potential friction reduction for a micro-structured air keeping surface for ships. It further describes the experimental setup of the visualization flow tank to investigate velocity profiles and the validation of the CFD code by simulating the HSVA HYKAT and preliminary friction reduction results from the SVA friction tunnel experiments.

1. Introduction

Active air lubrication is considered as an energy saving technology of high potential for the shipping industry. It is well known that frictional forces are proportional to fluid viscosity, giving rise to a strong motivation to lower the viscosity of the fluid. Without bubble size regulation and monitoring, inducing air in form of bubbles into the boundary layer mainly modulates the viscosity of water *Busse and Sandham (2012), Verschoof et al.* (*2016)*. Experiments with injecting small bubbles can produce a drag reduction of up to 22%, *Butterworth et al. (2015), Van den Berg et al.* (*2005)*. Active air lubrication system are already commercially available and demonstration tests show net average energy efficiency savings of up to 4.3 %, *Shell (2015)*. Such active air lubrication systems require injection of air upstream in order to maintain a finite mass flow, *Elbing et al. (2008)*.

1.1. A bioinspired air keeping surface

Contrary to active air lubrication, the aim of the current EU project AIRCOAT (Air Induced friction Reducing ship Coating) is to develop a passive air lubrication technology inspired by nature. The bioinspired technology mimics the floating water fern ‘Salvinia molesta’, which forms a permanent air layer when submerged in water *Barthlott et al. (2010)* and is able to maintain a stable air layer under pressure, *Gandyra (2020).* The special surface structure and resulting properties of the coating suffice to establish and retain an air layer. This means that no additional air or energy have to be supplied and the air layer also remains effective when the ship is not moving, setting AIRCOAT apart from bubble inducing systems available on the market.

Based on this so called Salvinia effect, that is enabled by specific surface topology (and a combination of hydrophilic and hydrophobic areas), the team of nanotechnologists from the Karlsruhe Institute of Technology (KIT) developed an artificial surface that can maintain an air layer under water for several years. This technology was transferred onto self-adhesive foils in AIRCOAT and can be used to coat ships, boats and other marine structures, Fig.1. For an overview of the concept see Fig.2 in *Oeffner et al. (2020)*. The AIRCOAT foil creates a thin permanent air layer between the immersed hull and the surrounding water, resulting in two major benefits. On the one hand, there will be a significant reduction in frictional resistance. The potential is massive: Estimations assuming friction coefficient reduction scenarios from 2-20% for an AIRCOAT foil applied to the global IMO-registered fleet could reduce annual fuel cost by millions of Euros, *Oeffner et al. (2020)*. On the other hand, the air layer will form a physical barrier for marine organisms, preventing the attachment of biofouling and thus the increase of frictional resistance over time.

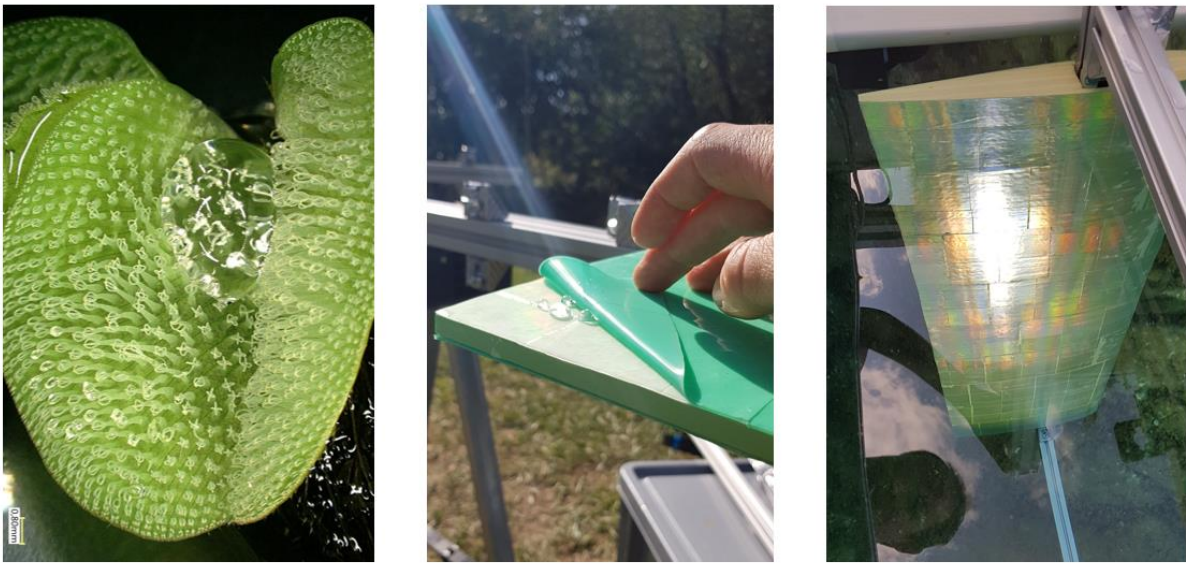

Fig.1: Images of the biological template (‘Salvinia molesta’) with a water droplet (indicating the Salvinia effect) on its surface with the characteristic eggbeater shaped structures (left); the AIRCOAT foil with a water droplet on its surface on land (middle) applied on a foil section and submerged in water (right). Here, the rainbow coloured reflections show the air layer.

Transferring the small microstructure characteristics of a Salvinia plant onto sea going ships (e.g. container ships) – which are among the largest maritime macrostructures – and demonstrating its effectivity is an ambitious task that involves a well-defined validation method. The AIRCOAT project does this by means of combining experimental and numerical methods to upscale results from laboratory prototypes to application of full-scale solutions in operational environments. Here, small- and large-scale laboratory experiments will investigate the air retaining and friction reducing capabilities of the surface. Visualisation techniques will be used to determine the phenomena occurring at the air-water interface. In parallel, a set of numerical studies at different levels (small, large and full scale) will be carried out to estimate the drag reduction for a sea going ship coated with AIRCOAT.

1.2. Friction Reduction of AIRCOAT

A fluid flowing along an immovable solid wall is subject to the no-slip condition and thus forms a boundary layer through which the fluid velocity increases from zero (at the wall) to freestream velocity normal to the surface. If the fluid flows along a liquid/gas interface the conditions differ. In the case of AIRCOAT, where an air layer exists between liquid and solid surface, a reduction in normal velocity gradient occurs. One can say, that part of the boundary layer lies within the air layer which allows a certain amount of slip between the wall and the water, the so-called slip velocity, Fig.2.

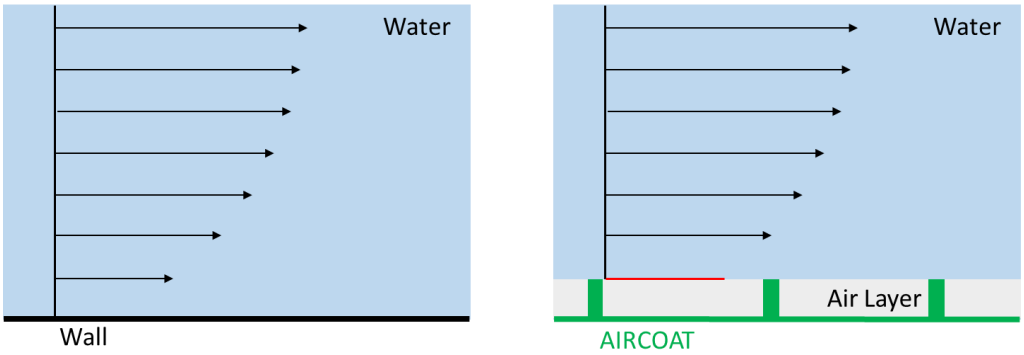

Fig.2: Boundary layer of surface without and with AIRCOAT applied. Black arrows indicate velocity profile normal to a solid wall with zero velocity due to no-slip-condition (left) and normal to an air layer (right), where slip velocity (red)occurs at the air/water interface.

Since the velocity gradient at the phase boundary determines the shear stress and the gradient is at its maximum at the wall, friction is reduced, *Busse and Sandham (2012)*. Ideally, the boundary layer would be entirely contained in the air layer. However, the resulting air layer would be unstable. Additionally, the air needs to adhere to the hull which necessitates areas of contact between the hull and the water on the microscopic scale. This physical constraint further lowers the achievable reduction in friction, the quantification of which is a major task of the AIRCOAT project.

1.3. Validation difficulties

One of the major challenges in this validation process is reaching Reynolds numbers in the order of magnitude typical for ships (approx. 10^9). In model tests a low viscosity fluid can be used to increase the Reynolds number for friction experiments. Since the air water interface is of particular importance in this case, changing the fluid is not an option which limits the achievable Reynolds number during experiments to about 10^7. The second experimental option would be to build a full-scale prototype which is not realistic within the time and budget of the project.

Due to the novelty of the AIRCOAT technology, the laws for scaling the effects from small to full scale application are yet to be determined. Thus, it is not known if and how the effects of AIRCOAT depend on the Reynolds number.

It was therefore decided to employ numerical methods and simulate a ship at full scale to demonstrate the efficiency of the technology. However, resolving the microscopic surface structure and associated physics in such a macroscopic model is practically impossible. To overcome this drawback, the properties of the coating will be incorporated into a wall function. A combination of computational fluid dynamics (CFD) and experiments is utilised to design and validate this wall function.

2. AIRCOAT's drag reduction validation concept

Starting from low Reynolds numbers (10^0) and small probe lengths (10^{-2} m), test body dimensions and flow speed during the experiments will be gradually increased for the various experiments until reaching the maximum lengths of 8 m and Reynolds numbers of Re = 10^7, respectively.

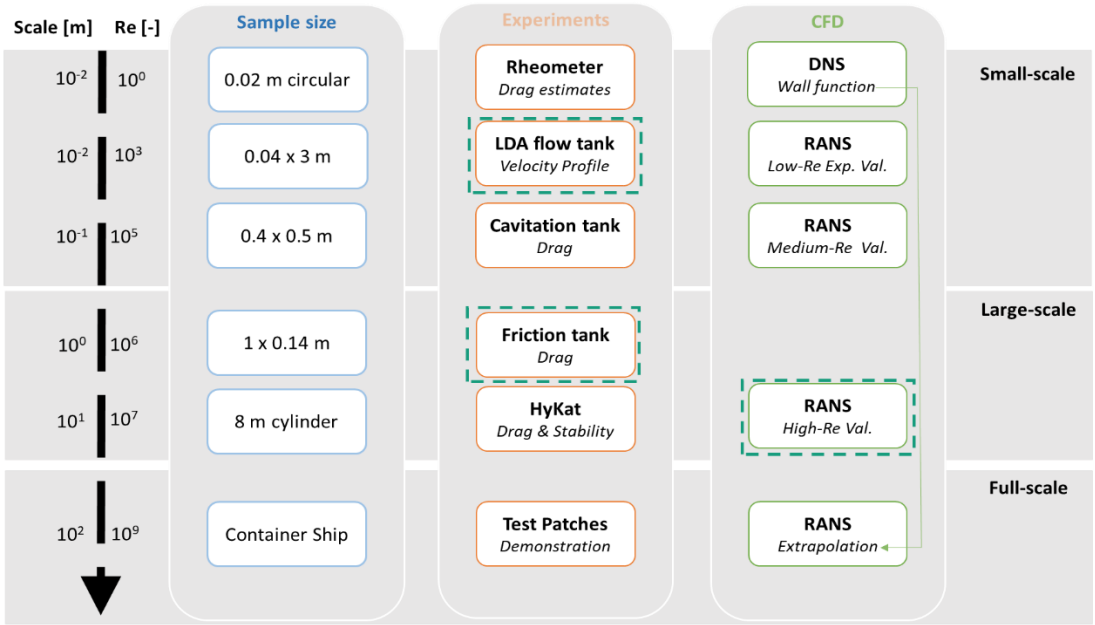

Fig.3: AIRCOATs validation process chain from micro to macroscopic scales (top to bottom) by means of increasing sample sizes and Reynolds numbers at different experiments which are validated by numerical simulations (CFD) in order to allow for a final full-scale extrapolation. Green dashed boxes represent the focus items of this paper.

Investigations will be conducted at three scales: Small- and large-scale laboratory experiments will investigate the air retaining and friction reducing capabilities of the surface. Visualization techniques will be used to determine the phenomena occurring at the air-water interface. In parallel, a set of numerical studies at different levels (small-, large- and full-scale) will be carried out in order to validate the codes and gain additional insight into the flow phenomena around the phase boundary. Experiments and Numerical simulations complement each other.

The final full-scale validation to estimate the drag reduction for a sea going ship virtually coated with AIRCOAT will be conducted with a RANS code equipped with an AIRCOAT specific wall function. The entire process chain for validation of AIRCOAT is depicted in Fig.3 and further described in the following subchapters.

This paper will focus on three items of the above explained process chain for which Fraunhofer CML is in charge within the AIRCOAT project: LDA flow tank design, friction tank experiments and AIRCOAT RANS model validation (see dashed green boxes in Fig.3).

2.1. Small-scale

Small-scale experiments with max samples size of 0.2 sqm allow for quick testing in incremental steps while the AIRCOAT surface is constantly readjusted in parallel based on test results. Very low Reynolds number experiments (Re ~ 6) with Rheometer will be done to get drag estimates. To develop the wall function, results from rheometer measurements, DNS simulations and advanced visualization techniques will be coupled. For the latter, Laser Doppler Anemometry (LDA) experiments at low Reynolds numbers (Re ~ 9000) will be done to determine an actual velocity profile normal to the AIRCOAT surface. Furthermore, cavitation tank experiments at medium Reynold number ($Re = 2.27 \cdot 10^6$) shall give initial information on drag reduction at medium Reynolds numbers.

2.1.1. LDA flow tank design

In order to perform the LDA experiments, a gravity driven flow tank has been designed by Fraunhofer CML, Fig.4. A main objective with this experiment is gathering information on the velocity profile, which requires establishing an undisturbed, fully developed flow in the measurement section. Consequently, the tank is designed to reach a maximum flow velocity of 0.5 m/s. Water is supplied to the main inlet from an overflow tank which is fed by a pump. Excess water is lead into another overflow basin to keep the water level in the main inlet constant, Fig.4, top left. These measures are taken to avoid inducing any turbulence and create a constant flow velocity. After acceleration in the vertical tube the flow is deflected to a horizontal direction and led through a rectifier to eliminate any off-axis flow. The length of the rectifier is defined by the diameter of the pipe and has to be minimum two times dI.

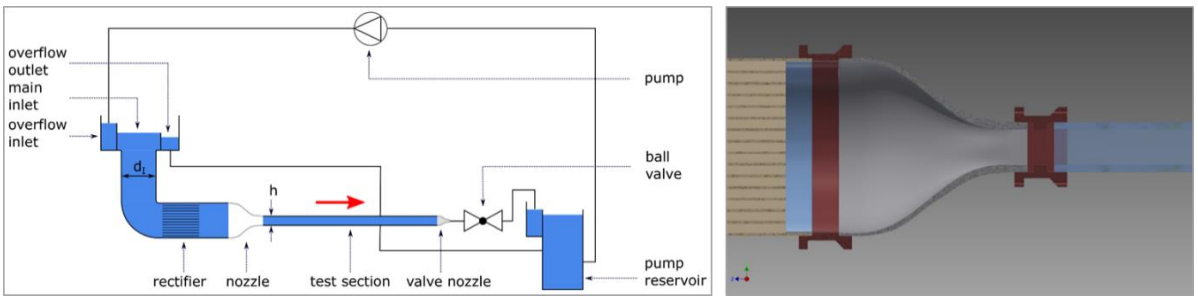

Fig.4: Schematic drawing of the LDA flow tank with major parts and flow paths. The red arrow indicates main flow direction (top left) and detailed rendering of the nozzle with 3D-printed connectors and adjacent parts (top right).

Before entering the test section, a specially manufactured nozzle (see Fig.4, top right) changes the cross section from the round pipe to a square channel. The nozzle is specially designed to accelerate the water as homogenously as possible. The test section is a tube of 3 m length with quadratic cross section (4 x

4 cm). This length (75h) is required to ensure a fully developed boundary layer at its end where the LDA measurement will be performed. The lid of the test section can be removed and will be coated with AIRCOAT. A valve is located behind the test section to adjust the flow speed before the water exits into a tank from where it overflows into the pump reservoir. The setup was designed to the needs of fitting an LDA profile sensor (ILA, LDV fp50 unshifted system) to determine a velocity profile. The boundary layer size was estimated based on the channel height, the flow speed and fluid properties. Based on the minimal resolution of the LDA five to ten measurement points are expected to be located inside the viscous sublayer, allowing for extrapolation of the speeds towards the air-water phase boundary.

2.2. Large-scale

Large-scale hydrodynamic tests allow for high precision measurement of friction drag reduction in a near-operational environment. Here, AIRCOAT surface is investigated with two different setups with different benefits: The SVA friction tunnel reaches relatively large Reynold numbers with small sample sizes, the HSVA HYKAT allows for operational tests, visual control and hydrodynamic conditions closer to real conditions.

2.2.1. Friction tank experiments

The friction tank of SVA Potsdam creates a narrow (~ 12 mm thick) rectangular channel by means of two opposing test plates and determines drag reductions via pressure difference measurement. A full test series allows measuring at a number of pre-set steps in a speed range from 1 m/s up to 18 m/s. The measurement cycle is repeated three times. Twelve pressure sensors measure the pressure. From the pressure difference, the shear stress is derived, which is then translated to a drag coefficient by dividing by dynamic pressure. This allows comparison to the ITTC friction line (*ITTC, 2002)*, which in turn enables extrapolating the results to ship operation conditions, see *Schulze & Klose, 2017* for details.

A production process specifically designed for AIRCOAT was used by KIT to produce air keeping surfaces by structuring thermoplast foils. Additionally, the same production process was used to produce unstructured foils of the same material that act as control for the experiments. Aluminum plates with the dimension of 1m x 0.16 m were coated with the samples using tesa® 4967 double sided tape (0.05 m rolls). Stripes of tesa had to be aligned and samples were carefully applied, however small air bubbles between coating and plates could not prevented. The leading edge of the samples were bend around the sharp leading edge and fixed on the other side. Test plates were installed in the friction tank and measurements were performed.

2.2.2. HYKAT cavitation tunnel

The HYKAT at HSVA, *Weitendorf and Friesch (1990)*, is a closed circulating cavitation tunnel with test section dimensions of (L x W x H) 11 m x 2.8 m x 1.6 m. It can be equipped with a 7.5m long axisymmetric underwater test body located in the center of the test section to conduct friction experiments at medium to large Reynolds numbers ($Re = 10^8$) with respective water speeds of 20 kn. The flow conditions are close to those of real ocean-going ships. The HYKAT allows to coat a larger area with AIRCOAT and the ability to adjust the pressure (between 2.5 and 0.15 bar) facilitates investigating air layer thickness, air retention, air reloading and foil adhesion at varying application depths.

The test body of the HYKAT will be covered with AIRCOAT foil to investigate the drag reduction effect of the air keeping surfaces. Reference measurements with a flat coated test body have been done and act as a validation instrument for the CFD code development as described in the following.

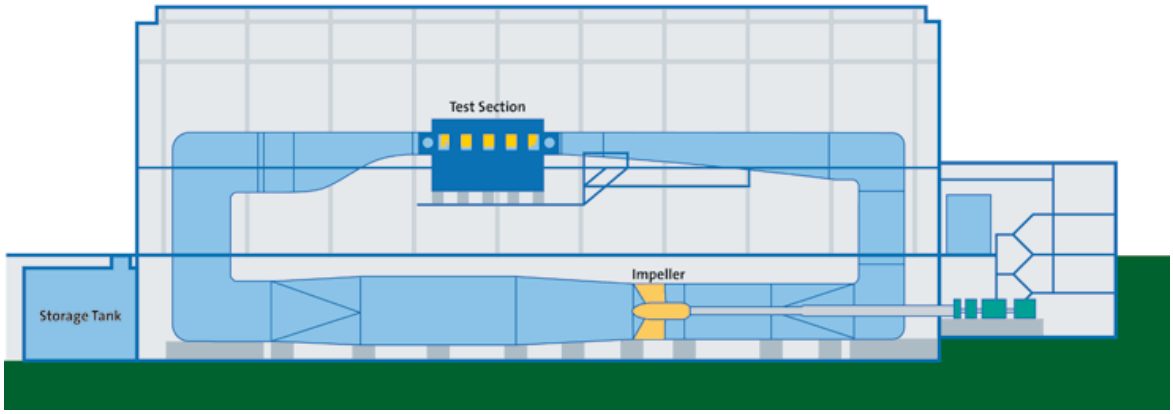

Fig.5: Schematic drawing of the HYKAT cavitation tunnel setup

2.3. Full-scale

Normally, in order to determine the total resistance of a ship, model tests are conducted in ship model basins and results are upscaled to full-size. The associated scaling process has been standardized by the International Towing Tank Conference, *ITTC (2002)*. Therefore, towing tank tests are carried out at Froude similarity, which enables direct transfer of the measured residuary resistance coefficient from the model to the ship. In such an experiment, viscous forces such as friction will not be captured to scale since they depend on the Reynolds number and it's not possible to fulfil Froude and Reynolds similarity simultaneously in a model test. To overcome this issue, friction correlation formulas (such as the ITTC friction line) have been derived which are used to separate residuary from frictional resistance components for the model and determine the frictional resistance of the full-scale ship. The total resistance of the ship is then determined by applying the residuary resistance from the model test and the frictional resistance from the friction correlation formula.

This is not applicable to AIRCOAT as the laws for scaling the effects from small-scale experiments to full-scale are yet to be determined for air keeping surfaces. As AIRCOAT can only reduce viscous resistance, towing tank experiments – which have a significant wave drag component, and are restricted in Reynolds numbers range – are not feasible. Hence, to maximise the measurable effect, AIRCOAT will only be analysed in closed loop cavitation tank experiments (such as the HYKAT), where wave drag components are not existent and total forces are directly related to friction forces. Hence, a reduction of forces would directly represent AIRCOAT friction reduction. Results will be cross-validated by a CFD code that targets to estimate the total effect on a real ship.

Numerically simulating the interaction of the microstructured AIRCOAT surface with a turbulent flow in a three-dimensional volume at transient and two-phase (water and air) flow conditions comes at very high-computational cost. Nevertheless, to understand the drag reducing effect it is crucial to investigate the influence of AIRCOAT on turbulent structure and momentum transfer from water to the surface. Therefore, it will be done on very small scales via Direct Numerical Simulation (DNS) at small Reynolds numbers of Re ~ 300 within the project.

As the final goal is to verify the drag reducing effect, it will be extrapolated and scaled-up to large ocean-going ships numerically. Such ships operate at high Reynolds numbers (Re ~ 10^9), hence a RANS CFD code including a turbulence model will be used. The designed wall function will be incorporated in the developed AIRCOAT RANS model.

2.3.1. AIRCOAT RANS model

OpenFOAM v1806 is used to solve the Reynolds-Averaged Navier-Stokes equations. Turbulence is modelled using the k-ω-SST turbulence model and wall functions are used to resolve the boundary layer. The simpleFoam solver with second-order Gauss linear upwind schemes is employed.

A finite-volume approach has been utilized in this study, *Ferziger and Perić (2002)*. Fully unstructured hex-dominant meshes are generated using CFMesh, *Juretic (2015)*. The six steps as shown in Table I will be performed to validate the model.

Table I: The six steps of the AIRCOAT RANS code validation

#	Setup	Re	Flow	Surface	Validation of
1	HYKAT	High	Single-phase	unstructured	AIRCOAT RANS code
2	Container Ship	Very High	Two-phase	unstructured	Literature data (KCS model)
3	Cavitation tank	Medium	Two-phase, WF	AIRCOAT	RANS + Wall function
4	LDA flow tank	Low	Two-phase, WF	AIRCOAT	Velocity profile
5	HYKAT	High	Two-phase, WF	AIRCOAT	Drag Reduction
6	Container Ship	Very High	Two-phase, WF	AIRCOAT	AIRCOAT full-scale

2.3.2. High-Re Validation

In this paper the first step will be described which is to verify the established CFD model by comparing experiment and simulations, this being the prerequisite to use the code for future simulations. Therefore, HYKAT experiments with smooth surface, which represents the facility with hydrodynamic conditions as closest as possible –but controllable– to real operation are to be validated. If model and experiment align, results from experiments with AIRCOAT surface can be numerically upscaled to allow estimating the full-scale AIRCOAT potential.

Only the test section of the HYKAT experiment, Fig.5, has been replicated for the simulations. A sketch of the setup can be seen in Fig.6. The underlying coordinate system is right-handed rectangular cartesian. The origin lies in the center of the numerical tank. The positive z-axis points upwards and the positive x-axis points towards the inlet. The flow enters the test section from the left, i.e. along the negative x-direction.

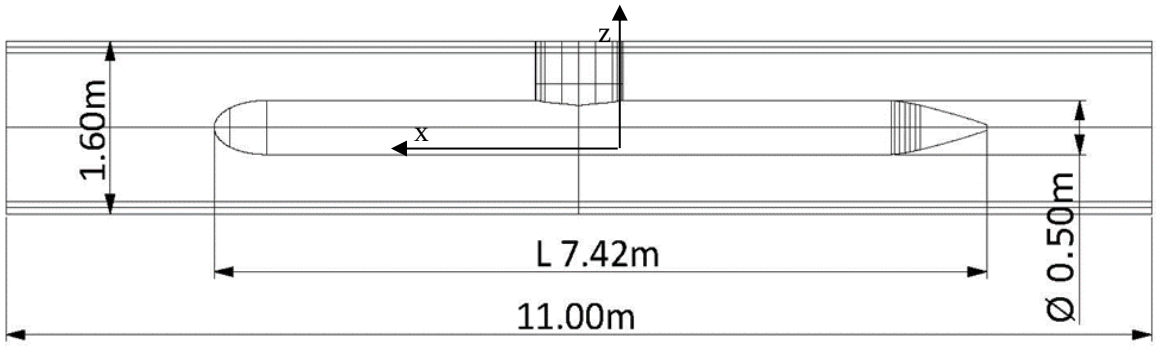

Fig.6: Sketch of case setup with the test body located inside the test section

A grid study with five different meshes was done to investigate the sensitivity of the solution towards the resolution of the geometry at a Reynolds number of $Re = 1.6 \cdot 10^7$. The mesh size with the best resolution to computational cost ratio was used for a validation study, which was performed at five speeds to cover the entire range of the experimental tests from $Re = 1.6 \cdot 10^6$ to $Re = 7.5 \cdot 10^7$. In order to keep the non-dimensional wall distance y+ constant, five grids (one per speed) were created ranging from 12 up to 15 million cells.

3. Results

3.1.1. LDA flow tank design

The flow tank was constructed based on the described design, Fig.7. Validation experiments without AIRCOAT are currently undertaken in order to verify the setup. Later, the lid of the test section will be coated with AIRCOAT foil and LDA measurements will be done in order to investigate the velocity

profile and obtain valuable information on slip length and drag reduction effects and to cross-validate the above described CFD code.

Fig.7: Image of the constructed the LDA flow tank with major parts and flow paths. The red arrow indicates main flow direction (top left) and detailed rendering of the nozzle with 3D-printed connectors and adjacent parts (top right).

3.1.2. Friction Tank

Standard test procedures (for details see *Schulze & Klose, 2017)* were used for the control at speeds ranging from 2 to 17 m/s, corresponding to Reynolds number between $Re = 6.3 \cdot 10^5$ and $Re = 5.62 \cdot 10^6$. During first measurements with higher speeds, the control foil detached from the plate, water flowed under the foil and the foil locally ruptured. The reason for this failure was likely bending of the relatively stiff thermoplast at leading edge, where small cracks were visible before installation. Hence, control measurements existed only up to $Re = 2 \cdot 10^6$.

Therefore, the test procedure for the AIRCOAT samples installed in the tank, Fig.8, was modified, and runs with reduced speed up to 6.5 m/s, reps. $Re = 3.16 \cdot 10^6$ to were successfully performed. The air layer was still intact after these runs. Another test with standard test procedures revealed detachment of the foil, Fig.8.

Fig.8: Images of the friction tank experiments at SVA. Left: Flat control installed in the friction tank. Middle: AIRCOAT foil submerged in water after experiments done at 6 m/s – note the clearly visible, silvery shining air layer. Right: AIRCOAT foil installed in the friction tank before (top) and after the last experiment with maximum velocity of 17 m/s (below).

Comparing the drag coefficient values of control and AIRCOAT for the speed range with successful measurements resulted in drag reduction (DR) values between 1% and 3 % drag reduction, Table II.

Table II: Drag reduction (DR) of AIRCOAT foil compared to unstructured control at different Reynolds number (Re) range in the friction tank. Negative values indicating reduction.

Re [-]	$6.3 \cdot 10^5$	$7.1 \cdot 10^5$	$7.9 \cdot 10^5$	$8.9 \cdot 10^5$	$1.0 \cdot 10^6$	$1.1 \cdot 10^6$	$1.3 \cdot 10^6$	$1.4 \cdot 10^6$	$1.5 \cdot 10^6$	$1.8 \cdot 10^6$	$2.0 \cdot 10^6$
DR [%]	-3.0%	-1.6%	-1.2%	-1.3%	-1.5%	-1.6%	-1.5%	-1.2%	-1.0%	-1.2%	-2.4%

3.1.3. High-Re Validation

Deviations from 1% to 10% are found between experiment and simulation, Fig.9, depending on flow speed. Furthermore, the accuracy of the numeric solution is found to increase significantly with speed, Fig.10, which is ascribed to the presence of laminar flow in the experiment, especially at lower speeds.

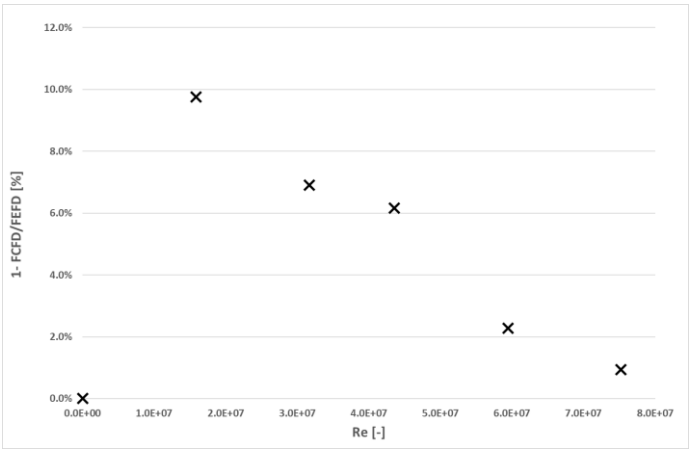

Fig.9: Results of the validation of simulation and experiment. Relative resistance difference of simulation to experiment per Reynolds number.

The decrease of the frictional resistance coefficient with Reynolds number is well documented, *Spurk and Aksel (2010)*, and used in empirical friction correlation formulas such as the ITTC'57 friction line, *ITTC (2002)*. A relatively lower frictional resistance will also reduce viscous pressure resistance.

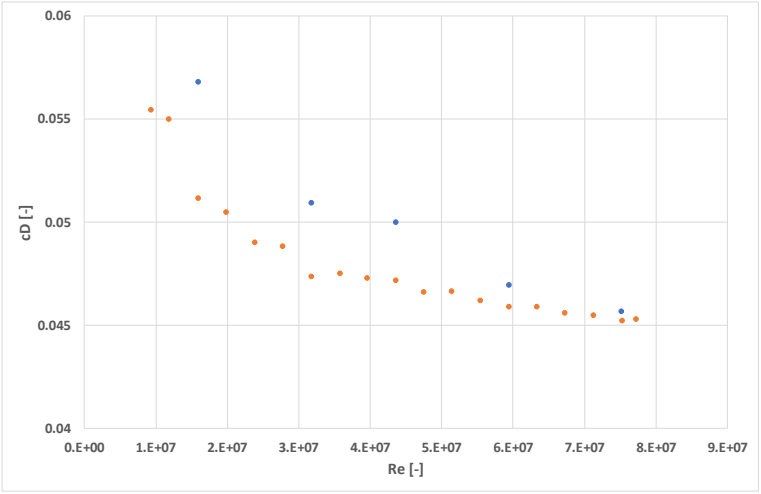

Fig.10: Results of the validation of simulation and experiment. Drag coefficient c_D over Reynolds number for experiment (orange dots) and simulation (blue dots).

If the fluid loses less momentum along the body the pressure peak at its end rises. However, when looking at Fig.12, which shows a comparison of the pressure fields normalized with dynamic pressure in order of increasing Reynolds number, this cannot be observed. The pressure field around the back half of the body remains unchanged. Instead, the pressure around the front and below the front half of the test body decreases with increasing Reynolds number. Furthermore, there is a low-pressure region below the test body that coincides with the longitudinal position of the attachment strut and increases in size with increasing Reynolds number.

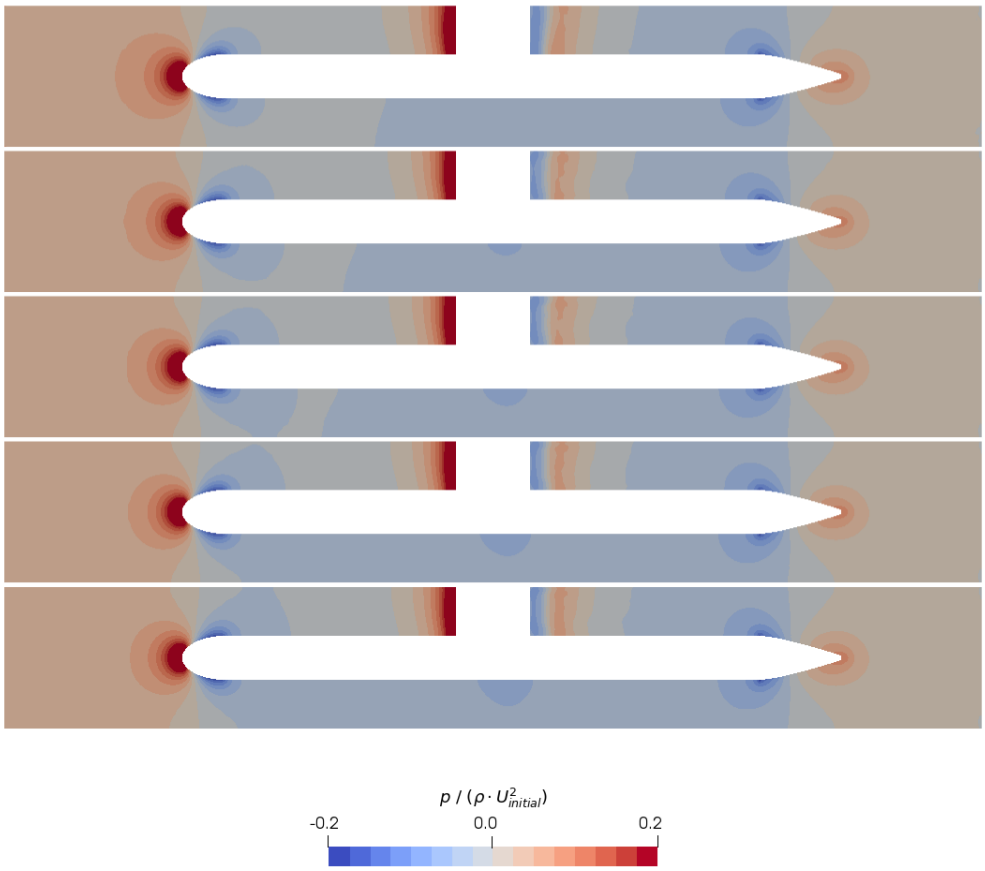

Fig.11: Normalized pressure fields around test body for Reynolds numbers ranging from $1.59 \cdot 10^7$ (top) to $7.5 \cdot 10^7$ (bottom).

Fig.12 shows a comparison of the pressure fields around the nose of the test body between the two extremes of the Reynolds number range investigated in this study. At Re = $7.5 \cdot 10^7$ there is relatively lower pressure around the nose, which is associated with lower pressure resistance.

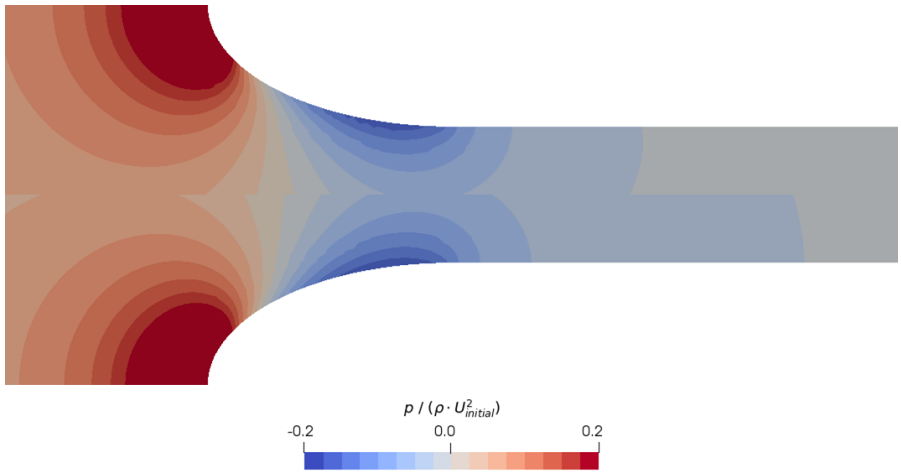

Fig.12: Comparison of pressure field above nose of test body between Re = $1.59 \cdot 10^7$ (top, inverted) and Re = $7.5 \cdot 10^7$ (bottom)

Hence, experiments can be replicated more accurately at higher Reynolds numbers, which are closer to the actual operating conditions of ships and are therefore of particular interest for the final full-scale validation. The code can be considered as validated for unstructured surfaces in the used setups. Hence, the first step of Table I is done. Subsequently, two-phase, freestream simulations of ships under

operational conditions will be simulated (Table I, step 2). Furthermore, the customized wall functions will be included into the code and then compared to experiments with AIRCOAT surface from the cavitation tank, LDA flow tank and HYKAT to validate the final code necessary to perform the full-scale container ship validation.

4. Conclusion & Outlook

The AIRCOAT RANS code was validated with experimental data of the HYKAT. This is the prerequisite to compare the still-outstanding large-scale AIRCOAT HYKAT experiments with the still-outstanding numerical simulation that include a wall function to simulate the effect of AIRCOAT. The pure viscous drag coefficients retrieved from the simulation showed good alignment with the ITTC'57 friction line, following the curve with slightly higher drag coefficients. Furthermore, experiments at SVA friction tunnel resulted in drag coefficients also following the ITTC'57 friction line, Fig.13. Therefore, the experimental and numerical tools considered and the validation concept designed seem a promising approach to tackle the large set of challenges accompanying the novelty of passive air lubrication with bioinspired technologies.

It was validated that AIRCOAT does reduce frictional resistance. However, friction tunnel experiments only showed a slight reduction of maximum 3% to the control. The experimental setup gives a first drag estimate but may be not perfectly suitable for the investigated samples. The structured and unstructured samples were made of thermoplasts in a laboratory setup, which resulted in thickness changes of about 0.4 mm across the entire sample area. Furthermore, the application processes led to trapped air bubbles between sample backside and aluminium, which created further unwanted surface height changes. In a nutshell, samples were not completely level. This created an unknown parameter for calculating drag force calculations of the test setup with a 12 mm narrow channel breadth.

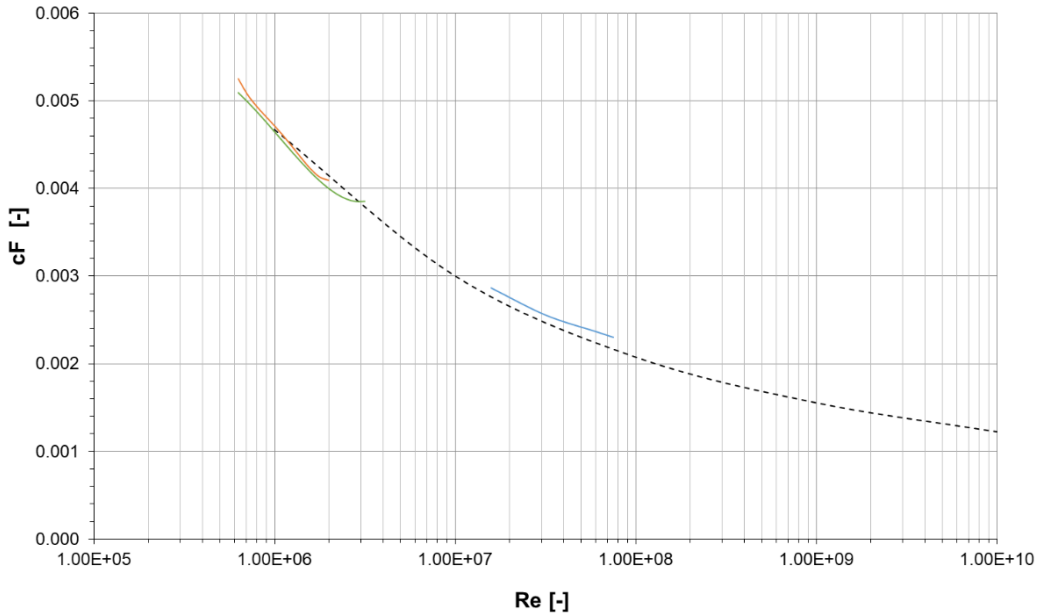

Fig.13: Comparing viscous friction drag (cF) values from friction tank experiments with AIRCOAT (green line) and with the unstructured control (orange line) as well as from numerical simulations of a HYKAT experiments with flat (unstructured) surfaces (blue line). Here, the results for the third grid with slightly higher cF values are not shown. The black dotted line represents the friction ITTC'57 friction line, *ITTC (2002).*

The entire test section is enclosed by the aluminium plates, hence there is no possibility to visually control the behaviour of the AIRCOAT surface during the experiment. It is possible that the air layer was not existent during these experiments as the run-in time of the experiments with undersaturated

water (~ 89 % Oxygen saturation), that is necessary to fill the pressure sensor chambers, may have resulted in air layer loss. Both AIRCOAT and control show an increase of drag coefficient values after a critical Reynolds number (rising above the ITTC line). This is typical for coatings with surface roughness's, and show that both surfaces are not completely smooth and could even back the hypothesis that the air layer was lost and that the drag reduction was only due to the remaining (but now wetted) surface structures of AIRCOAT.

To get deeper insight into this, experiments with visible controls such as with the LDA flow tank and the cavitation tunnel are necessary to get a better understanding of the drag reduction capabilities of AIRCOAT. Those should be backed by future friction tunnel experiments with AIRCOAT that are level and already have a self-adhesive backside in order to reduce surface height changes and thus foil detachment. Finally, future HYKAT experiments at high Reynolds number will give insights to both drag reduction as well air layer stability (via visual control) to extrapolate the effect by "virtually coating" a ship with AIRCOAT in order to evaluate the true potential of AIRCOAT.

Acknowledgements

The AIRCOAT project has received funding from the European Union's Horizon 2020 research and innovation programme under grant agreement N° 764553.

References

BARTHLOTT, W.; SCHIMMEL, TH.; WIERSCH, S.; KOCH, K.; BREDE, M.; BARCZEWSKI, M.; WAHLHEIM, S; WEIS, A.; KALTENMAIER, A.; LEDER, A.; BOHN, H.F. (2010), *The Salvinia paradox: superhydrophobic surfaces with hydrophilic pins for air retention under water,* Advanced Materials *22*(21), pp.2325–2328

BUSSE, A.; SANDHAM, N. D. (2012), *Influence of an anisotropic slip-length boundary condition on turbulent channel flow,* Physics of Fluids *24*(5), pp.55111

BUTTERWORTH, J.; ATLAR, M.; SHI, W. (2015), *Experimental analysis of an air cavity concept applied on a ship hull to improve the hull resistance,* Ocean Engineering 110, pp.2-10

ELBING, B.R.; WINKEL, E.S.; LAY, K.A.; CECCIO, S.L.; DOWLING, D.R.; PERLIN, M. (2008), *Bubble-induced skin-friction drag reduction and the abrupt transition to air-layer drag reduction,* J. Fluid Mechanics 612, pp.201-236

FERZIGER, J.H.; PERIĆ, M. (2002), *Computational methods for fluid dynamics,* Springer

GANDYRA, D.; WALHEIM, S.; GORB, S.; DITSCHE, P., BARTHLOTT, W. SCHIMMEL, T. (2020), *Air Retention under Water by the Floating Fern Salvinia: The Crucial Role of a Trapped Air Layer as a Pneumatic Spring,* Small, 2003425

ITTC (2002), *Guidelines: Testing and Extrapolation Methods: Resistance-Uncertainty Analysis, Example for Resistance Test,* Int. Towing Tank Conf.

JURETIC, F. (2015), *cfMesh v1.1 user Guide,* Creative Fields, Ltd., Zagreb,

OEFFNER, J.; JALKANEN, J.P.; SCHIMMEL, T. (2020), *From nature to green shipping: Assessing the economic and environmental potential of AIRCOAT on low-draught ships,* Transport Research Arena, Helsinki

SCHULZE, R.; KLOSE, R. (2017), *Friction Measurements of different Coatings in a Friction Tunnel,* 2nd Hull Performance & Insight Conf. Ulrichshusen

SHELL (2015), *Silverstream Air Lubrication Technology delivers significant energy savings*. https://www.shell.com/business-customers/trading-and-supply/trading/news-and-media-releases/silverstream-air-lubrication-technology.html

SPURK, J. H.; AKSEL, N. (2010), *Strömungslehre: Einführung in die Theorie der Strömungen*, Springer

VAN DEN BERG, T.H.; LUTHER, S.; LATHROP, D.P.; LOHSE, D. (2005), *Drag reduction in bubbly Taylor-Couette turbulence*, Physical Review Letters 94(4), pp.44501

VERSCHOOF, R.A.; VAN DER VEEN, R.C.A.; SUN, C.; LOHSE, D. (2016). *Bubble Drag Reduction Requires Large Bubbles*, Physical Review Letters 117(10), pp.104502

WEITENDORF, E.; FRIESCH, J. (1990), *Der HYKAT die neue Versuchsanlage der HSVA-Einsatzmöglichkeiten und erste Ergebnisse*, Jahrbuch der Schiffbautechnischen Gesellschaft

Antifouling Efficacy and Skin Friction Drag of 3D-printed Microstructured Surfaces

Mattias Berglin, RISE Research Institutes of Sweden, Göteborg/Sweden, mattias.berglin@ri.se
Patrik Stenlund, RISE Research Institutes of Sweden, Göteborg/Sweden, patrik.stenlund@ri.se
Lena Granhag, Chalmers University of Technology, Göteborg/Sweden, lena.granhag@chalmers.se

Abstract

The advent of new technologies within 3D-printing provide novel opportunities to produce micro-patterned surfaces in the appropriate hierarchical length scale needed to control both biological response and thereby ultimately prevent biofouling based on physical interference and at the same time reduce skin frictional drag. This paper describes parameter studies for a sharkskin-replica coating. Although initial effective in preventing barnacle settling in field tests, after three months all surfaces became seriously fouled. This indicates the need for either improved morphology design or combination with other antifouling technology.

1. Introduction

Marine biofouling is the unwanted accumulation of marine organisms on man-made surfaces in the marine environment, Fig.1. It is a global problem causing hydrodynamic drag and increased fuel consumption for ships, transport of harmful non-indigenous species, corrosion of metal surfaces, reduced function of submerged structures like marine energy production plants, desalination plants, cooling systems and aquaculture installations, *Videla and Characklis (1992)*, *Eashwar et al. (1992)*, *Yebra et al. (1992)*, *Fitridge et al. (2012)*, *Sangeetha et al. (2010)*. Equally important is the problem of the present use of unsustainable antifouling technologies based on coatings that release toxic compounds that have a detrimental effect on marine and coastal life worldwide, *Alzieu et al. (1986)*. In addition to marine life, the use of toxic antifouling treatments in desalination plants and aquaculture might put human health at unacceptable risk, *Fitridge et al. (2012)*.

Fig.1: Biofouling (own and https://safety4sea.com/onr-sponsored-research-targets-ship-biofouling/)

The current use of toxins in biofouling protection is questioned and has motivated the search for more sustainable antifouling technologies where biologically inspired antifouling strategies may offer novel solutions. Here surface microstructure present on the organisms has been suggested to have an adverse effect on biofouling settling and adhesion. Abiotic man-made surfaces with microstructures have produced encouraging results and in laboratory studies reduced settling of diatoms, *Vucko et al. (2013)*, algae, *Schumacher et al. (2007)*, barnacles, *Andersson et al. (1999)*, *Berntsson et al. (2000)*, and tube worms, *Scardino and De Nys (2011)* have been observed. A surface micropattern that has been evaluated in several laboratory studies is the diamond shaped unit cell with protruding ridges showing similarities to the placoid scale of fast swimming marine animals, such as dolphins and

sharks, *Schumacher et al. (2007)*. This surface design not only showed reduced settlement of biofouling, but also reduced skin friction drag at certain water velocities. The combination of environmentally benign antifouling protection and reduced skin friction saving fuel upon operation is an attractive concept.

The conclusion of current studies is that the best reduction of settling is achieved when the size of the geometrical protrusions interferes with size of colonizing organism or it's attachment organ. In the marine environment a diverse range of biofouling organisms with settling stages and attachment organs that span several orders of magnitude in size are present. Thus, surfaces having micro-structuring on several length scales acting in concert are more likely to perform satisfactory compared with surfaces having microstructures of a uniform length scale. However, the potential of such multi-scaled microstructured surfaces has not been adapted or fully explored, mainly due to limiting manufacturing techniques.

The advent of new technologies within 3D-printing including extrusion based additive manufacturing, digital light processing, 2-photon polymerization or laser lithography provide novel opportunities to produce micro- as well as nanopatterned surfaces in numerous polymers having differences in both surface properties (i.e. chemical functional groups) as well as mechanical properties *Selimis et al. (2015), Tumbleston et al. (2015)*. But most importantly, the surfaces can be patterned with geometries with appropriate hierarchical length scales which might be needed to prevent the settling of several different fouling organisms and thereby ultimately prevent biofouling based on physical interference. The objectives of this paper were, (I) to evaluate if a sharkskin replica could be produced in an acrylate based polymer by using an DLP (digital light processing) 3D-printer, and (II) to evaluate if the addition of an uniaxial undulation on a different length-scale than the protrusion ridges of the sharkskin replica influence biofouling accumulation and (III) study the effect on skin friction in a flow-chamber set-up.

2. Materials and Methods

2.1 Microstructuring via 3D-printing

The microstructures were modeled and up-scaled by pattern generation using Autodesk® Fusion 360™ and NETFABB 2019 software (Autodesk Inc., San Rafael, CA, US). The generated STL-files (Fig.2) were finalized for printing by translation to light matrix job files typical for DLP-printing systems, using the software Perfactory RP (EnvisionTEC GMBH, Gladbeck, Germany). A layer thickness of 15 µm was defined, and microstructured panels of dimensions L=80 mm, W=50 mm and H=2 mm, were printed without support in a liquid photopolymer material known as EnvisionTEC R11 using a Perfactory 4 mini XL printer (EnvisionTEC, GMBH, Gladbeck, Germany) with a 75 mm lens installed. The prints were cleaned in an ultrasonic bath of isopropanol for 5 minutes and then repeated with fresh isopropanol. Thereafter the panels were dried for 24 h in room temperature before the post-hardening treatment were initiated by exposing the printed panels for 2 x 2000 flashes in an Otoflash G171 system (EnvisionTEC, GMBH, Gladbeck, Germany). Three panels of each microstructure, i.e. shark and undulated shark, as well as a smooth reference control were printed for further analysis and field studies.

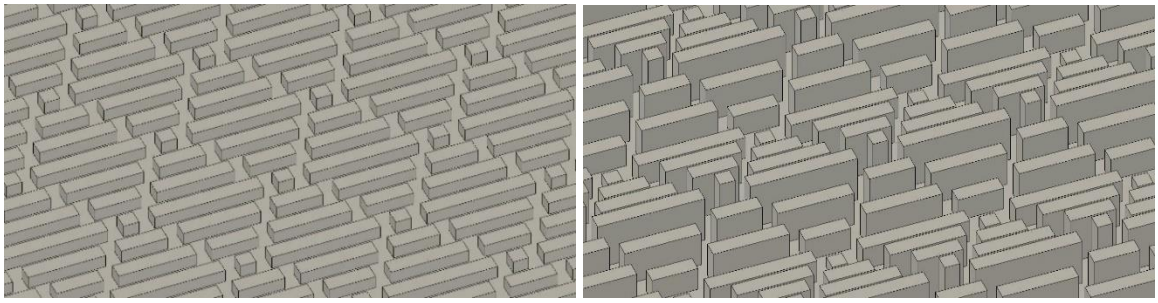

Fig.2: Tilted view of shark STL-files (left) and undulated shark (right)

2.2 Geometrical assessment

Light microscopy images were obtained using a stereomicroscope, Olympus, Japan. Images were taken perpendicular to the surface protrusions at x86 magnification. Higher magnification images (x300) were obtained by scanning electron microscopy (SEM) using a Supra 40VP microscope (Zeiss, Germany) equipped with a Gemini electron source. The microscope was operated at 2 kV and secondary electrons were detected by using the SE2 detector at a working distance of 2-4.5 mm. All samples where coated with a thin layer of gold (Agar sputter coater B7340, UK) prior to analysis to avoid artifacts due to charging. The 3D surface appearance was analyzed using a non-contact optical profiler (S neox from Sensofar, Spain). An area of 1.5 by 1.2 mm was scanned in confocal variation mode. The maximum slope that could be measured with this technique was 86˚ and unmeasureable points in the dataset were adjusted by assuming straight line between closest measured points. For light microscopy, SEM and optical profilometry at least three different positions on the surface were analysed and the appearance of the microstructures were compared.

2.3 Skin frictional drag performance of microstructured panels

The drag performance of smooth and 3D-printed panels was evaluated in small-scale channel flowcell constructed at Chalmers University of Technology. For more information regarding design and performance of the flowcell, *Turkmen et al. (2020), Yeginbayeva et al. (2019)*. In short, by measuring the channel height (H) and pressure drop as a function of distance from inlet (dp/dx) the wall shear stress (τ_w) can be calculated according to Eq.(1). The skin frictional drag (C_f) is then calculated by Eq.(2), in which ρ is the density of the medium, i.e. water 998 kg m^{-3} at 22°C, and *U* is the mean streamwise velocity in the channel. Calculation of Reynold number (Re_m) based on H and U was calculated according to Eq.(3) where ν is the kinematic viscosity of water, 0.908 x 10^{-6} m^2 s^{-1}.

$$\tau_w = -\frac{H}{2}\frac{dp}{dx} \quad (1)$$

$$C_f = \left(\frac{\tau_w}{0.5\rho U^2}\right) \quad (2)$$

$$Re_m = \frac{HU}{\nu} \quad (3)$$

It should be stressed that the 3D-printed panels where smaller than the testing section in the flowcell chamber. To be able to carry out the measurement four 3D-printed panels were glued to a supporting glass panel resulting in three “seams” present perpendicular in the flow stream. Even though care was taken to pattern fitting this resulted in high drag penalty. By assuming similar penalty an internal ranking between smooth and microstructured panels were done.

2.4 Field Study

A field study was carried out at Sven Loven centre for marine infrastructure on the west coast of Sweden (58°52'33.6"N 11°08'47.2"E). Microstructured 3D-printed panels were deployed by hanging them with a tie strap on frames (180 cm x 200 cm) using pre-drilled holes on the corners of the panels. The panels were randomly distributed on the frame both achieving a random vertical and lateral distribution. Water depth ranged from 25 cm to 75 cm. The field study was initiated early June when the fouling pressure is known to be highest. The panels were visually inspected and photographed at different time intervals for a full fouling season (~15 weeks). The panels were further evaluated until 52 weeks of immersion. The degree of fouling and species was calculated based on visual inspection and photographs using a modified ASTM D6990-05 method in which the cover of each major macrofouling type was documented. Statistical analyses were done by t-test assuming equal variances with a significant level of 0.05.

3. Results and Discussion

3.1 Geometrical assessment of 3D-printed microstructured panels

Light microscopy analysis revealed the presence of the diamond-like unit cell on the sharkskin, Fig.3. The ridges are of constant length and separated from neighboring ridges. Ridges of the undulated surface was wider resulting in narrower space between them. The smooth reference surface showed a "pixelated" appearance. This result originates from the way the printing process works. In the digital STL-file the smallest design element is a three-dimensional cuboid with x-y-z dimensions of 44x44x15 µm. The pixelated appearance of the smooth surface indicates that there is a difference between the perfect cuboid in the digital STL-file and the final printed cuboid. The printed cuboid shows some round edges, which add to some structuring of the surface.

The higher magnification SEM images corroborate the observations made by light microscopy with separated slightly rounded ridges on sharkskin. Fig.3. On the undulated sharkskin the ridges are higher and occasional thin bridges of polymer between some of the ridges were observed. Extensive washing procedure did not improve the appearance indicating this material to be at least partly cured and believed to originate from scattering of light during the printing process.

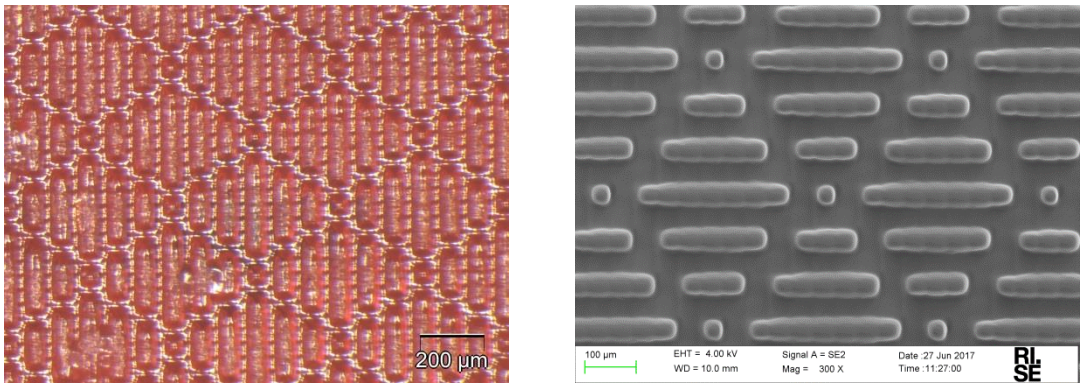

Fig.3: Light microscopy (left) and scanning electron microscopy (right) of 3D-printed sharkskin panels

Optical profilometry provides a three-dimensional view of the printed surfaces allowing more detailed geometrical analyses, Fig.4. The ridges present on the sharkskin surface were evenly distributed with an average center-to-center distance of 86.9 ± 2.0 µm, which is close to the expected distance of 88.0 µm. The average height of the ridges was measured to 35.2 ± 1.2 µm. Small variation in height between ridges was measured but the average height was lower than the expected. It was also noted that the ridges was wider at the base (49.0 ± 5.1 µm) compared to width at the top (28.4 ± 1.8 µm) giving the ridges a somewhat "trapezoid" shape with a sharp incline from the valley to the top rather than the expected cuboid shape. The appearance of the undulated sharkskin is comparable with the sharkskin with evenly distributed ridges with a center-to-center distance of 83.9 ± 6.2 µm. As with the sharkskin the ridges were lower than expected but varied according to design pattern giving rise to a sinusoidal wave or an undulation at a measured wavelength of 525.9 ± 6.5 µm and amplitude of 78.5 ± 1.9 µm. The optical profilometry measurements verified the presence of rounded edges of the cuboid, which resulted in a valley-to-top structuring in the order of 1 µm on the smooth reference.

The profile extracted from the digital STL-file was superimposed on top of the measured profiles, and the difference in "digital" profile area and "printed" profile area was assessed. The main difference was the appearance of the ridges. As discussed above, the ridges are somewhat smaller at the top than at the base and are not as high as in the digital STL-file. One plausible reason for this appearance could be the lack of support structures during printing. To counteract the lack of support a higher pressure was used to assure proper adhesion between the building plate and printed structures. The higher pressure might affect the size of the cuboid in the z-direction leading to thinner deposited layers and reduced height of the printed structures.

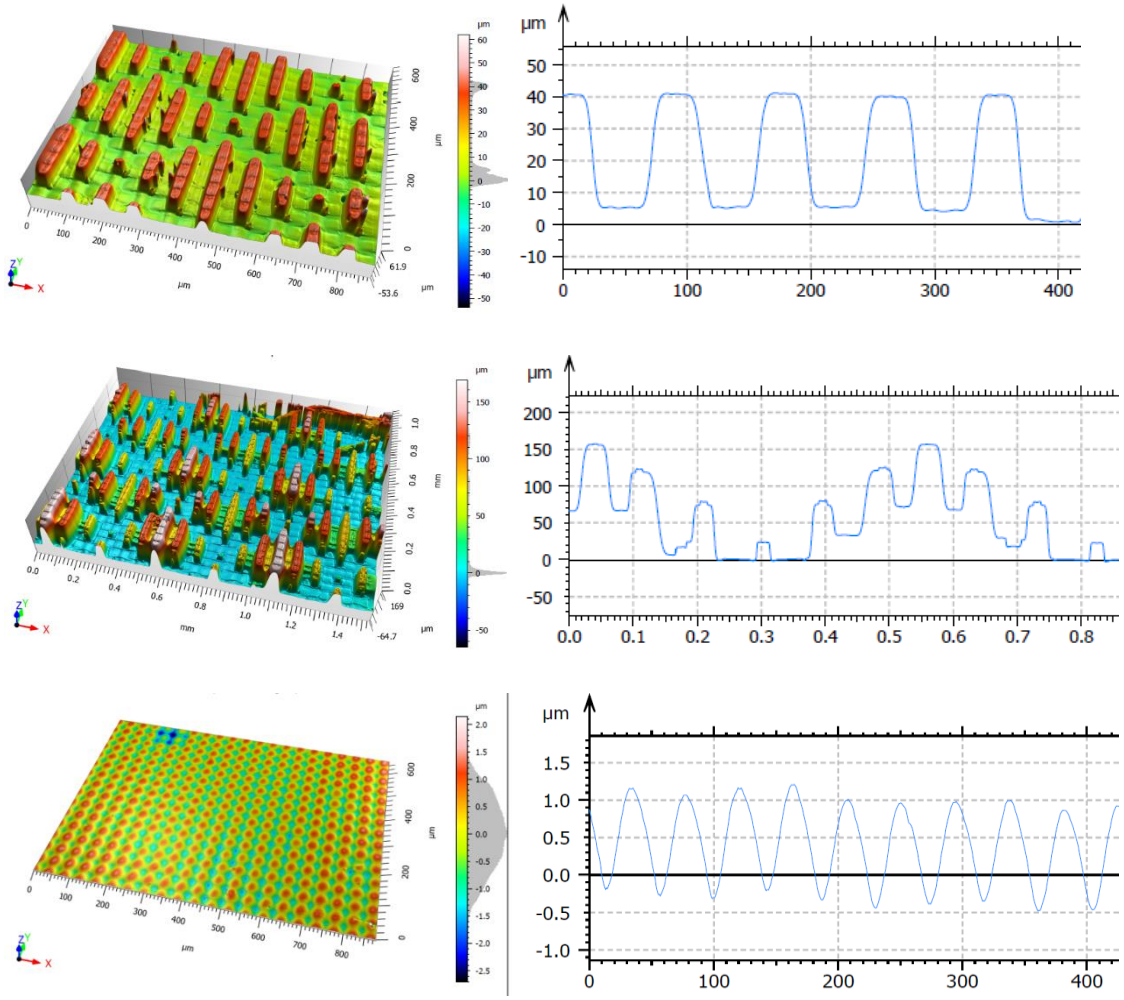

Fig.4: Representative appearance of the shark (top), undulated shark (middle) and smooth (bottom) 3D-printed panels as determined by optical profile measurements.

As the center-to-center distance of the ridges is close to the expected we conclude that only minor shrinking of the polymer takes place during printing and the following post-treatment procedure. Adding up the extracted profile areas outside and areas inside and comparing with the expected digital STL-file resulted in a discrepancy in the order of 13%, which can be considered acceptable for printing at this resolution.

When analyzing the dimensional accuracy of the undulated sharkskin, in addition to reduced height of the ridges, extra material between the parallel ridges of high amplitude was observed. Although the general appearance of the surface was acceptable, the reduced height and extra material resulted in a discrepancy between digital and printed profile in the order of 40%. The areas lacking material and the areas with extra material contributed each with 20% to this discrepancy, almost as the material was redistributed by taking material from the top of the ridge and moving it to the valley. It can also be noted that the center-to-center distance between high ridges was shorter than expected. This was not observed between shorter ridges. It can be speculated that during the post-processing treatment the extra material in between the ridges shrinks to some extent during curing and by this pulling the high ridges together i.e. making them slightly tilted.

Overall, the dimensional accuracy of the two microstructured surfaces was well within the acceptable range for the purpose of the planned field and drag performance study. The dimensional accuracy might be further improved by adjusting printing parameters and post-treatment protocols.

3.2 Skin frictional drag of microstructured panels

The skin frictional drag (C_f) as a function of Reynolds number (Re_m) of 3D-printed panels is presented in Fig.5. As comparison, the Cf of a smooth acrylic panel is presented. As can be seen the C_f of the smooth 3D-printed panels was at least three orders higher compared with the smooth acrylic. We believe this difference to originate from the experimental set-up with seams between the 3D-printed panels as discussed above and only internal rankling was performed. However, these preliminary results at least corroborate previous studies showing lower drag is possible to achieve at certain flow regimes with appropriate microstructure. Outside this flow regime the microstructure instead increases drag. This was also observed in our data when comparing the undulated shark with the smooth reference panel. At low to average flow the measured C_f is lower for the undulated shark panel while a rapid increase in C_f is observed at high flow. Nevertheless, the undulated shark is quite rough with protrusions of up to 150 µm from the lowest point still shows lower skin frictional drag than the smooth reference with structuring in the 1 µm range.

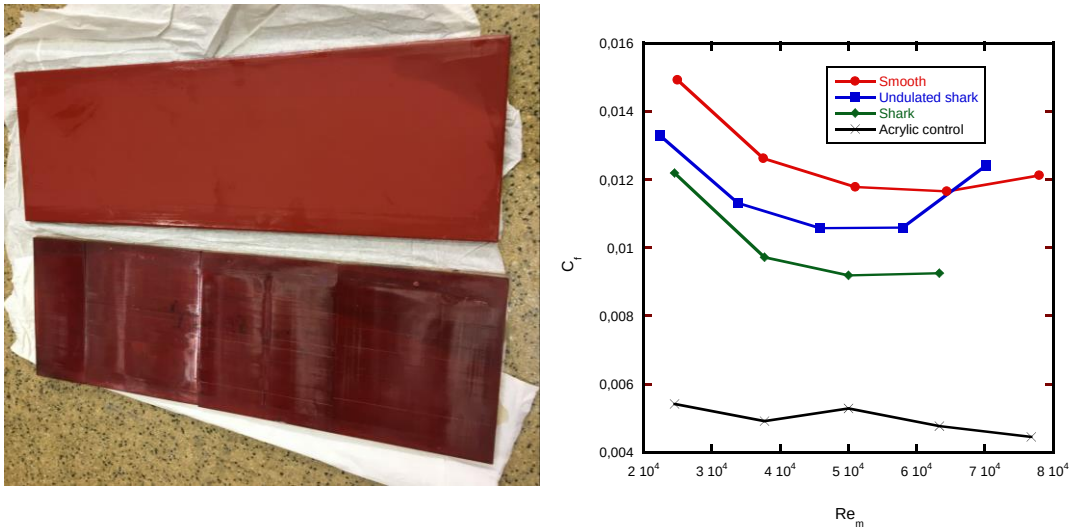

Fig.5: Photograph of 3D-printed sharkskin panel and reference coating (left) and results from skin frictional drag (C_f) measurements (right)

3.3 Antifouling efficacy

Panels where inspected after 2 weeks, 1 month and 3 months of immersion and the degree of fouling (total biofouling and barnacle coverage) were assessed on panels with microstructure (i.e. shark and undulated shark), smooth reference as well as smooth "backside".

After two weeks of immersion the only fouling organism present on the panels was barnacles. The degree of settling was highest on smooth reference with 246 ± 32 and smooth backside with 241 ± 19 individuals/dm^2. The degree of barnacle settling on smooth reference was statistically higher than the degree of settling on for example shark skin surface with 193 ± 16 individuals/dm^2 ($p = 0.006$) and the undulated sharkskin with 150 ± 43 individuals/dm^2 ($p = 0.002$). The number of settled barnacles on the sharkskin surface was statistically higher than number of barnacles settled on the undulated sharkskin ($p = 0.04$).

After 1 month of immersion the number of settled barnacles was higher on all panels, but again, except some filamentous algae barnacles were the only fouling organism present. At this time point no statistical difference in barnacle settling between smooth reference (341 ± 46) and sharkskin (298 ± 42) was observed ($p = 0.11$). The number of settled barnacles on the undulated sharkskin (273 ± 54) was still significantly lower compared with the smooth reference ($p = 0.04$).

After 3 months of immersion the panels were heavily fouled. In addition to barnacles, mussels, tunicates, tubeworm, filamentous algae and encrusting bryozoans were found on the surfaces. As barnacles are opportunistic, they are usually the first organism found on surfaces. Many other fouling organisms then use the already settled barnacles as holdfast when they colonize the surface. Preventing the attachment and following growth of barnacles can prolong the efficacy of an antifouling coating.

4. Conclusions

With regular bench-top DLP 3D-printer it was possible to produce panels with microstructures in the bioactive range for performing initial effect studies such as antifouling and skin friction drag.

Geometrical assessment of microstructures verified acceptable similarities between the digital STL-file and the 3D-printed. Deviations mainly being round edges on the produced microstructures as well as problem with separation between high aspect microstructures.

For the skin friction measurements panels were stitched resulting in high drag penalty during experiments. Internal ranking was performed showing the possibility of reducing drag by microstructuring.

The 3D-printed panels showed initial better antifouling performance compared with a smooth reference. Adding microstructuring on different length scales also improved the performance. Nevertheless, after 3 months of testing all panels independent of structuring were severely fouled.

The ease of designing and producing surfaces with nano/microstructures using 3D-printing is encouraging for further studies.

References

ALZIEU, C.; SANJUAN, J.; DELTREIL, J.P.; BOREL, M. (1986), *Tin Contamination In Arcachon Bay - Effects On Oyster Shell Anomalies*, Marine Pollution Bulletin 17(11), pp.494-498

ANDERSSON, M.; BERNTSSON, K.; JONSSON, P.; GATENHOLM, P. (1999), *Microtextured surfaces: towards macrofouling resistant coatings*, Biofouling 14(2), pp.167-178

BERNTSSON, K.M.; ANDREASSON, H.; JONSSON, P.R.; LARSSON, L.; RING, K.; PETRONIS, S.; GATENHOLM, P. (2000), *Reduction of barnacle recruitment on micro-textured surfaces: Analysis of effective topographic characteristics and evaluation of skin friction*, Biofouling 16(2-4), pp.245-261

EASHWAR, M.; SUBRAMANIAN, G.; CHANDRASEKARAN, P.; BALAKRISHNAN, K. (1992), *Mechanism For Barnacle-Induced Crevice Corrosion In Stainless-Steel*, Corrosion 48(7), pp.608-612

FITRIDGE, I.; DEMPSTER, T.; GUENTHER, J.; DE NYS, R. (2012), *The impact and control of biofouling in marine aquaculture: a review*, Biofouling 28(7), pp.649-669

SANGEETHA, R.; KUMAR, R.; DOBLE, M.; VENKATESAN, R. (2010), *Barnacle cement: An etchant for stainless steel 316L?*, Colloids and Surfaces B-Biointerfaces 79(2), pp.524-530

SCARDINO, A.J.; DE NYS, R. (2011), *Mini review: Biomimetic models and bioinspired surfaces for fouling control*, Biofouling 27(1), pp.73-86

SCHUMACHER, J.F.; CARMAN, M.L.; ESTES, T.G.; FEINBERG, A.W.; WILSON, L.H.; CALLOW, M.E.; CALLOW, J.A.; FINLAY, J.A.; BRENNAN, A.B. (2007), *Engineered antifouling microtopographies - effect of feature size, geometry, and roughness on settlement of zoospores of the*

green alga Ulva, Biofouling 23(1), pp.55-62

SELIMIS, A.; MIRONOV, V.; FARSARI, M. (2015), *Direct laser writing: Principles and materials for scaffold 3D printing*, Microelectronic Engineering 132, pp.83-89

TUMBLESTON, J.R.; SHIRVANYANTS, D.; ERMOSHKIN, N.; JANUSZIEWICZ, R.; JOHNSON, A.R.; KELLY, D.; CHEN, K.; PINSCHMIDT, R.; ROLLAND, J.P.; ERMOSHKIN, A., SAMULSKI, E.T.; DESIMONE, J.M. (2015), *Continuous liquid interface production of 3D objects*, Science 347(6228), pp.1349-1352

TURKMEN, S.; ATLAR, M.; YEGINBAYEVA, I.A.; BENSON, S.; FINLAY, J.A.; CLARE, A.S. 2020), *Frictional drag measurements of large-scale plates in an enhanced plane channel flowcell*, Biofouling 36(2), pp.169-182

VIDELA, H.A.; CHARACKLIS, W.G. (1992), *Biofouling And Microbially Influenced Corrosion.* International Biodeterioration & Biodegradation 29(3-4), pp.195-212

VUCKO, M.J.; POOLE, A.J.; SEXTON, B.A.; GLENN, F.L.; CARL, C.; WHALAN, S.; DE NYSET, R. (2013), *Combining a photocatalyst with microtopography to develop effective antifouling materials*, Biofouling 29(7), pp.751-762

YEBRA, D.M.; KIIL, S.; DAM-JOHANSEN, K. (2004), *Antifouling technology - past, present and future steps towards efficient and environmentally friendly antifouling coatings*, Progress in Organic Coatings 50(2), pp.75-104

YEGINBAYEVA, I.A.; GRANHAG, L.; CHERNORAY, V. (2019), *Review and historical overview of experimental facilities used in hull coating hydrodynamic tests*, J. Engineering for the Maritime Environment 233(4), pp.1240-1259

MASS Autonomous Ships: Current Status, Developments and Pitfalls!

Giampiero Soncini, IB Marine, Rapallo/Italy, g.soncini@ib-marine.com

Abstract

There are unmanned trains, and there are and will be more and more in the future unmanned cars. So why not unmanned ships? The technology is there today. What is needed is some changes in the rules, some redundant machinery on the ships, and some pioneering spirit and entrepreneurship in the industy.

1. Introduction

Not everybody may (yet) be familiar with the terminology in unmanned and autonomous shipping. MASS means 'Maritime Autonomous Surface Ship', i.e. a ship which, up to a certain degree, can operate independently of human interaction. In other words, it is a technical definition of an autonomous ship, which can operate without a crew, or at least with a very reduced one (3-5 persons).

For MASS vessels, The IMO has established four degrees of autonomy:

- Degree one: Ship with automated processes and decision support: Seafarers are on board to operate and control shipboard systems and functions. Some operations may be automated and at times be unsupervised but with seafarers on board ready to take control.
- Degree two: Remotely controlled ship with seafarers on board: The ship is controlled and operated from another location. Seafarers are available on board to take control and to operate the shipboard systems and functions.
- Degree three: Remotely controlled ship without seafarers on board: The ship is controlled and operated from another location. There are no seafarers on board.
- Degree four: Fully autonomous ship: The operating system of the ship can make decisions and determine actions by itself

The IMO's Strategic Plan (2018-2023), http://www.imo.org/en/About/strategy/Pages/default.aspx, has a key Strategic Direction to "Integrate new and advancing technologies in the regulatory framework". This involves balancing the benefits derived from new and advancing technologies against safety and security concerns, the impact on the environment and on international trade facilitation, the potential costs to the industry, and finally their impact on personnel, both on board and ashore.

In 2017, following a proposal by several Member States, IMO's Maritime Safety Committee (MSC) agreed to include the issue of marine autonomous surface ships on its agenda. This would be in the form of a scoping exercise to determine how the safe, secure and environmentally sound operation of Maritime Autonomous Surface Ships (MASS) may be introduced in IMO instruments.

2. Historic perspective

MASS vessels (under whatever term the concept was used) are by no means a new idea, but have gained more and more traction in recent years. Milestones have been:

1980	Ships and Shipping of Tomorrow, book by Rolf Schönknecht
1988 - 2005	Feasibility study on Intelligent traffic system – Japan
2007	Waterborne European project - A cluster of European maritime stakeholders, published a vision paper for the future development of the maritime industry regarding competitiveness and innovation on autonomous ships

2011	Korean project Multipurpose Unmanned ship named Krisco is launched
2012 - 2015	MUNIN Maritime Unmanned Navigation through Intelligence in Networks
2013	DNVGL and Transnova – ReVolt Project for an electrical unmanned vessel
2015	Rolls-Royce launches Advanced Autonomous Waterborne Applications
2016	Lloyd's Register launches the first guidance doc on Cyber-enabled ships
2016	Norwegian Forum for Autonomous Ships (NFAS) – a forum initiative of the Norwegian Maritime Authority, Coastal Administration, Industry and MARINTEK, was established. An agreement was signed for unmanned ships testing
2017	MOL (Mitsui O.S.K Lines), and Mitsui Engineering & Shipbuilding Co. and the Japanese government, launches R&D on autonomous ocean transport systems.
2017	Rolls-Royce and towage Svitzer demonstrated the world's first remotely operated commercial vessel in the port of Copenhagen, Denmark, the Svitzer Hermod
2017	China Classification Society (CSS) and HNA Technology Logistics Group launched an unmanned cargo ship development alliance in China
2017	Norwegian Kongsberg Seatex launched the Hull 2 Hull (H2H) project with funding from the European GNSS Agency under the European Union's Horizon 2020. H2H will help mariners take correct navigation decisions
2017	Korean project Krisco was successfully tested
2018	20000 TEU container ship, MV COSCO Shipping Aries, built by the Chinese venture Nantong COSCOS KHI Ship Engineering, Co. (NACKS) was the first ever to receive LR's cyber-enabled ship (CES) descriptive note "Cyber AL3 SECURE PERFORM" for its energy management system.
2018	United States' Defense Advanced Research Projects Agency (DARPA) successfully completed its Anti-Submarine Warfare (ASW) Continuous Trail Unmanned Vessel (ACTUV) and officially transferred the technology demonstration vessel, called Sea Hunter, to the Office of Naval Research (ONR)
2018	Norwegian group Wilhelmsen and Kongsberg joined forces to establish the world's first autonomous shipping company: Massterly.
2018	Announcement of the first ever zero emission autonomous ship called Yara Birkeland, a cooperation effort between Kongsberg and Yara, working along with the newly announced Massterly Company. The vessel will be the first ever fully electric autonomous container ship
2018	Rolls-Royce and AXA Corporate Solutions sign a LOI to explore ways in which they can combine their respective products utilizing Rolls-Royce Ship Intelligence systems and equipment and AXA's risk analytics capabilities to support current sailing and future vessels
2018	IMO took the first step towards addressing autonomous ships, looking into how safe, environmentally sound and secure MASS may be.

2018 DNV-GL released and Autonomous and Remotely Operated Ship Guideline to help build a safety culture around these new technologies

2019 Japan's NYK Group companies NYK, MTI and Keihin Dock along with Japan Marine Science have been selected to participate in a remotely controlled ship demonstration project for the practical implementation of autonomous ships by 2025

2019 The autonomous vessel “Maxlimer” by the British company Sea-Kit set a successful sail from the UK to Belgium, hauling beer and oysters

2019 Mayflower Autonomous Ship (MAS) will also set sail on 2020. Built entirely by the British company M Subs and funded by the ProMare Foundation.

And the evolution continues as we speak (or read the HIPER proceedings). Japan has NYK testing its first MASS-related technology on a ro-ro vessel, https://www.youtube.com/watch?v=QUKbMA5sjSA&feature=youtu.be, and China reports also MASS testing, https://www.youtube.com/watch?v=EtcSjXSvYG8.

3. Is this a revolution?

3.1. Not everything is so new

Increasing ship autonomy is old hat for the navies of this world. For example, the NATO “RV Alliance”, https://en.wikipedia.org/wiki/Italian_ship_Alliance_(A_5345), Fig.1, built in 1986, was the first vessel in the world with:

- GPS
- DGPS
- INS
- Combined CMMS and CBM
- Very advanced automation system
- Hull mounted Doppler sonar

Fig.1: “RV Alliance”

Even computers are much older than we usually imagine. The Antikythera mechanism, https://en.wikipedia.org/wiki/Antikythera_mechanism, is an ancient (2200 years old) Greek analogue computer used to predict astronomical positions and eclipses for calendar and astrological purposes decades in advance. It could also be used to track the four-year cycle of athletic games which was similar to an Olympiad, the cycle of the ancient Olympic Games. Detailed imaging of the mechanism suggests that it had 37 gear wheels enabling it to follow the movements of the moon and the sun through the zodiac, to predict eclipses and even to model the irregular orbit of the moon, where the Moon's velocity is higher in its perigee than in its apogee. This motion was studied in the second century BC by astronomer Hipparchus of Rhodes.

3.2. Why now?

So, why is unmanned shipping now such a hot topic, when basic ideas have been around for ages? After all, technology allowing unmanned ships has been around at least 30 years. Unmanned trains have been operating now for over 20 years. Cars are being tested for 4-5 years now. It is normal that also ships will be affected by this "movement". The difference is that today technology is much cheaper, much easier, much more powerful. The combination of these three factors (price, access, power) makes the vision of unmanned shipping now a reality within reach.

3.3. How will it evolve

But why do we want unmanned ships at all? There may be many reasons given, including:

- Who wants to go at sea today? We will face a shortage of qualified seafarers in the future.
- It is not effective. We keep crews 24 h on board to work 8/10.
- 75% of marine accidents are caused by human errors. Computers are much more diligent and stress resistant.
- We can work more efficiently like in the aviation industry. Airplanes required just a crew of 3 for the flying of the airplane.
- Technology allows us to do so. Most systems needed are at least in the prototype stage.

Of course, the theme of replacing men by machines is emotional and evokes time-honoured emotional replies from Luddites, https://en.wikipedia.org/wiki/Luddite, such as:

- "It" kills! see the Boeing max 800 issue!
- Wait until you will have the first ship being idle in the middle of the ocean!
- All those poor seafarers without a job!
- No machine can replace a man!
- A captain will always be needed!
- It will never happen!

These arguments have been used time and time again when we moved on to new technologies. Let's have a look at facts and numbers:

- Number of seafarers worldwide: ~1.5 million
- Number of jobs created by autonomous technology worldwide: 28 million (developers only)

Let's face it: Machines have replaced men, for all tedious and repetitive jobs. And the art of navigating a vessel is not an art anymore.

Do you miss cowboys? Or horse shoemakers? Yet, when the car was invented, they all lost their jobs. When cars were created, cowboys, horse traders, dung cleaners, corral builders, saddle makers, etc… They all lost their jobs. but then we had to build roads, traffic lights, road signs, barriers, tolls etc.

4. Final thoughts

So, how will autonomous ship technology evolve? Some thoughts that come to my mind are:

1. It will take time. between 10 to 20 years. but the first unmanned ships will be sailing 5 years from now.
2. Not all ships can and will be totally unmanned. It could be that none would be "totally" unmanned. Probably we will keep a crew of 3 on board, mainly for insurance/ownership purposes.
3. Don't say "the rules will never change" because they are changing already.
4. Remember mp3, apple, amazon, google, booking.com. But remember also horses, carts, the advent of the steam engines, the train, and the airplane.

Even in a traditionally conservative industry, innovation and progress shouldn't be bad words:

- Every time there is something new, there are enemies.
- The resistance to change is always very strong, especially in the work environment. But those opposing innovation, oppose the company they work for.
- Innovation allows us to work better, in a more effective and efficient way.

The maritime industry has always innovated. Remember:

- When UMS was introduced
- When OMBO was introduced
- When GPS was introduced
- When GMDSS was introduced
- When ECDIS was introduced

Some countries are ahead of the game, among them Japan. There, government, industry, classification society, and research centers are all working together. Their approach is:

- Analyze problems and issues
- Create new standards to solve them
- Cooperate to build

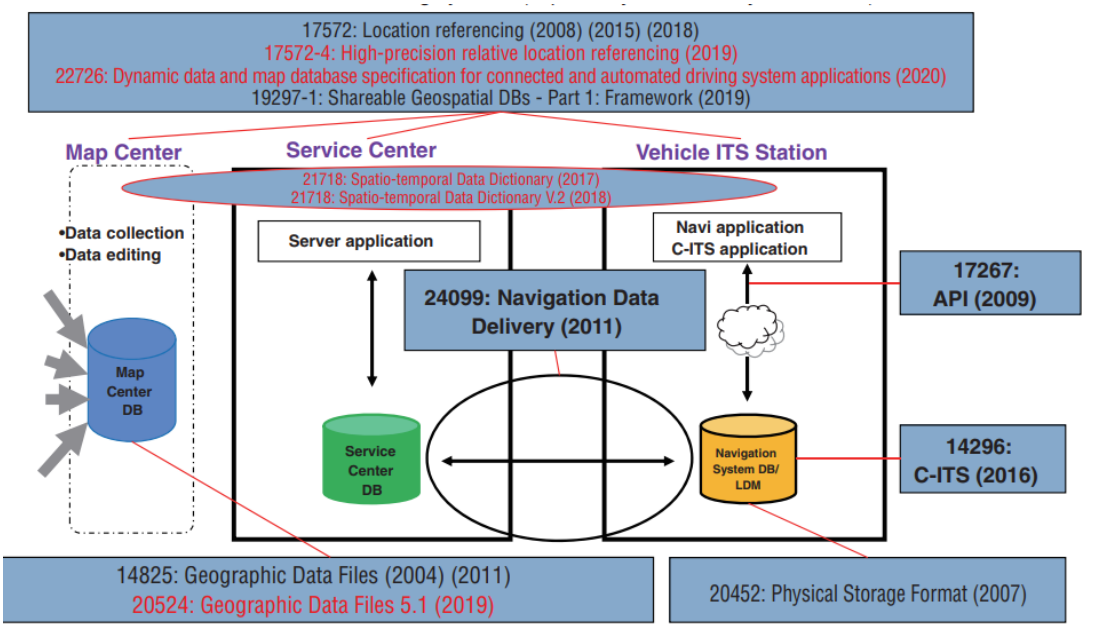

Fig.2: Schematic for Intelligent Transportation Systems

In full cooperation with ISO, the Japanese Industrial Standards Committee (JISC) has set workshops to revise and design a new set of programs to minimize, simplify and rationalize ITS (Intelligent Transport Systems) in cars, ships and other vehicles, Fig.2.

What are the biggest issues slowing us down? The answer is not surprising, as MASS technology is a young industry and young industries face typically these issues:

- Regulations, Legal, Flag States and PSC lag behind technology
- Insurance is hesitant as insurance business is based on experience (statistics for risk assessment)
- Lack of standardization. Standardization is a “must”, and that is why Japan is ahead of the game.

There is no digitalization of a fleet, unless information is standardized, and data is made openly available.

Wind Assisted Ship Propulsion Enabling Zero-Emission Shipping

Guus van der Bles, Conoship International BV, Groningen/The Netherlands, guus@conoship.com
Frank Nieuwenhuis, Econowind BV, Groningen/The Netherlands, nieuwenhuis@econowind.nl

Abstract

This paper describes how Wind Assisted Ship Propulsion (WASP) based on eConowind-units and VentiFoils™ enables Zero Emission Shipping for cargo vessels in the coming years. The development and principle of the eConowind-unit and VentiFoils™ are introduced, based on the 'Suction-Wing'-principle. Recent experience is presented on retrofitting stand-alone VentiFoils™ on existing vessels, enabling those vessels to reduce fuel consumption and CO2 emissions up to levels of 20 % in favorable Bft 5 wind conditions. Future developments are presented on larger VentiFoils™ in new concept-designs of Conoship, that can save more than 50% on fuel and CO2 emissions in favorable wind conditions.

1. Introduction

Wind Assisted Ship Propulsion is as old as mankind and after more than a century of primarily coal and fuel oil driven ship propulsion, wind energy is re-discovered as a promising energy source for zero emission shipping. The basic idea for Wind Assisted Ship Propulsion (WASP) is that the generated wind-driven thrust is reduced on the propeller thrust by decreasing the fuel to the engine: maintaining an equal economical speed while reducing the fuel consumption and emissions. This paper highlights the development of WASP devices by Conoship and Econowind for application on seagoing vessels, the VentiFoils™ and eConowind-unit, and their future application in zero emission ship concepts.

As innovative Ship Design office, Conoship has always had a strong focus since its founding in 1952 on designing fuel-efficient vessels, optimising hull lines and propulsion systems. Realising that wind is freely available at a lot of routes at sea, Conoship started R&D projects in 2009 to develop fuel-saving auxiliary wind propulsion systems for seagoing vessels, considering to keep the impact on the operations of the vessel limited. This led to the founding of Econowind BV in 2016 for dedicated development, production, and delivery of wind propulsion systems for ships.

The next section presents an overview of the development of the eConowind-unit with two foldable VentiFoils™, Fig.1, based on the 'Suction wing'-principle, followed by a section on retrofitting of VentiFoils on existing vessels and the resulting savings in fuel consumption and emissions.

Fig.1: eConowind-unit on General cargo vessel (photo by Flying Focus)

The final section focusses on a new concept design based on hybrid propulsion combining WASP and other zero emission propulsion technologies like batteries and hydrogen powered fuel cells. Including wind as an important energy source, helps to reduce both OPEX and CAPEX of the other required zero emission propulsion technologies, enabling the future realisation of zero emission shipping.

2. Development of VentiFoils™ and eConowind-unit

Various systems have been, and are still being, developed for wind propulsion of cargo vessels, mostly assisting the primary propulsion system of the propeller driven by an engine. After investigating a variety of relevant WASP Systems and their major characteristics related to application on cargo vessels, the 'suction wing'-principle was selected as most promising by Conoship. The first maritime application of the 'Suction-wing'-principle was developed by Jacques Cousteau and French scientists between 1980 and 1985 and it was applied in the 'Turbosail'-system on vessels of the Cousteau Foundation, Fig.2.

2.1. The Suction-wing principle

The Cousteau Turbosail consists of a vertical 'Suction-wing-profile' with a large thickness and a small chord-length, resulting in an egg-shaped cross-section, Fig.3. It is not a rotating cylinder, the direction of the leading edge (the 'sharp nose' of the egg-shaped cross-section) is just adjusted to an optimal angle of attack to the apparent wind. To control the airflow around the extreme 'thick' foil-shape, boundary-layer-suction is applied, for which a ventilator is installed inside the Suction-wing profile. The system generates approx. 5-6 times the force per square meter compared to a normal sail.

Fig.2: Turbosails on the Alcyone

The generated thrust force depends on a combination of variables like the ventilator power (related to wind-speed), effective boundary-layer suction, position and size of suction holes, shape of the profile, angle of attack of apparent wind, etc. This is a challenging issue in theoretical modelling, in model testing in a wind-tunnel and in translation to full scale practice on a vessel at sea. The Suction-wing system can be as compact as a Flettner rotor, generating comparable thrust forces for equal sizes and wind conditions. It can be fully automated and can have low impact on cargo handling operations by careful positioning on the vessel. As it is a lightweight structure and not rotating, there are no gyroscopic forces that require heavy foundation structures.

2.2. CFD analysis of VentiFoils

A CFD-analysis was performed on the Suction-wing by a MSc student of Delft University of Technology at the MARIN institute in Wageningen, The Netherlands. The influences of variations of (wind)angle of attack and of the boundary-layer-suction were investigated by analysing the pressure distribution around the VentiFoil™, Fig.3, at wind speeds of 6 m/s (~ wind force Bft 3), 10 m/s (~ Bft 5) and 14 m/s (~ Bft 6/7). In this figure, the incoming wind from the bottom-left corner has an angle of attack of 30 degrees and is bended along the pressure-side (underside in the figure) guided by a 'flap' at the trailing edge (right side of the profile in the figure).

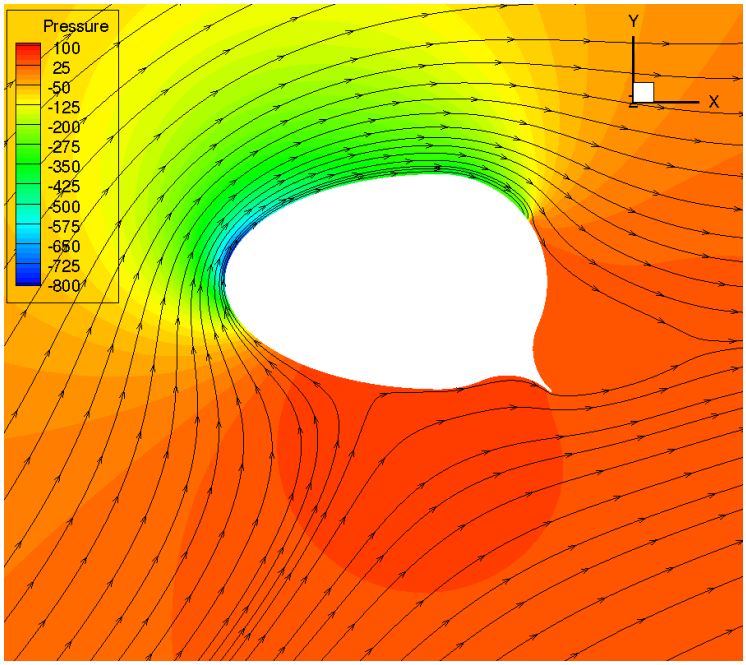

Fig.3: CFD analysis pressure distribution (from TU Delft graduation Anton Kisjes)

At the leading edge (left side of the profile, the 'nose' of the egg-shaped cross-section) the airflow is accelerated leading to very low pressure on the top-left side of the profile and all along the suction-side (upper side in the figure. This is the result of the boundary-layer-suction through small openings in the surface of the profile in the top-right corner, opposite to the position of the 'flap'. A ventilator inside the VentiFoil™ generates the under-pressure forcing an airflow from the boundary layer into the profile, accelerating the boundary layer and preventing separation of the air flow on the suction side of the profile. This leads to high lift forces for the compact profile and lift-coefficients of 7 to 8 (for infinite span) depending on angle of attack and suction-efficiency. CFD calculations for a VentiFoil™ with an aspect ratio of 5.5 result in a lift coefficient between 5 and 6.

Based on these results the potential reductions in CO_2 emission and fuel consumption were calculated for example vessels in various operational conditions, resulting in polar diagrams like Fig.4. This figure indicates the reduction in Kilowatt of the main engine, for keeping an equal speed of 11 kn, while using 4 VentiFoils™ of 10 m height (in 2 eConowind-units) in 3 windspeeds from various directions. The 0 degree on top means a headwind for the vessel, leading to zero reduction, and the 90 degrees on the right side indicate a beam wind from starboard side, with the true wind direction at an angle of 90 degree from the heading of the vessel. The reduction of engine power is indicated in circles, ranging from 0 kW in the centre to 450 kW in the largest circle. The yellow line of the widest contour is indicating the kW-reduction at a true windspeed of 14 m/s (Bft 6/7), indicating a reduction of abt. 420 kW for this windspeed from 90 degree's starboard side. The red line of the middle contour indicates for the same wind direction a reduction of abt. 220 kW at the windspeed of 10 m/s (Bft 5) and the blue line of the smallest contour a reduction of abt. 140 kW at the windspeed of 6 m/s (Bft 4).

In parallel to the research and the CFD analysis a test- model was constructed to be tested in real wind conditions.

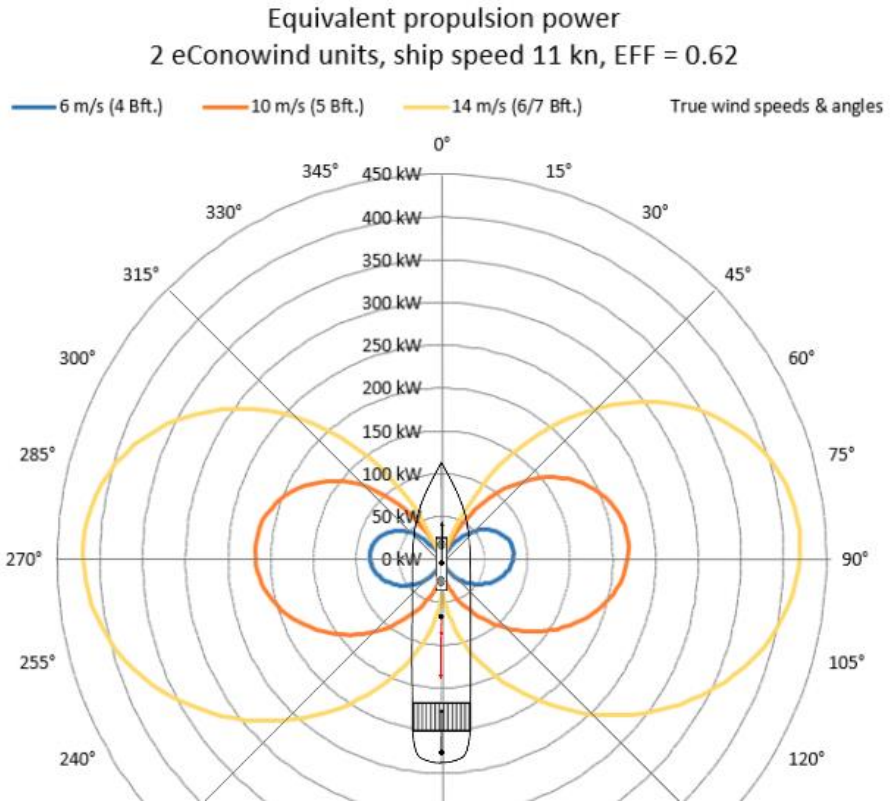

Fig.4: Reduction in engine power using 2 eConowind-units (= 4 VentiFoils™)

2.3. Test model and prototype of the eConowind-unit

Conoship International BV and HCP holding founded the company Econowind BV in 2016 for development, construction, testing, optimization and commercialisation of VentiFoils™ and eConowind-units. Field tests were performed during 2017 with a test model of a VentiFoil™, Fig.5, with a height of 5,5 m and a chord length of 1 m., partly parallel to the CFD analysis.

Fig.5: Test model of VentiFoil

The acquired knowledge and testing experience led to the development and building in 2018 of a full-scale prototype of the eConowind-unit based on a 40 ft open-top container with two foldable 10 m VentiFoils™. In upright position the VentiFoils™ convert wind to thrust for the vessel and when not in operation they can be folded downwards and be stored horizontally in the container. Multiple eConowind-units can be positioned on a variety of General cargo vessels, on container fitted hatch covers as quickly as 40 ft containers. After field tests in October, Fig.6, the first sea trial of the eConowind-unit was in November 2018, on the Short Sea General cargo vessel 'MV Lady Christina', Fig.1, of shipowner WijnneBarends of Delfzijl, The Netherlands. The first test trial was a roundtrip from Emden (Germany) to Plymouth (UK) and Finland and it was followed by additional test trips on the same vessel in the first half of 2019.

Fig.6: Prototype of the eConowind-unit

The test results confirmed the Suction-wing theory: at favourable wind conditions fuel savings of 800 litre/day were recorded at an equal speed of 13 kn. This is comparable to abt. 150 kW reduction of engine power, with only one prototype eConowind-unit, with two 10 m VentiFoils™. Since then the eConowind-unit is tested on a variety of vessels: a container vessel, RoRO-vessel and several other types. The fact that the eConowind-unit is based on a 40 feet container simplifies the logistical issues to get the unit to and on the vessels.

3. Retrofitting VentiFoils on existing vessels reducing fuel consumption and CO2 emissions

During 2019 the development of larger VentiFoils was initiated at Econowind BV, to generate larger thrust from wind than can be possible with the 10 m VentiFoils in the 40 feet container that is limiting their dimensions.

3.1. VentiFoils of 16 m on 'MV Ankie'

The first two stand-alone VentiFoils were developed with a height of 16 m and a chord-length of 2 m. In January 2020 the 10 m basic sections were fitted on a pre-fabricated subframe on the aft side of the forecastle of the Short Sea General cargo vessel 'MV Ankie' of Van Dam Shipping of Spijk, The Netherlands, Fig.7. Later in 2020 the additional 6 m extensions will be fitted.

Fig.7: Stand-alone VentiFoils on the ‘MV Ankie’

Once the VentiFoils are at their design length of 16 m, each VentiFoil will be able to deliver the same thrust as an eConowind-unit with two 10 m VentiFoils. In that situation at a wind- force of 5 Bft from a favourable beam direction, calculations show that the VentiFoils provide abt. 20% of the required thrust for sailing 10 kn with the ‘MV Ankie’. The VentiFoils can be utilized up to wind-force 7 Bft, delivering maximal thrust, and will be turned off and folded down at higher wind speeds and in head winds. They can be folded down aftwards to a horizontal position, supported by (removeable) rests on the forward hatch covers, avoiding wind resistance and hazardous situations in storms.

Analysing the measured thrust-forces on ‘MV Ankie’ with the 10 m VentiFoils, her number of sailing days and sailing routes in the Baltic and North Sea and the long year statistical weather information on that routes, a yearly average saving on fuel and CO2 emissions is predicted between 6 and 8 %.

3.2. Flexible positioning of VentiFoils on Short Sea vessels in relation to cargo-handling

The positioning of WASP devices on Short Sea General cargo vessels is challenging, because they may influence the cargo handling efficiency during loading and unloading. Most vessels of this type have large cargo holds that can be opened completely, leaving very little space for extra installations on deck. Usually the wheelhouse is positioned on the aft ship and SOLAS regulations on the visibility from the bridge have to be considered.

For the compact and slender VentiFoils™ the bridge visibility is usually not the largest challenge: four to six VentiFoils™ could be positioned in upright position on typical example vessels that were investigated. In ports and area’s with dense traffic, the VentiFoils™ can be folded down to the horizontal position to regain the complete original view from the bridge.

When multiple VentiFoils™ are applied to maximize reduction of emissions and fuel consumption, the operational efficiency of cargo handling operations may become a challenge. The optimal balance will be influenced by the specific deck lay-out of the vessel, the type of hatch covers, availability of a crane, and by the operational profile and trading area of the vessel. Regarding the variety of Short Sea General cargo vessels, several options are developed for the positioning of VentiFoils™ on the vessels:

- The eConowind-unit as mentioned above, that can be handled by a crane to be positioned on and off the hatches;
- The stand-alone VentiFoils on a fixed sub-frame on the aft part of the forecastle, like on 'MV Ankie', that can be folded down to the aft side when the hatches are closed, and also folded down to the forward side above the forecastle during cargo-handling with open hatches;
- Foldable VentiFoils on a flat-rack, that can be (re)positioned over the hatch covers in downfolded situation using the hatch-cover crane of the vessel, as will be installed on the 'MV Frisian Sea 'of Boomsma Shipping, Sneek, The Netherlands, Fig.8, where the (red coloured) hatch-cover crane is positioned in front of the deckhouse

Fig.8: VentiFoils on flatracks on the '*MV Frisian Sea'*

New developments of larger VentiFoils for larger vessels give new challenges and opportunities.

3.3. Larger VentiFoils for larger vessels

For the application on larger tankers and bulk carriers, VentiFoils up to a length of 20 m are under development and investigations have started for VentiFoils XL of 30 m length. Those VentiFoils will be mounted on subframes that will be designed and adapted to the construction of the vessel, and they will be foldable downwards to (near) horizontal position, to prevent wind resistance in headwinds and hazards in storms. As most bulk carriers and tankers are sailing at moderate speeds between 10 and 13 kn, initial calculations for some examples of existing vessels show quite positive results.

Preliminary concept studies on the application of 6 VentiFoils XL of 30 m length on different types of bulk carriers, Fig.9, indicate potential savings in fuel consumption and CO2 emission that are ranging from 25 to 65% in positive situations of wind force 5 Bft from favourable directions. This first studies were based on limited data on the vessels and variations in results are related to the size of the example vessels, but also to differences in speed-power characteristics between older vessels and more recent designs. The annual average savings that may be expected for these vessels are strongly dependent on their operational navigation routes: when sailing worldwide there are navigation areas with the favourable 'Tradewinds', but also areas with long periods with very limited winds. For a reference route crossing the (quite windy) North Atlantic, the studies indicate possible annual average savings on fuel and CO2 emission between 10 and 25%, encouraging further investigations.

As the free deck space for mounting VentiFoils, also in down-folded position, seems to be available on most tankers, they are an interesting ship type for further investigation, just like bulk carriers that usually

have relatively small hatches with quite some space in between. Integrating of VentiFoils in the deck arrangement of existing vessels and new designs will require quite some attention and input from the operational departments of shipowners and charterers, with regard to cargo handling during loading and unloading operations and other operational modes that are specific for the ship type.

Fig.9: 6 VentiFoils XL 30 m on a bulk carrier

3.4. Upcoming Regulations effecting the application of VentiFoils and other WASP devices

Items like wheelhouse visibility and stability issues will also need detailed and careful consideration, but actual studies focus on possible yearly average savings on fuel consumption and CO2 emission. Both are closely related, but for the longer term it is to be expected that the actual emphasis of most ship owners and charterers on saving of fuel costs, will gradually shift to reduction of CO2 emission, due to upcoming Regulations.

Both the European Commission and the IMO are preparing regulations with the aim to reduce CO2 emission of shipping, varying from a tax or a levy on emitted CO2, and/or including shipping in the European Trading System (ETS) for CO2-emission rights, to IMO regulations on maximising the CO2 output per 'ton-mile sailed'. Proposals indicate that IMO may define an 'EEXI', an 'Energy Efficiency Index for eXisting vessels', comparable to the EEDI (the Energy Efficiency Design Index that is in force for new built vessels) that maximizes the CO2 emission in gram per ton-mile for a specific vessel, depending on its deadweight. The maximum limit for the allowable CO2 emission may be gradually reduced, and the obvious way for existing vessels to fulfil these requirements seems to be 'slow steaming'.

Another important promising option is the application of VentiFoils or other WASP-devices on existing vessels, generating 'wind-driven-thrust' that can be added to the (reduced) thrust from the propeller that is powered by the engine, emitting CO2. In a situation where the speed of an existing vessel is required to be reduced to fulfil future EEXI-requirements on CO2 emission caused by the main engine, the VentiFoils may be used to increase this speed again in windy circumstances. This may increase the 'transport efficiency' and related economics, without increasing the CO2 emissions.

The proposals for the definition of the EEXI regulations are still developing, and additional careful consideration (and possibly influencing of proposals) is required, to get the possible positive impact of

VentiFoils and other WASP-devices included in the Regulations in a correct way. This will be an interesting subject for another paper, the next section elaborates possible concepts to realize zero emission ocean-going shipping in the future.

4. Hybrid propulsion combining WASP and zero emission technologies

The investigation on the effects and applicability of VentiFoils XL of 30 m length was extended with preliminary concept studies aiming at zero emission ocean-going shipping, a 'Kamsarmax' bulkcarrier of 82.000 TDW with a length of 229 m and a "St. Lawrence Seaway max" Dry Cargo vessel of 33.000 TDW with a length of 220 m and a (quite narrow) Beam of 23.75 m, limited by the locks of the St. Lawrence Seaway from the North Atlantic Ocean to the Great Lakes in the US and Canada.

4.1. Hybrid installation on Kamsarmax concept combining WASP, LNG or Methanol propulsion and future CO2 capturing

The preliminary concept study on the Kamsarmax focused on the application of 10 VentiFoils XL with a length of 30 m on a typical Kamsarmax hull, Fig.10. First studies on the effect of the 10 VentiFoils XL in this concept indicate a possible 'wind-driven-thrust' that is equivalent to a reduction in engine power up to 2700 kW in the situation of sailing with a speed of 10 kn in wind force 5 Bft from a favourable direction. This would mean that the vessel could be able to sail abt. 10 kn in that situation, without using additional engine power, which is quite promising but unlikely and requires additional research. In this preliminary study the effects of the hull lines in the forward part of the hull on the resulting drift angle due to the side forces of the VentiFoils was not yet included. The resulting drift-related added resistance will have a negative impact and requires further investigation, in relation to optimisation of the hull lines in the forward part of the hull.

Fig.10: Ten VentiFoils XL 30m on an 82.000 TDW Kamsarmax bulk carrier concept

For wind conditions on a 'benchmark-North-Atlantic-route' the study indicates a possible annual average 'wind-driven-thrust' that is equivalent to a reduction in engine power of around 1000 kW, based on a vessel speed of 10 kn. On most other routes this value will be lower, so additional thrust from the propeller is required to be able to realize an average service speed of 10 kn. The required engine power to generate that propeller-thrust (and the related fuel consumption and CO2 emission) can be minimized by optimization of the propulsive efficiency of propeller and hull.

To optimize the propulsive efficiency of the combination of aftship lines and propeller, the application of a 'Large Diameter Propeller'(LDP) was investigated, based on the results of a European research project. In that project Conoship collaborated a.o. with MARIN and Chalmers University, leading to an efficiency gain of up to 15% on propulsive efficiency, by application of an LDP for the reference vessel. This was compared to a well-designed conventional propeller and aftship of the same vessel. The conventional design could already attain an EEDI-value that was only 93% of the maximum allowable

value for the Phase 3 regulation, while the LDP design achieved an even lower EEDI-value of just 78% of that allowable value.

Initial investigations on a conventional state-of-the-art Kamsarmax concept indicate a possible gain of abt. 8 % on the propulsive efficiency by application of the LDP concept, leading to the same reduction of the 'non-wind-driven-power-part' that is predicted to give the vessel an economical service speed of 10 kn. This power should be supplied by a propulsion plant with limited CO2 emission, for which a slow speed, 2-stroke Dual Fuel (DF) main engine is considered, fuelled by LNG or (bio)methanol. This was not elaborated in the preliminary concept study, but Conoship research on the possibilities of future capturing of CO2 on board of LNG fuelled vessels is quite promising.

As CO2 capturing from exhaust gasses is a proven technology in land-based installations, the capturing of CO2 on board of vessels can be considered technically feasible. Advantages of LNG fuelled vessels are the relatively clean exhaust gasses (compared to HFO installations) and the availability of LNG at abt. minus 160 degrees Centigrade. The 'available cold' in the LNG can be used to cool down and liquify the captured gaseous CO2 and the liquified CO2 can be stored in regular CO2 tanks at minus 20 gr.C at a pressure of 20 bar. In a future scenario the liquid CO2 can be unloaded in port during the bunkering of LNG and be stored deep in the earth in offshore wells, resulting in a 'CO2-neutral'shipping concept.

The future economic feasibility of this concept should be considered in comparison to other CO2 neutral or zero emission technologies. The application of the 10 VentiFoils XL enables to use wind (whenever it is available) to reduce the required energy from the main engine. Depending on the operational area and related wind conditions, this may reduce the required capacity of the installation for the methanol or LNG system, reducing the CAPEX of that installations and the OPEX for the fuels.

4.2. CONOSHIP 33000 ZE, combining WASP, batteries and green hydrogen for wind powered zero emission shipping

The initial results of the application of 10 VentiFoils XL of 30 m length and the resulting optimized hull lines from the LDP research in cooperation with MARIN, inspired the preliminary concept study for a CONOSHIP 33000 TDW Zero Emission concept, Fig.11.

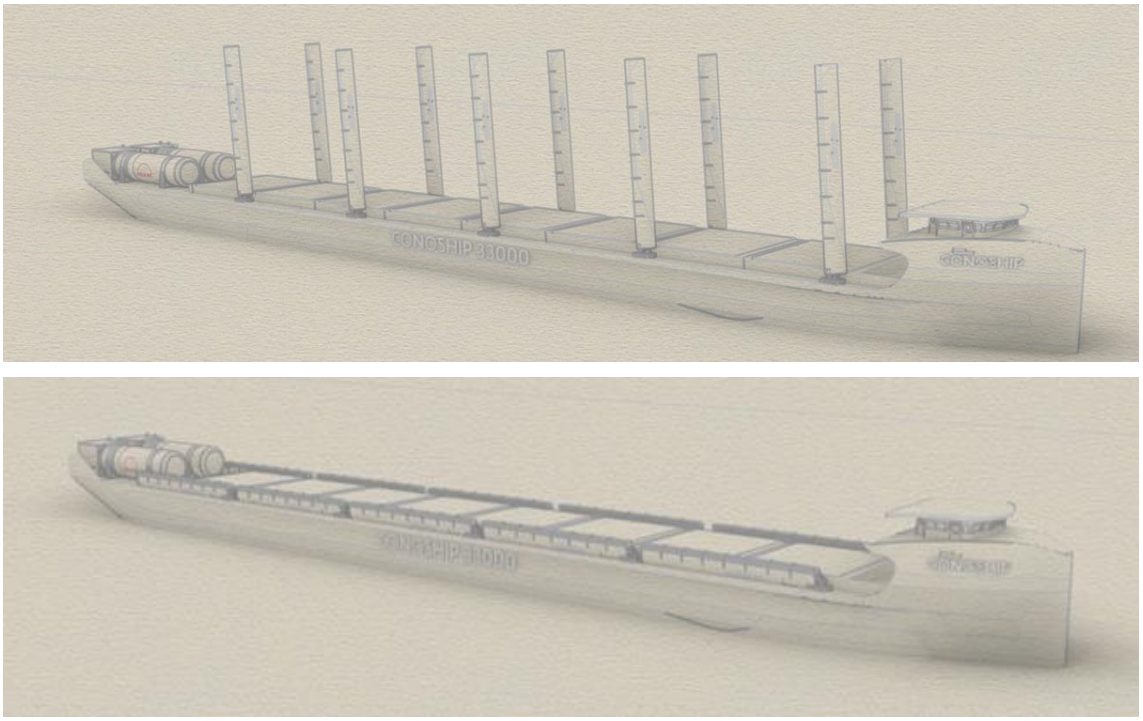

Fig.11: CONOSHIP 33000 ZE with 10 VentiFoils XL

The slender hull with reduced breadth, limited by the dimensions of the locks in St. Lawrence Seaway, was optimized for propulsive efficiency according to the LDP concept and tank tested at MARIN for sailing in heavy weather on the North Atlantic. The slender bow has good seakeeping characteristics and is considered to be promising in relation to limiting the resulting drift angle due to the side forces of the VentiFoils. The same goes for the resulting drift-related added resistance, although this was not investigated yet and requires further research.

The arrangement with the forward wheelhouse gives free visibility not impeded by VentiFoils, but the large hatch openings require the challenging positioning of the VentiFoils next to the hatches on the gangway, folding down longitudinally in head winds and heavy storms. Integrating the VentiFoils XL in this concept design requires additional investigations in next phases of the project.

Studies on the effect of the 10 VentiFoils XL in this concept indicate a possible 'wind-driven-thrust' that is ~25% more than required for sailing at the service speed of 11 kn in the situation of sailing in wind force 5 Bft from a favourable direction. This would mean that the vessel could be able to sail faster than 11 kn in that situation, without using additional engine power, which is quite promising and not necessary for the intended operation. It is considered 'less unlikely' than in the previous concept study mentioned above, but also requires additional research in a next phase.

For wind conditions on the 'benchmark-North-Atlantic-route' the study indicates a possible annual average 'wind-driven-thrust' that is equivalent to a reduction of abt. 40 % in engine power, based on a vessel speed of 11 kn. For the concept study it is considered that in wind conditions between 5 and 7 Bft. the speed is kept around 11 kn and the propeller will be used as a 'water-turbine': the flow of water will turn the propeller, transmitting driving power to the electric propulsion motor that will act as a generator, providing electrical energy for charging a large battery bank in the vessel. During periods of less wind than abt. 5 Bft., the batteries will provide the required power to the electric propulsion motor to keep on sailing ~11 kn.

During longer periods of limited wind speeds, the electrical power for the 2500 kW propulsion motor will be supplied by a stack of PEM fuel cells that are powered by hydrogen in this concept study. The hydrogen is considered to be stored at minus 253 degrees Centigrade, in specially designed tanks for liquid hydrogen (that are actually being designed and produced in Sweden for a different application).

The complex hydrogen system will require additional research and development, just like the other systems in the concept, but preliminary calculations based on energy content, indicate that the concept should be able to cross the North Atlantic from Rotterdam to Quebec with an amount of liquid hydrogen that can be stored in 2 tanks of 400 m^3 This is considered to be a rather limited amount of hydrogen, requiring a weight and space that can be integrated in the design of the zero emission concept.

Application of the 10 VentiFoils XL on this windy route is indicated to provide on average a relevant part of the required thrust and energy for crossing the Atlantic at an average speed of 11 kn. The LDP concept reduces the required power of the electric motor to a modest 2500 kW, (more than) enough to sail at a speed of 11 kn without wind on a flat sea. Preliminary calculations indicate that the capacity of 2 tanks of 400 m^3 of liquid hydrogen should be sufficient for crossing the Atlantic on the benchmark-route, even if there is only little wind available. In a situation without any wind for weeks, it may be wise to reduce speed to 10 or 9 kn.

5. Conclusion

Although the mentioned subjects require additional research and development, the concept study on a CONOSHIP 33000 ZE concept is considered to be promising for technical feasibility of zero emission shipping, based on the hybrid combination of VentiFoils XL and zero emission propulsion technology that is available or can be available in the near future. Economical feasibility in a future situation will be determined by rules and regulations on preventing of emission to save the climate and the planet.

Acknowledgements

Special acknowledgements go to the ship owners WijnneBarends that offered the ‘MV Lady Christina’ for the first seagoing tests, Van Dam Shipping for data from the ‘MV Ankie’, and Boomsma Shipping for the ‘MV Frisian Sea’. MARIN and TU Delft were very supportive in providing practical and theoretical support and the following companies provided data and support for the concept study on zero emission shipping: Nedstack on PEM fuel cell technology, SPBES on batteries and MAN Cryo on bunker tanks for liquid hydrogen.

The development of the VentiFoils™ was co-financed by the European Fund for Regional Development and the provinces of Groningen, Fryslan and Drenthe of the Netherlands, through a VIA-subsidy coordinated by SNN.

Index by Authors

13th Symposium on

High-Performance Marine Vehicles – "Technologies for the Ship of the Future"

HIPER

Tullamore / Ireland, 13-15 September 2021



Topics: ultra-efficient & zero-emission ships / alternative fuels / 2030 & 2050 target technologies / electric ships
advanced design & production technology / shipyard 4.0 / future materials /
future use of oceans / blue economy / future shipping scenarios / intelligent & connected ships /
unconventional designs & propulsion concepts / biomimetic marine technologies

Organiser: Volker Bertram (volker@vb-conferences.com)

Advisory Committee:

Catherine Austin	I-Tech	**Robert Dane**	Ocius	**Kohei Matsuo**	NMRI
Carlo Bertorello	Naples University	**Stefan Harries**	Friendship Systems	**Christian Oldendorff**	Amplifier
Carsten Bullemer	Maritime Data Systems	**Robert Hekkenberg**	TU Delft	**Prasanta Sahoo**	FIT
Emilio Campana	CNR	**Thomas Hildebrandt**	Numeca	**Pierre Sames**	DNV GL
Roy Campe	CMB	**Jan Kelling**	Hasytec	**Noah Silberschmidt**	Silverstream Technologies
Andrea Coraddu	Strathclyde Univ	**Jiulun Liu**	Wuhan Univ Technology	**Teus van Beek**	Wärtsilä

Venue: The conference will be held at the "Bridge House Hotel" in Tullamore/Ireland

Format: Papers to the above topics are invited and will be selected by a selection committee.
Proceedings will be electronic pdf version in colour.

Deadlines:

anytime	Optional "early warning" of interest to submit paper
8.6.2021	First round of abstract selection (1/3 of available slots)
8.7.2021	**Second round of abstract selection (remaining 2/3 of slots)**
8.9.2021	Payment due for authors
8.9.2021	Final papers due (50 € surcharge for late submission)

Fees:

650 € / 350 €	regular / PhD student – early registration (by 15.9.2020)
750 € / 400 €	regular / PhD student – late registration

Fees are subject to VAT
Fees include proceedings, lunches and coffee breaks, and conference dinner
Fees apply also to authors

Sponsors: Tutech Innovation, Hasytec – further to be announced

Media Partner: Hansa

Information: volker@vb-conferences.com